



**THE** SPECIAL ISSUE  
**IIOAB**  
**JOURNAL**

**VOLUME 7 : NO 11 : DECEMBER 2016 : ISSN 0976-3104**

**Institute of Integrative Omics and  
Applied Biotechnology Journal**

Dear Esteemed Readers, Authors, and Colleagues,

I hope this letter finds you in good health and high spirits. It is my distinct pleasure to address you as the Editor-in-Chief of Integrative Omics and Applied Biotechnology (IIOAB) Journal, a multidisciplinary scientific journal that has always placed a profound emphasis on nurturing the involvement of young scientists and championing the significance of an interdisciplinary approach.

At Integrative Omics and Applied Biotechnology (IIOAB) Journal, we firmly believe in the transformative power of science and innovation, and we recognize that it is the vigor and enthusiasm of young minds that often drive the most groundbreaking discoveries. We actively encourage students, early-career researchers, and scientists to submit their work and engage in meaningful discourse within the pages of our journal. We take pride in providing a platform for these emerging researchers to share their novel ideas and findings with the broader scientific community.

In today's rapidly evolving scientific landscape, it is increasingly evident that the challenges we face require a collaborative and interdisciplinary approach. The most complex problems demand a diverse set of perspectives and expertise. Integrative Omics and Applied Biotechnology (IIOAB) Journal has consistently promoted and celebrated this multidisciplinary ethos. We believe that by crossing traditional disciplinary boundaries, we can unlock new avenues for discovery, innovation, and progress. This philosophy has been at the heart of our journal's mission, and we remain dedicated to publishing research that exemplifies the power of interdisciplinary collaboration.

Our journal continues to serve as a hub for knowledge exchange, providing a platform for researchers from various fields to come together and share their insights, experiences, and research outcomes. The collaborative spirit within our community is truly inspiring, and I am immensely proud of the role that IIOAB journal plays in fostering such partnerships.

As we move forward, I encourage each and every one of you to continue supporting our mission. Whether you are a seasoned researcher, a young scientist embarking on your career, or a reader with a thirst for knowledge, your involvement in our journal is invaluable. By working together and embracing interdisciplinary perspectives, we can address the most pressing challenges facing humanity, from climate change and public health to technological advancements and social issues.

I would like to extend my gratitude to our authors, reviewers, editorial board members, and readers for their unwavering support. Your dedication is what makes IIOAB Journal the thriving scientific community it is today. Together, we will continue to explore the frontiers of knowledge and pioneer new approaches to solving the world's most complex problems.

Thank you for being a part of our journey, and for your commitment to advancing science through the pages of IIOAB Journal.



Yours sincerely,

*Vasco Azevedo*

**Vasco Azevedo**, Editor-in-Chief  
Integrative Omics and Applied Biotechnology  
(IIOAB) Journal





**Prof. Vasco Azevedo**  
Federal University of Minas Gerais  
Brazil

## Editor-in-Chief

### Integrative Omics and Applied Biotechnology (IIOAB) Journal Editorial Board:



**Nina Yiannakopoulou**  
Technological Educational Institute of Athens  
Greece



**Jyoti Mandlik**  
Bharati Vidyapeeth University  
India



**Rajneesh K. Gaur**  
Department of Biotechnology, Ministry of Science and Technology  
India



**Swarnalatha P**  
VIT University  
India



**Vinay Aroskar**  
Sterling Biotech Limited  
Mumbai, India



**Sanjay Kumar Gupta**  
Indian Institute of Technology  
New Delhi, India



**Arun Kumar Sangaiah**  
VIT University  
Vellore, India



**Sumathi Suresh**  
Indian Institute of Technology  
Bombay, India



**Bui Huy Khoi**  
Industrial University of Ho Chi Minh City  
Vietnam



**Tetsuji Yamada**  
Rutgers University  
New Jersey, USA



**Moustafa Mohamed Sabry Bakry**  
Plant Protection Research Institute  
Giza, Egypt



**Rohan Rajapakse**  
University of Ruhuna  
Sri Lanka



**Atun RoyChoudhury**  
Ramky Advanced Centre for Environmental Research  
India



**N. Arun Kumar**  
SASTRA University  
Thanjavur, India



**Bui Phu Nam Anh**  
Ho Chi Minh Open University  
Vietnam



**Steven Fernandes**  
Sahyadri College of Engineering & Management  
India

ARTICLE

# EFFECT OF ORGANIC MANURE ON THE HYDRO-BIOLOGICAL CHARACTERISTICS OF FISH POND

S. Kumar\* and S. Godara

Department of Zoology, CRM Jat (PG) College, Hisar-125001, INDIA

## ABSTRACT

The availability of nutrients in the ponds, artificial feed and recycling of the nutrients regulates the fish productions. In the present investigations, different organic manure i.e vermicompost @ 15,000 kg/ha/yr, vermicompost @ 10,000 kg/ha/yr, cow dung @ 10,000 kg/ha/yr, poultry manure @ 6,000 kg/ha/yr, pig manure @ 4,000 kg/ha/yr used to monitored their effect on water quality parameters, bacterial population and growth performance of Catla catla, Labeo rohita and Cirrhinus mrigala. The maximum values of dissolved oxygen (5.81 to 8.65 mg/l), turbidity (35.96 to 16.30 cm), phytoplanktons (99 to 5,786 no/l) and zooplanktons (186 to 2,046 no/l) observed in pond waters treated with vermicompost @ 10,000 kg/ha/yr. While that of pH (5.63 to 5.80), alkalinity (200.00 to 360.62 mg/l), hardness (173.06 to 292.02 mg/l) found to be maximum in vermicompost @15,000 kg/ha/yr. Free CO<sub>2</sub> (1.40 to 3.40 mg/l) and nitrogen (0.990 to 0.170 mg/l) found to be maximum in the pond waters treated with cow-dung @ 10,000 kg/ha/yr. Temperature (26.53 to 34 oC), potassium (3.24 to 23.94 mg/l) and phosphorous (0.72 to 0.199 mg/l) found to be maximum in the pond waters treated with poultry manure @ 4,000 kg/ha/yr. The range of water parameters increased significantly ( $P<0.05$ ) in the pond waters treated with different manures. Pond fertilized with vermicompost @ 10,000, found to be best as compare to vermicompost @ 15,000, followed by cow dung @ 10,000, poultry manure @ 6,000 and pig manure @ 4,000 kg/ha/yr, respectively..

## INTRODUCTION

**KEY WORDS**  
Vermicompost,  
bacteria, alkalinity,  
phytoplankton,  
manures, population

The over increasing demand for quality food especially the protein sources can be satisfied only through improved production of protein rich products. The aquaculture products could be one of the most import source of protein. Therefore, the improvement of aquaculture is only possible by increasing the integrated large network of man-made as well as natural reservoirs. The sustainable integrated management of such reservoirs could only increase the production of aquaculture products per unit area. The fish production mainly depends over the natural or inherits productivity of natural or manmade ponds. Various types of nutrients can be artificially provided to the fish ponds through addition of manures, fertilizers and supplementary feed. Nowadays, the natural productivity of the ponds are being enhanced through the artificial application of numerous types and dosages of natural or synthetic fertilizers and manures to meet the nutritional requirements, selection of high productivity fish species and their stocking ratios, alteration of the feeding ratio and frequency. Improving the production of beneficial phytoplankton, algae also boots the productivity of the fish as these microscopic phytoplankton sustain the primary productivity of an aquatic food chain [1]. Improvement in the various water quality parameters suitable for the fish growth, have been reported due to increased fertilization except the fluctuation of dissolved oxygen due to the application of high manuring rate [2]. The nitrogen, phosphorous and potassium released during the decomposition of organic manures in the water which serve as primary nutrients for the growth of all types of phytoplankton The improvement in the growth of decomposers such as bacteria and fungi have been found due to addition of organic fertilizers and such decomposers are critical to the removal of various types of toxic waste produced and accumulate due to the use of artificial fish feeds [3]. The maintenance of doses of organic manures in the fish ponds are also crucial as the decomposition of such material consumes all the dissolved oxygen thus water quality is deteriorated. Similarly, the use of organic manures and fertilizer in excess results depletion of dissolved oxygen which results in production of various types toxic gases such as H<sub>2</sub>S, NH<sub>3</sub>, CO<sub>2</sub>, etc. Increase of such gases in the aquaculture ponds results higher growth of pathogenic microorganisms thus the aquaculture is reduced due to parasitic diseases [4]. The use of vermi compost is as organic fertilizer in agro-ecosystems as well as in aquaculture has also found improving the production. The quick availability of nutrients present in the vermin compost are 'ready- to-uptake forms which is a major advantage [5].

## MATERIALS AND METHODS

A series of experiments carried out using earthen ponds with the size of 18ft × 20 ft from Sept., 2013 to Aug., 2014. The ponds cleaned with lime @ 200kg/ha/yr and filled with inland ground water obtained from deep tube wells and allowed to stabilize for about 15 days. The combination of different fish (C. catla as surface feeder, L. rohita as column feeder and C. mrigala as bottom feeder) species selected for experiments. The Indian major carp's fingerlings collected from Satroad fish farm situated at Hisar and stocked in tubs. Fingerlings acclimated in aquarium room for 10 days prior to the commencement of experiment. All fish fed daily twice @ 2% BWd<sup>-1</sup> for the whole experimental duration of 12 months. Fish growth was monitored after regular 15 days interval in term of weight and length gain and feeding rate adjusted accordingly to APHA [6]. To fertilize the ponds with semi dried pig manure @ 4,000 kg/ha/yr (T2), poultry manure @ 6,000 kg/ha/yr (T3), cow-dung @10,000 kg/ha/yr (T4), vermicompost @10,000 kg/ha/yr (T5), vermicompost @15,000 kg/ha/yr (T6) and control (T1) applied at 25% initial and remaining

\*Corresponding Author  
Email:  
suresh\_sang@yahoo.com  
Tel.: +91- 9466547018

Published: 10 Oct 2016



split doses given at biweekly intervals in ponds. The various feed ingredients, used in the present study fish meal, processed soybean, rice bran, mustard oil cake and wheat flour. All the ingredients grounded and powdered prior to the preparation of experimental diets. The water quality parameters like dissolved oxygen, pH, alkalinity, turbidity, temperature, hardness, free CO<sub>2</sub>, potassium, nitrogen, phosphorus, phytoplankton and zooplanktons population were recorded at 15 days intervals according to method as describe by APHA [6]. The results compared using 'Completely Randomized Design' [7]. A 10 liters volume of pond water was filtered through a 125 µm mesh size plankton net and further concentrated to 40 ml in small plastic bottles. The filtrated planktons were immediately preserved and the plankton abundance were expressed as organisms per liter. A 1 ml volume of the concentrated plankton sample was transferred to the cell cavity of Sedgwich rafter cell and allowed to settle. Randomly 10 selected fields of chamber were counted under the microscope and the number of the planktons were calculated as follows:

$$\text{Number of plankton/l} = (P \times C \times 100) / L$$

Where

- P = the number of plankton counted from ten aquaria  
C = Volume of final concentration of sample (ml)  
L = the volume of water sample (l) filtered

## RESULTS AND DISCUSSION

Camel The production of aquaculture products depends on the water quality which are one the most important factors responsible for the fish growth throughout the cultivation period. The high production of fish in only possible if the survival, growth, and reproduction of the fish will be high. Which depends on the water quality of the aquaculture ponds. The fish production will be reduced in the poor water. Indian major carp namely *C. catla*, *L. rohita* and *C. mrigala* stocked to evaluate the response of treated pond [8]. In the present study, a significant difference in dissolved oxygen observed between the treatments. The vermicompost @10,000 kg /ha/yr used in present study seemed to act as oxygen promoters as these caused significant increase in dissolved oxygen in pond water. The effect of vermicompost @ 10,000 kg/ha/yr was better than vermicompost @ 15,000 kg/ha/yr followed by cow-dung @ 10,000 kg/ha/yr, poultry manure @ 6,000 kg/ha/yr, and pig manure @ 4,000 kg/ha/yr, respectively. On the other hand, pond fertilized with vermicompost @ 15,000 kg/ha/yr showed dissolved oxygen increase up to 8.5 mg/l as compare 7.90 mg/l in the pond water in control treatment [Fig. 1]. Similar results were observed by Bansal [9] and Kaur [10]. They also reported significantly higher dissolved oxygen in vermicompost as compared to other organic manure (cow-dung). During the present investigation dissolved oxygen showed the negative and highly significant correlation with the water temperature in all the treatments.

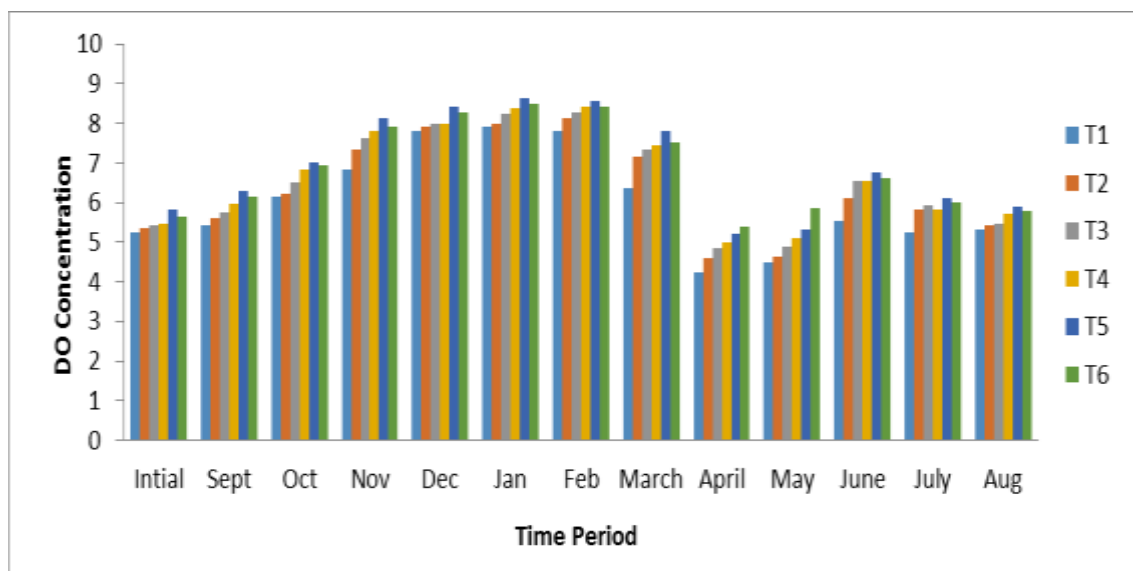


Fig. 1: Variation in dissolve oxygen (DO) during Sept. 2013 to Aug. 2014 in fish pond

The variation in pH level depending on a number of factor including species composition and plant communities. It can cause stress, increase susceptibility to disease, low production levels and poor growth [11]. The pH range between 5 and 10 in most of the natural waters [12] however, the pH is influenced by several factors such as discharge of wastewaters, acid rains, increase dissolution of atmospheric CO<sub>2</sub> and fish respiration. In the present study, a significant difference in pH observed between all the treatments and control. The pH found to be maximum in vermicompost @ 15,000 followed by vermicompost @10,000, cow-dung @ 10,000, poultry @ 6,000 and pig manure @ 4,000 kg/ha/yr, respectively [Fig. 2].

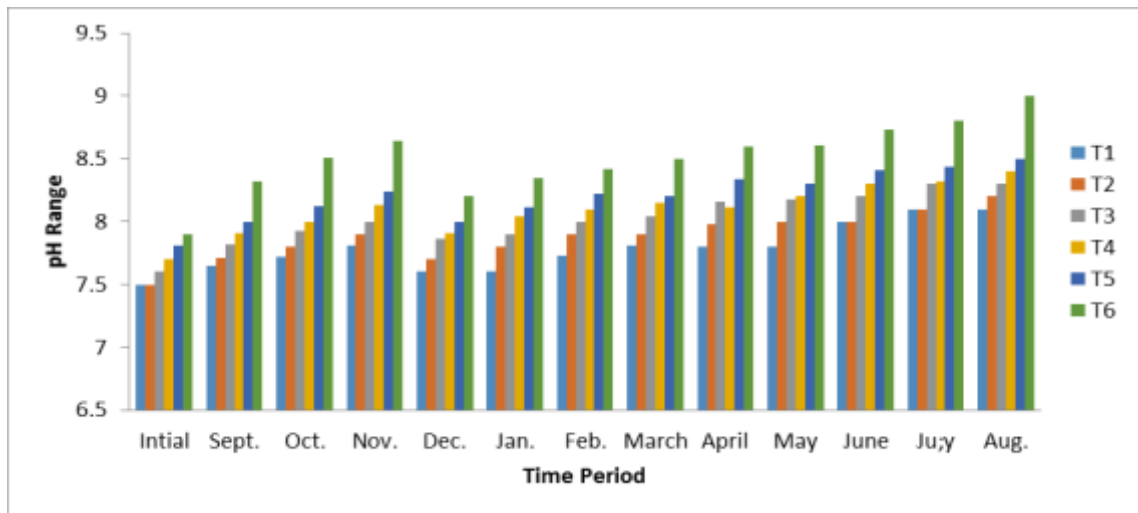


Fig. 2: Variation in pH during Sept. 2013 to Aug. 2014 in fish pond

On the other hand, pond fertilized with vermicompost @10,000 kg/ha/yr had pH 8.50. The pH was 8.10 in the ponds under control treatment. Throughout the experimental period, seasonal variation in pH was observed which varied from 7.5 to 9.0 in all the treatments due to respiration and photosynthetic activities. A positive and significant correlation among the pH and planktonic biomass was observed in all the treatments which are in accordance with the findings of Mahboob and Sheri [13]. The alkalinity of pond increased and reached up to 360.62 mg/l in the pond treated with vermicompost @ 15,000 kg/ha/yr. The alkalinity found to be maximum in treatment

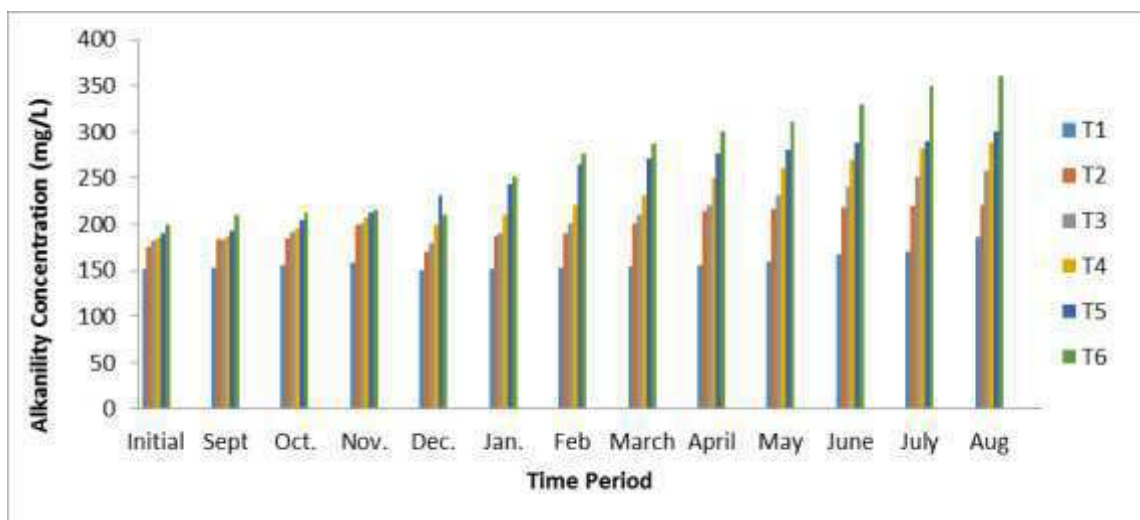


Fig. 3: Variation in water alkalinity during Sept. 2013 to Aug. 2014 in fish pond

vermicompost @ 15,000 kg/ha/yr followed vermicompost 10,000 kg/ha/yr, cow-dung @10,000 kg/ha/yr , poultry manure @ 6,000 kg/ha/yr and pig manure @ 4,000 kg/ha/yr [Fig. 3]. Similarly, pond fertilized with vermicompost @ 10,000, cow-dung @ 10,000, poultry @ 6,000 and pig manure @ 4,000 kg/ha/yr showed alkalinity increased up to 300.00, 288.41, 258.20, 220.80 mg/l as compared to 186.60 mg/l in the control fish pond.

Similar observations were reported by Kaur and Ansal [14]. Compared to other organic manure i.e. cow-dung, Kaur and Ansal [14] reported significantly higher alkalinity in vermicompost. Therefore, throughout the experimental periods the pond water was remained alkaline in all the treatments. Terziyski et al. [15] reported that the presence of carbonates and bicarbonates also make the pond water slightly alkaline which has been found to be favorable for the growth of the aquatic organism.

The hardness of pond increased and reached up to 292.02 mg/l in the ponds treated with vermicompost @ 15,000 kg/ha/yr. The hardness was found to be maximum in vermicompost @ 15000 followed by vermicompost @ 10000, cow-dung @ 10000, poultry manure @ 6000 and pig manure @ 4000 kg/ha/yr [Fig. 4]. The hardness was 178.20 mg/l in the ponds under control treatment.

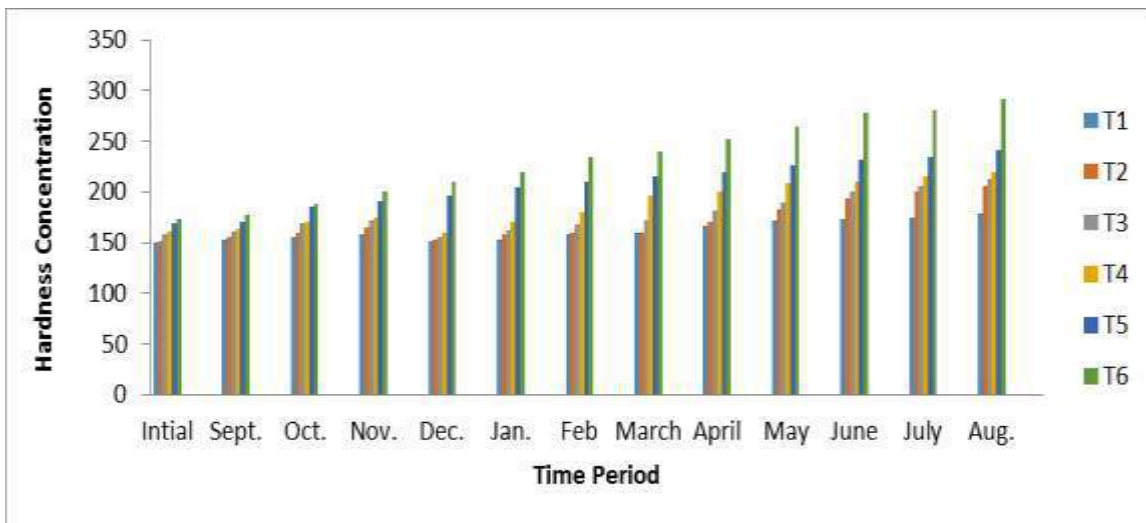


Fig. 4: Variation in hardness of water during Sept. 2013 to Aug. 2014 in fish pond

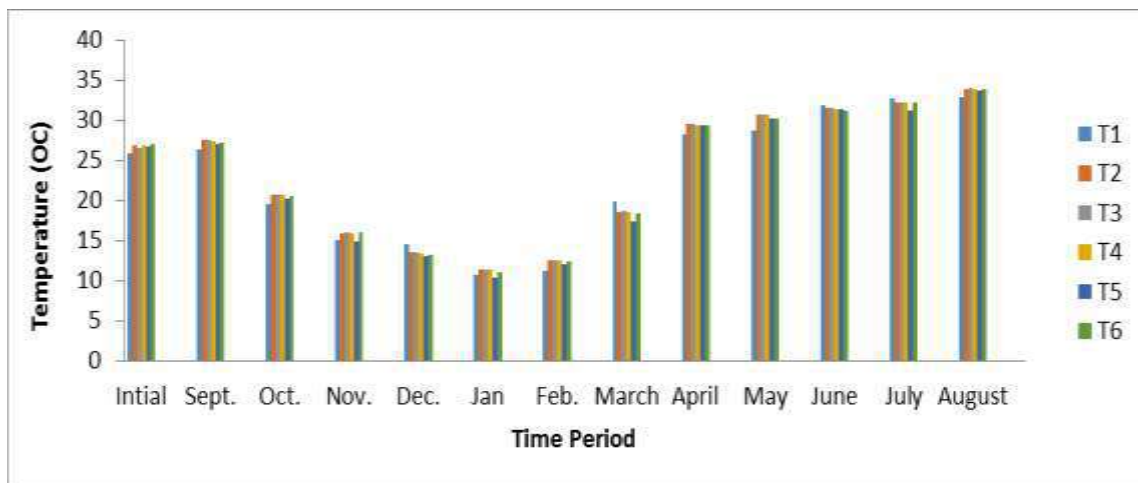


Fig. 5: Variation in Temperature of water during Sept. 2013 to Aug. 2014 in fish pond

The temperature of the water temperature was comparatively 2-5°C lower than the air during the experimental durations. . In the present study, the water temperature ranged between 10.7-34.0°C [Fig. 5]. A significant difference observed in temperature between the vermicompost @15,000 kg/ha/yr, vermicompost @ 10,000 kg/ha/yr, cow-dung @ 10,000 kg/ha/yr, poultry manure @ 6,000 kg/ha/yr, pig manure @ 4,000 kg/ha/yr and control treated ponds in different proportions. The temperature of pond increased and reached up to 34 °C in the ponds treated with poultry manure @ 6,000 kg/ha/yr. The treatment poultry manure used in present study showed an enhancing effect as it caused significant increase in temperature of pond water due to decomposition of manure. The temperature was found to be maximum in poultry manure @ 6,000 kg/ha/yr followed by pig manure @ 4,000 kg/ha/yr, cow-dung @ 10,000 kg/ha/yr, vermicompost @ 15,000 kg/ha/yr and vermicompost @ 10,000 kg/ha/yr . The temperature was 32.82 °C in the ponds under control. Hayat et al. [16] reported a positive and significant correlation between planktonic biomass and the water temperature. The planktonic biomass and water temperature both are the important parameters which directly corresponds primary productivity of pond ecosystem thus responsible for the fish growth and yield. In the present investigation, the overall range of water turbidity was 35.96 to 11.20 cm. The turbidity of pond decreased and reached up to 14.30 cm in the ponds treated with cow-dung @10,000 kg/ha/yr. The turbidity was found to be maximum in vermicompost @ 10,000 kg/ha/yr followed by vermicompost @ 15,000 kg/ha/yr, cow-dung @ 10,000 kg/ha/yr, poultry manure @ 6,000 kg/ha/yr and pig manure @ 4,000 kg/ha/yr [Fig. 6]. On the other hand, pond fertilized with vermicompost @ 15,000 kg/ha/yr, cow-dung @ 10,000 kg/ha/yr, poultry manure @



6,000 kg/ha/yr and pig manure @ 4,000 kg/ha/yr showed decrease up to 15.00, 14.30, 13.00, 13.00 cm.

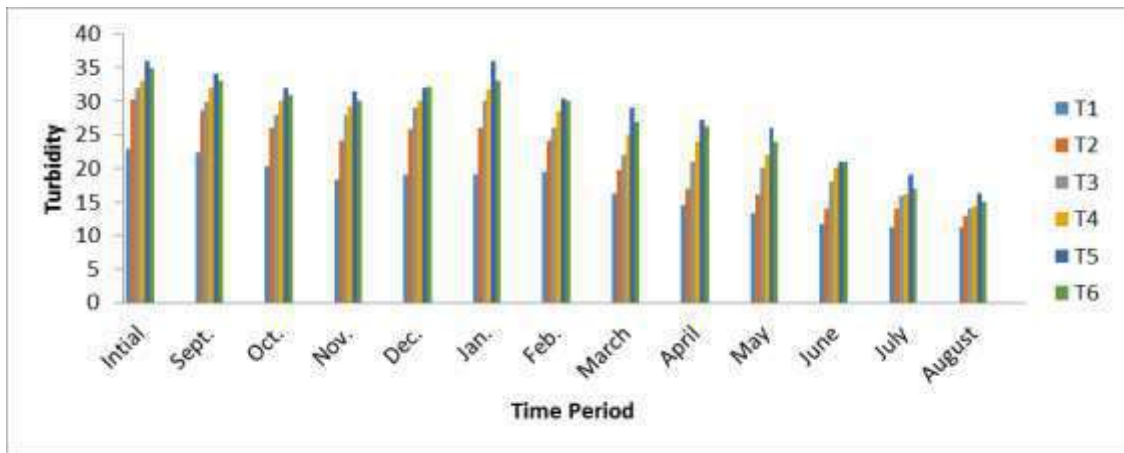


Fig. 6: Variation in water turbidity during Sept. 2013 to Aug. 2014 in fish pond

The mean values of turbidity in the pond water of control remained in a range of 22.90 to 11.20 cm. The primary productivity of water bodies depends on the light penetration therefore; it is also one of the limiting factors. The availability of light, essential nutrients and water temperature regulates various metabolic processes of aquatic organisms thus corresponds the overall biological productivity of a pond ecosystem which is a measure of planktonic [17 & 18].

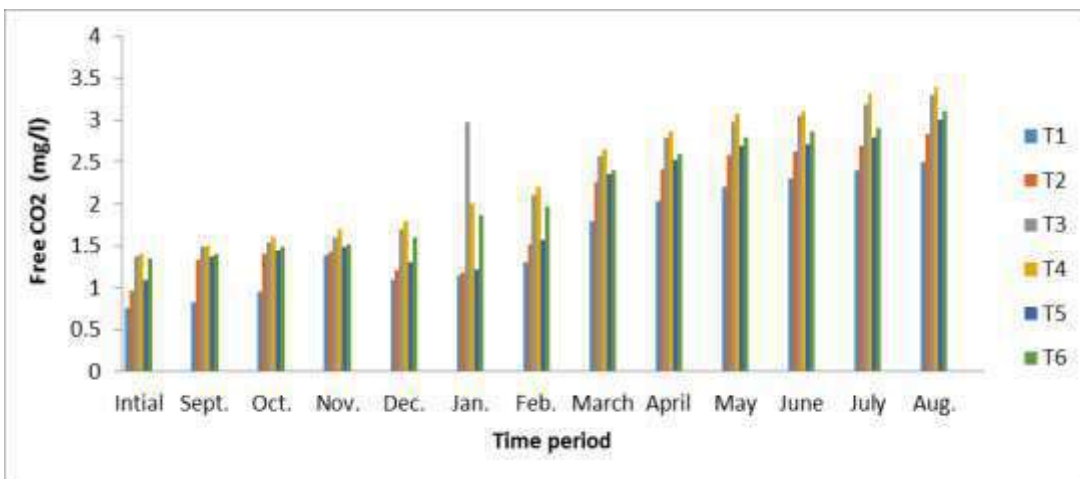


Fig. 7: Variation in free CO2 during Sept. 2013 to Aug. 2014 in fish pond

The treatment cow-dung used in present study showed an enhancing effect as it caused significant increase in free CO<sub>2</sub> of pond water. The free CO<sub>2</sub> was found to be maximum in cow-dung @ 10,000 kg/ha/yr treatment followed by poultry @ 6,000 kg/ha/yr and vermicompost @ 15,000 kg/ha/yr, vermicompost @ 10,000 kg/ha/yr, pig manure @ 4,000 kg/ha/yr [Fig. 7]. On the other hand, pond fertilized with treatment poultry manure @ 6,000 kg/ha/yr, vermicompost @ 15,000 kg/ha/yr, vermicompost @ 10,000 kg/ha/yr and pig manure @ 4,000 kg/ha/yr showed increase up to 3.30, 3.10, 3.00, 2.84 mg/l. The free CO<sub>2</sub> was 2.50 mg/l in the ponds under control treatment. Similar results were observed by Kaur [10] on free CO<sub>2</sub> in vermicompost as compared to other organic manure (cow-dung).

The potassium of fish pond increased and reached up to 23.94 mg/l in the poultry manure@ 6,000 kg/ha/yr treated fishes. The poultry manure used in present study seemed to have potassium enhancing effect as it caused significant increase in potassium in fish pond. The effect of poultry manure @ 6,000 kg/ha/yr was better than pig manure @ 4,000 kg/ha/yr, cow-dung @ 10,000 kg/ha/yr, vermicompost @ 15,000 kg/ha/yr and vermicompost @ 10,000 kg/ha/yr [Fig. 8]. On the other hand, pond fertilized with pig manure @ 4,000 kg/ha/yr, cow-dung @ 10,000 kg/ha/yr, vermicompost @ 15,000 kg/ha/yr and vermicompost @ 10,000 kg/ha/yr showed increase up to 19.98, 18.36, 15.65, 14.27 mg/l values of potassium. The potassium was 7.78 mg/l in the ponds under control quantities exits in ponds is very complex because of the many states in which nitrogen can exist: NH<sub>3</sub>, NH<sub>4</sub><sup>+</sup>, N<sub>2</sub>, N<sub>2</sub>O, NO, N<sub>2</sub>O<sub>3</sub>, N<sub>2</sub>O<sub>5</sub>,

NO<sub>2</sub><sup>-</sup>, and NO<sub>3</sub><sup>-</sup>, nitrates are usually most important because living cells contain about 1-10% total nitrogen by dry weight. In the present study, a significant difference in NH<sub>4</sub>-N was observed between all six the treatments [Fig. 9]. The NH<sub>4</sub>-N of fish pond increased and reached up to 0.170 mg/l in the cow-dung @ 10,000 kg/ha/yr treated fishes. Over all, NH<sub>4</sub>-N also found to increase in Indian major carp fed on a diet containing cow-dung@10,000 kg/ha/yr. The effect of cow-dung @ 10,000 kg/ha/yr was better than vermicompost @ 15,000 kg/ha/yr, vermicompost @ 10,000 kg/ha/yr, poultry manure @ 6,000 kg/ha/yr and pig manure @ 4,000 kg/ha/yr. On the other hand, pond fertilized with vermicompost @ 15,000 kg/ha/yr, vermicompost @ 10,000 kg/ha/yr, poultry manure @ 6,000 kg/ha/yr and pig manure @ 4,000 kg/ha/yr showed increase up to 0.140, 0.135, 0.081, 0.070 mg/l value of NH<sub>4</sub>-N. The NH<sub>4</sub>-N was 0.050 mg/l in the ponds under control treatment [19, 20].

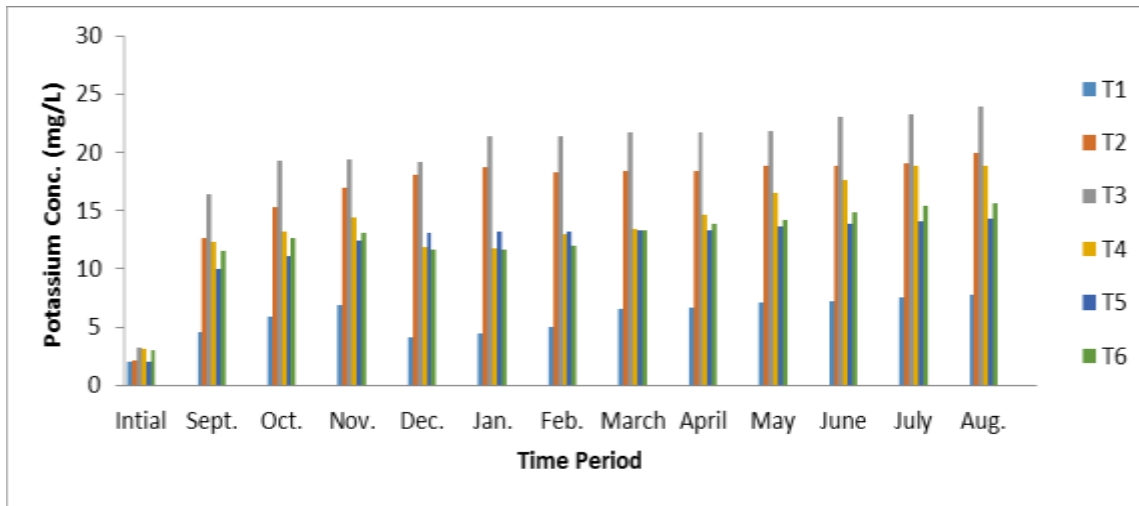


Fig. 8: Variation in water potassium concentration during Sept. 2013 to Aug. 2014 in fish pond

The amount of phosphorous of fish pond increased and reached up to 0.199 mg/l in the poultry manure @ 6,000 kg/ha/yr treated fishes. Over all, phosphorous was also found to increase in Indian major carp fed on diet containing poultry manure @ 6,000 kg/ha/yr. The treatment poultry manure used in present study seemed to have phosphorous enhancing effect as it caused significant increase in Indian major carp pond [Fig. 10]. The effect of poultry manure @ 6,000 kg/ha/yr was better than vermicompost @ 15,000 kg/ha/yr, vermicompost @ 10,000 kg/ha/yr, cow-dung @ 10,000 kg/ha/yr and pig manure @ 4,000 kg/ha/yr. On the other hand, pond fertilized with vermicompost @ 15,000 kg/ha/yr, vermicompost @ 10,000 kg/ha/yr, cow-dung @ 10,000 kg/ha/yr and pig manure @ 4,000 kg/ha/yr showed increase up to 0.186, 0.182, 0.175, 0.089 mg/l values of phosphorous. The phosphorous was 0.047 mg/l in the ponds under control treatment. A similar result was observed by Bansal [9] who found that vermicompost contained all the major nutrients compounds and high plankton occurred in ponds treated with organic manure mainly due to the content of phosphate.

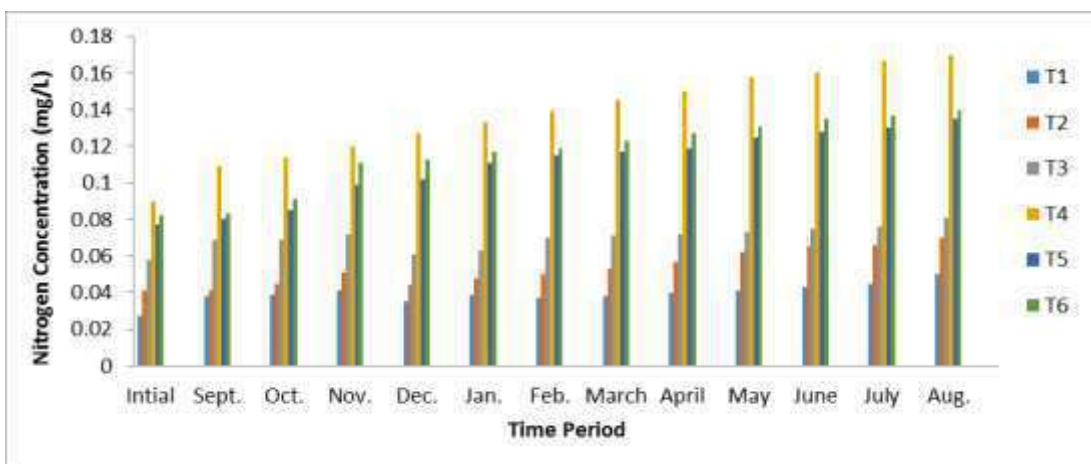


Fig. 9: Variation in water Nitrogen concentration during Sept. 2013 to Aug. 2014 in fish pond

The population density of zooplankton of fish pond increased and reached up to 2,046 no/l in the pond treated with vermicompost @ 10,000 kg/ha/yr [Fig. 11]. Vermicompost @ 10,000 kg/ha/yr used in present study seemed to have zooplankton enhancing effect as it caused significant increase in amount of nutrients in the pond. The effect of treatment vermicompost @ 10,000 kg/ha/yr was better than

vermicompost @ 15,000 kg/ha/yr, cow-dung @ 10,000 kg/ha/yr, poultry manure @ 6,000 kg/ha/yr and pig manure @ 4,000 kg/ha/yr. The zooplankton was 686 no/l found in the ponds under control treatment. The correlation between the total solids and planktonic biomass remained positive and significant in all the treatments noted.

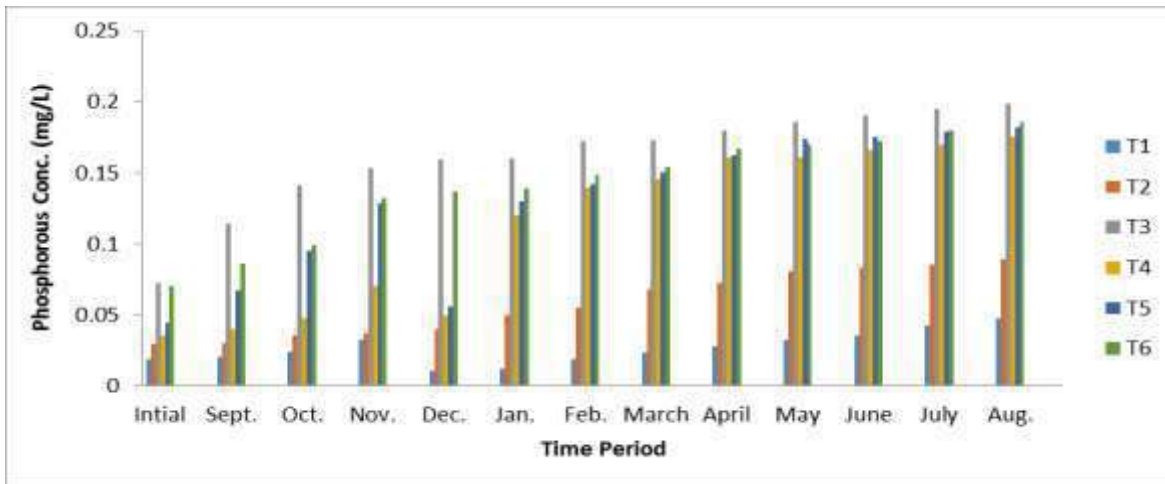


Fig. 10: Variation in water Phosphorous concentration during Sept. 2013 to Aug. 2014 in fish pond

The addition of fertilizers and natural manures in the aquaculture ponds provides basic nutrients and elements in ready to uptake form to the phytoplankton and zooplanktons which serve as a major source of food for fish [21]. The increased phytoplankton and zooplankton density can be correlated with the fish productivity. Chakrabarty et al. [4 & 22] also recorded significantly higher plankton production in vermicompost treated ponds as compare to traditionally use organic manure and inorganic fertilizers that ultimately enhances the fish growth. Cow-dung manure caused a marked increase in planktonic biomass in cow-dung @10,000 kg/ha/yr, which is an indication of well pond productivity. The population density of phytoplankton of fish pond increased and reached up to 5,786 no/l in the pond treated with vermicompost @ 10,000 kg/ha/yr [Fig. 12]. The vermicompost @ 10,000 kg/ha/yr used in present study seemed to have phytoplankton enhancing effect as it caused significant increase in amount of nutrients in the pond. The effect of treatment T5 was better than vermicompost @ 15,000, cow-dung @ 10,000, poultry manure @ 6,000, poultry manure @ 6,000 and pig manure @ 4,000kg/ha/yr. On the other hand, pond fertilized with vermicompost @ 15,000, cow-dung @ 10,000, poultry manure @ 6,000, poultry manure @ 6,000 and pig manure @ 4,000kg/ha/yr showed increase up to 4,839, 3,510, 2,988 and 1,122 no/l values of phytoplankton. The phytoplankton was 870no/l in the control treatment of pond water.

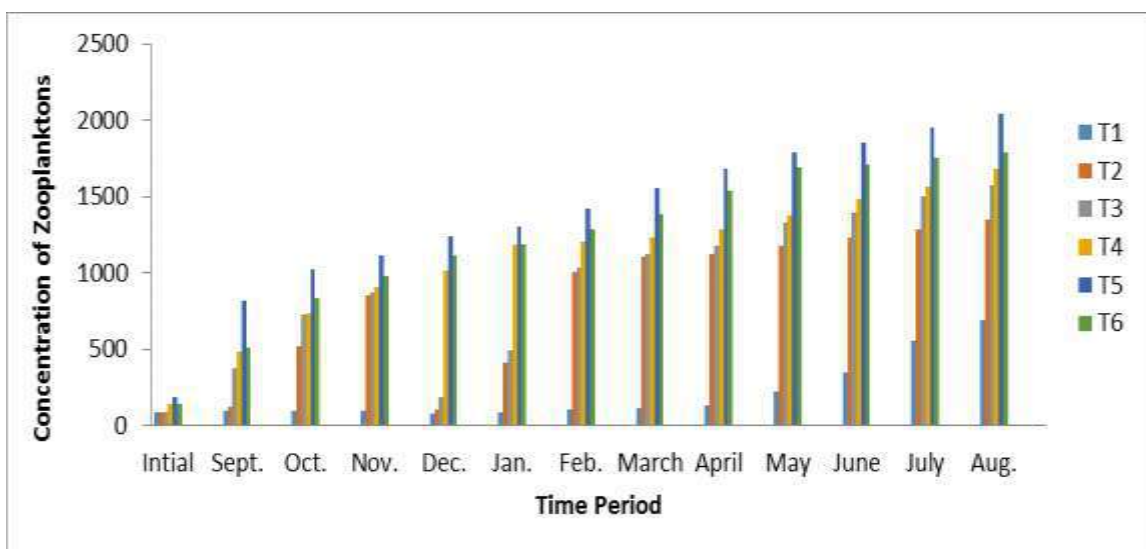


Fig. 11: Variation in Zooplanktons during Sept. 2013 to Aug. 2014 in fish pond

The correlation between the total solids and planktonic biomass remained positive and significant in all treatments noted.

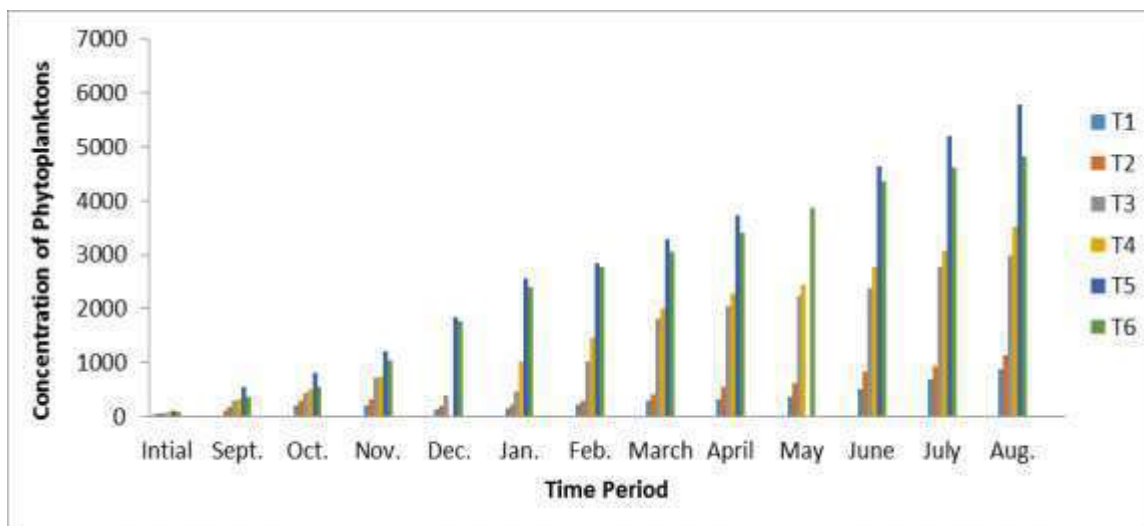


Fig. 12: Variation in Phytoplanktons during Sept. 2013 to Aug. 2014 in fish pond.

## CONCLUSION

Fish can play a vital role in providing nutritional diet to the people especially in the present circumstances. This is especially true when one thinks about the growing population of the country and at the same time degraded varieties of the agriculture products due to over use of chemicals such as pesticides, fertilizers etc. looking to world's economy status, to increase the better fish production by using cheap and easily available resources like organic manure as pond fertilizers which enhance the algal bloom that ultimately increases the fish growth. Despite the known usefulness of vermicompost in aquaculture as organic manure for more production of carps, available information on the use of vermicompost in India, especially Haryana perspectives in rather scanty. All hydro-biological parameters were found to be in optimal range in vermicompost T5 as compared to others. The findings of the present study clearly demonstrated that water temperature played a major role towards fish growth among all the parameters. Comparatively higher increase in the fish body weight was observed during summer than the winter for all the treatments

## CONFLICT OF INTEREST

There is to certify that there is no conflict of interests, technical or financial.

## ACKNOWLEDGEMENTS

The authors are thankful to the Principal, CRM Jat (PG) College, Hisar for providing necessary facilities.

## FINANCIAL DISCLOSURE

None

## REFERENCES

- Purohit Garg SK, Bhatnagar A. [2000] Effect of fertilization frequency on pond productivity and fish biomass in still water ponds stocked with *Cirrhinus mrigala* (Ham.). *Aquaculture Research*, 31: 409-414.
- Wahab MA, Azim ME, Ali MH, et al. [1999] The potential of periphyton-based culture of the native major carp *Labeo calbasu* (Ham.). *Aquaculture Research*, 30: 409-419.
- Wurts WA. [2004] Organic fertilization in culture ponds. *World Aquaculture*, 35 (2): 64-65.
- Chakrabarty D, Das MK, Das SK. [2008] Growth performance of *Cyprinus carpio* Linn. in intensively different organic manures. *International Journal of Environmental Research*, 2: 419-424.
- Nath SS, nd Lannan JE. [1992] Dry matter-nutrient relationships in manures and factors affecting nutrient availability from poultry manures. In: Egna, H., McNamara, M., Bowman, J. and N. Astin (Eds), Tenth Annual ADMIN.Report, 1991-1992. PD/A CRSP, Office of International Research and Diversity, Corvallis, Oregon. pp. 110-119.
- APHA, [1998]. Standard methods for the examination of water and waste water, 19th Ed. American public health association, Washington, DC. *Aquaculture Research*, 37: 1360-1371.
- Rahman MM. [2008] Food web interaction and nutrients dynamics in polyculture ponds. Ph.D. Thesis, Wageningen University, Netherlands, pp-175.
- Bansal N. [2010] Effect of vermicompost as pond fertilizer on growth performance of common carp [*Cyprinus carpio* Linn.]. M.Sc. Thesis. Dept. of Zoology, CCSHAU, Hisar. pp 43.
- Kaur JS. [2011] Impact of vermicompost as pond fertilizer on the growth performance of Indian major carps. M.Sc. Thesis. Dept. of Zoology, CCSHAU, Hisar. pp 50.
- Piper RG, McElwain IB, Orme LF, et al. [1982]. *Fish hatchery management*. US. Fish and Wildlife Service, Washington D.C. pp 71-82.
- Boyd CE. [1990] *Water quality in ponds for aquaculture*. Alabama Agricultural Experimental Station, Auburn University Auburn, AL. pp-482.
- Mahboob S, Sheri AN. [2002]. Influence of fertilizers and artificial feed on the seasonal variation in physico-chemical factors in fishponds. *Pakistan Journal of Zoology*, 34(10): 51-56.
- Kaur S, Ansa, MD. [2010]. Efficacy of vermicompost at fish pond manure, its effect on water quality and growth of *Cyprinus carpio* [Linn.]. *Bioresource Technology*, 101[15]:6215-6218.

- [14] Hayat S, Javed M, Hanif K. [1996] Impact of poultry droppings fertilization of fish ponds on the physico-chemistry of water. *Pakistan Journal of Livestock Poultry*, 2(2): 199-208.
- [15] Rafique RM, Hussain N, Mahboob S. [2003] Limnological variation in River Jhelum at Dulahi Muzaffarabad. *Journal of Natural Science*, 1(1): 107-112.
- [16] Liti DM, Mugo, RM Munguti JM, et al. [2006] Growth and economic performance of Nile tilapia [*Oreochromis niloticus* L.] fed on three brans [maize, wheat and rice] in fertilized ponds. *Aquaculture Nutrition*, 12: 239-245.
- [17] Hassan M, Javed M, Mahmood G. [2000a] Response of different levels of nitrogen from broiler manure fertilization of ponds. *Pakistan Journal of Livestock Poultry*, 2(2): 65-71.
- [18] Hassan M, Javed M, Mahmood G. [2000b] Response of different levels of nitrogen from broiler droppings towards planktonic biota of major carps rearing ponds. *Pakistan Journal of Biological Sciences*, 3(10): 1712-1715.
- [19] Javed M, Sial MB, Javed K. [1990] Effect of artificial feed on the growth performance of major carps. *Pakistan Journal of Agricultural Sciences*, 30(2): 167- 172.
- [20] Chakrabarty D, Das MK, Das SK. [2009] Relative efficiency of vermicompost as direct application manure in pisciculture. *Paddy Water Environment*, 7: 27-32.



## ARTICLE

# DETERIORATING AIR QUALITY AND INCREASED HEALTH RISKS IN DELHI: THE DECISIONS BEING DELAYED

Avdesh Bhardawaj\*, Gazala Habib, Annada Padhi, Abhishek Anand, Neeta Mahala, Badresh Kumar Singh

Department of Civil Engineering, Indian Institute of Technology Delhi, Hauz Khas, New Delhi, INDIA

## ABSTRACT

Delhi is sitting on a virtual environmental health epidemic waiting to explode due to deteriorating air quality and related health effects. With about 80 deaths attributed daily to air pollution in the capital city of India, the menace is even higher than terrorism or natural disasters. Aerosols, especially PM<sub>2.5</sub>, are responsible for major illnesses like respiratory problems, cardiovascular diseases, strokes, cancers and even deaths. The present study is a review of the existing air quality situation in Delhi, its causes and related health, environmental and socio-economic impacts. The focus is placed on chinks in the decision making process and critically examines avoidable delays that instigate losing scientifically gained grounds to political and bureaucratic lobbies. A historical perspective of events leading to the present status of the air quality and policies has been elucidated. The roles of different stakeholders like governments, judiciary, bureaucrats, NGOs, media and public pertaining to framing, implementing and sustaining related laws and policies have been discussed. Recommendations have been put forth for improving the air quality, monitor health aspects, develop strategies to combat related health effects, policy making and further research in the subject. The paper is expected to propound the current status of scientific research and related policies in air quality and health aspects in Delhi and offer viable solutions to tackle the problem posed as well as fill the gaps in policy development and implementation for improving the air quality and consequently health of the people.

## INTRODUCTION

Air pollution has become a prominent avoidable reason of disease and death worldwide. It has emerged as one of the prime killers in recent times and the world's single largest environmental health risk. It has been ranked in top six as a major risk factor of morbidity and mortality consistently. Around 5.5 million people worldwide including 1.4 million in India die prematurely due to fine PM [1] or more commonly called as PM<sub>2.5</sub> (Particulate Matter having aerodynamic diameter  $\leq 2.5 \mu\text{m}$ ). Global Burden of Disease (GBD) report that came out in 2013 has ranked outdoor air pollution as the 5th biggest cause of death in India [2]. The report attributed around 6.2 lakh premature deaths per year due to air pollution induced illnesses, which is a six-fold escalation since year 2000. This translates into a staggering figure of about 71 deaths per hour or 1.18 deaths per minute. India has the dubious distinction of having half of the world's top 20 worst polluted cities from 3000 cities in 103 countries studied with Delhi at 11th Place in the list in terms of PM<sub>2.5</sub> and 25th Place in terms of PM<sub>10</sub> [3]. Delhi's polluted air accounts for nearly 10 to 30 thousand deaths per year [4], which is about 80 deaths per day or 3.33 deaths per hour. On an average, Delhi's air kills more people annually there than terrorism or natural disasters.

PM<sub>2.5</sub> penetrates deep into the lungs, bronchioles and alveoli and might get deposited there or pass on to the blood stream and be carried to different organs and cause various diseases like chronic bronchitis, COPD (Chronic Obstructive Pulmonary Disease), cancers of throat, lung and other organs, stroke and heart diseases like arrhythmia, ischemia, Heart Rate Variability (HRV), myocardial infarction etc. [5, 6, 7, 8, 9, 10, 11, 12, 13, 14, 15, 16]. PM<sub>2.5</sub> is regarded as the benchmark cause of air pollution induced morbidity and mortality by World Health Organization (WHO) [3]. As per GBD, 2013, ischemic heart diseases have claimed to be more fatal compared to respiratory diseases in India due to pollution from PM<sub>2.5</sub> [2]. Particulate matter was categorized as carcinogenic and leading cause of human death by cancer by International Agency for Research on Cancer (IARC) in the year 2013 which is a specialized body of WHO [17]. Global Health Risks report [5] concluded that developing countries face more risk of such diseases than the developed countries. There has been a lot of concern regarding air quality in India and that has also resulted in the formation of an Air Quality Index (AQI) for India in the year 2015 to provide an indication of health risks due to criteria air pollutants.

Delhi has witnessed a consistent spurt in cardiovascular and respiratory diseases in Delhi of late, which are correlated with air pollution levels. Delhi's deteriorating air quality is ascribed to bio-mass burning, industrial exhausts and thermal power plants apart from vehicles. According to the official website of Delhi government [18] around 8.5 million vehicles ply on the roads with approximately 1,500 new vehicles adding to the woes and stress of air pollution in the city. The average life expectancy of Indians is being lowered by 3.2 years due to excess pollution [19]. In India, 660 million people now reside at places exceeding permissible PM<sub>2.5</sub> concentrations. The urban poor, children and elders are the most vulnerable sections of the society in the context of air pollution's detrimental effects on health. This is so because children engage in a lot of outdoor activities like sports and also their breathing rates are higher during that time period. The poor section does not have facilities of air purifiers or hygienic conditions. The elderly are usually very prone to such diseases due to lower immunity and existing illnesses and medical histories. Hence policy makers must include the references and impacts on these vulnerable sections of the society while framing policies.

### KEY WORDS

Aerosols; Delhi; health risk; cardiovascular illness; odd even scheme; PM<sub>2.5</sub>

Published: 10 Oct 2016

### \*Corresponding Author

Email:  
avdeshiitd@gmail.com  
Tel.: +91-11-26597330  
Fax: 91-11-26581117

## ADVERSE HEALTH EFFECTS OF AIR POLLUTION IN DELHI

The preliminary symptoms of air pollution's adverse effects are seen on the eyes, skin, and cavities of the nose with sustained exposure leading to permanent impairments. Now with majority of high pollution causing factories having been put out of Delhi, air pollution is taken as a direct resultant of vehicular traffic, re-suspension, biomass burning, etc. The deterioration of air quality in Delhi is correlated to the number of vehicles, their design, maintenance, fuel quality, etc. The major share of vehicles in Delhi are propelled Delhi by twin-stage engines which exemplify seriousness of the situation and the reforms needed in the relevant policies. These engines being very inefficient have exhausts laden with dangerous smoke and particles that are inhaled by the people. In the 1980s, a lot of laws came into being in Delhi to tackle the menace of pollution but their effect was very limited on curbing Delhi's air pollution. In fact, air quality declined during this time period. This was so because even though there were environmental laws, but poor compliance neutralized all the gains.

Augmentation in certified deaths was seen from 11.4% to 20.4% and 3.8% to 4.6% owing to cardiovascular and respiratory illnesses respectively; both of which were directly linked to air pollution between 2006 and 2009 [20]. In the first half of 1990's decade, morbidity and mortality owing to heart and lung illness were allied to prevalent air quality and estimated to be more than 51,400 human lifetime years annually [21]. For certain age groups, especially the vulnerable section, a 0.23% intensification in per day deaths for every 10  $\mu\text{g}/\text{m}^3$  rise in total suspended particles was observed owing to such illness [21]. Respiratory problems have been seen more in people residing in more polluted zones in Delhi than cleaner ones [22, 23]. Greater pervasiveness of asthma indications was observed in school going kids who studied in schools close to traffic crossings [24, 25].

Increased air pollution as TSP in a time series analysis induced an increase in emergency room visits over a two-year period for asthma (by 21.3%), COPD (by 24.9%), and acute coronary events (by 24.3%) in AIIMS, a prominent government hospital in Delhi [26]. In another interesting study done at St Stephens Hospital Delhi, it was found that children aged 9 to 24 months living in proximity of elevated air pollution levels are at 54% greater chance of getting vitamin D insufficiency than those in cleaner environment [27] thus suggesting the role of air pollution in such cases. In 2007, a research found that pollutant concentrations will cross dangerous levels due to a surge in number of automobiles in Delhi and hence a cap on them is a must especially those running on diesel [28]. Asthma was detected in 7.7% of 3,500 children aged 7 to 15 in a four year study done in Delhi, suggesting higher pollution's role with asthma spurt [29]. An exposure-response study correlated indoor air pollution with a drop in lung functions of Delhi's children [30]. There has been a manifestation of effects of both outdoor and indoor pollution. Chittaranjan National Cancer Institute (CNCI) and Central Pollution Control Board (CPCB) did a study from 2002 to 2005 and concluded 43.5% of 11,628 school going kids in schools aged 4 to 17 years had reduced or limiting lung functioning [31] primarily attributed to air pollution exposure in Delhi.

National Capital Region Planning Board (NCRPB) found in 2009 that air pollutants concentrations Delhi and surrounding areas exceeded permissible limits [32]. Delhi saw significantly improved respiratory health for a short in years 2000 to 2002 owing to [33] switch over of CNG in commercial automobiles, and phasing out of factories from suburban areas. Symptoms of elevated respiratory disorder were observed among students living in different parts of Delhi [34, 35]. In 2012 CPCB published a detailed health study correlating air pollution with health effects [36]. According to its results, Upper Respiratory Symptoms (URS) were present in 21.5% and Lower Respiratory Symptoms (LRS) were 1.8 times greater in people of with Respirable Suspended Particulate Matter (RSPM) positively correlating to LRS. A third of Delhi's residents reported breathing issues with impaired pulmonary abilities and COPDs around 40 % and 4 % respectively.  $\text{PM}_{10}$  concentrations were a causative influence on high blood pressures which subsequently lead to heart related and neurological ailments. Investigation on the contents of polynuclear aromatic hydrocarbons (PAHs), in airborne particulate matter of Delhi revealed higher pollution in suburban zones here than those in other nations [35]. Source apportionment of air-borne contaminants for the duration of 19th Commonwealth Games held at New Delhi reported high contribution from vehicular pollution [37]. A study established that amending norms of usage in land area of Delhi rose air pollution significantly in the vicinity of Gurgaon, Noida, Faridabad and Ghaziabad [38]. In February 2015, Greenpeace carried out an air-quality monitoring survey in 5 schools throughout Delhi and concluded that  $\text{PM}_{2.5}$  exceeded 4 and 10 times acceptable limits prescribed in India and by WHO respectively, with an average of 205.8  $\mu\text{g}/\text{m}^3$  [39].

## CURRENT AND FUTURE PERSPECTIVES-SCIENCE AND POLICY

There have been some positive developments in India in the last two years since new government took over. In November 2014, Indian Prime Minister announced that air quality data would be made accessible to the public and new emissions standards will be set for power plants. India launched its Air Quality Index (AQI) on 6<sup>th</sup> April, 2015 which was based upon System of Air quality and weather Forecasting and Research (SAFAR). This gives a visual status of prevailing real time air quality and possible health impacts for even a layman to understand. It also predicts the air quality for the next day. This is an appreciable and positive step in the right direction. This would not only create awareness but also reduce exposure of people to dangerous air pollutants, and in the long run aid in meeting the requisite air quality standards. If the standards set by WHO could be met by Delhi, then majority of related

premature deaths can be avoided. Across India, annually 400 thousand premature deaths can be avoided if the WHO standards are satisfied [40]. This offers a gigantic challenge to rectify the situation. It is high time that scientific research and policy implementations work hand in hand.

## RESPONSIBILITIES OF THE DIFFERENT STAKEHOLDERS

The onus of good health of the citizens is not the sole responsibility of the government; it is rather an agglomeration of efforts of a lot of stakeholders including judiciary, bureaucracy, NGO's, health care sector and the public at large.

### Responsibilities of the government

The government has the responsibility of framing laws to control pollution and improve healthcare of the citizens. But this task can't be done in isolation. It involves the inputs from experts of a wide array of specialties including doctors, scientists, law professionals, etc. In India, the laws are framed so strict that they are hard to implement in practicality. Therefore, the need is to have not punitive but flexible and participatory laws to be framed. In the 1980s, the Indian Parliament passed numerous laws like Air (Prevention and Control of Pollution) Act 1981, for protecting the air we breathe. Formation of air pollution policy alarmed with rising pollution from a plethora of sources and reluctance on the part of the government to deal with this problem urged a famous environmental lawyer Mr. M. C. Mehta to approach the Supreme Court requesting protection of fundamental constitutional rights and to clean air in December 1985. The court directed ministries and departments in the government to implementation of the Air Act, 1981 in Delhi. Many more acts followed, including the Environmental (Protection) Act of 1986, Air Act (amended) 1987, Motor Vehicles Act 1988, and Central Motor Vehicle Rules 1989. The 1988 Motor Vehicles Act and the 1989 Central Motor Vehicle Rules empowered the government to set guidelines for vehicular emissions both for manufacturers as well as users in India. In 1993, the Ministry of Environment and Forests (MoEF) introduced the first set of standards regarding vehicular mass emissions for India. From 1994–1998, the Supreme Court vehemently worked towards implementation of three key reforms namely phasing out of gasoline with lead, premixed fuels and taking out commercial vehicles older than fifteen years off Delhi roads. The policies for leaded gas and premixed fuels after surmounting resistance from certain sections were ultimately adopted but the ban on 15-year-old commercial vehicles still hasn't seen the light of the day fully. Such a huge delay in implementation of laws does make a mockery of environmental system management and continues to diminish the air quality. Another failure on the part of the Delhi government was the creation of a Mass Rapid Transport System (MRTS) and Bus Rapid Transit (BRT) corridor. MRTS was conceived to lower the use of private vehicles and deal with the rising demand of transportation. The bypass was expected to reduce exposure to polluting trucks and buses that passed through Delhi. Owing to the faulty implementation of the designs and delays the BRT system is being dismantled and all the efforts gone into its making going into vain. Environment Pollution (Prevention and Control) Authority (EPCA) was established in 1998 and was authorized to consider policy and provide specific recommendations especially of technical nature to the courts. This has done some commendable work and has also been acknowledged by the Supreme Court of India. The ambitious scheme Odd-Even scheme of Delhi government has been more or less regarded as having insignificant effect on controlling air pollution levels [41, 42, 43, 44]. It is expected that the new central government with the motto of "make in India" would in all seriousness frame and implement the laws and policies to arrest the spurt in air pollution level and health impacts particularly in the capital city of the country-Delhi.

### Responsibilities of the Judiciary

Judiciary has multiple responsibilities in the context of air pollution norms. In the absence of the government taking a lead in the implementation of the laws, the judiciary has the authority in India to issue orders to the government. In Indian society, it is perceived to be an autonomous and comparatively less corrupted guardian of fundamental rights. The courts are also supposed to hear grievance cases in the non-implementation or wrongful prosecutions in some cases, providing relief and reparations for indemnity to people, property and associated matters. The first intrusion by the Apex court in India, the Supreme Court was in early 1990 to forcibly relocate hazardous, heavy, toxic and big polluting category "H" industries from Delhi according to the second master plan for Delhi accepted by the then central government in 1990 [45]. But with government's laxity and strong industrial lobby many deadlines passed yet the industries remained at their locations in Delhi. With perseverance of the Court though, these industries were finally relocated out of Delhi by 1997. The nexus of some political sections and industries is one of the stumbling blocks in strict decision making. Then a historic Apex Court judgment in 1998 forced every community level transport automobiles in Delhi to use Compressed Natural Gas which lowered RSPM levels significantly, although in due course of time, all the improvements in air quality levels have been dissipated. In the year 1995 mean RSPM level in Delhi was 409  $\mu\text{g}/\text{m}^3$  which reduced upto 190  $\mu\text{g}/\text{m}^3$  and 160  $\mu\text{g}/\text{m}^3$  in the years 2000 and 2007 respectively but in a 2016 report by WHO, it stands at 225  $\mu\text{g}/\text{m}^3$  which is about 6 times the safe limit of WHO [3]. Herein raises the question as to what caused such loss of covered ground so quickly. The answer lies in the delays of the decisions to be implemented. In India a dedicated Nation Green Tribunal (NGT) was formed in the year 2010 to speedily deal with all cases pertaining to environment, including air pollution and to reduce the burden of litigation in the higher courts. A recent case in point is National Green Tribunal's (NGT) direction to prohibit petrol

and diesel vehicles older than 15 and 10 years respectively from plying in Delhi and surrounding areas. This has been in controversy for past some time because a section of the government is concerned with specific lobby and giving reference of public and essential services as a scapegoat. But the Supreme Court is welcoming the ban as are the scientific experts. But in the meantime while the decision is being taken, the delay is already caused and gained grounds are lost. Courts also perform an important role in law enforcement. The toll on heavy and light diesel trucks plying through Delhi at night will be imposed from November 1, 2015 to check the high PM levels due to their exhausts. This order has come directly from the Supreme Court of India. There has been a welcome positive progress in the attitude of the judiciary towards environmental decision making process. In India, penalties for pollution are in fact so severe that they are hardly ever enforced. The delays will hopefully be avoided henceforth and political or electoral commitments shouldn't dilute the scientific achievements.

### Responsibilities of the bureaucracy

The bureaucracy is a vital cog in the entire scheme of decision making and execution of environmental decisions and policies. They act as a connecting link between the government policies and ground level accomplishments. This link has traditionally been the one where the decisions were mostly delayed, but of late the pressures of the media and stricter governance have made this important area smoother functioning and less corrupt. A lot of cases are seen in the media where the bureaucrats take a lead in championing the environmental causes. If this aspect of governance can take a lead in faster execution of environmental plans then a major part of the entire delay can be avoided and better management achieved.

### Responsibilities of the NGOs

The courts also act with the vigilant eyes of an active NGO community in India that continues to give unbiased views and at the ground level suggestions, keeping the entire system on their toes. The contribution of NGO's in the environmental systems decision making in India has been phenomenal. Apart from creating awareness among the masses regarding environmental issues and working out projects, these NGO's keep relentless pressure on the authorities to execute the plans and laws. In Delhi the contribution of NGO's like Centre for Science and Environment (CSE) and environmental lawyers filing Public Interest Litigations (PIL) have been instrumental in keeping the work going. An illustration of this is the complete ban on blue line buses from Delhi roads. The role played by media including newspapers (press), magazines, television, and radio. With the advent of social media the potential role of sites like Facebook and WhatsApp has increased considerably. With signature movements to file petitions becoming common online, it appears to be start of an upcoming digital environmental protection age. The ultimate responsibility of health remains with the people at large. It is their task to avoid pollution, pressurize governments to take actions to regulate environmental standards and take precautions to minimize exposure. The recent initiatives like *Raahgiri days* (Pedestrian's days) in Delhi and Gurgaon is a welcome step where no traffic is allowed on specified and notified roads and these are dedicated towards fun activities, street plays, awareness campaigns, safety trainings, etc. Similar scheme in Gurgaon having car free days every Tuesday has seen some positive change coming to public life.

## CONCLUSION

It can be concluded that the gains of scientific knowledge, experiences of epidemiological studies and the efforts put in by different stakeholders are neutralized and sometime buried by political inaction, bureaucratic apathy and vested interests. This has turned Delhi's air into slow breathing poison and the stage is being set for a major public health disaster waiting to happen. It is high time that tough decisions be made and strictly implemented quickly without any delay for improving air quality in Delhi and saving millions of lives.

## RECOMMENDATIONS: THE ROAD AHEAD

The National Ambient Air Quality Standards (NAAQS) should be made legally binding in all regions with hefty penalties for any violations. The implementation of a color coded Air Quality Index (AQI) with health advisories (now available only for ten cities in India) should be implemented at all places in India because air pollution is rarely a confined or local issue as the polluted air from a surrounding area like Gurgaon, Ghaziabad or Noida can easily affect Delhi's air and health of its people. As soon as possible, switching should be done to Euro V and Euro VI standards. Curb must be exercised on diesel vehicles as diesel is now regarded as class I cancer causing agent by WHO. Until then diesel retro fitment must be done on such vehicles. Subsidies and policy assistance must be extended to swop to CNG, battery operated vehicles non-motorized transport and other relatively cleaner modes of transport. Public transport like buses and metro rails should be extended to reach out to entire population so as to reduce dependence on private vehicles. Lead-free fuel should be made easily available, all polluting vehicles regardless of its age should be banned, and stricter parking norms must be evolved along with to signal-free roads. With the availability of a lot of health cost estimation models proper estimation of illnesses caused by air pollution should be an integral part in decision making. Media and specially social media which has deep penetration and reach should be involved in creating awareness and educating the masses regarding this



important issue and pollution emergencies measures on the same lines as disaster management plans. Polluter's pay principle must be implemented in the strictest possible means to act as deterrent for defaulters. Possibilities in Clean Development Mechanism (CDM) must be explored in this area. Majority of Delhi's premature non-accidental deaths can be avoided by taking precautionary steps in controlling air pollution to come within national ambient air quality and WHO standards. Epidemiological studies have confirmed PM<sub>2.5</sub> as the most harmful air pollutant for health effects hence its regular monitoring must be done at all places. Starting immediately, all children in Delhi should undergo lung function test, blood pressure monitoring and ECG at least once in a year, and those detected with problems must be monitored regularly. This must be recorded with air pollution data of that place. Subsequently, this should be extended to all citizens and data maintained and analyzed scientifically on regular basis to evolve policies. Mass transit, pedestrian walking zones, and bicycle lanes should be included in all city and township planning. Above all, the decisions pertaining to environment must not be delayed for the road ahead to development is a bumpy and challenging one.

#### CONFLICT OF INTEREST

All the authors declare no conflict of interest whatsoever.

#### ACKNOWLEDGEMENTS

None

#### FINANCIAL DISCLOSURE

All the authors declare no conflict of financial interest.

## REFERENCES

- [1] Brauer M. [2016] The Global Burden of Disease from Air Pollution. In: 2016 AAAS Annual Meeting (February 11-15, 2016).
- [2] Global Burden of Disease (GBD) Report, 2013. Available at: [http://www.healthdata.org/sites/default/files/files/policy\\_report/2013/GBD\\_GeneratingEvidence/IHME\\_GBD\\_GeneratingEvidence\\_FullReport.pdf](http://www.healthdata.org/sites/default/files/files/policy_report/2013/GBD_GeneratingEvidence/IHME_GBD_GeneratingEvidence_FullReport.pdf).
- [3] Global Urban Ambient Air Pollution Database (update 2016). Available at: [http://www.who.int/phe/health\\_topics/outdoorair/databases/cities/en/](http://www.who.int/phe/health_topics/outdoorair/databases/cities/en/)
- [4] Apte JS, Marshall JD, Cohen AJ, Brauer M. [2015] Addressing global mortality from ambient PM<sub>2.5</sub>. *Environmental science & technology* 49(13): 8057-8066
- [5] Brunekreef B, Hoffmann B. [2016] Air pollution and heart disease. *The Lancet*.
- [6] Ierodiakonou D, Zanobetti A, Coull BA, Melly S, Postma DS, Boezen HM, Hallstrand TS. [2016] Ambient air pollution, lung function, and airway responsiveness in asthmatic children. *Journal of Allergy and Clinical Immunology* 137(2): 390-399.
- [7] Kaufman JD, Adar SD, Barr RG, Budoff M, Burke GL, Curl CL, Kronmal R. [2016] Association between air pollution and coronary artery calcification within six metropolitan areas in the USA (the Multi-Ethnic Study of Atherosclerosis and Air Pollution): a longitudinal cohort study. *The Lancet*.
- [8] Tsangari H, Paschalidou AK, Kassomenos AP, Vardoulakis S, Heaviside C, Georgiou KE, Yamasaki EN. [2016] Extreme weather and air pollution effects on cardiovascular and respiratory hospital admissions in Cyprus. *Science of the Total Environment* 542:247-253
- [9] Halonen JI, Blangiardo M, Toledano MB, Fecht D, Gulliver J, Anderson HR, Tonne C. [2016] Long-term exposure to traffic pollution and hospital admissions in London. *Environmental Pollution* 208: 48-57.
- [10] To T, Zhu J, Larsen K, Simatovic J, Feldman L, Ryckman K, Villeneuve PJ. [2016] Progression from Asthma to Chronic Obstructive Pulmonary Disease (COPD): Is Air Pollution a Risk Factor? *American journal of respiratory and critical care medicine*, (ja).
- [11] Nascimento LFC, Vieira LCP, F Mantovani KCC, Moreira DS. [2016] Air pollution and respiratory diseases: ecological time series. *Sao Paulo Medical Journal*, (AHEAD), 0-0.
- [12] To T, Zhu J, Villeneuve PJ, Simatovic J, Feldman L, Gao C, Miller AB. [2015] Chronic disease prevalence in women and air pollution—A 30-year longitudinal cohort study. *Environment international* 80:26-32.
- [13] Diaz-Sanchez D. [2015] Can particulate pollution affect lung function in healthy adults? *American journal of respiratory and critical care medicine* 191(6): 610-612.
- [14] Shrey K, Suchit A, Deepika D, Shruti K, Vibha R. [2011] Air pollutants: the key stages in the pathway towards the development of cardiovascular disorders. *Environmental toxicology and pharmacology* 31(1):1-9.
- [15] Mills NL, Donaldson K, Hadoke PW, Boon NA, MacNee W, Cassee FR, Newby DE. [2009] Adverse cardiovascular effects of air pollution. *Nature clinical practice Cardiovascular medicine* 6(1): 36-44.
- [16] Brook RD. [2008] Cardiovascular effects of air pollution. *Clinical science*, 115(6): 175-187.
- [17] Loomis D, Grosse Y, Lauby-Secretan B, El Ghissassi F, Bouvard V, Benbrahim-Tallaa L, Straif K. [2014] IARC evaluation of the carcinogenicity of outdoor air pollution. *Environnement, Risques & Santé*, 13(4): 347-352.
- [18] Delhi govt. (2015) Total Vehicle registration. Available at: [http://delhi.gov.in/wps/wcm/connect/doi\\_transport/Transport/Home/Vehicle+Registration/Total+Vehicle+Registered.Accessed:14/October/2015](http://delhi.gov.in/wps/wcm/connect/doi_transport/Transport/Home/Vehicle+Registration/Total+Vehicle+Registered.Accessed:14/October/2015).
- [19] Greenstone M, Nilekani J, Pande R, Ryan N, Sudarshan A, Sugathan A. [2015] Lower pollution, longer lives life expectancy gains if India reduced particulate matter pollution. *Economics and Political Weekly* 8: 40-46.
- [20] DoES, [2010] Annual Report on Registration of Births and Deaths in Delhi. Directorate of Economics and Statistics, Government of Delhi, New Delhi, India.
- [21] Cropper ML, Simon NB, Alberini A, Arora S, Sharma PK. [1997] The health benefits of air pollution control in Delhi. *American Journal of Agricultural Economics* 1625-1629.
- [22] Chhabra S K, Chhabra P, Rajpal S, Gupta RK. [2001] Ambient air pollution and chronic respiratory morbidity in Delhi. *Archives of Environmental Health: An International Journal* 56(1): 58-64.
- [23] Rajkumar P. [1999] Effect of air pollution on respiratory system of auto rickshaw drivers in Delhi. *Indian Journal of Occupational and Environmental Medicine* 3(4):171-3.
- [24] Paramesh H. [2002] Epidemiology of asthma in India. *The Indian Journal of Pediatrics* 69(4):309-312.
- [25] Chhabra SK, Bhatnagar S. [2002] Bronchodilator Responsiveness in Asthma Chronic Obstructive Pulmonary Disease c. *Indian J Chest Dis Allied Sci* 44:91-971
- [26] Pande JN, Bhatta N, Biswas D, Pandey RM, Ahluwalia G, Siddaramaiah NH, Khilnani GC. [2002] Outdoor air pollution and emergency room visits at a hospital in Delhi. *Indian Journal of Chest Diseases and Allied Sciences*, 44(1): 13-20.
- [27] Agarwal, KS, Mughal MZ, Upadhyay P, Berry JL, Mawer EB, Puliyl JM. [2002] The impact of atmospheric pollution on vitamin D status of infants and toddlers in Delhi, India. *Archives of disease in childhood* 87(2):111-113.
- [28] Mohan M, Kandya A. [2007] An analysis of the annual and seasonal trends of air quality index of Delhi. *Environmental monitoring and assessment* 131(1-3):267-277.
- [29] Rajkumar, Jitendra K Nagar, Harsh Kumar, et al.[ 2007] Association of indoor and outdoor air pollutant level with respiratory problems among children in an industrial area of



- Delhi, India. Archives of Environmental & Occupational Health 62 (2); 75-80.
- [30] Rajkumar, Jitendra K. Nagar, Alka Singh Kushwah, Neelima Raj, Mahesh Meena, SN Gaur. Indoor air pollution and respiratory fun 20(1): 36 48.
- [31] CPCB [2008] Study on ambient air quality, respiratory symptoms and lung function of children in Delhi.
- [32] NCRPB. [1999] A Report on National Capital Region Growth and Development.
- [33] Foster A, Kuma, N. [2011] Health effects of air quality regulations in Delhi, India. Atmospheric Environment 45(9):1675-1683.
- [34] Mathew J, Goyal R, Taneja KK, Arora N. [2012] Correlation between Air Pollution and Respiratory Health of School Children in Delhi. 2nd WAO International Scientific Conference (WISC 2012) pp. 16.
- [35] CPCB. [2012] Epidemiological study on effect of air pollution on human health (adults) in Delhi.
- [36] Khillare PS. [2013] Investigation on the contents of polynuclear aromatic hydrocarbons (PAHs), in airborne particulate matter of Delhi.
- [37] Marrapu P, Cheng Y, Beig G, Sahu S, Srinivas R, Carmichael GR. [2014] Air quality in Delhi during the Commonwealth Games. Atmos. Chem. Phys, 14, 10619-10630.
- [38] Kumar N, Linderman M, Chu A, Tripathi S, Foster AD, Liang D. [2014]. Environmental Interventions and Air Pollution (Re) distribution in Delhi, India. India (June 8, 2014).
- [39] S Greenpeace [2015 ] Delhi children breathe toxic air. Available at: <http://www.greenpeace.org/india/en/Press/-Delhi-children-breath-toxic-air-reveals-Greenpeace-air-monitoring-survey-in-schools/>
- [40] Hoy D, March L, Brooks P, Blyth F, Woolf A, Bain C, Buchbinder R. [2014] The global burden of low back pain: estimates from the Global Burden of Disease 2010 study. Annals of the rheumatic diseases, annrheumdis-2013.
- [41] Sehgal M, Gautam SK. [2016] Odd even story of Delhi traffic and air pollution. International Journal of Environmental Studies 73(2): 170-172.
- [42] Gupta M, Raheem S. [2016] Delhi Air Pollution–A Review. Journal of Environmental Engineering and Studies, 1(1).
- [43] Pavani VS, Aryasri AR. [2016] Pollution Control through Odd-Even Rule: A Case Study of Delhi. Indian Journal of Science, 23(80):403-411.
- [44] Jha S. [2015] Oddity of Managing Air Pollution in Delhi: Public Policy Myopia. Apeejay School of Management–Centre for Public Policy & Governance Discussion Paper, 1.
- [45] Bell RG, Mathur K, Narain U, Simpson D. [2004] Clearing the air: how Delhi broke the logjam on air quality reforms. Environment: Science and Policy for Sustainable Development, 46(3): 22-39.

## ARTICLE

# ASSESSMENT OF SEASONAL VARIATION OF SURFACE WATER QUALITY: ENVIRONMETRIC AND INDEXING APPROACH

Mayuri Chabukdhara<sup>1\*</sup>, Sanjay Kumar Gupta<sup>2</sup>, Arvind Kumar Nema<sup>2</sup>

<sup>1</sup>Dept. of Environmental Biology and Wildlife Sciences, Cotton College State University, Guwahati, Assam-INDIA

<sup>2</sup>Environmental Engineering Laboratory, Department of Civil Engineering, Indian Institute of Technology, Hauz Khas, New Delhi, INDIA

## ABSTRACT

The seasonal variation of water quality of the river Hindon in Ghaziabad, India was evaluated using environmetric techniques and metal pollution index. Various environmetric methods were tested for source apportionment and identifying the variables responsible for seasonal variations in river water characteristics. Source analysis indicated that in the pre-monsoon period, the metal contamination in river water was due to the disposal of industrial and urban wastewater. The order of metals as per River Metal Pollution Index (RMPI) as follows  $Pb > Cd > Zn > Cr > Cu > Fe > Ni$ . The RMPI indicated high pollution at S-3, S-5 and S-6 ( $IMPI > 2$ ) and moderate pollution at S-1, S-2 and S-4 ( $IMPI \leq 2$ ). Based on IMPI ranking, the order of all the monitored sites was as follows:  $S-3 > S-5 \geq S-6 > S-4 > S-1 > S-2$ . This finding of the present study demonstrated the necessity and usefulness of integration of environmetric analysis and pollution index method in monitoring river water quality.

## INTRODUCTION

The deterioration of river water have become a crucial environmental issue in most of the countries therefore, it is one of the most threatened freshwater resources in the present scenario. In most of the countries including India, the river water is used for domestic, agricultural and numerous industrial purposes. However, due to the disposal of untreated or partially treated domestic and industrial wastewater in to surface water, the vulnerability to the contamination is very high. Several factors including geological morphology, vegetation, atmospheric inputs, climatic conditions, anthropogenic activities directly or indirectly affects the river water quality [1-2]. Along with various physico-chemical water quality parameters, contamination of heavy metals in the water bodies is also of a serious concern. Industrial and urban discharges, agricultural activities, atmospheric deposition and geologic weathering of rocks and minerals etc are the major sources of heavy metals contamination in water bodies [3-5].

Thus, there is an urgent need to control and maintain the safe ambient river water quality because its deterioration reduces the usability of these precious resources [6]. Such maintenance requires pollution control through point and diffused sources and regular monitoring as well. However, the water quality monitoring, analysis and interpretation of the large number of measured variables and influencing factors it is a major challenge [7]. Therefore other than analytical tools, various statistical methodologies are required to obtain conclusive monitoring results for preparing appropriate management strategies. The application of environmetric methods not only helps in source apportionment but also avoid misinterpretation of monitoring data. These methods are also helpful in decision making process in terms of effective management of the water resources through appropriate strategies [7-9]. The present study was undertaken to assess the seasonal variation of Hindon river water quality in terms of physico-chemical parameters and heavy metals distributions. The probable pollution sources were identified using environmetric methods. Further, river metal pollution index (RMPI) was estimated to understand the influence of metal contamination on river water quality.

## MATERIALS AND METHODS

### Study area

River Hindon originates in the lower Himalayas in Saharanpur district of Uttar Pradesh, India. This is a tributary of river Yamuna and flow through Ghaziabad district ( $28^{\circ} 40' N$  and  $77^{\circ} 25' E$ ), located in the middle of Ganga-Yamuna doab at about 1.5 km east of the river. Ghaziabad is one of the fastest growing industrial cities of the country with more than 300 industrial units in the city. Details of the industries are given elsewhere [10]. The Hindon river water is predominantly used for domestic, agricultural and industrial purposes in Ghaziabad. The climate of this region is tropical to temperate and the rainfall usually starts in the end of the June and normally it rains till October.

### Sampling, monitored parameters and analytical methods

Total six sites [Fig. 1], along the Hindon River and an artificial canal branch (Hindon Cut, S5) were selected for sampling of river water for this study. A GPS (Garmin® eTrex® Vista Cx, Taiwan) was used to record the

### KEY WORDS

Environmetric techniques; Metal pollution index; Hindon; Discriminant Analysis; Industrial and urban sources

Published: 10 Oct 2016

### \*Corresponding Author

Email:  
mayuri\_chabukdhara@ya  
hoo.co.in  
Fax: + 91-361-2733502

location (longitudes and latitudes) of each site. Water samples were collected in pre-cleaned polypropylene bottles and stored at 40C during the transit period. Selected physico-chemical parameters were analyzed following standards method of water and wastewater analysis (APHA). Heavy metals analysis was performed by atomic absorption spectrophotometer (ECIL, India) following acid digestion method as described by APHA [11].

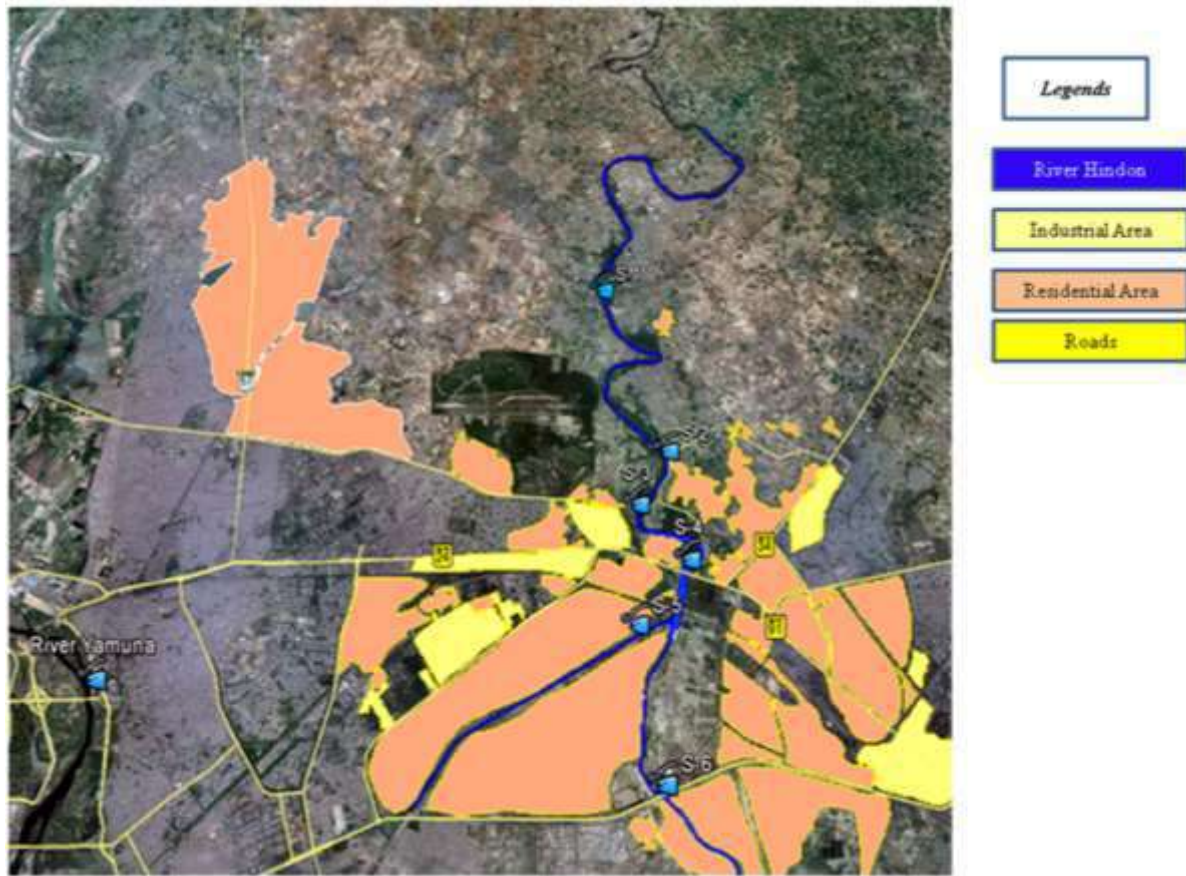


Fig. 1: Map showing sampling sites

### Reagents and standards

Throughout the study, analytical grade chemicals were used. All the reagents and standards were prepared by ultrapure water (TKA, Germany). The metal standards were prepared from certified stock solution of 1000 mg/l (E-Merck, Germany) and used for the calibration purposes. All the analysis was carried out in triplicate.

### Data treatment and environmetric methods

The water quality monitoring data were analyzed using a statistical package SPSS® (Window Version 17.0) and with XIStat, an add-in package of Microsoft Excel 2011. Correlation analyses were performed on the different datasets depending upon the nature of data. Environmetric multivariate analyses including principal component analysis (PCA), and discriminant analysis (DA) was used for selected data sets. Detailed information about environmetric techniques is given elsewhere [10]. The normality of data for all metals was checked prior to multivariate analysis and logarithmic transformation was used wherever required.

### River metal pollution index

The metal pollution index is applied to compare seasonal variations of metals at different sites in Hindon River. River metal pollution index (RMPI) was calculated as per following equation.

$$RMPI = C_{rmc} / C_{smc} \quad (1)$$

where RMPI is the river metal pollution index;  $C_{rmc}$  is the measured metal concentration ( $\mu\text{g/l}$ ) in river water;  $C_{smc}$  is the standard metal concentration ( $\mu\text{g/l}$ ) in surface water. All the standard values ( $\mu\text{g/l}$ ) were adopted from USEPA acute values [12] for protection of freshwater aquatic life which are as follows: 13 for Cu, 2 for Cd, 120 for Zn, 1000 for Fe and 470 for Ni, respectively. The standard values adopted for Cr was 11 and 32

for Pb [13]. The monitoring site is regarded as polluted if RMPI > 1; otherwise, non-polluted. Integrated Metal Pollution Index (IMPI) is defined as the mean values for all the Pollution Indexes (PI) of all considered metals [14] and calculated as follows.

$$IMPI = \sum RMPI/n \quad (2)$$

where, n is the number of metals considered in the study. The river water at different sites were classified as low contaminated if the IMPI ≤ 1.0, moderate contaminated if the 1.0 < IMPI ≤ 2.0 or high contaminated when IMPI > 2.0 [15].

## RESULTS AND DISCUSSION

### Basic physico-chemical characteristics of river

The physico-chemical parameter represents the quality of river water. Statistical summary of analyzed parameters in pre- and post-monsoon season are shown in [Table 1]. Compared to the Central Pollution Control Board (CPCB) guideline values for inland surface water [15], BOD and NO<sub>3</sub><sup>-</sup> levels were found above the safe limits. High load of NO<sub>3</sub><sup>-</sup> in the surface water may cause eutrophication. The total dissolved solids (TDS) levels in both the pre and post-monsoon seasons exceeded the CPCB' class A guideline value whereas the mean DO value was lower than the prescribed limit for inland surface water [Table 1]. Low DO in river may pose threat to the existence of aquatic life. TDS in water originates from both natural sources as well as anthropogenic sources such as urban and industrial discharges.

**Table 1:** Summary of physico-chemical characteristics of river Hindon and its comparison with the CPCB guideline values

Physico-chemical parameters	Pre-monsoon		Post-monsoon		Overall mean	CPCB, 1995 Inland Surface water Classification (Class A-E)*				
	Mean ± SD	Range	Mean ± SD	Range		A (Drinking water without conventional treatment but after design)	B (Outdoor bathing)	C (Drinking water with conventional treatment and after design)	D (Propagation of wild life, fisheries (recreation and aesthetic))	E (Irrigation, industrial cooling and controlled waste disposal)
pH	7.32±0.3	6.8–7.85	7.8±0.36	7.25–8.55	7.56	6.5–8.5	6.5–8.5	6.5–8.5	6.5–8.5	6.5–8.5
EC (mS/cm)	0.68±0.34	0.31–1.42	0.37±0.11	0.22–0.74	0.53	-	-	-	1	2.25
Turbidity (NTU)	30.3±18.99	11–82.6	29.4±13.35	10.8–68	30.0	-	-	-	-	-
SO <sub>4</sub> <sup>2-</sup> (mg/l)	40.2±25.35	14.6–108.5	24.6±15.53	8.0–58	32.4	400	-	400	-	1000
NO <sub>3</sub> <sup>-</sup> (mg/l)	30.1±15.08	10.6–77.8	24.9±7.25	10.5–40	27.5	20	-	50	-	-
TA (mg/l)	314.6±138.31	48–556	284.2±79.87	186–410	299.4	-	-	-	-	-
TH (mg/l)	245.3±83.28	148–412	215.2±62.6	132–304	230.3	-	-	-	-	-
Ca (mg/l)	63.4±22.81	32–110	52.7±16.53	30–80	58.1	-	-	-	-	-
Cl (mg/l)	236.5±260.07	46.6–788	88.0±89.78	26–351	162.2	250	-	600	-	600
DO (mg/l)	3.3±1.20	1.04–5.09	4.61±1.28	2.74–6.14	3.97	6	5	4	4	-
COD (mg/l)	136.8±66.89	58–270.5	90.3±23.7	44–132	113.6	-	-	-	-	-
BOD (mg/l)	36.4±16.44	12–78	26.5±7.17	14–40	31.5	2	3	3	-	-
TDS (mg/l)	443.2±195	170–874	458.7±266.3	200–1278	451	500	-	1500	-	2100

### Metals concentrations in river water

Statistical summary of the mean metals concentrations in the river water for both the seasons are shown in [Table 2]. The Mean values of all metals were lower in post-monsoon season which could be due to dilution effect of rainwater. The results heavy metals analysis clearly demonstrated that among different sites, the site 3 (S-3) was most polluted whereas site-1 (S-1) was least polluted. The total metal concentrations in



water was recorded in the order of Fe > Zn > Pb > Mn > Ni > Cr > Cu > Cd [Table 3]. During the monitoring, it was noticed that a drain carrying industrial and urban wastewater was getting mixed with the Hindon river near the sampling point no. S-3. This could be reason for higher metal concentrations in water at S-3 location. The concentration of copper (Cu) was above the maximum permitted limits [12] for protection of aquatic life at S-3, S-4, S-5 and S-6 [Table 3]. Similarly, the lead (Pb) and cadmium (Cd) concentrations were also found higher at all sites than the prescribed limits Pb and Cd for protection of aquatic life [12]. Throughout all the sampling sites, the zinc (Zn) concentrations were also exceeded the USEPA permitted limits however it was well within CPCB prescribed safe limits [14]. Further, except one sampling location (S-1), the iron (Fe) concentrations were also above the USEPA maximum permitted concentrations at all sites.

**Table 2:** Metal concentrations ( $\mu\text{g/l}$ ) in river Hindon in two different seasons

Metals	Pre-monsoon		Post-monsoon	
	Mean $\pm$ SD	Range	Mean	Range
Cu	30.2 $\pm$ 19.85	7-76	6.4 $\pm$ 3.83	2-18
Cr	31.7 $\pm$ 10.38	12-47	12.1 $\pm$ 14.32	2-57
Pb	193.4 $\pm$ 115.17	55-435	160.6 $\pm$ 79.35	55-314
Cd	10.5 $\pm$ 11.44	1.5-37	3.6 $\pm$ 1.25	2-6.5
Zn	423.5 $\pm$ 251.62	137-1067	311.5 $\pm$ 179.94	48-719
Mn	128.5 $\pm$ 65.09	30.5-256	106.5 $\pm$ 43.01	3-164
Fe	1541 $\pm$ 676.46	838-2780	1036.8 $\pm$ 498.27	400-2024
Ni	106.7 $\pm$ 64.61	42-249	33.6 $\pm$ 29.1	2-94

**Table 3:** Summary of site-wise metal concentrations ( $\mu\text{g/l}$ ) in river Hindon

Site	Cu	Cr	Pb	Cd	Zn	Mn	Fe	Ni	Ref.
S-1	10.3	13.8	210.8	3.9	313.4	89.8	972	31.4	
S-2	8.8	11.9	137.3	3.3	351	79.1	1192	40.6	
S-3	24.6	35.5	252.7	12.9	273.3	194.1	1488.5	118.7	
S-4	13.6	20.7	167.3	3.5	436.7	117.2	1141	67.4	
S-5	21.1	20.3	119.3	10.7	594.7	108	1766	98.1	
S-6	31.4	29.2	174.6	7.9	236	116.9	1723	64.8	
Acute values for protection of freshwater aquatic life	13	-	-	2	120	-	1000	470	[12]
Class A	1500	-	100	-	15000	-	300	-	[14]
Class B	-	-	-	-	-	-	-	-	
Class C	1500	-	100	-	15000	-	50000	-	
Class D	-	-	-	-	-	-	-	-	
Class E	-	-	-	-	-	-	-	-	

\*CPCB Class

\*\*CPCB classes are same as given in [Table 1]

### Correlation analysis of the physico-chemical parameters and metals

The Spearman's rank correlation analysis enabled the identification of possible common characteristics of physico-chemical parameters (not shown) and heavy metals in river water [Table 4]. During pre-monsoon period, the electrical conductivity (EC) values showed strong positive correlations with pH, turbidity, Sulphate (SO<sub>4</sub><sup>2-</sup>), nitrate (NO<sub>3</sub><sup>-</sup>), total alkalinity (TA), total hardness (TH), chloride (Cl<sup>-</sup>), chemical oxygen demand (COD) and total dissolved solids (TDS). The conductivity indicates the presence of positive and negative ions in water therefore the existing relationship is expectable. However, in post-monsoon season, the EC did not show any positive relation with other observed physico-chemical parameters. This could be due to dilution effect in post-monsoon. A significant correlation ( $p < 0.01, 0.05$ ) was found among SO<sub>4</sub><sup>2-</sup>, NO<sub>3</sub><sup>-</sup>, TA, TH, Cl<sup>-</sup> and TDS in pre and post- monsoon season indicating the pollution due to a common wastewater discharges. The BOD and COD showed significant relationships with TA, TH and Cl<sup>-</sup> in both, pre and post-monsoons.

Among various heavy metals, except Zn, other metals were found closely associated with each other in pre-monsoon season whereas in post-monsoon, Cu showed significant correlation with Cr, Pb and Mn while Cr with Cd and Ni and Pb with Zn, Mn and Fe [Table 4].

**Table 4:** Spearman's rank correlation matrix for metals in river Hindon

	Cu	Cr	Pb	Cd	Zn	Mn	Fe	Ni
Pre-monsoon								
Cu	1							
Cr	0.83**	1						
Pb	0.59**	0.54**	1.000					



Cd	0.84**	0.76**	0.47**	1				
Zn	-0.29	-0.23	-0.58**	-0.29	1			
Mn	0.37*	0.57**	0.07	0.45**	0.22	1		
Fe	0.68**	0.66**	0.39*	0.46**	-0.3	0.33	1	
Ni	0.72**	0.78**	0.36*	0.69**	0.15	0.66**	0.57**	1
Post-monsoon								
Cu	1							
Cr	0.49**	1						
Pb	0.34*	-0.06	1					
Cd	0.28	0.48**	0.2	1				
Zn	0.09	-0.32	0.68**	-0.18	1			
Mn	0.47**	0.31	0.56**	0.19	0.27	1		
Fe	0.26	-0.16	0.87**	0.16	0.59**	0.58**	1	
Ni	0.25	0.51**	-0.67**	0.11	-0.71**	-0.25	-0.7**	1

\*\*Correlation is significant at the 0.01 level (2-tailed).

\*Correlation is significant at the 0.05 level (2-tailed).

### PCA for physico-chemical parameters and metals in river Hindon

The PCA analysis revealed that in pre-monsoon EC, turbidity, NO<sup>3-</sup>, Cl<sup>-</sup>, TH and TDS showed strong positive loadings and moderate loadings for SO<sub>4</sub><sup>2-</sup> in PC1 that explained 36.4% of the total variance. Similarly, PC2 explaining 22% of the total variance which showed strong loadings for COD and BOD and moderate loadings for Cl<sup>-</sup> and SO<sub>4</sub><sup>2-</sup>. The source of PC1 parameters could be mainly from industrial discharges while PC2 may have dominant domestic sources, SO<sub>4</sub><sup>2-</sup> and Cl<sup>-</sup> may have come from mixed sources. The pH, TA and DO were dominated in PC3 that explained 19.8% of the total variance. In post-monsoon EC, SO<sub>4</sub><sup>2-</sup>, TA, Cl<sup>-</sup>, TH, TDS, COD and BOD were dominated in the first component (PC1) explaining 43% of the total variance. In PC2, turbidity and NO<sup>3-</sup> showed strong positive loadings while SO<sub>4</sub><sup>2-</sup>, Cl<sup>-</sup> and BOD showed moderate loadings indicating mixed origin for these parameters. The DO showed negative loadings in PC2 whereas PC3 is dominated by EC. The physico-chemical parameters such as EC, TA, TH and TDS may have dominant contribution from industrial sources while COD and BOD may have major contribution from municipal or urban discharges. The SO<sub>4</sub><sup>2-</sup> and Cl<sup>-</sup> may have come from mixed sources [Table 5].

In order to have clear visualization of the data trends, PCA results of metals is depicted by loadings and score plot. The scores and loadings of the principal components of metals for both the seasons are presented in [Fig. 2a and b]. In pre-monsoon, PC1 explaining 52.6% of the total variance [Fig. 2a] which showed the strong positive loadings for Cu, Cr, Cd, Fe and Ni suggesting different anthropogenic sources for these metals. The results also depicted that Cu, Cr, Fe and Ni may have mainly come from industrial sources such as textiles, foundries, electroplating or galvanizing industries, tanneries, pharmaceutical industries etc. The Cd might have come from electroplating and galvanizing, metal processing industries, dye and dyes, urban discharges etc. The Pb and Zn were dominated in PC2 that explained 24.5% of the total variance [Fig. 2a] but Pb showed negative loading in PC2 indicating an unique source for this metal. Beside various metal processing and pesticide industries, several lead re-processing (>25 units) and induction and foundries (>75 units) are situated there in Ghaziabad industrial area. The wastewater discharges from these industries in to the Hindon river could be responsible for very high Pb contamination. A portion of the industrial particulate emissions of heavy metals directly reaches to the river whereas its substantial amount get settle down on the nearby soil surface and finally get mixed with river water through run-off. The Zn contribution is particularly from electroplating and galvanizing, metal processing, pharmaceutical, textiles, pulp and paper, and pesticide industries as well as from urban wastes also. The Mn showed moderate loadings in PC1 and PC2 indicating mixed sources.

In post-monsoon, Pb, Zn and Fe showed strong positive loadings in PC1 (explains 43.1% of total variance) and negative loadings for Ni suggesting unique source for Ni [Fig. 2b]. These metals may have dominant anthropogenic sources even in post-monsoon period. The Cu, Cr and Cd were dominated in PC2 explaining 28.8% of the total variance and these metals might have come from natural sources as the concentration were much lower in post-monsoon due to dilution effect.

**Table 5:** Variance explained and components for physico-chemical parameters in river Hindon

Physico-chemical	Pre-monsoon			Post-monsoon		
	PC1	PC2	PC3	PC1	PC2	PC3
pH	-0.15	-0.14	0.88	0.73	-0.45	0.31
EC	0.76 <sup>a</sup>	0.32	0.55	-0.05	0.18	0.96

Turbidity	0.77	-0.1	-0.05	0.44	0.75	-0.02
SO <sub>4</sub> <sup>2-</sup>	0.52	0.43	0.24	0.7	0.64	0.08
NO <sub>3</sub> <sup>-</sup>	0.8	0.19	-0.08	-0.03	0.83	0.13
TA	0.2	0.16	0.76	0.93	0.25	-0.05
TH	0.81	0.31	0.37	0.91	0.05	-0.11
Cl <sup>-</sup>	0.74	0.52	0.33	0.65	0.59	0.4
COD	0.06	0.93	0.19	0.86	0.24	-0.09
BOD	0.09	0.94	-0.11	0.64	0.51	-0.08
TDS	0.9	-0.02	0.09	0.82	0.1	0.41
DO	-0.45	-0.39	-0.6	-0.07	-0.77	-0.52
<i>Eigen values</i>	4.37	2.64	2.38	5.17	3.23	1.66
<i>Total variance</i>	36.4	22	19.8	43	27	13.8
<i>Cumulative %</i>	36.4	58.8	78.3	43	70	83.8

Extraction Method: Principal Component Analysis  
 aBold values indicate strong and moderate loadings, respectively

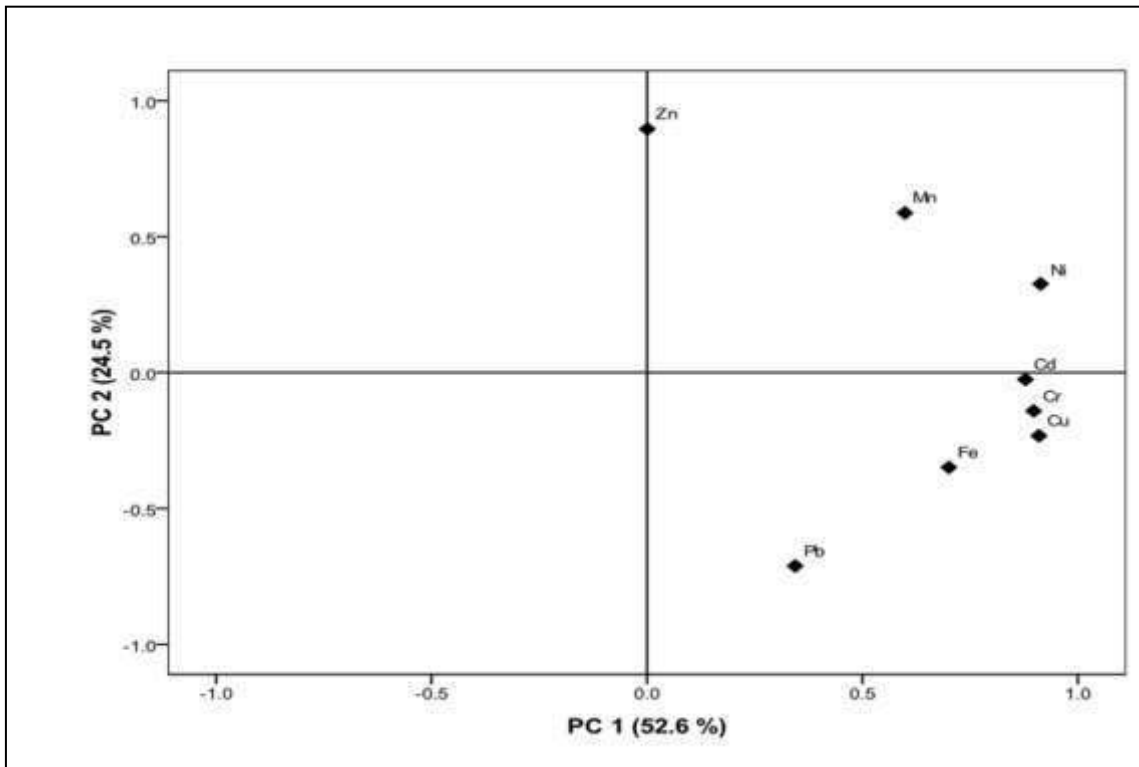


Fig. 2: (a). PCA loadings and score plots of heavy metals in (a) pre-monsoon period

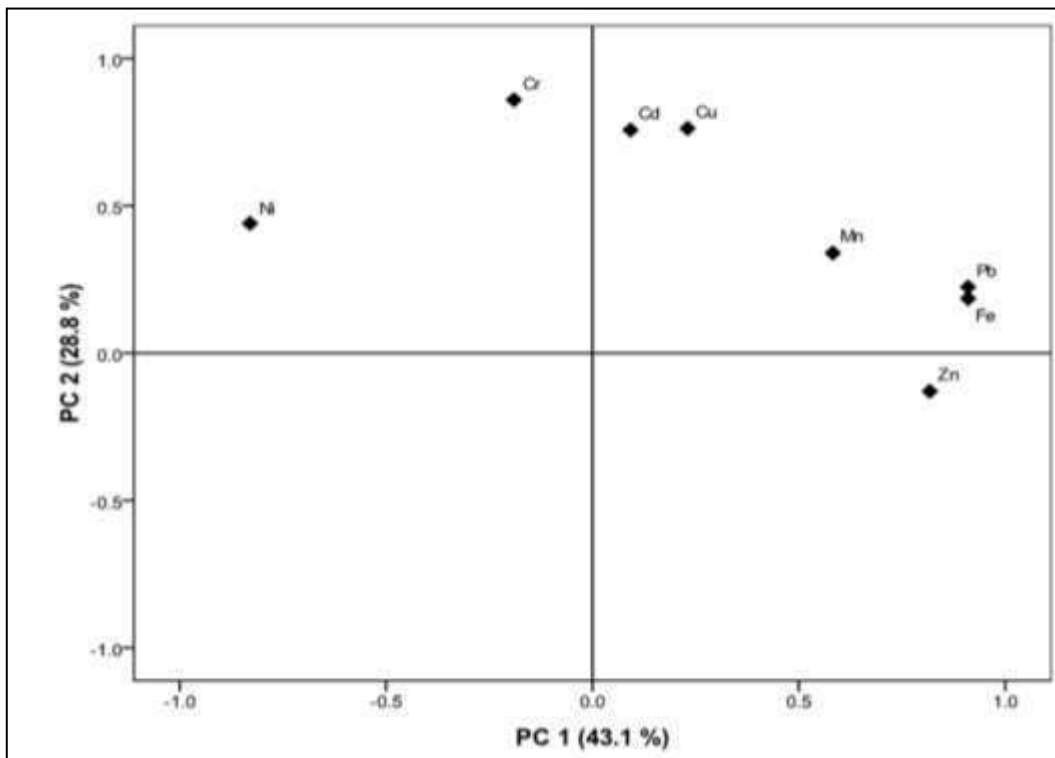


Fig. 2: (b). PCA loadings and score plots of heavy metals in post-monsoon period

### Seasonal dissimilarity using DA for physico-chemical parameters and metals

To evaluate seasonal variation of different parameters including heavy metals in river water, DA was applied on the raw data matrix by using the standard and backward stepwise modes. The raw data set was classified into two groups comprising pre and post-monsoon. The seasons were the grouping (dependent) variables, while physico-chemical parameters and heavy metals were considered as independent variables. Discriminant functions coefficients obtained from the standard and backward stepwise modes of DA are shown in [Table 6]. The standard and backward stepwise DA showed that among physico-chemical parameters, pH, SO<sub>4</sub><sup>2-</sup>, TH, Ca, COD and BOD were significant discriminant variables of seasonal variation among two seasons while among metals Cu, Cr, Pb, Mn, Fe and Ni were the significant discriminant variables of seasonal variation [Table 6]. The DA showed significant differences between two seasons, which were represented in terms of 8 discriminating parameters. Such seasonal variation of various physico-chemical parameters could be due to urban and industrial discharges at various points along the river. Hence, DA rendered a reduction in dimensionality of data set by identification of the most important discriminating variables responsible for seasonal variability.

Table 6: Classification function coefficients for seasonal variations of physico-chemical parameters and heavy metals in Hindon river

	Standard mode		Backward stepwise mode	
	Pre-monsoon	Post-monsoon	Pre-monsoon	Post-monsoon
pH	347.148	361.847	193.086	206.590
EC	627.916	628.128		
Turbidity	-0.078	-0.131		
SO <sub>4</sub> <sup>2-</sup>	8.420	8.996	1.142	1.385
NO <sub>3</sub> <sup>-</sup>	9.139	8.846		
TA	-1.328	-1.355		
TH	1.285	1.417	0.145	0.261
Ca	-5.234	-5.838	-0.395	-0.919
Cl <sup>-</sup>	-0.263	-0.242		
COD	-1.049	-1.407	-1.374	-1.656
BOD	4.874	5.583	1.730	2.316
TDS				
DO	63.229	64.599		
Cu	7.142	7.564	2.293	2.584

Cr	-5.679	-6.365	-0.925	-1.475
Pb	0.126	0.083	-0.339	-0.380
Cd	-22.866	-23.160		
Zn	0.381	0.381		
Mn	0.417	0.530	0.825	0.924
Fe	-0.186	-0.199	-0.092	-0.105
Ni	1.252	1.093	-0.689	-0.847
Constant	-1597.663	-1678.211	-654.611	-733.713

### Metal pollution index (RMPI) analysis

The RMPI depicts the suitability of river water quality for its various uses and also indicates the level of pollution. The RMPI values of pre-monsoon indicated that all sites were contaminated with metals (RMPI > 1) except for Ni at all sites and Cu at S-2. In post-monsoon, all the sites were comparatively less contaminated. Overall metal pollution was found in order of Pb > Cd > Zn > Cr > Cu > Fe > Ni.

The IMPI also indicated that the metal pollution degree was comparatively higher in pre-monsoon season and the highest at S-3 [Fig.3]. Based on the IMPI, three sites i.e. S-1, S-2 and S-4 showed moderate pollution (IMPI ≤ 2) whereas the rest of the three sites i.e. S-3, S-5 and S-6 showed high pollution level (IMPI > 2). Based on IMPI, the order of the polluted site was as follows S-3 > S-5 ≥ S-6 > S-4 > S-1 > S-2. The maximum IMPI was noted for S-3 which could be due to mixing of the urban-industrial wastewater to the river while S-5 is the diverted canal from the main river and S-6 is the downstream site of the river that could receive additional metals from various sources all along the river and lesser dilution due to diversion at S-5.

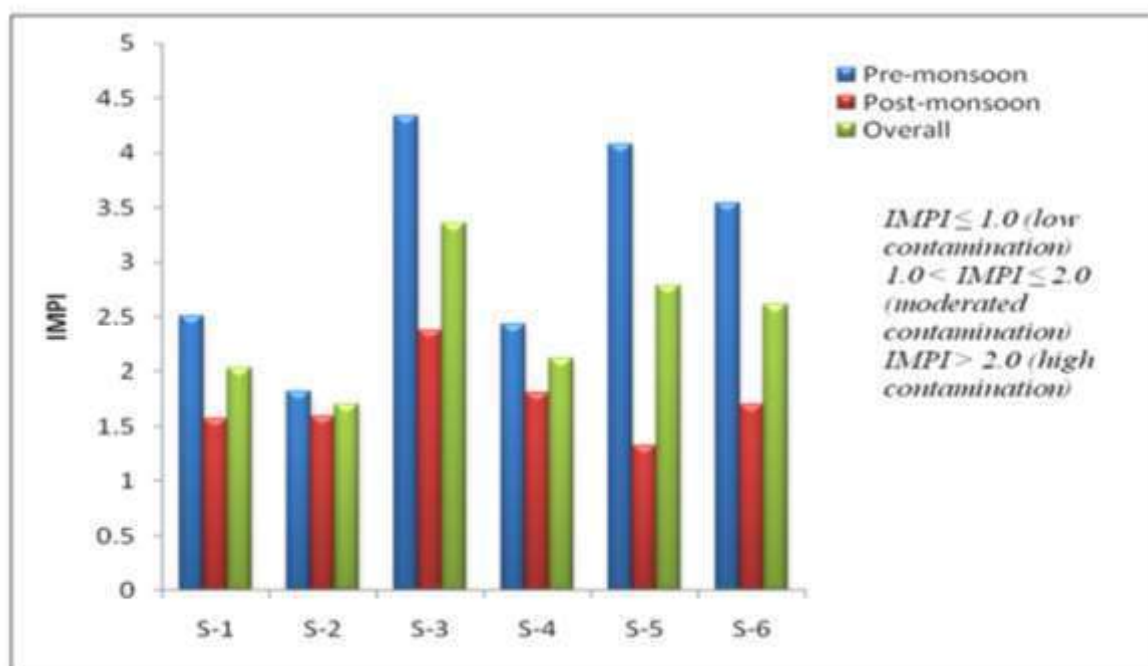


Fig.3: Seasonal trend of integrated metal pollution index (IMPI) in the river Hindon

### CONCLUSION

Present study showed that application of environmetric techniques for the evaluation of various types of pollutants and characterizing its sources. The physico-chemical analysis and heavy metals data were segregated and useful information were extracted on possible sources of contamination, seasonal variation patterns and characterization of river water quality with the help of environmetric techniques. Integrated metal pollution index (IMPI) was used for the assessment of the heavy metal contamination at various sites of Hindon river and the IMPI indicated severe pollution in pre-monsoon season compared to post-monsoon. The findings of this study clearly revealed that the water quality of Hindon river is very poor and cannot be used for domestic purposes. The high load of selected metals may even pose threat to the aquatic life. This kind of integrated study is very important for regular monitoring of rivers water quality and evaluation of pollution load as well as sources. Such type of integrated monitoring programs may help to take effective measures to control pollution in time and managing the water bodies.

#### CONFLICT OF INTEREST

There is no conflict of interest.

#### ACKNOWLEDGEMENTS

The authors acknowledge the support of the Department of Civil Engineering, Indian Institute of Technology Delhi, for providing laboratory facilities for this study.

#### FINANCIAL DISCLOSURE

None.

## REFERENCES

- [1] Purohit Jarvie HP, Whitton BA, Neal C. [1998] Nitrogen and phosphorus in east-coast British rivers: Speciation, sources and biological significance. *Sci Tot Environ* 210: 79-109.
- [2] Brezonic P, Hatch K., Mulla L, Perry D. [1999] Management of diffuse pollution in agricultural watersheds lessons from the Minnesota river basin. *Water Sci Tech* 39: 323-330.
- [3] Li S, Xu Z, Cheng X, Zhang Q. [2008] Dissolved trace elements and heavy metals in the Danjiangkou Reservoir, China. *Environ Geol* 55: 997- 983.
- [4] Dragun Z, Roje V, Mikac N, Raspor B [2009] Preliminary assessment of total dissolved trace metal concentrations in Sava river water. *Environ Monit Assess* 159: 99-110
- [5] Yilmaz S, Sadikoglu M. [2011] Study of heavy metal pollution in seawater of Kepez harbor of Canakkale (Turkey). *Environ Monit Assess* 173: 899-904
- [6] Fulazzaky MA [2005] Assessment of river water quality degradation of the Citarum and Brantas rivers by using a new developed water quality index system. In: *The 2nd Southeast Asia Water Forum: Better Water Management Through Public Participation, Proceeding, Bali, Indonesia*
- [7] Simeonov V, Einax JW, Stanimirova I, Kraft J. [2002] Envirometric modeling and interpretation of river water monitoring data. *Analy Bioanal Chem* 374: 898-905.
- [8] Lambrakis N, Antonakos A, Panagopoulos G. [2004] The use of multicomponent statistical analysis in hydrological environmental research. *Wat Res* 38: 1862-1872.
- [9] Kotti ME, Vlessidis AG, Thanasoulas NC, Evmiridis NP. [2005] Assessment of river water quality in Northwestern Greece. *Wat Res Manage* 19: 77-94.
- [10] Chabukdhara M and Nema AK. [2012] Assessment of heavy metal contamination in Hindon River sediments: A chemometric and geochemical approach. *Chemosphere* 87: 945-953.
- [11] APHA [1998] Standard methods for the examination of water and wastewater analysis (20th ed.) APHA, AWWA
- [12] USEPA [2006] National Recommended Water Quality Criteria. United States Environmental Protection Agency. Office of Water, Office of Science and Technology
- [13] Rios-Arana JV, Walsh EJ, Gardea-Torresdey JL. [2003] Assessment of arsenic and heavy metal concentrations in water and sediments of the Rio Grande at El Paso-Juarez metroplex region. *Environ Int* 29:957-971.
- [14] Chen TB, Zheng YM, Lei M et al. [2005] Assessment of heavy metal pollution in surface soils of urban parks in Beijing, China. *Chemosphere* 60: 542-551.
- [15] Central Pollution Control Board, CPCB [1995]. Classification of Inland surface waters (CPCB Standards) *Water Quality Parivesh* 1(4), 29-26.



## ARTICLE

# EVALUATING PLASTIC WASTE DISPOSAL OPTIONS IN DELHI USING MULTI CRITERIA DECISION ANALYSIS

Saurav Bhagat\*, Avdesh Bhardawaj, Piyush Mittal, Prateek Chandak, Mohammad Akhtar, Paaras Sharma

Department of Civil Engineering, Indian Institute of Technology Delhi, Hauz Khas, New Delhi, INDIA

## ABSTRACT

Continuous rise in the population of India has led to a steep increase in the amount of solid waste generated, particularly from urban areas which ultimately deteriorates soil and water due to unscientific disposal methods. Plastic forms an important constituent in the composition of the urban MSW because of its increasing use in our everyday lives and therefore requires the selection of a sustainable management option which is currently absent in the existing policy framework of India. This study uses the Multi Criteria decision analysis approach (MCDA) in order to evaluate different options for waste disposal for arriving at the most sustainable option for management and disposal of plastic waste in Delhi. A panel of nine members, who were faculty, researchers and students from the Indian Institute of Technology (IIT), Delhi was made and they evaluated seven disposal options against a set of environmental, health, financial and legislative criteria. The seven options included Landfill, Recycling, Incineration, Pyrolysis and a combination of two processes each from the first three mentioned in the study. The panel weighed the criteria and scored the options on them to arrive at an overall aggregate score for the best option. The study reveals that MCDA is a very effective and transparent measure of involving and encouraging public participation in decision making with highly successful results in the context of waste management. The panel suggested that a blend of recycling along with incineration was the best option which was followed by recycling and incineration. The worst method in the panel's consideration was the open landfilling currently practiced in Delhi which is a big source of soil contamination. The paper suggests that MCDA approach for evaluation of waste disposal options can arrest soil contamination to a great extent by providing the best waste management choice.

## INTRODUCTION

**KEY WORDS**  
Delhi, Landfill, Multi  
Criteria Decision Analysis  
(MCDA), Plastic, Waste  
Management

India ranks second as the most populated country with the population anticipated to increase at an average annual rate of 1.2% from 1029 million to 1.65 billion from 2001 to 2026 [1]. With an overwhelming rise in population, it is anticipated that the amount of municipal solid waste (MSW) in the coming future will increase as India strives towards achieving the status of an industrialized nation [2-4]. With the present unscientific methods of waste disposal, this humongous waste will ultimately contaminate the soil.

The amount of waste generated is related to factors like life standards of people, extent of industrialization and urbanization as well as the economic activities being carried out in and around an area. With a change in the lifestyle of people and increasing urbanization, the extent of MSW generation in Indian cities is now ~ 8 folds than what was at the time of independence [5]. Economic prosperity and a greater urban population proportion in India is linked with higher waste generation evident from the figures of about 114,576 tonnes/day of MSW in 1996, predicted to increase fourfold to about 440,460 tonnes/day by 2026 [6]. Table-1 summarizes the quantity and per capita solid waste generated in different states/ UT in India [10].

The National Capital Region (NCR) of India, which is a conglomeration of Delhi and the neighbouring urban areas of Haryana, Rajasthan and Uttar Pradesh, forms one of the largest commercial and residential hubs in the country thus contributing to increased MSW generation from this area. The residents of Delhi generated MSW of about 7000 tons/day in 2007 which is expected to increase rise to around 17,000 – 25,000 tons/day by 2021 [7]. If it were even possible to use composting and incineration and for maximum waste reduction, there would still be a minimum of 4000 – 5000 tons of waste per day that would have to be landfilled in 2021 [8]. Management of such a huge quantity of waste plan requires the presence of a strong policy framework in pertaining to waste management and disposal operations along with significant cooperation from the public to lead to efficient enforcement. With this perspective in mind, the Municipal Corporation of Delhi (MCD) did a study to know the viability and came up with a Master Plan (MP) for first treatment and then subsequent disposal of MSW during 2005–2021 in order to get sustainable MSW management options for Delhi. Composting and biomethanation are the technologies proposed in the MP (2005– 2021) for dealing with the MSW [9]. However, the success of developing sustainable and effective waste management options depends upon the extent of cooperation and involvement of the people.

The physical composition of MSW generated in Delhi from 1982-2002 has been given in [Table 2]. There is a wide variety in the composition of MSW which subsequently opens up multiple options and processes of waste disposal or waste to energy conversions. The most commonly used of these are landfilling, recycling, thermal conversion - incineration, pyrolysis and gasification - and bio-chemical processes such as composting, vermicomposting, and anaerobic digestion [11]. Plastic waste, however, forms an important component of MSW because of its everyday use in essential items. Post the industrial production of plastic

\*Corresponding Author

Email:  
saurav.bhagat01@gmail.com  
Tel.: +91-07838836939  
Fax: +91-11-26581117

Published: 10 Oct 2016

in the 1940s, the usage, and hence the waste generation rate of plastic solid waste (PSW) has augmented at a rapid rate of up to 3 % in Europe [12].

Furthermore, it can be seen that the fraction of plastic and non-biodegradables has been escalating in the Indian MSW mix [Table 2] which could be attributed to increased plastic packaging due to rise in living standards of the people [7]. It is highly imperative that we design use sustainable methods to dispose off plastic in an economically and environmentally feasible way.

**Table 1:** MSW generation in different states/ Union Territory (UT) in India [10]

S. No	Name of State/UT	Municipal population	Municipal solid waste (ton/day)	Per capita generated (kg/day)
1	Andaman & Nicobar	380,581	50	0.131378077
2	Andhra Pradesh	84,580,777	11500	0.1359647
3	Arunachal Pradesh	1,383,727	93.802	0.067789383
4	Assam	31,205,576	1146.28	0.036733179
5	Bihar	104,099,452	1670	0.016042352
6	Chandigarh	1,055,450	380	0.360036004
7	Chhattisgarh	25,545,198	1167	0.045683733
8	Daman Diu & Dadra	586,956	41	0.069851914
9	Delhi	16,787,941	7384	0.439839525
10	Goa	1,458,545	193	0.132323651
11	Gujarat	60,439,692	7378.775	0.122084921
12	Haryana	25,351,462	536.85	0.021176294
13	Himachal Pradesh	6,864,602	304.3	0.044328863
14	Jammu & Kashmir	12,541,302	1792	0.142887876
15	Jharkhand	32,988,134	1710	0.051836821
16	Karnataka	61,095,297	6500	0.106391168
17	Kerala	33,406,061	8338	0.249595425
18	Lakshadweep	64,473	21	0.325717742
19	Maharashtra	112,374,333	19.204	0.000170893
20	Manipur	2,855,794	112.9	0.039533664
21	Meghalaya	2,966,889	284.6	0.095925395
22	Mizoram	1,097,206	4742	4.321886683
23	Madhya Pradesh	72,626,809	4500	0.061960591
24	Nagaland	1,978,502	187.6	0.094819212
25	Orissa	41,974,218	2239.2	0.053347033
26	Puducherry	1,247,953	380	0.304498647
27	Punjab	27,743,338	2793.5	0.10069084
28	Rajasthan	68,548,437	5037.3	0.073485264
29	Sikkim	610,577	40	0.065511803
30	Tamil Nadu	72,147,030	12504	0.173312748
31	Tripura	3,673,917	360	0.09798806
32	Uttar Pradesh	199,812,341	11.585	5.79794E-05
33	Uttarakhand	10,086,292	752	0.074556636
34	West Bengal	91,276,115	12557	0.137571587
	<b>Total</b>	<b>1,210,854,977</b>	<b>127485.107</b>	<b>8.194978662</b>

Previous studies have shown that there are a number of sustainable and green methods of PSW handling viable from environmental and monetary point of view [13] and could be used to ensure proper PSW management. However, in a large number of cities in India, plastic disposal is carried out in open and unlined dumping areas in the vicinity of cities without any concern to environment. Alternative options for the disposal and treatment of plastic are required due to the increasing cost and decreasing space of landfills [14].

## OBJECTIVES OF THE STUDY

The objective of the present this study is to utilize a simple multi criteria decision analysis (MCDA; elaborated further in this paper for examining and evaluating plastic waste disposal options in Delhi which is generally indiscriminately disposed off and contaminates the soil, depriving of its natural quality in addition to posing high risk to human health and environment. A panel of experts and residents of Delhi

was formed and an assessment of plastic waste management options in Delhi was made by examining health, environmental effects of the different disposal processes considered. The disposal processes considered in the study are as follows: i) Landfilling, ii) Recycling, iii) Incineration and iv) Pyrolysis. Apart from these processes, a combination of landfilling and recycling, landfilling and incineration, recycling and pyrolysis have also been considered to arrive at a better outcome by using a combination of multiple methods and techniques. The criteria and the sub criteria considered for the analysis have been given in [Table 5].

**Table 2:** Physical constitution of MSW (as wt. %) in Delhi. Sources: [15-17]

S. No.	Parameters	2002	1995	1982
1	Biodegradable	38.6	38.0	57.7
2	Paper	5.6	5.6	5.9
3	Plastic	6.0	6.0	1.5
4	Metal	0.2	0.3	0.6
5	Glass and Crockery	1.0	1.0	0.3
6	Non-biodegradable (leather, rubber, bones, and synthetic material)	13.9	14.0	5.1
7	Inert (stones, bricks, ashes, etc.)	34.7	34.8	28.9

This paper is divided into the different sections. Section 3 gives us a review of MCDA and its need as policy framing and analysis tool along, use of MCDA in waste management options and an insight of plastic waste and its disposal options. Section 4 highlights the methodology adopted in this study. Section 5 gives an analysis and explanation of the results and discussions.

## LITERATURE REVIEW

### Multi- Criteria Decision Analysis

Multiple- Criteria Decision Analysis (MCDA) is a mechanism for assessing and understanding complex problems by breaking them down into simpler individual pieces and then using data to give an assessment on those individual pieces which when finally reassembled and combined present a coherent overall picture to decision makers [18]. In other words, it allows a complex problem to be appraised based on certain criteria (selected by the panel members) that have relative weightage (again assigned by the panel members) and uses a final sum of the weighted score of each option to offer the best elucidation. The panel is made up of a combination of experts and local residents who discuss and subjectively assign weightage to the criteria considered in the problem. The MCDA process has the following major stages [18]:

1. Setting up the aims of MCDA analysis; identifying decision makers, experts and other stake holders.
2. Establishing the context of MCDA and designing the socio-technical system for conducting it.
3. Identifying the various options that have to be evaluated and selecting the criteria for evaluating the options under consideration.
4. Prioritizing the criteria and assigning weights to determine their relative importance in decision making
5. Score the options on the criteria considered and then calculate overall weighted scores.
6. Examine the results and check their consistency; Discuss on the outcome achieved and make recommendations by carrying out sensitivity analysis.

MCDA has been used in the regulatory framework by many countries [19, 20], in a review of the decision analysis mechanism of United States Environmental Protection Agency (USEPA), a Multi-criteria Integrated Resource Assessment (MIRA) has been recognized as an substitute framework in place of current existing decision analysis methodologies. MCDA was utilized while carrying out Environmental Impact Assessment (EIA) in the Netherlands [21]. Furthermore, applications of MCDA can also be seen in the United Kingdom from evaluations of overseas trade being conducted by the National Audit Office to local authorities using MCDA modelling in order to decide the three-year strategic plan for management of their social care budget [18]. The key advantages of an MCDA include the following [22]:

- It invokes active participation of the stakeholders during the decision evaluating process and their interactive learning to appreciate viewpoints of others.

- It allows exploration of multiple dimensions of a problem taking into account the complexities associated with each proposed solution.
- It allows both quantitative as well as qualitative criteria to be taken into account. Thus it offers transparency in terms of analysis of a problem by including the importance of the qualitative social impact of the choices of a problem.

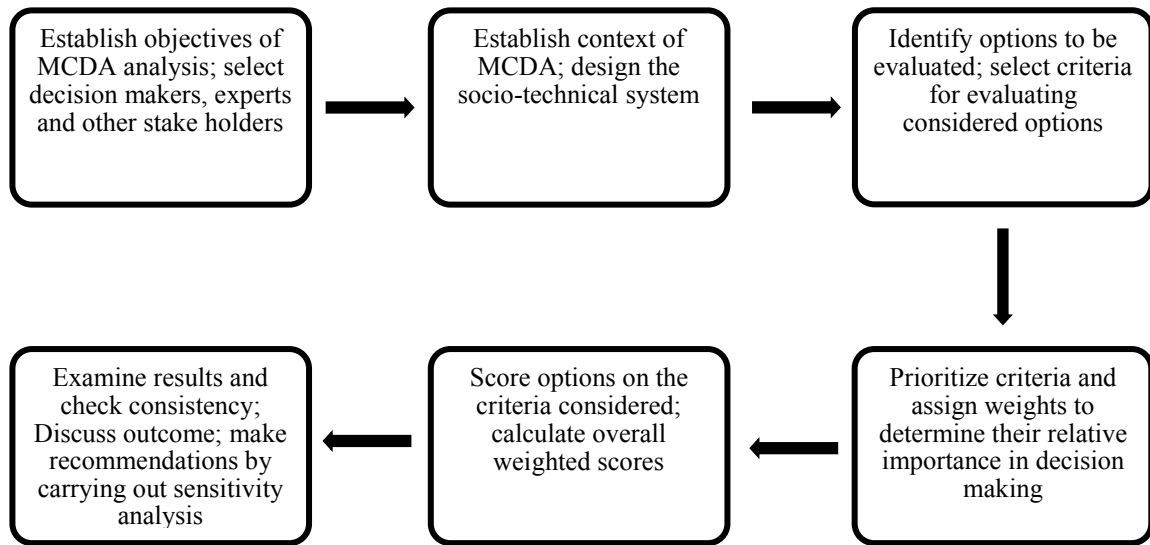


Fig. 1: The stages involved in an MCDA process

However, in spite of all its benefits the MCDA has been criticized because of the subjectivity that it imparts to the decision making process. At times, there is no fixed rationale for determining the weights assigned to criteria and this allows decision making to border on uncertainty in some cases. Also, several problems such as domination of the MCDA panel by certain individualistic stake holders, presence of a certain bias in the minds of the panel deter in reaching a coherent and socially optimal decision. Furthermore, MCDA is incapable to quantify whether one decision crafts greater human prosperity than alternative decision [23].

#### Applications of MCDA in management of waste

Multiple- Criteria Various studies have been carried out by researchers in different countries that have used MCDA in order to determine waste disposal options. Janssen, 2001 [21] studied the application of MCDA while conducting EIA in Netherlands, and established the necessity of transparency in the decision process which can be done by imparting information to the stakeholders in a manageable and simple way. MCDA was utilized to analyze the waste disposal options for the management of paper waste on the Isle of Wight in the United Kingdom [23]. In that study seven waste management and disposal ways were evaluated by the panel on the basis of several criteria like: environment, finance, legislation and society. They concluded that gasification of waste on the island was the option that was most preferred by the panel members and MCDA was efficient technique to engage public in the decision making process for waste management. Similarly Powell et al. 1996, [24] examined six waste disposal options namely landfilling, incinerating and refuse-derived fuel (RDF), each with and without recycling) for management of waste in the UK. The analysis resulted in RDF with recycling coming out to be the best option and the results changing to landfilling when the weightage of cost of disposal technique was increased.

López, 2010 [25] carried out an MCDA for evaluating ways of energy recovery from waste in Reading, UK. The criteria that his study incorporated were financial (capital and running costs) and environmental (odour, noise, pollution) and inferred that gasification with a combination of heat and power to be the best method of waste management. The stake holders are influenced greater by economical factors than environmental. In another case at Saharawi refugee camps in Algeria, Garfi et al. 2009 [27] compared different waste management solutions in for arriving at a decision making method. Their study employed a mathematical technique, the analytical hierarchy process (AHP), for multi-criteria strategy making.

In a study conducted at an Indian city Dakar, MCDA was applied for studying solid waste management options in households [26]. The criteria considered in the study included generation, accumulation and treatment of waste along nine city zones and suggested different methods of waste disposal in these areas. Although difficulties were reported in generating consistent and significant data but conclusions were drawn such as adoption of measures such as increased recycling and reducing the source of waste [23].

Apart from these studies several other studies have been carried which give us a detailed idea of the importance of public participation in waste management [28], trade-offs made sometimes because of the

diverging aims of policy makers with regards to little environmental impacts and expenditures [29]. With regards, to the Indian context there hasn't been a lot of work regarding the application of MCDA in waste management and the study aims to showcase effective application of MCDA to plastic waste management options thereby encouraging active public participation in policy enactment.

## Methods of Plastic Waste Management

### Landfilling

Multiple- Criteria Various studies Landfilling is the process in which wastes are deposited over an area of land thus degrading its soil quality from small to a large extent. The purpose of landfills is to avert contamination of the environment by the disposed waste, specifically the groundwater. Landfills are of following types: Open dumps, Semi-operated landfills & Sanitary landfills. Open, unlined, unengineered and unsanitary landfills are prevalent in India, resulting in contamination of soil, groundwater, foul smell and air pollution apart from dangerous levels of health risks. Other challenges of landfilling are limited availability of land for waste disposal and low awareness in public. Usually a high percentage of the solid waste along with plastics has been landfilled all over the world. However, landfill disposal has become unviable due to legislative reasons in some countries (which have targets of landfilling reduction by 35% in the time range of year 1995 to 2020), escalating maintenance expenditures, generation of GHGs like CH<sub>4</sub> and low degrading capacity of major disposed wastes [30]. Landfill gases contain around 0.01 - 0.6% cancer causing VOCs [31, 32].

### Recycling

Recycling of plastic waste is reprocessing of the expended plastics for creating new products carried out in a way to cut down environmental pollution, thus enhancing efficiency during the process. There are multiple types of recycling processes, for example to cycle plastics- primary, secondary, tertiary and quaternary techniques may be employed [33].

Mechanical Recycling is a combination of primary and secondary recycling resulting in conversion of plastic waste into products with characteristics either similar to those of original product or different from that. Although the process seems to be an eco-friendly mechanism, the reprocessing process is uneconomical and inefficient as it requires lofty energy for intermediate processes leading to making of a new usable product [34]. Chemical recycling or tertiary recycling involves manufacture of fuels and chemicals from plastic waste. Its primary function is to transform waste polymers into their simpler forms and then into chemicals which is useful for catering to a diversity of industrial applications/fuels. Quaternary recycling recovers energy from waste plastics utilizing aerobic combustion at high temperatures called incineration thus reduce the CO<sub>2</sub> burden on the environment indirectly[35]. This method is presently not popular in India.

### Incineration

Incineration is the process of combustion of waste substances which converts to ash residue and gases. The principle of generating energy from plastics waste incineration is useful for waste polymers that are recuperated and replace fossil fuels and thereby reducing CO<sub>2</sub> emissions virtually. The energy content and calorific value of polyethylene is almost same as traditional fuel oil and hence such substitution is feasible. Local authorities prefer incineration over other methods as energy recovery option since there is monetary profit in sales of plastic waste as fuel [36]. In India incineration is a poor option for MSW as the wastes are mostly unsegregated and consists of mainly high organic (40- 60%), inert (30-50%) and moisture content (40-60%) alongwith low calorific value (800-1100 kcal/kg). Additionally, the construction and operational costs of incineration plants are high [37]. However, using incineration as a means of disposing plastic is now being suggested in various places due to the reduction in volume this process achieves. Currently India doesn't have legislation or dedicated government departments to control this new sector of waste to energy incineration. But still this option is considered as a viable procedure for seeing off and managing disposal of waste under controlled conditions because of the primary reduction in the quantity of waste.

### Pyrolysis

Pyrolysis is defined as anaerobic combustion at high temperatures. In plastic pyrolysis, the macromolecular polymers break down to simpler species and syngas (mixture of CO, H<sub>2</sub>, CH<sub>4</sub> and higher hydrocarbons). It depends upon factors like temperature, retention residence time, catalysts etc. [35]. Plasma Pyrolysis is a novel technique which integrates thermochemical properties of plasma with the pyrolysis process. The extreme heat generation potential of PPT enables it to set out various kinds of plastic wastes by a dependable and secure manner. Thus segregation of waste is not a prerequisite in Plasma Pyrolysis Technology [33]. By this mechanism, there is a more than 99% chance of conversion of waste into non-toxic gases. Plasma Pyrolysis Technology is not extensively used in India.



## MATERIAL AND METHODS

### Formation of the MCDA panel

The MCDA panel consisted of faculty, researchers and students of the different departments at IIT Delhi, one of the premier technical institutions in the country with feedback and suggestions from experts in the field of waste. Also, there was no political representation (such as counselors or members of the Municipal Corporation of Delhi) of any involvement of laymen from outside. The contact with the panel members was established verbally by approach and a panel of nine members upon their subsequent agreement with assurance of confidentiality of their identity. Details regarding the members of the panel have been given in [Table 3].

**Table 3: Details of the panel members involved in the MCDA analysis**

Panel Member No	Qualification	Discipline
1	PhD	Environment Engineering
2	PhD	
3	M.Phil, M.Sc	Environmental Sciences
4	M.Phil, M.Sc	
5	M.Phil, M.Sc	
6	M.Tech	Environment Engineering
7	M.Tech	
8	M.Tech	
9	M.Tech	

### Panel Meeting & Discussion

The discussion among the panel members took place on a working day. The members of the panel were briefed on the problems created by improper management and disposal techniques of plastic waste. The procedure of an MCDA was thoroughly explained to all the members of the panel. After an initial briefing of the MCDA technique, the panel members were introduced to the following options considered for plastic management of waste disposal:

- Landfilling of the total plastic waste in the nearby landfills of Okhla, Bhalaswa and Gazipur
- Mechanical recycling of plastic waste
- Thermal recycling in the incineration units of Narela and Ghazipur
- Pyrolysis

Three more options which included i) Combination of incineration and landfilling. ii) Combination of mechanical recycling and landfilling and iii) Combination of incineration and landfilling were also provided to the panel in case a mixed solution was considered to be more appropriate than individual techniques.

An approach similar to the one used by Hanan et. al (2012) [23] was followed. The criteria used for MCDA were modifications of the ones used by Hannan et al. (2012) [23] whose criteria were in turn based on work done by Hirschberg et al. 2007 [38] in developing Bollinger and Pictet's (2008) criteria [39].

The members of the panel were asked to consider the following criteria (and add any one of their own if they deemed necessary) and allocate a total of 100 marks between these criteria (given in Table 4) in accordance to their relative significance during decision making procedure:

- Environmental criteria such as air, water and land pollution caused by the management techniques
- Health and Social Parameters which included the toxicity, aesthetic factors and cleanliness of the area
- Financial parameters which included the overall implementation cost of the technique used (inclusive of cost of collection and transport) and benefits from the by-products obtained from the process
- Confirmation to the prescribed legislative standards including local and national policies
- Practical implementation and feasibility of the proposed solution in terms of the number and capacity of the treatment plants in Delhi.



**Table 4:** Criteria considered for MCDA of plastic waste management

Serial No.	Criteria Considered	Sub – Criteria
1	Environmental	Pollution of air
		Degradation of water and land
2	Health and Social Parameters	risk/ chronic diseases capability - (individual)
		Aesthetic effects - (Cleanliness)
3	Financial	Cost of Collection, Transport and Implementation
		Economic Benefits from by products (if any)
4	Conforming to prescribed Legislative Standards	Local Policies
		National Standards
5	Practical Application & implementation	Feasibility of proposed solution
		Number of plants in the nearby area

For aiding the decision making process, the members of the panel were given the following information:

- An introduction about the common methods of waste disposal management [35].
- Environmental impacts of waste disposal of plastic through the considered options. This was provided in the form of an eco profiles for six divergent techniques in of disposing the plastic which included environmental impact in terms of global warming, solid waste generation, ozone depletion and nutrient enrichment (phosphorus and nitrogen) which have been given in [Table 5] [40]. Social parameters such as cleanliness were also obtained by correlating Area degradation with solid waste quantity.
- Relative cost of implementation of the techniques and their benefits (if any) were provided by waste management experts from IIT Delhi. Though exact quantitative data with regards to this wasn't available, an economic demarcation between the techniques could be made.
- To find the feasibility of the applied solution, data pertaining to the number, locations and capacity of landfills and incineration units in Delhi was provided to the panel.

**Table 5:** Environmental effects (as person equivalents) of the six disposal options [40]

Environmental Effect	Process					
	Recycling vision/ chemical separation	Recycling Dissolvent Separation	Recycling non- separation	Landfilling	Incineration with heat recovery	Pyrolysis
Global Warming	-39.56	-67.26	52.65	0.00	-12.21	145.39
Stratospheric Ozone Depletion	0.00	0.00	0.00	0.00	0.00	0.00
Acidification	-120.46	-128.64	23.02	0.00	-94.24	22.14
Nutrient Enrichment (nitrogen)	-62.50	-61.26	-0.19	0.00	-39.73	-2.28
Nutrient Enrichment (phosphor)	-2.06	-2.06	0.00	0.00	0.00	0.00
Photochemical ozone formation	-270.04	-302.22	75.88	0.00	-130.85	161.37
Solid Waste	386.87	375.92	269.30	2173.91	-193.83	887.28

Values are expressed in  $\mu\text{PE}/\text{kg}$

The panel was asked to consider the options presented to them and rank each of them with respect to the criteria mentioned previously. The panel members rated the options on a scale ranging from 1 to 10 with 1 being the least preferred and 10 being the highest or most preferred. Once the panel members had scored the options, an aggregate of the scores for all the options was done and the options were compared. The outcome of the MCDA was discussed by the panel members who concluded that the option was correct in their combined opinion. A sensitivity analysis was carried out to see the impacts of changing relative weights of the criteria on the outcome.

## RESULTS

The MCDA provides a clear and transparent mechanism to evaluate and arrive at the best possible option for disposal and management of plastic waste in Delhi. The weights that were assigned by the panel to the various criteria have been given in [Table 6]. A pie chart given in [Fig. 2] has also been plotted which allows us to assess the relative importance of the criteria considered by the panel. The scores given by the members of the panel have been given in [Table 7]. The aggregate total of the disposal option has been given in [Table 8] and another bar graph [Fig. 3] allowing us to compare the relative performance of each of the options.

From the results, we can show that the panel shows a clear preference for the combined option of recycling + incineration to be the preferred mechanism of handling solid plastic waste. Recycling of plastic as an option came in a close second which was followed by incineration. The reason could be that the panel thought that the combination would allow them to come up with a solution that would have the benefits of both the technologies and as a result would be better suited to handle the waste. Landfilling with recycling came in to be next perhaps because the panel considered that the option would have a high feasibility. The use of pyrolysis as a technique was not preferred by the panel and one of the major reasons for this were high chronic disease and air pollution associated with the technique. Open Landfilling, the way it is carried out in India, was considered to be the least preferred option.

**Table 6:** Weightage allotted to the criteria in the MCDA analysis

Serial No	Criteria Considered in MCDA analysis	Weightage considered
1	Pollution of air	15
2	Degradation of water and land	20
3	Risk/ chronic diseases capability - (individual)	15
4	Aesthetic effects - (Cleanliness)	8
5	Cost of Collection, Transport and Implementation	15
6	Economic Benefits from by products (if any)	8
7	Local Policies	4
8	National Standards	4
9	Feasibility of proposed solution	6
10	Number of plants in the nearby area	5
	Total	100

## DISCUSSION

This study has been used to evaluate waste disposal options from a series of given alternatives to arrive at the best solution to disposing plastic waste options in the city of Delhi. The major advantage that an MCDA offers is that allows us to include qualitative criteria in addition to the quantitative criteria and also encourages a greater participation of the public as stakeholders in the decision making process. The involvement of the people ensures a greater chance of success in the implementation of the actions made by the policy makers.

The panel did not have the presence of decision making people such as counselors or people from the Municipal Corporation of Delhi (MCDA) who are actively involved in the decision making process. Thus, the panel lacked that key area of decision maker expertise. In spite of the above limitation, the panel was still able to arrive at a coherent decision of choosing a combination of recycling and incineration as the best options for plastic waste disposal and management. The relative importance or weights assigned to the criteria have an important role in deciding the outcome of the analysis. In the present study, the panel members awarded the highest importance to environmental and health based criteria in contrast to the financial criteria. This shows that the main focus of the panel was in evaluating and considering the impact of qualitative parameters like health and environment over the cost which indicates a more robust and holistic thinking. Legislative criteria were awarded lower importance perhaps due to a lack of data on that front. However, the panel also did not very highly weigh the practicality of the proposed solution to be an important parameter because they felt that the methods mentioned in the study were practical enough to

be executed in the regions of Delhi. Also, the members of the panel were also guided by their personal feelings and intuitive knowledge in certain cases.

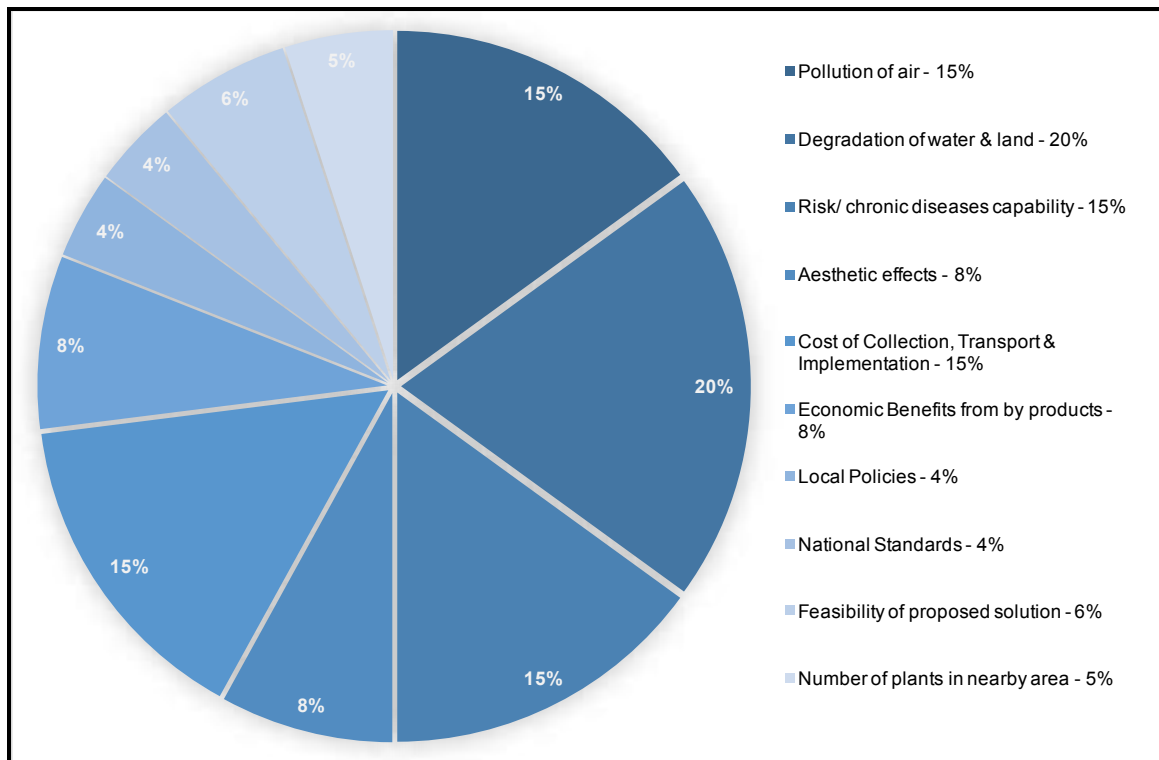


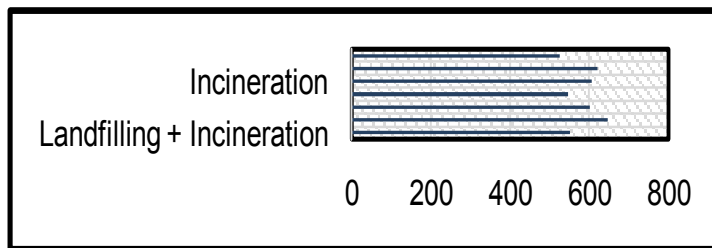
Fig. 2: Relative importance of the criteria in the MCDA analysis

Table 7: Scores given by the panel to various options considered in the MCDA

S No	Criteria considered for MCDA analysis	Landfill	Recycling	Incineration	Pyrolysis	Landfill + Incineration	Recycling + Incineration	Landfill + Incineration
1	Pollution of air	6.5	7	4.5	4	6.5	6.5	6.5
2	Degradation of water and land	2	5.5	8	6	5	7.5	4
3	Risk/chronic diseases capability (individual)	6.5	6.5	6	5.5	6.5	6.5	6
4	Aesthetic effects (cleanliness)	2	7	7	6	5.5	7	5.5
5	Cost of collection, Transport and Implementation	8	5	4.5	5.5	7	5	6.5
6	Economic Benefits from by products (if any)	2	7.5	7	6.5	4.5	7	4.5
7	Local Policies	7	6	6	5.5	6.5	6	6.5
8	National Standards	7	6	6	5.5	6.5	6	6.5
9	Feasibility of proposed solution	7.5	6	5.5	5	6	6	6
10	Number of plants in nearby area	7.5	6.5	5.5	5.5	6.5	6	6.5

**Table 8:** Aggregate scores for various plastic management and disposal options

S No		Total Score
1	Landfilling	525.5
2	Recycling	620
3	Incineration	605.5
4	Pyrolysis	546.5
5	Landfilling + Recycling	600.5
6	Recycling + Incineration	646
7	Landfilling + Incineration	550.5



**Fig. 3:** Overall Score of the disposal options

A combination of recycling and incineration came out to be the best option and the panel discussed this towards the end of the meeting. The panel felt that a combination of the two processes provided a solution with the benefits of one counterbalancing the shortcomings of the other. The recycling option was seen to be better in reduced air pollution, economic benefits due to use of reprocessed plastic and feasibility because of a large number of recycling units present in the Delhi NCR. On the other hand, the reduction in waste volume carried out by incinerating it was seen to cause reduced land and water pollution and the technique scored fairly high in maintaining aesthetic quality of the land. Thus a combination of the two was preferred as the best option. Only recycling emerged as a superior option in comparison to only incineration since the benefits of recycling mentioned above seemed to outnumber those of incineration.

Landfilling was ranked as the lowest or the least preferred option. The reason for this was that the method of dumping is followed in the name of landfilling in the areas around Delhi. This criterion was least preferred as it contributed the most to land and water pollution and also had very few benefits from by products in comparison to the other methods. On the other hand, the simplicity and ease of dumping meant that the criteria scored very high in the financial category because of its low cost, ease of application and practicality. On the other hand, the panel members also scored pyrolysis as not a good method. This was because of the bias that existed in the minds of the people with regards to anaerobic combustion of plastic which was instinctively thought to be a hazardous condition. Though, the panel conceded that techniques like Plasma Pyrolysis Technology (PPT) which were very clean and efficient were also prevalent but these were ruled out because they were not very practical and therefore could not be implemented in India.

In the study here, we haven't considered a sensitivity analysis by varying the relative weightage of the criteria. This can be considered as a scope for future research to test the robustness of the MCDA procedure.

## CONCLUSION

The MCDA in spite of adding a lot of subjectivity to decision making allows us to come to a consensus and achieve a robust option for the management of plastic waste and hence soil quality conservation. It can be concluded that such methodological approaches must be encouraged in decisions especially pertaining to environmental management and conservation.

### CONFLICT OF INTEREST

All the authors declare no conflict of interest whatsoever.

### ACKNOWLEDGEMENTS

The authors sincerely acknowledge the panel members for sparing their valuable time for discussions on the topic for MCDA.

## FINANCIAL DISCLOSURE

All the authors declare no conflict of financial interest.

## REFERENCES

- [1] Bongaarts J. [2009] Human population growth and the demographic transition. *Philosophical Transactions of the Royal Society of London B: Biological Sciences*, 364(1532), 2985-2990.
- [2] Sharma S, Shah KW. [2005]. Generation and disposal of solid waste in Hoshangabad. In: *Book of Proceedings of the Second International Congress of Chemistry and Environment*, Indore, India, 749-751.
- [3] Central Pollution Control Board (CPCB), [2004] *Management of Municipal Solid Waste*. Ministry of Environment and Forests, New Delhi, India
- [4] Shekdar AV, Krshnawamy KN, Tikekar VG, Bhide AD. [1992] Indian urban solid waste management systems - jaded systems in need of resource augmentation. *Journal of Waste Management* 12 (4):379-387.
- [5] Sharholy M, Ahmad K, Mahmood G, Trivedi RC. [2008] Municipal solid waste management in Indian cities - A review, *Waste Management* 28:459-467.
- [6] Hoorweg D, Laura T. [1999] What a waste: solid waste management in Asia. Working Paper Series No. 1. Urban Development Sector Unit, East Asia and Pacific Region, The World Bank, Washington, DC.
- [7] Talyan V, Dahiya RP, Sreekrishnan TR. [2007] State of municipal solid waste management in Delhi, the capital of India, *Waste Management* 28:1276-1287.
- [8] DUEIP, 2001. Delhi urban environment and infrastructure improvement project. Government of National Capital Territory of Delhi and Government of India Ministry of Environment and Forests (MoEF), India.
- [9] MCD, 2004. Feasibility study and master plan report for optimal solid waste treatment and disposal for the entire state of Delhi based on public and private partnership solution. Municipal Corporation of Delhi, Delhi, India.
- [10] CPCB, 2012. Status report on municipal solid waste management.
- [11] Singh RP, Tyagi VV, Allen T, Hakimi M I, Kothari R, [2011] An overview for exploring the possibilities of energy generation from municipal solid waste (MSW) in Indian scenario, *Renewable and Sustainable Energy Reviews* 15: 4797-4808
- [12] Al-Salem S M, Lettieri P, Baeyens P. [2009] Recycling and recovery routes of plastic solid waste (PSW): A review, *Waste Management* 29:2625-2643.
- [13] Howard GT, [2002] Biodegradation of polyurethane: a review. *International Bio-deterioration and Biodegradation* 49 (1):245-252.
- [14] Zia KM, Bhatti HN, Bhatti IA. [2007] Methods for polyurethane and polyurethane composites, recycling and recovery: a review. *Reactive & Functional Polymers* 67 (8):675-692
- [15] TERI, [2002] *Performance Measurements of Pilot Cities*. Tata Energy Research Institute, New Delhi, India.
- [16] NEERI, 1996. *Solid Waste Management in MCD Area*. National Environmental Engineering Research Institute, Nagpur, India.
- [17] IHPH, [1982] *Studies of Institute of Hygiene and Public Health*. Calcutta Metropolitan Development Authority, Calcutta, India.
- [18] Department for Communities and Local Government, 2009. *Multi-Criteria Analysis: A Manual*. Department for Communities and Local Government, London, UK
- [19] Stahl CH, Cimorelli AJ, Chow AH. [2002] A new approach to environmental decision analysis: Multi-criteria integrated resource assessment (MIRA). *Bulletin of Science, Technology and Society* 22:443-459
- [20] Stahl CH. [2003] *Multi-criteria integrated resource assessment (MIRA): A new decision analytic approach to inform environmental policy analysis [thesis]*. Wilmington (DE), USA: University of Delaware.
- [21] Janssen R. [2001] On the use of multi-criteria analysis in environmental impact assessment in The Netherlands. *Journal of Multi-Criteria Decision Analysis* 10:101-109.
- [22] Diakoulaki D, Grafakos S. [2004] Multi-criteria analysis. Work Package 4 Report, Externalities of Energy. <<http://www.externe.info/expolwp4.pdf>> (accessed 30.03.12).
- [23] Hanan D, Burnley S, Cooke D. [2012] A multi-criteria decision analysis assessment of waste paper management options, *Waste Management* 33: 566-573.
- [24] Craighill A, Powell J. [1996] Life cycle assessment and economic evaluation of recycling: a case study. *Resources, Conservation and Recycling* 17:75-96
- [25] López, P.I. [2010] Decision-support tool for energy-from-waste plants in development projects. In: 23rd International Expert Group for Life Cycle Assessment for Integrated Waste Management. Environment Agency, Bristol, UK.
- [26] Kapepula KM, Colson G, Sabri K, Thonart P. [2007] A multiple criteria analysis for household solid waste management in the urban community of Dakar. *Waste Management* 27: 1690-1705.
- [27] Garfi M, Tondelli S, Bonoli A, [2009] Multi-criteria decision analysis for waste management in Saharawi refugee camps. *Waste Management* 29:2729-2739
- [28] Hung M-L, Ma H-W, Yang W-F. [2007] A novel sustainable decision making model for municipal solid waste management. *Waste Management* 27 (2):209- 219.
- [29] Chang YH, Chang N. [1997] A fuzzy goal programming approach for the optimal planning of metropolitan solid waste management systems. *European Journal of Operational Research* 99:303-321
- [30] Garforth AA, Ali S, Martı́nez JH, Akah A. [2004] Feedstock recycling of polymer wastes. *Current Opinion in Solid State and Materials Science* 8(6):419-25
- [31] Residua, Landfill Information Sheet, Warmer Bulletin, May 2000.
- [32] Montague P. [1998] Landfills are dangerous. *Rachel's Environment and Health Weekly*, 617
- [33] Central Pollution Control Board (CPCB), India, Report on Plastic Waste Management - Chapter 11.
- [34] Mantia PL, Handbook of Plastic Recycling, Fransecso, [2002] ISBN: 1859573258, 9781859573259
- [35] Achyut K. Panda, RK Singh, DK Mishra, [2009] Thermolysis of waste plastics to liquid fuel A suitable method for plastic waste management and manufacture of value added products—A world prospective. *Renewable and Sustainable Energy Reviews* 14 (2010) 233-248.
- [36] Scott G. Polymers and the environment. *Royal Society of Chemistry*; 1999978-1-84755-172-6 [online]
- [37] Agnihotri AK. [2014] Current scenario of Indian Landfill and its solution through Biotechnological approaches 2nd International Congress on Green Urban Futures 2014 The session on Biotechnological Approaches for Enhancing Functional Quality of Urban Landscapes. The Energy and Resources Institute (TERI) New Delhi.
- [38] Hirschberg S, Bauer S, Burgherr P, Dones A, Simons A, Schenler W, Bachmann TM, Gallego Carrera D, [2007] Environmental, economic and social criteria and indicators for sustainability assessment of energy technologies. In: Project Co-funded by the European Commission Within the Sixth Framework Programme (2002-2006). Paul Scherrer Institute, Villigen PSI, Switzerland
- [39] Bollinger D, Pictet J. [2008]. Multi criteria decision analysis of treatment and land-filling technologies for waste incineration residues. *Omega* 36:418-428.
- [40] Molgaard C, [1996] Environmental impacts by disposal of plastic from municipal solid waste. *Resources, Conservation and Recycling* 15:51-63.



# ARTICLE

## MEASUREMENT OF CARBON MONOXIDE (CO) AND ESTIMATION OF % COHB AT SELECTED HIGH TRAFFIC JUNCTIONS OF AHMEDABAD CITY

Chauhan Kinjal<sup>1</sup>, Shah Dipsha<sup>2</sup>, Pandya Minarwa<sup>3</sup>

<sup>1</sup>L. D. College of Engineering, Gujarat Technological University (GTU)

<sup>2</sup>Faculty of Technology, CEPT University

<sup>3</sup>Environmental Engineering Department, L. D. College of Engineering, GTU

### ABSTRACT

The carbon monoxide (CO) is a vital criterion of pollutants, universal in environment. It generally produces due to incomplete combustion of fuels. Roughly, 80-90% of absorbed CO binds with hemoglobin to form Carboxy hemoglobin (COHb). The intimacy of hemoglobin with carbon monoxide is 200-250 times more than oxygen. The effect of CO poisoning on human health are headache, nausea to the loss of attentiveness and collapse, if the exposures are prolonged and with high concentration. The ambient CO exposure may affect various people such as drivers, traffic polices, street sellers, parking servants, pedestrians and cyclists [4]. Ahmadabad has become a mega city. In Ahmedabad, the rapid population growth rate and vehicular growth rate cause serious traffic congestion on streets and roads during peak hours leads to air pollution. Carbon Monoxide concentration is measured at high vehicular traffic junction in Ahmedabad city by using Carbon monoxide analyzer. CO Concentration is measured at 1.5 m height during the 10 AM to 7 PM of every 15 minutes. The CO investigation occurred during 21<sup>st</sup> April to 19<sup>th</sup> May 2015. The fifteen heavy traffic junctions had been selected in Ahmedabad city. Out of 15 traffic junctions, at 13 traffic junctions, CO concentration exceeds the one hour National Ambient Air Quality Standards (NAAQS) in peak hours due to heavy traffic of school time and office time and cumulate 8 hrs CO concentration exceeds the NAAQS at nine traffic junctions out of total 15 selected traffic junctions. Estimated %COHb is not more than 1%, so it is not contributed to any serious health effect.

### INTRODUCTION

Carbon monoxide (CO) produces due to incomplete combustion of carbon fuels and vehicular emission is the major source of generation of CO. % contribution of cities' high traffic congestion in generation of CO is of 95. CO concentration inside vehicles is inversely proportional to vehicles' speed. CO concentration may increase from 25 ppm to 45 ppm, when vehicles stop. Various literature reviews reveal that in areas with high traffic density and the high retention of vehicular traffic on the road, CO concentrations are high [1].

In the last few decades, Ahmedabad city has seen a rapid growth in vehicular population, urban infrastructure and industrial sector resulted in rising pollution levels in the city. Vehicular pollution accounts for 60-70% of total air pollution loads in urban India. Unlike industrial emissions, vehicular pollutants are released at ground level and hence, their impacts are likely to be more significant. Out of total number of vehicles in Ahmedabad as on 31<sup>st</sup> December 2013, 19, 74,452 are motorcycles, 2,72,393 are mopeds, 1,52,168 are auto rickshaws, 4,56,778 are four wheelers, 36,305 are trucks and 52,663 are tempos. % wise graphical representation of the same is depicted as [Fig. 1].

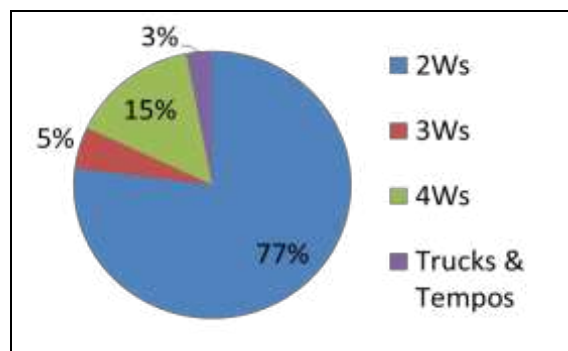


Fig. 1. Compositions of types of vehicles in Ahmedabad city

For the Ahmedabad city, % contribution of CO, HC, NO<sub>x</sub>, SO<sub>2</sub> and PM is approximately works out to be 61%, 23%, 14%, 1% and 1% respectively. The graphical presentation of the same is depicted in [Fig. 2].

#### KEY WORDS

Measurement of CO;  
Ahmedabad; Effect of  
Pollution on Traffic  
Polices; Air Pollution;  
Vehicular Pollution

Published: 10 October 2016

#### \*Corresponding Author

Email:  
dipsha.shah@gmail.com  
dipsha.shah@cept.ac.in  
Tel.: +91-7567369548  
Fax: +079-26302470

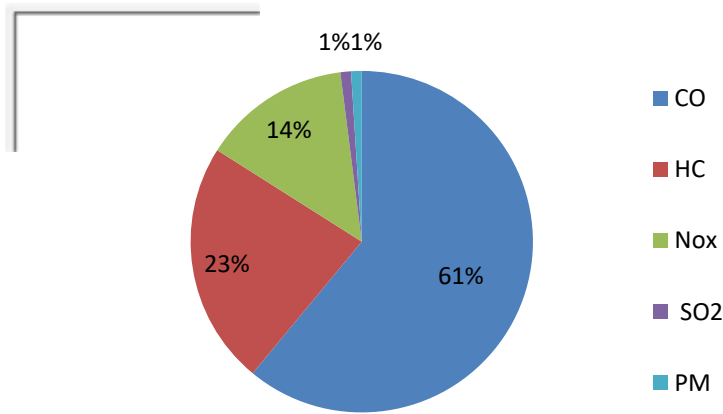


Fig. 2. % Contribution of air pollutants in total emission load due to vehicles for Ahmadabad City

Considering the nature and location of work place of traffic police, exposure of CO and resultant health risks are significantly high than the other people. In particular, traffic policemen are a population group under risk due to their inhalation for minimum 8 hrs. /day of CO [2, 3]. There is a severe effect of CO on human health only when CO concentration is higher than 10 ppm.

## METHOD

### Selection of high traffic junctions

Carbon Monoxide concentration is measured at high traffic junction in Ahmedabad city by using Carbon monoxide analyzer of HTC Company having range from 0 to 1000 ppm with 1 ppm resolution. The areas have been selected considering the residential, commercial, industrial and mixed zone. [Table 1] represents the list of selected traffic junctions along with CO measurement date and type of area. CO Concentration measured at 1.5 m height during 10 am to 7 pm. CO was measured every 15 minutes and cumulated the CO concentration of every hour. Every hour concentration was compared with 1 hour standard. Cumulated 8 hours (10am – 6pm and 11am – 7pm) CO concentration and compared with the 8 hours standard. The CO measurement has been done during 21<sup>st</sup> April to 19<sup>th</sup> May 2015.

Table 1: Selected traffic junctions of Ahmadabad city

Sr no.	Selected Junction	Measurement Date	Types of Area
1	Incometax Circle	21/4/2015	Commercial
2	Panchvati cross road	23/4/2015	Commercial are + Residential
3	Kalapur cross road	24/4/2015	Commercial
4	Anjali cross road	4/5/2015	Commercial + Residential
5	Astodiya Darwaja	5/5/2015	Commercial
6	Helmet circle	6/5/2015	Commercial
7	Visat junction	8/5/2015	Commercial + Residential
8	Memco cross road	9/5/2015	Commercial + industrial
9	Narol cross road	11/5/2015	Commercial + Industrial
10	Subhash bridge circle	12/5/2015	Commercial
11	Tilak baug	14/5/2015	Commercial
12	IskonCross road	15/5/2015	Commercial
13	Delhi Darwaja	16/5/2015	Commercial + Residential
14	Panjrapol cross road	18/5/2015	Residential + Sensitive

15	Kankariya Lake Gate No. 1	19/5/2015	Residential + Sensitive
----	---------------------------	-----------	-------------------------

**% COHb Estimation based on CO concentration**

The percentage of COHb has been estimated as function of inhaled CO (in ppm), from the duration of exposure by using following formula;

$$\%COHb = [CO]_{air} \cdot K \cdot T$$

Where,  $[CO]_{air}$  - Air concentration of CO in ppm

K - Constant that varies from 0.018 at rest to 0.048 at light work (usually depend on physical activity)

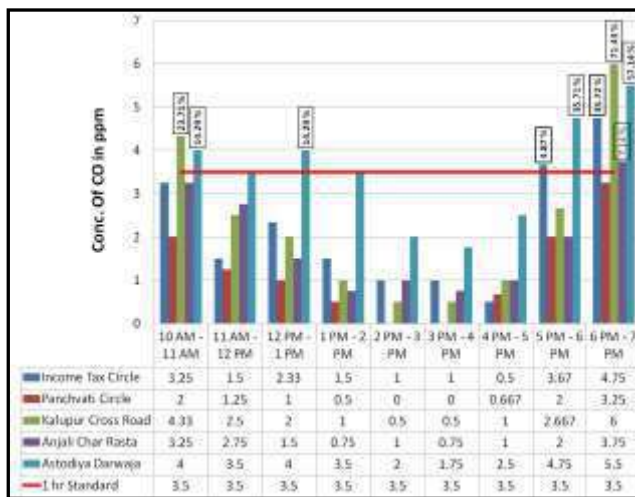
T - Duration of exposure in hours

**RESULTS**

**Hourly concentration of CO at selected junction**

Hourly concentration of CO is measured at selected area of Ahmedabad city during the 10 a.m. – 7 p.m. Each hour CO concentration has been compared with 1 hr National Ambient Air Quality Standard. 8 hours cumulate CO concentration, from 10 a.m. to 6 p.m. and from 11 a.m. to 7 p.m. has been compared with 8 hrs National Ambient Air Quality Standard.

At Income tax circle, hourly CO concentration was measured on 21st April 2015. The data obtained from CO measurement indicate that from 5 p.m. to 6 p.m. and 6 p.m. to 7 p.m., CO concentration is more than 1 hour standard. At Panchvati circle, hourly CO concentration was measured on 23rd April 2015. The data obtained through CO measurement indicate that for this location concentration of CO is within 1 hour standard. At Kalupur cross road, hourly CO concentration was measured on 24th April 2015. The CO measurement data indicate that from 10 a.m. to 11 a.m. and from 6 p.m. to 7 p.m., concentration of CO is more than 1 hour standard. At Anjali cross road, hourly CO concentration was measured on 4th may 2015. The data obtained through CO measurement indicate that from 6 p.m. to 7 p.m., CO concentration is more than 1 hour standard. At Astodiya darwaja, hourly CO concentration was measured on 5th may 2015. The data obtained through CO measurement indicate that from 10 a.m. to 11 a.m., 12 p.m. to 1 p.m., 5 p.m. to 6 p.m. and 6 p.m. to 7p.m. concentration of CO is more than 1 hour standard which is due to high vehicular traffic, narrow street roads and densely populated area. The graphical representation of hourly concentration of CO of above five traffic junctions (Income tax circle, Panchvati cross road, Kalupur cross road, Anjali cross road and Aastidiya Darwaja) in the form of bar chart is represented as [Fig. 3].



**Fig. 3.** Hourly Concentration of CO at Selected Junctions of Ahmedabad City

At Helmet circle, hourly CO concentration was measured on 6th may 2015. The data obtained through CO measurement indicate that from 6 p.m. to 7 p.m. concentration of CO is more than 1 hour standard. At Visat junction, hourly CO concentration was measured on 8th may 2015. The Co measurement data indicate that concentration of CO is within 1 hour standard at Visat junction. At Memco cross road, hourly CO concentration was measured on 9th may 2015. The CO measurement data indicate that from 6 p.m. to 7 p.m., concentration of CO is more than 1 hour standard. At Narol circle, hourly CO concentration was measured on 11th may 2015. The data obtained through CO measurement indicate that from 10 a.m. to 11 a.m., 11 a.m. to 12 p.m., 5 p.m. to 6 p.m. and 6 p.m. to 7 p.m., CO concentration is more than 1 hour standard. At Subhash bridge circle, hourly CO concentration was measured on 12th may 2015. The CO measurement data indicate that from 6 p.m. to 7 p.m., concentration of CO is more than 1 hour standard. The graphical representation of hourly concentration of CO of these five traffic junctions (Helmet circle,

Subhas bridge circle, Visat junction, Memco cross road and Narol circle) in the form of bar chart is represented as [Fig. 4].

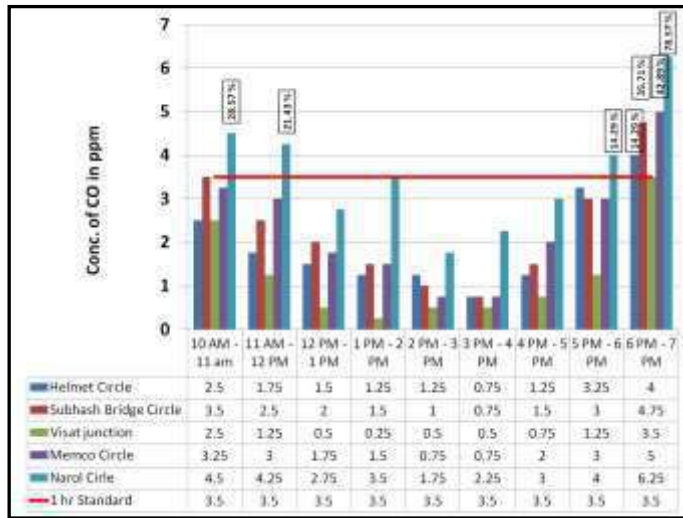


Fig: 4. Hourly Concentration of CO at Selected Junctions of Ahmedabad City

At Tilak baug, hourly CO concentration was measured on 14th may 2015. The data obtained through CO measurement indicate that from 6 p.m. to 7 p.m., concentration of CO is more than 1 hour standard. At Iscon circle, hourly CO concentration was measured on 15th may 2015. The CO measurement data indicate that from 6 p.m. to 7 p.m., concentration of CO is more than 1 hour standard. At Delhi Darwaja, hourly CO concentration was measured on 16th may 2015. The data obtained through CO measurement indicate that from 6 p.m. to 7 p.m., concentration of CO is more than 1 hour standard. At Panjrapol cross road, hourly CO concentration was measured on 18th may 2015. The data obtained through CO measurement indicate that from 6 p.m. to 7 p.m., concentration of CO is more than 1 hour standard. At Kankariya Lake; gate no. 1, hourly CO concentration was measured on 19th may 2015. The data obtained through CO measurement indicate that form 10 a.m. to 11 a.m., 11 a.m. to 12 p.m., 5 p.m. to 6 p.m. and 6 p.m. to 7 p.m., concentration of CO is more than 1 hour standard. The graphical representation of hourly concentration of CO of these five traffic junctions (Tilak baug, Iscon circle, Delhi Darwaja, Panjarapole cross road and Kakariya Lake) in the form of bar chart is represented as [Fig. 5].

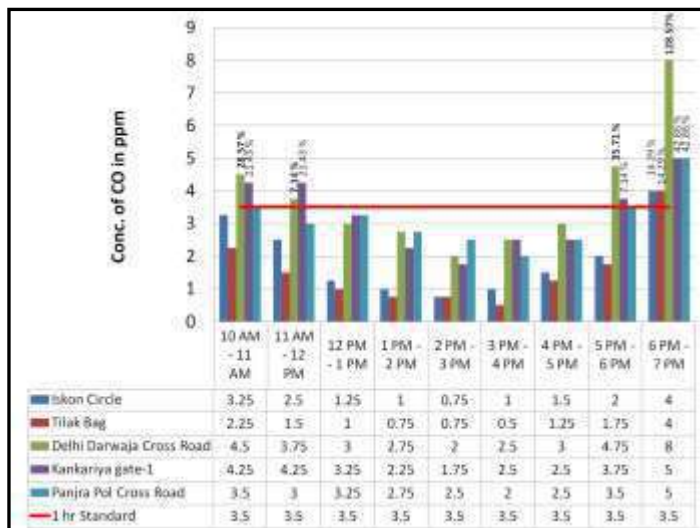


Fig: 5. Hourly Concentration of CO at Selected Junctions of Ahmedabad City

### 8 hours CO concentration at 15 selected junctions

The data obtained through CO measurement indicate that cumulate 8 hours (10 a.m. to 6 p.m.), CO concentration is more than 8 hours standard due to high vehicular traffic at Income tax circle (5.14%), Kalupur cross road (3.543%), Astodiya darwaja (85.71%), Subhash bridge circle (12.51%), Memco circle

(14.29%), Narol circle (85.71%), Delhi darwaja (91.09%), Kankariya Lake gate no 1 (75.03%) and Panjrapol char rasta (64.29%). So, total at 9 traffic junctions out of 15 traffic junctions, CO concentration exceeding the 8 hours NAAQS.

From the data obtained through CO measurement indicate that cumulate 8 hours (11 a.m. to 7 p.m.), CO concentration is more than 8 hours standard due to high vehicular traffic at Income tax circle (16%), Kalupur cross road (15.43%), Astodiya darwaja char rasta (96.47%), Subhash bridge circle (21.43%), Memco circle (26.8%), Narol circle (98.23%), Delhi darwaja char rasta (116%), Kankariya Lake gate no 1 (80.34%) and Panjrapol char rasta (75.03%).

The graphical representation of cumulative 8 hours (10 a.m. to 6 p.m. and 11 a.m. to 7 p.m.), CO concentration of 15 selected traffic junctions in the form of bar chart is represented as [Fig. 6].

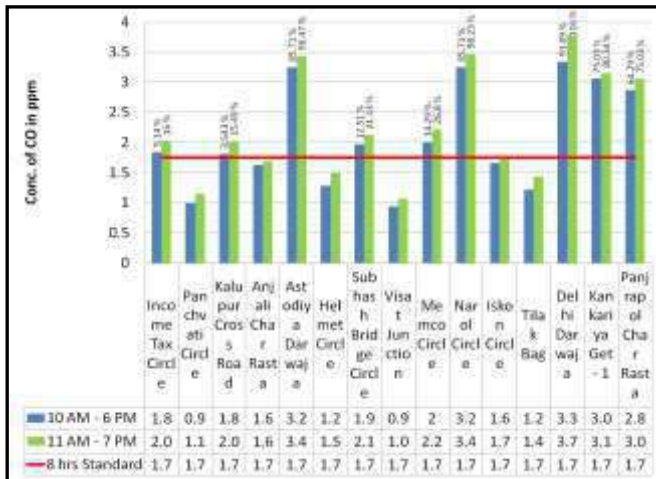


Fig. 6. 8 Hours concentration of CO at selected junctions of Ahmadabad city

### 3.3. % COHb Estimation in Blood

Based on cumulative 8 hours CO concentration, % COHb in blood of human beings has been estimated using the formula shown in method for 15 selected traffic junctions and tabulated as [Table 2].

Table 2: Level of % COHb in Blood Due to Exposure of CO for 8 hours

Sr. No.	Areas	10 A.M. – 6 P.M.		11 A.M. – 7 P.M.	
		Conc. in ppm	% COHb	Conc. in ppm	% COHb
1	Income Tax Circle	1.84	0.29	2.03	0.3248
2	Panchvati Circle	0.99	0.158	1.146	0.183
3	Kalupur Cross Road	1.812	0.2899	2.021	0.352
4	Anjali Char Rasta	1.625	0.26	1.688	0.27
5	Astodiya Darwaja	3.25	0.52	3.438	0.55
6	Helmet Circle	1.28	0.205	1.5	0.24
7	Visat Junction	0.9375	0.15	1.063	0.17
8	Memco Circle	2	0.32	2.219	0.355
9	Narol Junction	3.25	0.52	3.469	0.555
10	Subhash Bridge Circle	1.9	0.304	2.125	0.34
11	Tilak Baug	1.219	0.195	1.437	0.2299
12	Iskon Circle	1.656	0.265	1.75	0.28
13	Delhi Darwaja Char Rasta	3.344	0.535	3.78	0.605
14	Panjrapol char rasta	2.875	0.46	3.063	0.49
15	Kankariya Gate-1	3.063	0.49	3.156	0.505

CO measurement, it was observed that at most of the traffic junctions, hourly concentration of CO exceeding



the National Ambient Air Quality Standards during peak hours (10:00 a.m. to 11 a.m., 5:00 p.m. to 7:00 p.m.). This is due to high vehicular traffic, traffic congestion, more vehicular retention period, more no. of heavy duty vehicles and narrow street roads. So, to reduce the vehicular air pollution, heavy duty vehicles should not be allowed to congested areas during peak hours (Office Hours). The % COHb has been determined based on 8 hours CO concentration which comes out to be less than 1% in all selected traffic junctions, so no severe health effect due to CO concentration. To reduce the CO concentration in the atmosphere, more no. of trees should be grown on roads in highly populated areas, in the industrial areas and high vehicular traffic areas. To reduce the CO concentration, public transport facility should be improved and people should be encouraged to maximum use of public transport.

## CONCLUSION

From the study it concluded that

- 1) It is observed that out of the fifteen selected heavy traffic junction of Ahmedabad city, at thirteen traffic junctions, CO concentration exceeds the 1 hour standard and places are Income tax circle, Kalupur cross road, Astodiya darwaja char rasta, Subhash bridge circle, Memco circle, Narol circle, Delhi darwaja char rasta, Kankariya Lake gate no. 1, Panjrapol char rasta, Anjali char rasta, Helmet circle, Iskon circle and Tilak baug.
- 2) It is observed that out of the fifteen selected heavy traffic junction of Ahmedabad city, nine traffic junctions, CO concentration exceeds the 8 hours standard and places are Income tax circle, Kalupur cross road, Astodiya darwaja char rasta, Subhash bridge circle, Memco circle, Narol circle, Delhi darwaja char rasta, Kankariya gate-1 and Panjrapol char rasta.
- 3) It is observed that in most of the selected traffic junctions, during peak hours 10 a.m. to 11 a.m. and 5 p.m. to 7 p.m., CO concentration exceeds the 1-hr standard.
- 4) Based on the results CO, 1 hour concentration and 8 hours concentration not more than 10 ppm. So that it is not occurred any sign & symptoms on health (based on table 1).
- 5) The level of % COHb in blood for 8 hours, level of % COHb is not more than 1%. So it is not contributing any serious health effect.

## CONFLICT OF INTEREST

There is no conflict of interest.

## ACKNOWLEDGEMENTS

For this research work, we are thankful to Ahmedabad City Police – Traffic Police for their cooperation and Mr. Jagdish Chauhan of Nisarg Enviro Consultant for giving us instrument (CO Analyzer) to measure CO concentration.

## FINANCIAL DISCLOSURE

During this research work, we have not taken any financial help from any institute or from person.

## REFERENCES

- [1] G Mohan Kumar, S Sampath, VS Jeena and R Anjali [2008] Carbon Monoxide Pollution Levels at Environmentally Different Sites” Journal Ind Geophys 12:31-40
- [2] Maynard RL, Waller R. [1999] Carbon Monoxide. In: Holgate ST, Samet JM, Koren HS & Maynard RL (eds) Air Pollution and Health Academic Press: Harcourt Brace & Company, Publishers, pp. 749-796.
- [3] Yanan Liu, Shu Tao, Yifeng Yang, Han Dou, Yu Yang, Raymond M. [2007] Coveney Inhalation exposure of traffic police officers to polycyclic aromatic hydrocarbons (PAHs) during the winter in Beijing, China; Journal: Science of the Total Environment 383: 98-105
- [4] <http://www.mindfully.org/Health/Carbon-Monoxide-Health1sep01.htm>

## ARTICLE

# DETERMINATION OF SUSTAINABILITY THRESHOLDS FOR RIVER YAMUNA AND ITS FLOODPLAINS DUE TO THE CONSTRUCTION ACTIVITIES IN DELHI

Sumanth Chinthala and Priyajit Pandit

Indian Institute of Technology Delhi, New Delhi, INDIA

## ABSTRACT

Nature has a limited capacity to provide resources and absorb pollutants with time. Thus it's important to identify environmental threshold values, since it's important to know about the critical zones before actual tipping points in the system are reached. These Environmental Thresholds can be defined as a point or zone where there is a dramatic change in the state of matter or a system. In a threshold response, a minor change in the independent variable results in a dramatic change in the dependent variable. This research paper focuses on the determination of threshold levels for the river Yamuna and its floodplains with reference to the construction and operation of the Metro link between Nizamuddin Railway station and Yamuna Bank Metro Station in Delhi which would transect the River Yamuna through an elevated track. The study aims to identify the environmental thresholds with respect to the ecology of the river and its floodplains through identification of specific indicators which could be used to monitor the change which could lead to a further breakdown of an already stressed environment. It also seeks to quantify these thresholds so that they could be monitored more effectively through indicators.

## INTRODUCTION

The floodplains and the Yamuna riverbed are considered to be one of the sensitive locations due to their vital role in maintaining the groundwater levels in the vicinity of Delhi. The construction of the third phase of the Delhi metro rail link at the flood plain near Hazrat Nizamuddin will further affect the flood plain of the river Yamuna which is already stressed due to the existing structures and bridges. The third phase of Delhi Metro's master plan proposes to connect the Nizamuddin railway station to the Yamuna bank metro station which involves the construction of a bridge across the river Yamuna and a maintenance depot on the right bank. In addition to this, a bund shall also be constructed along the east bank. The proposed metro line along with the tentative location of the depot is shown in the [Fig.1]. The study has been done through the following stages:

- i. Identify threshold areas: The identification of areas, along/ in the river and its floodplains where there is likelihood of occurrence of environmental issues pertaining to air, water, land use and noise will exceed the threshold limits
- ii. Selection of thresholds and establishment indicators: From the chosen threshold areas, a set of indicators will be established, which are susceptible to change and have crossed the permissible limits. The major and minor thresholds would influence the identification of major and minor indicators.
- iii. Explore inter-relationship between indicators: Creation of sets and subsets to explore the inter-relationship between the indicators, in order to determine those indicators which are most susceptible to change. The thresholds can be directly linked to environmental resources, pressure/stress on the environment and underlying driving force. Measurement of threshold levels: Quantification of threshold levels for determining the critical points for environmental sustainability. The detailed methodology has been shown in the [Fig. 2].

## MATERIALS AND METHODS

### Construction methods adopted by Delhi Metro

The Delhi metro uses the following methods for construction of the Metro Link. The construction involves the building of the piers and the laying of the over head track. During the construction of the piers on the wetland, the position of the pillars is first identified on the ground and marked. After this, a special technique called "well sinking" is employed to construct the pillars. At a later stage, when the track is constructed, a special technique known as Incremental Launching is used. The technique involves the construction of the bridge in segments, as opposed to constructing it in irregular parts. The entire segment is first cast on a casting bed and then pulled over the pillars of the bridge by jacking. The construction technique is ideal for busy cities because it allows construction without any major disruption of traffic.[3]

### Determination of the state of the Eco-system

The domain area shown in the figure 1 is bounded by NH24 on the north and DND flyover towards the south and Sarai kale khan bus station in the west and Noida in the east. Within the enclosed domain a wide variety of species were present. It has been reported that *Typha angustata*, *Eichhornia crassipes* and *Sachharum munja* were distributed all along the fringes of the river in this area. The largest areas

**KEY WORDS**  
Sustainability; Threshold;  
Indicators

Published: 10 October 2016

\*Corresponding Author  
Email:  
mithrudu31@gmail.com  
Tel.: +91-9278275215

were occupied by *Typha angustata* (1.72 sq. km.) and *Eichhornia crassipes* (0.26 sq. km.). Smaller areas were occupied by *Nymphaea stellata* (0.95 sq. km.), *Sachharum munja* (0.03 sq. km.), *Carex fedia* (0.03sq. km.) and *Polygonum glabrum* (0.03 sq. km.) Over the entire river stretch, *Typha angustata* was the most common semi-aquatic plant and reached the highest abundance in this area.

### Impact assessment of the structures over the Yamuna

[Fig. 3] shows the impacts of the construction of structures over the river (Babbar, 2001). Many primary and secondary effects have been noticed in and around the near bed due to the construction activities. The construction of bridges has resulted in a change in the surface water profiles which significantly affect the aquatic systems. Further, the river experiences complex patterns of scouring in the vicinity. Moreover, this has found to have significant effect on the biodiversity and soil in the surrounding areas. It has also been observed that in the long run, the noise and air pollution in the surroundings increased due to increased flow of traffic. Hence the construction of every structure on the river causes many indirect and direct impacts.

## RESULTS

### Determination of the state of the ecosystem and calculation of the stresses

The method for determining the additional stress is as shown in the [Fig. 4]. The methodology includes the determination of stresses due to water quality, air quality, noise, and biodiversity and land degradation.

#### Water quality

The discharge from 22 drains joining river Yamuna at NCT – Delhi was 49.57 m<sup>3</sup>/sec in 2000 which reduced to 42.65 m<sup>3</sup>/sec in 2005. Correspondingly there was reduction of about 25% in BOD load contributed by these drains. From the description above and the graphs it is clear that the stretch under consideration is the most polluted with the DO levels approximately close to zero. Hence we can conclude that the health of the river is under severe stress.

Since the water quality parameters have already exceeded the permissible value, it is difficult to estimate the stresses based on the changes in those parameters. Hence, the water quality index can be calculated as follows:

$$\text{Water Quality Index} = (a/A) \times W \quad (1)$$

Where,

a = area of water body affected (m<sup>2</sup>), A= Total area (m<sup>2</sup>)

W= Weightage factor = (Stress factor x Fraction of species affected)/ Maximum stress factor

Where the maximum value of the Stress factor is 2.25 (justification of this value) times the number of species since the total value from each species cannot exceed 2.25. The value is obtained as 23 x 2.25 = 51.75 for the total species present. From the above formula, the weightage factor is obtained as (23x40)/ (42 x 51.75)\* (14.27/100) = 0.0602

#### Air pollution

Table 1 shows the predominant pollutant concentrations at the ITO intersection which is the nearest measuring station for the selected domain.

The Air quality index has been calculated by using the following formula

$$AQI = [SO_x / SO_xStd] + [NO_x / NO_xStd] + [Particulates / ParticulatesStd] + [CO / COStd] \quad (2)$$

The air quality index for the average pollutant concentrations during the years 1989-97 and for the years 2000-06 has been obtained as 6.17 and 5.20 respectively. Assuming that the pollutant concentrations will not exceed three times the permissible concentration, the total factor will not exceed a value of 12. For this case the average value of the index is 5.68.

#### Noise pollution

The main sources of noise from the operation of trains includes: engine noise, cooling fan noise, noise due wheel rail interaction, electric generator and miscellaneous noise like passenger's chatting. The roughness of the contact surfaces of rail and wheel and train speed are the factors, which influence the magnitude of rail wheel noise. The vibration of concrete structures also emits noise. Hence total noise level would be about 80.4dB (A). The permissible standards for a silence zone is 50dB where as the site will be exposed to a value very much greater than the permissible value. Hence the value of one is considered as a factor that should be multiplied with the noise impact.

#### Land use in the flood plain

The land use pattern in the river bed in the stretch under consideration has been shown in the [Table 1]. The east bank is occupied by the unauthorized colonies and agriculture in many zones. The west bank is

more diverse with archeological structures, landfills and recreational facilities. Due to the proposed metro line and the construction of bund, the land use pattern is expected to change. [2]

The approximate change in the area has been calculated by making the following considerations.

The reduction in the river bed area is equal to the number of piers times the diameter of each pier. The area of each pier and the number of piers are assumed to be same as that of the existing Delhi metro bridge that has been constructed near the Yamuna bank metro station

The area of the bund is calculated as 16 hectares.

The area of the metro depot proposed is considered to be equal to that of the built up area because the existing two depots have an areas of 39 hectares and 72 hectares. Hence a value closer to the average value has been chosen.

The total area of the metro track has been calculated based on the total width of the metro tracks in the existing alignments. The value is obtained as six hectares. The change in the land use pattern has been shown in the [Table 2].

Determination of the land use Index is given as

$$\text{Landuse Index} = \sum (\text{change in area} / 100) * \text{factor for land use} = 0.1522$$

### Biodiversity

Among the four different zones listed, the effect of the construction activities on the aquatic and terrestrial species has been quantified. It has been estimated that there are forty two aquatic species and thirty two terrestrial species present in the riverbed (Babbar, 2001). Out of those, twenty three aquatic species and eighteen terrestrial species are located in the zone where the construction activities are going to take place. For each species present in the zone III, a factor has been multiplied to calculate the effect of the activities on the particular species. The factors are calculated as follows

If the species is located only in zone III and absent in all other zones, a factor of 2 is considered

If the species is present in more than one zone, then a factor of 1 is used. The effect on the same species present in the adjacent zone becomes half of the original value.

The total effect is calculated as the product of the fraction of the species present in the zone to the total weightage obtained.

For the case of terrestrial species, the effect will be confined only to the immediate zones. The species if absent in the adjacent zone will not carry any effect on to the zone ahead.

**Table 1:** Pollutant concentration at the ITO intersection (Source: www.envforc.nic.in)

Year (Permissible concentrations)	SOx(µg/m3) (80)	NOx(µg/m3) (80)	Particulates (µg/m3) (100)	CO(µg/m3) (2000)
1989	8.7	18.5	373	2905
1990	10.2	22.5	338	2688
1991	13.3	27.2	317	3464
1992	18.4	30.4	377	3259
1993	18.5	33.2	372	4628
1994	19.5	33.0	377	3343
1995	19.0	34.1	407	3916
1996	19.0	33.7	387	5587
1997	16.2	33.0	370	4847
2000-2006	10.9	80	234	3450

**Table 2:** Change in the land use pattern due to the proposed construction activities

	Area (Hectares)	% of Area	Area (Hectares)	% of Area	% change in Area
River	150.63	14.28	150.63-0.0854=150.5436	14.27	-0.01
Agriculture	775.71	73.55	722.01-16=706.01-6= 700.01	66.37	-7.18
Built up area	53.70	5.09	2(53.70)+6=113.4	10.75	+5.64
DND	47.14	4.47	47.14	4.47	+0.00
Protection structures	17.79	1.69	17.79+16=33.79	3.2	+2.39
Hindon cut	9.63	0.91	9.63	0.91	+0.00
	1054.60		1054.60		

The weightage factor is calculated using the formula described below.

$$\text{Weightage factor} = (\text{Stress factor} \times \text{Fraction of species affected}) / \text{Maximum Stress Factor (3)}$$

Where the maximum value of the Stress factor is 2.25 times the number of species since the total value from each species cannot exceed 2.25. The value is obtained as 40.50 for the total species present.

From the above formula, the weightage factor is obtained as  $(31.50 \times 18) / (32 \times 40.50) = 0.437$ . The total land in the domain is 1054.60 and the area occupied by species which is directly affected is 700.01 hectares. Thus we get the Biodiversity Index value as 0.29. Since air and water have the maximum impact on the sustainability threshold of the ecosystem under study five scenarios emerged which may be undertaken for analysis as shown below [Table 3].

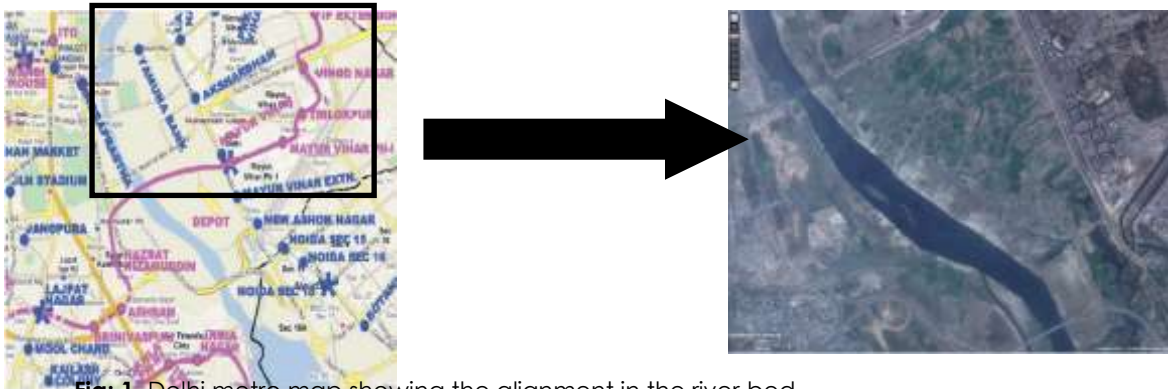


Fig. 1. Delhi metro map showing the alignment in the river bed

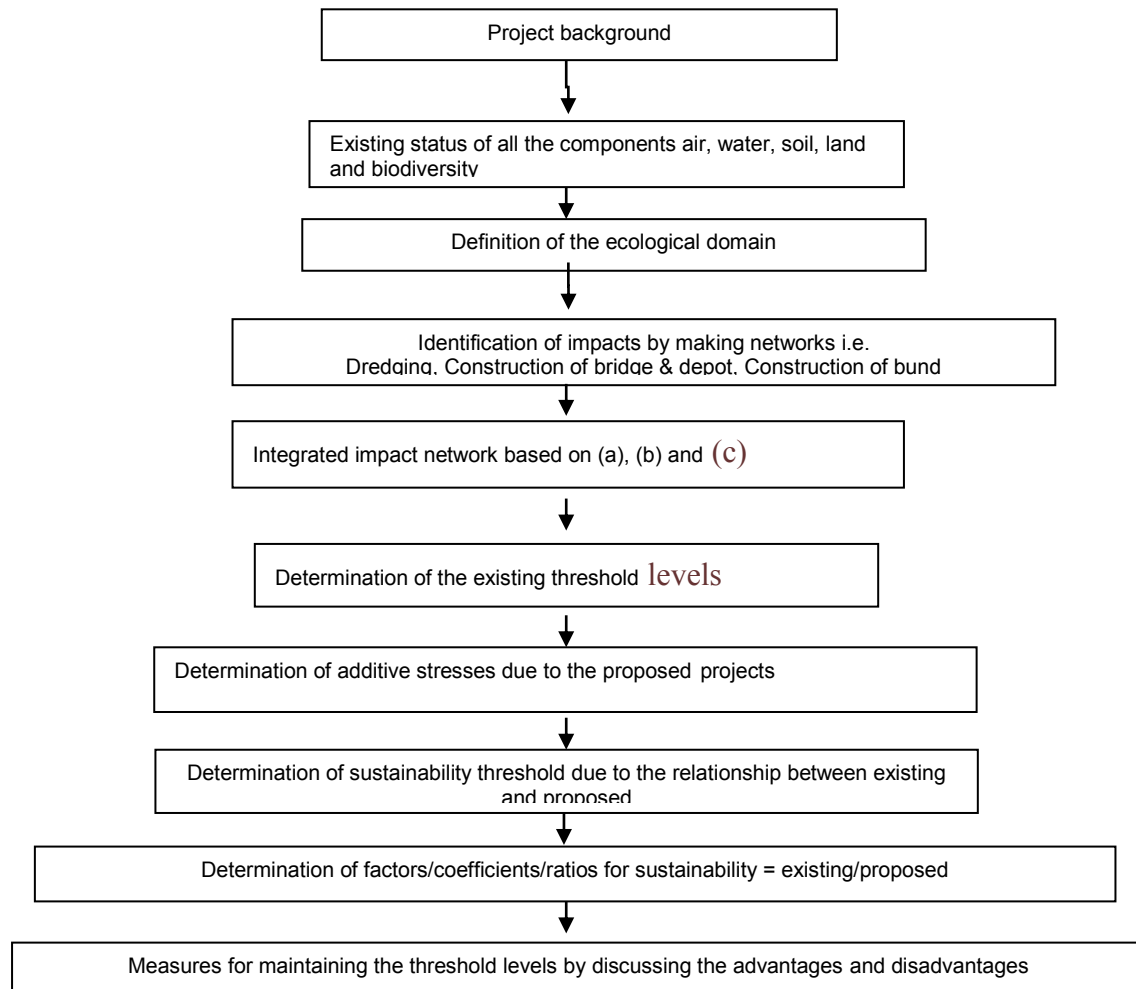


Fig. 2. Methodology for quantifying the sustainability threshold for the domain

Table 3: Possible Scenarios for the analysis of threshold levels for the current site

Sl no	Component	Scenario-I (Max-Max)	Scenario-II (Mid-Mid)	Scenario-III (Min- Max)	Scenario-IV (Min-Min)	Scenario-V (Max-Min)
1	Air	0.4	0.3	0.2	0.1	0.4
2	Water	0.4	0.3	0.4	0.1	0.4
3	Land	0.2	0.2	0.2	0.05	0.1
4	Biodiversity	0.2	0.2	0.1	0.1	0.1
5	Noise	0.2	0.1	0.1	0.1	0.05



Bubble diagram of impacts

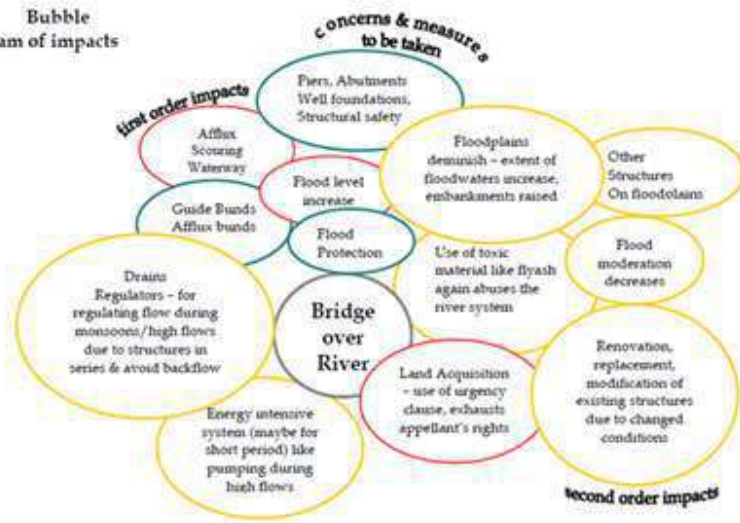


Fig. 3. Conceptual Diagram showing the effect of structures on the river [1]

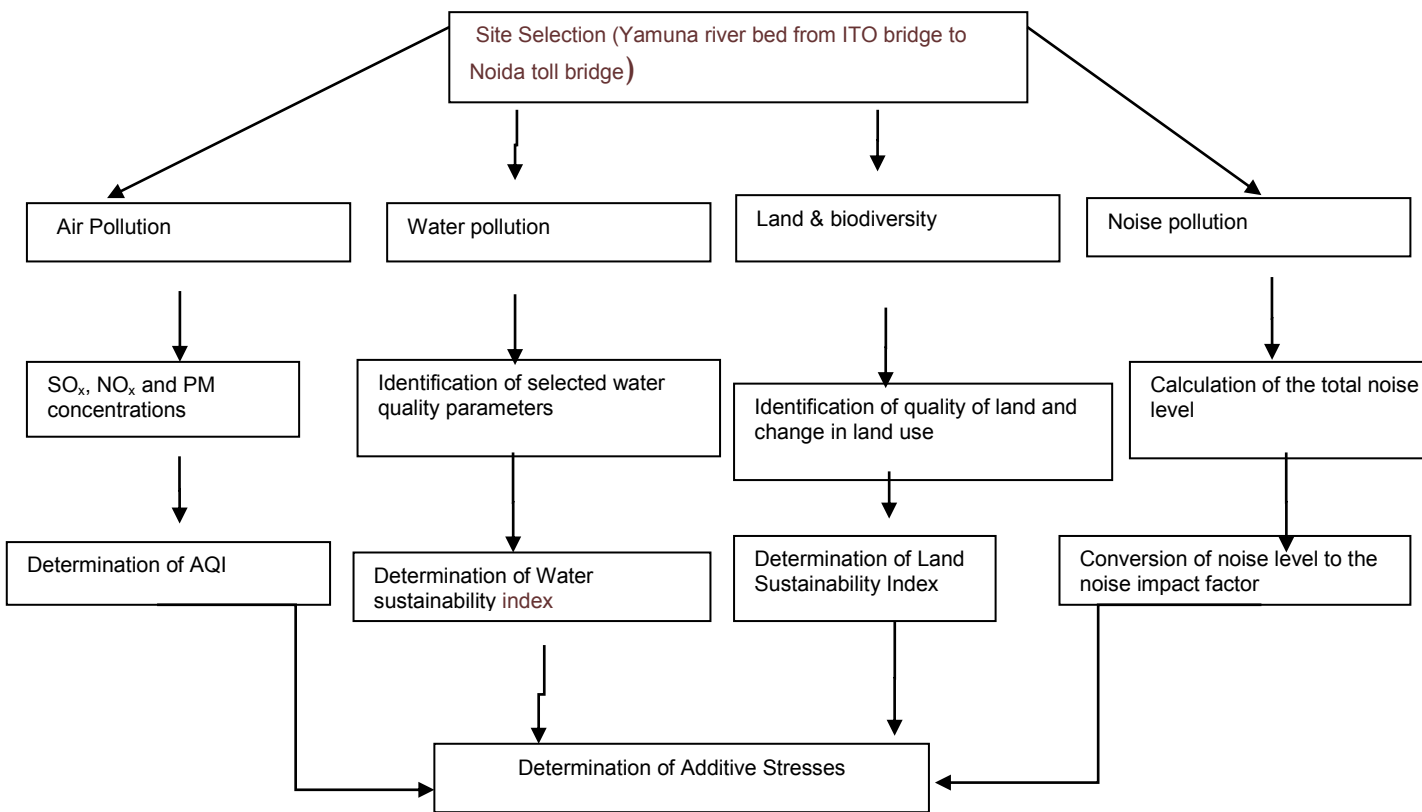


Fig.4: Methodology for determination of additive stresses

## DISCUSSION

### 1. Pressure indicators

In this case the pressure indicators identified are the large scale human interference which would be further enhanced through the construction of the Delhi Metro.

### 2. State indicators

According to the state of the ecosystem it can be safely concluded that most of the components including soil and water have already crossed the acceptable concentrations of their sustainability. Any further intervention especially on the flood banks or the wetland zone would not only threaten the state of the air and soil but also cause long term impacts to the biodiversity and water.

### 3. Threshold indicators

These indicators relate pressure and state indicators. They are “distance-to-target” type of indicators.

## CONCLUSION

The threshold indicators can be summarised thus:

Total Stress on the Ecosystem (The total index) =  $A \times AQI + B \times WQI + C \times LQI + D \times NQI$

In our case the actual Stress on the eco-system,

$S = 5.68 + 0.0602 + 1.608 + 0.1522 + 0.437 = 7.92$

The Maximum Stress on the Eco-System =  $12 + 1 + 3 + 1 + 1 = 18$

Therefore the Sustainability Threshold Index is,

Sustainability Threshold Index =  $7.92 / 18 = 0.44$

The tipping points for the Sustainability of each identified component can be calculated as;

Threshold index = Actual Stress / Maximum permissible Stress

1. Air =  $5.68 / 12 = 0.4733$

2. Water =  $0.0602 / 1 = 0.0602$

3. Noise =  $1.608 / 3 = 0.536$

4. Land =  $0.1522 / 1 = 0.1522$

5. Biodiversity =  $0.437 / 1 = 0.437$

Hence the tipping point would be close to the 1/3rd of the maximum value. This value is assumed on the basis of the ability to regenerate without a change in state of the renewable and non-renewable sources, in order to enable them to withstand stress conditions.

### CONFLICT OF INTEREST

There is no conflict of interest.

### ACKNOWLEDGEMENTS

The authors are thankful to Hon'ble Dean and Management

### FINANCIAL DISCLOSURE

None

## REFERENCES

- [1] Ameet Babbar, Landscape engineering measures for nature conservation :The flood plains and engineering techniques /measures for flood control with special reference to river Yamuna, 76-79, Advanced Landscape engineering report, School of Planning and Architecture, Newdelhi, India (2005).
- [2] Ecologic Institute and SERI, [2010] Establishing Environmental Sustainability Thresholds and Indicators, Final report to the European Commission's DG Environment, (2010).
- [3] DMRC, EIA for Delhi Gurgaon Metro rail, Delhi metro Rail Corporation, New Delhi, India (2011).

## ARTICLE

# NOISE REDUCTION AND HEARING LOSS IN PETROCHEMICAL WORKERS: A CASE STUDY

Rashi Gupta<sup>1</sup>, Amit K Gupta<sup>2\*</sup> and Byeong-Kye Lee<sup>1</sup>

<sup>1</sup>Department of Civil and Environmental Engineering, University of Ulsan, Ulsan 680-749, KOREA

<sup>2</sup>Ministry Of Environment, Forests and Climate Change, Regional Office (Eastern), Bhubneswar, INDIA

### ABSTRACT

The petrochemical plants workers have a high risk of noise induced hearing loss (NIHL). This study focused on the workers working for 10hrs daily in noisy environment of petrochemical plant. This study analyzed the data obtained, based on the survey queries of basic information and symptoms associated with noisy environment and the audiometry test of different noise situations. Workers exposed to high intensity of noise are suffering from many difficulties related to hearing loss. Out of 400 workers from the three plants of petrochemical plants, 44 were reported hearing loss as well as hearing difficulty. Analysis of the data also found that the workers who have been exposed to an excessive noise had a substantially poor audition and if they were exposed to noisy environment for a longer period of time, there would be more chances of hearing loss. Among the affected workers only few were subjected to the test and the rest were left for their own protection. This means that substantially many workers were still passive in protecting their hearing ability. Moreover, as the company spent more on the noise prevention facilities to protect the worker's hearing ability, their hearing ability gets no longer worse.

### INTRODUCTION

**KEY WORDS**  
Schistosoma Hearing loss; Noise; Hearing ability; Exposure  
Noise induced hearing loss (NIHL); decibel (dB); temporary threshold shift (TTS); permanent threshold shift (PTS)

Noise has assumed alarming proportions and has become even more dangerous than water and air pollution. Noise pollution is a slow and insidious killer. It is a serious health hazard but still the noise level is rising higher and higher in modern societies. Thus, noise is no less pollutant than the toxic chemicals in our environment [1]. Noise arising from the petrochemical plants affects the efficacy of communications; interfere with public address and alarm systems or, at high levels, cause damage to employees' hearing. Exposure to high level of noise creates the hazard to human health and even produces hearing loss to the workers of heavy industries.

The word noise comes from the Latin word nausea meaning seasickness and is often used to mean – "Sound that is unwanted by the listeners" or it is a meaningless sound of greater than usual volume [2]. Noise is usually a complex a periodic sound wave having indefinite pitch that bears no information. In other words noise is defined as a signal that interferes with the detection of or quality of another signal because there is no instrument that can distinguish between a sound and a noise. However, noise can be detected by the human's reaction. Noise is generally originated by human activities like industrialization, urbanization and transportation. Fast industrialization not only made the society more affluent but it has also created the environmental pollution and industrial calamity, which has affected the health, behavior and safety of the people who are working in the industrial sites. However, people living in cities and near to industrial areas can also be the victim of the noise problem [3,4]. People working in several industries like in petrochemical plants are directly exposed to the noise pollution sources. Noise pollution can cause annoyance and aggression, hypertension high stress level, hearing loss and adverse physiological and psychological impacts [5, 6]. High noise level can contribute to cardiovascular effects like coronary heart disease (CHD) which involves narrowing of small blood vessels that supply blood and oxygen to heart and its risk factor includes diabetes, high blood pressure altered blood lipid etc [7].

The other effect is noise induced hearing loss (NIHL) caused by chronic exposure to noise. NIHL is a sensorineural hearing loss. Prolonged exposure to high intensity noise can damage and destroys sensory hair cells of the inner ear leading to irreversible hearing loss [8]. Hearing damage is related to duration and intensity of noise exposure and it occurs at levels of 80dB or greater than that. Surveys indicated that more than half of industrial machines generate noise up to levels of 90dB or 100dB or above that which presents a definite health hazard to workers Noise having sound level below 80dB is reasonably safe [9]. If we have the exposure to high noise temporarily then we will lose hearing sound called as "temporary threshold shift (TTS)". When we get rest then it can be recovered, if the exposure is for a long time then we will have noise hearing impaired, called as "permanent threshold shift (PTS)" which cannot be recovered. Employee noise exposure can be assessed for the entire workforce by combining noise levels within areas or modules (either predicted or measured) with typical employee working patterns. Even though there are relevant safety rules to protect the workers, who are exposed to various noise levels, from getting hearing loss [4]. Numerous companies also showed a passive attitude with the investment to noise reduction. Many of the workers would not wear noise protecting equipments because of discomfort or nuisance. Thus lots of industrial workers exposed to high noise

Published: 10 October 2016

**\*Corresponding Author**  
Email:  
amitenv@yahoo.com  
Tel.: +91-674-2302452

levels for a long time might get difficulty in hearing without hearing aids. This study will help in preventing from the hearing impaired on factory noises with the example of petrochemical plants in Korea.

The objective of the present study is to determine the effect of noise on human health and how to reduce its level. The aims of the study were (1) to determine the % frequency level of noise in the workers working in different companies of the petrochemical companies (2) to determine the effect of noise on human health, along with the diseases faced by the workers and (3) to establish the various methods of noise reduction.

## MATERIALS AND METHODS

### Study area description

This study was performed in the petrochemical industrial complex (PC-IC) in Ulsan, which is the second largest port city and the largest industrial city in Korea. The PC-IC zone has many oil refineries, chemical plants, propylene and epoxy resin production plants, dye and pigment production plants, waste treatment plants and landfills. The petrochemical outputs produced from Ulsan almost reached to 45% of the entire petrochemical production in Korea. A lot of people in Ulsan work at industrial complex (IC) including heavy industries like petrochemical plants and a large number of workers in these companies have been exposed to serious noise levels.

Three petrochemical plants (A, B and C) located in the PC-IC area were chosen for this study in Ulsan. Plant A is specific for producing raw materials of petrochemical products and the total numbers of workers were 40. This plant has only one process (process AA) and this was started lately in 1990's. Plant B was established in 1980 and is mainly comprised of producing three types of synthetic resins through three different processes (process BA, BB and BC) with the help of 250 workers. Plant C, started in late 1990's with 110 workers, mainly manufactures liquid products through three processes (processes CA, CB and CC). Each plant has different processes which are shown in [Table 1].

**Table 1:** Showing the production and the processes of the different plants (A, B, C).

Plant	Hearing difficulty workers	Number and fractions of NIHL workers				
		Low NIHL	Medium NIHL		High NIHL	
			One ear	Both ear	One ear	Both Ear
Plant A	8	8 (100%)	0	0	0	0
Plant B	20	11 (55%)	4 (20%)	4 (20%)	1 (5)	0
Plant C	16	9 (56.3%)	3 (18.8%)	3(18.8%)	1 (6.1%)	0
Total	44	28(63.6%)	7 (15.9%)	7 (15.9%)	2 (4.6%)	0

### Noise measurement and protocols

The processes included in these plants were responsible for producing the loud noise which was found above the level of hearing capacity of a normal person. A survey was done on these workers and it was found that the behavior of some workers has changed; some are facing hearing difficulty and some were seen normal. Then a doctor's team was called to monitor those people who were showing the abnormal features and each person was kept on monitoring for a few years. Then at some frequency levels like 500, 1000, 2000 and 4000Hz their hearing capability of both the ears were measured to find out how much the people are affected by noise induced hearing loss (NIHL). A sound arresting meter (897 Dosimeter, Simpson) was utilized to examine the size of noise as well as hearing loss (NIHL) in the workers related to these plants. Workers involved in each process of each plant as well as those who were not involved in processes (e.g. people working in the supporting area of the plants) were also monitored for the test of NIHL. On the basis of above experiment the affected persons were selected and they were monitored for few days and their behavior and response against noise was observed at the above given each frequency level (produced in each process of their plant) continuously. Firstly test was done at low level of frequency and then after week by week frequency level and its period were increased. After the few weeks of observation the authors found that from each plant some workers were found affected by NIHL. Then these workers were kept on monitoring again and some queries were done related to the problems arising through the noise exposure. These series of analysis showed that plant A, B and C had 8, 20 and 16 affected workers, respectively, particularly including one worker who showed high NIHL.

## RESULTS AND DISCUSSION

### Average noise level and the effected workers

[Table 2, 3, 4] showed that the plant A has produced the average noise range of 84.8-94dB, among the total included workers 31 the affected were 8 in the AA process. The highest noise range was produced from a storage process and the supportive area has 58-65dB range noise with no effected persons.

**Table 2.** Company A: Average sound produced by different processes and % of effected workers.

Processes	Average Noise (dB)	Total number of workers	Number of effected workers	Effected workers (%)
AA process	84.8-94	31	8	25.8
Supportive area	58-65*	4	0	0
Average	84.8-94	35	8	22.9

\* Supportive area average is not included in the total average

**Table 3.** Company B: Average sound produced by different processes and % of effected workers

Processes	Average Noise (dB)	Total number of workers	Number of effected workers	Effected workers (%)
BA process	73.5-84.6	25	7	28.0
BB process	87.8-93.1	28	5	17.9
BC process	85.6-89.3	57	6	10.5
Supportive area of the plant	62-70*	140	2	1.4
Average	82.1-89.0	250	20	8.0

\* Supportive area average is not included in the total average

**Table 4:** Company C: Average sound produced by different processes and % of effected workers

Processes	Average Noise (dB)	Total number of workers	Number of effected workers	Effected workers (%)
CA process	63.5	20	8	40.0
CB process	76.4	24	5	20.8
CC process	63.3	23	1	4.3
Supportive area	61-68*	40	2	5.0
Average	67.5	107	16	15.0

\* Supportive area average is not included in the total average

Plant B which polymerizes synthetic resins showed average noise level of 82.1-89.0dB and 20 effected workers out of 250. Among three processes in plant B, process BA having lower average noise range 73.5-84.6dB, showed a higher rate of effected workers (28.0%) than those (17.9 and 10.5%) in process BB and BC, which had relatively, high average noise ranges (87.8-93.1dB and 85.6-89.3dB). This is because process BA include a separation process which showed the highest noise range 90-102dB than the cutting activity in process BB and BC which showed the highest noise level of 91-97dB. The supporting area having an average noise range 62-70dB, showed even 2 effected workers out of 140 (1.4%) to NIHL.

Plant C which produced liquid products by chemical reactions showed a large variation in fractions of effected workers to NIHL. Even though the average noise level 63.5dB in process CA was much lower as compared to those processes in plant B, its fraction of the effected workers to NIHL was much higher than those of other process in this study. Process CB for neutralization and refining showed average noise level of 76.4dB and 20.8% of effected workers to NIHL with the 2 effected workers out of 40 from the supportive area which showed noise range of 61-68Db which is a relatively higher rate as that in plant B. This showed that each process has their own sections which was responsible for producing the highest noise range that was affecting the workers involved in that process.

### Noise induced hearing loss in the workers

[Table 5] showed the survey results of the noise hearing loss in both the ears of the workers who are directly related to the processes of each plant. This showed that workers of B and C plant have high NIHL of 5% and 6.1% respectively and the 100% lowest NIHL was shown by plant A 55% by plant B and 56.3% by plant C. These workers were working without any noise protecting equipment. Even though the noise levels observed in the plant A process were 84.8-94dB, all the effected workers only showed low NIHL. However, the effected workers in plant B with noise levels of 82.1-89Db showed low, medium and high NIHL of 55, 40 and 5%, respectively. Even though



the average noise levels were relatively lower than those in plant A the NIHL levels were much higher than those in plants B and C. This is because the workers in process BB and BC in plant B were exposed to high noise levels of 85.6-93.1dB, as compared to other processes. The workers in plant C with average noise levels of 67.5dB, which is much lower levels as compared to plants A and B, showed low, medium and high NIHL workers of 63.6, 31.8 and 4.6% to their total effected workers, respectively. Their medium and high NIHL fractions were slightly lower than those in plant B. This phenomenon may be associated with other factors, such as biological age and working periods to noise environment, rather than physical factors like noise levels.

Table 5: Showing the percentage of the workers having noise induced hearing loss (NIHL)

Plant	Hearing difficulty workers	Number and fractions of NIHL workers				
		Low NIHL	Medium NIHL		High NIHL	
			One ear	Both ear	One ear	Both Ear
Plant A	8	8 (100%)	0	0	0	0
Plant B	20	11 (55%)	4 (20%)	4 (20%)	1 (5)	0
Plant C	16	9 (56.3%)	3 (18.8%)	3(18.8%)	1 (6.1%)	0
Total	44	28(63.6%)	7 (15.9%)	7 (15.9%)	2 (4.6%)	0

### Medical survey according to the Working time period and age of the workers

The workers who were found affected by NIHL their survey was done according to their working time period, age and their education. The detail is given in table 6. The total affected workers were 44 among 44, 43 persons were undergone through some tests and medical survey and the rest one doesn't want to have any test. From 43 the 3 persons were from supportive department and the rest 40 were from the different processes of plants A, B and C.

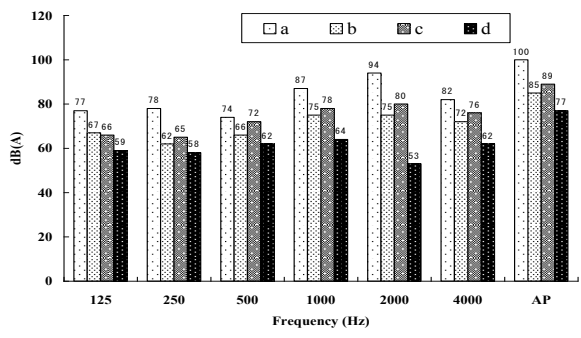
Table 6: Showing the detail of the affected workers according to age, education and working period

Plant	Working area		Age (years)			Education			Working period (years)		
	Process	Supportive area	40	40-50	50	Middle School	High School	College	5	5-10	10
Plant A	8	0	4	3	1	0	7	1	0	1	7
Plant B	18	2	2	18	0	0	16	4	0	1	19
Plant C	14	1	5	5	5	0	13	2	0	9	6
Total	40	3	11	26	6	0	36	7	0	11	32

So, the maximum affected persons were from the age between 40 to 50 yrs and their working period was more than 10 years. This means that the middle age workers are more sensitive towards the high level of noise and when they were exposed for many years they were found effected from NIHL. These total 43 workers were asked several questions regarding health, noise difficulty and noise level, protection equipments about NIHL and noise reduction as well as regarding the change of the department. Regarding the health checkup for noise in last year 90.7 to 97.7% were responded positively and when they were asked that were they facing any difficulty due to hearing loss and about it's cure then maximum (53.5- 88.4%) answered No. But still many (83.7%) were not ready for the cure for NIHL. Again they were questioned about the health effect due to exposure to noise then 41.9% workers were unaware of this and they were not able to assure about the problems they were facing due to noise exposure. Many workers were unknown from the effects of noise exposure and about the protection from NIHL (51.2%) still they were aware of their own protection and were themselves using the noise protecting equipment to protect them from NIHL, because when they were asked that were they forced by the manager to wear the equipment then 90.7% answered No but they (76.7%) never requested about any protection from noise at their work place. After knowing each and every thing still 95.3% denied to change their department. These queries and their result percentage showed these workers are conscious about their health and are coming forward so that their problems can be cured. The queries and their answer by the 43 workers are summarized below in [Table 7].

### Noise protection / reduction Facilities

After survey and doctor's query plant A has established some noise protection facilities such as noise absorption wall to the workers of its plant, a detailed noise measurement was conducted with the help of some central frequencies. The noise level at each fixed frequency before protection facility detected at every central frequency of 125, 250, 500, 1000, 2000 and 4000Hz was 77, 78, 74, 87, 94 and 82dB respectively. The noise levels, after establishing the noise protection facilities, were measured with two different environment including blocking and unblocking the noise produced from surroundings. The change in noise levels before and after establishing the noise protection facilities was summarized in figure 1. After providing the noise protection facility to the workers, the identified noise levels without blocking the noise from surroundings showed the loss of 11dB at 125Hz, 13dB at 250Hz, 2dB at 500Hz, 9dB at 1000Hz, 14dB at 2000Hz and 10dB at 4000Hz. This is explained in [Table 8]. This result shows that noise protection equipment can reduce a great amount of noise in the workers.



a: Level before protection facility, b: Target noise level, c: Level after protection without covered surrounding, d: Level after protection with covered surrounding.

Fig. 1. Showing noise level difference before and after the establishment of noise protection facility

Table 7: Survey for the affected workers to noise

Questions asked to affected workers	Yes		No	
	No of people	%	No of people	%
1. Do you have special health check for noise last year?	41	95.3	2	4.7
2. Do you remember the results from the last year test?	42	97.7	1	2.3
3. Did the abnormal symptoms are observed from the test?	39	90.7	4	9.3
4. Are you facing any difficulty in your life due to hearing loss problems?	5	11.6	38	88.4
5. Do you think further hearing loss will occur in future?	20	46.5	23	53.5
6. As compared to your colleagues did they get the cure for hearing loss?	18	41.9	25	58.1
7. Do you think you need regular check up for special test of hearing ability?	36	83.7	7	16.3
8. Is the special test necessary for you?	32	74.4	11	25.6
9. Is NIHL be cured?	7	16.3	36	83.7
10. Could you explain well the health effect due to exposure to noise?	25	58.1	18	41.9
11. Were you measured the noise level at your work place?	37	86.0	6	14.0
12. Did you realize the noise level at your work place?	32	74.4	11	25.6
13. Could you tell the noise level?	27	62.8	16	37.2
14. Did you always take your hearing protection equipment during work?	36	83.7	7	16.3
15. Had you ever took out your equipment while working?	36	83.7	7	16.3
16. Is your manager force you to wear the protecting equipment?	4	9.3	39	90.7
17. Did you wear themselves the protecting equipment without the force of manager?	39	90.7	4	9.3
18. Is the hearing protection equipment effective?	40	93.0	3	7.0
19. Did you like the hearing protection equipment?	36	83.7	7	16.3
20. Did you have enough knowledge about the protection from NIHL?	21	48.8	22	51.2
21. Did you have any training or education?	31	72.1	12	27.9
22. Did you want any training or education?	34	79.1	9	20.9
23. Have you ever thought about the methods for noise reduction?	41	95.3	2	4.7
24. Did you try to avoid going at the noisy places?	27	62.8	16	37.2
25. Did you ever request to your manager for the protection from the noise at your work place?	10	23.3	33	76.7
26. Did you want to work in other department of the same plant because of the noise?	2	4.7	41	95.3
27. Even though the noise level is severe problem you have to work their because of your family living?	9	20.9	34	79.1

Table 8: Reduced noise level after providing the noise protecting equipment

Methods	Frequency in Hz						
	125	250	500	1000	2000	4000	All Pass
Level of noise before the Protection facility(dB)	77	78	4	87	94	82	100
Target (Db)	67	62	66	75	75	72	85
Delta of target and noise level Before protection (Db)	10	16	8	12	19	10	15
Noise level after protection in Closed area (Db)	59	58	62	64	53	62	77
Noise level after protection in open area (Db)	66	65	72	78	80	72	89
Difference between protection in closed area and before the protection	18	20	12	23	41	20	23
Difference between protection in open area and before the protection	11	13	2	9	14	10	11

Hearing test results before and after using protection

This study compares the hearing test results of the workers of plant A at 400Hz before and after establishing the noise protection facilities. In years 2002, 2003 and 2004 no protection facility was provided and in year 2005 the workers were provided with noise protecting facility. An average of noise levels of both the ears of effected workers was taken before the establishment of protection facilities and compared with the noise levels of the both the ears of the same workers after the establishment of protection facilities. On comparison of the noise levels at 400Hz a remarkable result was detected. There was relative decrease in the noise levels of the left ear of all the 7 workers after the establishment of noise protection facility, only one worker out of 8 did not show any difference on the left ear before and after the establishment of noise protection facility. For the right ear out of 8 workers 3 showed relative decreases in noise level and one did not show any difference but 3 workers showed a little increase in their noise level after the establishment of noise protection facility. This is explained in table 9. Overall result explains that noise protection facility decreases the noise level of the both the ears of the workers up to a large extent and is safe as well as helpful in protecting their ears from the exposure of noise.

**Table 9:** Hearing test results of Plant A workers

Persons	Frequency at 400Hz				Difference before and after noise protection facility	
	Average of noise levels of 3 years		Noise level of year 2005		Left ear	Right ear
	Left ear	Right ear	Left ear	Right ear		
Mr X	50	23.3	45	15	-5	-8
Mr Y	46.7	53.3	45	55	-2	+2
Mr XY	66.7	41.7	60	40	-7	-2
Mr XX	60	75	60	80	0	+5
Mr XZ	51.7	55	45	50	-7	-5
Mr YX	30	46.7	25	50	-5	+3
MrZ X	43.3	11.7	40	10	-3	-2
Mr YY	52.5	60	40	60	-12	0

## CONCLUSION

The above study is helpful in explaining the noise induced hearing loss in the workers of petrochemical plants who have been exposed to high noise for a long time. These workers were working in noisy environment without the noise protection equipment and thus their both the ears were exposed continuously to the particular noise which lead them towards the noise induced hearing loss as well as other health defects. After establishing the noise protection facilities in the work place as well as to their ears, the noise level was much decreased and could minimize the noise pollution. Thus; this study explains that noise protection equipment as well as noise protection facilities are very much helpful to cope up with the dreadful condition of NIHL

### CONFLICT OF INTEREST

There is no conflict of interest.

### ACKNOWLEDGEMENTS

This work was supported by the research funds by the University of Ulsan, Ulsan, Korea.

### FINANCIAL DISCLOSURE

None

## REFERENCES

- [1] Bhatia SC, [2007] Book: Textbook of Noise Pollution and Its Control.
- [2] Plog BA, [1998] Fundamental of Industrial Hygiene (Third Edition), Edited by National Safety Council. Pg-163.
- [3] Singh N, Dawar SC, [2004] Noise pollution – Sources, Effects and Control, J Hum Eco, 16(3):181-187.
- [4] Barba MCD, Jurkiewicz AL, Zeigelboim BS, et al. [2005] Audiometric findings in petrochemical workers exposed to noise and chemical agents. Noise and Health, 5 (29):7-11.
- [5] Mitzelfelt R, Albuquerque's environmental story, Environmental topic: noise. Albuquerque, NM, City of Albuquerque. Available from: [www.cabq.gov/aes/s5noise.html](http://www.cabq.gov/aes/s5noise.html) 1996, (accessed 19 March, 2010).
- [6] Miller GT. [1998] living in the Environment, tenth ed. Wadsworth, New York.
- [7] Mead MN. [2007] Noise pollution: The sound behind heart effect, Environ health perspect, 115(11):A536-A532.
- [8] Lusk SL, [1997] Noise exposures, effects on hearing and prevention of noise induced hearing loss. Journal of American Association of Occupational Health Nurses 45:397-408.
- [9] Cheremisnoff PN, [1993] Industrial noise control, Edited by PTR (pg-1).

## ARTICLE

# MUNICIPAL SOLID WASTE MANAGEMENT IN INDIA: A CASE STUDY OF POST CONSUMED TETRA PAK CARTONS IN DELHI NCR

Ashish Jain<sup>1</sup>, Radha Goyal<sup>2\*</sup>, Shyamli Singh<sup>3</sup>, Lolita Pradhan<sup>4</sup>

<sup>1</sup>Director, Indian Pollution Control Association, 4 DDA Shopping Complex, Hargobind Enclave, Vikas Marg, New Delhi, INDIA

<sup>2</sup>Deputy Director, Indian Pollution Control Association, 4 DDA Shopping Complex, Hargobind Enclave, Vikas Marg, New Delhi, INDIA

<sup>3</sup>Faculty Indian, Institute of Public Administration, Indraprastha Marg, Ring Road New Delhi, INDIA

<sup>4</sup>Research Associate, Indian Pollution Control Association, 4 DDA Shopping Complex, Hargobind Enclave, Vikas Marg, New Delhi, INDIA

## ABSTRACT

The per capita waste generation in Indian cities is increasing everyday with increase in their population size, change in their life style and standards of living. Therefore the problems of waste management are hitting our country and they are becoming the issues of national concerns. However, the management of municipal solid waste is still very much neglected in our country as compare to other issues of national concern. In current scenario of municipal waste, the quantity of organic waste is declining, whereas the quantity of inorganic waste (Tetra Pak, PET, paper, plastic, metaletc) is accelerating, which indicates the high preference of packed food amongst the modern society. However in lieu of disposing the urban waste in India, the present study aims to explore the possibilities and opportunities to make best use of tetrapak carton's waste as a resource to generate wealth and reduce the environmental damages which it may cause if disposed on landfills. To achieve the aim, an attempt has been made to analyze the entire value chain of Tetra Pak cartons collection and recycling and identify the roles and responsibilities of each stakeholder involved for developing a sustainable business model for Tetra Pak cartons collection and recycling for the mega cities, which are actually facing the problem of post consumed cartons disposal. The results of the study indicates some positive environmental benefits, i.e. 1496.8 tons of GHG reduction and 4138 cubic meter of Landfill savings was achieved from collection and recycling of 1663.2MT of Tetra Pak cartons.

## INTRODUCTION

The increasing population and rapid urbanization in India has led to a significant increase in the waste quantity. In most of the urban cities with change in lifestyle and standards of living, per capita waste generation has increased tremendously and the nature of the waste being generated in the domestic sector has also changed. The literature reveals that almost 90% of the total generated waste is disposed of in a truly unscientific manner in open dumps, which are non engineered, unsanitary landfills in India [1]. It results into serious damages to public and environmental health as it attract birds, rodents and flies to the waste dumping site and create highly unhygienic conditions[2]. Further, the degradation of the solid waste results in the emission of carbon dioxide (CO<sub>2</sub>), methane (CH<sub>4</sub>) and other trace gases, which are the main green house gases [3]. The per capita/ per day waste generation rate in India varies from small town to large towns, for example, in small towns, per capita waste generations is nearly 100 grams/ day, whereas in large towns or cities like Delhi, per capita waste generation is almost 500 grams/ day[4].

In India Municipal Solid waste (MSW) is usually disposed of in low-lying areas without segregation and taking any precautionary measures before disposing. In places where there is no proper sanitation facilities, there streets serve as dumping grounds for both human and animal fecal matter and manure. The poor collection system and inappropriate facilities for transportation is making every nook and corner of cities occupied with waste. Furthermore, streets are widely been made useful for even dumping all kind of Construction & Demolition waste. Though the Solid Waste Management (SWM) includes activities, starting from generation, segregation, storage and collection, transfer and transport, treatment and disposal, most of the cities follow only four steps for managing their waste, i.e. generation, collection, transportation and disposal, which are also not in efficient manner[5]. Therefore, due to inefficient collection system (only 70% waste is collected), the uncollected waste often mixed with animal and human excreta dumped on streets, in drains and roads, leading to flooding, breeding grounds for insects, rodents and spread harmful diseases[ 6, 7, 8, 9, 10]. Thus waste management is becoming a crucial environmental problem in Indian metro cities. Further, in cities like Delhi, the land availability for waste disposal is very limited [11].

Although municipalities have the sole responsibility for managing MSW in their cities but they are failing to fulfill their duties and responsibilities. Their inefficiency in managing MSW is ultimately affecting human health, deteriorating environment and degrading our society. Now a days in the domestic sector the quantity of organic waste is declining whereas the quantity of that of inorganic waste (Tetra Pak, PET, paper, plastic, metal etc) is accelerating indicating that there is high preference of packed food amongst the modern society [12]. Thus with such waste generation scenario we require more and more land for its final disposal and land being a non-stretchable resource is shrinking with burgeoning population.

**KEY WORDS**  
Waste generation; Tetra pak; Delhi-NCR; Domestic sector; Solid Waste management; Recycling

Published: 10 October 2016

\*Corresponding Author  
Email:  
radhagoyal@gmail.com  
Tel.: 91-11-42207478

Tetra pak which is a six layered packaging box made up of internal polyethylene layer that seals in the liquid, polyethylene layer for lamination process, aluminum foil that creates a barrier for oxygen, light and flavors, polyethylene adhesion layer needed for lamination, followed by paperboard that gives stability and strength and finally the polyethylene layer that protects food from external moisture. Every Tetra Pak carton is primarily made up of paper with 75% made up of paperboard remaining 20% of polyethylene and 5% of aluminum. These three materials are compressed together and layered by means of heat and pressure to form a six layered armor which protects the contents from light, oxygen, dirt, air and moisture. The design of cartons is not just to protect the contents but to also prevent the content from being wasted while distribution [12]. But the only issue with Tetra Pak cartons is the outermost polyethylene layer, that makes it non-biodegradable and make them stay in the ambient environment for thousands of years till they eventually degrade. The mixed paper mills only recycle the paper content of the tetra pak carton, therefore there is a complete loss of aluminum and polyethylene content due to lack of technology at mixed paper recycling units. Though in countries like UK initiatives have been taken for segregation and recycling of the waste Tetrapak but in India the main problem is lack of awareness amongst the waste collectors and scrap dealers to segregate tetra pak's carton from the mixed paper waste so that it can 100% recycled and they can also be benefitted by generating more revenue. The waste should be segregated into three separate streams namely bio-degradable or wet waste, non bio-degradable or dry waste and domestic hazardous wastes by the waste generators as per MSW rules, 2015-16 [13]. However, these rules are rarely practiced in the metro cities, which further aggravate the problem. The Tetra Pak cartons being non-biodegradable in nature, when reach landfill sites continues to stay for 1000 of years and cause continuous GHG emissions[14]. Moreover most of the landfill sites of Delhi has exhausted and do not have any alternative left for the waste disposal. The problem related to solid waste management in Delhi may become even worse in the near future if we don't take correct actions. A trained and motivated group of stakeholders are needed to collectively help in managing solid waste. To combat this problem of non-biodegradable nature of Tetra Pak cartons the present paper showcases the attempt made by Indian Pollution Control Association (IPCA) to create a sustainable model for post consumed TetraPak carton collection and recycling in Delhi NCR region. A regularized system of source segregation followed by collection, sorting, bailing and finally recycling Tetra Pak cartons helped to enhance the social and economic status of the waste collectors involved in managing Tetra Pak cartons.

## SITE DESCRIPTION

The project was implemented in Delhi NCR region which is located in northern India between the latitudes of 28°-24'-17" and 28°-53'-00" North and longitudes of 76°-50'-24" and 77°-20'-37" East. It has an area of 1,483 sq. km, with a maximum length of 51.90 km and greatest width of 48.48 km. The site is between the borders of two states i.e. Uttar Pradesh and Haryana. The specific site locations of project area are clearly shown in [Fig. 1].

## METHODS

The case study of post consumed Tetra Pak cartons in Delhi NCR has been undertaken by the Indian Pollution Control Association (IPCA), a not-for-profit, non-government organization working on Solid waste Management, Rain Water Harvesting and several other environmental issues, to understand the opportunities for improving the status of municipal solid waste in Indian cities, which was evaluated by Indian Institute of Public Administration (IIPA), New Delhi. IPCA in collaboration with Tetra Pak had initiated collection and recycling of Tetra Pak cartons across Delhi NCR. In this process a total of 500 waste collectors were involved who worked with IPCA is collecting Tetra Pak cartons from different locations all across Delhi. After collection and further segregation these cartons were sent to bailing site located at Dallu Pura village, Mayur Vihar. At this site, daily 1-1.5 tons of tetra pak cartons were bailed into blocks. After converting the cartons into bails they were sent for recycling to different recycling units. There these bails were separated and fed into a large tank with water, where it was swirled around. The fibers absorb water and convert into slurry form (watery fiber). Any non- paper element such as plastic, aluminum etc. usually sink or separate out of the slurry. The slurry was then poured on thin flat surface to make recycled paper which can be used to produce other useful products. The plastic (polymer) and aluminum foil was further processed to produce the poly-al sheets. This process of recycling Tetra Pak cartons and recovering maximum of the paper, plastic and aluminum contents is a good practice and has many scope of improvement. The overall steps of recycling has been detailed in the subsequent section

## Value chain analysis of Tetrapak collection and Recycling

### Collection System

The trained waste collectors collect the Tetra Pak cartons generated from houses, institutions, commercial complexes and others. Cluster wise collection was done which helped in connecting different waste collectors in one location enabling maximum collection maximum. These small clusters work together and collect cartons from different locations within their range.





## RESULTS AND DISCUSSION

IPCA initiated systematic cluster wise collection of Tetra Packs from 2011 since then there has been a marked increase in collection which is reflected in Table , which indicate that Tetra Pak collection has increased every year with a rise of 35%[14]. This increase in collection is possible through combined efforts of IPCA team and waste collectors. Training and workshop sessions has helped them in understanding the need for collection and recycling, which is depicted in increasing collection rate.

Environmental analysis of Tetra Pak collection and recycling

Green House Gas emission savings/ Carbon savings

The Tetra Pak collection and its 100% recycling, is resulting into carbon savings. The waste which was otherwise ending into landfills, drains and water streams and accelerating the rate of carbon emissions into the environment is now reduced through proper channel of collection and recycling these cartons. Through collection and recycling process carbon savings of 1496.8 tons have been achieved till date and with increasing collection rate every year it is expected to increase the GHG emission savings here forth. Formula used for calculating carbon footprint is as follows-

Carbon footprint (tons of CO<sub>2</sub> eq) = Activity \* Emission factor (CO<sub>2</sub> e per unit)

[1]

$$= 1663.20MT * 0.9 = 1496.8 \text{ tons of CO}_2 \text{ equivalent}$$

Table 1: Tetra Pak Collection (Metric Tons)

S. No.	Year	Collection of Tetrapak (MT)
1	2011	80
2	2012	165
3	2013	419.715
4	2014	450.089
5	2015	548.402

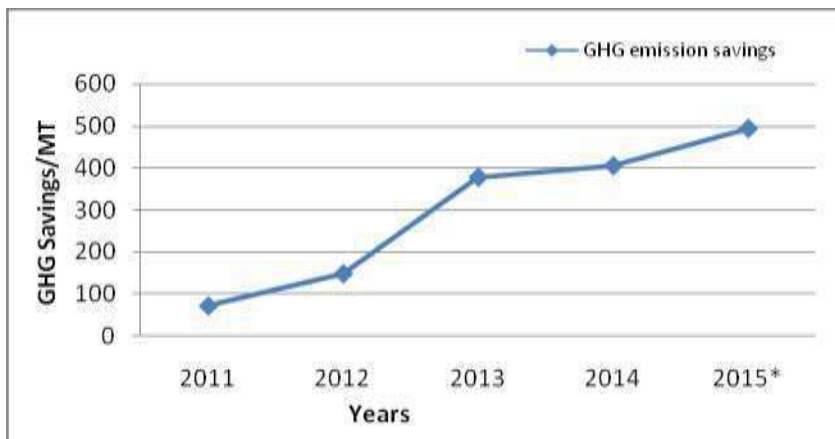


Fig: 2. GHG emission savings

### Landfill savings

The usual practice in most of the countries is that whatever is of no use is ultimately dumped into landfills. In Delhi we have three landfill sites which are floating beyond its capacity. With such a situation there will be no space left at landfills to assimilate the waste generated by the city. Thus looking into the present scenario and future concerns something can be done. Only through Tetra Pak collection, sorting, bailing and recycling approximately 4138 m<sup>3</sup> of landfill site have been saved since 2011 and it is expected to increase in the coming years with increasing collection rate every year. Relationship used in calculating landfill savings is taken from a study done by Tetra Pak, Europe of beverage cartons. The study depicts that by recycling one ton of beverage cartons we can save 2-3cubic meters of landfill(Source: Recycling of used beverage cartons in Europe, Tetra Pak)

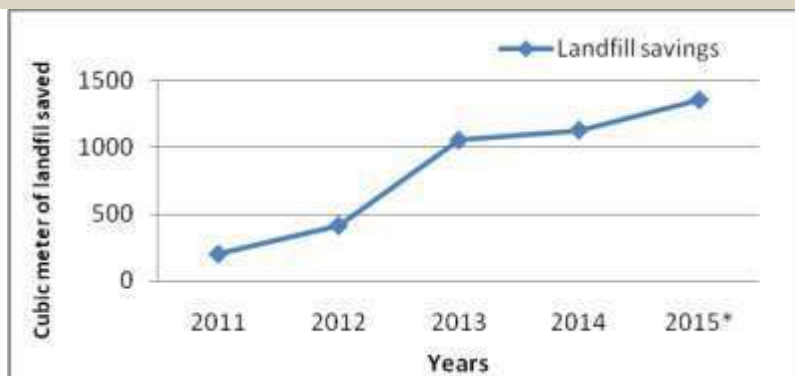


Fig.3: Landfill savings

## CONCLUSION

Tetra Pak collection and recycling as practiced by IPCA is a very sustainable business model which can be adopted in mega cities where the Tetra Pak generation rates are high and its disposal is a major problem. Being non-biodegradable in nature untreated Tetra Pak cartons can stay for 1000 years landfill sites and cause continuous GHG emissions. If practiced systematically and regularly the sustainable model developed by IPCA can mitigate problems like Tetra Pak cartons littering, dumping in drains which eventually block the drains and cause other health problems. However, lack of waste segregation by the waste generator is the biggest challenge in the model developed since Tetra Pak cartons come under the category of dry waste and if waste segregation is not practiced at the point of generation, the waste collector team have to put a lot of effort in its segregation. Thus if source segregation is done at point of generation, a lot of waste recovery can be done along with lesser health exposures to waste collectors. Moreover, the study also reflects that till date IPCA had been able to achieve collection of 1663.2MT of Tetra Pak cartons, which is turn has benefited the members involved in its value chain. Also, the increasing collection rate is also reflecting some positive environmental benefits like 1496.8 tons of GHG reduction and 4138 cubic meter of Landfill savings was achieved from 1663.2MT of Tetra Pak collection and recycling. Thus if this process continues we can save the carbon footprints and in turn reduce environmental load from Tetra Pak cartons.

Besides there is an urgent need to create more clusters of waste collectors and spread awareness about Tetra Pak cartons amongst more waste collectors, so as to increase the collection all across Delhi NCR. More R&D needs to be promoted to identify potential technological options to recover maximum paper content out of the post consumed Tetra Pak cartons, which currently is only 40-50% out of total 75% paper. If this recovery is increased to 60% it can create huge revenue opportunities for the recyclers and the waste collectors. Waste segregation campaigns should be initiated first at household level and then replicated to commercial areas. This practice can help recover higher Tetra Pak cartons from the dry waste stream without much wastage. Technological options for recycling poly-al part of Tetra Pak cartons should also be explored. Some economically viable technologies should be identified to attract more and more recyclers to indulge in its recycling.

## CONFLICT OF INTEREST

There is to certify that there is no conflict of interests.

## ACKNOWLEDGEMENTS

We acknowledge Tetra Pak India Pvt. Ltd for providing the opportunity to be able to work on the project. The support and guidance given by the Director IIPA, Dr. T.Chatterjee is highly acknowledged.

## FINANCIAL DISCLOSURE

None

## REFERENCES

- [1] Sharholly Mufeed et al. (2008). "Municipal solid waste management in Indian cities- A review." Waste Management 28(2): 459-467.
- [2] Sharholly Mufeed, et al. (2007). Municipal solid waste characteristics and management in Allahabad, India. Waste management, 27(4): 490-496.
- [3] Mor S, Ravindra K, Visscher AD, Dahiya RP, Chandra A. [2006] Municipal solid waste characterization and its assessment for potential methane generation: a case study. Journal of Science of the Total Environment 371(1):1-10.Sharma,
- [4] Shah S and Shah KW. (2005) Generation and disposal of solid waste in Hoshangabad." Book of proceedings of the second International Congress of Chemistry and Environment, Indore, India.
- [5] Siddiqui TZ, Siddiqui FZ, Khan E. [2006] Sustainable development through integrated municipal solid waste management (MSWM) approach – a case study of Aligarh District. In: Proceedings of National Conference of Advanced in Mechanical Engineering (AIME- 2006), Jamia Millia Islamia, New Delhi, India, pp. 1168-1175.

- [6] Gupta S, Mohan K, Prasad R, Gupta S, Kansal A. [1998] Solid waste management in India: options and opportunities. Resources, conservation and recycling, 24(2):137-154.
- [7] Das, D., Srinivasu, M., Bandyopadhyay, M., 1998. Solid state acidification of vegetable waste. Indian Journal of Environmental Health 40 (4), 333-342.
- [8] Kansal A, Prasad RK, Gupta S. [1998] Delhi municipal solid waste and environment – an appraisal. Indian Journal of Environmental Protection 18 (2): 123-128
- [9] Chakrabarty, P, Srivastava, VK, Chakrabarti, SN. [1995] Solid waste disposal and the environment – a review. Indian Journal Of Environmental Protection 15 (1):39-43
- [10] Khan RR. [1994] Environmental management of municipal solid wastes. Indian Journal of Environmental Protection 14 (1), 26-30.
- [11] Sharholy M, Ahmad K, Mahmood G, Trivedi RC. [2006] Development of prediction models for municipal solid waste generation for Delhi city. In: Proceedings of National Conference of Advanced in Mechanical Engineering (AIME-2006), Jamia Millia Islamia, New Delhi, India, pp. 1176-1186.
- [12] Magzoub M, Alla G, Elsharief AG. [2014]. Production of hardsheets from municipal solid waste. International Journal of Technical Research and Applications, e-ISSN: 2320-8163, 2(5) (Sep-Oct 2014), : 94-96, Source: [www.ijtra.com](http://www.ijtra.com) MSW rules, 2015-1016
- [13] Department of Economic Affairs (2009). Position Paper on the Solid Waste Management Sector in India. Public Private Partnerships in India.
- [14] IPCA [2015] Opportunities for improving the status of municipal solid waste in Indian cities: A case study of post consumed Tetra Pak cartons in Delhi NCR



ARTICLE

# TEMPERATURE CONTROL FOR SUSTAINED MICROBIAL ACTIVITY IN ANAEROBIC BIOGAS DIGESTERS

Neena Ahuja<sup>1\*</sup>, Dipali Bansal<sup>1</sup>, Khwaja M Rafi<sup>2</sup>

<sup>1</sup>Department of EEE, Manav Rachna International University, Faridabad, Haryana, INDIA

<sup>2</sup>Jahangirabad Institute of Technology, Barabanki, Uttar Pradesh, INDIA

## ABSTRACT

Exhaust gases from biogas powered internal combustion engine coupled to an alternator with temperature in the range of 450 to 650°C can be utilized to maintain biogas digester temperature at the desired operating point for the optimized activity of anaerobic methanogenic bacteria in locations experiencing varied temperatures throughout the year. Charts designed would provide handy information on the time interval for which the gases need to be introduced into the digester to maintain 37°C temperature within it by mathematical analysis. For every kilogram of digester slurry exhaust gases at 600°C are required to be introduced into the digester through boiler tubes of surface area 0.1 m<sup>2</sup> for 1.03 seconds for initially raising the digester's temperature to the set 37°C temperature, followed by a second gas introduction period of 0.0044 seconds to account for the heat lost to the outer digester surface and later for 0.0046 seconds every 7.6 seconds to compensate for the heat lost to the air outside the digester for the region of Faridabad in the month of January with a normal temperature of 14.3 °C. This exercise will provide help for the designing, engineering and commissioning of heating systems for varied sizes of biogas plants.

## INTRODUCTION

**KEY WORDS**  
Biogas, Digester,  
Microbial activity,  
Sustained,  
Temperature Control

Ministry of Power of The Government of India in its July 2016 report has confirmed the country's total installed electric power generation capacity as on 30 June 2016 at 303,118 MW. The contribution from Private Sector has been the highest at 41.45% of the total installed capacity followed by State Sector at 33.59% and Central Sector at 25.17%. In terms of fuel used; Thermal Power contributed 69.8% of the total installed capacity power, Hydro-14.1%, Renewable energy sources comprising small hydro projects, biomass gasifier, biomass power, urban and industrial waste power-14.1% and Nuclear-1.9%. Electricity Generation target has been set at 1178 Billion Unit for the year 2016-2017, 999 Billion Unit from Thermal Power, 134 Billion Unit from Hydro power, 40 Billion Unit from nuclear, and 5 Billion Units are imported from Bhutan. The deficit in energy availability was recorded as 2.1% in the year 2015 -16 while the peak demand deficit was recorded as 3.2%. The 2016-17 energy deficits stood at 0.9% till June 2016 with -2% deficits in the peak demand [1]. Government of India foresees a state with adequate electricity supply to its citizens by March 2019. "Power for All" scheme launched by the government aims to provide uninterrupted electric power to all residential and commercial establishments by improvising and creating necessary infrastructure [2] [3]. Several initiatives have been launched for the development of "Solar Cities" to cater to the growing demand of Electric energy in the country. Solar city projects based on renewable fuel resources like solar, small hydro, biomass, wind, waste to energy etc. and employment of energy efficiency techniques are primarily aimed to reduce at least 10% of the projected electric power demand from traditional energy resources in a targeted span of five years. Out of the 60 cities identified by the Ministry as potential Solar cities, the city of Faridabad from Haryana state figures among the 31 cities sanctioned approval to prepare a master plan for the same [4]. A Solar city would need to employ a variety of renewable energy resources decentralized at various locations depending on the availability of the resource to ensure 24 x 7 supply throughout the year. Small hydro needs availability of continuous flow of stream while wind farms need the availability of wind above a particular speed. Solar energy needs continuous supply of sunlight. The idea of distributed power either stand alone or grid integrated especially from biomass/organic waste could be looked upon as a viable solution to uninterrupted renewable energy electric power resource that could be relied upon throughout the year. Constant power from a biogas generator requires the flow of set volume of methane in biogas produced which depends on the type of substrate fed to it, its C/N ratio, the maintenance of constant temperature range, pH of the reactor environment, agitation of the digester contents, concentration of total solids (TS) in the influent, hydraulic retention time (HRT), type of system single stage or multistage etc. for which it is designed [5] [6] [7] [8] [9]. Provided these parameters are controlled, the country could boost of cheap electric supply throughout the year as the fuel powering this biogas power unlike before lies in every household's dustbin - organic kitchen waste.

Published: 20 October 2016

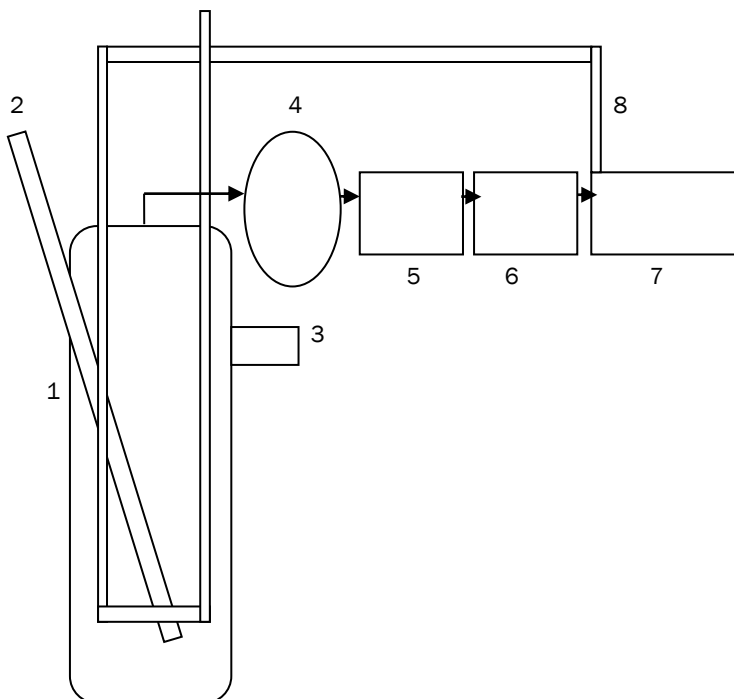
\*Corresponding Author  
Email:  
nina\_ahuja@rediffmail.com  
Tel.: +919650581155

Of all the factors affecting the yield of biogas temperature of the digester environment is the most important. The temperature of the region decides the group of *methanogenic bacteria* that shall be stimulated for production of methane. *Mesophilic* organisms are active in the 25°C to 40°C temperature range while *thermophilic* operate in the 45°C - 60°C temperature range and the *psychrophilic* bacteria operate below 25°C range [10]. Maintaining constant temperature within the digester helps in maintaining the sustainability of the respective bacterial environment and any temperature fluctuations can inactivate the bacteria resulting in reduced biogas production. Temperature control therefore becomes an important design criterion while designing anaerobic biogas digesters. Use of digester insulation, maintaining temperature in the digester via heat exchangers, heating elements, placing digesters inside a water bath, and injecting steam in the digester are some of the means of maintaining temperature of the digester in



its operating range [11] [12]. Temperature within the digester has also to be brought back to the maintained set point as soon as possible as it hinders the digestion process [13].

Energy from biomass is a hidden source of energy still largely untapped and unscientifically disposed by Municipal Corporation of Faridabad because of the huge amount of Municipal Solid waste generated every day and inadequate disposal methods and land unavailability. Distributed biomass treatment plants across the city either in the form of a community biogas plant or in the verandah of individual households to supply fuel to the kitchens or to biogas generators to produce electricity is the most viable solution to the clean and green environmental maintenance of the city. The hurdle to the continuous operation of biogas plants the world over especially in the developing and undeveloped countries lies in the inability to maintain stable biogas production from these digesters resulting in unacceptability of tapping this abundantly available resource. To sustain production of a constant methane throughput from such anaerobic digesters the health and vitality of the microorganism thriving in the digester environment that reduce its contents into biogas primarily the methane component need to be provided a stable environment both in terms of the substrate they are happy to feed on as well as the temperature and pH environment that aids to their increased activity [7] [14] [15]. Temperature control in this city is a constraint to the adaptability of this technology as the city lies in the northern hemisphere of the country and is exposed to extremes of temperature both during winters and summers. The idea exploited here is to reintroduce the hot exhaust gases emerging from biogas generators that produce electricity from biogas into the digester via boiler tubes that act as heat exchanger carrying heat from the exhaust gases to digester contents [Fig. 1].



1. Biogas Digester
2. Inlet pipe
3. Outlet pipe
4. Biogas Storage Balloon
5. H<sub>2</sub>S Removal Unit
6. Water Vapour Removal Unit
7. Biogas Generator
8. Exhaust gas pipeline to biogas digester with vent into the atmosphere.

→ Arrow shows direction of flow of biogas from biogas anaerobic digester to storage balloon and finally to the generator via a H<sub>2</sub>S removal unit and Water Vapour Removal Unit.

**Fig.1:** Schematic Diagram showing reintroduction of exhaust gas into the biogas digester from 100% biogas generator.

Biogas power plants essentially have a process of cleansing the biogas produced of its Hydrogen Sulfide component (trace amounts) and water vapour to avoid corrosion of metal parts [16]. Biogas electric plants particularly those employed at the community and/or household level are small alternators coupled to internal combustion engines.

In the absence of temperature control production of biogas would fall during winters. While 35 °C provides optimum activity temperature for *methanogenic bacterium*, increasing temperature up to 37°C temperatures reduces digestion time of substrate within the anaerobic digester. Biogas production rate falls with the further increase of temperature i.e. above 37°C [17].

During the otherwise warm months maintaining the temperature constant would boost the production of biogas as all living organisms in the universe operate best under steady state conditions. Changes in environment affect their activity. Maintaining temperature within the digester at 37°C throughout the year

shall be targeted as this temperature decreases substrate digestion time. Power output from a biogas generator depends directly on the volume of biogas injected into it. Biogas production on the other hand is a function of Volatile Solids present in the influent and the digestion efficiency. Volatile solids are expressed as percentage of Total Solids present in the influent. Assuming that 1m<sup>3</sup> of biogas generates 1 kWh of electricity; power produced by a 100% Biogas Generator for different temperature ranges have been formulated [18].

The generalized formula for power output from the generator during weather conditions when temperature is within 35 – 40°C which is an optimal range for *mesophilic* bacteria producing biogas under anaerobic conditions thus turns out as;

Power generated between 35-40°C temperature range = (%VS x %TS x input biomass in kg x digestion efficiency)/Biogas density x 10<sup>6</sup>

Every 10 degree drop in temperature decreases the biogas output yield by 50% [14]. Averaging it over 5 degree gives a drop in biogas production of 25%. Power generated within 30 to 35°C temperature range is thus formulated as;

Power generated within 30-35°C temperature range = (%VS x %TS x input biomass in kg x digestion efficiency) x 0.75/Biogas density x 10<sup>6</sup>.

F.R. Hawkes et al. reported that a decrease in temperature from 30°C to 20°C in laboratory scale experiment with a 9-12 day retention time for biogas production from mechanically separated cattle slurry resulted in reduction of biogas yield by 36 to 39% for every 5°C drop in temperature [19]. Assuming a 39% drop in biogas production within the [20 – 30] °C range for every 5°C drop in temperature the power generated can be arrived as;

Power generated within 25-30°C temperature range = [1-0.39] (%VS x %TS x input biomass in kg x digestion efficiency) x (0.75)/Biogas density x 10<sup>6</sup>

=0.61(%VS x %TS x input biomass in kg x digestion efficiency) x (0.75)/Biogas density x 10<sup>6</sup>

=0.46(%VS x %TS x input biomass in kg x digestion efficiency)/Biogas density x 10<sup>6</sup>

Power generated within 20-25°C temperature range = [1-0.39] x 0.46(%VS x %TS x input biomass in kg x digestion efficiency)/Biogas density x 10<sup>6</sup>

=0.28(%VS x %TS x input biomass in kg x digestion efficiency)/Biogas density x 10<sup>6</sup>

Power generated within 15-20°C temperature range = almost zero.

Based on the above formulae power generated by a 100% Biogas generator producing 1kWh of electric power every m<sup>3</sup> of biogas injected into it from a biogas digester per kg of kitchen waste throughout the year for the city of Faridabad is calculated and tabulated [Table1].The percentage of *Total Solids(TS)* in the feedstock is assumed as 10% of which 88% are composed of *Volatile Solids (VS)*. Efficiency of biogas production in the digester is assumed as 60% and biogas density is assumed as 1.227 kg/m<sup>3</sup> [7] [20] [21].

The normal temperature in Faridabad throughout the year is never in the optimal range of 35 – 37°C [Table 1].Temperature within the digester can be maintained at 37°C by passing hot exhaust gases from the generator through boiler tubes into the digester and vented out into the atmosphere. Heat transfer would follow the scheme shown in [Fig 2].

**Table 1:** Electric power generation potential /kg kitchen waste for the city of Faridabad, Haryana,India [22]

Month	Normal Temp in °C	Avg. Biogas Power kWe/day
January	14.3	0
February	16.8	0
March	22.3	0.012
April	28.8	0.02
May	32.5	0.032
June	33.4	0.032
July	30.8	0.032
August	30	0.032
September	29.5	0.02
October	26.3	0.02
November	20.8	0.012
December	15.7	0

Heat from the digester flows to the external surface of the digester via conduction because of the temperature gradient and is finally transferred to the air surrounding the digester which is continually replaced by cooler air. This warrants the need of passing the exhaust gases into the digester environment after specific intervals of time to maintain the targeted temperature within the digester.

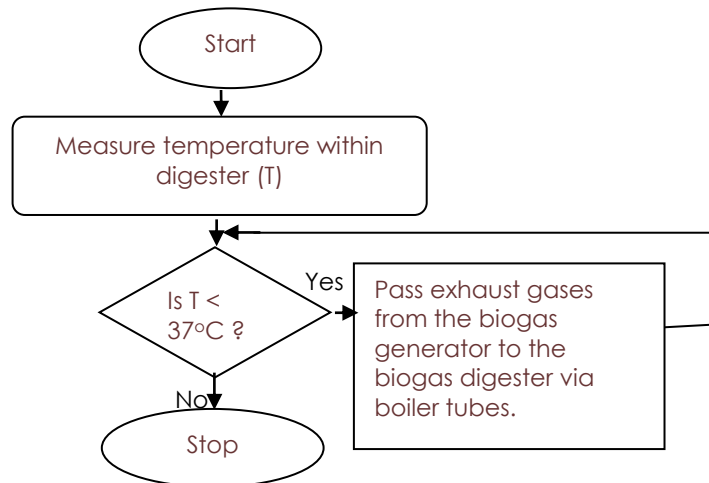


Fig.2: Heat transfer scheme in a biogas digester

## MATERIALS AND METHODS: MATHEMATICAL ANALYSIS

The objective was to maintain 37°C within the digester throughout the year to provide a stable environment to the microorganism population within the digester. Internal combustion engines coupled to alternators in 100% Biogas generators emanate exhaust gases at around 450-650°C [23].

Boiler tubes are excellent conductors of heat which can carry these exhaust gases into the digester. For this study the temperature of the exhaust gases is assumed as 600°C; the thermal conductivity of boiler tubes as 50 W/m °C [24] and its outer diameter as 31.75 mm (0.03 metres approximately) [25]. The transfer of heat energy from the exhaust gas carrying boiler tubes to the digester contents is via the process of conduction.

Surface Area of boiler tube walls per meter through which heat can be dissipated to the outer digester contents =  $2 \times \pi \times r \times h = \pi \times d \times h = 3.14 \times 0.03 \times 1 = 0.0942 \text{ m}^2$  (0.1 m<sup>2</sup> approx.). Heat dissipated through the boiler tubes through conduction per second during the month of January when the ambient temperature is 14.3°C = Thermal Conductivity of Boiler Tubes x Surface Area of boiler tube walls x (Exhaust gas temperature - Temperature of surrounding material) / diameter of boiler tubes

$$= 50 \times 0.0942 \times (600 - 14.3) / 0.03 = 91954.9 \text{ J/s} \text{ ----- (Eq. 1)}$$

Assuming 90% water content in the digester, the specific heat capacity of water is considered for calculating the heat absorbed by the digester contents.

Total heat that gets transferred to the digester contents = mass of digester material x specific heat capacity of digester contents x (Temperature required to operate the digester under *mesophilic* conditions - ambient temperature)

=  $1 \times 4186 \times (37 - 14.3) = 95022.2 \text{ J}$  per kilogram of digester contents. This is the heat required by the system to reach 37°C during the month of January.

Time required to transfer the required heat to raise the temperature of digester environment to 37°C = Heat required by the digester contents to raise their temperature to 37°C / Heat dissipated by the boiler tubes =  $95022.2 / 91954.9 = 1.03$  seconds.

A generalized Formula can be arrived at for determining the amount of time required to introduce the exhaust gases into the system reduces down to the following

Mass of Digester contents in kg x Specific Heat capacity of Digester contents x (Temperature to be maintained within the digester - Ambient Temperature) / Thermal Conductivity of boiler tube x surface area of boiler tube per metre x (exhaust gas temperature - Ambient Temperature) / diameter of boiler tube.

Time required to introduce the exhaust gases at 600°C into the digester with Total Solid content of 10% and boiler tube diameter of 0.03 m throughout the year reduces down to:

$$T = \{1 \times 4186 \times (37 - \text{Ambient Temperature})\} / \{50 \times 0.0942 \times (600 - \text{Ambient Temperature}) / 0.03\}$$

$$= 26.7 (37 - \text{Ambient Temperature}) / (600 - \text{Ambient Temperature})$$

Based on the above Formula time required in seconds to pass the exhaust gases per meter of boiler tube having a diameter 0.03 metres to raise the temperature of 1 kilogram of digester contents is calculated [Table 2].

Temperature within the digester is higher than the ambient. This will result in flow of heat from the digester walls to the air outside. The air outside shall be continuously replaced by convection. The next series of calculations are aimed at calculating the drop in temperature from the targeted 37°C within the digester and the amount of time to reintroduce the hot exhaust gases to bring back the desired temperature within the digester.

**Table 2:** Exposure of exhaust gases for raising temperature within the digester to 37°C

Month	Average Temperature in °C	Gas Introduction in seconds
January	14.3	1.03
February	16.8	0.924
March	22.3	0.679
April	28.8	0.38
May	32.5	0.212
June	33.4	0.169
July	30.8	0.291
August	30	0.328
September	29.5	0.351
October	26.3	0.498
November	20.8	0.747
December	15.7	0.973

For the determination of the amount of heat lost to the outer surface of the digester and eventually to the air outside the following assumptions are taken into account:

Thickness of walls of the digester: 50 mm=5 cm=0.05 m

Thermal Conductivity of Water Tank material =  $k = 0.19W/mK$  [26]

A PVC tank of diameter = 1 metre and height = 1 metre

Surface area of this tank =  $2\pi r^2 + 2\pi rh = 2 \times \pi \times r \times (r + h) = 2 \times 3.14 \times 0.5 \times (0.5+1) = 4.71 m^2$

Heat dissipation through the digester to its outer surface which is at ambient temperature takes place via conduction and is given by the formula: Thermal Conductivity of PVC digester x Surface Area of Biogas Digester (Temperature inside Digester - Ambient Temperature) / Thickness of digester

=  $0.19 \times 4.71 \times (37-14.3)/0.05 = 406.28 W=406.28 J/s$  for the month of January ----- (Eq. 2)

Heat dissipated through the boiler tubes through conduction per second during the month of January when the ambient temperature is 14.3°C = 91954.9 J (From Eq.1)

To compensate for 406.28 J (Eq. 2 ) lost to the digester's outer surface per second the time the exhaust gases need to be reintroduced into the digester =  $1 \times 406.28/91954.9 = 0.0044$  seconds.

This states that to keep the digester maintained at 37°C, the exhaust gas at 600°C needs to be supplied for additional 0.0044 seconds to account for the heat transferred to the external surface of digester.

The general formula for determination of time for reintroduction of exhaust gas into the digester is arrived as;

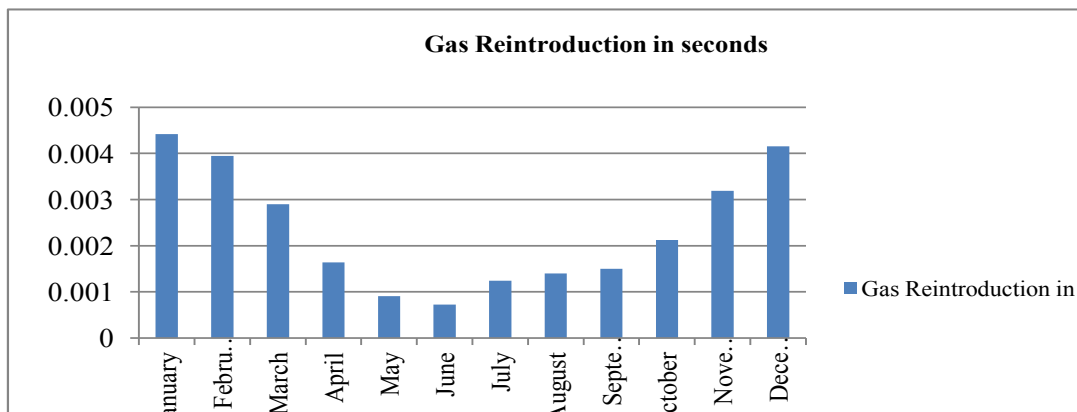
(Thermal Conductivity of digester material x Surface Area of Biogas Digester (Temperature inside Digester - Ambient Temperature)) / Thickness of digester/ {Thermal Conductivity of Boiler Tubes x Surface Area of boiler tube walls x (Exhaust gas temperature-Temperature of surrounding material)/diameter of boiler tubes}

=  $\{0.19 \times \text{Surface Area of Biogas Digester (Temperature inside Digester - Ambient Temperature)} / \text{Thickness of digester}\} / \{\text{Thermal Conductivity of Boiler Tubes} \times \text{Surface Area of boiler tube walls} \times (\text{Exhaust gas temperature-Temperature of surrounding material})/\text{diameter of boiler tubes}\}$

With surface area and thickness of the biogas digester as 4.71 m<sup>2</sup> and 0.05metres respectively, the thermal conductivity of boiler tubes as 50W/m°C, exhaust gas temperature as 600°C, diameter of boiler tubes as 0.03 metres and surface area of boiler tubes as 0.0942 metres, the general formula for gas reintroduction reduces down to:

$0.114 (37- \text{Ambient Temperature})/(600-\text{Ambient Temperature})$

The span of time that the exhaust gas at 600°C should be introduced for an extra time to compensate for the heat lost due to conduction across the digester walls for the entire year to maintain a temperature of 37°C inside the digester is plotted [Fig. 3].



**Fig. 3:** Second introduction of exhaust gases into the digester

The air surrounding the digester is in direct contact with the digester's outer surface. However the specific heat capacity of air is 0.025 W/mK which is 7.6 times lower than that of PVC Biogas Digester. It will take 7.6 seconds to dissipate the 406.28 Joules of energy transferred to the outer digester surface from the internal digester environment to the surrounding medium i.e air.

The amount of heat energy required to raise the temperature within the digester by 1°C per kg of digester contents = Mass of Digester contents x Specific Heat capacity of water x (Temperature maintained within the digester – Temperature lower than that maintained by 1°C.)

$$= 1 \times 4186 \times (37-36) = 4186 \text{ J} \text{----- (Eq.3)}$$

This is the energy required by the digester contents to raise the temperature within the digester by 1°C.

In one second 406.28 J has passed to outer surface of digester as derived in Eq.2

And the energy required to raise the temperature of digester contents by 1°C = 4186 Joules (Eq. 3)

Drop in temperature resulting because of the loss of 406.28 J of heat energy to the surroundings is therefore given as  $406.28 \times 1/4186 = 0.097^\circ\text{C}$  drop in 7.6 seconds. The new temperature of the digester decreases down to  $36.903^\circ\text{C}$ . In order to maintain a stable  $37^\circ\text{C}$  environment within the digester the lost heat 406.28 J needs to be compensated for. The heat flow from the exhaust gas to the digester content after temperature has dropped down to  $36.903^\circ\text{C}$  is calculated below:

Energy required to raise the temperature of the digester contents by  $0.097^\circ\text{C}$

$$= 4186 \times 0.097 = 406.042 \text{ J} \text{----- (Eq.4)}$$

Amount of heat that will be transferred across the boiler tubes carrying exhaust gases to the digester contents after temperature within the digester has dropped down to  $36.903^\circ\text{C} = 50 \times 0.0942(600-36.903)/0.03 = 88406.229 \text{ J / second}$

Time for which the exhaust gases need to be passed for 406.042 J of heat energy to be conducted across the boiler tubes to raise the temperature of the digester environment by  $0.097^\circ\text{C} = 406.042/88406.229 = 0.00459$  seconds

For the month of January exhaust gas at  $600^\circ\text{C}$  needs to be sent into the digester via boiler tubes for a period of 1.03 seconds per Kg of digester contents to bring up the temperature of the digester to  $37^\circ\text{C}$ . An extra 0.44 seconds of reintroduction of exhaust gasses would be warranted to account for the heat lost by conduction from the internal digester environment to the external digester walls. This heat is transferred consecutively to the air outside the digester every 7.6 seconds. Therefore heat needs to be again introduced into the system every 7.6 seconds by introducing the exhaust gases at  $600^\circ\text{C}$  for 0.00459 seconds. Thereafter, this cycle of replenishing the lost heat shall be repeated after every 7.6 seconds.

A general formula devised for maintaining  $37^\circ\text{C}$  environment within the digester is:

Heat dissipation from internal digester environment to digester surface = Thermal Conductivity of PVC digester x Surface Area of Biogas Digester x (Temperature inside Digester - Ambient Temperature) / Thickness of digester

$$= 0.19 \times 4.71 \times (37-\text{Ambient Temperature})/0.05 = 1.7898(37-\text{Ambient Temperature})$$

Drop in internal temperature within the digester = Heat dissipation from internal digester environment to digester surface / Amount of heat energy required to raise the temperature within the digester by  $1^\circ\text{C}$  per kg of digester contents =  $1.7898(37-\text{Ambient Temperature})/4186$

$$= 0.000428(37-\text{Ambient Temperature})$$

New Temperature within Digester =  $37 - 0.000428(37-\text{Ambient Temperature})$

Reintroduction of exhaust gas for temperature maintenance due to heat lost to atmosphere every 7.6 seconds = Amount of heat energy required to raise the temperature within the digester by  $1^\circ\text{C}$  per kg of digester contents x Drop in internal temperature within the digester / Heat dissipated through the boiler tubes through conduction per second after temperature drop in digester

$$= 4186 \times \text{Drop in internal temperature} / 157(600 - \text{New Temperature within Digester})$$

$$= 26.66 \times \text{Drop in internal temperature} / (600 - \text{New Temperature within Digester})$$

The calculated values based on the derived formulae for the reintroduction of exhaust gases into the digester to compensate for heat transfer to the atmosphere every 7.6 seconds is tabulated [Table 3].

**Table 3:** Extra time in seconds required for exhaust gas to be introduced into the digester to compensate for heat transfer to the atmosphere every 7.6 seconds

Month	Normal Temperature in ° C.	Energy requirement in Joules	Drop in temperature in ° C.	Dropped Temperature within digester in °C	Time of reintroduction of exhaust gas in seconds
January	14.3	406.28	0.097	36.903	0.0045925
February	16.8	361.54	0.086	36.914	0.0040718
March	22.3	263.10	0.063	36.937	0.0029830
April	28.8	146.76	0.099	36.01	0.0047095
May	32.5	80.54	0.019	36.981	0.0008997
June	33.4	64.43	0.015	36.985	0.0007103
July	30.8	110.97	0.026	36.974	0.0012311
August	30	125.29	0.030	36.7	0.0014199
September	29.5	134.24	0.032	36.68	0.0151445
October	26.3	191.51	0.046	36.95	0.0021781
November	20.8	289.95	0.069	36.93	0.0032670
December	15.7	381.23	0.091	36.91	0.0043085



## RESULTS

Power output from a biogas generator falls down to 0 kilowatts during the cold months of December January and February for the region of Faridabad [Table 1] when the temperature is in the range of [14-17]°C. November and March which are less cooler than December to February with temperature in the range of [20 - 23]°C, the average biogas power improves to 0.12 kWe/day per kilogram of bio waste fed to the anaerobic digester. Still warmer months of September, October and April with a temperature range of 26 to 30°C a further improvement in biogas power can be obtained at 0.2 kWe/day for every 1 kg of organic feedstock fed to it. The four consecutive months from May to August with a temperature in the range of 30 - 34°C provide a calculated power output of 0.032 kWe /day per kilogram of bio waste particularly kitchen waste.

Exhaust gases at 600°C passed through the boiler tubes of diameter 0.03 metres and height 1 metre (or boiler tubes of surface area 0.1 m<sup>2</sup> approximately) for 1.03 seconds help to raise the temperature within the digester for every kilogram of digester contents to 37°C during the month of January when the normal temperature is around 14.3°C. An additional inflow for 0.00441830 seconds of the exhaust gases per kg of the digester contents through the specified boiler tubes would be required in the month of January to account for the heat lost to the digester's outer surface due to conduction. Every 7.6 seconds exhaust gases would be needed to be introduced into the digester for 0.0045925 seconds per kg digester contents to account for the heat lost to the air. December and February are a little less cooler than January and the time of introduction of exhaust gases for raising digester's internal temperature to 37°C, for heat lost to the digester's outer surface and finally to the atmosphere are lower than that required in the month of January at 0.973, 0.00415574, 0.00430848 and at 0.924, 0.00394856, 0.0040718 seconds respectively. November and March with a higher average temperature within [20-23]°C have further lower gas introduction times of 0.747, 0.00318854, 0.00326698 and 0.679, 0.00290081, 0.0029830 for raising temperature to 37°C, for heat lost to the digester outer surface and finally to the atmosphere respectively per kilogram of digester contents. October, April and September months within the temperature range of 26 to 30°C the respective timings for gas introduction for raising internal temperature of digester to 37°C heat lost to the digester outer surface and finally to the atmosphere every 7.6 seconds would amount to; 0.498, 0.00212620, 0.00217807; 0.38, 0.00163656, 0.0047095 and 0.351, 0.00149869, 0.01514450; gas introduction times decreasing with the increase in ambient temperature. The months of May, June, July and August which exhibit temperatures within [30-34] °C exhibit the corresponding values of gas introduction for raising internal temperature of digester to 37°C heat lost to the digester outer surface and finally to the atmosphere at 0.212, 0.00090396, 0.0008997; 0.169, 0.00072432, 0.0007103; 0.291, 0.00124174, 0.00123113 and 0.328, 0.00140000, 0.00141985 seconds per kg of digester contents respectively.

This exercise provides a guideline to design heating system for the anaerobic digester and its associated valve opening and close timings. An anaerobic biogas digester treating 100 kg of bio waste per day with a 20 day retention time would have an accumulated content of 20 x 100 = 2000 kg. To maintain the requisite 37°C temperature within the digester would require the exhaust gases to be introduced for 2000 x 1.03 seconds (= 2060 seconds = 34.3 minutes) through boiler tubes with surface area of 0.1 m<sup>2</sup> approximately. An additional inflow for 200 x 0.00441830 seconds (= 0.88366 seconds) of the exhaust gases per kg of the digester contents through the specified boiler tubes would be required in the month of January to account for the heat lost to the digester's outer surface due to conduction. Every 7.6 seconds exhaust gases would be needed to be introduced into the digester for 200 x 0.0045925 seconds (= 0.9185 seconds) per kg digester contents to account or the heat lost to the air.

## CONCLUSION

The proper maintenance of temperature without fluctuations would result in the flourishing of microorganisms within the digester. Exploiting the energy released as heat in the exhaust gases of a 100% Biogas Generator for maintaining the temperature is a practically feasible approach requiring the operation of a properly timed valve leading to the entry of exhaust gases into the digester. A portion of the heat could also be utilized by a Combined Heat and Power system wherein steam could be generated to run a turbine and generate power on a larger scale. In the smaller version the heat could be used to heat water and warm buildings or houses or even cook food by placing the food in a hot water jacket. The purpose of this exercise is to provide a guideline for the development of prototypes and commissioning of biogas power plants using exhaust gas heat as a source for maintaining requisite temperatures within the biogas digester. The per unit value calculations could serve as a tool for the design and development of the biogas digester heating system for any sized biogas plant.

### CONFLICT OF INTEREST

None amongst the authors.

### ACKNOWLEDGEMENTS

Manav Rachna International University, Faridabad; Alfalah University, Faridabad

FINANCIAL DISCLOSURE  
No financial support was received.

## REFERENCES

- [1] Government of India, Ministry of Power, "Power Sector at a Glance All India, Available [Online]: <http://powermin.nic.in/en/content/power-sector-glance-all-india>
- [2] Wikipedia, "Electricity sector in India," Available [Online]: [https://en.wikipedia.org/wiki/Electricity\\_sector\\_in\\_India](https://en.wikipedia.org/wiki/Electricity_sector_in_India)
- [3] The Economic Times, "States resolve to provide 24x7 power to everyone by March 2019," Available [Online]: <http://economictimes.indiatimes.com/industry/energy/power/states-resolve-to-provide-24x7-power-to-everyone-by-march-2019/articleshow/52802534.cms>
- [4] Government of India, Ministry of New and Renewable Energy Resources, "Solar/Green Cities," Available [Online]: <http://mnre.gov.in/schemes/decentralized-systems/solar-cities/>
- [5] S Mohan, BK Bindhu, [2008] Effect of phase separation on anaerobic digestion of kitchen waste, *Journal of Environmental Engineering and Science*, 7(2): 91-103, 10.1139/S07-039 [Online] Available: <http://www.nrcresearchpress.com/doi/abs/10.1139/S07-039>
- [6] A R Tembhurkar, V A Mhaisalkar, Studies on Hydrolysis and acidogenesis of Kitchen waste in Two Phase Anaerobic Digestion," *Journal of the IPHE ,India*, 2007-08( 2) [Online] Available: <http://re.indiaenvironmentportal.org.in/files/Kitchen%20waste.pdf>
- [7] Neena Ahuja, Dipali Bansal, Khwaja M Rafi. [2016] "Compacting Biogas Digester for Installation in the Backyard," *International Journal of Applied Engineering Research* ISSN 0973-4562, 11( 9):6219-6226 © Research India Publications [Online] Available: [http://www.ripublication.com/ijaer16/ijaerv11n9\\_25.pdf](http://www.ripublication.com/ijaer16/ijaerv11n9_25.pdf)
- [8] IJ Dioha, CH Ikeme, T Nafi'u, NI Soba and Yusuf MBS.[ 2013] Effect of Carbon to Nitrogen Ratio on Biogas Production," *International Research Journal of Natural Sciences* , 1 ( 3), European Centre for Research Training and Development UK, September pp.1-10, [Online] Available: <http://www.eajournals.org/wp-content/uploads/EFFECT-OF-CARBON-TO-NITROGEN-RATIO-ON-BIOGAS-PRODUCTION.pdf>,
- [9] Musa I. Tanimu, Tinia I. Mohd Ghazi, Razif M. Harun, and Azni Idris, "Effect of Carbon to Nitrogen Ratio of Food Waste on Biogas Methane Production in a Batch Mesophilic Anaerobic Digester," *International Journal of Innovation, Management and Technology*, Vol. 5, No. 2, April 2014, [Online] Available: <http://www.ijimt.org/papers/497-H1008.pdf>
- [10] Ramansu Goswami, Pritam Chattopadhyay, Arunima Shome, Sambhu Nath Banerjee, Amit Kumar Chakraborty, Anil K. Mathew, Shibani Chaudhury," An overview of physico-chemical mechanisms of biogas production by microbial communities: a step towards sustainable waste management," *3 Biotech*. 2016 Dec; 6(1): 72., Published online 2016 Feb 16. DOI: 10.1007/s13205-016-0395-9, [Online] Available: <http://www.ncbi.nlm.nih.gov/pmc/articles/PMC4755961/>
- [11] EnergyPedia, "Digester Heating," [Online] Available: [https://energypedia.info/wiki/Digester\\_Heating](https://energypedia.info/wiki/Digester_Heating)
- [12] "Waste Digester Design Instructor Materials," *Hand On Educational Activities From NSF Succeed Work*, [Online] Available: <https://sites.google.com/a/ncsu.edu/civil-freshman-activities/waste-digester-design/waste-digester-design-instructor-materials>
- [13] Aquafix, "Anaerobic Digester Upset & Troubleshooting," [Online] Available: <https://teamaquafix.com/anaerobic-digester-upset-troubleshooting/>
- [14] Nehru National Urban Renewal Mission, "Faridabad City Development Plan –Appraisal Report," [Online] Available: [http://jnnurm.nic.in/wpcontent/uploads/2010/12/Faridabad\\_CEPT.pdf](http://jnnurm.nic.in/wpcontent/uploads/2010/12/Faridabad_CEPT.pdf)
- [15] Municipal Corporation Faridabad, "Solid Waste Management," [Online] Available: <https://www.mcfbd.com/solid-waste-management>
- [16] extension, "Biogas Utilization and Cleanup," [Online] Available: <http://articles.extension.org/pages/30312/biogas-utilization-and-cleanup>
- [17] Adrian Eugen Ciobla, Ioana Ionel, Gabriela-Alina Dumitrel and Francisc Popescu," Comparative study on factors affecting anaerobic digestion of agricultural vegetal residues," *Biotechnology for Biofuels* 2012, DOI: 10.1186/1754-6834-5-39, [Online] Available: <https://biotechnologyforbiofuels.biomedcentral.com/articles/10.1186/1754-6834-5-39>
- [18] Charles Banks, "Optimizing Anaerobic Digestion," [Online] Available: <http://www.kingdombio.com/Optimizing%20anaerobic%20digestion.pdf>
- [19] Hawkes FR Rosser, BL Hawkes, DL Statham M "Mesophilic anaerobic digestion of cattle slurry after passage through a mechanical separator: factors affecting gas yield". *Agricultural Wastes* 1984 Vol.10 No.4 pp.241-256 ref.14, [Online] Available: <https://www.cabdirect.org/cabdirect/abstract/19842422074>
- [20] David House, "The Complete Biogas Handbook," ISBN 0-915238-47-0
- [21] New World Encyclopedia, "Density," [Online] Available: <http://www.newworldencyclopedia.org/entry/Density>
- [22] Weather statistics for Faridabad, Haryana (India), [Online] Available: <https://www.yr.no/place/India/Haryana/Faridabad/statistics.html>
- [23] Wikipedia, "Combined cycle," [Online] Available: [https://en.wikipedia.org/wiki/Combined\\_cycle](https://en.wikipedia.org/wiki/Combined_cycle)
- [24] Albrecht Kaupp, "The Soot and Scale Problems," pp 7 , [Online ] Available: [http://heating.danfoss.com/PCMPDF/BC\\_Kaupp\\_report\\_VFGIA102.pdf](http://heating.danfoss.com/PCMPDF/BC_Kaupp_report_VFGIA102.pdf)
- [25] Plymouth Tube Company, "Carbon & Alloy Tubing", [Online ] Available: <http://www.plymouth.com/media/8896/Boiler%20Tubing%20Info%20Sheet.pdf>
- [26] The Engineering Toolbox, "Thermal Conductivity of some common Materials and Gases," [Online ] Available: [http://www.engineeringtoolbox.com/thermal-conductivity-d\\_429.html](http://www.engineeringtoolbox.com/thermal-conductivity-d_429.html)

ARTICLE

STATE ESTIMATION OF PERMANENT MAGNET SYNCHRONOUS MOTOR DRIVE USING NON-LINEAR FULL ORDER OBSERVER

Ramana Pilla<sup>1\*</sup>, Alice Mary Karlapudy<sup>2</sup>, Surya Kalavathi Munagala<sup>3</sup>

<sup>1</sup>Department of EEE, GMR Institute of Technology, Rajam, Andhra Pradesh, INDIA

<sup>2</sup>Department of EEE, Gudlavalleru Engineering College, Gudlavalleru, Andhra Pradesh, INDIA

<sup>3</sup>Department of EEE, JNTUH College of Engineering, Hyderabad, Telangana, INDIA

ABSTRACT

This paper presents stability analysis, robust control and estimation of damper winding currents for a non-salient pole permanent magnet synchronous motor (PMSM). The proposed work combines State feedback Controller (SFC) with a Non-linear Full order Observer (NFO) based on rotor reference frame model. The inputs to the observer are motor voltages, currents and speed. The proposed observer estimates all the four states such as damper winding currents ( $i_{dr}$  &  $i_{qr}$ ) as well as stator winding currents ( $i_{ds}$  &  $i_{qs}$ ) of PMSM with fair amount of accuracy. In addition to this, a state feedback controller is designed in order to control the system performance. To provide stability, a pole placement technique is used in order to shift all poles to the left half of the s-plane. The speed and position of the rotor are estimated using an encoder. By providing all these, permits the successful design of control system, which is able to maintain stability and robustness in spite of uncertainties in system dynamics and parameter imperfections.

INTRODUCTION

KEY WORDS

Non-linear controller, Non-linear full order observer, Permanent Magnet synchronous Motor, PI controller,

In drive mechanism, the electrical machine plays a vital role. Nowadays, DC motors are of minor importance, since recent advances in power semiconductor and microprocessor technology increased the relevance of Induction and Electrically Commutated (EC) Motors for electrical drives. The EC motor like PMSM can be controlled by power electronics together with a pole position sensor and works like a DC machine. In Induction Motor (IM), the stator current contains magnetizing as well as torque producing components, whereas in PMSM due to the usage of permanent magnets on rotor magnetizing current component is absent, therefore the stator current provides only torque producing component [1]. Due to this, the PMSM can be operated at high power factor. PMSM drives are used in robotics, machine tools, pumps, ventilators, compressors etc. due to various features like good dynamic performance, easy controllability, high torque to inertia ratio, high efficiency and improved power factor [2].

In this paper, PMSM with damper windings is provided in order to damp out natural frequency of oscillations. The existence of inverse-field under transient conditions is compensated by counteracting magneto motive force of damper currents, but these currents are immeasurable. Due to this, the damper winding currents are to be estimated with fair amount of accuracy. To get stability and control, SFC [3] is designed based on a linear state feedback control [4] law and the closed loop stability is obtained using pole placement technique. In order to implement SFC, the knowledge of all the states is needed. For this purpose a non-linear full order observer [5 - 7] is designed to estimate both accessible and inaccessible states.

MODELING OF PMSM

The advantage of modelling of any machine is to limit the complexity of calculations for machine with non-constant mutual inductances and also it decouples the stator and rotor windings in order to control independently [8] [9]. For modelling of any machine, two kinds of transformation are required i.e., a 3-phase to 2-phase transformation and stationary to arbitrary rotating coordinate system [2]. The transient behaviour of a high-performance vector controlled PMSM drive is obtained using d-q model of the PMSM. The modelling of PMSM is done in rotor reference frame model, since this model is useful to control the switching elements and power on the rotor side.

The modelling equations of PMSM in rotor reference frame are given as below:

$$v_{qs} = r_a i_{qs} + l_{qs} p i_{qs} + l_{aq} p i_{qr} + \omega_r l_{ds} i_{ds} + \omega_r l_{ad} i_{dr} \tag{1}$$

$$v_{ds} = r_a i_{ds} + l_{ds} p i_{ds} + l_{ad} p i_{dr} - \omega_r l_{qs} i_{qs} - \omega_r l_{aq} i_{qr} \tag{2}$$

$$v_{dr} = r_{dr} i_{dr} + l_{dr} p i_{dr} + l_{ad} p i_{ds} \tag{3}$$

$$v_{qr} = r_{qr} i_{qr} + l_{qr} p i_{qr} + l_{aq} p i_{qs} \tag{4}$$

The electrical torque developed is,

\*Corresponding Author

Email: pramana.gmrif@gmail.com, ramana.pilla@gmit.org  
Tel.: +91-9491569956  
Fax: +91-08941251591

$$T_e = \frac{3}{2} \times \frac{P}{2} [(l_{ad} - l_{aq})i_{ds}i_{qs} + l_{ad}i_{qs}i_{dr} - l_{aq}i_{qr}i_{ds}] \quad (5)$$

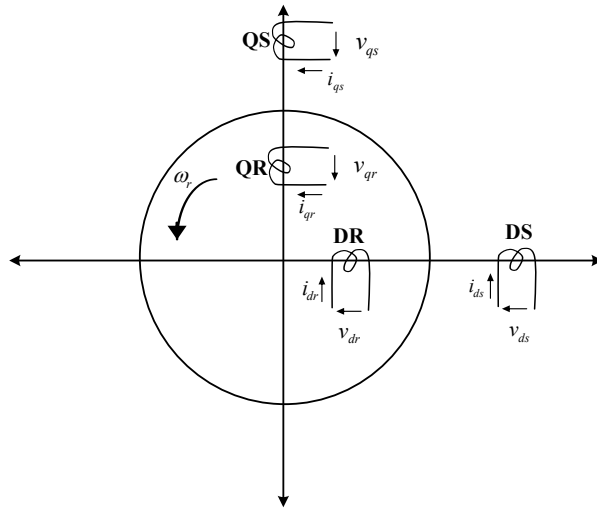


Fig: 1. Schematic of PMSM with damper windings

And the torque balance equation for no. of poles, P=4 is taken as

$$p\omega_r = \frac{2}{J} [T_e - T_l - \frac{B\omega_r}{2}] \quad (6)$$

$$\begin{bmatrix} v_{qs} \\ v_{ds} \\ v_{qr} \\ v_{dr} \end{bmatrix} = \begin{bmatrix} r_a + l_{qs}p & \omega_r l_{ds} & l_{aq}p & \omega_r l_{ad} \\ -\omega_r l_{qs} & r_a + l_{ds}p & -\omega_r l_{aq} & l_{ad}p \\ l_{aq}p & 0 & r_{qr} + l_{qr}p & 0 \\ 0 & l_{ad}p & 0 & r_{dr} + l_{dr}p \end{bmatrix} \begin{bmatrix} i_{qs} \\ i_{ds} \\ i_{qr} \\ i_{dr} \end{bmatrix} \quad (7)$$

$$\begin{bmatrix} l_{qs} & 0 & l_{aq} & 0 \\ 0 & l_{ds} & 0 & l_{ad} \\ l_{aq} & 0 & l_{qr} & 0 \\ 0 & l_{ad} & 0 & l_{dr} \end{bmatrix} \begin{bmatrix} pi_{qs} \\ pi_{ds} \\ pi_{qr} \\ pi_{dr} \end{bmatrix} = \begin{bmatrix} r_a & \omega_r l_{ds} & 0 & \omega_r l_{ad} \\ -\omega_r l_{qs} & r_a & -\omega_r l_{aq} & 0 \\ 0 & 0 & r_{qr} & 0 \\ 0 & 0 & 0 & r_{dr} \end{bmatrix} \begin{bmatrix} i_{qs} \\ i_{ds} \\ i_{qr} \\ i_{dr} \end{bmatrix} + \begin{bmatrix} v_{qs} \\ v_{ds} \\ v_{qr} \\ v_{dr} \end{bmatrix} \quad (8)$$

Thus, above equation can be written in the form of,

$$A_y \dot{x} = A_x x + B_x u \quad (9)$$

or it will be modified as,

$$\dot{x} = Ax + Bu \quad (10)$$

with  $A = (A_y^{-1} A_x)$  &  $B = (A_y^{-1} B_x)$

Where

$$A_x = \begin{bmatrix} r_a & \omega_r l_{ds} & 0 & \omega_r l_{ad} \\ -\omega_r l_{qs} & r_a & -\omega_r l_{aq} & 0 \\ 0 & 0 & r_{qr} & 0 \\ 0 & 0 & 0 & r_{dr} \end{bmatrix} \quad (11)$$

$$A_y = \begin{bmatrix} l_{qs} & 0 & l_{aq} & 0 \\ 0 & l_{ds} & 0 & l_{ad} \\ l_{aq} & 0 & l_{qr} & 0 \\ 0 & l_{ad} & 0 & l_{dr} \end{bmatrix} \quad (12)$$

$$x = [i_{qs} \quad i_{ds} \quad i_{qr} \quad i_{dr}]^T \quad (13)$$

$$B_x = \begin{bmatrix} 1 & 0 \\ 0 & 1 \\ 0 & 0 \\ 0 & 0 \end{bmatrix} \quad (14)$$

## DESIGN OF A NON-LINEAR FULL ORDER OBSERVER

Development of a high performance controller-observer needs an accurate estimation of machine states. So far, numerous methods have been presented [10-14] to estimate the states of synchronous machine. Out of all, observers are desirable, which augment or replace sensors in a control system. An Observer [10] can be defined as an algorithm that produces observed signals from the sensed signals with the knowledge of the control system. These signals are accurate, less expensive and more reliable than sensed signals. In PMSM, four states such as stator and damper winding currents have to be estimated to implement SFC. For this purpose, a NFO [15-17] is designed. The design of NFO is as follows:

The system equations of PMSM in state space form

$$\dot{x} = Ax + Bu \quad (15)$$

$$y = Cx \quad (16)$$

Let a new vector  $\zeta$  of dimension 'n' (n=no. of states) be defined as,

$$\zeta = Lx \quad (17)$$

where L = transformation matrix and the dimension of 'x' is 4x1 as it associated with  $i_{qs}$ ,  $i_{ds}$ ,  $i_{qr}$  and  $i_{dr}$  vectors, ' $\zeta$ ' will be 4x1 as it has to estimate all the four states and the dimension of 'L' will be 4x4. Then, the equations (16) and (17) can be combined as,

$$\begin{bmatrix} y \\ \hat{\zeta} \end{bmatrix} = \begin{bmatrix} C \\ L \end{bmatrix} x \quad (18)$$

From the above equation, the estimated states  $\hat{x}$  can be written as,

$$\hat{x} = \begin{bmatrix} C \\ L \end{bmatrix}^{-1} \begin{bmatrix} y \\ \hat{\zeta} \end{bmatrix} \quad (19)$$

A full order observer [7] can be represented by,

$$\dot{\hat{\zeta}} = D\hat{\zeta} + Gu + Fy \quad (20)$$

Here, F to be chosen as

$$F = F_1 + (\omega_r - \omega_d)F_2 \quad (21)$$

The nonlinearity of observer can be cancelled by choosing the matrix  $F_2$  as

$$F_2 = L(A_y^{-1})F_3 \quad (22)$$

Here, the design constant  $\omega_d$  can be chosen as the average operating speed; resulting the non-linear term magnitude remains small. Now, the matrix  $F_3$  is chosen as,

$$F_3 = \begin{bmatrix} 0 & -l_{ds} \\ l_{qs} & 0 \\ 0 & 0 \\ 0 & 0 \end{bmatrix} \quad (23)$$

Differentiating equation (17) and using equations (20) and (15), the error in the estimate of  $\zeta$  can be given as,

$$\dot{\tilde{\zeta}} = \dot{\hat{\zeta}} - \dot{\zeta} = D\hat{\zeta} + (G - LB)u + [F_1C + (\omega_r - \omega_{d2})F_2C - L(A_1 + \omega_{d2}A_2) - (\omega_r - \omega_{d2})LA_2]x \quad (24)$$

For an accurate estimate of  $\zeta$

$$\tilde{\zeta} \rightarrow 0 \text{ or } \hat{\zeta} \rightarrow \zeta, \text{ as } t \rightarrow \infty$$

In the above equation (24), the effect of 'u' can be eliminated by choosing

$$G = LB \quad (25)$$

Substituting equations (21) and (25) in equation (24) and rearranging,

$$\dot{\tilde{\zeta}} = D(\hat{\zeta} - \zeta) - [LA_d - F_1C - DL + (\omega_r - \omega_{d2})L(A_2 - A_y^{-1}F_3C)]x \quad (26)$$

For the error estimation of  $\zeta$ ,  $\tilde{\zeta} = \hat{\zeta} - \zeta$  to decay,

$$(i) L(A_2 - A_y^{-1}F_3C) = 0 \quad (27)$$

$$(ii) LA_d - F_1C - DL = 0 \quad (28)$$

(iii) D should be a stable matrix such that

$$\{\lambda_i\}_D \neq \{\lambda_i\}_A \quad (29)$$

The matrices D, L and  $F_1$  can selected using the above three conditions. To satisfy condition (i), the matrix L is chosen as

$$L = \begin{bmatrix} l_{11} & l_{12} & l_{13} & l_{14} \\ l_{21} & l_{22} & l_{23} & l_{24} \\ l_{31} & l_{32} & l_{33} & l_{34} \\ l_{41} & l_{42} & l_{43} & l_{44} \end{bmatrix} \quad (30)$$



Where, one possible solution is given as

$$\begin{aligned}
 l_{11} &= \frac{\Delta_1}{r_a l_{qr}}, & l_{12} &= \frac{\Delta_2}{\omega_{d2} l_{qs} l_{dr}}, & l_{13} &= \frac{\Delta_1}{r_a l_{aq}}, & l_{14} &= \frac{\Delta_2}{\omega_{d2} l_{qs} l_{ad}} \\
 l_{21} &= \frac{\Delta_1}{\omega_{d2} l_{ds} l_{qr}}, & l_{22} &= \frac{\Delta_2}{r_a l_{dr}}, & l_{23} &= \frac{\Delta_1}{\omega_{d2} l_{aq} l_{ds}}, & l_{24} &= \frac{\Delta_2}{r_a l_{ad}} \\
 l_{31} &= \frac{\Delta_1}{r_{qr} l_{aq} l_{qs} l_{qr}}, & l_{32} &= \frac{\Delta_2}{\omega_{d2} l_{aq} l_{dr}}, & l_{33} &= \frac{\Delta_1}{r_{qr} l_{aq} l_{qs}}, & l_{34} &= \frac{\Delta_2}{\omega_{d2} l_{aq} l_{ad}} \\
 l_{41} &= \frac{\Delta_1}{\omega_{d2} l_{ad} l_{qr}}, & l_{42} &= \frac{\Delta_2}{r_{dr} l_{ad} l_{ds} l_{dr}}, & l_{43} &= \frac{\Delta_1}{\omega_{d2} l_{ad} l_{aq}}, & l_{44} &= \frac{\Delta_2}{r_{dr} l_{ad} l_{ds}}
 \end{aligned}$$

with

$$\begin{aligned}
 \Delta_1 &= l_{qs} l_{qr} - (l_{aq})^2 \\
 \Delta_2 &= -(l_{ad})^2 (l_{ds} + l_{dr} - 2l_{ad})
 \end{aligned}$$

To find the matrices  $F_1$  and  $D$ , we can solve the simultaneous equations from conditions (i) and (ii), where

$$F_1 = \begin{bmatrix} f_{11} & f_{12} \\ f_{21} & f_{22} \\ f_{31} & f_{32} \\ f_{41} & f_{42} \end{bmatrix} \tag{31}$$

$$D = \begin{bmatrix} d_{11} & d_{12} & d_{13} & d_{14} \\ d_{21} & d_{22} & d_{23} & d_{24} \\ d_{31} & d_{32} & d_{33} & d_{34} \\ d_{41} & d_{42} & d_{43} & d_{44} \end{bmatrix} \tag{32}$$

## DESIGN OF A CONTROL SYSTEM

[Fig. 2] shows block diagram of the proposed control system [18] in the conventional two-loop structure; the outer speed loop and the inner current loop for an SPWM voltage source inverter fed PMSM drive.

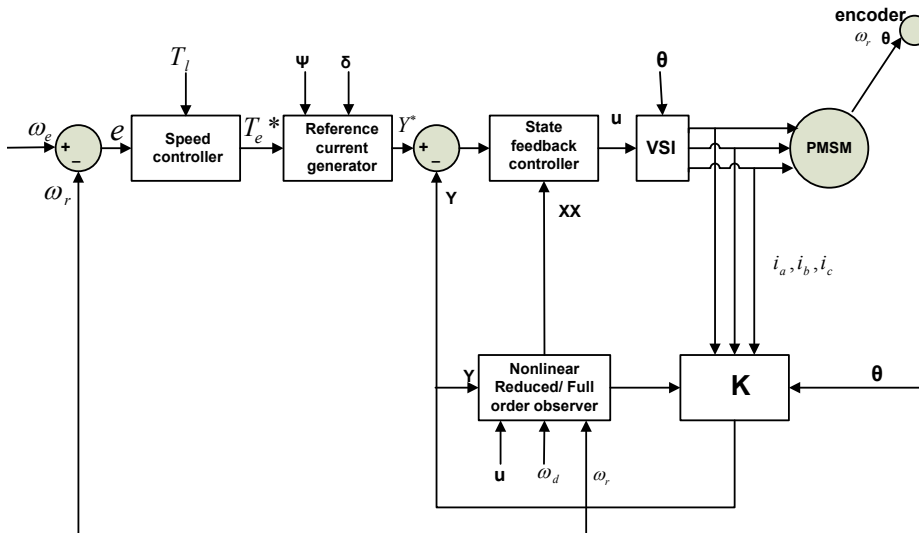


Fig. 2: Block diagram of the proposed control system

### Design of Speed Controller

In the outer loop, PI controller is used as speed controller and the output of this controller is reference torque  $T_e^*$ , from which the reference currents  $i_q^*$  and  $i_d^*$  are generated. The PI controller gain constants are designed as given below:



Substituting  $v_{qs}$  and  $v_{ds}$  values in eqn. (42)

$$\tan \delta = \frac{-r_a i_{ds} - l_{ds} p i_{ds} - l_{ad} p i_{ds} + \omega_r l_{qs} i_{qs} + \omega_r i_{aq} i_{qr}}{r_a i_{qs} + l_{qs} p i_{qs} + l_{aq} p i_{qr} + \omega_r l_{ds} i_{ds} + \omega_r l_{ad} i_{dr} + \omega_r \Psi} \quad (43)$$

Under steady state condition all p or  $\frac{d}{dt}$  terms as well as  $i_{dr}$  and  $i_{qr}$  assumed to be zero. So

$$\tan \delta = \frac{\omega_r l_{qs} i_{qs} - r_a i_{ds}}{r_a i_{qs} + \omega_r l_{ds} i_{ds} + \omega_r \Psi} \quad (44)$$

Also,

$$i_{ds} = i_{qs} \tan \psi \quad (45)$$

With a permanent magnet on the rotor, the motor has a constant flux linkage ( $\Psi$ ). Three sets of formulae for reference currents are derived-one with specified  $\delta$ , second one with specified  $\psi$  and the third one for field oriented case.

The reference currents with  $\delta$  specification are given as

$$i_{qs}^* = \frac{T_e^*}{3(l_{ad} - l_{aq})i_{ds} + \Psi} \quad (46)$$

$$i_{ds}^* = \frac{-q_2 \pm \sqrt{q_2^2 - 4q_1 q_3}}{2q_1} \quad (47)$$

where

$$q_1 = 3(l_{ad} - l_{aq})(-r_a - \omega_r l_{ds} \tan \delta)$$

$$q_2 = -3(l_{ad} - l_{aq})\omega_r \Psi \tan \delta + 3\Psi(-r_a - \omega_r l_{ds} \tan \delta)$$

$$q_3 = -3\Psi^2 \omega_r \tan \delta - (r_a \tan \delta - \omega_r l_{qs})T_e^*$$

The reference currents with  $\psi$  specification are given as

$$i_{qs}^* = \frac{-3\Psi \pm \sqrt{9\Psi^2 + 12T_e^*(l_{ad} - l_{aq}) \tan \psi}}{6(l_{ad} - l_{aq}) \tan \psi} \quad (48)$$

$$i_{ds}^* = i_{qs}^* \tan \psi \quad (49)$$

The reference currents for field oriented case are given as

$$i_{qs}^* = \frac{T_e^*}{3\Psi} \quad (50)$$

$$i_{ds}^* = 0 \quad (51)$$

### State Feedback Controller

For the regulator model of given multivariable system, the linear feedback control [4, 20] law is applied with a gain matrix of K. In addition, to have complete control over the system dynamics a pole placement technique [19] is used.

Now partitioning K into  $K_{bs}$  and  $K_{is}$ , multiplied with the regulator model, the control signal 'u' can be given as

$$\dot{u}_2 = Kz = \begin{bmatrix} K_{bs} & K_{is} \end{bmatrix} \begin{bmatrix} \dot{x} \\ y - y_r \end{bmatrix} \quad (52)$$

Integrating and simplifying the above equation, the control law becomes

$$u_2 = K_{bs}x + K_{is} \int_0^t (y - y_r) dt \quad (53)$$

From the above equation, it is concluded that IOE feedback makes the controller as robust from the modelling imperfections and step like disturbances.

### Pole Placement by State Feedback

In order to have complete control over the system dynamics the controller has been designed by placing the poles of the closed loop system at the desired locations in the s-plane.

For a linear time invariant system represented by

$$\dot{x} = Ax + Bu_2 \quad (54)$$

with the state feedback control law as

$$u_2 = K_2x \quad (55)$$

the closed loop system becomes

$$\dot{x} = (A + BK_2)x \quad (56)$$

which can have arbitrary or prescribed eigen values, if and only if, the pair (A, B) is controllable.

## RESULTS AND DISCUSSION

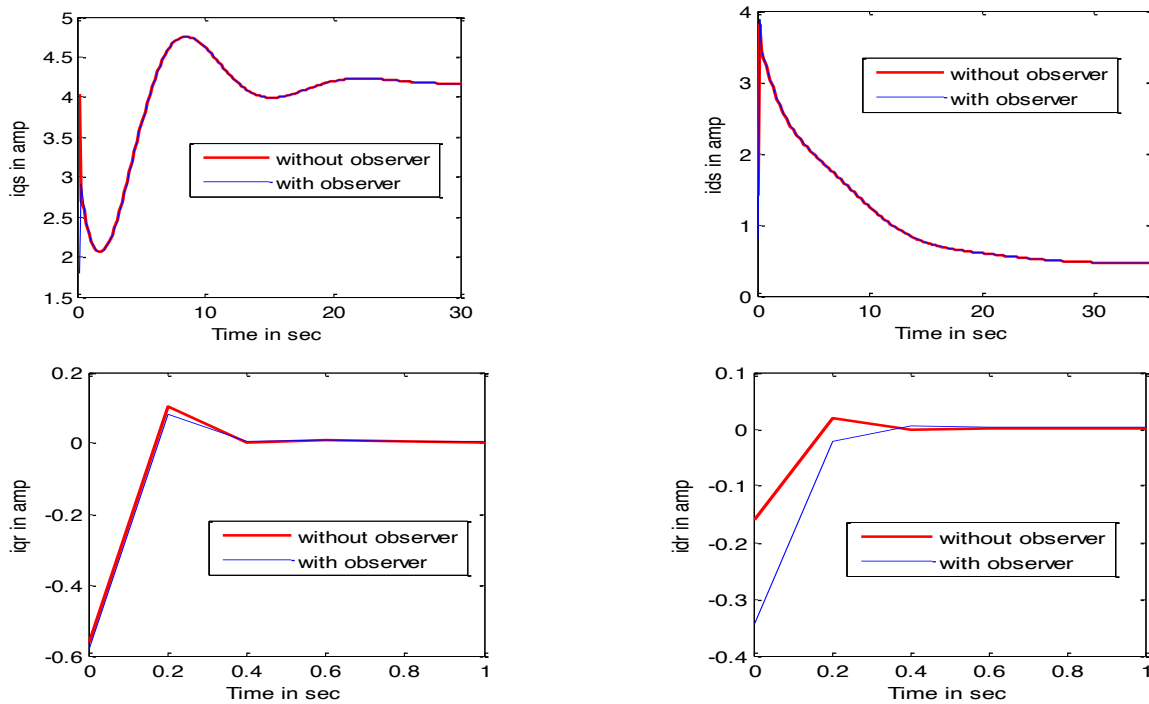


Fig. 4: Simulations results of PMSM drive with and without non-linear full order observer

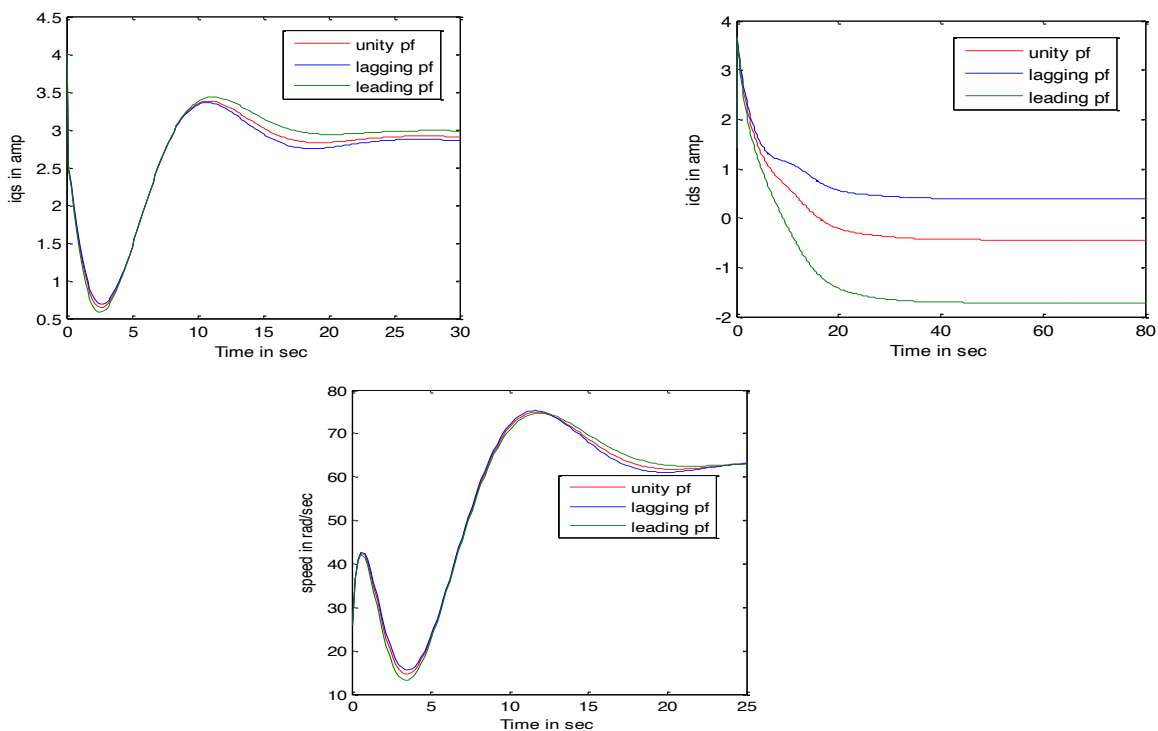
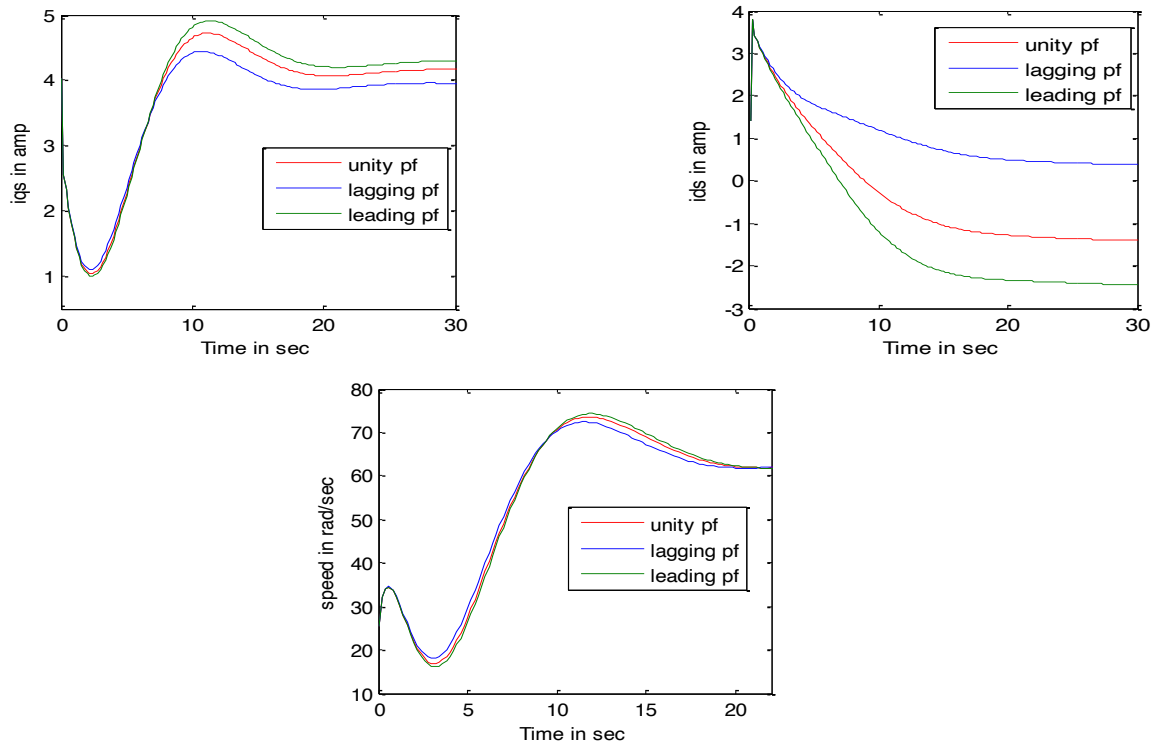


Fig.5: Simulation results of PMSM drive for delta variation (a)  $\delta=8.735^\circ$  (u.p.f) (b)  $\delta=5^\circ$  (lagging p.f) (c)  $\delta=15^\circ$  (leading p.f)



**Fig. 6.** Simulation results of PMSM drive for  $\psi$  variation (a)  $\psi = -19.1^\circ$  (u.p.f) (b)  $\psi = 5^\circ$  (lagging p.f) (c)  $\psi = -30^\circ$  (leading p.f)

From the results shown in [Fig. 4], the estimated damper winding currents (i.e.  $i_{qr}$  &  $i_{dr}$ ) in its steady state are observed as zero; the initial currents are only affected, as damper currents exist only under transient conditions and goes to zero at steady state. The transient response of these currents is oscillatory in nature and very close to that with the actual states. The other estimated states such as stator currents (i.e.  $i_{qs}$  &  $i_{ds}$ ) are nearly similar to the actual states. [Fig. 5 and 6] shows the simulation results of the drive for different values of  $\psi$  and  $\delta$  resulting in variation of power factor from lagging to leading including unity. From the results it is clear that the settling values of  $i_{ds}$  has large variations for different values of power factor, which clearly indicates the effect of magnetizing current for corresponding values of power factor.

**Table 1.** Performance PMSM drive with and without non-linear full order observer

Variable	Actual values			Estimated values		
	Initial peak value	Steady state value	Settling time (sec)	Initial peak value	Steady state value	Settling time (sec)
$i_{qs}$	4.03	4.188	40	2.91	4.188	40
$i_{ds}$	3.81	0.44	41	3.88	0.44	41
$i_{qr}$	0.105	0.00	01	0.08	0.00	0.4
$i_{dr}$	0.021	0.00	01	0.006	0.00	0.3

**Table 2.** Performance figures of PMSM with variable  $\delta$

Design Specifications	Achieved performance figures									
	$\delta$ (deg.)	$\psi$ (deg.)	$\phi$ (deg.)	$\cos\phi$	Variable	Change in $\omega_r$		Change in $T_l$		Settling time (sec.)
						S.S. Value	Peak Value	S.S. Value	Peak Value	
$\delta = 3.8^\circ$ (min.)	3.8	19.6	23.4	-0.14	$i_{qs}$	3.87	4.5	3.87	4.62	26.0
					$i_{ds}$	1.38	3.8	1.38	3.6	38.5
					$\omega_r$	62.83	74.7	62.83	76.1	39.0
$\delta = 8.73^\circ$	8.73	-8.73	0.0	1.0	$i_{qs}$	2.91	3.37	2.99	3.40	25.5
					$i_{ds}$	-0.42	3.66	-0.37	3.52	33.5
					$\omega_r$	62.8	74.9	62.8	75.5	37.0
$\delta = 35^\circ$ (max.)	35.0	-40.6	-5.6	0.78	$i_{qs}$	4.54	5.22	4.54	5.3	27.0
					$i_{ds}$	-3.89	3.72	-3.89	3.4	35.0
					$\omega_r$	62.83	77.2	62.83	78.3	38.0



Table 3. Performance figures of PMSM with variable  $\psi$

Design Specifications	Achieved performance figures									
	$\delta$ (deg.)	$\psi$ (deg.)	$\phi$ (deg.)	$\cos\phi$	Variable	Change in $\omega_r$		Change in $T_l$		Settling time (sec.)
						S.S. value	Peak value	S.S. value	Peak value	
$\psi=-49^\circ$ (min.)	43.67	-49	-5.33	0.76	$i_{qs}$	4.54	5.55	4.8	5.92	26.4
					$i_{ds}$	-5.23	3.75	-5.5	3.56	29.5
					$\omega_r$	62.84	78.3	62.83	80.0	24.16
$\psi=-19.1^\circ$	19.1	-19.1	0.0	1.0	$i_{qs}$	4.16	4.72	4.22	4.83	27.6
					$i_{ds}$	-0.38	3.67	-1.42	3.6	29.6
					$\omega_r$	62.8	74.9	62.9	74.5	24.14
$\psi=62^\circ$ (max.)	-14.73	62.0	47.27	-0.99	$i_{qs}$	3.39	3.9	3.39	4.07	27.8
					$i_{ds}$	6.37	6.5	6.38	6.5	29.7
					$\omega_r$	62.77	69.7	62.83	71.4	24.16

From [Table 1] it is clear that, the initial peak values of estimated variables are low when compared to the actual values. The steady state values are equal in both actual and estimated, also settled at equal time. But in case of estimated damper winding currents the settling time is very low i.e, the observer converges very fast.

From [Table 2] it is clear that, for the design specifications of torque angle  $\delta$ , the motor reaches its speed at a steady value of  $20\pi$  rad/sec either as a result of change in reference frequency or load torque. Here the settling time lies between 25sec-39sec.

From [Table 3] it is clear that, for the design specifications of internal p.f angle  $\psi$ , the motor reaches its speed at a steady value of  $20\pi$  rad/sec either as a result of change in reference frequency or load torque. Here the settling time lies between 24sec-30sec.

## CONCLUSION

In order to implement sophisticated control schemes for PMSM drive, the state feedback approach is usually employed. The implementation of state feedback control requires that all the system states are available for feedback. So, a non-linear full order observer is designed for the estimation of both accessible and inaccessible states in orders to feedback all the states to state feedback controller. By designing full order observer, the information which is provided by sensors is completely eliminated from the control system. Although in the particular design, because of the special structure of the system matrices, the non-linear term automatically gets cancelled through the full order observer design. Due to this, the system becomes less expensive, more accurate and reliable.

### Appendix-A: Machine Ratings

Rated voltage=400V, Rated current=2.17A, Rated speed=1500rpm, No. of poles=4, Power rating: 1.2/1.5 kW, 0.8/1.0 p.f

#### CONFLICT OF INTEREST

There is no conflict of interest.

#### ACKNOWLEDGEMENTS

None

#### FINANCIAL DISCLOSURE

None

## REFERENCES

- [1] Pillay P and Krishnan R. [1988] Modeling of Permanent Magnet Motor Drives. *IEEE Transactions on Industrial Electronics*, 55(4): 537-541.
- [2] Pillay P and Krishnan R. [1989] Modeling, simulation and analysis of Permanent magnet motor drives, Part-I: The Permanent Magnet Synchronous Motor Drive. *IEEE Transactions on Industry Applications*, 25(2): 265-273.
- [3] Shyu KK, Lai CK and Hung JY. [2001] Totally Invariant State Feedback Controller for Position Control of Synchronous Reluctance Motor. *IEEE Transactions on Industrial Electronics*, 48(3): 615-624.
- [4] Hasirci U and Balikli A. [2009] Nonlinear and adaptive state feedback control of variable speed PMSM drives. *7<sup>th</sup> IEEE Asian Control Conference*, 1605-1610.
- [5] Brandstetter P, Rech Pand Simonik P. [2010] Sensorless Control of Permanent Magnet Synchronous Motor Using Luenberger Observer. *PIERS Proceedings, Cambridge, USA*, pp.424-428.
- [6] Jorge A. Solsona and Maria I.[2003] Disturbance and Nonlinear Luenberger Observers for Estimating Mechanical Variables in Permanent Magnet Synchronous Motors Under Mechanical Parameters Uncertainties,"

- IEEE Transactions on Industrial Electronics, 50( 4):717-725.
- [7] Ramana P, Alice Mary K, Surya Kalavathi M and Hareesh Kumar J.[2016] Design of a Non-linear Reduced and Full order Observers for an Inverter Fed Permanent Magnet Synchronous Motor Drive. *Indian Journal of Science and Technology*, 9(9):01-08.
- [8] Kron G.[1930] Generalized theory of electrical machinery. *Transactions of the American Institute of Electrical Engineers*, 49(2):666-683.
- [9] Krishnan R. [2010] Electric motor drives: Modeling analysis and control. *Prentice Hall*, 2<sup>nd</sup> edition.
- [10] J Solsona, MI Valla and C Muravchik.[2005] A Nonlinear Reduced Order Observer for Permanent Magnet Synchronous Motors. *IEEE transactions on industrial electronics*, 43(4):492-497.
- [11] Junfeng Xu, Yinglei Xu, Jianghua Feng and Fengyan Wang. [2004] Direct torque control of Permanent Magnet Synchronous Machines using Stator flux Full order State Observer. *IEEE International Symposium on Industrial Electronics*, 2:913-916.
- [12] Fanglai Zhu.[2007] The Design of Full-order and Reduced-order Adaptive Observers for Nonlinear Systems. *IEEE International Conference on Control and Automation*, 529 - 534.
- [13] Comanscu M and Todd D Batzel. [2010] Full Order EMF Observer for PMSM Design-Analysis and Performance under Improper Speed Signal. *4<sup>th</sup> annual IEEE system conference*, 86 - 90.
- [14] P Ramana, K Alice Mary, M Surya Kalavathi and A Swathi. [2015] Parameter Estimation of Permanent Magnet Synchronous Motor-A Review. *i-manager's Journal on Electrical Engineering*, 9(4):46-56.
- [15] M Hinkkanen, T Tuovinen, L Harnefors, and J Luomi. [2010] A reduced order position observer with stator-resistance adaptation for PMSM drives. *IEEE International Symposium on Industrial Electronics*, 3071-3076,
- [16] P.Ramana, K. Alice Mary, M.Surya Kalavathi and M.Phani Kumar.[2011 ] Design of a Non-linear Observer for VSI Fed Synchronous motor,International Journal of Electrical and Electronics Engineering, 5(4): 268-271.
- [17] K G Lee, J S Lee and K B Lee. [2015] Wide-Range Sensorless Control for SPMSM Using an Improved Full-Order Flux Observer. *Journal of Power Electronics*, 15(3):721-729.
- [18] K Alice Mary, A Patra, NK De and S Sengupta.[2002] Design and Implementation of the Control System for an Inverter-fed Synchronous Motor Drive. *IEEE Transactions on Control Systems Technology*, 10(6): 853-859.
- [19] K Alice Mary.[2009] Speed Control of An SPWM inverter Driven Non Linear PMSM Drive with Pole Placement Technique-II. *IEEE International conference on Electrical energy systems and power electronics in emerging economics*,413-417
- [20] P Ramana, K Alice Mary and M Surya Kalavathi.[2016] State Feedback Linearization of a Non-linear Permanent magnet Synchronous motor drive. *Indonesian Journal of Electrical Engineering and Computer science*, 1(3): 234-542.

## ARTICLE

# ISOLATED WORD RECOGNITION SYSTEM FOR SPEECH TO TEXT CONVERSION USING ANN

Sunanda Mendiratta<sup>1</sup>, Neelam Turk<sup>2</sup>, and Dipali Bansal<sup>3</sup>

<sup>1</sup>YMCA University of Science and Technology, Faridabad, INDIA

<sup>2</sup>Department of Electronics, YMCA University of Science and Technology, Faridabad, INDIA

<sup>3</sup>Electronics Engineering Department Faculty of Engineering and Technology, Manav Rachna International University, Faridabad, INDIA

## ABSTRACT

The capacity of a device or a program to listen, identify various sounds is referred as Speech recognition and recognize some known languages from the spoken words and for human machine interface the Automatic Speech Recognition (ASR) system is helpful. In recent periods, for the ASR system, lot of research works has been developed but the concerns in that system are vast, because of the improper techniques used for the feature selection. Proper features are selected in this paper in order to develop a superior ASR system and convert the spoken word into corresponding text. Three phases are comprised in the proposed system; preprocessing, feature extraction and classification. Initially, from the source the spoken word is detected by the preprocessing phase and the noise level is reduced. Then, totally eight features are extracted containing five statistical features and three common in the feature extraction phase. Then, the classifier is trained by using these features referred as artificial neural network (ANN) with back propagation (BP). The eight features are use as the training dataset for BP algorithm and based on this feature the corresponding text displayed at the output of the proposed ASR system. The proposed system is implemented in the working platform of MATLAB. The implementation result prove that the system provide superior classification and converts the text properly. The classification accuracy examined based on performance metrics. Ultimately, the overall performance of the proposed ASR system is superior and well suitable for human machine interface.

## INTRODUCTION

Speech recognition (SR) is the process by which a computer (or other machine) identifies spoken words [1]. Basically, it refers to talking to your computer and it correctly recognizes what you are saying. The SR techniques are also referring as computer Speech Recognition (CSR), or Automatic speech recognition (ASR) [2]. Usually, the process of converting speech signals to a sequence of words occur through an algorithm implemented using a computer program. About the mechanisms for mechanical realization of human speech capabilities for reasons ranging from technological curiosity, to desire to automate simple a task which necessitates human machine interactions and research in automatic speech recognition by machines has fascinated a high deal of attention for sixty years [3].

The most part of research has been motivated by People's desire in speech processing to construct mechanical models for imitating human verbal communication capabilities [4]. The fundamental objective of Speech recognition area is to create techniques and methods for speech input to machine [5]. Today, the automatic speech recognition methods find broad application in tasks based on significant advances in statistical modeling of speech that need human machine interface contains query based information methods and automatic call processing in telephone networks provide updated travel data, stock price quotations, climatic reports etc., [6]. In common, environmental noise can easily influence the free space communication signals like the speech signal [7].

In ASR method, numerous conceivable types of environmental distortion remains a challenging issue in noisy environments and compensate these distortions precisely is difficult [8]. Using some essential features the speech signal is trained and then based on the trained feature the speech signal tested or recognized. Subsequently, training and testing are the two major process of basic speech signal recognition method [9]. For poor recognition performance in noise the mismatch between test condition and training was the important purpose [10]. Numerous strategies are created in order to improve the performance and to lower this mismatch. For grouping these methods, the two fundamental categories are model adaptation method and Feature enhancement method [11]. Using Model adaptation techniques the probability distributions of the recognizer is remunerated straightly and in presence of noise the feature extraction methods are helpful in speech recognition [12-14]. Short-term energy, formants, Pitch, MFCCs, cross-section areas and Teager energy operator-based features are the most fascinating features for the significant speech recognition [15].

Denosing feature vectors received at the test time can work as the feature recognition strategies and these are normally trained from clean speech, so that they match the recognizer's acoustic models [17]. As the computation of these methods are simpler than model domain techniques they are more attractive and the recognizer independently implemented. For instance, at the spectrum level methods such as spectral subtraction [18] work, spectral-MMSE [19] work on the features specifically. Generally, a prior speech model is used by a class of techniques in Gaussian mixture model (GMM) to assist the

### KEY WORDS

Automatic Speech Recognition (ASR); speech signal preprocessing; feature extraction; isolated word recognition; speech to text conversion; statistics features; back propagation (BP) algorithm.

Published: 20 October 2016

### \*Corresponding Author

Email: sunandamendiratta712@gmail.com

enhancement process. For instance, stereo recordings of noisy and clean speech is used by SPLICE and using a GMM from noisy to clean speech a piecewise linear mapping was studied [20]. Whereas, enhanced performance have been indicated by front-end techniques on numerous tasks make point-estimates of the clean speech features. Additionally mismatch between the acoustic model and the features are because of errors in these estimates, resulting in performance degradation. These methods can enhance recognition accuracy in noisy conditions [21], [22] and obtain superior execution.

The remaining paper is summarized as follows. The recent research works related to the ASR system is examined in Part 2. Part 3 explains the proposed ASR system for speech to text conversion. Part 4 demonstrates the experimental implementation and performance comparison. Then, finally resulting sections gives the conclusion and references.

## RELATED WORK

Based on the speech intelligibility some of the recent work is listed below:-

Yixiong Pan et al. [23] have recognized three emotional states: happy, sad and neutral. The actual researched characteristics consist of: vitality, message, linear predictive range html coding (LPCC), Mel-frequency range coefficients (MFCC) and Mel-energy range powerful coefficients (MEDC). The German Corpus (Berlin Database of Emotional Speech) and self-built Chinese emotional databases are used by Support Vector Machine (SVM) classifier for training. In unlike databases, the various combinations of features are compared in the resultant section. The complete investigational consequences exposed that the feature combination of MFCC+MEDC+ Energy had the highest accuracy rate on both Chinese emotional database and Berlin emotional database.

Navdeep Kauret al. [24] has proposed a system to identify the speech dependent on the best possible element as well as in addition to the dialect. Speaker recognition is used to recognize a person from a spoken phrase. The SR system developed based on the neural network and they utilized twenty three phrases to the SR when using the taken out characteristics LPCC, REMOTE CONTROL and LPC by talk transmission as well as element vectors are created. For identification processes of various speakers and languages and for training, Neural Network back propagation learning algorithm is used. 25 speakers are comprised in the database used for that system .575 neurons are contained in the ANN model input layer and 25 neurons in the output layer and through the experimental verification the average recognition score was 93.38%.

Ant Colony Optimization method used in feature selection algorithm has been proposed by C. Poonkuzhali et al. [25] for automatic speech recognition. Consider the input as the appeared actual speech signal and through MFCC feature extraction approach, extracts 39 coefficients using MFCC. The unwanted features are withdrawn by the Ant Colony Optimization (ACO) technique. The fresh confirmation with their methodology exhibited that the last number connected with features removed significantly.

Petko N. Petkov et al. [26] has proposed a speech pre-enhancement method based on matching the recognized text to the text of the original message. This qualifying measure was appropriately estimated due to the probability with the appropriate transcription provided a good estimate with the noisy speech features. Along with drop in the actual signal-to-noise relation, in the profile of atmospheric noise speech intelligibility diminishes. They have carried out speech pre-enhancement system that optimizes the actual proposed qualifying measure to the variables of a couple different speech modification strategies within a good energy-preservation restriction. In earlier knowledge of transcription the process proposed was necessary with the transported message and acoustic speech models from a computerized speech recognition system. This performance demonstrated a major development exceeding healthy speech and a reference point system that optimizes perceptual-distortion-based aim intelligibility measure.

An automatic speech recognition (ARS) technique have been presented by Siddhant C. Joshi et al. [27] using back propagation neural network. The strategies designed in that paper may expand to some common applications including sonar target recognition, missile tracking and grouping of submerged acoustic signals. Back-propagation neural network algorithm used the proposal training trials and their ideal result convictions to perceive specific patterns by changing the real service beliefs linked with the nodes and weight several links relating its nodes. A real trained network appeared later uses feature recognition inside ASR program

Deniz Baskent et al. [28] has presented a study on speech enhancement system for the hearing impaired persons based on phonemic restoration (PR). To measure the speech signal interrupted intermittently two conditions are used and its recognition are interruptions stay quiet and with high noise break interruptions are loaded. They used linear amplification whereas several contemporary hearing aids (HAs) gave compressive amplification. Behind this choice the reason was that the study was the chief to give baseline PR data with hearing-impaired (HI) listeners, and compressive solutions could have had sudden impacts because of their nonlinear nature.

Cross adaptation of language model was investigated by X. Liu et al. [29], either carry out as a stand-alone system combination method or used together with acoustic model cross adjustment to improve large

vocabulary continuous speech recognition (LVCSR) method. Three kinds are in language models that includes a multi-level LM that both syllable as well as word arrangements are modeled, a word level neural network LM, and the linear combination of the two were cross adjusted. The investigational results on a state-of-the-art speech recognition task suggested complimentary features exist on multiple layers of the progressive hierarchy among highly diverse sub-frameworks.

Wooil Kim et al.[30] have presented three approaches acquired using missing-feature techniques to enhance the speech recognition accuracy. The first innovation of that paper was Frequency-dependent classification, which engage independent classification. The second innovation was Colored-noise generation using multi-band partitioning, which involved the use of masking noises with artificially-introduced spectral and temporal variation in training the Bayesian classifier. The third innovation was an adaptive method to assess the priori values of the mask classifier, which determined if a specific time-frequency section of the test data was solid or not. It demonstrates that these advancements provide improved speech recognition accuracy on a small vocabulary test.

## PROPOSED ASR SYSTEM

The common objective of the automatic speech recognition system (ASR) is to enhance performance in man machine interaction. Motivates the proposed ASR system to classify the signal and convert the classified signals the corresponding text signal. Four stages are comprised in the proposed system they are preprocessing, feature extraction, optimal feature selection and recognition. The architecture of the proposed ASR system is shown in [Fig. 1].

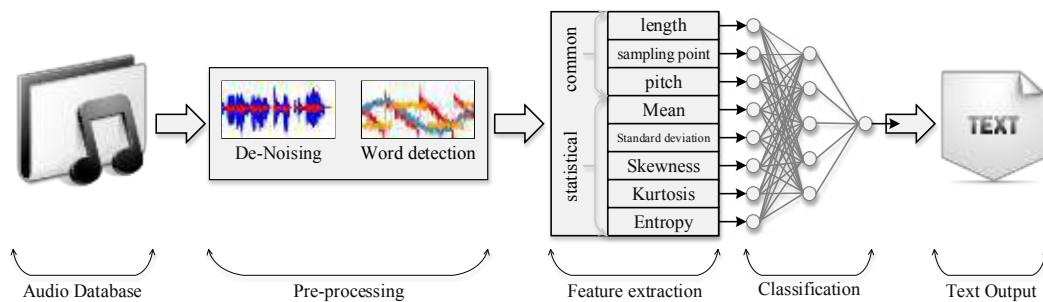


Fig. 1: Architecture of Proposed ASR system

Preprocessing the input recoded audio signal for removing noise and to detect the word. Then, the features are extracted such as sampling point, word length, pitch and the five statistical features like Mean, Variance, Skewness, Kurtosis, and Entropy. Subsequently, select the optimal level of features for the classifier training. Then, recognize the spoken word and displays the corresponding text. The detailed descriptions of the proposed ASR system is given in following sections

### Input Database

The input database contains dissimilar persons spoken various speech signals. For the proposed ASR system, consider these stored speech signals as the input signal and equation (1) represents the input speech signal given beneath as,

$$S_i = x_i(t) \mid i = 1, 2, \dots, N \quad (1)$$

Where, ' $S_i$ ' is  $i^{th}$  input signal in database and ' $N$ ' represents the total no of speech signals in database.

### Preprocessing

In ASR method, preprocessing is the first phase where analog speech signal is managed at the recording time, which varies with time. The signal is processed by digital means, as it is important to sample the continuous-time signal into a discrete-time discrete valued (digital) signal. The speech is partitioned into frames or a sequence of uncorrelated segments as the properties of a signal change gradually with time and the sequence is processed as if properties of each frame has fixed. Under this postulation, the features of each frame is removed based on the sample inside the frame. Moreover, the original signal will be replaced by the feature vector in the additional processing, which means the speech signal converted from a time varying analog signal into a sequence of feature vectors. The method of varying speech samples sequences into feature vectors characterizing events in the probability space known as Signal Modeling [31].



The function of preprocessing is to derive a set of parameters presented from the transmission medium in a form to represent speech signals advantageous for subsequent processing and the sampled speech signal is processed and representation is produced independent on amplitude variations, speaker stress and noise. Both the frequency and time domain methods are used in the preprocessing step, amid this Time domain approaches are usually easy to implement and directly dealing with the speech signal's waveform with parameters of zero crossing rates and energy. Some form of spectral analysis are involved by Frequency domain approaches that are not straightly obvious in the time domain. In speech recognition the most widely used are the latter methods.

### Background Noise Removal

In the genuine situations, the background noise is normally created through fans, air conditioning, fluorescent lamps, type writers, PC's, back conversation, footsteps, traffic, opening and shutting the entryways etc., the speech recognition method's designers frequently have less control over these things. Except for impulse noise sources like type writers, certain kind of noise in nature is additive and they are usually steady state [32]. Based on the environment, about 60 dB to 90 dB the levels of noise will vary. The most commonly used technique is Head mounted close speaking microphone to reduce the impact of the background noise. At normal conversational level when a speaker generating speech and the microphone filtering the speech signal then the average speech level increment by around 3dB each time. To remove the background noise the filter is given by Equation (2).

$$E_s = 10 \times \log_{10} \left\{ \epsilon + \frac{1}{N} \sum_{n=1}^N S^2(n) \right\} \quad (2)$$

Where, the ' $E_s$ ' is log energy of a block of ' $N$ ' samples and ' $\epsilon$ ' is a small positive constant added to prevent the computing of log zero. ' $S(n)$ ' be the  $n^{th}$  speech sample in the block  $N$  samples.

### Speech Word Detection

The speech recognition want to process the utterance consisting of silence, speech and other background noise is need to process in. The presence of speech detection entrenched in the background noise and dissimilar non-speech events known as an end point detection or speech activity detection or speech detection. For numerous reasons, a fine end point detection algorithm influences the performance of framework for accuracy and speech. First, before recognition the silence frame is removed and for both speech and noise the accumulated utterance likelihood score focus more on the speech portion of an utterance [33]. Second, it is difficult to precisely model silence and noise in altering environments [34] and limit this effect using background noise frame in advance. Third, non-speech frames are removed, when the computation time is considerably lowered the number of non-speech frames is large [35-39].

Steps for speech word detection are as follows:

**Step 1:** Measurements for endpoint detection

Zero crossing count, NZ is the number of zero crossing the block. Equation (2) denotes the log energy  $E_s$  of a block of length  $N$  samples. Equation (3) characterizes the normalization auto-correlation coefficient at unit sample delay  $C_1$ .

$$C_1 = \frac{\sum_{n=1}^N S(n)s(n-1)}{\sqrt{\left[ \sum_{n=1}^N S^2(n) \right] \times \left[ \sum_{n=0}^{N-1} S^2(n) \right]}} \quad (3)$$

**Step 2:** Filter for end point detection

Assume one utterance may have possible pauses separate several speech segments. To determine each segment detect a pair of endpoints named segment beginning and ending points. There is reliably a starting point is followed by a raising edge and a descending edge before an ending point on the energy contours of utterance. In the methodology at first, the edge is detected and after that the equivalent endpoints are detected. For accurate and robust endpoint detection a detector is required to detect all possible endpoints from energy feature. Equation (4) postulates the endpoint detection has the feature for one dimensional short term energy in the data sample as given beneath

$$E(l) = 10 \times \log_{10} \sum_{j=n(l)}^{n(l)+l-1} o(j) \quad (4)$$

Where, ' $o(j)$ ' is data sample, ' $l$ ' is window length, ' $E(l)$ ' is frame energy in decibel, ' $n(l)$ ' is number of first data sample in the window.

Step 3: Energy normalization

The purpose of normalization of energy is to normalize the utterance energy  $E_l$ . Equation (5) specifies the normalization of energy for finding the maximum energy value  $E_{\max}$  over the words as,

$$E_{\max} = \max(E_l), 1 \leq l \leq L \quad (5)$$

Subtracting  $E_{\max}$  from  $E_l$  to give  $\hat{E}_l = E_l - E_{\max}$ . In this way the peak energy value of each word is zero decibels and the recognition system is relatively insensitive to the difference in gain between different recordings. There is a restriction in performing the above calculations that word energy contour normalization cannot take place until locating the end of the word.

### Feature Extraction

In the ASR method Feature Extraction is a crucial process, based on the feature of the system provides the precise recognition of words. The clarity of the recognized speech is enhanced based on the feature extraction and selection. Feature extraction is exceptionally focused in this proposed ASR system. The common features such as sampling point, word length, pitch and the statistical features such as Standard deviation, Mean, Kurtosis, Skewness and Entropy of the speech signal are considered.

### Statistical Feature Extraction

**Mean:** Mean is the statistician's jargon for the average estimation of a signal represented as  $\mu$  (a lower case Greek mu) and found generally as you would expect as all samples are collectively added, and divide by N. These are represented as a mathematical form in Equation (6).

$$\mu = \frac{1}{N} \sum_{i=0}^{N-1} x_i \quad (6)$$

**Standard deviation:** Similar to the average deviation is the standard deviation, but instead of amplitude the averaging occurs with power. This is achieved by squaring each deviation before taking the average (bear in mind, power  $\propto$  voltage<sup>2</sup>). To compensate for the beginning square, take square root in order to complete the process. As an equation form it is represented in Equation (7).

$$\sigma = \frac{1}{N-1} \sum_{i=0}^{N-1} (x_i - \mu)^2 \quad (7)$$

**Skewness:** Skewness is a measure of the asymmetry of the probability distribution of a real-valued random variable about its mean in probability theory and statistics. The value of skewness can be negative or positive, or even undefined. For n sample values, a natural method for moment's estimator of the population skewness is shown in eqn. (8) as given beneath

$$\gamma = \frac{\frac{1}{N-1} \sum_{i=0}^{N-1} (x_i - \mu)^3}{\sigma^3} \quad (8)$$

**Kurtosis:** Kurtosis is any measure of the "peakedness" of the probability distribution of a real-valued random variable in probability theory and statistics. Kurtosis is a descriptor with the shape of a probability distribution, with the same idea of skewness and distinctive methods for evaluating it for a theoretical distribution and relating methods for estimating it from a population sample, same as skewness. Primarily peakedness are the various interpretations of Kurtosis (width of peak), lack of shoulders and tail weight (distribution primarily peak and tails, not in between) the precise measures are interpreted. The Kurtosis is calculated using equation (9) as,

$$Kurt = \frac{\frac{1}{N-1} \sum_{i=0}^{N-1} (x_i - \mu)^4}{\sigma^4} \quad (9)$$

**Entropy of the speech signal:** Entropy of the speech signal is valuable to estimate the differential entropy of a method or process with some observations in dissimilar engineering fields includes image investigation, independent component investigation, speech recognition, genetic investigation, time delay estimation and manifold learning. Histogram-based estimation is the simplest and the most commonly used approach in this paper. The formula used for calculating the histogram-based entropy estimation is given in Equation (10).

$$Entropy = - \sum_{i=0}^{N-1} x_i \log \left( \frac{x_i}{w(x_i)} \right) \quad (10)$$

Where, w is the width of the  $i^{th}$  bin.

## Word Identification

In this phase, the identified spoken words is converted into text. The identification accuracy greatly depends on the classification technique and the accuracy is identified highly. To tackle this problem an artificial intelligence (AI) is penetrated. The AI algorithm used in this paper for classification is artificial neural network (ANN).

## ANN Based Word Recognition

Duplicating the neural structure and working of the human brain is the principal aim of the programmed computational model, ANN. It consist of an interrelated structure of artificially created neurons that for data exchange it function as pathways. Artificial neural networks are adaptive and flexible, adjusting and learning every different external or internal stimulus. In sequence artificial neural networks are used, and data processing, pattern recognition systems, modeling and robotics. The ANN comprises of a single output layer and a single input layer and to one or more hidden layers. Except the input layer all nodes are composed with neurons. Depending on the issue the number of nodes in each layer differs. The architecture complexity of the network is dependent upon the number of nodes and hidden layers. ANN training is to find a set of weights that would give desired values at the output when at its input presented a dissimilar pattern. Training and testing is the two main process of an ANN. An example of a simple artificial neural network is shown in [Fig.2].

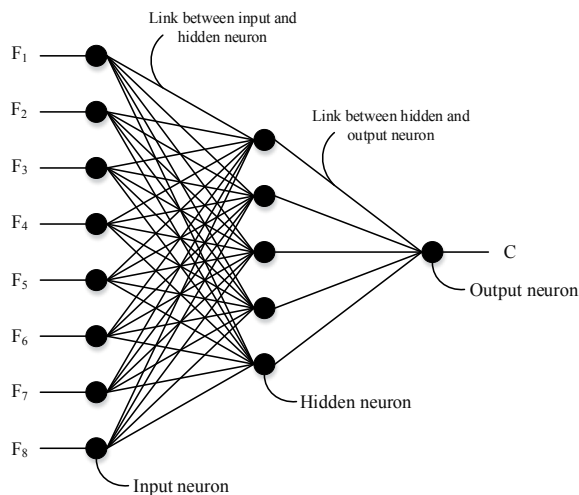


Fig. 2: Structure of ANN

The input for the ANN gets total of eight features and as the output of the ANN corresponding text can be obtained. Three common features and five Statistical features are included in the eight features. Statistical features such as standard deviation, mean, kurtosis, skewness and the common features such as sampling point, word length, and pitch. Thus, eight inputs (eight features) and corresponding word output is contained in the proposed ANN architecture. The two main process of a classification algorithm is training and testing.

## Training and Testing of ANN

In this phase, using the extracted features the ANN is trained. In training, the input and the output is defined and then fix the appropriate weight so that in the testing phase the classifier (ANN) can able to predict the apt object (word). In a common classifier algorithm the major part is the training phase. In the proposed system the back propagation (BP) algorithm is used for training. In the training the process involved is given as follows and [Fig. 3] shows the architecture of back propagation neural network (BPNN).

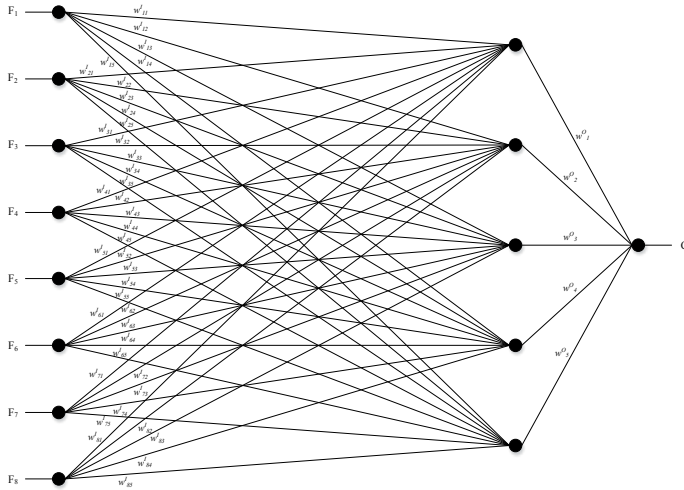


Fig. 3 : Proposed back propagation neural network

The proposed ANN consist of one output units, eight input units and  $M$  hidden units ( $M=5$ ). In the back propagation algorithm's forward pass, first to the hidden layer the input data is transmitted and then to the output layer. In the hidden layer each node gets input from the input layer and with appropriate weights multiplexed and summed. Using the equation (11) the output of the neural network is achieved which is given below.

$$C = \sum_{j=1}^M \frac{w_j^O}{1 + \exp\left(-\sum_{i=1}^N F_i w_{ij}^I\right)} \quad (11)$$

In eqn. (11), ' $F_i$ ' is the  $i^{th}$  input value and ' $w_j^O$ ' is the weights assigned between hidden and output layer, ' $w_{ij}^I$ ' is the weight assigned between input and hidden layer and  $M$  is the number of hidden neurons. The non-linear transformation of the resulting sum is the output of the hidden node. The same process is followed by the output layer. From the output layer the output values are compared with target values and for the neural network calculate the learning error rate, which is given in eqn (12) as

$$\partial_k = \frac{1}{2}(Y - C)^2 \quad (12)$$

In eqn. (12),  $\partial_k$  is the  $k^{th}$  learning error of the ANN,  $Y$  is the desired output and  $C$  is the actual output. The error between the nodes is transmitted back towards the hidden layer by the backward pass of the back propagation algorithm. Then, for some other training dataset the training is repeated by changing the weights of the neural network.

The following steps describe the minimization of error by back propagation algorithm.

- i. First, to hidden layer neurons the weights are assigned. The input layer has a constant weight, for the output layer neurons the weights are randomly chosen. Then, using Eqn. (11) the output is calculated.
- ii. Then, compute the back propagation error using the Eqn. (13).

$$BP_{error} = \sum_{k=1}^Z \partial_k \quad (13)$$

Where, ' $BP_{error}$ ' is Back Propagation error, ' $\partial_k$ ' learning error rate of  $k^{th}$  training data set. Then the weight deviation in the hidden neuron is finding by using the equation (14).

$$\Delta w = BP_{error} \cdot \gamma \cdot \delta \quad (14)$$

Where, ' $\Delta w$ ' is the weight deviation, ' $\gamma$ ' is the learning rate, which usually ranges from 0.2 to 0.5, ' $\delta$ ' is the average of hidden neurons output.

$$\delta = \frac{1}{T} \cdot \sum_{n=1}^T H_n \tag{15}$$

Here,  $H_n = \frac{1}{1 + \exp\left(-\sum_{i=1}^N F_i w_{in}^I\right)}$

Where, ‘ $\delta$ ’ is the average of hidden neurons output. ‘ $N$ ’ is the total no of input neurons, ‘ $T$ ’ is the total no of training and ‘ $H_n$ ’ is the  $h^{th}$  output at hidden neuron or activation function at input side. Then find the new weights by using the equation (16) given below.

$$w^{new} = w + \Delta w \tag{16}$$

Where, ‘ $w^{new}$ ’, the new weight or updated weight and ‘ $w$ ’ is the current weight.

Then repeat the process until the BP error gets minimized and it satisfies  $BP_{error} < 0.1$ . If the BP error reaches a minimum value, then the ANN is ready for classification.

Subsequently, process the testing, in testing the ANN undertaken for the verification of classification accuracy. In this phase, other than the data used in the training a new set of data is verified by the classifier. Once the classification accuracy is satisfied by ANN it can be used for the live application for the intended classification.

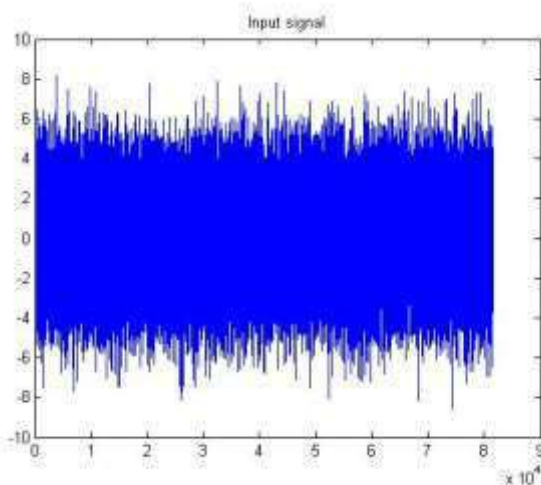
## RESULTS

The proposed system for the automatic speech recognition is implemented in the working platform of MATLAB with the following system specification.

Processor : Intel i5 @ 3GHz  
RAM : 8GB  
Operating system : windows 7  
Matlab version : R2013a

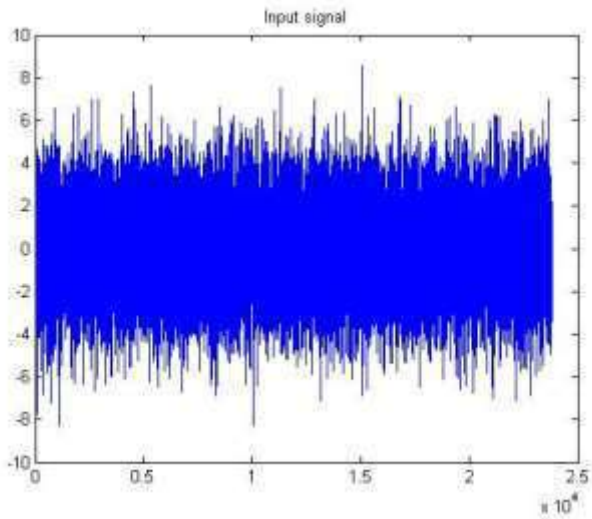
The ASR system is a peculiar process to made interface between man and machine .The normal machines don't have any sense to identify the attitude of a common man. One can make a system to interact with human with the help of artificial intelligence. Everyone could interact with or control the machine but for the interaction among various attitudes speech is one of the special and easiest way. A speech recognition system is important in this case in order to identify the speech or spoken word precisely. Consequently, by converting these recognized words or speech into the corresponding electrical signal the machine could realize the speech of an ordinary man. An ASR system is developed in this paper to recognize the spoken word and convert it to corresponding text. For implementing the proposed system the research tool in this section is Matlab. Using some recorded speech signals the recognition performance is analyzed.

In the input audio database we have stored 68 recorded speech signals. Amongst 68, for the performance analysis three signals such as Apple, Badam and Cow are used. The input speech signal apple, Badam and Cow are shown in [Fig. 4].

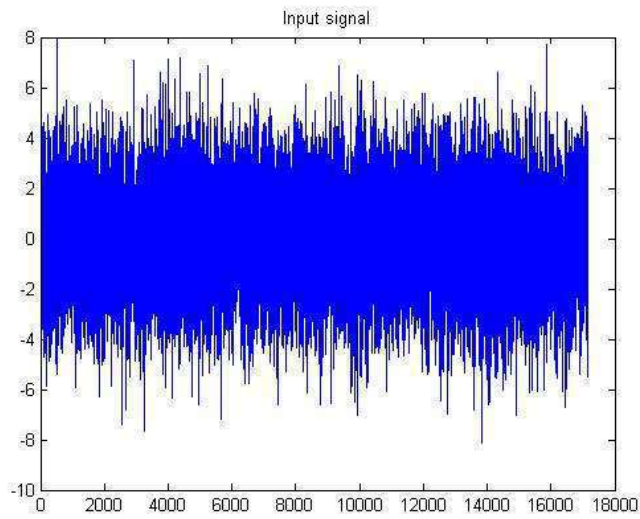


(a)Apple



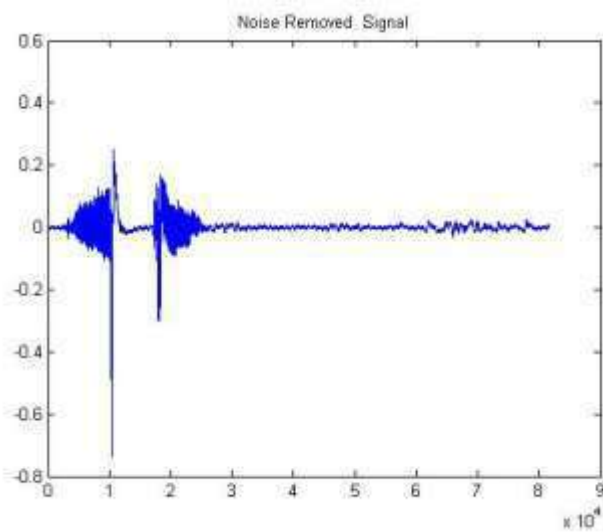


(b)Badam

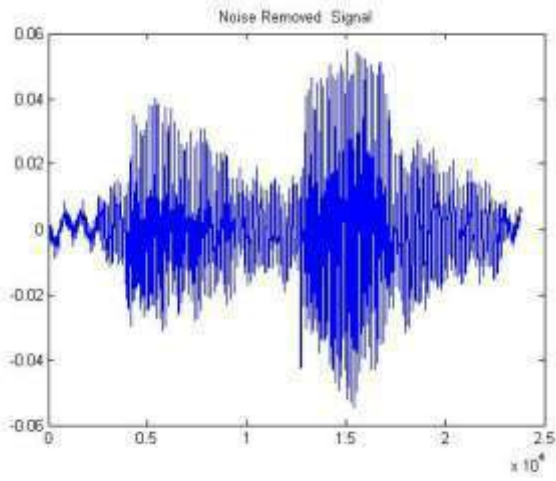


(c)Cow

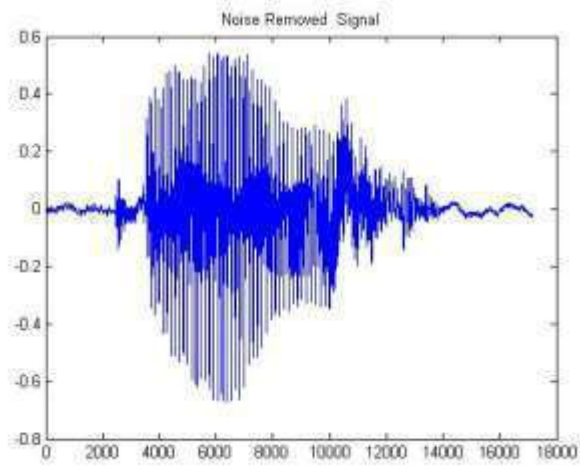
Fig. 4: Input speech signal :(a) Apple, (b) Badam, (c) Cow



(a)

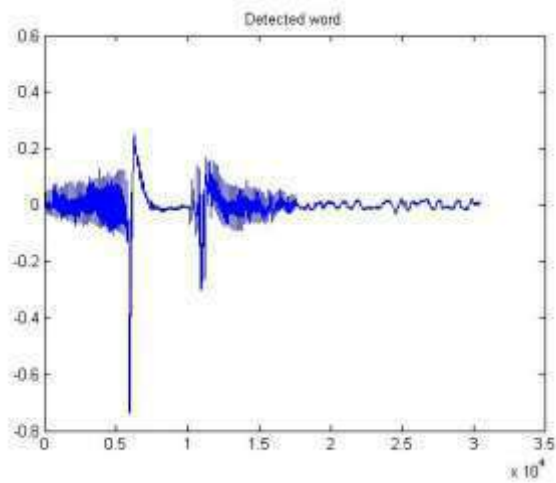


(b)

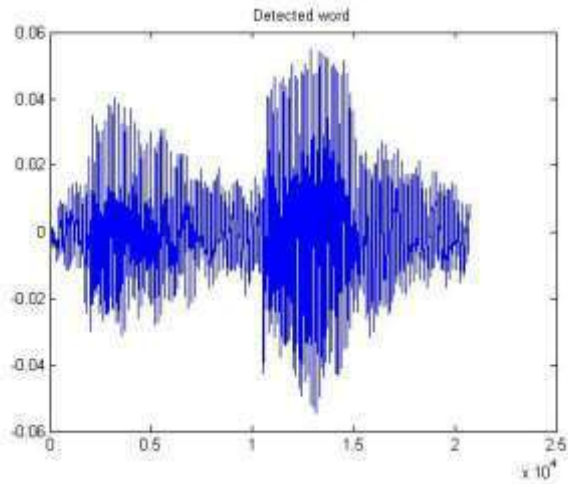


(c)

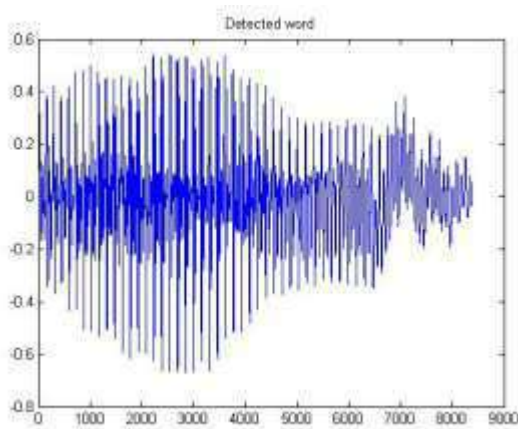
(i):(a) Apple, (b) Badam, (c) Cow



(a)



(b)



(c)

(ii): (a) Apple, (b) Badam, (c) Cow

**Fig. 5:** Preprocessed signal; (i) De-noised and (ii) Detected word

In [Fig. 5] the pre proposed signal shown for three different speech signals Apple, Badam and Cow. To detect the isolated word and for noise removal the preprocessing step is used. The statistical and the common features of the spoken signal are followed after the preprocessing stage. After preprocessing the common features are obtained easily .Using the eqn. (6) to eqn. (10) the statistical features are obtained and [Table 1] gives the obtained statistical values.

**Table 1:** Values of Statistical features

Features	Numerical value of Signal Samples		
	Apple	Badam	Cow
Mean	-0.0000077	0.0022	-0.00033
Variance	0.0011	0.0549	0.0173
Skewness	-0.00000023	-0.0000087	-0.0000057
Kurtosis	0.0000000017	0.000028	0.00000071
Entropy	5683.3	15510	5242.4

The eight features including common and statistical are given to the ANN to display the corresponding text and for the classification of signal. The proposed ASR system's obtained output was shown in [Fig. 6]. The corresponding text of spoken word is the outcome of ASR system.

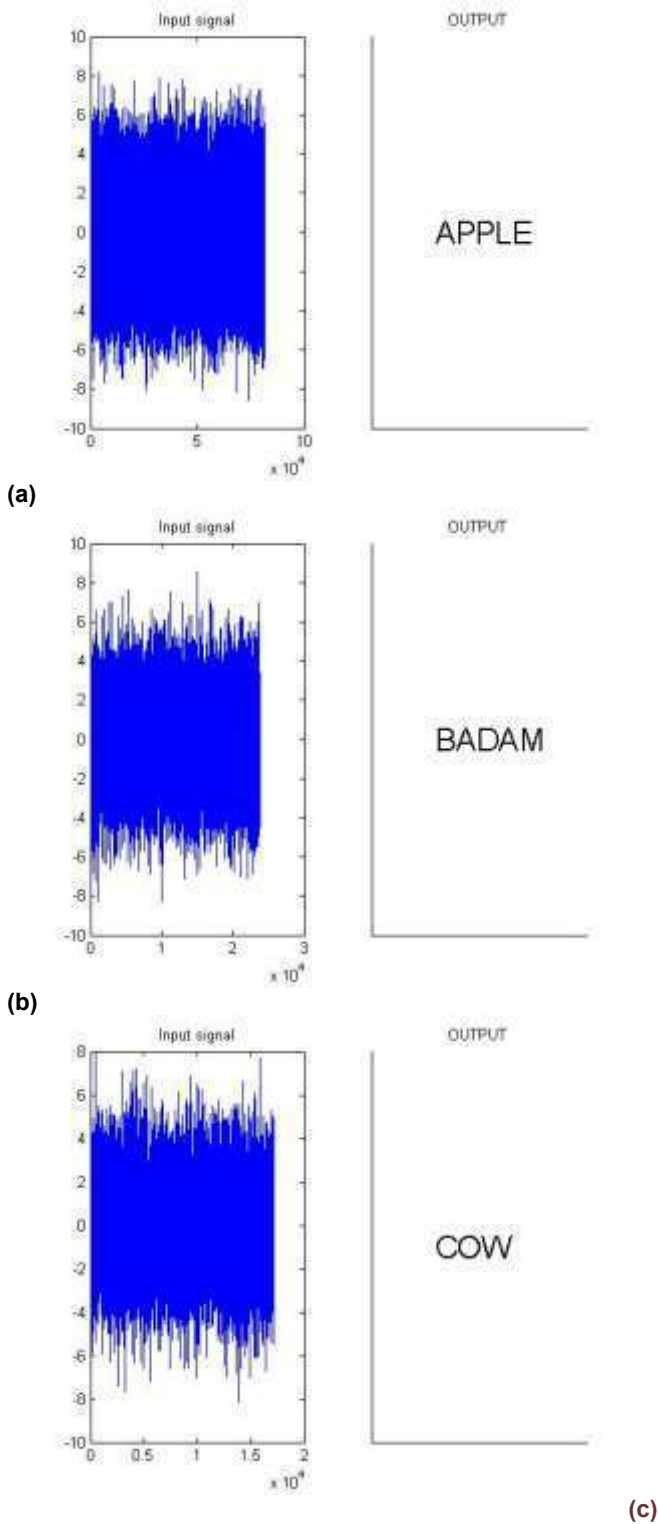


Fig. 6: Text display; (a) Apple, (b) Badam, (c) Cow

Then, analyze the performance of ANN classifier based on the Sensitivity, classification Accuracy, Specificity, Negative Predictive Value (NPV), Positive Predictive Value (PPV), False Discovery Rate (FDR), Matthews Correlation Coefficient (MCC) and False Positive Rate (FPR). For these performance measures the graphical representation is shown in [Fig. 7].

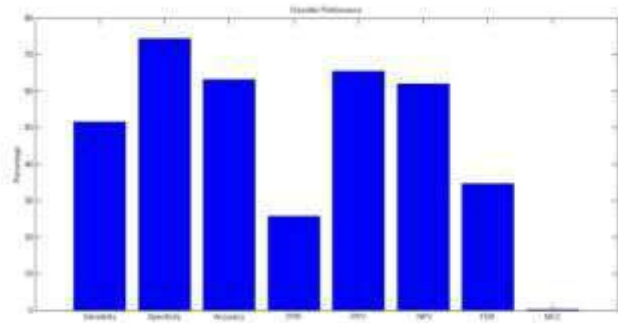


Fig.7: Classification Performance of proposed ASR

The classifier performance of the proposed ASR system is shown in [Fig. 7]. The performance obtained for Specificity, Sensitivity, FPR, Accuracy, NPV, PPV, MCC and FDR are 74%, 50%, 26%, 62%, 60%, 65%, 0.19% and 35% respectively. These results displays that the proposed ASR system can satisfy the required performance like accuracy sensitivity and specificity for identifying the spoken word. We can show that the proposed system is a suitable approach for automatic speech recognition from these performance analyses and result.

## CONCLUSION

The spoken speech signal is converted in to corresponding text by the proposed automatic speech recognition system. Three stages are comprised in the proposed ASR system; at first stage preprocessing the spoken speech signal to detect the isolated word and to remove noise. The sum of eight features such as sampling point, word length, Mean, pitch, Skewness, Variance, Entropy and Kurtosis are extracted in the second stage. In the final level, the word spoken gets recognized with the help of features extracted in the previous stage and the corresponding text is displayed. With back propagation training using ANN classifier the identification of word occurs. The proposed system's performance was scrutinized for three signal samples like Badam, Apple and Cow explained the corresponding waveform. Then based on the accuracy, classification accuracy and specificity the classifier's performance was analyzed. The complete performance shows that for the man machine interaction the proposed system for the ASR is the best option. The ASR system we proposed provide enhanced performance so it is suitable for a real time human and machine interaction over speech. The ASR system's performance will further improved by the influence of a novel classifier approach in future.

## CONFLICT OF INTEREST

There is no conflict of interest.

## ACKNOWLEDGEMENTS

The authors are thankful to Hon'ble Dean and Management

## FINANCIAL DISCLOSURE

None.

## REFERENCES

- [1] Bedros, Renee, Charles PB, Arch WB, Francis MC, Brian AI, George HQ, David Spoor, Stephen RS, and David JW. [1993] Multimedia interface and method for computer system. U.S. Patent 5,208,745, issued May 4, 1993.
- [2] Trentin, Edmondo, and Marco Gori. [2001] A survey of hybrid ANN/HMM models for automatic speech recognition. *Neurocomputing*, 37(1):91-126.
- [3] Furui and Sadaoki. [2005] 50 years of progress in speech and speaker recognition. *SPECOM 2005*, Patras, 1-9.
- [4] Childers DR, Cox V, DeMori R, Furui S, Juang BH, Mariani JJ, Price P, Sagayama S, Sondhi MM, and Weischedel R. [1998] The past, present, and future of speech processing. *IEEE signal processing magazine*, 15(3):24-48.
- [5] Gaikwad, Santosh K, Bharti WG, and PravinYannawar. [2010] A review on speech recognition technique. *International Journal of Computer Applications*, 10(3):16-24.
- [6] JuangBH, and Rabiner LR.[2005]Automatic speech recognition—a brief history of the technology development. Georgia Institute of Technology.Atlanta Rutgers University and the University of California, Santa Barbara, 1.
- [7] Krim Hamid, and Mats Viberg. [1996] Two decades of array signal processing research: the parametric approach. *Signal Processing Magazine*, 13(4):67-94.
- [8] Li Jinyu, Li Deng, Dong Yu, Yifan Gong, and Alex Acero. [2009] A unified framework of HMM adaptation with joint compensation of additive and convolutive distortions. *Computer Speech & Language*, 23(3):389-405.
- [9] Anusuya MA, and S.K. Katti SK. [2009] Speech Recognition by Machine: A Review. *International Journal of Computer Science and Information Security*, 6(3):181-205.
- [10] Viikki, Olli, and Kari Laurila. [1998] Cepstral domain segmental feature vector normalization for noise robust



- speech recognition. *Speech Communication*, 25(1):133-147.
- [11] Kalinli, Ozlem, Michael LS, and Alex Acero. [2009] Noise adaptive training using a vector Taylor series approach for noise robust automatic speech recognition. In Proceedings of IEEE International Conference on Acoustics, Speech and Signal Processing, 3825-3828.
- [12] Leggetter CJ, and Woodland PC. [1995] Maximum likelihood linear regression for speaker adaptation of continuous density hidden Markov models. *Computer Speech Languages*, 9(2):171-185.
- [13] Gauvain J-L, and Lee CH. [1994] Maximum a posteriori estimation for multivariate gaussian mixture observations of Markov chains. *IEEE Transactions on Speech Audio Process*, 2:291-298.
- [14] Dupont, Stéphane, and JuergenLuettin. [2000] Audio-visual speech modeling for continuous speech recognition. *IEEE Transactions on Multimedia*, 2(3):141-151.
- [15] Ververidis, Dimitrios, and Constantine Kotropoulos. [2006] Emotional speech recognition: Resources, features, and methods. *Speech communication*, 48(9):1162-1181.
- [16] Kyung Hak Hyun, Eun Ho Kim and Yoon-Keun Kwak. [2007] Emotional Feature Extraction Based On Phoneme Information for Speech Emotion Recognition. In Proceedings of 16th IEEE International Symposium on Robot and Human Interactive Communication, 802-806.
- [17] Kalinli, Ozlem, Michael LS, Jasha Droppo, and Alex Acero. [2010] Noise adaptive training for robust automatic speech recognition. *IEEE Transactions on Audio, Speech, and Language Processing*, 18(8):1889-1901.
- [18] Boll S. [1979] Suppression of acoustic noise in speech using spectral subtraction. *IEEE Transactions on Acoustic Speech Signal Process*, 27(2):113-120.
- [19] Yu D, Deng L, J Droppo J, Wu J, Gong Y, and Acero A. [2008] A minimum-mean-square-error noise reduction algorithm on mel-frequency cepstra for robust speech recognition. In Proceedings of ICASSP, Las Vegas, NV, 4041-4044.
- [20] Deng L, Acero A, Plumpe M, and Huang X. [2000] Large-vocabulary speech recognition under adverse acoustic environments. In Proceedings of ICSLP, Beijing, China, 806-809.
- [21] Saon G, Huerta JM, and Jan EE. [2001] Robust digit recognition in noisy environments: The IBM Aurora 2 system. In Proc. Interspeech, Aalborg, Denmark, 629-632.
- [22] Cui X and Alwan A. [2005] Noise robust speech recognition using feature compensation based on polynomial regression of utterance SNR. *IEEE Transaction on Speech Audio Processing*, 13(6):1161-1172.
- [23] Yixiong Pan, Peipei Shen and Liping Shen. [2012] Speech Emotion Recognition Using Support Vector Machine. *International Journal of Smart Home*, 6(2):101-108.
- [24] Navdeep Kaur and Sanjay Kumar Singh. [2012] Data Optimization in Speech Recognition using Data Mining Concepts and ANN. *International Journal of Computer Science and Information Technologies*, 3(3):4283-4286.
- [25] Poonkuzhali C, Karthiprakash R, Valarmathy S, and Kalamani M. [2013] An Approach To Feature Selection Algorithm Based on Ant Colony Optimization For Automatic Speech Recognition. *International Journal of Advanced Research in Electrical, Electronics and Instrumentation Engineering*, 2(11):5671-5678.
- [26] Petko NP, Gustav EjeHenter, Bastiaan Kleijn W. [2013] Maximizing Phoneme Recognition Accuracy for Enhanced Speed Intelligibility in Noise. *IEEE Transaction on Audio, Speech and Language Processing*, 21(5):1035-1045.
- [27] Siddhant CJ, Cheeran AN. [2014] MATLAB Based Back-Propagation Neural Network for Automatic Speech Recognition. *International Journal of Advanced Research in Electrical, Electronics and Instrumentation Engineering*, 3(7):10498-10504.
- [28] Deniz Baskent, Cheryl L, Eiler and Brent Edwards. [2010] Phonemic restoration by hearing-impaired listeners with mild to moderate sensorineural hearing loss. *Hearing Research*, 260(1-2):54-62.
- [29] Liu X, Gales MJF, and Woodland PC. [2013] Language model cross adaptation for LVCSR system combination. *Computer Speech and Language*, 27(4):928-942.
- [30] Wooil Kim and Richard MS. [2011] Mask classification for missing-feature reconstruction for robust speech recognition in unknown background noise. *Speech Communication*, 53(1):1-11.
- [31] Picone L. [1993] Signal modeling technique in Speech Recognition. *IEEE ASSP Magazine*, 81(9):1215-1247.
- [32] Hwang T, and Chang S. Energy Contour enhancement for noisy speech recognition. *International Symposium on Chinese Spoken Language Processing*, 1:249-252.
- [33] Rabiner L, and Sambur M. [1976] Some Preliminary experiments in the recognition of connected digits. *IEEE Transactions on Acoustics, Speech and Signal Processing*, 24(2):170-182.
- [34] Abdulla W. [2002] HMM-based techniques for speech segment extraction. *Scientific programming*, IOS Press, Amsterdam, The Netherlands, 10(3):221-239.
- [35] Becchetti C, and Ricotti L. [2004] *Speech Recognition Theory and C++ Implementation*. John Wiley & Sons, Wiley Student Edition, Singapore, 121-188.
- [36] Ney H. [2003] An optimization algorithm for determining the end points of isolated utterances. In Proceedings of IEEE International Conference on Acoustics, Speech, and Signal Processing (ICASSP), 7(3):26-41.
- [37] T Yuvaraja, M Gopinath. [2014] Fuzzy Based Analysis of Inverter Fed Micro Grid in Islanding Operation. *International Journal of Applied Engineering Research* ISSN 0973-4562 9(1)16909-16916.
- [38] Yuvaraja Teekaraman, Gopinath Mani. [2015] Fuzzy Based Analysis of Inverter Fed Micro Grid in Islanding Operation-Experimental Analysis. *International Journal of Power Electronics and Drive System (IJPEDS)* 5(4): 464-469
- [39] T Yuvaraja, K Ramya. [2016] Implementation of Control Variables to Exploit Output Power for Switched Reluctance Generators in Single Pulse Mode Operation. *IJE TRANSACTIONS A: Basics* 29(4): 505-513.

## ARTICLE

# INVESTIGATION ON QUALITY ASSURANCE & QUALITY CONTROL IN HIGH RISE BUILDINGS

P Siva Sankar<sup>1</sup>, K J Brahma Chari<sup>2\*</sup>, Tanmai R<sup>3</sup>, V Ranga Rao<sup>4</sup>

<sup>1,3</sup>Dept of Civil Engineering, Chirala Engineering College, Chirala, AP- 523157, INDIA

<sup>2,4</sup>Dept of Civil Engineering, K L University, Vaddeswaram, Guntur, AP-522502, INDIA

### ABSTRACT

Quality control in construction typically involves insuring compliance with minimum standards of material and workmanship in order to insure the performance of the facility according to the design. These minimum standards are contained in the specifications described in the previous section. For the purpose of insuring compliance, random samples and statistical methods are commonly used as the basis for accepting or rejecting work completed and batches of materials. Constructions of high rise building provide the comfort living standard for the people and also help in the planning of the cities. Defects or failures in constructed facilities can result in very large costs. Even with minor defects, re-construction may be required and facility operations impaired. Increased costs and delays are the result. In the worst case, failures may cause personal injuries or fatalities. The main purpose of this paper is to present the Quality Assurance & Quality Control in High Rise Buildings. Specifications of work quality are an important feature of facility designs. Also for the high rise building the requirements and laboratory tests that are essential for it are mentioned. This chapter also shows the importance of analytical quality assurance during the construction process and presents an introduction to successful and economic method development.

### INTRODUCTION

Infection Quality is an important factor when it comes to any product or service. With the high market competition, quality has become the market differentiator for almost all products and services. Therefore, all manufacturers and service providers out there constantly look for enhancing their product or the service quality. In order to maintain or enhance the quality of the offerings, manufacturers use two techniques, quality control and quality assurance. These two practices make sure that the end product or the service meets the quality requirements and standards defined for the product or the service. There are many methods followed by organizations to achieve and maintain required level of quality. Some organizations believe in the concepts of Total Quality Management (TQM) and some others believe in internal and external standards. The standards usually define the processes and procedures for organizational activities and assist to maintain the quality in every aspect of organizational functioning. When it comes to standards for quality, there are many. ISO (International Standards Organization) is one of the prominent bodies for defining quality standards for different industries. Therefore, many organizations try to adhere to the quality requirements of ISO. In addition to that, there are many other standards that are specific to various industries.

As an example, SEI-CMM is one such standard followed in the field of software development. Since standards have become a symbol for products and service quality, the customers are now keen on buying their product or the service from a certified manufacturer or a service provider. Therefore, complying with standards such as ISO has become a necessity when it comes to attracting the customers.

- A high standard or level
- Degree of excellence
- Distinguishing feature
- Satisfaction of a customer's needs or requirements
- Quality is "totally of characteristics of an entity that bear on its ability to satisfy stated and implied

Quality inspections on site (Site Supervision):

- Attend contractor(s) progress meetings
- Review and check the contractor(s) methods and techniques
- Monitor the contractor(s) QA/QC procedures
- Review and witness all fields tests and inspections

Quality Control:

The operational techniques and activities that are used to fulfill requirements for quality and various statistical analyses used to verify continued system performance.

For the (whole) project execution, the contractor shall maintain a quality system that is based upon international accepted standards. This quality system is described (by the contractor) in a specific "Project Quality Plan", which should include subjects as project organization, procedures to be applied during engineering, procurement, fabrication, construction and commissioning and a summary of quality control plans.

Many people get confused between quality control (QC) and quality assurance (QA). Let's take a look at quality control function in high-level. As we have already discussed, organizations can define their own internal quality standards, processes and procedures; the organization will develop these over time and then relevant stakeholders will be required to adhere by them. The process of making sure that the stakeholders are adhered to the defined standards and procedures is called quality control. In quality control, a verification process takes place. Certain activities and products are verified against a defined set

#### KEY WORDS

Schistosoma nasale,  
cross H.F cow, Anthioma  
line

Published: 20 October 2016

\*Corresponding Author  
Email  
chari.k285@gmail.com

of rules or standards. Every organization that practices QC needs to have a Quality Manual. The quality manual outlines the quality focus and the objectives in the organization. The quality manual gives the quality guidance to different departments and functions. Therefore, everyone in the organization needs to be aware of his or her responsibilities mentioned in the quality manual.

Quality Assurance:

In order to deliver products which continuously meet the requirements, (sub) contractors have to produce according to a quality control plan. These quality control plans have to include all certified material deliveries, component manufacturing steps, factory acceptance tests and site acceptance tests. Quality Assurance is a broad practice used for assuring the quality of products or services.

There are many differences between quality control and quality assurance. In quality assurance, a constant effort is made to enhance the quality practices in the organization. Therefore, continuous improvements are expected in quality functions in the company. For this, there is a dedicated quality assurance team commissioned. Sometimes, in larger organizations, a 'Process' team is also allocated for enhancing the processes and procedures in addition to the quality assurance team. Quality assurance team of the organization has many responsibilities. First and foremost responsibility is to define a process for achieving and improving quality. Some organizations come up with their own process and others adopt a standard processes such as ISO or CMMi. Processes such as CMMi allow the organizations to define their own internal processes and adhere by them. Quality assurance function of an organization uses a number of tools for enhancing the quality practices. These tools vary from simple techniques to sophisticated software systems. The quality assurance professionals also should go through formal industrial trainings and get them certified. This is especially applicable for quality assurance functions in software development houses. Since quality is a relative term, there is plenty of opportunity to enhance the quality of products and services. The quality assurance teams of organizations constantly work to enhance the existing quality of products and services by optimizing the existing production processes and introducing new process

## ABOUT MY HOME ABHRA

- Heart Of Modern Hyderabad
- Well Connected To Other Parts Of The City Through A Network Of Wide Roads Bustling Shopping And Entertainment Hub
- A Host Of Hospitals, Schools, Banks, ATM's And Sports Institutions In Close Proximity
- Swift Access To Airport Via Outer Ring Road
- Investment Goldmine

### Expanse

- Private Home Theater Lounge
- Marble Flooring Of Premium Quality
- Serene And Safe Ground Level With Minimal Vehicular Movement
- Floor To Floor Height Of 10'4"
- Dry And Wet Kitchen In Selected Apartment
- Accommodation For Domestic Help In Select Apartments
- 73% Open Space

### Comfort

- Jogging track
- Indoor air-conditioned squash & shuttle courts
- Basketball court
- Indoor swimming pool
- Gym & spa
- Library & secured
- Outdoor & indoor children's play area
- Landscaped central plaza
- Reticulated pipe gas system
- Metered water and electricity
- Garbage disposal system and servant toilets at every alternate mid-landing level

- Provision for centralized VRV system for air-conditioning
- Car wash area and centralized laundry
- 24x7 security system
- Access ramps at all entrances provided for physically challenged
- Sewage treatment plant
- 

#### Home features

- Living, Dining and family room
- Amalgamated/ imported marble flooring of reputed make
- Smooth putty finish with 2 coats of premium acrylic emulsion paint of reputed make over a coat of primer
- Teak wood/granite door frames with veneered flush door shutters, melamine finish & reputed hardware
- UPVC door frames with clear float glass paneled shutters and designer hardware of reputed make for French doors
- UPVC window site with clear float glass with suitable finishes as per design, with provision for mosquito mesh track
- Aesthetically designed mild steel (M.S) grills with enamel paint finish

#### Bed room

- 600 x 600 mm size double charged vitrified tiles / wooden flooring
- Smooth putty finish with 2 coats of premium acrylic emulsion paint off reputed make over a coat of primer
- Teak wood / granite door frames with veneered flush door shutters, with melamine finish & reputed hardware
- UPVC window system with clear float glass that are equipped with sliding shutters and a provision for mosquito mesh track

#### Bath rooms

- Acid resistant, anti-skid ceramic tiles of reputed make. Glazed ceramic tile dado of reputed make up to 7'-4" height
- Kohler, Roca, Depravity or equivalent fittings
- Vanity type counter top
- EWC with flush valve of best brands
- Single lever with wall mixer cum shower of best brands
- Provision for geysers in all bathrooms

#### Kitchen

- 600 x 600 mm size double charged vitrified tiles
- Smooth putty finish with 2 coats of premium acrylic emulsion paint of reputed make over a coat of primer
- Glazed ceramic tiles dado up to 2'-0" height above kitchen platform of reputed make
- Supply of gas from centralized gas bank to all individual flats with pre-paid gas meters
- Granite platform with stainless steel sink
- Provision for fixing of water purifier, exhaust fan & chimney
- Provision for geyser for hot water near the sink
- Basketball Courts, Children's Play Area
- Indoor Air-Conditioned Badminton And Squash Courts
- Fully-Equipped State-Of-The-Air Gym / Spa
- Indoor Swimming Pool

#### Specifications

- Number of towers 5
- Number of floors per tower G+17
- Number of flats 387
- Number of flats per floor 2 and 5
- Land area 5 Acres
- Sizes:
- 3 & 4 BHK lifestyle apartments ranging from 2310 to 4650 S.ft
- Parking: 2 level parking (Basement I and Basement II)
- Number of lifts per tower 3
- Earthquake resistance structure
- Vaastu compliant and eco-friendly building

#### Structure

- R.C.C framed structure : R.C.C framed structure to withstand wind and seismic loads
- Superstructure: 8" thick solid blocks for external walls and 4" thick blocks for internal walls

#### Plastering

- Internal : 1 coat of plastering for walls
- External : 2 coats of plastering for external walls

#### Doors

- Main door: Teak wood / granite door frames with veneered flush door shutters, melamine finished & reputed hardware
- Internal doors: Teak wood / granite door frames with veneered flush door shutters, melamine finished & reputed hardware
- French doors (if any): UPVC door frames with clear float glass paneled shutters and designer hardware of reputed make
- Windows: UPVC windows system with clear float glass with suitable finishes as per design, with provision for mosquito mesh track
- Grills: Aesthetically designed, mild steel (M.S) grills with enamel paint finish

#### Paintings

- External: Textured / smooth finish with two coats of exterior emulsion paint of reputed make
- Internal: smooth putty finish with 2 coats of premium Acrylic emulsion paint of reputed make over a coat of primer

#### Flooring

- Living, dining: Amalgamated marble / imported marble flooring of reputed make
- All Bedrooms & kitchen: 600 x 600 mm size double charged vitrified tiles
- Bathrooms: Anti-skid ceramic tiles – of reputed make
- All Balconies: Rustic vitrified tile to reputed make
- Staircase/corridor: Marble

#### Dadoing

- Dadoing in kitchen: Glazed ceramic tiles dado up to 2'-0" height above kitchen platform of reputed make
- Bathrooms: Glazed ceramic tile dado of reputed make up to 7'-4" height
- Servants' rooms & utility: Rustic vitrified tile of reputed make

#### Parking management

- Entire parking is well designed to suit the number of cars parks, provision of parking signage's at required places for ease of driving

#### Fire and Safety

- Fire hydrant and fire sprinkler system in all floors and basements
- Fire alarm and public address system in all floors and parking areas (basements)
- Control panel will be kept at main security



## Facilities for physically Challenged

- Access ramps at all entrances shall be provided for physically challenged

### Kitchen:

- Tiles dado up to 3' height in utility wash areas
- Granite platform with stainless steel sink
- Provision for fixing of water purifiers, exhaust fan & chimney
- Provision for geyser for hot water near the sink

### Utilities / wash

- Dish washer and washing machine provision in the utility area

### Bathrooms

- Vanity type wash basin / counter top
- EWC with flush tank of best brands
- Single lever fixtures with wall mixer cum shower of best brands
- Provision for geysers in all bathrooms
- All C.P fittings are chrome plated of best brands

### Electrical

- Concealed copper wiring of best brands
- Power outlets for air-conditioners in all rooms
- Power outlets for geysers in all bathrooms
- Power plug for cooking range chimney, refrigerator, microwaves ovens, mixer / grinders in kitchen, washing machine and dish washer in utility area
- Three phase supply for each unit and individual meter boards
- Miniature circuit breakers (MCB) for each distribution boards are of best brands

### Telecom / Internet / Cable TV:

- FTH with Wi-Fi internet DTH, Telephone & intercom.

### Lifts

- High speed automatic passenger lifts with rescuer device with V3F for energy efficiency
- One service lifts with V3F for energy efficiency for each tower. Entrance with granite / marble cladding.

### WTP & STP

- Fully treated water made available through exclusive water softening and purification plant in case of bore-well water, water meters for each unit
- A sewage treatment plant of adequate capacity as per norms will be provided inside the project, treated sewage water will be used for the landscaping and flushing purpose

### Generator

- D.G set backup with acoustic enclosure & A.M.F

### Security / BMS

- Sophisticated round-the-clock security system
- Panic button and intercom is provided in the lifts connected to the security room
- Solar power fencing around the compound
- Surveillance cameras at the main security and entrance of each block & in all lifts
- Video door phone for each apartment connected to security for screening for the visitors

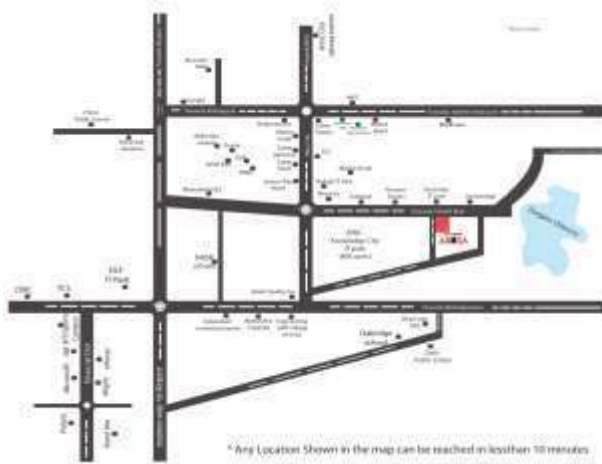


Fig. 1: Location map

**LPG:**

- Supply of gas from centralized gas bank to all individual flats with pre-paid gs meters
- Centralized Air-Conditioning:
- Provision for centralized VRV system for all rooms as per the requirement of approved make.

S.No	Trial No	Amount of cement	Amount of water	Depth of penetration
1	1	500 grams	150 mm <sup>3</sup>	16 mm
2	2	500 grams	155 mm <sup>3</sup>	9 mm
3	3	500 grams	160 mm <sup>3</sup>	5 mm

**METHODOLOGY**

**CONCRETE**

Building material in use since Roman times, made up of four main ingredients: coarse aggregate (gravel, usually more than 4.75 mm), fine aggregate (sand, usually less than 4.75 mm), Portland cement, and water. Air too plays an important part, and often special additives (called admixtures) are also added to improve or modify the concrete's properties.

Concrete in various forms is being commonly used in the constructional field these days. The use of cement concrete is becoming more and more popular in construction engineering where strength and durability are of prime importance. Plain cement concrete, Reinforced cement concrete and per-stressed cement concrete are replacing other construction material due to their better appearance, high crushing strength, more durability, imperviousness, quickness and ease of monolithic construction, less maintains cost etc.

**QUALITY ASSURANCE**

For the quality assurance we are conducted laboratory tests on cement, aggregate and hardened concrete. The tests on Cement conducted are Fineness, Consistency, Initial and final setting time, Soundness. The tests on Aggregates conducted are Sieve analysis, Water absorption, Aggregate abrasion value, Aggregate impact value, Aggregate crushing value. The tests on Hardened Concrete conducted are Non-destructive tests, Rebound hammer, Ultrasonic pulse velocity, and Compression test.

**RESULTS**

The following tests are conducted on cement for the quality assurance.

**Tests on cement**

**FINENESS:**

W1=Total weight of cement

W2=Total weight of residue  
Total weight of cement w1=100g  
Total weight of residue w2=13.4g  
% of fines=86.6%

**CONSISTENCY:**

Taking fresh samples of cement and different quantities of water until the reading on the Vicat apparatus gauge 5 to 7mm.  
We made three trials to achieve our result of the normal consistency using fresh cement in each trial.

**Table 1:** Determination of consistency of cement

S.N	DETAILS	TRAIL
1	WEIGHT OF AGGREGATE SAMPLE IN CYLINDRICAL MEASURE, W1 G (EXCLUDING EMPTY WEIGHT OF CYLINDRICAL MEASURE)	0.350
2	WEIGHT OF CRUSHED AGGREGATES AFTER PASSING THROUGH 2.36MM SIEVE W2 G	0.030
3	AGGREGATE IMPACT VALUE [W2/W1 * 100]	8.57%

Express the amount of water as a percentage of the weight of dry cement to the first place of decimal.

**INITIAL AND FINAL SETTING TIME:**

**Table 2:** Determination of Initial & Final setting time

S.No	Time	Penetration
1	5 min	0 mm
2	20 min	1 mm
3	35 min	5 mm
4	55 min	6 mm
5	70 min	7 mm

The initial setting time is 35 min  
The final setting time is 10 hours.

**TESTS ON AGGREGATES**

The results of the sieve analysis may be recorded graphically on a semi-log graph with particle size as abscissa (log scale) and the percentage smaller than the specified diameter as ordinate.  
The results should be calculated and reported as:

- The cumulative percentage by weight of the total sample
- The percentage by weight of the total sample passing through one sieves and retained on the next smaller sieve, to the nearest 0.1 percent.

**Table 3:** Sieve Analysis

S. No	SIEVE SIZE	MASS RETAINED (G)	% RETAINED	CUMULATIVE % RETAINED	CUMULATIVE % PASSING
1	13.20MM	0	0	0	100
2	9.50MM	371.80	18.60	18.60	81.40
3	6.70MM	392.50	19.60	38.20	61.80
4	4.75MM	222.10	11.10	49.30	50.70
5	2.36MM	387.50	19.40	68.70	31.30
6	1.70MM	97.90	4.90	73.60	26.40
7	1.18MM	109.10	5.50	79.10	20.90
8	4.25µM	170.80	8.60	87.70	12.30
9	300µM	45.80	2.30	90.00	10.00
10	150µM	76.70	3.80	93.80	6.20
11	<150µM	123.00	0.00	0.00	0.00
	TOTAL	1992.20	100		

**AGGREGATE ABRASION VALUE:**

Grade of the material = B  
Number of Spheres Used = 11  
Weight of charge = 4580  
Size of the aggregate = Passing through 20 & retained on 12.5mm  
Number of revolutions = 500  
Speed of rotation= 30-33 rpm

**AGGREGATE IMPACT VALUE:**

The Impact value of the given aggregate is 8.57% . Which lies <10%. Hence, the aggregates are exceptionally strong.

Table 4: Determination of aggregate impact value

**Aggregate Crushing Value:**

Size of the aggregate: passing through 12.5mm & retained on 10mm IS sieve. Rate of application of load: 4 tons/min  
Total load applied: 40 tons

Table 5: Determination of aggregate crushing value

S.No	Details	Trail
1	Weight of aggregate sample in the cylindrical measure. W1 gm	3.250kg
2	Weight of crushed aggregates after passing through 2.36mm seive , W2g	0.610kg
3	Aggregate crushing value [W2/W1 * 100]	8.76kg

**TESTS ON HARDENED CONCRETE:**

**NON-DESTRUCTIVE TESTS:**

**REBOUND HAMMER:**

The rebound reading on the indicator scale has been calibrated by the manufacturer of the rebound hammer for horizontal impact, that is, on a vertical surface, to indicate the compressive strength. When used in any other position, appropriate correction as given by the manufacturer is to be taken into account.

**ULTRASONIC PULSE VELOCITY:**

The quality of concrete in terms of uniformity, incidence or absence of internal flaws, cracks and segregation, etc., indicative of the level of workmanship employed, can thus be assessed using the guidelines given below, which have been evolved for characterizing the quality of concrete in structures in terms of the ultrasonic pulse velocity.

Table 6: Determination of concrete quality

S.No	PULSE VELOCITY (KM/SECOND)	CONCRETE QUALITY (GRADING)
1	ABOVE 4.5	EXCELLENT
2	3.5 TO 4.5	GOOD
3	3.0 TO 3.5	MEDIUM
4	BELOW 3.0	DOUBTFUL

**QUALITY CONTROLLING:**

For the quality controlling the Workability test, Slump cone test, Compacting factor test, Vee-Bee test, Compressive strength, Split Tensile Strength, Flow Test tests are conducted on Fresh Concrete.

**FRESH CONCRETE:**

When the binding material (Cement or lime), fine aggregate (generally sand), Coarse aggregate (such as crushed stones, broken bricks etc) and water are mixed together in suitable proportions, they form an easily workable mix, known as plastic, wet or green concrete. Which is easy with which concrete will flow Following are the important properties of fresh concrete

- Workability
- Bleeding and segregation
  - a) Bleeding
  - b) Segregation
  - c) laitance
- Hydration
- Air entrainment

**4 SITE OBSERVATION**

The following observations are noted in field for the quality control and quality assurance

**5.1 P.C.C: Plain Cement Concrete:**

Plain cement concrete (PCC) is used to provide rigid impervious bed to RCC in foundation where the earth is soft and yielding. PCC can be used over brick flat soling or without brick flat soling. Plain cement concrete can also called only "cement concrete (CC)" or "binding concrete"

- Check the dimensions of form work of PCC before mixing concrete.
- Check polythene sheet is laid over PCC bed.
- Check the concrete slump (maximum slump should be 75mm)
- Check the thickness level of PCC before casting by putting steel pegs in concreting area or putting level pillar of fresh concrete at suitable distance
- Check the finish level of PCC by thread fixing with nails in form work.
- Inspect if the concrete is placing gently

## 5.2 RCC: Reinforced Cement Concrete

The following observations assurance Footing, Column Starters Columns, Beams, Slabs, Shear walls, Stair Cases are noted in field for the quality control and quality.

### Footings:

Footings are structural elements that transmit column or wall loads to the underlying soil below the structure. Footings are designed to transmit these loads to the soil without exceeding its safe bearing capacity, to prevent excessive settlement of the structure to a tolerable limit, to minimize differential settlement, and to prevent sliding and overturning.

Footings are laid above the PCC to support the structure according to the dimensions given in the plan with Reinforcement

- Marking of Footings
- Laying of footings
- Checking of Footings

### Marking of footing:

According to the grid lines marked on the site the PCC is laid, that grids are transferred to the PPC and by that reference the marking of the footing is done

### Laying of Footing:

Laying of footing is done on PPC, it required all the shuttering works and the reinforcement works

### hecking of Footings:

1. Reinforcement check
2. Shuttering checks

### Reinforcement Checks:

1. Steel Placing: The steel has to be placed in a proper way as per the drawings
2. Spacing: After placing the steel the spacing should be checked properly with the reference of the markings and weather there are as per the drawings or not
3. Number of Bars: Check whether the given number of bars is placed or not
4. Diameter of Bars: This is the important factor that will consider mainly while laying of the reinforcement. The diameter of the bars has to be placed in the same direction as given in the drawings.
5. Chair height calculations: Mainly chairs are provided to avoid the contact of the top mat to the bottom mat. The height of the chairs is dependent on the depth of footing
6. Alignments: In this reinforcement checks the alignments are checked by considering the covers on the all sides of the footing

## 5.3 Shuttering Checks:

1. Profile (level): Weather the top of the footing is level or not has to be checked in these checks.
2. Alignments: The footings are to be laid in the same alignments, if not there may be a chances of changing the position of the footing
3. Plumb: The vertical of the footing is checked by using the plump
4. Dimensions: The dimensions of footing as to be laid same in the site as per the drawings given. For that, the dimensions of the footings can be accurately checked
5. Diagonal : After marking the footing dimensions on the PCC it has to be checked diagonally  
Supports: After providing the shuttering works it has to support by some supports, so that can avoid the leakage of the concrete when it is poured. For providing this supports the excavations has to be done 1 feet extra excluding the dimension of the footing not in the depth.
6. Gaps: The gaps between the shuttering works has to be avoided, so when the concrete is poured the leakage can be arrested
7. Covers: After laying of the reinforcement the covers has to be checked. If it is not, there may be chances of increasing the cover at one side and decreasing the cover at other side

### COLUMN STARTERS:

This work is done immediately after the completion of the footing. It is done just to support the column shuttering. The height of the column starters are in between 3" to 6"

Advantages of Column Starters:

- It will support the shuttering in the proper position
- Leakage of the concrete is controlled by using this starters

COLUMN: Column or pillar in architecture and structural engineering is a structural element that transmits, through compression, the weight of the structure above to other structural elements below

Checks conducted for the columns

- Reinforcement Checks
- Shuttering Checks



#### Reinforcement Checks:

- 1 Steel Placing: The steel has to be placed in a proper way as per the drawings
- 2 Spacing: After placing the steel the spacing should be checked properly with the reference of the markings and weather there are as per the drawings or not.
- 3 Number of Bars Check whether the given number of bars are placed or not.
- 4 Diameter of Bars: This is the important factor that will consider mainly while laying of the reinforcement. The diameter of the bars has to be placed in the same direction as given in the drawings

#### Lapping:

- Steel reinforcement usually comes in 6m (200 ft) and 12m (40ft) lengths. In such cases where the steel reinforcement is required to exceed these lengths, or other cut lengths then a splice is required. This lap length as we would discuss varies depending on the bars sizes as there are various bar sizes and where the bars are lapped and/or which structural member or element the lapping occurs.

#### Shuttering Checks

**Alignments:** The footings are to be laid in the same alignments; if not there may be chances of changing the position of the footing

**Plumb:** The vertical of the footing is checked by using the plumb

**Dimensions:** The dimensions of footing as to be laid same in the site as per the drawings given. For that, the dimensions of the footings can be accurately checked

**Diagonal:** After marking the footing dimensions on the pcc it has to be checked diagonally

**Supports:** After providing the shuttering works it has to supported by some supports, so that can avoid the leakage of the concrete when it is poured. For providing this supports the excavations has to be done 1 feet extra excluding the dimension of the footing not in the depth

**Gaps:** The gaps between the shuttering works has to be avoided, so when the concrete is poured the leakage can be arrested

**Covers:** After laying of the reinforcement the covers has to be checked. If it is not, there may be chances of increasing the cover at one side and decreasing the cover at other side.

**BEAMS:** A beam is a structural member which spans horizontally between supports and carries loads which act at right angles to the length of the beam. Furthermore, the width and depth of the beam are "small" compared with the span. Typically, the width and depth are less than span/10

#### Types of beams used in these constructions:

1. Inverted beam
2. Concealed beam
3. T- beams

**Inverted beam:** The beam whose bottom level is same that of slab called inverted beam, likely to be used only in top slab of the building to give good view for inner face of the building

**Concealed beam:** The Hidden beam is a means to describe the load dispersion on to supporting slab. Hidden beams are generally inserted within the suspended slabs where slab thickness is considerable. The hidden beam is not a beam and the only means to spread the concentrated load of the walls on the slab area. Hidden beam between balcony and room is very common to facilitate easy inclusion of balcony into room space later. It is also known as "Concealed Beam".

#### T-beam:

Concrete alone is brittle and thus overly subject to the shear stresses a T-beam faces where the web and flange meet. This is the reason that steel is combined with concrete in T-beams.

**SLAB:** A slab is structural member, whose dimensions are small compared to its length. A concrete slab is a common structural element of modern buildings. Horizontal slabs of steel reinforced concrete, typically between 100 and 500 millimeters thick, are most often used to construct floors and ceilings, while thinner slabs are also used for exterior paving.

#### Types of Slabs:

1. PT Slabs
2. RCC slab
3. Flat Slabs
4. Grade Slabs

#### PT Slabs:

Post-tensioned concrete is a term heard more and more in the construction industry today. This method of reinforcing concrete enables a designer to take advantage of the considerable benefits provided by pre stressed concrete while retaining the flexibility afforded by the cast-in-place method of building concrete structures

- PT slabs are used for longer span instead of using beams
- PT slab consist of tendons as per design
- Tendon consist of number of stand as per design
- The diameter of each tendon is 12.7mm
- Tendons are laid along/parallel with the longer span
- In PT slab we consider live load only
- At the supports, tendons will be placed over the top reinforcement and in the middle, tendons will be laid over the bottom reinforcement
- After laying tendons concreting is done
- After attaining 100% strength, stressing of tendons is done. Later grouting is done



Fig 2: Reinforcement System

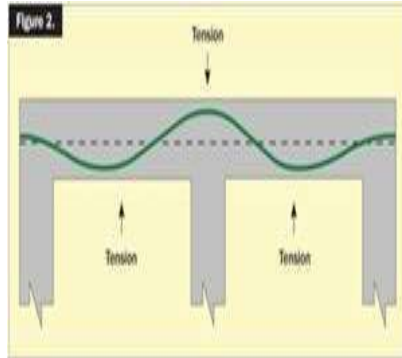


Fig. 3: Tension line of acting in a beam

#### 5.4 Rcc slabs:

Reinforced concrete can be in-situ concrete or precast concrete.

For understanding behavior of reinforced concrete, we shall consider a plain concrete beam subjected to external load.

##### Flat Slab:

Fast and cheap construction using simple form work. Reinforced concrete flat slabs are commonly used in construction as they provide a number of benefits to the designer including:

- Thin sections allowing for greater roof heights and lighter floors.
- Exposed ceilings
- Flexible column arrangements, this is more difficult to achieve for a beam-column design

However, flat slabs have a lower stiffness in comparison to a beam-column floor plan which can lead to relatively large deflections. In addition to this, the shear capacity can also be reduced in particular around the column head where large shear forces can develop.

There are two main failure modes of flat slabs:

- Flexural Failure
- Punching Shear Failure

**Grade Slab:** The slab foundation commonly used for sheds is called a slab-on-grade foundation. This combines a 3 1/2"-to 4"-thick floor slab with a 8"-to 12"-thick perimeter footing that provides extra support for the walls of the building.

#### 5.5 Shear walls:

- Shear walls are vertical elements of the horizontal force resisting system. Shear walls are typically wood frame stud walls covered with a structural sheathing material like plywood.
- Shear walls have four parts:
- Framing members
- Sheathing
- Nails
- Hold-downs

#### 5.6 STAIRCASES:

Staircases provide means of movement from one floor to another in a structure. Staircases consist of a number of steps with landings at suitable intervals to provide comfort and safety for the users.

Some common types of stairs are shown. These include straight-flight stairs, quarter-turn stairs, half-turn stairs, branching stairs, and geometrical stairs.

##### PRINCIPLES TO BE OBSERVED WHILE PLANNING AND DESIGNING A STAIR

1. Width of Stair: It should not be less than 1.00m.
2. Length of flight: The number of steps in a single flight should not be more than 12.
3. Pitch of the stair: It should be 25 to 40
4. Width of landing: It should be 150mm, more than the width of stair.
5. Winders or kite steps: Odd shaped steps should be avoided and incase found necessary. These should be provided at the start of a stair.

6. Hand-rails: It should be 750 to 850 mm in height from the top of respective step or landing.
  7. Step proportions: The size of rise and tread in a stair should be kept uniform throughout the whole stair.
  8. Headroom: Minimum of 2000mm of clear headroom is required above the pitch line
- Following proportions are recommended:
- (i) Residential buildings- Tread=250 mm  
Rise=160 mm

(ii) Public buildings - Tread=300 mm  
Rise=150 mm

(iii) Industrial buildings, Railway station,  
etc Tread =not less than 250 mm  
=250 to 300 mm  
Rise =not less than 150 mm  
=150 to 190 mm

Otherwise work out the sizes of rise and tread by using any one of the following proportions

(i)  $(2 \times \text{Rise}) + (\text{Going})$ , In mm=550 to 600 mm

(ii) Rise x tread, both in cm = 400 to 410 cm<sup>2</sup>.

(iii) With basic proportion of going 300 mm and rise 150 mm, add 10 mm to rise for every 20 mm deduction from going e.g. For a going of 280 mm the rise will be 160 mm.

The above rules act as guide but the actual sizes depend upon the availability of space, while planning stairs practical-field.

- Balusters: The smaller posts fitted between the stair and the handrail, usually decorative, and in timber or steel.
- Bull nose Step: The step at the base of a stair which usually has a protruding semi-circular end
- Capping: The piece of timber that forms the edge or border for the carpet or other floor coverings, located at the edge of the floor on upper level
- Closed Stair: A stair that has treads and risers
- Cut Stringer: Stringers that are cut to follow the profile of the treads and risers.
- Handrail: The shaped or molded piece of timber you hold on to as you walk up or down the stair.
- Handrail Scroll: The decorative handrail piece at the start of the stair that curls around and sits above the bullnose step
- Handrail Wreaths: The sections that curve around corners to form a continuous handrail
- Landing: The flat platforms usually located where a stair changes direction.
- Newel Posts: The larger square posts at the start and the corners of a stair. They are usually turned, fluted, paneled or decorated in some way.
- Open Stair: A stair that has no risers
- Risers: The vertical pieces which are the solid infill between the treads
- Stringers: The main beams that support treads and risers
- Tread Bracket: The decorative pieces that fit to the face of a cut stringer in the more traditional type of stair
- Tread Nose: The rounded leading edge of a step
- Treads: These are simply the steps you walk on
- Winder Steps: The triangular treads used to change the direction of the stair, usually around right-angle corners

## 5.7 INTERIORS:

Brick Work  
Plastering Plaster Of Paris  
Tiling  
Fall ceiling

**Brick Work:** Brickwork is masonry produced by a bricklayer, using bricks and mortar in a variety of patterns with a variety of mortar joints. Typically, rows of bricks called courses are laid on top of one another to build up a structure such as a brick wall

## 5.8 AAC:

Autoclaved Aerated Concrete (AAC) is a certified green building material, which can be used for commercial, industrial and residential construction. It is porous, non-toxic, reusable, renewable and recyclable.

### QUALITY CHECKS FOR AAC:

Dimension, Plumb, Drop test, Color test, Damages, Should be free from oil, Black spots

**Plastering:** Plaster is a building material used for coating walls and ceilings. Plaster is manufactured as a dry powder and is mixed with water to form a paste when used. The reaction with water liberates heat through crystallization and the hydrated plaster then hardens. Plaster can be relatively easily worked with metal tools or even sandpaper. These characteristics make plaster suitable for a finishing, rather than a load-bearing material.

## 5.9 CHECK LIST FOR PLASTERING WORK

- Check sand quality: Check the fineness of sand as recommended in construction manual.
- Check sand are dust or dirt free.

- Check cement quality: Check the grade of cement as specified in your construction manual.
- Cleanness of mortar-mixing platform: Check the platform, on which plaster mortar will be mixed, is properly cleaned. The platform should not be wetted. It should be plain and dry.
- Screening of sand: Check sand is screened before mixing with cement. So that any big particles from the sand can be removed.
- Cement-Sand Ratio: Check cement and sand ratio is maintained for mixing as recommended in construction manual.
- Mortar Mixing: Cement and sand should be mixed in dry condition. Check the dry mix is properly mixed before adding water. There is a tendency of masons to add water before mixing the mortar properly in dry condition.
- Water content in mortar: Water content in mix should not be less or more. It should be appropriate as needed.
- Mortar using time: Cement's initial setting time is 45 minutes. So, check the mortar is being used within 45 minutes after adding water. If necessary, separate some cement sand mix in dry condition. If you need it later you can add water with that. You can maintain a resister for tracking mortar mixing time.
- Thickness of plaster: Suggested plaster thickness is 1/2 inch. But due to size variation of masonry block it can be 3/4 to 1 inch and above. If above one inch thick plaster is required in anywhere that should be done in two coats. After doing 1st coat that should be roughed. And 2nd coat should be done next day.
- Lighting availability: When plastering inside a building, check enough lighting is available there.
- Make a level mark: Before doing plaster inside a room, make level marks with fresh mortar on all four walls. So that, after plastering room size is truly square or truly rectangular. Otherwise, when you'll fix floor tiles you'll face difficulties.
- If you plan to plaster on ceiling, do the same for that also. In this case, make the level mark on beams around the ceiling portion.
- Smoothness of plaster surface: after plastering check the smoothness of plaster surface. If you plan to fix tiles on plaster then make it scratched.
- Level of plaster: check the level of plaster with an aluminum bar. If you need you can use torch light.
- Reduce mortar wastage: During plaster work some mortar can be fallen down. To collect them, lay empty cement bag or polythene sheet below. So that you can reuse fallen mortar. These should be collected and reuse every 30 minutes.
- Sharpness of Edges and corners: Check all edges and corners are sharp and straight.
- Groove and other design work: Check the drawing if there is any groove work or design work on plaster surface. Make the grooving sharp and straight.
- Window border: Check the window border with plumb bob or spirit level that those are straight.
- Check the sharpness of window-opening edges. Check the borders are in right angle.
- Window sill: Check the window sill is plain and even.
- Water proofing admixture: During outside plastering, make sure water proofing agent is mixed with mortar.

#### 5.10 Dadoing:

- In architectural terminology, the dado is the lower part of a wall, below the dado rail and above the skirting board. The word is borrowed from Italian meaning "die" (as an architectural term) or plinth.
- **False ceiling:** A false ceiling is actually a secondary ceiling that hangs below the main ceiling to increase the aesthetics of the room. There should be approximately 1 feet distance between the false ceiling and the primary ceiling. The false ceiling should have at least a height of 8 ½ feet from the floor level.

#### 5.11 MEP: Mechanical Electrical and Plumbing

MEP systems must satisfy multiple objectives and criteria for design, installation, commissioning, operation, and maintenance. Different types of specialty contractors (e-g., process piping, HVAC piping, WAC ductwork, plumbing, electrical, fire protection, controls) are responsible for these systems. Example of diverse criteria for system design include spatial (avoiding interferences), functional within a system (flow or gravity drainage), adjacency or segregation, system installation (layout dimensions, space and access for installation productivity), and testing (ability to isolate).

#### 5.12 Tower Crane:

Tower cranes are a modern form of balance crane that consist of the same basic parts. Fixed to the ground on a concrete slab (and sometimes attached to the sides of structures as well), tower cranes often give the best combination of height and lifting capacity and are used in the construction of tall buildings. The base is then attached to the mast which gives the crane its height. Further the mast is attached to the slewing unit (gear and motor) that allows the crane to rotate. On top of the slewing unit there are three main parts which are: the long horizontal jib (working arm), shorter counter-jib, and the operator's cab.

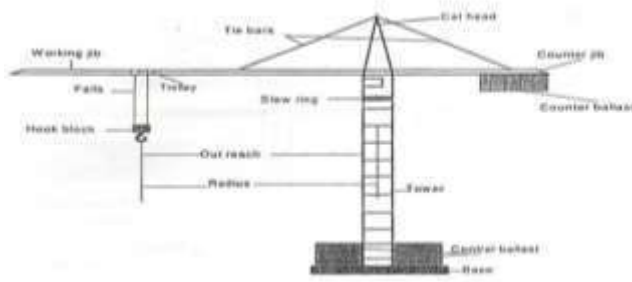


Fig 4: A modern form of balance crane

#### Fire protection system:

The purpose of fire protection systems is to make the building fire resistant and to facilitate the speedy evacuation of occupants in the event of a fire. For fire protection systems, the design parameters are set in accordance with NFPA-13 (National Fire Protection Association). These are the minimum requirements. Fire protection systems designers must also contact local jurisdiction officials, and the owner's insurance rating agency (Factory Mutual, Industrial Risk Insurer etc.) for requirements beyond the minimum standard required by NFPA and Uniform Building Code (UBC) as amended by that jurisdiction.

#### Electrical system:

For electrical system designers, the design parameters are set in accordance with the National Electric Code (NEC). These are the minimum requirements that must be met. Electrical system designers must also adhere to NFPA 13, and the UBC for requirements beyond the minimum set forth by the NEC. The major categories of the electrical system are supply, distribution, and lighting.

#### Plumbing system:

The plumbing system consists of three major categories - gravity drained waste systems, pressure driven systems, and pumped waste. Plumbing design must meet the Uniform Plumbing Code (LPC). The gravity drain systems include sloped lines which must have a natural grade line. In addition, the gravity drained systems require vent lines for the entire system, to allow for open channel flow in the drainage network. The pressure driven systems include hot and cold water supply lines the various locations in the building. Lastly, pumped waste systems include all waste lines that must be driven by pressure rather than by gravity. All pumped waste systems must run in double contained piping systems.

#### Objectives of Work Permit

- Ensuring proper authorization of designated work
- Provide recommendations on how to plan and execute potentially hazardous jobs in a safe manner.
- Achieve the desired degree of safety when carrying out work
- Making clear to people carrying out work about
  - Nature of job, Hazards involved & Control measures
  - Scope of the specific work
- Time during in which the job may be carried out.
- Ensuring the Project Site In charge is aware of the work being done
- Providing a formal procedure to ensure safe completion of work
- Objectives of Work Permit
- Ensuring proper authorization of designated work
- Provide recommendations on how to plan and execute potentially hazardous jobs in a safe manner.
- Achieve the desired degree of safety when carrying out work
- Making clear to people carrying out work about
  - Nature of job, Hazards involved & Control measures
  - Scope of the specific work
  - Time during in which the job may be carried out
- Ensuring the Project Site In charge is aware of the work being done
- Providing a formal procedure to ensure safe completion of work

#### Permit is applicable

- Working at Heights
- Hot work [ Welding , Cutting Wrapping coating etc ]
- Working with Electricity
- Ground Disturbance [ Excavation]
- Confined Space Entry [ Shaft work / Networking



## CONCLUSION

Our project deals with Quality control and Quality assurance on the high rise buildings which gives the total description of how the control is done in the each and every activity of the construction. This is done based on the ISO 9001-2008.

In high rise buildings the construction process includes quality control and quality assurances. The present construction practices in India is still adopt the methodology of as a when required resources management. Lack of professionalism leading to lack of detail when meticulous planning and decision making as per site management is concerned leading to under utilization of resources to a great extend. Still now project resources planning is only limited to planning and scheduling with time but resources mobilization and usages planning according to their capacity and availability ahead of timing the planning stage is still now nobody concern. In order to assess capabilities for utilization of resources and track their productivity the first step should be to keep and maintain their real time record from the ongoing project this is already done project their four planning and scheduling will be same type of project which nearly equal Total Quality Managements.

## CONFLICT OF INTEREST

There is no conflict of interest.

## ACKNOWLEDGEMENTS

The authors wish to thank Dr. Syed Kamaluddin, Principal Chirala Engineering College, Chirala & Dr.P.Suresh Babu Principal Chalapathi Institute of Engineering Technology, Guntur for the enormous support. We thank Head of Department, Civil Engineering for sharing their pearls of wisdom with us during the course of this research, and we thank teaching and non-teaching members of Civil Engineering Department for supported or partially supported.

## FINANCIAL DISCLOSURE

None.

## REFERENCES

- [1] Development of BIM-based evacuation regulation checking system for high-rise and complex buildings Original Research Article Automation in Construction, Volume 46, October 2014, Pages 38-49 Jungsik Choi, Junho Choi, Inhan Kim
- [2] Li tang, [2006] study of high rise building in japan, ph.d thesis, Tongji University, shanghai.
- [3] Zhao yuqin, hebi college vocation and technology.
- [4] Indian standard, fir safety of building (general): details of construction code of practice (first revision), is 1642:1989.
- [5] Arthur w t leung, divison of building and technology, city university of hong kong Dr. C m tam, department of building and construction, city university of hong kong. Orange city fire department, fire prevention division. Rober gifford, de-partment of psychology and school of environmental studies, university of victoria.
- [6] This illustrative pay factor schedule is adapted from R.M. Weed, "Development of Multicharacteristic Acceptance Proce-dures for Rigid Pavement,"Transportation Research Record 885, 1982, pp. 25-36.
- [7] BA Gilly, A Touran, and T Asai, [1987] Quality Control Circles in Construction," ASCE Journal of Construction Engineering and Management, 113( 3): 432.
- [8] See Improving Construction Safety Performance, Report A-3, The Business Roundtable, New York, NY, January 1982.
- [9] Hinze, Jimmie W., Construction Safety,, Prentice-Hall, 1997.
- [10] This example was adapted from E. Elinski, External Impacts of Reconstruction and Rehabilitation Projects with Implications for Project Management, Unpublished MS Thesis, Department of Civil Engineering, Carnegie Mellon University, 1985.
- [11] American Association of State Highway and Transportation Officials, Guide Specifications for Highway Construction, Washington DC, Section 714.01, pg. 244
- [12] HG Poulos, Piled-raft foundation: design and applications (2001) Géotechnique, 51, pp. 95-113.
- [13] J Hanisch, R. Katzenbach, G. König, Kombinierte Pfahl-Plattengründungen (2002) Ernst & Sohn Verlag, Berlin, Germany.
- [14] R Katzenbach, Optimised design of high-rise building foundations in settlement-sensitive soils (2005) International Geotechnical Conference of Soil-Structure Interaction, 26-28 May, St. Petersburg, Russia, pp. 39-46.
- [15] MF Randolph, Design of piled raft foundation (1983) International Symposium on recent developments in laboratory and field tests and analysis of geotechnical problems, 6-9 December, Bangkok, Thailand, pp. 525-537.
- [16] RW Cooke, Piled raft foundations on stiff clays - a contribution to design philosophy (1986) Géotechnique, 36, pp. 169-203.
- [17] MF Randolph, P. Clancy, Efficient design of piled rafts (1993) 5th International Conference on Deep Foundations on Bored and Auger Piles, 1-4 June, Ghent, Belgium, pp. 119-130.
- [18] JL Briaud, M. Ballouz, G. Nasr, Static capacity prediction by dynamic methods for three bored piles (2000) Journal of Geotechnical and Geo environmental Engineering, Vol. 126, July, ASCE, Reston, Virginia, USA, pp. 640-649.
- [19] R Katzenbach, G. Bachmann, S. Leppla, H. Ramm,[2010] Chances and limitations of the observational method in geotechnical monitoring (2010) 14th Danube-European Conference on Geotechnical Engineering, 2-4 June, Bratislava, Slovakia, 13 p.
- [20] O Reul, In-situ Messungen und numerische Studien zum Tragverhalten der Kombinierten Pfahl-Plattengründung (2000) Mitteilungen des Institutes und der Versuchsanstalt für Geotechnik der Technischen Universität Darmstadt, Heft 53.
- [21] Development of BIM-based evacuation regulation checking system for high-rise and complex buildings Original Research Article Automation in Construction,

- Volume 46, October 2014, Pages 38-49 Jungsik Choi, Junho Choi, Inhan Kim.
- [22] Quality control and standardization of embryo morphology scoring and viability markers Review Article Reproductive BioMedicine Online, Volume 31, Issue 4, October 2015, Pages 459-471 Kersti Lundin, Aisling Ahlström
- [23] Analysis of concentration fluctuations in gas dispersion around high-rise building for different incident wind directions Original Research Article Journal of Hazardous Materials, Volume 192, Issue 3, 15 September 2011, Pages 1623-1632 X.P. Liu, J.L. Niu, K.C.S. Kwok
- [24] T Yuvaraja, K. Ramya Implementation of Control Variables to Exploit Output Power for Switched Reluctance Generators in Single Pulse Mode Operation IJE TRANSACTIONS A: Basics Vol. 29, No. 4, (April 2016) 505.
- [25] Safety Aspects, Quality Control, and Quality Assurance using Microwave-Assisted Sample Preparation Systems Microwave-Assisted Sample Preparation for Trace Element Analysis, 2014, Pages 345-38 Peter A. Fecher, Gerhard C. Schlemmer, Kerstin S. Schoeberl.
- [26] T Yuvaraja, M Gopinath. [2014] Fuzzy Based Analysis of Inverter Fed Micro Grid in Islanding Operation International Journal of Applied Engineering Research ISSN 0973-4562 9(22) :16909-16916.
- [27] Yuvaraja Teekaraman\*, Gopinath Mani\*\* Fuzzy Based Analysis of Inverter Fed Micro Grid in Islanding Operation-Experimental Analysis International Journal of Power Electronics and Drive System (IJPEDS) Vol. 5, No. 4, April 2015, pp. 464~469

## ARTICLE

# PV BASED BOOST - SEPIC CASCADED INVERTER FED INDUCTION MOTOR SYSTEM WITH LOW CURRENT RIPPLE

Jasmine David<sup>1</sup> and Gopinath Mani<sup>2</sup>

<sup>1</sup>Dept Of Electrical and Electronics Engineering, St. Peter's University, Chennai, INDIA

<sup>2</sup>Dept. Of Electrical and Electronics Engineering, Dr. N.G.P Institute of Technology, Coimbatore, INDIA

## ABSTRACT

Induction motor IM is a low cost motor with high ruggedness required in paper and textile mills. This paper deals with comparison of performances of Boost-Boost inverter fed IM drive system with boost SEPIC inverter fed IM drive system. The output of PV system is boosted using boost SEPIC converter. The output of SEPIC is converted to seven level output using an inverter. Boost - SEPIC converter is proposed to reduce the ripple in the input current. Boost-SEPIC cascaded inverter is proposed in the present work.

## INTRODUCTION

THE electric vehicles (EV) and Hybrid Electric Vehicles (HEV) currently seem to constitute an increasingly effective alternative to the conventional vehicles, allowing to the vehicle manufacturers to be able to fulfill the requirements required by the users of vehicles (dynamic performances and fuel consumption) and the environmental constraints (reduction of the pollutant emissions). The electric propulsion system is the heart of EV [1]. It consists of the motor drive, transmission device, and wheels. In fact, the motor drive, comprising the electric motor, the power converter, and the electronic controller, is the core of the EV propulsion system. The motor drive is configured to respond to a torque demand set by the driver.

The induction motor seems to be a very interesting solution for EV's propulsion. Field Oriented Control (FOC) [2] and Direct Torque Control (DTC) [3-4] have emerged as the standard industrial solutions to achieve high dynamic performance. However some drawbacks of both methods have motivated important research efforts in the last decades. Particularly for DTC, the high torque ripple and the variable switching frequency introduced by the hysteresis comparators have been extensively addressed [5-6]. In addition, several contributions that combine DTC principles together with PWM and SVM have been reported to correct these problems. This approach is based on the load angle control, from which a voltage reference vector is computed which is finally modulated by the inverter [7]. Although one major feature of classic DTC is the absence of modulators and linear controllers, this approach has shown significant improvements and achieves similar dynamic performance.

On the other hand, the power converter technology is continuously developing, and cascaded multilevel inverters have become a very attractive solution for EV applications, due to its modular structure, higher voltage capability, reduced common mode voltages, near sinusoidal outputs, and smaller or even no output filter [8]. In general, cascaded multilevel inverter may be classified in two groups. The first one refers to the amplitude of isolated DC sources devoted to supply each H-bridge cell. If the amplitude of all sources is equal, then the inverter is called symmetrical, otherwise, if at least one of the sources present different amplitude, then it will be called asymmetrical. The second classification label the multilevel inverter whether hybrid or not. If the converter is implemented with different technologies of semiconductor devices (IGBTs, SCRs, GTOs, IGCTs), different nature of DC sources (fuel cells, batteries and super capacitors) and/or if it presents a hybrid modulation strategy, then it is classified as hybrid [9-10]. This structure greatly simplifies the converter complexity.

The proposed control algorithm eliminates the need of additional isolated DC sources. The control strategy regulates the DC link voltages of capacitors connected to the smallest voltages of a two cells 7-level cascaded H-bridge inverter. The obtained results validate the voltage control strategy and confirm the high dynamic performance of the proposed method, presenting very low torque ripple. Two viable Schemes for induction motor torque control is given by Casadei [11]. Control of a hybrid asymmetric multilevel inverter for competitive medium-voltage industrial drives is given by Veestra [12]. A cascade MLI using a single fuel cell DC source is given by Du [13]. A cascade MLI H-bridge inverter utilizing capacitor voltages sources is given by Corzine [14]. Cascaded H-bridge multilevel inverters- A re-examination is given by Liao [15]. The above literature does not deal with Boost-SEPIC seven level inverter fed induction motor drive. This work proposes cascaded Boost-SEPIC converter.

## MATERIALS AND METHODS

### MULTILEVEL INVERTER TOPOLOGY

The block diagram of the existing system is illustrated in [Fig. 1]. The inverter is composed by the series connection of power cells, each one containing an H-bridge inverter and an isolated dc-source. In the particular case of asymmetric inverters these sources are not equal ( $V1 > V2$ ). The asymmetry of the input voltages can

**KEY WORDS**  
Solar Power, SEPIC, Open loop control, THD, MLI, Boost Converter

Published: 20 October 2016

\*Corresponding Author  
Email:  
jas.malli@gmail.com,  
mgopinath\_10@yahoo.co  
.in  
Tel.: +91-9943327722  
Fax: 0422-2369118

reduce, or when properly designed, eliminate redundant output levels, maximizing the number of different levels generated by the inverter.

Therefore this topology can achieve the same output voltage quality with less number of semiconductors, space, costs and internal fault probability than the symmetric fed topology. A particular cell  $i$  can generate three voltage levels ( $+V_i, 0, -V_i$ ). The total inverter output voltage for a particular phase  $j$  is then defined by

$$v_{in} = \sum_{j=1}^n v_{ij} = \sum_{j=1}^n v_j = (s_{j1} - s_{j2}), \quad i \in \{a, b, c\}$$

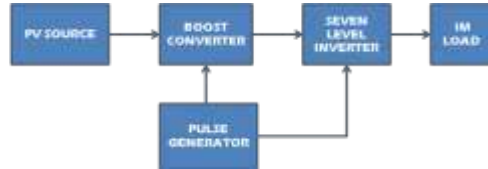


Fig.1: Block diagram of existing system

Where  $v_{in}$  is the total output voltage of phase  $i$  (respectively, the neutral of the inverter  $N$ ), is the output voltage of cell of phase, and the switching state associated to cell. Note how the output voltage of one cell is defined by one of the four binary combinations of the switching state, with "1" and "0" representing the "On" and "Off" states of the corresponding switch, respectively.

The inverter generates different voltage levels (e.g. an inverter with  $m = 4$  cells can generate  $(2m+1 - 1 = 31)$  different voltage levels). When using three-phase systems, the number of different voltage vectors is given by  $3n(n-1) + 1$ , where  $n$  is the number of levels. For example, for the  $m = 4$  case with 31 levels there are 2791 different voltage vectors. Table I summarizes the output levels for an asymmetric 7-level inverter using only  $m=2$  cells per phase (only phase is given). An example of the voltage waveform generation for an asymmetric seven-level inverter is illustrated in [Fig. 2].

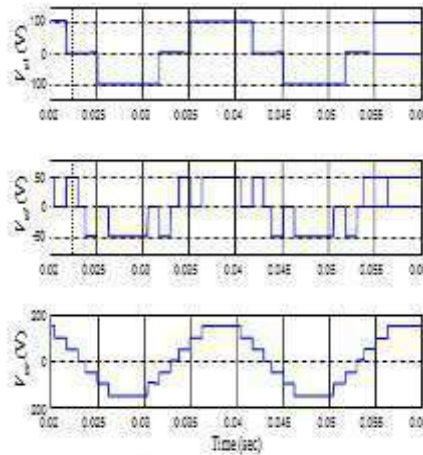


Fig. 2. Asymmetric multilevel inverter with 7-levels output voltage synthesis.

Table I. 7-LEVEL ASYMMETRIC CASCADED INVERTER SWITCHING STATES

n1	cell 1		cell 2		total		
	$S_{11}$	$S_{12}$	$V_{a1}$	$S_{21}$	$S_{22}$	$V_{a2}$	$V_{aN}$
1	1	0	$3V_{dc}$	0	0	0	$3V_{dc}$

2	1	0	$3V_{dc}$	0	1	$-V_{dc}$	$2V_{dc}$
3	0	0	0	1	0	$-V_{dc}$	$V_{dc}$
4	0	0	0	0	0	0	0
5	0	0	0	0	1	$-V_{dc}$	$-V_{dc}$
6	0	0	$-3V_{dc}$	1	0	$V_{dc}$	$-2V_{dc}$
7	0	1	$-3V_{dc}$	0	0	0	$-3V_{dc}$

### SYSTEM DESCRIPTION

The block diagram of proposed system is shown in [Fig. 3]. Boost converter is replaced by Boost-SEPIC converter to increase the control range and reduce input current ripple.

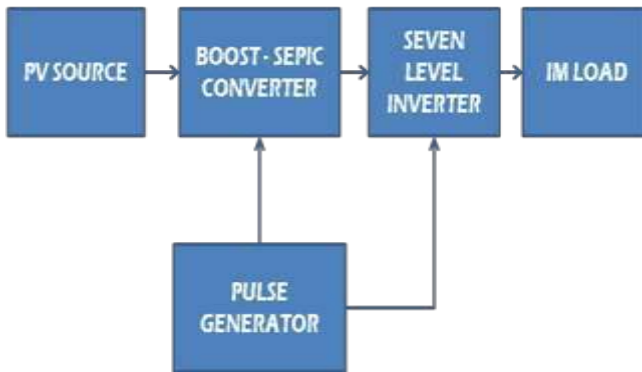


Fig.3: Block diagram of proposed system

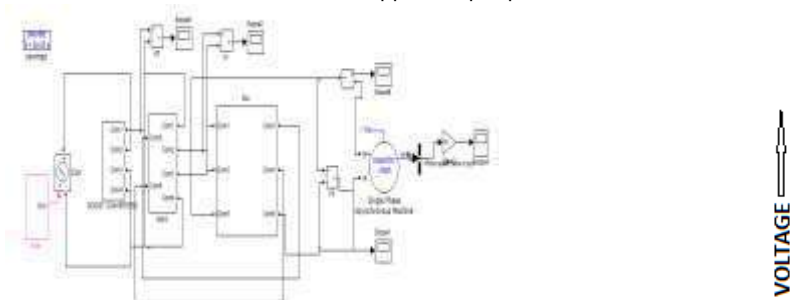
## RESULTS

### SIMULATION RESULTS

Boost-SEPIC cascaded multi level inverter system is shown in [Fig.4.1]. The output of PV is stepped up in two stages using Boost and SEPIC converters. A single phase induction motor is used as the load. Output voltage of solar system is shown in [Fig.4.2]. Boost converter circuit and its input current ripple are shown in [Figs.4.3&Fig.4.4 ]respectively. The output voltage of the Boost converter is shown in [Fig.4.5].

SEPIC converter and its input current ripple are shown in [Figs.4.6 and 4.7] respectively. The peak to peak ripple is 5A. The output voltage of SEPIC converter is shown in Fig.4.8 and its value is 100V. Switching pulses for M1 and M3 of MLI are shown in [Fig. 4.9]. The output voltage of MLI is shown in Fig.4.10. The peak value is 200V. The speed response is shown in [Fig. 4.11]. The speed settles at 1400RPM. The frequency spectrum for the output is shown in [Fig. 4.12]. The THD is 16.72%.

The comparison of Boost – Boost and Boost - SEPIC systems are given in Table 1. The comparison is done in terms of current ripple, output power and THD.







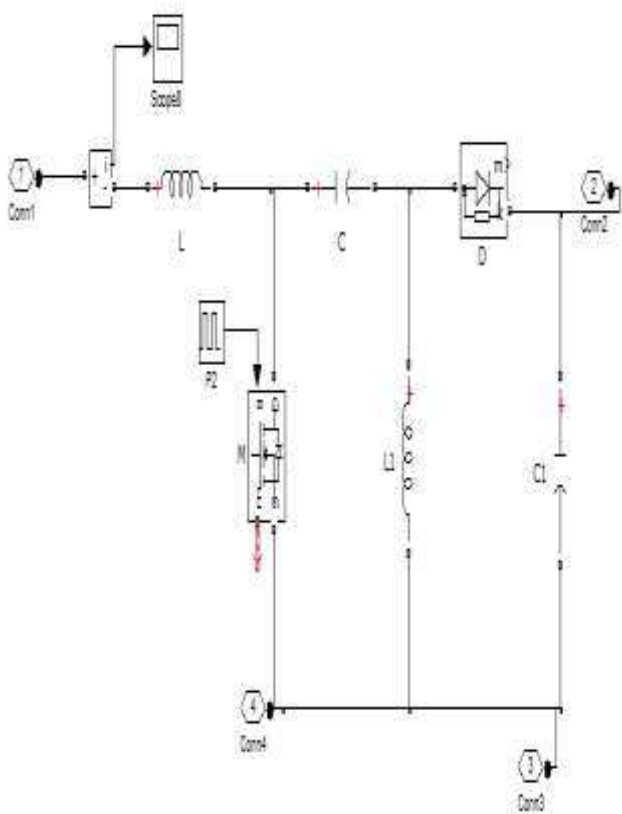


Fig. 4.6 :SEPIC converter circuit

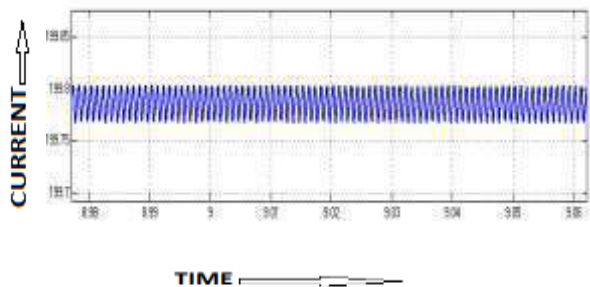


Fig. 4.7 :Input current ripple of SEPIC

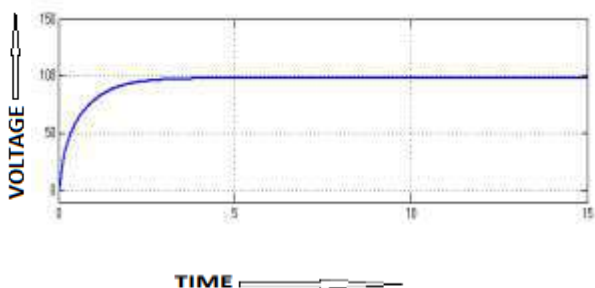


Fig. 4.8: Output voltage of SEPIC converter

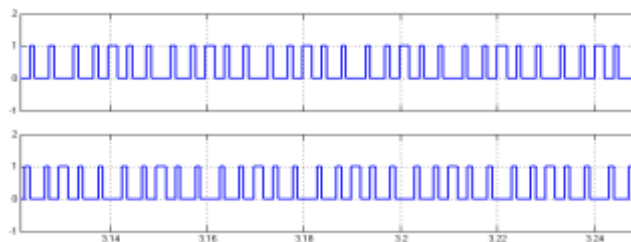


Fig. 4.9 :Switching pulse for M1 & M3 of MLI

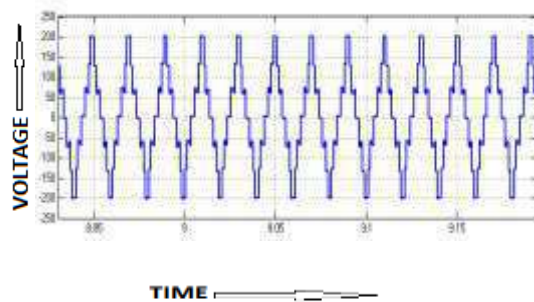


Fig.4.10 :Output voltage

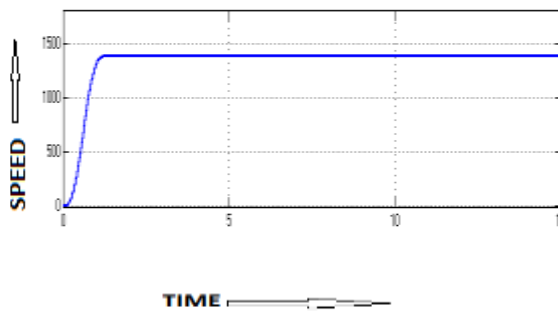


Fig.4.11: Motor Speed

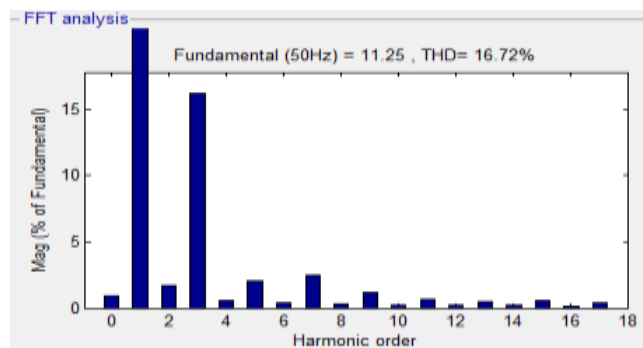


Fig. 4.12: Frequency Spectrum

Table 1: Comparison of Current ripple & Output Power

converter	Input current ripple	Power (Po)	THD
Boost	3.5A	3125W	24.16%
SEPIC	0.04A	3320W	16.72%

## RESULTS

The snap shot for complete hardware system is shown in [Fig.4.25]. The hardware is realized with 230/15V,230/5V transformer,PIC 16F84, IR2110, IRF840 and MCT2E. The output voltage of solar system is shown in fig.4.26. The output voltage of boost converter and SEPIC converter are shown in [Fig. 4.27] and [Fig. 4.28] respectively. Switching pulses for M1 and M3 is shown in [Fig. 4.29]. Switching pulses for M5 and M7 is shown in fig.4.30.The output voltage of seven level inverter is shown in [Fig. 4.31]. The results given in [Figs. 4.10 and Fig. 4.31] indicates that the experimental results are similar to the simulation results.



Fig. 4.25: Hardware snap shot

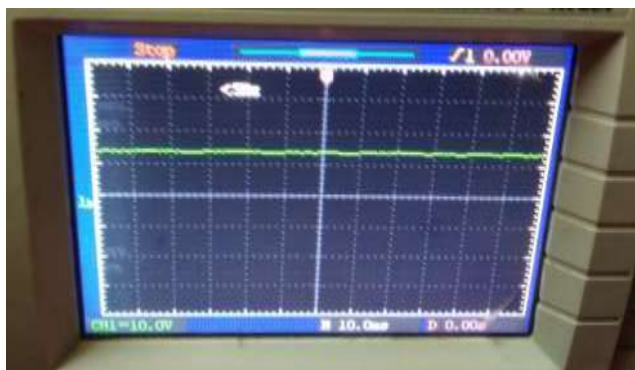


Fig.4.26: Input voltage

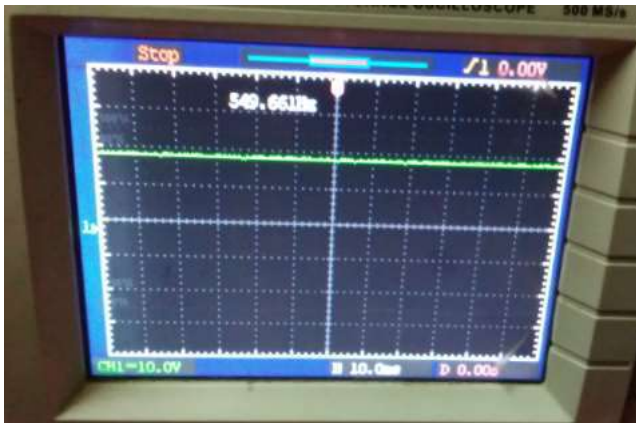


Fig.4.27: Output voltage of boost converter

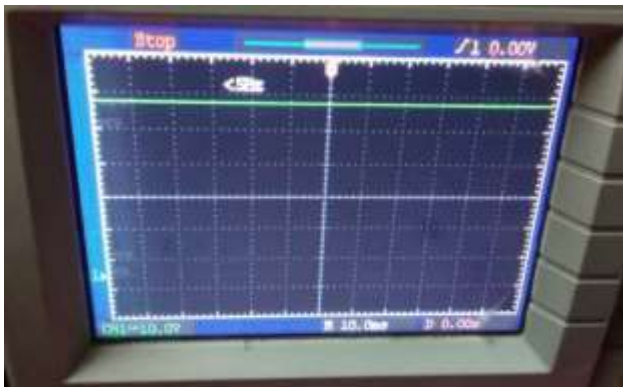


Fig.4.28: Output voltage of sepic converter



Fig.4.29: Switching pulse for M1,M3

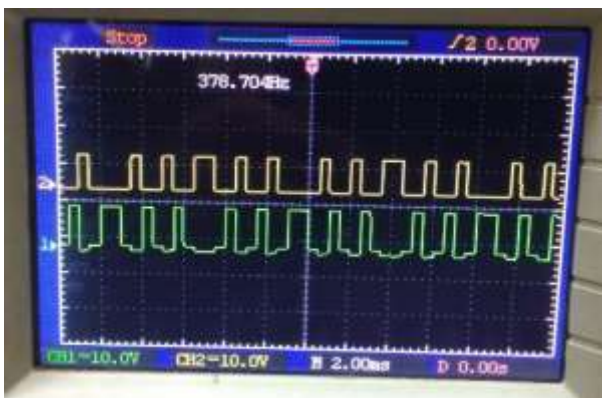


Fig.4.30: Switching pulse for M5, M7

THE IIOAB3 JOURNAL

## CONCLUSION

PV based Boost – Boost and Boost- SEPIC cascaded inverter fed induction motor drive systems are designed, modelled and simulated using Matlab and the results are presented. The comparison indicates that the output power is higher & THD is lower with Boost-SEPIC cascaded inverter system.

The disadvantage of the proposed system is that the number of stages are increased. This paper deals with investigations on open loop system. The closed loop system will be investigated in future.

### CONFLICT OF INTEREST

There is no conflict of interest.

### ACKNOWLEDGEMENTS

None

### FINANCIAL DISCLOSURE

None.

## REFERENCES

- [1] Purohit MEH Benbouzid et al.[ 2006] Electric motor drive selection issues for HEV propulsion systems: A comparative study," IEEE Trans. Vehicular Technology, 55(6): 1756-1764
- [2] DO Neacsu et al.[ 2001 ] Comparative analysis of torque-controlled IM drives with applications in electric and hybrid vehicles vehicle," IEEE Trans. Power Electronics, 16(2): 240-247.
- [3] A Haddoun et al.[2007] loss-minimization DTC scheme for EV induction motors," IEEE Trans. Vehicular Technology, 56(1):81-88
- [4] D Casadei et al.[ 2003] Performance analysis of a speed-sensorless induction motor drive based on a constant switching-frequency DTC scheme," IEEE Trans. Industry Applications, 39(2): 476-484.
- [5] CA Martins et al.[ 2002] Switching frequency imposition and ripple reduction in DTC drives by using a multilevel converter," IEEE Trans.Power Electronics, 17( 2):286-297
- [6] J Rodriguez et al.[ 2008] Direct torque control with imposed switching frequency in an 11-level cascaded inverter," IEEE Trans. Industrial Electronics, 51(4): 827-833
- [7] GS Buja et al. [2004.] Direct torque control of PWM inverter-fed ac motors—A survey," IEEE Trans. Industrial Electronics, 51(4): 744-757
- [8] J Rodriguez et al.[ 2002] Multilevel inverters: A survey of topologies, controls and applications," IEEE Trans. Industrial Electronics, 49(4): 724-738.
- [9] F Khoucha et al., "Hybrid cascaded H-bridge multilevel inverter motor drive DTC control for Electric Vehicles," in Proceedings of the ICEM'08, Vilamoura (Portugal), pp. 1-6, September 2008.
- [10] C Rech et al.[ 2007] Impact of hybrid multilevel modulation strategies on input and output harmonic performance," IEEE Trans. Power Electronics, 22(3): 967-977,
- [11] D Casadei et al.[ 2002]Two viable schemes for induction motors torque control," IEEE Trans. Power Electronics, vol. 17(5): 779-787
- [12] M Veenstra et al.[2005] Control of a hybrid asymmetric multilevel inverter for competitive medium-voltage industrial drives," IEEE Trans. Industry Applications, 41(2): 655-664.
- [13] Z Du et al.[ 2006] A cascade multilevel inverter using a single fuel cell DC source," in Proceedings of the IEEE APEC'06, Dallas (USA),1: 426-430
- [14] KA Corzine et al. [2003] A cascaded multilevel H-bridge inverter utilizing capacitor voltages sources," in Proceedings of the IASTED ICPE'S'03, Palm Springs (USA), pp. 290-295, February.
- [15] J Liao et al., "Cascaded H-bridge multilevel inverters - A reexamination," in Proceedings of the IEEE VPPC'07, Arlington USA), pp. 203-207, September 2007.
- [16] J Chavarria, D Biel, F Guinjoan, C Meza, and JJ Negroni. [2013] Energy- balance control of PV cascaded multilevel grid-connected inverters un- der level-shifted and phase-shifted PWMs," IEEE Trans. Ind. Electron., 60(1): 98-111
- [17] J Pereda and J. Dixon, "High-frequency link: A solution for using only one DC source in asymmetric cascaded multilevel inverters," IEEE Trans. Ind. Electron., vol. 58, no. 9, pp. 3884-3892, Sep. 2011.
- [18] NA Rahim, K Chaniago, and J Selvaraj,[ . 2011] Single-phase seven-level grid-connected inverter for photovoltaic system," IEEE Trans. Ind. Electr., 58(6): 2435-2443
- [19] Y Ounejjar, K Al-Hadded, and LA Dessaint, [2012] A novel six-band hysteresis control for the packed U cells seven-level converter: Experimental validation," IEEE Trans. Ind. Electron., 59(10): 3808-3816
- [20] J Mei, B Xiao, K Shen, and LM Jian Yong Zheng, [2013] Modular multilevel inverter with new modulation method and its application to photovoltaic grid-connected generator," IEEE Trans. Power Electron., 28( 11): 5063-5073
- [21] I Abdalla, J Corda, and L Zhang.[ 2013]Multilevel DC-link inverter and control algorithm to overcome the PV partial shading, IEEE Trans. Power Electron., 28(1): 11-18
- [22] JM Shen, HL Jou, and JC Wu, Novel transformer-less grid- connected power converter with negative grounding for photovoltaic gen- eration system," IEEE Trans. Power Electron27, no. 4, pp. 1818-1829, Apr. 2012.
- [23] R Gonzalez, J Lopez, P Sanchis, and L Marroyo.[ 2007] Transformerless inverter for single-phase photovoltaic systems," IEEE Trans. Power Elec- tron 22(2): 693-697.
- [24] T Yuvaraja, K. Ramya Implementation of Control Variables to Exploit Output Power for Switched Reluctance Generators in Single Pulse Mode Operation IJE TRANSACTIONS A: Basics 29( 4):505.



## ARTICLE

# ENERGY MANAGEMENT OF MICRO GRID USING SUPPORT VECTOR MACHINE (SVM) MODEL

Rambabu M<sup>1\*</sup>, Nagesh Kumar GV<sup>2</sup>, Siva Nagaraju S<sup>3</sup>

<sup>1</sup>GMRIT-Rajam, INDIA

<sup>2</sup>GITAM-university-vizag, INDIA

<sup>3</sup>JNTUK-Kakinada, INDIA

## ABSTRACT

Micro grids (MG) are currently getting great consideration and measured the future trend for power distribution, consumption and storage; intended to meaningfully improve the self-sustainability of future electric dissemination of grids. In this paper the effective predictive energy organization model for micro-grid is implemented on the basis of generation model, energy storage scheme and load demand. Generation model comprises of a solar photovoltaic (PV) and wind turbine (WT), whereas hybrid power supply scheme comprises of battery and fuel cells (FCs). The goal is to ensure the load demand totally while sustaining the scheme constraints. The proposed optimized model is based on the SVM calculation. The SVM prediction model is prophesied the output on the basis of that produced the training dataset from the projected scheme restraints. The SVM can prophesied the control signal to converter for monitoring the power flow, then projected controllers can achieve the power signal and preserves the linear power transmission in a numerous load demand. Lastly, the application is performed by the MATLAB/Simulink platform and the presentation of the projected model is investigated on the basis of the two cases namely linear, non-linear load burdens and stable, non-stable produced power. The optimal power signal assessment investigation is achieved with dissimilar outmoded methods such as ANN, fuzzy over the reference signal.

## INTRODUCTION

This period is predictable to observe unparalleled growth and encounters in power generation, delivery, and usage. Ecologically responsive (renewable and clean alternatives) power generation skills will show a significant part in future power supply because of augmented worldwide public consciousness of the requirement for ecological defense and wish for less requirement on fossil fuels for energy manufacture [1]. These machineries comprise power generation from renewable energy (RE) resources, PV, micro hydro (MH), namely wind, biomass, ocean wave, geothermal, and tides, and clean alternative energy (AE) specifically FCs, power generation skills and micro turbines (MTs) [2]. The assistances of RE penetration comprise a reduction in outside energy dependence, reduction in transmission and alteration losses and further progress the scheme reliability, etc. [3][4]. To upsurge the energy dependability, wind and solar energy are utilized as dual energy sources. Though, seasonal climatic circumstances and geographic circumstances disturb the wind-solar energy output [5]. Consequently, a third energy scheme is desirable to progress the energy supply reliability. Therefore, the PEM FC preferably fulfils the necessity for any twitch up power. After the wind and the solar scheme energy are inadequate output then the FCs backups the delivery scheme [6]. An overall power scheme utilizes battery energy storage to evade a power outage or power surges produced by usual ecological influences.

The latest tendency of RE expansion is an amalgamation of disseminated power sources and energy storage subsystems to custom a small micro-grid that can decrease loss of energy from power broadcast lines over long distances [7]. A renewable-based micro grid can be implicit as a specific case of a more overall idea known as a 'smart grid' that is an interdisciplinary name for a group of technological results for electric power scheme management [8]. The modern idea of micro grid is extremely talented as a result to the issue because of shortage of fossil fuel in future in conservative power generation. Micro grid is a platform to assimilate DERs into circulation network. The DERs may comprise DGs and distributed storage (DS) [9]. The MGs function in grid-connected or island mode, and may involve distribution networks with inhabited or commercial end-consumers, in rural or urban parts [10][11]. Process of micro grid is on the basis of prosperous integration of DERs that is associated with numerous factors such as power quality problems. The power quality problems should be sagely distributed with to attain sensible values of voltage and frequency in grid associated and islanded mode of micro grid in firm state and also at the time of dynamic state i.e. conversion from grid associated mode to islanded mode and vice versa [12] [13].

The energy accomplished from the RES is fresh and generates no pollution, but on another aspect it is stochastic and subsequently problematic to control. Because of this disadvantage, a high diffusion of the RES can create reliability, stability, and power quality issues in the chief electrical grid. Thus, an optimum way of assimilating the energy proficient from the RES must be intended [14, 15]. In this aspect, the hybrid scheme, fashioned by intersecting small, modular generation and storage devices has demonstrated to be the best means of gathering the energy demand with high dependability, flexibility and cost efficiency [16], [17]. Energy organization of hybrid energy schemes is vital for safeguarding optimal energy application and energy sustainability to the supreme extent. Additionally, the upsurge in infiltration of RE in power schemes, chiefly at the distribution level, presents novel encounters for frequency and voltage regulation as they can alteration the generation/demand balance of the network almost promptly as associated with conventional alternators whose dynamics are governed using their inertia constant [18][19]. Dynamic

### KEY WORDS

SVM, REMS, Micro grid, Power transfer, PV, WT, Energy management, battery, fuel cells.

Published: 20 October 2016

### \*Corresponding Author

Email: m.rambabu2001@gmail.com  
Tel.: +919985456004  
Fax: +91-08941251591

communications amongst the load claim then the RE source can prime to critical issues of stability and power quality. Consequently, handling the flow of energy throughout the hybrid scheme is indispensable to upsurge the operating life of the membrane and to safeguard the unceasing energy flow. The cumulative number of RE sources and disseminated generators necessitates novel approaches for their operations for maintaining the energy balance amongst the renewable sources and utility grid or micro-grid [20].

At this time, I have envisioned to suggest an artificial intelligence (AI) method for energy management of combined RE scheme resources with MG. The projected combined RE system is on the basis of PV scheme, WT, Batteries and UC system correspondingly. The projected control method will be holding the power flows amongst the collective RE sources and the grid. It will be encountering the existing RE power and to preserve the grid power claim from the grid operator. The electrical power desirable by the grid operator is provided as a reference to the input of micro grid. The projected approach must be dispersed the total power reference among the scheme portions properly. In the projected method, the objective performance will be well-defined by the scheme information subject to equivalence and dissimilarity restraints. The constraints will be the obtainability of the PV power, wind power, power demand and the SoC (states of charge) of storage rudiments. Batteries will be used as an energy source, to alleviate and allow the renewable power scheme units to keep running at a firm and steady output power.

## RECENT RESEARCH WORK: A TRANSITORY REVIEW

Amounts of research work are heretofore occurred in literature that on the basis of the energy management of RE scheme with micro grid. Some of the works are studied here.

an Energy Management System (EMS) for hybrid systems (HS) collected by a amalgamation of renewable resources with the provision of dissimilar storage devices (battery and hydrogen system) that permit its operation without the requirement of grid connection (i.e. a stand-alone system) was proposed by Juan P.Torreglosa et al. [21].The prominence of the projected EMS lies in considering economic problems that disturb to the decision of that device of the HS must function in each moment. Linear programming was utilized to encounter the objective of decreasing the net present value of the operation cost of the HS for its whole lifespan. The complete operation costs on the basis of mainly on the reposition charges of its mechanisms.

A Genetic Algorithm (GA) is used to apply a tri-objective design of a grid independent PV/Wind/Split-diesel/Battery hybrid energy scheme for a characteristic residential building with the objective of decreasing the Life Cycle Cost (LCC), CO<sub>2</sub> emissions and dump energy was described by A.S.O.Ogunjuyigbe et al.[22]. To attain some of these objectives, small split Diesel generators are utilized in place of single big Diesel generator and are agreeable on the basis of convinced group of principles on the basis of existing RE resources and SOC of the battery. The algorithm was used to study overhead five situations for a characteristic load profile of a inhabited house with the help of typical wind and solar radiation information.

The implementation of a meta-heuristic algorithm specifically Cuckoo Search (CS) in the arena of a hybrid energy organization design issue was elucidated by Sarangthem Sanajaoba et al.[23]. Solar and wind power on the basis of hybrid energy scheme with energy storage unit gives a dependable and cost effective energy alternative above the conservative diesel generator on the basis of scheme usually utilized by remote users. The efficiency of Cuckoo Search algorithm in resolving hybrid energy scheme design issue was inspected and its function was associated with other well-known optimization algorithms such as GA and Particle Swarm Optimization (PSO) algorithm. At this time, the consequence of wind turbine generator (WTG) force outage rate (FOR) on the optimal scheme dependability and economics.

A Energy Management System (EMS) for a micro grid on the basis of four energy bases: a WT, PV solar panels, a battery, and a hydrogen system, that was collected of a FC and an electrolyser was described by Pablo Garcia et al.[24]. That control approach enhances the complete cost of the hybrid scheme via lifetime assessments designed hourly for each energy storage device. That control approach links the anticipated lifetime of the energy sources to their generation costs, i.e., if the lifetime was low, the generation cost upsurges and, subsequently, that energy source will surprise to be utilized less.

An Improved Harmony Algorithm (IHA) for optimal allocations and sizing of capacitors in numerous distribution schemes was proposed by E.S.Ali et al.[25]. Initially, Power Loss Index (PLI) was familiarized to attain the uppermost candidate buses for fixing capacitors. At that time, the IHA was engaged to resolve the most optimum locations of capacitors and their sizing from the designated buses using PLI. The objective performance was premeditated to decrease the entire cost and losses and accordingly, to upsurge the net saving per year. The algorithm was verified on three dissimilar radial distribution schemes. A hybrid many optimizing liaisons (MOL) and the teaching learning based optimization (TLBO) based optimization of integrated hybrid renewable energy sources (IHRES) for techno-economic-socio investigation was demonstrated by Ranjeeta Khare et al.[26]. Optimal sizing of IHRES was performed based on solar irradiation, wind speed, demand load, reliability index, loss of load probability (LOLP) then the CO<sub>2</sub> emission over diesel generator. Annual cost of the system (ACS) was assessed via the existing hybrid algorithm. Sovereignty of the recommended hybrid technique for optimal sizing of hybrid scheme was demonstrated by associating the solutions with other optimization systems such as TLBO, ITLBO, PSO, MOL and SGA.

A Flower Pollination Algorithm (FPA) for optimum distributions and sizing of capacitors in numerous dissemination schemes was proposed by A.Y.Abdelaziz et al.[27]. Initially the most applicant buses for connecting capacitors were recommended by Loss Sensitivity Factors (LSF). Formerly the FPA was engaged to assume the sites of capacitors and their sizing from the chosen buses. The algorithm was associated with others to focus the assistances of the algorithm in decreasing total cost and exploiting the net saving.

The evaluation of the current investigation work displays that, energy organization of hybrid RE storage devices for MG. For the energy administration, dissimilar renewable devices are encompassed typically PV and wind power generators, together with a diesel power generator. In the energy management scheme, the purpose of the size of PV, wind, and diesel power generators is tremendously challenging. The organisation of the energy sources is talented by the energy supervisory scheme. It is accountable for monitoring the energy sources of the RE scheme and their power converters. This is mostly because of a great amount of factors complicated in the problem, the instability developing from the renewable resources and the demand load, and the multifaceted interaction between issues. Conservatively, there are numerous methods are utilized to energy management strategies such as fuzzy, neuro-fuzzy and optimization algorithms. By utilizing fuzzy logic controller (FLC) for a WT /PV/hydrogen/battery REMS on the basis of the energy management, that provides better solutions but it does not illustrate the exclusive nature of fuzzy schemes theory. On another aspect, PSO has been established to have decent worldwide search ability. Though, in PSO algorithm, the velocity equation comprises of stochastic variables so the worldwide best value is changing hesitantly. Consequently, a RE scheme control approaches are mostly intended to track the required power, to usage optimally the energy sources and to standardize the DC bus voltage of the REMS. Consequently, a combined RE scheme is obligatory for an auspicious result to overawed this encounter. In literature very scarce methods on the basis of works are accessible to solve this issue; these disadvantages and issues have encouraged doing this research analysis.

### PROPOSED RENEWABLE ENERGY MANAGEMENT SYSTEM (REMS)

The representation figure of the REMS under deliberation is shown in [Fig. 1]. It is expected that MG comprises dissimilar kinds of distributed generators (DGs) such as WT, PV and energy storage system (ESS) like UC, battery and FC. The incorporation of these DGs and ESS is generally interfaced with the load and the chief grid by power electronic converters. The dissimilar topologies of power converter are essential to control power flow to be appropriate for the load power claim. The REMS organization is familiarized to direct the enhanced values of each source to power converter control circuit bearing in mind the outputs instructions from the Support Vector Machine (SVM).

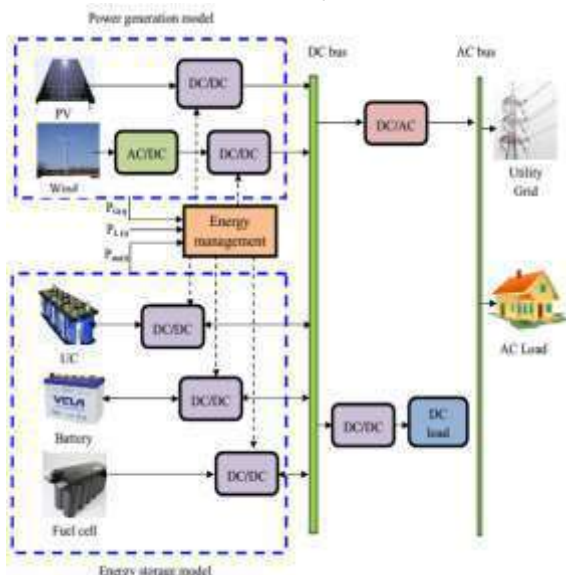


Fig. 1: Proposed schematic diagram of the REMS

The SVM algorithm for organization and regression is the last preparation in the name of the support vectors that abbreviates the large training information to a meaningfully lesser subspace of SVs. The training dataset are generated on the basis of the projected organization parameters then the function is investigated also associated with other out-dated approaches specifically ANN and fuzzy.

### POWER GENERATION MODEL

### Photovoltaic array

The PV cell is demonstrated as a corresponding circuit that comprises of an ultimate current source  $I_{cs}$  in parallel with a diode and resistance  $R_p$  all in sequences with resistor  $R_s$ . The diode models the semiconductor material, and  $R_s$  models the resistance amongst the contactor and semiconductor material [28]. The overriding equations (1), (2), (3) and (4) are,

$$V_d = V_{cell} + I_{pv}R_s \quad (1)$$

$$I_{pv} = I_{cs} - I_s \left[ e^{\frac{(qV_d)}{AKT_{pv}}} - 1 \right] - \frac{V_d}{R_p} \quad (2)$$

$$I_s = I_{s,r} \left( \frac{T_{pv}}{T_r} \right)^3 e^{\frac{qE_{bg}}{AK} \left( \frac{1}{T_r} - \frac{1}{T_{pv}} \right)} \quad (3)$$

$$I_{cs} = \left[ I_{s,r} + K_I (T_{pv} - T_r) \right] \frac{S_{pv}}{1000} \quad (4)$$

Where,  $V_d$  and  $V_{cell}$  are the diode voltage and PV cell voltage, correspondingly;  $I_{pv}$  is the PV cell output current, and  $I_s$  is the cell saturation current;  $q$ ,  $A$  and  $K$  are an ideal factor, an electron charge, and the Boltzmann's constant, correspondingly;  $I_{s,r}$  is the cell's reverse saturation current at reference temperature  $T_r$ ;  $E_{bg}$  is the band-gap energy of the semi conductor;  $K_I$  is the cell's short circuit current temperature coefficient,  $S_{pv}$  represents that the irradiance of the PV. The cell model is ascended to a PV arrangement by bearing in mind  $\eta_{pv}$  cells in sequences, thus the assortment power is specified as equation (5),

$$P_{pv} = \eta_{pv} V_{cell} I_{pv} \quad (5)$$

For brevity, we only abridge the PV model equations (1) to (5). Note that a maximum power point tracking (MPPT) algorithm is typically engaged to progress PV efficacy. Then additional renewable energy source wind turbine model is enlightened below.

### Wind turbine power model

The WTs detention portion of the kinetic energy of winds and translate it into electrical energy. This abstraction of energy produces a wind energy scarcity amongst the wind leaving the turbine and the wind arriving in front of the turbine. Henceforth, a discount of power output is fashioned at down WTs [29]. The WT power  $P_w$  is demonstrated with the help of a non-linear expression that fundamentally on the basis of the wind speed and the wind turbine features is designated as equation (6),

$$P_w = \frac{1}{2} \rho A C_p (\lambda_1) v^3 \quad (6)$$

Where,  $\rho$  is the air density ( $kg.m^{-3}$ ),  $A$  is the surface of the turbine blades ( $m^2$ ) and  $C_p$  is the power coefficient, which is given by equation (7),

$$C_p(\lambda_1) = 0.5176 \left( \frac{116}{\lambda_1} - 0.4\beta - 5 \right) e^{\frac{-21}{\lambda_1}} + 0.0068\lambda_1 \quad (7)$$

$$\text{Where, } \frac{1}{\lambda_1} = \frac{1}{\lambda_1 + 0.08\beta} - \frac{0.035}{\beta^3 + 1} \quad (8)$$

And,  $\lambda_1$  is represented as the tip-speed ratio, that revenues that the ratio amongst the tangential speed of the tip of a blade and the real speed of the wind  $v$ . Then the tip speed ratio is designated as equation (9),

$$\lambda_1 = \frac{\Omega R}{v} \quad (9)$$

Where,  $R$  is the helix radius (m),  $\Omega$  is the angular mechanic speed ( $rad.s^{-1}$ ). The anticipated energy storage scheme can switch the power flow of the micro grid on the basis of the parameters of the scheme. The output of the scheme can be measured on the basis of the SVM that is trained on the basis of the

input parameters of the generator and storage scheme. The storage model is utilized some storage schemes specifically battery, UC, FCs. The energy storage scheme model is designated below.

### Energy storage system model

On the basis of the load demand curve, the batteries in a conventional stand-alone solar scheme are substituted archetypally. An enormous battery scheme is recommended to cater for the peak power and also to extend the battery lifespan. The dilapidation in battery lifespan is because of the unpredictable battery charging using the solar energy source, by way of the output of the source is deeply reliant on weather circumstance. The output of the solar energy source alters rendering to the intensity of the light, subsequently an inconsistent battery charging and settling cycle [30]. Heavy current satisfying because of the heavy load necessities will also distress battery life. The stress factor on the battery similarly asymmetrical discharging rate and widespread time at the low SOC could upsurge the rate of impairment to the battery. The distinguished damage contrivances are associated to battery electrolyte stratification and also irreparable sulphating that significantly abridges battery lifespan.

The DC/DC converter associated with the FC is a high-step up boost-type topology functioning in incessant conduction mode. The control approach utilized in the DC/DC converter understands a single current loop to control the output power inoculated into the micro grid [32]. The full-bridge inverter continuously performs as a current source whether the micro grid functions in impartial or grid linked mode, being a slave converter. The inverter is well-ordered by two loops i.e. a current loop and a voltage loop. The anticipated SVM depended on energy management system needs dataset for the training procedure that is enlightened below

### Dataset Generation for classification training and testing

The REMS hinge on upon the RE sources of the REMS on the basis of the power need of the grid and the load with the help of the power production model and the energy storage schemes. At this time, we utilizing the SVM organization and testing model is attained the REMS. The projected SVM model can produce the training dataset and measured the output of the SVM. The training datasets are on the basis of the actual produced power of the natural generators such as PV array and wind turbine and the load claim at the specific duration [33]. Primarily the generator model power is designated as equation (10),

$$P_G(t) = P_{PV}(t) + P_W(t) \quad (10)$$

And the storage system model is demonstrated as equation (11),

$$P_{sto}(t) = P_{BAT}(t) + P_{UC}(t) + P_{FC}(t) \quad (11)$$

The training dataset decides the reference power necessary from the RE sources and the storage strategies. The fashioned power can be designated through the equation (12).

$$P_p(t) = P_G(t) + P_{sto}(t) \quad (12)$$

In which,  $P_G(t)$  signifies the entire power produced from the PV and wind energy from time interval;  $P_p(t)$  represents the entire power of the accessible sources in the REMS from time  $t$  interval and  $P_{sto}(t)$  indicates the total power from the storage devices from time  $t$  interval;  $P_{PV}(t)$  characterizes the power produced from the PV scheme from time  $t$  interval;  $P_{WT}(t)$  characterises the power produced from the WT from time  $t$  interval;  $P_{BAT}(t)$  suggests the power needed from the battery from time  $t$  interval;  $P_{UC}(t)$  narrates to the power mandatory from the UC from time  $t$  interval and  $P_{FC}(t)$  resembles to the power needed from the FC from time  $t$  interval [34]. On the basis of the above equations, the training dataset of the SVM has been industrialized that is displayed in the equation (13).

$$\begin{bmatrix} P_G(0), P_L(1) \\ P_G(1), P_L(2) \\ \vdots \\ P_G(t-1), P_L(t) \end{bmatrix} = \begin{bmatrix} P_{ref}(0) \\ P_{ref}(1) \\ \vdots \\ P_{ref}(t) \end{bmatrix} \quad (13)$$

At this time, the SVM inputs are may be the preceding prompt power generation from the produced RE sources  $P_G(t-1)$  and the load demand  $P_L(t)$  and the output panel is reference influence of the REMS  $P_{ref}(t)$ . By engaging the relative parameters, the new ANFIS method has been able to produce the rules and tuned proficiently. The produced dataset is used for training the SVM and it accomplishes the energy of the REMS at the challenging time. The SVM on the basis of energy management is enlightened below

### Support Vector Machine



To apply the load profile documentation, a SVM model that appropriately classifies the actual load profile from the SVR load profile models is skilled and authenticated. This again, comprises the 3 stages as declared above: information pre-processing, model assortment, and cross-validation and grid search. SVM is an extensively utilized machine learning algorithm for organization and reversion investigation. It is on the basis of the organizational risk minimization belief rather than the experiential risk minimization principle that can decrease the experiential jeopardy and self-assurance interval instantaneously so as to confirm the generalization presentation of learning [35]. The chief benefit of the SVM algorithm for organization and deterioration is the final origination in the name of the support vectors, which shortens the large training information to a meaningfully lesser subspace of SVs. Furthermore, the preparation does not necessitate any computationally intensive accurate operations. SVM alters the learning issue to an optimization issue of arched quadratic programming that can acquire the worldwide optimal result theoretically and the arrangement is demonstrated in [Fig. 2].

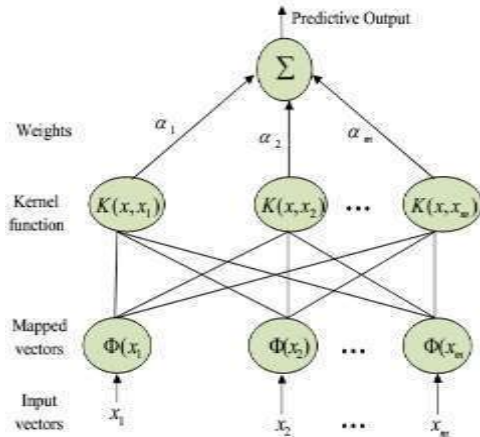


Fig.2: Structure of SVM training model

Specified a training sample set  $T = \{(x_i, y_i), i = 1, 2, \dots, n\}$ , where,  $x_i$  is the  $i^{th}$  input sample,  $x_i \in R^n$ ,  $y_i$  is the consistent output,  $y_i \in \{1, -1\}$  and  $n$  is the number of samples. The primitive optimization issue is expressed in equation (14),

$$\min_{w, b} \frac{1}{2} \|w\|^2 \quad (14)$$

Subject to,

$$y_i(w \cdot x_i + b) - 1 \geq 0, i = 1, 2, \dots, n$$

For making the result of the primitive issue more modest and feasible, it is malformed to a dual issue. The Lagrange performance is familiarized and demonstrated in equation (15),

$$L(w, b, \alpha) = \frac{1}{2} \|w\|^2 - \sum_{i=1}^n \alpha_i \{y_i [(w \cdot x_i) + b] - 1\} \quad (15)$$

Where, is the Lagrange multiplier; By manipulative the partial derivative for ; constructing them equal to 0, the subsequent dual issue can be attained as equation (16),

$$\max_{\alpha} \sum_{j=1}^n \alpha_j - \frac{1}{2} \sum_{i=1}^n \sum_{j=1}^n y_i y_j \alpha_i \alpha_j (x_i \cdot x_j) \quad (16)$$

Subject to,

$$\sum_{i=1}^n y_i \alpha_i = 0, \alpha_i \geq 0, i = 1, 2, \dots, n$$

Following that issue (15) is solved; the optimal gratifies the equation (17),

$$w^* = \sum_{i=1}^n \alpha_i^* y_i x_i \quad (17)$$

And the decision performance is articulated as equation (18),

$$f(x) = \text{sgn} \left[ \sum_{i=1}^n \alpha_i^* y_i (x_i \cdot x) + b^* \right] \quad (18)$$

For realizing the SVM in nonlinear condition, samples should be represented from the original nonlinear space to the high dimensional linear space. This nonlinear mapping can be comprehended with the help of the kernel performance is provided as equation (19),

$$K(x_i, x_j) = \phi(x_i) \cdot \phi(x_j) \quad (19)$$

The nonlinear alteration comprehended by the kernel performance can significantly diminish the computational difficulty. At that time, the issue can transmute to equation (20),

$$\max_{\alpha} \sum_{j=1}^n \alpha_j - \frac{1}{2} \sum_{i=1}^n \sum_{j=1}^n y_i y_j \alpha_i \alpha_j K(x_i, x_j) \quad (20)$$

Matter to,

$$\sum_{i=1}^n y_i \alpha_i = 0, 0 \leq \alpha_i \leq C, i = 1, 2, \dots, n$$

In which,  $C$  is the consequence co-efficient;  $C$  is utilized to regulator the chastisement degree for erroneously categorized samples. By resolving the quadratic programming issue (20), the subsequent decision performance can be acquired as equation (21),

$$f(x) = \text{sgn} \left[ \sum_{i=1}^n \alpha_i^* y_i K(x_i, x) + b^* \right] \quad (21)$$

The mapping  $\phi$  is frequently nonlinear and unknown. As an alternative of computing  $\phi$ , the kernel function  $K$  is utilized to calculate the inner product of two vectors  $x_i$  and  $x_j$  in the feature space  $\phi(x_i)$  and  $\phi(x_j)$ , that is provided in equation (19). The sophistication of using the kernel performance is that one can compact with feature spaces of random dimensionality without having to calculate the map  $\phi(x)$  obviously [36]. Any performance sustaining Mercer's condition can be utilized as the kernel performance. The succeeding are three frequently utilized kernel functions as equations (22), (23) and (24),

$$\text{Linear: } K(x_i, x_j) = x_i \cdot x_j \quad (22)$$

$$\text{Polynomial: } K(x_i, x_j) = (1 + x_i \cdot x_j)^\rho, \rho > 0 \quad (23)$$

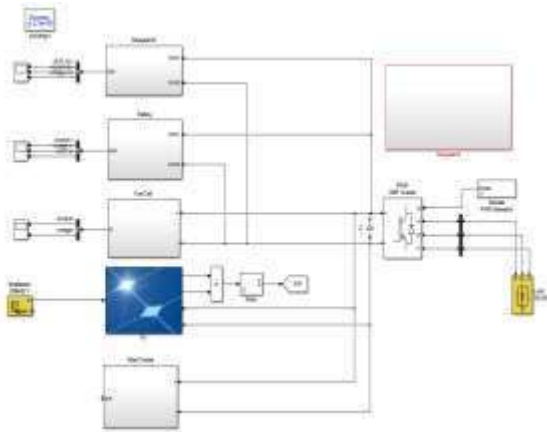
$$\text{Radial basic function (RBF): } K(x_i, x_j) = \exp\left(-\gamma \|x_i - x_j\|^2\right) \quad (24)$$

At this point,  $\rho$  and  $\gamma$  are adaptable kernel parameters. The kernel parameter should be prudently selected as it subliminally describes the structure of the great dimensional feature space  $\phi(x)$  and therefore panels the complication of the final result. Additionally, the function of the model is seriously reliant on the regulation parameter  $C$ , the width of the tube  $\epsilon$  and the parameter of the selected kernel performance. From the application point of view, training is corresponding to disentangling a linearly embarrassed quadratic programming (QP) with the number of variables twice that of the input information dimension.

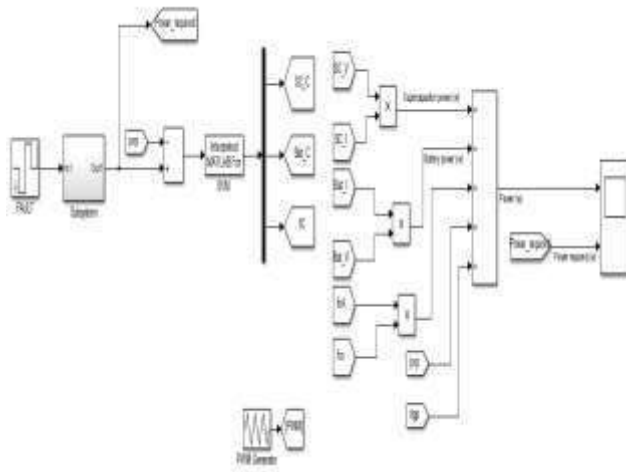
The anticipated technique exploits these recompenses of the SVM to attain a computationally effectual assessment algorithm. This stage involves information acquisition, information alteration and format adaptation for the SVM arrangement model applied to accomplish the information facts from each of the load profiles. These information points are then rehabilitated into the feature variables of the input vector. Then it pacts with the assortment of the optimal kernel has to be applied in the classification model of the load profile. Numerous kernels are assessed and the one with optimized parameter that provides the uppermost accurateness with lowest number of SVs is selected. Lastly, the cross validation is performed and the groups of information are utilized as the testing information while the others are utilized for training determination. This permits the classification accurateness to better reproduce the model's capability in categorizing novel information. The performance investigation of the projected technique is appraised and elucidated in segment 4.

## RESULTS AND DISCUSSION

In this segment designated the result and discussion of the projected technique with the SVM organization algorithm. In that the projected scheme is applied with Intel(R) core(TM) i5 processor, 4GB RAM and MATLAB/Simulink 7.10.0 (R2015a) platform. The projected scheme is applied and the simulation diagram is demonstrated in [Fig. 3]. At this time, the projected technique restrained the actual parameters and preserves the stable power slow for the grid connected scheme. The controlling parameters are measured hinge on the SVM classifier. In this segment, the measured parameters are appraised to the function of the anticipated scheme and associate with other approaches and to assess the efficiency of the scheme. In this investigation, the procedures have two cases on the basis of the load and output power of the scheme. Primarily, the non-linear power and linear load parameters are assessed and evaluated secondly, the linear power and non-linear load. The parameters are assessed and to preserve the power flow on the basis of the SVM training dataset.



(a)



(b)

**Fig. 3:** The Simulink structure of (a) the projected model (b) SVM prediction model

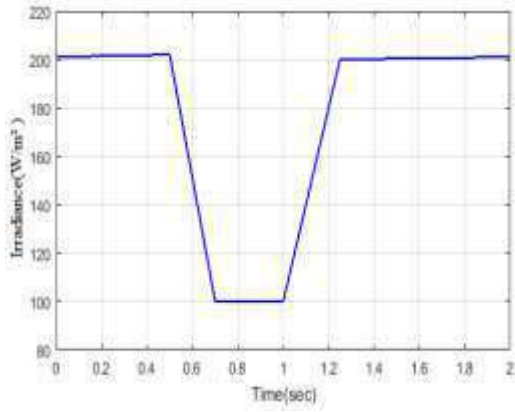
**Table.1:** The simulation parameters

No	Parameters	values
1.	PV rated power	3.78kW
2.	PV open circuit voltage	64.2V
3.	PV short circuit current	5.96A
4.	WT rated power	1kW
5.	FC rated power	1.26kW
6.	FC nominal stack efficiency	55%
7.	Battery nominal voltage	26.4V
8.	Battery rated capacity	6.6Ah
9.	UC rated voltage	16V
10.	UC rated capacitance	500F

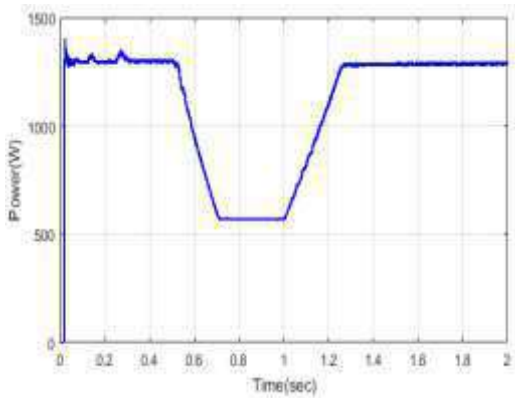
**Performance investigation of the projected method**

Case1: Linear load demand with non-linear power generation

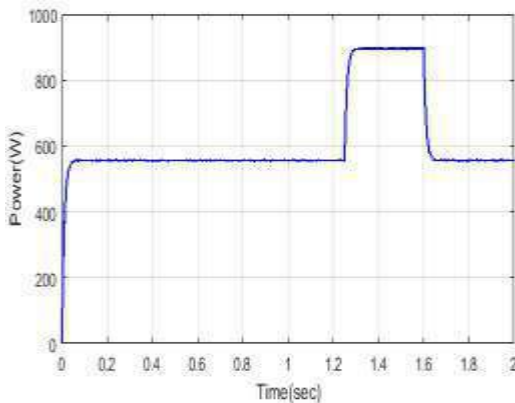
The projected scheme application parameters are tabularised in [Table. 1]. In this parameters are utilized in an application progression. The actual parameters are appraised and assess the reference parameters of the training dataset and then it will train with the help of SVM. The assessed parameters are exemplified in subsequent. Primarily the case 1 like non-linear power and linear load condition is accessible and appraised.



(a)



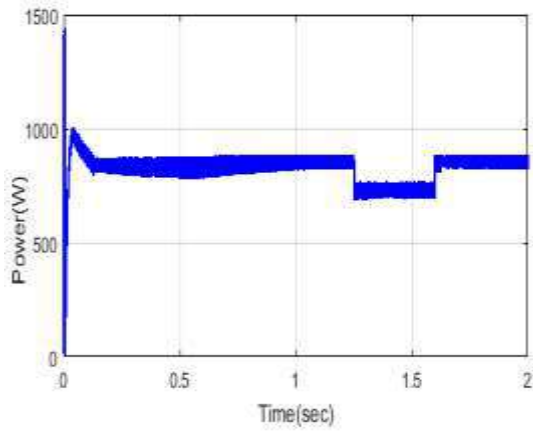
(b)



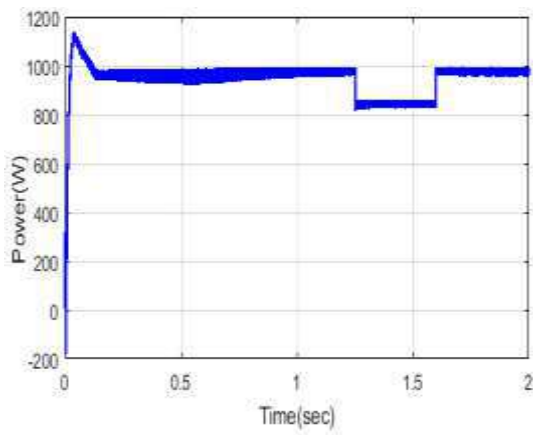
(c)

Fig.4: Power fashioned from the generation model (a) Irradiation, (b) PV power, (c) Wind power in case 1.

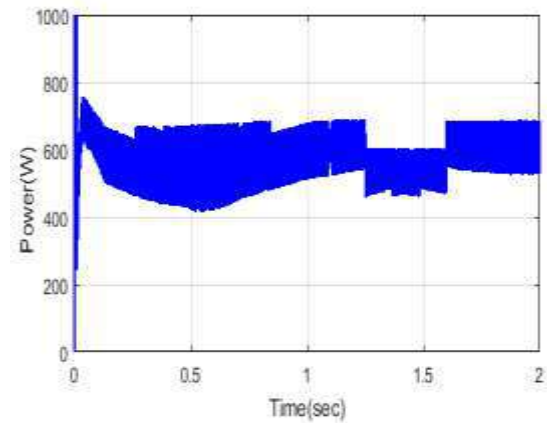
.....



(a)



(b)



(c)

**Fig.5:** Power fashioned from the storage model (a) Battery, (b) UC, (c) FC in case 1.

.....



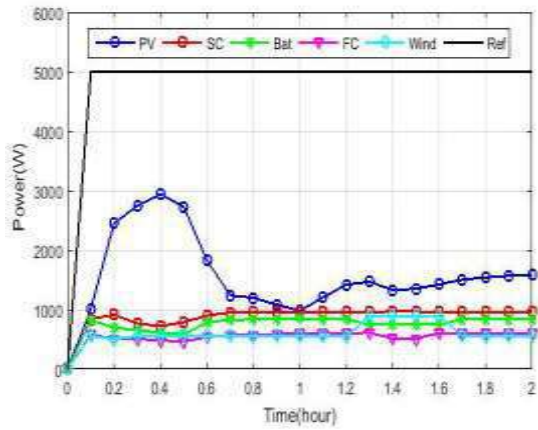


Fig. 6: Power produced from the existing sources SC, Battery, FC, PV and WT in case 1.

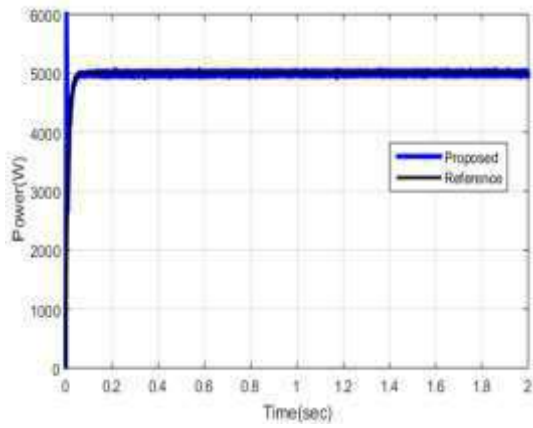


Fig. 7: Projected technique load power contrast in case 1.

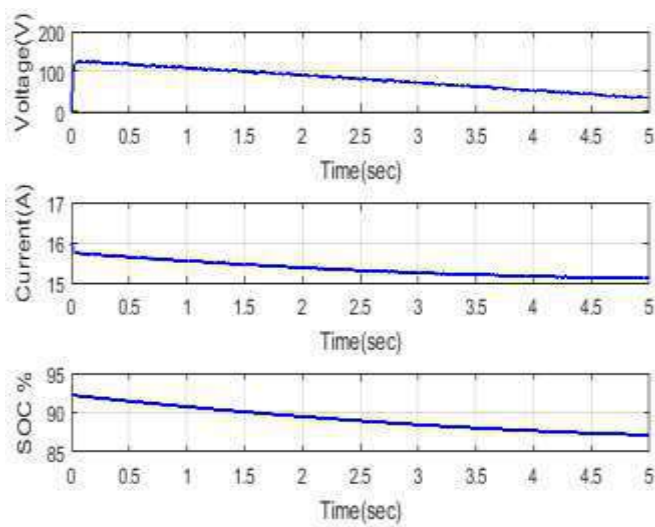


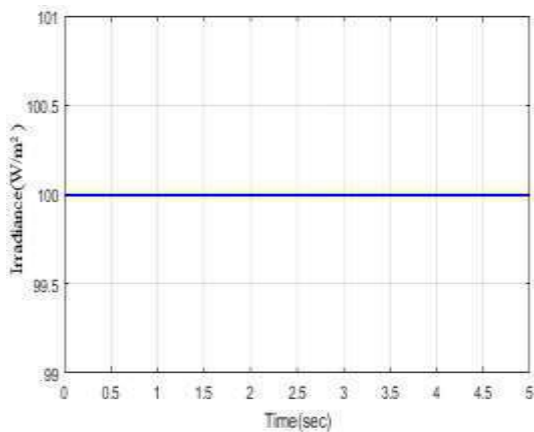
Fig. 8: Battery states of charge in case 1.

In case 1 is the generated power is unbalanced condition and the output load is linear circumstance. The power generation of a generation scheme model is assessed and demonstrated in [Fig. 4]. In a figure declared that the variation of the irradiations, PV power and WT model is designated. Then the storage scheme model power is restrained and plotted in [Fig. 5]. In that the battery, UC and FC power variation is demonstrated. If the power of the battery is deposited the energy and control the flow of the micro grid.

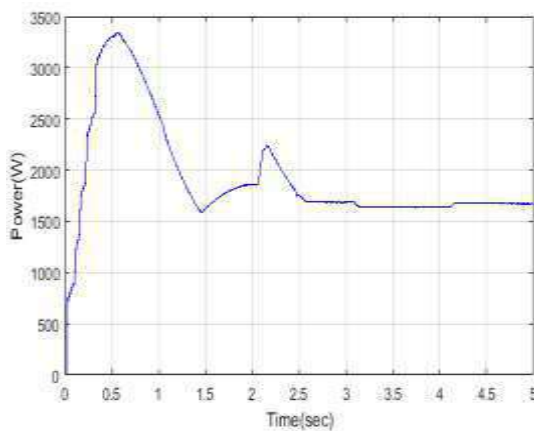
The power assessed from the manufactured and stored scheme model is exemplified in [Fig. 6]. In this figure, demonstrated the generated model and storage model power and declared and associated with the reference power of the projected scheme. The efficiency of the projected model with this case 1 on the basis of the linear load demand is demonstrated in [Fig. 7]. Then the storage scheme battery state of charge is designated in [Fig. 8]. SoC is generally utilized if conferring the current state of a battery in usage when conferring the lifetime of the battery after recurring usage. Frequently, SoC cannot be restrained directly but it can be assessed from direct measurement variables. Lastly the second case is restrained and also assessed the parameters of the influence of the structure.

### Case2: Non- linear load demand with linear power generation

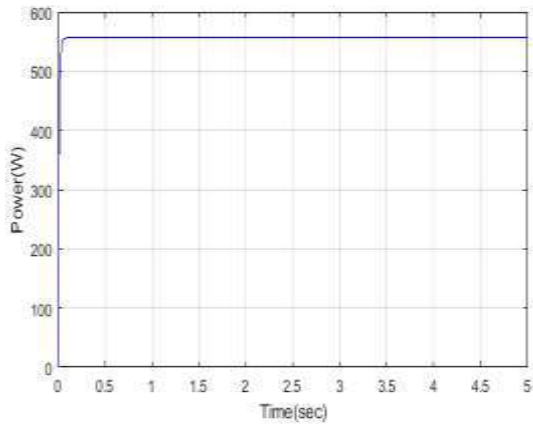
In the case2 encompasses of the linear power output and non-linear load circumstance of the projected scheme that revenue that the output of the PV and WT power is stable condition. In this condition, the power of the irradiance, PV and WT are restrained and exemplified in [Fig. 9]. The irradiance of the solar is unwavering and it preserves normal values. The power of the PV and WT is originally high value and it preserves the stable values. The solar irradiance is 100, PV power upholds 1700 watts and the WT upholds the 550 watts for generation model. Then the storage scheme model is restrained and appraised in case 2 so the output load demand is fluctuating and it cannot be unhinged.



(a)



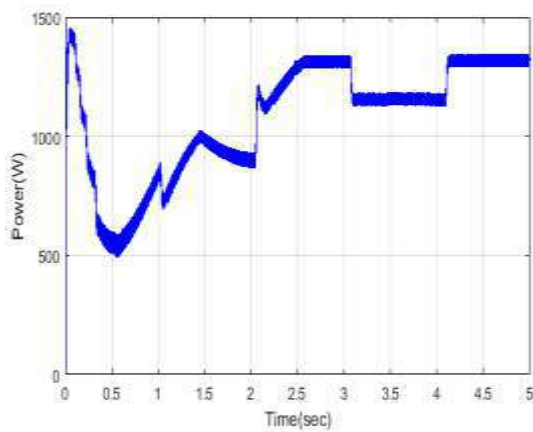
(b)



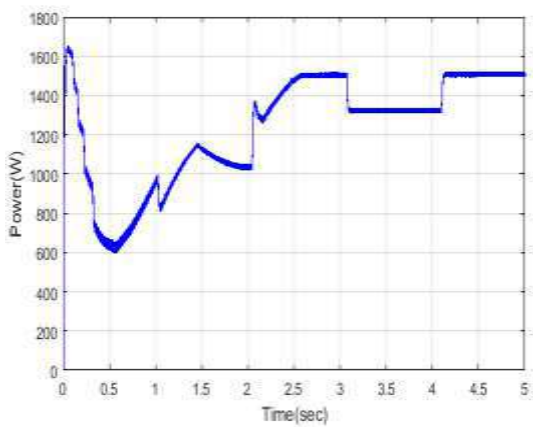
(c)

Fig. 9: Power fashioned from the generation model (a) Irradiation, (b) PV power, (c) Wind power in case 2.

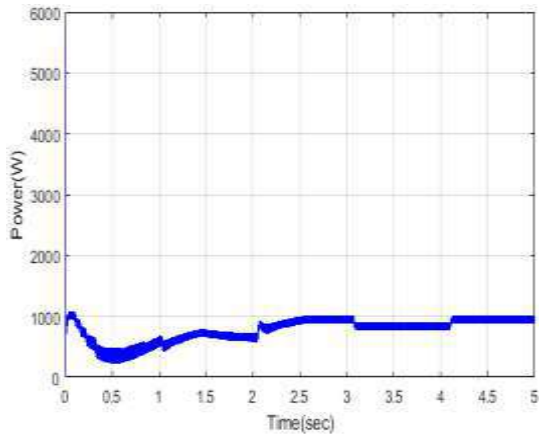
The restrained power of the battery, UC and FCs are assessed in [Fig. 10]. The power of the battery is differs from 500 watts and the UC is differs from 600 to 1500 watts and then the power of the FC is hesitated less than 1000 watts. Lastly, the assessed power of the renewable sources and the energy storage schemes are associated with the reference power signal that is designated in [Fig. 11].



(a)



(b)



(c)

Fig.10: Power produced from the storage model in case 2 (a) Battery, (b) UC and (c) FCs.

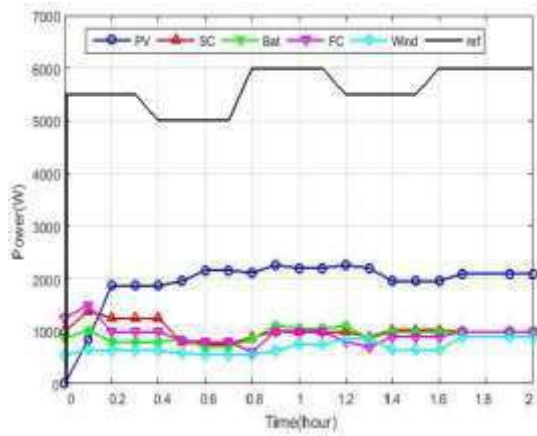


Fig.11: Power produced from the existing sources UC, Battery, FC, PV and WT

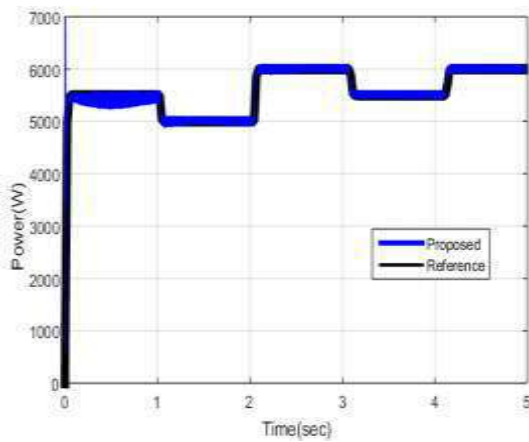


Fig.12: Projected technique load power assessment in case 2.

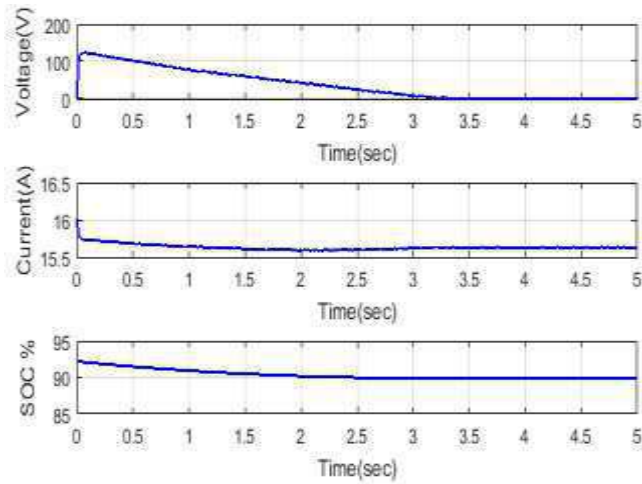


Fig.13: Battery states of charge in case 2.

In the present case 2 the awaited system efficacy with the load demand is associated in [Fig. 12]. Then, the monitoring power storage scheme states of charge is demonstrated in [Fig. 13] that displays the voltage, current and state of charge for battery is revealed. In this battery charge can progresses the power control of the MG on the basis of demand of the loads. The association with the load demand is assessed and appraised below.

**Comparison with the reference signal**

In this sub segment, the comparison investigation of the projected model with the dissimilar traditional models such as ANN and fuzzy, this associated with the reference power signal of the projected model. The projected model assessment investigation is designated in [Fig. 14], that the optimal power flows of the projected method consistent with the reference signal. At that time, the energy organization is associated with the traditional methods that demonstrated in [Fig. 15]. In this figure, encompasses the efficiency of the projected model can transformed the power conforming the load claim of the MG model. In this segment, designated about the function of the projected technique for the load demand and the projected predictive model are greater to other methods. In this technique, function is enhanced on the basis of the load demand also the battery life span of the storage scheme.

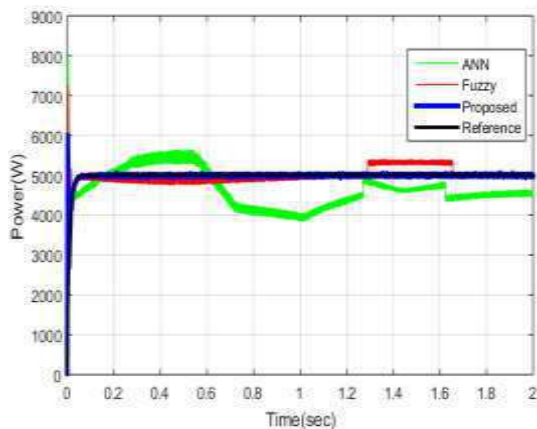


Fig.14: The comparison investigation of the generated power with dissimilar methods



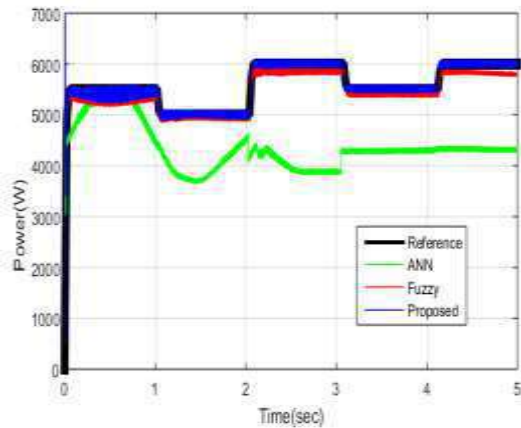


Fig.15: Energy management assessment with the help of dissimilar methods

The power flow of the MG is joined with the converter utilized for power alteration of the MG. Henceforth; the contrast investigation is shown that the projected forecast model is better operative for the linear, non-linear load ultimatum. Then the projected model is determined in segment 5.

## CONCLUSION

This article suggested an energy management model for micro-grid implementation on the basis of the SVM expectation model. The projected model is associated with the generation classical then the energy stowage model. The production model comprises of a solar PV and WT, the energy storage scheme comprises the UC, battery, and FCs. The SVM prognostic model is produce the dataset on the basis of the projected energy organization scheme restraints for training the extrapolation model. Then the projected scheme is enhanced the power necessities by considering a photovoltaic power accessibility, battery bank SOC and load power request. The function of the projected model is investigated on the basis of the two cases similarly linear and non-linear load stresses and power generation. Lastly, the load power request association investigation is achieved with diverse traditional methods such as ANN, fuzzy complete reference signal. Formerly the association solutions are recognized that the anticipated technique is improved than the other out-dated methods.

## CONFLICT OF INTEREST

There is no conflict of interest regarding the publication of this paper.

## ACKNOWLEDGEMENTS

None

## FINANCIAL DISCLOSURE

No financial contribution for my manuscript.

## REFERENCES

- [1] M.H.Nehrir, C.Wang, K.Strunz, H.Aki, R.Ramakumar, J.Bing, Z.Miao and Z.Salameh,[2011] A Review of Hybrid Renewable/Alternative Energy Systems for Electric Power Generation: Configurations, Control, and Applications, IEEE Transactions on Sustainable Energy,2(04): 392-403.
- [2] Taher Niknam, Faranak Golestaneh and Ahmadreza Malekpour, [2012] Probabilistic energy and operation management of a micro grid containing wind/ photovoltaic/fuel cell generation and energy storage devices based on point estimate method and self-adaptive gravitational search algorithm, International Journal of Energy, 43(01): 427-437,
- [3] O.Erdinc and M.Uzunoglu, [2012] Optimum design of hybrid renewable energy systems: Overview of different approaches, International Journal of Renewable and Sustainable Energy Reviews, 16: 1412-1425.
- [4] M.Seddik, S.Zouggar, M.Oukili, T.Ouchbel, A.Aziz, M.L.Elhafyani and F.Z.Kadda, [2013] The Digital Energy Management of a Stand - Alone Hybrid System Photovoltaic-Wind, International Journal of Engineering and Innovative Technology, 3(03): 156-163.
- [5] Hanane Dagdougui, Riccardo Minciardi, Ahmed Ouammi, Michela Robba and Roberto Sacile,[2012] Modeling and optimization of a hybrid system for the energy supply of a "Green" building, International Journal of Energy Conversion and Management,64: 351-363.
- [6] Erkan Dursun and Osman Kilic, [2012] Comparative evaluation of different power management strategies of a stand-alone PV/Wind/PEMFC hybrid power system, International Journal of Electrical Power and Energy Systems,34: 81-89.
- [7] Yu-Kai Chen, Yung-Chun Wu, Chau-Chung Song and Yu-Syun Chen, [2013] Design and Implementation of Energy Management System with Fuzzy Control for DC Micro-Grid Systems, IEEE Transactions on Power Electronics,28(04): 1563-1570.

- [8] Rodrigo Palma-Behnke, Carlos Benavides, Fernando Lanas, Bernardo Severino, Lorenzo Reyes, Jacqueline Llanos, and Doris Saez, [2013] A Microgrid Energy Management System Based on the Rolling Horizon Strategy", IEEE Transactions On Smart Grid, 4(02): 996-1006.
- [9] H.S.V.S.Kumar Nunna and Suryanarayana Doolla, [2013] Multi Agent based Distributed Energy Resource Management for Intelligent Microgrids, IEEE Transactions on Industrial Electronics, 60(4): 1678-1687.
- [10] Yu Zhang, Nikolaos Gatsis and Georgios B.Giannakis, [2013] Robust Energy Management for Microgrids with High-Penetration Renewables, IEEE Transactions on Sustainable Energy, 4(4): 944-953.
- [11] Joydeep Sarkar and Pramod Yade, [2014] Structuring DC Micro-Grid for Integrating Renewable Energy in a DC Load Dominant Electrical Environment , International Journal of Engineering Sciences and Research Technology, 03(07): 609-613.
- [12] Prasenjit Basak, S.Chowdhury, S.Halder nee Dey and S.P.Chowdhury, [2012] A literature review on integration of distributed energy resources in the perspective of control, protection and stability of micro grid, International Journal of Renewable and Sustainable Energy Reviews,16: .5545-5556.
- [13] Mohammed Yekini Suberu, Nouruddeen Bashir, Ogunbola Matthew Adefemi and Umar Usman, [2013] Renewable Energy Distributed Electricity Generation and Microgrid Implementation in Rural Villages: A Review, ARPN Journal of Engineering and Applied Sciences, 8(02): 149-156.
- [14] A.Etxeberria, I.Vechiu, H.Camblong and J.M.Vinassa, [2012] Comparison of three topologies and controls of a hybrid energy storage system for micro grids, International Journal of Energy Conversion and Management, 54: 113-121.
- [15] Sreya Grace Mathew and Fossy Mary Chacko,[2014] Power Quality Improvement in a Grid Connected Renewable Energy System, International Journal of Electrical, Electronics and Data Communication,,2(10): 27-29.
- [16] Prabodh Bajpai and Vaishalee Dash, [2012] Hybrid renewable energy systems for power generation in stand-alone applications: A review, International Journal of Renewable and Sustainable Energy Reviews,16: 2926-2939.
- [17] Zeng Jun, Liu Junfeng, Wu Jie and H.W. Ngan, [2011] A multi-agent solution to energy management in hybrid renewable energy generation system, International Journal of Renewable Energy, 36:1352-1363.
- [18] Ahmed Mohamed and Osama Mohammed, [2013] Real-time energy management scheme for hybrid renewable energy systems in smart grid applications, International Journal of Electric Power Systems Research,96: 133-143.
- [19] John T.B.A.Kessels, Michiel Koot, Bram de Jager, Paul P.J.van den Bosch, P.I.Aneke, and Daniel B.Kok, [2007] Energy Management for the Electric Power net in Vehicles With a Conventional Drive train, IEEE Transactions on Control Systems Technology, 15(03): 494-505.
- [20] S.Merlin Joys Mary and S.Rajesh Babu, [2014] Energy management on grid connected hybrid renewable energy sources using fuzzy logic, International Journal of advanced research in electrical, electronics and instrumentation engineering, 3(4): 9275-9283.
- [21] Juan P.Torreglosa, Pablo Garcia-Trivino, Luis M.Fernandez-Ramirez and Francisco Jurado, [2016] Control based on techno-economic optimization of renewable hybrid energy system for stand-alone applications, International Journal of Expert Systems with Applications, 51: 59-75.
- [22] A.S.O.Ogunjuigbe, T.R.Ayodele and O.A.Akinola, [2016] Optimal allocation and sizing of PV/Wind/Split-diesel/Battery hybrid energy system for minimizing life cycle cost, carbon emission and dump energy of remote residential building, International Journal of Applied Energy,171: 153-171.
- [23] Sarangthem Sanajaoba and Eugene Fernandez, [2016] Maiden application of Cuckoo Search algorithm for optimal sizing of a remote hybrid renewable energy System", International Journal of Renewable Energy,96: 1-10.
- [24] Pablo Garcia, Juan P.Torreglosa, Luis M.Fernandez, Francisco Jurado, Roberto Langella and Alfredo Testa,[2016] Energy management system based on techno-economic optimization for microgrids, International Journal of Electric Power Systems Research, 131: 49-59.
- [25] E.S.Ali, S.M.Abd Elazim and A.Y.Abdelaziz, [2016] Improved Harmony Algorithm and Power Loss Index for optimal locations and sizing of capacitors in radial distribution systems," International Journal of Electrical Power and Energy Systems,80: 252-263.
- [26] Ranjeeta Khare and Yogendra Kumar, [2016] A novel hybrid MOL-TLBO optimized techno-economic-socio analysis of renewable energy mix in island mode", International Journal of Applied Soft Computing,43: 187-198.
- [27] A.Y.Abdelaziz, E.S.Ali and S.M.Abd Elazim,[2016] Flower Pollination Algorithm and Loss Sensitivity Factors for optimal sizing and placement of capacitors in radial distribution systems", International Journal of Electrical Power and Energy Systems, 78:207-214.
- [28] Li Ma, Nian Liu, Lingfeng Wang, Jianhua Zhang, Jinyong Lei, Zheng Zeng, Cheng Wang and Minyang Cheng, [2016] Multi-party energy management for smart building cluster with PV systems using automatic demand response, International Journal of Energy and Buildings,121: 11-21.
- [29] Victor Herrera, Aitor Milo, Haizea Gaztanaga, Ion Etxeberria-Otadui, Igor Villarreal and Haritza Camblong, [2016] Adaptive energy management strategy and optimal sizing applied on a battery-supercapacitor based tramway", International Journal of Applied Energy, 169: 831-845.
- [30] Nicu Bizon, Mihai Oproescu and Mircea Raceanu,[2015] "Efficient energy control strategies for a Standalone Renewable/Fuel Cell Hybrid Power Source, International Journal of Energy Conversion and Management,90: 93-110.
- [31] Vivek Mohan, Jai Govind Singh, Weerakorn Ongsakul, Nimal Madhu, M.P.Reshma Suresh, [2016] Economic and network feasible online power management for renewable energy integrated smart microgrid", International Journal of Sustainable Energy, Grids and Networks,7: 13-24.
- [32] Imene Yahyaoui, Amani Yahyaoui, Maher Chaabene and Fernando Tadeo, [2016] Energy management for a stand-alone photovoltaic-wind system suitable for rural electrification", International Journal of Sustainable Cities and Society, 25: 90-101.
- [33] Gokay Bayrak, [2015] A remote islanding detection and control strategy for photovoltaic-based distributed generation systems", International Journal of Energy Conversion and Management,96: 228-241.
- [34] T.Yuvaraja, M.Gopinath [2014] Fuzzy Based Analysis of Inverter Fed Micro Grid inIslanding Operation International Journal of Applied Engineering Research ISSN 0973-4562 9(22) : 16909-16916.
- [35] Yuvaraja Teekaraman\*, Gopinath Mani\*\*[2015] Fuzzy Based Analysis of Inverter Fed Micro Grid in Islanding Operation- Experimental Analysis International Journal of Power Electronics and Drive System (IJPEDS) 5(04): 464-469.

## ARTICLE

# ENERGY EFFICIENT SWITCHING CONTROL FOR HYBRID VEHICLES

Arockia Vijay Joseph<sup>1\*</sup>, Joselin Retna Kumar G<sup>1</sup>, Kabeelan S<sup>2</sup>, Eman Rose G<sup>2</sup>, Vishal G<sup>2</sup>,  
Siddharth N<sup>2</sup>

<sup>1</sup> ACCES LAB, Department of Electronics and Instrumentation Engineering, SRM University,  
Kattankulathur, Tamil Nadu, INDIA

<sup>2</sup>Department of Electronics and Instrumentation Engineering, SRM University, Kattankulathur, Tamil  
Nadu, INDIA

## ABSTRACT

Development of energy efficient and eco-friendly hybrid vehicle model is discussed in this paper. The power train test bed of a hybrid two wheeler system is physically modeled and a switching control methodology is developed to achieve electrical switching between electric motor and engine for efficient fuel consumption. The complete test bed for the power train of the hybrid vehicle is designed and fabricated. A conventional sequential and condition based switching control algorithm is developed to operate the system with electric motor at low speeds and the engine at higher speeds, using the speeds of the power components in terms of revolution per minute (rpm) as the parameter for switching. The analysis on the efficiency of the hybrid system resulted with a 21.4% efficient more than the conventional two wheeler system.

## INTRODUCTION

Improvements in fuel economy and emission reductions are the most important challenging goals that are presented before the automotive industry. The eco system is under potential threat due to the increase in the number of vehicles and its effect on environmental pollution with its emissions from internal combustion engines (ICE), used for their propulsion. The attempt of leaving the nature unaffected and allowing it to stay as it was, will bring us closer to the concept of hybridization. Hybrid electric vehicles (HEV) are beginning to demonstrate their capability to satisfy these requirements, and they will become a viable alternative to conventional vehicles in the future [3, 5]. The hybrid power train is an integrated system that may consist of the following components: an internal combustion engine (IC engine), a battery pack, and an electric machine (EM) which can be utilized as a traction motor or generator. In such a system, each sub-system is also a complex system which has its own functionality and desired performance [6]. These systems are versatile in nature and thus can be configured in different ways to deliver power. The different configurations of hybrid vehicles include Parallel Hybrid, Series hybrid, Series-Parallel or Combined hybrid and Plug-in Hybrid Electric Vehicle (PHEV) [4]. Generally the combined hybrid vehicles involve front wheel drive which is connected to the power sources through transmission systems and clutch in order to engage one of the sources to the wheel axle. The switching process is electro-mechanical in nature and power is transmitted through a dedicated transmission system. This system is limited to four wheelers such as cars and SUV's. Also a complete automatic switching mechanism is seldom implemented in such vehicles and this is the one highly required in field of biking sector for improved fuel efficiency. Hence considering all these factors, a simpler switching methodology is being adopted with the components matching the dynamics of a two wheeler and the sources being coupled by a chain transmission [1]. The focus of this paper is to develop energy efficient switching control strategy used to control combined HEVs.

## PROPOSED DESIGN

The test bed is a platform which houses the engine and the motor in a fixed position. The shaft of the engine is fitted with a toothed disc. Another toothed disc of same dimensions and teeth count is fitted to the motor shaft. The engine and the motor are placed such that they are a distance apart and their axis of rotation of the shafts is parallel to each other. Also the plane faces of the disc are maintained in the same plane and line, so that the two sources can be coupled effectively. The coupling is done using a chain. Thus when any one of the shaft is rotated, the other rotates in the same direction and speed. The parameter for switching is taken to be the speed of the shafts of motor and the engine individually in terms of rotations per minute (rpm). In order to read the speed of the shaft a Hall Effect sensor is incorporated in the shaft of both motor and the engine to read the number of rotations of the shaft. The motor speed is varied using a motor controller and the engine speed is varied using a throttle control system. In order to perform the throttle action of the engine, a servo motor is used to open the throttle valve to the pre-defined angle which provides the required amount of acceleration to the system. [Fig. 1] shows a schematic diagram of the simplified structure of a combined hybrid electric vehicle system considered in this paper and its technical specifications are shown in [Table 1].

### KEY WORDS

Hybrid vehicles,  
Switching Control,  
Efficiency, Power Train

Published: 20 October 2016

### \*Corresponding Author

Email:  
arockiavijay.j@ktr.srmuniv.ac.in  
Tel.: +91-9677002684

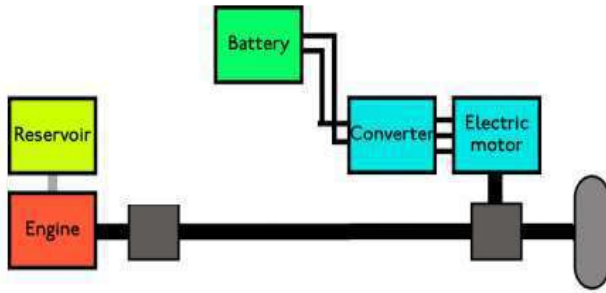


Fig. 1: Simplified structure of a combined hybrid electric vehicle

Table. 1: Technical specifications of the vehicle used in this work

Engine	Honda Activa – 109cc
Motor	Rating : 24V, 19.2A, DC Speed : 2750 rpm Power : 350W
Electronics Unit	Power Relay : 30 A Servo Motor : 5V, 300 mA Arduino Boards : 12V, 1A

### SYSTEM DESCRIPTION

The developed test bed for the proposed hybrid vehicle is shown in [Fig. 2] and the block diagram with various system components is depicted in [Fig. 4]. The various components involved in the system comprise of dedicated relays, servomotor, RPM measurement and display modules. This system also used an arduino based microcontroller in place of a full-fledged engine control unit. For ease of understanding the circuitry in the system can be broken down into different parts as follows,

1. RPM measurement and display modules
2. Relay switch modules
3. Servo motor
4. Control unit.



Fig. 2: Developed test bed for the hybrid vehicle

### RPM Measurement and Display Modules

The RPM measurement modules are arduino based, to which LCD panels serve the display function. This system uses separate and exclusive modules to measure the RPM of motor and engine. The RPM is measured using two Hall Effect sensors which are housed near the shafts of the engine and the motor, which constantly measure and feed the RPM data to the control unit. The control unit is already fed with a set RPM value in order to carry out switching in bi directional manner (i.e. motor to engine and engine to motor). The LCD displays the measured rpm values for ease of observation as shown in [Fig. 3].

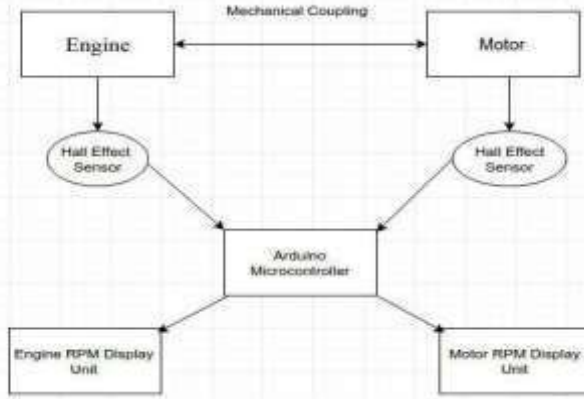


Fig. 3: Speed display module

Relay Switch Modules

The relay switches are the actual members that actuate the switching process by receiving signals from the controller when the set point is reached or crossed. Three dedicated relays are used for the purpose of engine start, engine stop and motor start/stop as shown in [Fig. 4]. The relays maintain normally open state when the system is idle. Thus they actuate either the engine or the motor when they receive a signal at their respective relay ports. The relays work such that when the system is switched ON; initially the motor relay closes first and actuates the motor until the motor reaches the set point, wherein the meantime the engine start and engine stop relays remain open. But when the set point is crossed the motor relay opens and the engine start relay closes and the engine starts immediately, picking up from the current rpm of motor where the motor has disengaged.

Servo Motor

As the engine takes on the system, the throttle wire is simultaneously pulled by actuating the servo motor which turns stepwise at defined angles. The actuating signal is given to the servo motor by and when the control unit senses that the set point is crossed. Once the servo has pulled the throttle to the maximum defined position, it returns back to null thereby causing deceleration of the engine. This gradually causes a decline in engine shaft rpm which falls below the set speed in the control unit, thereby rising a case to switch back to DC motor [7]. This operation can be related to the real time driving.

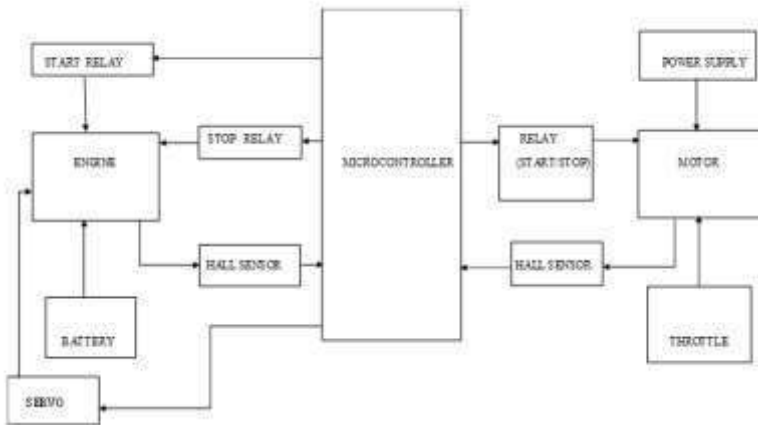


Fig. 4: System design

Control Unit

The control unit is fed with the defined speed as set point value and a condition based switching algorithm. The input parameter-(rpm values) is fed to the control unit for internal comparison and condition checking to enable bi-directional switching. Thus when there is an ascending crossover of the set point, the power is switched from DC motor to engine and when there is a descending crossover of the set point the power switches back to the DC motor from the engine, making the entire process completely automatic and repeatable for 'n' cycles [2].



### SWITCHING ALGORITHM

The flow chart of the switching algorithm is shown in [Fig. 5]. The algorithm mentioned is condition based programming. The switching process takes decisions based on the feedback values obtained from the engine and electric motor speed sensors. The vehicle is started using the electric motor to gain initial momentum and run until vehicle reaches the cutoff speed in rpm. Once the vehicle surpasses the cutoff speed, the engine is given the control to pull the vehicle switching off the motor. In case of deceleration, the controller checks for the feedback from speed sensor of engine shaft for cut off speed, to switch from engine to the electric motor. Once dropped below the cutoff, controller gradually loses the grip from the engine throttle servo motor and transfers the control to motor.

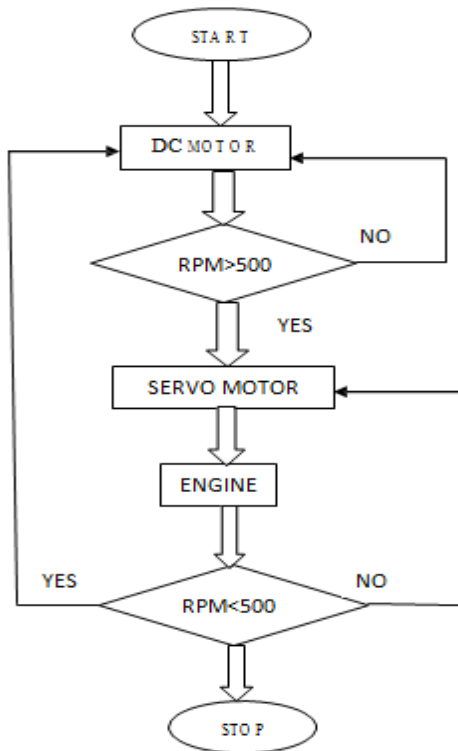


Fig. 5: Developed switching algorithm

### EXPERIMENTAL ANALYSIS

The proposed energy efficient hybrid system is implemented against the considered conventional gasoline two wheeler engine system and checked for mileage. For ease of observance 100 ml of petrol is kept as reference mark of input supply for the gasoline engine. The test bed is operated on the following two different modes,

1. Normal Mode
2. Hybrid mode

Here normal mode is the mode in which the test bed is operated with gasoline engine to understand the consumption rate of conventional gasoline two wheeler engine system under no load condition whereas the hybrid mode is the mode in which the gasoline engine is operated in conjunction with the electric motor under no load condition. Both the modes of operation are tested using continuous run test.

In order to run the hybrid mode testing, the throttle of the engine is controlled by a servo motor and the measured engine shaft speeds with respect to various servo angle position is tabulated and given in [Table 2] and [Table 3].

Table 2: Calibrated acceleration settings

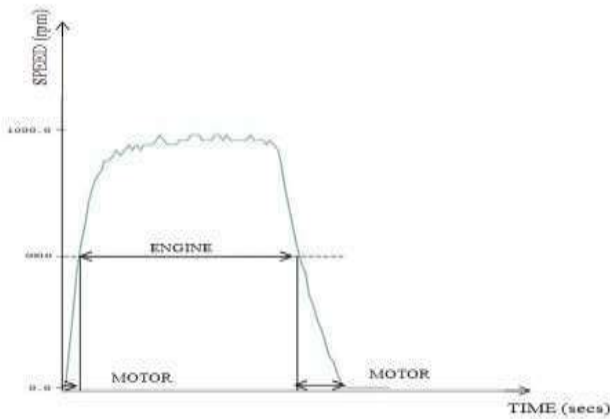
SERVO ANGLE (Degrees)	Speed (rpm)
180	0
160	300
120	1800

**Table 3:** Calibrated deceleration settings

SERVO ANGLE (Degrees)	Speed (rpm)
120	1800
160	300
180	0

**Continuous run test**

The system was run in two different modes. Initially the system was run in normal mode with 100ml of fuel and it was followed by the hybrid mode where the test was conducted with same amount of fuel as it was done in the normal mode. It was observed that the former mode of operation utilized a sizable amount of fuel to make the initial start and then regulated its consumption. In the latter system the initial speed was attained by electric motor and then it switches to engine to have the speed maintained with gasoline. The hybrid mode of operation consumed 20 ml less fuel compared to the normal mode drive. The output response of the hybrid mode operation of the test bed is logged and plotted in [Fig. 6].



**Fig. 6:** Output response of hybrid mode of operation

**DISCUSSION**

The results of the above experimental analysis are given in [Table 4].

**Table 4:** Mileage analysis on different modes

SYSTEM MODE	FUEL supplied in ml	Observed mileage in km
Normal Mode	100	4.2
Hybrid Mode	100	5.1

The above mentioned result is discussed having considered mileage as the parameter for efficiency. Thus comparing the mileage of the two systems, the efficiency value can be calculated as,  

$$\eta = (\text{mileage of the hybrid system} / \text{mileage of the conventional system}) \times 100$$
 i.e.  $(5.1/4.2) \times 100 = 121.4\%$   
 Since efficiency cannot be greater than 100, this calculation is understood as; hybrid system is 21.4% more efficient than the conventional gasoline engine for the same amount of fuel. The calculated distance covered is plotted and compared in [Fig. 7].

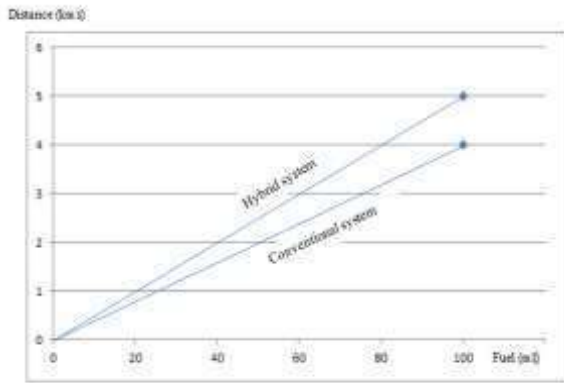


Fig. 7: Comparison of distance covered using different modes of operation

## CONCLUSION

This paper reviews briefly on the existing works in the area of hybrid modeling of various vehicles. This research shows the development of hybrid based two wheeler vehicle test bed and development of switching control strategy and its consideration towards the experimental proceedings. The results of the study analysis have presented a competitive area of research to provide solutions to the potential problems available in relation to the hybrid vehicles and energy efficient systems supporting the safer and cleaner environment.

The developed system lags the smoothness in switching which needed to be addressed by the modern and sophisticated control methodologies. Increased parameter considerations apart from engine and electric motor speed can fetch better switching and improved understanding on the behavior of the system and enables the control designer to enhance its switching dynamics. The system can also be provided with an option of simultaneous manual or automatic control based on the user's preference. Also hybrid two wheelers can be built and tested with this design and they can be further mass produced like the hybrid cars for a safer eco-system.

### CONFLICT OF INTEREST

The authors declare no competing interests in relation to the work.

### ACKNOWLEDGEMENTS

None

### FINANCIAL DISCLOSURE

This research is partially funded and supported by ACCES Lab, Department of Electronics and Instrumentation Engineering, SRM University.

## REFERENCES

- [1] Shimizu H, Harada J, Bland C, Kawakami K, Lam C. [1997] Advanced concepts in electric vehicle design. IEEE Trans. Ind. Electron.44: 14-18.
- [2] Masao Ono, Nobuhito Ohnuma, Jun Morimoto, Hiroko Yoshikawa, Akifumi Kurita, Osamu Watanabe. [2001] Hybrid Vehicle and method of controlling the travel of the vehicle. US 6,295,487 B1.
- [3] Chau KT, Wang YS. [2002] Overview of Power Management in Hybrid Electric Vehicles. Energy Convertors. Manage.43:1953-1968.
- [4] Ronald K Jurgen. [2002] Electrical and Hybrid-Electrical Vehicles. Society of Automotive Engineering 1:191- 195.
- [5] Bitsche O. and Gutmann G. [2004] System for Hybrid Cars. J Power Sources 127:8-15.
- [6] Licun Fang and Shiyin Qin. [2006] Optimal control of parallel hybrid electric vehicles based on theory of switched system. Asian Journal of Control 8:274-280.
- [7] Pau Muñoz-Benavent, Leopoldo Armesto, Vicent Girbés, J Ernesto Solanes, Juan Dols, Adolfo Muñoz and Josep Tornero. [2012] Advanced Driving Assistance Systems for an Electric Vehicle. International Journal of Automation and Smart Technology 2:329-338

# THE EXPERIMENTAL VERIFICATION OF BRIDGELESS TAPPED INDUCTOR SEPIC CONVERTER FOR BLDC MOTOR DRIVE APPLICATIONS

S Sathiyamoorthy<sup>1\*</sup> and M Gopinath<sup>2</sup>

<sup>1</sup>Department of Electrical and Electronics Engineering, St.Peter's University, Chennai, Tamilnadu, INDIA

<sup>2</sup>Department of EEE, Dr.N.G.P. Institute of Technology, Coimbatore, Tamilnadu, INDIA

## ABSTRACT

**Background:** This paper introduces a power factor corrected bridgeless tapped inductor SEPIC (BL TI-SEPIC) converter-fed brushless direct current (BLDC) motor drive in the form of a cost-economic solution for high-power applications. **Methods:** A mechanism of speed control of the BLDC motor through the control of the dc link voltage of the voltage source inverter (VSI) is exploited with a single voltage sensor. **Results:** A BL TI-SEPIC converter is presented that provides the removal of the diode bridge rectifier, thereby minimizing the conduction losses related to it. **Conclusions:** A BL TI-SEPIC converter is modelled to be operated in discontinuous current mode (DCM) to yield an intrinsic PFC at ac mains. **Applications:** The performance of the newly introduced driver is investigated under speed control with enhanced power quality at ac mains; in addition the validation of the BLDC driver proposed is done experimentally over a designed prototype.

## INTRODUCTION

### KEY WORDS

#### INDEX TERMS

Brushless Direct Current (BLDC), Power Factor Correction (PFC), Electronic Commutation, Discontinuous Current Mode (DCM)

Resourcefulness and being cost-economic are the important challenges in developing low-power motor drives aiming at household applications like fans, water pumps, blowers, mixers, etc. The usage of the brushless direct current (BLDC) motor in these applications is getting popular because of features like better efficiency, greater flux density per unit volume, lesser requirements for maintenance, and lesser electromagnetic-interference issues [1,2].

A BLDC motor consists of three phase windings on the stator in addition to permanent magnets on the rotor. The BLDC motor is also referred to as an electronically commutated motor since an electronic commutation dependent on rotor position is employed instead of a mechanical commutation that has demerits such as sparking and wear and tear of brushes and commutator assembly [3, 4].

A BLDC motor, while being powered by a diode bridge rectifier (DBR) with a large value of dc link capacitor obtains peaky current that can result in a THD of supply current of the magnitude of 65% and power factor as less as 0.8 [5]. Therefore, a DBR, which is followed by a power factor corrected (PFC) converter is used for boosting the power quality at ac mains. For the purpose of reducing the losses of the DBR, many bridgeless (BL) PFC rectifiers have been introduced for enhancing the rectifier power density and/or reduces noise emissions [6], [7] by means of the soft switching techniques.

The traditional BL PFC method of the BLDC motor drive uses a pulsewidth-modulated voltage source inverter (PWM-VSI) for speed control along with a continuous dc link voltage. This gives greater switching losses in VSI since the switching losses are increased in the order of a square function of the switching frequency. Since the speed of the BLDC motor is in direct proportion with the dc link voltage applied, the speed control is attained by the variable dc link voltage of VSI. This permits for the fundamental frequency switching of VSI (i.e., electronic commutation) and renders reduction in the switching losses.

## PROPOSED TOPOLOGY

This study demonstrates a new bridgeless SEPIC converter in addition to the tapped inductor (TI) model (BL TI-SEPIC) that has a wide gain range for the BLDC motor drive applications. The schematic diagram of the proposed BL TI-SEPIC converter along with the conventions of the circuit variables which are followed is shown in [Fig. 1].

The converter circuit proposed comprises of an input inductors  $L_1$  and  $L_2$ ; the main switches  $S_1$  and  $S_2$ ; intermediate capacitors  $C_1$  and  $C_2$ ; then a voltage multiplier cell is also included in the circuit, consisting of  $C_m$ ,  $D_{m1}$  and  $D_{m2}$ ; a Tapped Inductor (TI) of  $L_p$ ,  $L_s$ ; and a charge pump is also included in the circuit which contains  $C_3$ ,  $D_1$  and  $D_0$ , which feeds an output filter capacitor,  $C_0$ , and finally a voltage source inverter (VSI) fed BLDC motor drive.

In the proposed topology, the use of bridgeless configuration will reduce the losses corresponding to conduction and the voltage multiplier cell will then have a maximization of the gain and reduce the switch voltage stress. Hence, this novel topology boosts the efficiency on an overall. The proposed converter exploits two unidirectional switches ( $S_1$  and  $S_2$ ). Switch  $S_1$  is turned ON/OFF during the positive half-line

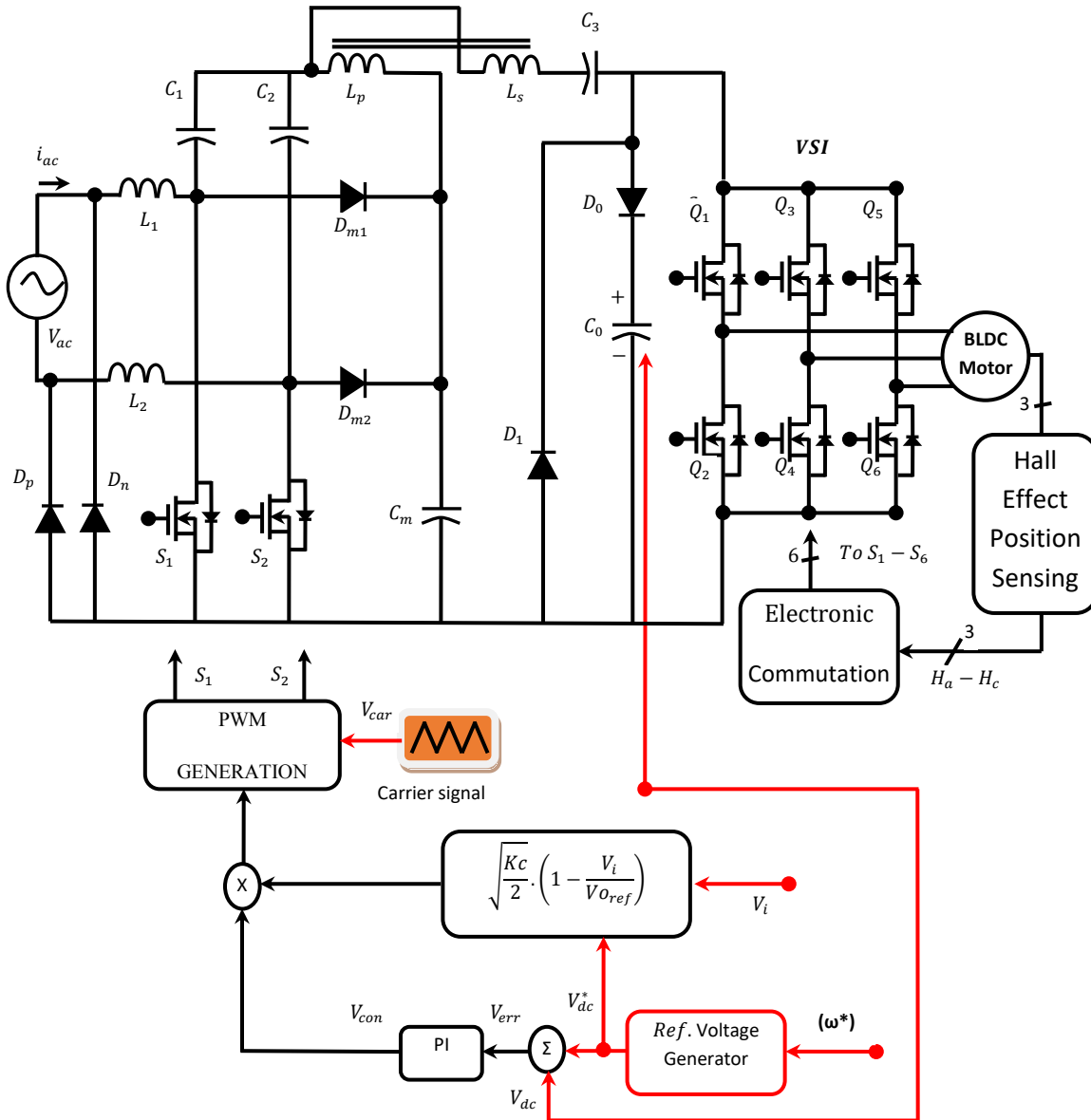
Published: 20 October 2016

\*Corresponding Author

Email:  
sathya2980@gmail.com

cycle with the current flowing back to the source through the diode  $D_p$ . During the time span of the negative half-line cycle, switch  $S_2$  is switched ON/OFF and then the current flows back passing through the diode  $D_n$ . Moreover, the two power switches  $S_1$  and  $S_2$  can be fed by the same control signal which assists in simplifying the control circuitry considerably.

**BL TI – SEPIC CONVERTER**



**Fig.1:** Schematic diagram of BL TI-SEPIC converter

**Voltage follower approach**

As illustrated from the [Fig. 1], a single voltage control loop (voltage follower mechanism) is employed for the BL-TI SEPIC converter. A reference dc link voltage ( $V_{dc}^*$ ) is generated as

$$V_{dc}^* = k_{volt} \times \omega^* \quad (1)$$

where  $k_{volt}$  and  $\omega^*$  indicate the respective the voltage constant and the reference speed of the motor.

The voltage error signal ( $V_{err}$ ) is produced by means of a comparison between the reference output voltage ( $V_{dc}^*$ ) and the output voltage sensed ( $V_{dc}$ ) expressed as

$$V_{err}(k) = V_{dc}^*(k) - V_{dc}(k) \quad (2)$$

In which (k) indicates the ( $k^{th}$ ) sampling instant. This error voltage signal ( $V_{err}$ ) is given as input to the voltage proportional-integral (PI) controller for generating a controlled output voltage ( $V_{con}$ ) as



$$V_{con}(k) = V_{con}(k - 1) + k_p\{V_{err}(k) - V_{err}(K - 1)\} + k_i V_{err}(k) \quad (3)$$

In which  $k_p$  and  $k_i$  stand for the corresponding proportional and integral gains of the voltage PI controller.

### Electronic commutation

An electronic commutation of the BLDC motor comprises of the correct switching of VSI such that a symmetrical dc current is received from the dc link capacitor for 120° and thereafter positioned symmetrically at the centre of each phase. A Hall-effect position sensor is used for the sensing of the rotor position with a 60° span which is required for the electronic commutation of the BLDC motor.

**Table 1:** Switching states based on hall effect position signals

$\theta^\circ$	HALL SIGNALS			SWITCHING STATES					
	$H_a$	$H_b$	$H_c$	$S_1$	$S_2$	$S_3$	$S_4$	$S_5$	$S_6$
NA	0	0	0	0	0	0	0	0	0
0-60	0	0	1	1	0	0	0	0	1
60-120	0	1	0	0	1	1	0	0	0
120-180	0	1	1	0	0	1	0	0	1
180-240	1	0	0	0	0	0	1	1	0
240-300	1	0	1	1	0	0	1	0	0
300-360	1	1	0	0	1	0	0	1	0
NA	1	1	1	0	0	0	0	0	0

A line current is got from the dc link capacitor whose magnitude is in accordance with the dc link voltage applied, back electromotive forces, resistances, and self-inductance and mutual inductance corresponding to the stator windings. [Table 1] shows the different switching states of the VSI that powers a BLDC motor based on the Hall-effect position signals ( $H_a - H_c$ ).

### EXPERIMENTAL EVALUATION

The performance of the new BL TI-SEPIC converter fed BLDC motor drive application is validated experimentally on a developed hardware prototype as illustrated in [Fig. 2]. A developed hardware prototype chiefly consists of 16 bit digital signal controller (dsPIC30F4011), MOSFET driver circuit for front end BL TI-SEPIC converter and VSI switches, Hardware arrangement of BL TI-SEPIC converter and VSI for power factor correction (PFC) and speed control operation correspondingly.

#### MOSFET driver circuit for BL TI-SEPIC converter and VSI switches

The switching signal for a MOSFET generally gets generated by means a logic circuit or a microcontroller that offers an output signal which is usually within a few mill amperes of current. As a result, a MOSFET, directly powered by such a signal would not be switching very fast, along with respective huge power loss. During the switching, the gate capacitor of the MOSFET may obtain current so rapidly that it creates a current overdraw in the logic circuit or microcontroller, leading to overheating, that again results in a permanent damage or even wholly destroy the chip. In order to avoid this, a MOSFET driver is placed between the microcontroller output signal and the power MOSFET. The MOSFET driver unit generally consists of transistor BC547, optocoupler 6N139 and MOSFET driver IC DS0026 as illustrated in [Fig. 3].

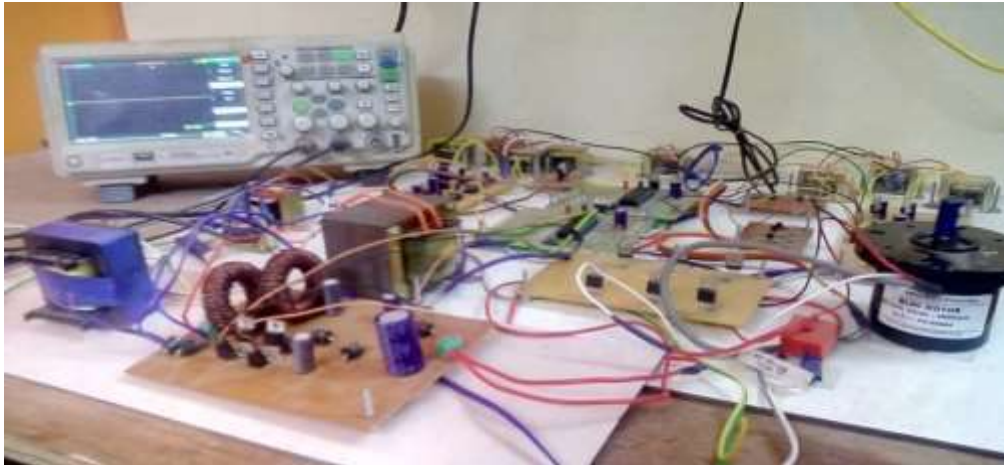


Fig.2: Proposed BLDC motor driver prototype test setup

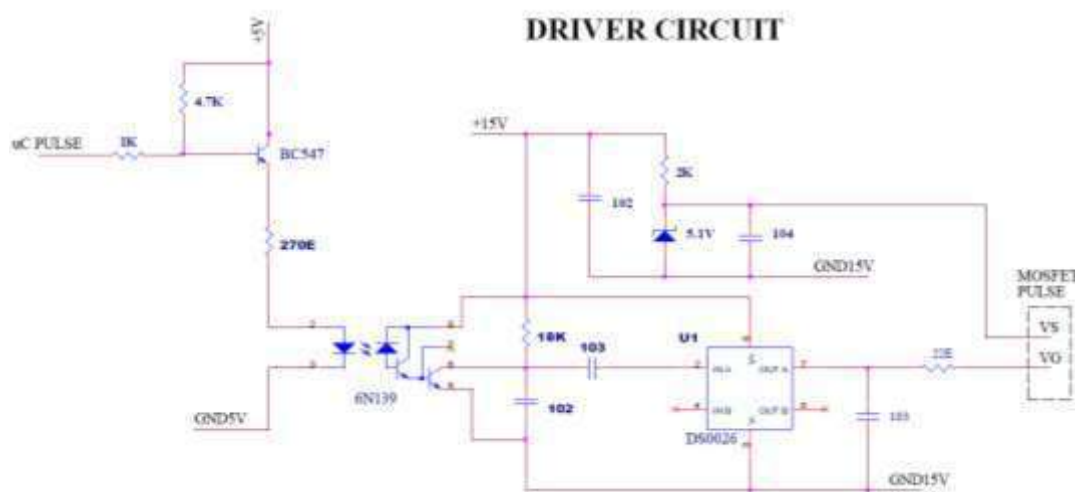


Fig.3: MOSFET driver circuit

In MOSFET driver unit BC547 is generally utilized for the amplification of current. It is an NPN bi-polar junction transistor. A transistor, symbolic for transfer of resistance, in which a small current at its base controls a bigger current at the collector & emitter terminals. BC547 is typically utilized for the purposes of amplification and switching. Its maximum current gain is of 800.

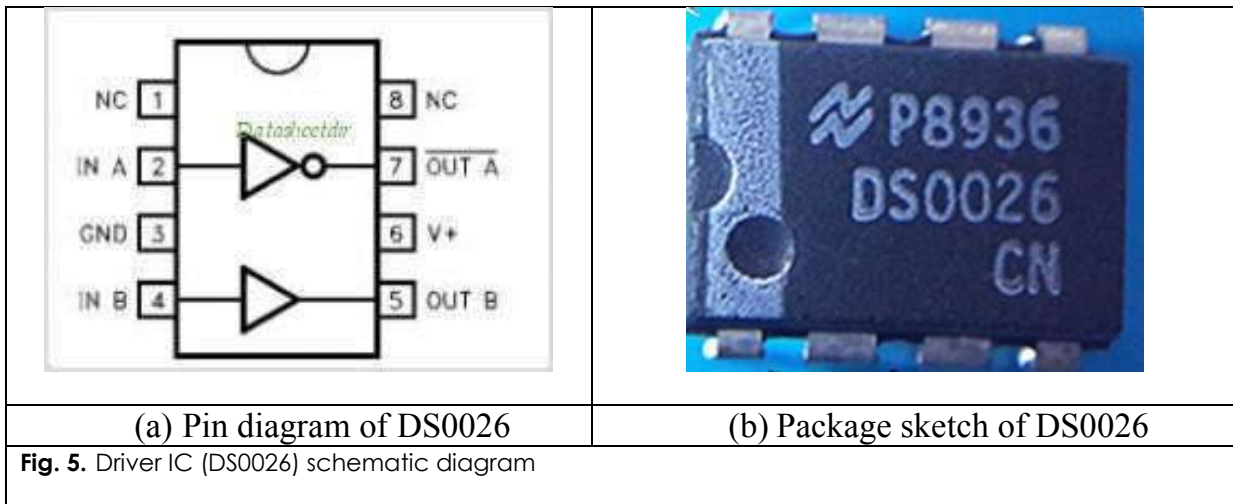
The transistor terminals need a constant dc voltage to be operated in the desired region of its characteristic curves. This is called as biasing. It is employed in common emitter configuration for amplifiers.

In a similar manner, the optocoupler TOSHIBA 6N139 comprises of an GaAlAs infrared emitting diode which is coupled with a split-Darlington output configuration. A high speed GaAlAs infrared manufactured with a distinct liquid phase epitaxial (LPE) junction, has the characteristic of rapid rise and fall time at low drive current. The pin configuration and package sketch of 6N139 optocoupler is illustrated in [Fig.4].

<p><b>PIN CONFIGURATION (Top view)</b></p> <p>1 : N.C. 2 : ANODE 3 : CATHODE 4 : N.C. 5 : GND 6 : OUTPUT 7 : OUTPUT BASE 8 : VCC</p> <p>(a) Pin diagram of 6N139</p>	<p>(b) Package sketch of 6N139</p>
--	------------------------------------

Fig. 4: Optocoupler (6N139) schematic diagram

In MOSFET driver unit, the part played by driver IC DS0026 is its use for the maximization of the switching speed. DS0026 is a cost economic monolithic high speed two phase metal oxide semiconductor (MOS) clock driver and interface circuit. This distinct circuit design gives very high speed operation along with the capability to drive huge capacitive loads. The device permits standard transistor-transistor logic (TTL) outputs and transforms them to MOS logic levels. DS0026 is bestowed with the features such as fast rise and fall times (20ns 1000 pF load), high output swing (20V) and high output current drive ( $\pm 1.5$  Amps). The pin configuration and package sketch of driver IC DS0026 is illustrated in [Fig. 5].



**Hardware arrangement**

A PFC BL TI-SEPIC converter is modelled in order to operate in discontinuous conduction so that the current in inductors ( $L_1$  and  $L_2$ ) tends to become discontinuous in a switching period. For a BLDC motor of power rating 30 W (entire specifications of the BLDC motor are provided in the [Table 2]). Corresponding to a huge variation in the dc link voltage (speed control), the output voltage is controlled ranging from a low value of 16 V ( $V_{out\_l}$ ) to the maximum value of 24 V ( $V_{out\_m}$ ). The average voltage that appears at the input ( $V_{in}$ ) is decided by equation (4)[8].

$$V_{in} = \frac{V_{ac} \times \sqrt{2} \times 2}{\pi} = \frac{12 \times 1.414 \times 2}{3.14} \cong 10.80 \text{ V}$$

Where ( $V_{ac}$ ) indicates the Rms value of supply voltage.

The speed control of BLDC motor is got by changing the duty ratio ( $d$ ) in the range of minimum ( $d_{mn}$ ) to maximum ( $d_{mx}$ ) as expressed by equation (5 to 7)[9].

$$d = \frac{V_{out}}{V_{in} + V_{out}}$$

$$d_{mn} = \frac{V_{out\_l}}{V_{in} + V_{out\_l}} = \frac{16V}{10.80V + 16V} \cong 0.59$$

$$d_{mx} = \frac{V_{out\_m}}{V_{in} + V_{out\_m}} = \frac{24V}{10.80V + 24V} \cong 0.689$$

The minimum and maximum duty ratios are computed as 0.59 and 0.69 correspondingly.

In order to have the the input inductance ( $L_1$  and  $L_2$ ) value estimated, and for operation in buck and boost mode in the BL TI-SEPIC converter, the equation (8 and 9)[10] is provided

$$L_1 = L_2 = \frac{(V_{out\_l})^2}{P_{out\_l}} \times \frac{(1 - d_{mn})^2}{2 \times f_s}$$

$$L_1 = L_2 = \frac{(16)^2}{14.4} \times \frac{(1 - 0.59)^2}{2 \times 10000} = 149.42 \mu\text{H}$$

Where ( $f_s$ ) refers to the switching frequency, ( $d$ ) indicates the duty ratio. So, the value of ( $L_1$  and  $L_2$ ) is computed at the minimum duty ratio of ( $d_{mn}$ ) so that the converter works in DCM even at conditions of very

low duty ratio. At minimum duty ratio, i.e., the LED Lamp that operates at 16 V ( $V_{out\_l}$ ), the power ( $P_{out\_l}$ ) is provided as 14.4 W. The values of input inductances  $L_1$  and  $L_2$  are considered to be less than 1/10th of the minimum critical value of inductance to guarantee a deep DCM condition [11]. Therefore, the input inductors  $L_1$  and  $L_2$  are chosen to be around 1/10th of the critical inductance and are considered as 14  $\mu$ H.

The value of the in-between capacitors ( $C_1, C_2, C_3$  and  $C_m$ ) is computed for the maximum duty ratio ( $d_{mx}$ ) as provided by equation (10 and 11) and is expressed as [9]

$$C_{1,2,3,m} = \frac{d_{mx} \times V_{cap}}{2 \times f_s \times \frac{(V_{out\_m})^2}{P_{out\_m}} \times \frac{\sim V_c}{2}}$$

Where ( $V_{cap} = V_{in} + V_{out\_m}$ ) represents the voltage across the capacitors ( $C_1$  or  $C_2$  or  $C_3$  or  $C_m$ ), and the allowable voltage ripple ( $\sim V_c$ ) is considered as 60% of ( $V_{cap}$ ).

$$C_{1,2,3,m} = \frac{0.69 \times (10.80 + 24)}{2 \times 10000 \times \frac{(24)^2}{18.67} \times \frac{20.4}{2}} = 3.815 \mu F$$

Therefore, the values of in-between capacitors ( $C_1$  or  $C_2$  or  $C_3$  or  $C_m$ ) are chosen to be 3.3 $\mu$ F.

The value of the coupled inductors ( $L_p$  and  $L_s$ ) for the admissible ripple current ( $\sim I_{out\_mx}$ ) in the coupled inductors, is considered to be 10% of output current ( $I_{out\_mx} = 0.715$  A) is computed as [12] and expressed in equation (12 and 13).

$$L_p = \frac{d_{mx} \times I_{out\_mx}}{f_s^2 \times 16 \times C_{int} \times \frac{(\sim I_{out\_mx})}{2}}$$

Where ( $C_{int}$ ) indicates intermediate capacitor value.

$$L_p = \frac{0.69 \times 0.715}{(10000)^2 \times 16 \times 3.815 \times 0.0398} = 2.03nH$$

Hence the values of coupled inductor ( $L_p$ ) got is (2.03nH). Moreover, the coupled inductor ( $L_s$ ) value is got on the basis of output voltage gain.

The output capacitors ( $C_0$ ) value is got by the equations (14 and 15) for the minimum duty ratio expressed as [9]

$$C_0 = \frac{I_{out\_mx}}{\sim V_{out\_min} \times \omega_l \times 2}$$

$$C_0 = \frac{0.733}{(0.03 \times 16) \times (2 \times 3.14 \times 50) \times 2} = 2371.94 \mu F$$

Where ( $\omega_l$ ) indicates the angular frequency, permitted ripple voltage ( $\sim V_{out\_min}$ ) in the output capacitors ( $C_0$ ), considered as 3%, therefore the output capacitors value of 2200  $\mu$ F is chosen.

**Table 2:** Proposed BLDC motor driver component specifications

S. No	BL TI-SEPIC converter fed BLDC motor driver component details	Operating values
1	Unidirectional N-Channel Power MOSFET (IRFZ44N)  ( $S_1$ and $S_2$ ) for PFC BL TI-SEPIC converter  ( $Q_1 - Q_6$ ) for VSI	50 V, 50 A
2	Input inductors ( $L_1$ and $L_2$ )  Core type: "Round"  Size : T45*26*15 ring Toroidal ferrite core	14 $\mu$ H

	Copper gauge : "25"	
3	In-between capacitors ( $C_1$ or $C_2$ or $C_3$ or $C_m$ ) Type: electrolytic	3.3 $\mu F$ , 50 V
4	Schottky power diode ( $D_p$ or $D_n$ or $D_{m1}$ or $D_{m2}$ or $D_1$ or $D_0$ ) Brand: Fairchild semiconductor Part no: SB550	50V, 5A
5	Coupled Inductors ( $L_p$ and $L_s$ ) Core type: "E-core" Size: E65*32*27 core Copper gauge: "19"	Ratio 1:2, Primary inductance value = 2.03nH, Secondary inductance value = 6nH
6	Output capacitors ( $C_o$ ) Type: electrolytic Brand: nichicon	2200 $\mu F$ , 50 V
7	Load: BLDC motor Model no: 2RB30AK	Dc voltage : 24V Power: 30W Speed : 3000 Rpm Torque: 1.2 Nm

## RESULTS AND DISCUSSIONS

A digital signal controller dsPIC30F4011 controller is utilized for developing the novel PFC BL TI-SEPIC converter-fed BLDC motor drive. The required circuitry for separation between dsPIC30F4011 controller and gate drivers of solidstate switches is designed making use of the optocoupler 6N139. A prefiltering and isolation circuit for the Hall-Effect sensor is also designed for the sensing of the Hall-effect position signals. The input and output specifications of the new system experimental verification is illustrated in

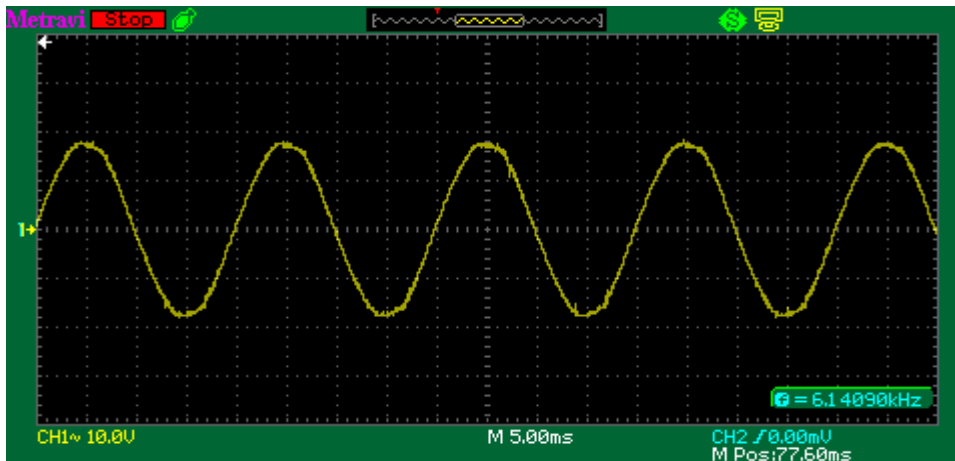
**Table 3:** The Test results are studied in the sections that follow

S. No	Input and output specifications of BL TI-SEPIC converter	values
BL TI-SEPIC converter operates in minimum output voltage		
1	Input supply voltage	12.02 V (Rms)
2	Input supply current	1.2 A (Rms)
3	Input power	14.4 W (Rms)
4	BL TI-SEPIC converter dc output voltage ( $V_{out\_l}$ )	16 V
5	BL TI-SEPIC converter dc output current ( $I_{out\_l}$ )	0.831 A
6	BL TI-SEPIC converter dc output power ( $P_{out\_l}$ )	13.3 W
7	BLDC motor speed (no load condition)	1000 Rpm
	Power Factor	0.993
BL TI-SEPIC converter operates in maximum output voltage		
8	Input supply voltage	12.02 V (Rms)

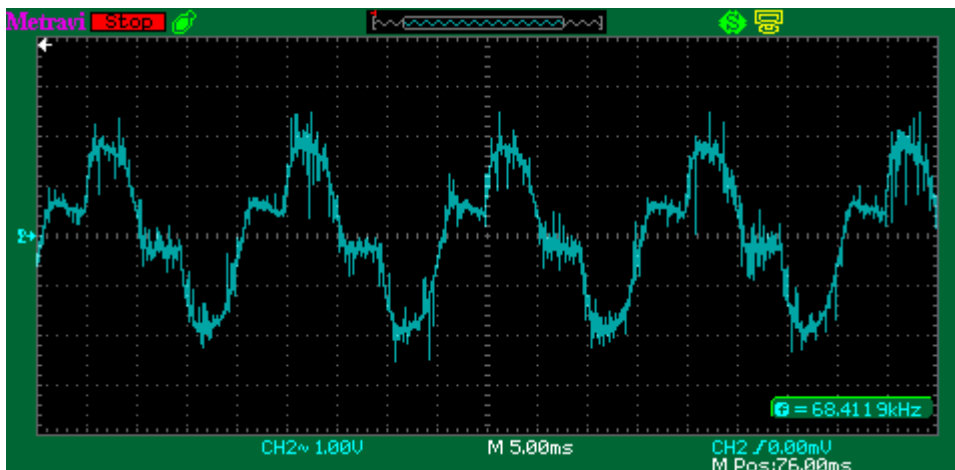


9	Input supply current	1.55 A (Rms)
10	Input power	18.67 W (Rms)
11	BL TI-SEPIC converter dc output voltage ( $V_{out\_m}$ )	24 V
12	BL TI-SEPIC converter dc output current ( $I_{out\_m}$ )	0.715 A
13	BL TI-SEPIC converter dc output power ( $P_{out\_m}$ )	17.16 W
14	BLDC motor speed (no load condition)	1500 Rpm
15	Switching frequency ( $f_{sw}$ )	10kHz
16	Supply frequency	50Hz
17	Efficiency of BL-IZC operates in maximum output voltage ( $\eta_{max}$ %)	91.91%
18	Efficiency of BL-IZC operates in minimum output voltage ( $\eta_{min}$ %)	92.33%
	Power Factor	0.991

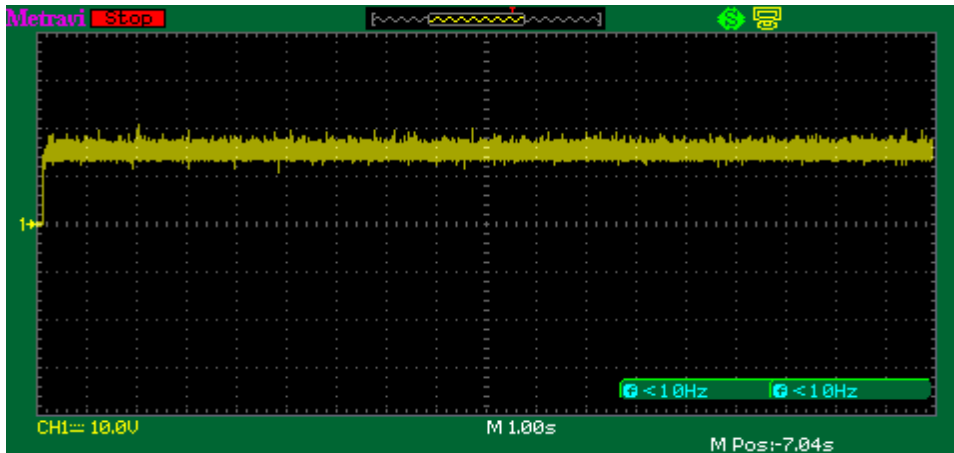
[Fig. 6] illustrates the operation of the newly introduced BLDC motor drive illustrating supply voltage, supply current, converter output voltage ( $V_{out\_l}$ ), motor speed, then the stator current and stator voltage for the dc link voltages of 16 V. A sinusoidal supply current approximately in phase with the supply voltage is accomplished for operating at minimum dc link voltage that indicates a near unity power factor at the ac mains.



(a) Supply voltage



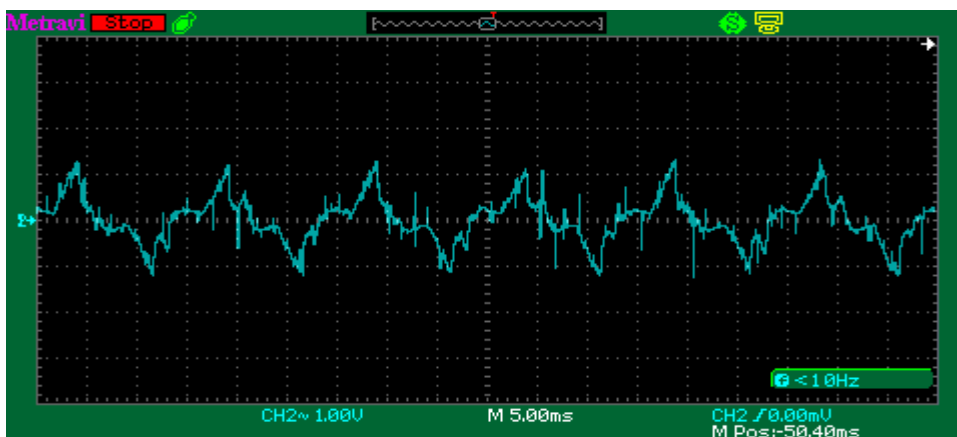
(b) Supply current



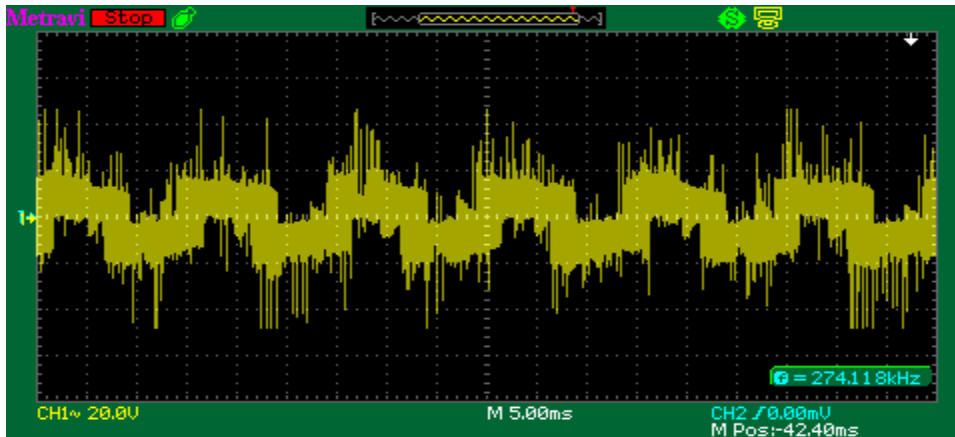
(C)BL TI-SEPIC converter output voltage ( $V_{out\_l}$ )



(d)BLDC motor speed in Rpm



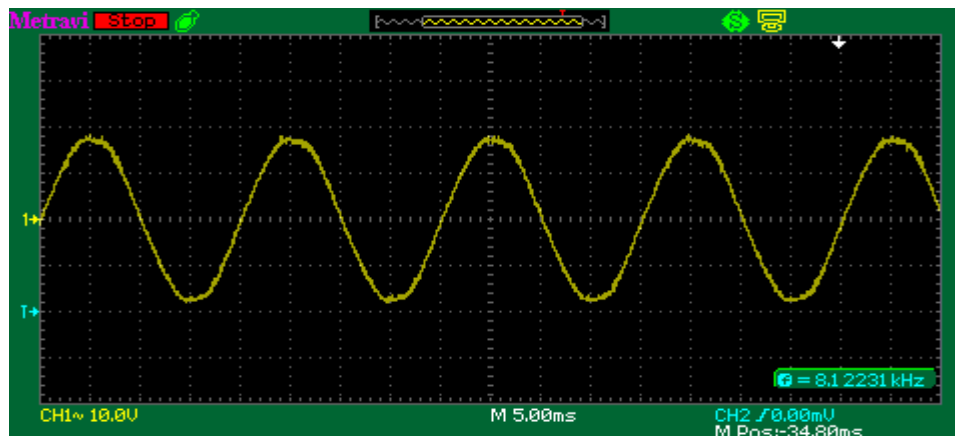
(e) BLDC motor Stator current



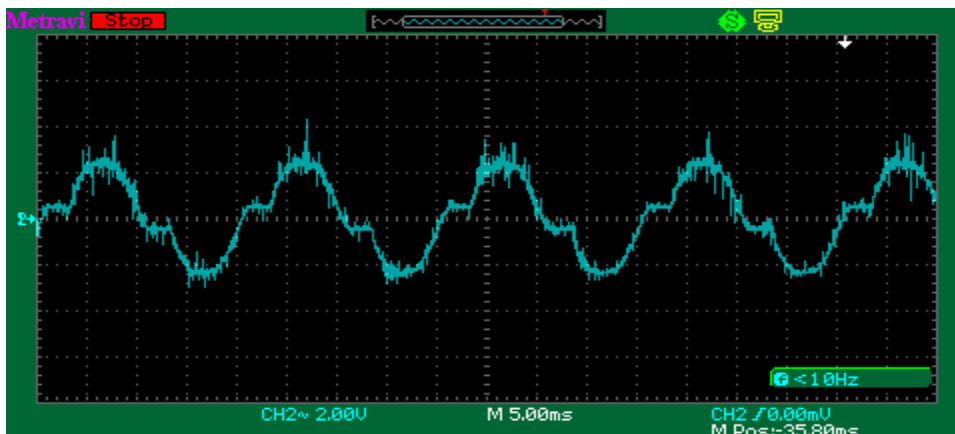
(f) BLDC motor stator voltage

Fig.6: Test results of proposed BLDC motor driver for the dc link voltage of 16 V

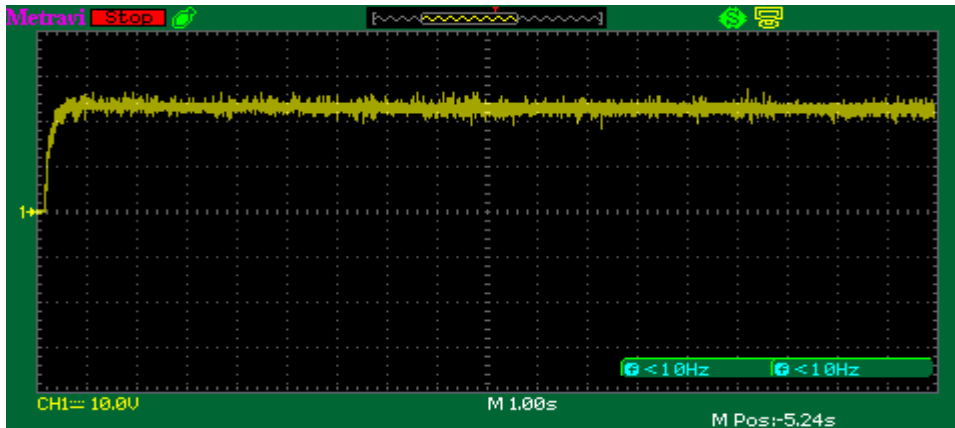
[Fig. 7] illustrates the operation of the newly introduced BLDC motor drive showing supply voltage, supply current, converter output voltage ( $V_{out\_m}$ ), motor speed, thereafter the stator current and stator voltage for the dc link voltages of 24V, correspondingly. A sinusoidal supply current approximately in phase with the supply voltage is attained for operating at minimum dc link voltage that indicates a near unity power factor at ac mains.



(a) Supply voltage



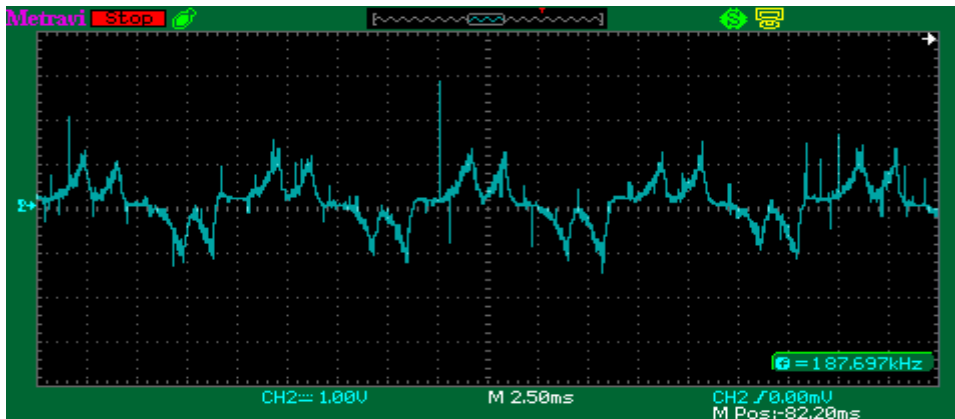
(b) Supply current



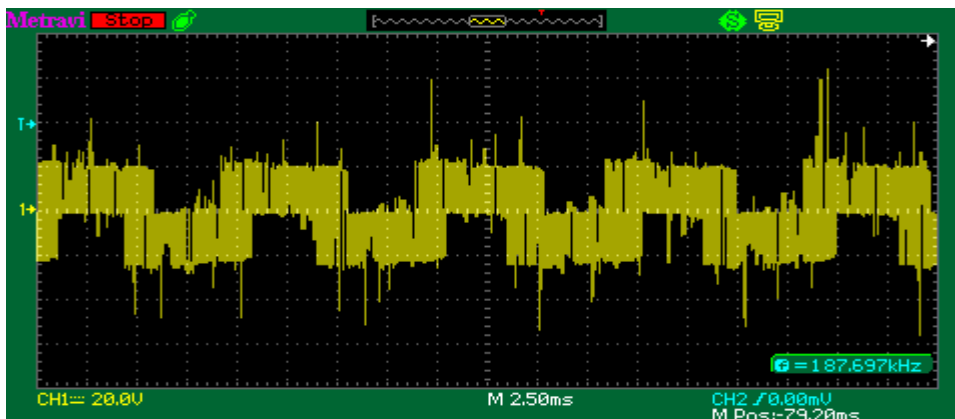
(c) BL TI-SEPIC converter output voltage



(d) BLDC motor speed in Rpm



(e) BLDC motor stator current



(f) BLDC motor stator voltage

Fig.7: Test results of proposed BLDC motor driver for the dc link voltage of 24 V

## CONCLUSION

A PFC BL TI-SEPIC converter-based VSI-fed BLDC motor drive has been introduced aiming at low-power applications. A novel technique of speed control has been used by regulating the voltage at dc bus and then operating the VSI at fundamental frequency for the electronic commutation of the BLDC motor in order to reduce the switching losses in VSI. The operation of the front-end BL TI-SEPIC converter has been done in DCM for attaining an intrinsic power factor correction at ac mains. A satisfying closed-loop performance has been accomplished for different speed control with enhanced power factor. At last, an experimental model of the drive proposed has been designed in order to verify the performance of the new BLDC motor drive under speed control with enhanced power quality at ac mains. The scheme proposed has revealed desired performance, and it is a solution recommended to be applied for high-power BLDC motor drives.

## REFERENCES

- [1] Xia CL. [2012] Permanent magnet brushless DC motor drives and controls. John Wiley & Sons.
- [2] Moreno J, Ortúzar ME and Dixon JW. [2006] Energy-management system for a hybrid electric vehicle, using ultra capacitors and neural networks. IEEE transactions on Industrial Electronics, 53(2):614-623.
- [3] Toliyat HA., and Campbell SG. [2003] DSP-based electromechanical motion control. CRC press.
- [4] Pillay P and Krishnan R. [1988] Modelling of permanent magnet motor drives, 35(4):537-541.
- [5] Singh S and Singh B. [2012] A voltage-controlled PFC Cuk converter based PMBLDCM drive for air-conditioners, IEEE transactions on industry applications, 48(2):832-838.
- [6] Chen YT, Chiu C L, Jhang, YR, Tang ZH, and Liang, RH. [2013], A driver for the single phase brushless dc fan motor with hybrid winding structure, IEEE Transactions on Industrial Electronics, 60(10):4369-4375.
- [7] Huang X, Goodman A, Gerada C, Fang Y, and Lu Q, [2012] A single sided matrix converter drive for a brushless dc motor in aerospace applications, IEEE Transactions on Industrial Electronics, 59(9): 3542-3552.
- [8] Simonetti DSL, Sebastian J, dos Reis FS, and Uceda J, [1992] Design criteria for SEPIC and Cuk converters as power factor pre-regulators in discontinuous conduction mode, Power Electronics and Motion Control., Proceedings of the 1992 International Conference, 1:283-288.
- [9] Mohan N, Undeland TM, and Robbins WP, Power Electronics: Converters, Applications and Design. Hoboken, NJ, USA: Wiley, 2003.
- [10] Emadi A, Khaligh A, Nie Z, and Lee YJ, [2009] Integrated Power Electronic Converters and Digital Control. Boca Raton, FL, USA: CRC Press.
- [11] Simonetti DSL, Sebastian J, dos Reis FS, and Uceda J, [1992] Design criteria for SEPIC and Cuk converters as power factor pre-regulators in discontinuous conduction mode, Power Electronics and Motion Control., Proceedings of the 1992 International Conference, 1:283-288..
- [12] Power Factor Correction in Bridgeless-Luo Converter-Fed BLDC Motor Drive Bhim Singh, Fellow, IEEE, VashistBist, Student Member, IEEE, Amrishi Chandra, Fellow, IEEE, and Kama



## ARTICLE

# FPGA IMPLEMENTATION OF HIGH SPEED AND LOW POWER CARRY SAVE ADDER

VS. Balaji<sup>1\*</sup>, Har Narayan Upadhyay<sup>2</sup>

<sup>1</sup>Department of Electronics & Instrumentation Engineering, INDIA

<sup>2</sup>Dept. of Electronics & Communication Engineering, School of EEE, SASTRA University, Thanjavur (TN), INDIA

## ABSTRACT

In recent years, the high speed adders play a vital role in any digital design of signal processing systems by performing much needed operations like subtraction, multiplication, and division, etc., along with the basic addition. Carry look-ahead adder (CLA), carry select adder (CSeA), carry-save adder (CSA) and carry-skip adder are the most popular high speed adders in digital signal processor and computer data path applications. This study demonstrates the efficiency of a carry-save adder with multi-operand addition using different majority voting circuit implementations in the place of carry out of a full adder. The carry is saved and propagated down to the next stage rather than passing within the same stage like in ripple carry adder (RCA). But the final sum is calculated with the help of carry ripple adder by propagating the carries appropriately. The final sum calculation stage in a carry save adder is implemented in this study using ripple carry adder (CSA-RCA), carry look-ahead adder (CSA-CLA) and carry select adder (CSA-CSeA) to compare better power, area and delay results. Addition of four 4-bit numbers, four 8-bit numbers, four 16-bit numbers, four 32-bit numbers and four 64-bit numbers are implemented on Altera EP4CE115F29C7 FPGA device using Quartus II synthesis software tool. Simulation results of adding four 32-bit numbers show that CSA-CSeA topology offers lower critical path delay as 34.823 ns compared with CSA-RCA topology (63.120 ns) and CSA-CLA topology (52.475 ns) at the expense of 221 logic elements (LEs) which is higher; the CSA-RCA topology and CSA-CLA topologies have only 192 LEs and 193 LEs respectively. It is also shown that the CSA-CLA topology has lower power dissipation as 170.54 mW compared with CLA-RCA (171.36 mW) and CSA-CSeA (174.68 mW).

## INTRODUCTION

### KEY WORDS

Carry save adder, FPGA, high speed adders, majority function, multi-operand addition, Quartus II.

In digital computer arithmetic, addition and subtraction are the most basic core operations, especially for digital signal processing applications. The other two fundamental operations like multiplication and division are too performed using addition and subtraction and hence they play a very important role in processors like microprocessors, microcontrollers and digital signal processors [1]. The fast adders can be used to speed up the arithmetic operations in a processor. There are numerous ways available to perform addition but with different trade-offs. Some are good in producing low power at the cost of area and some are best in offering performance (i.e., high speed) at the cost of power and/or area [2].

Arithmetic operations are essential building blocks in any system; either the system can be designed based on a processor, or an FPGA/ASIC [3]. The data path circuitries in a microprocessor, Multiply-Accumulate (MAC) operations in a digital signal processor and high speed integrated circuits in communication systems are the few application examples which would perform arithmetic operations especially using regular full adders [4]. The k-bit ripple-carry adder is the most simplest adder structure, which adds two words having k-bits. The delay of the RCA is very high since the carry is propagated (i.e., rippled) to the full adder stages to produce a final sum. If the value of k is very large, then the delay would be more. These RCAs are not suitable in situations where the speed data processing is involved. So the demand to design fast adders grows rapidly to meet the current high speed integrated circuits trend [5] [6].

This paper is organized as follows. The Section 2 contains the carry-save adder implementations with ten different majority voting circuits in the place of a carry out of a single-bit full adder in carry-save stages. The final sum is obtained using different circuits like carry look-ahead adder and carry-select adder in addition to the conventional ripple-carry adders, which are discussed in Section 3. The Section 4 obtains simulation results with FPGA implementation along with performance metrics like resource utilization report, critical path delay and power dissipation with Quartus II synthesis software tool using very high speed integrated circuits hardware description language (VHDL).

## MULTI-OPERAND ADDITION USING CARRY-SAVE ADDERS

The addition of more than two numbers would be done using carry-save adders based on the fact that a full-adder has 3 inputs and obtains 2 outputs and hence the full adder becomes the basic building block [6] [7]. The addition of four 4-bit numbers, four 8-bit numbers, four 16-bit numbers, four 32-bit numbers and four 64-bit numbers are exemplified using CSA principle in this study.

### Addition of four 4-bit numbers

A<sub>0-3</sub>, B<sub>0-3</sub>, C<sub>0-3</sub> and D<sub>0-3</sub> are the four 4-bit numbers which are used for addition. This is accomplished with the help of full adders (boxes) as in figure to obtain the overall sum as in [Fig. 1]. The carry from each stage is propagated down instead in the same stage and hence reduce the overall delay. These are known

Published: 2 December 2016

### \*Corresponding Author

Email: mjabala\_mtech@eie.sastra.edu,  
hnu@ece.sastra.edu  
Tel.: +918072496254

as “carry-save” stages and varies depend on the number of operands. Finally, the ripple-carry adder is used to obtain the final sum at the cost of delay [6] [8]. The complete schematic with full adder implementation (boxes) is shown in [Fig. 2].

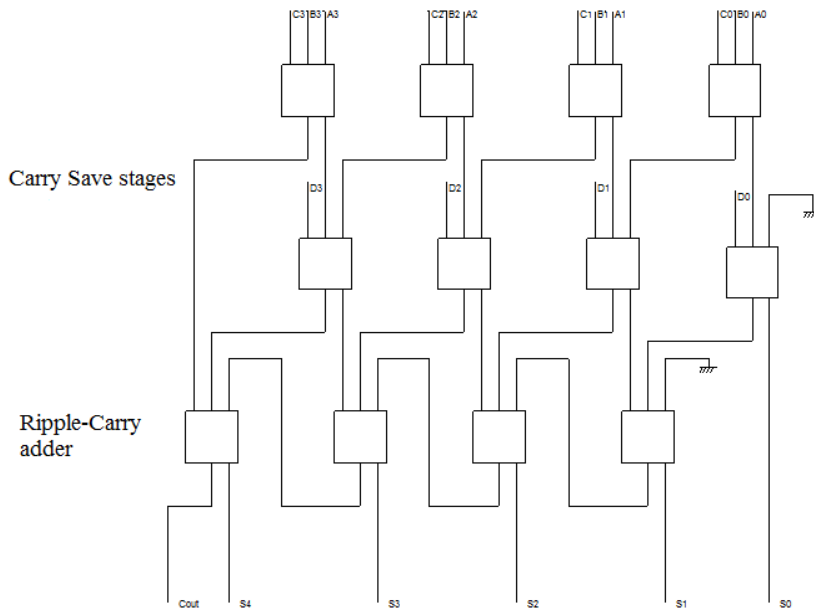


Fig. 1: Addition of four 4-bit numbers using CSA.

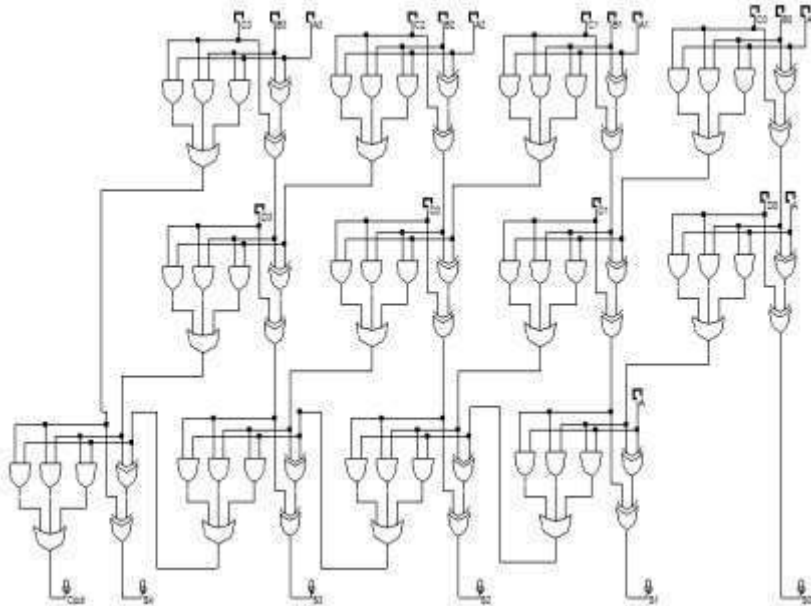


Fig. 2: Addition of four 4-bit numbers using full adders.

### Parity-checking and majority-voting of full adder

The sum and carry out of a full adder can be viewed as parity-checking and majority-voting circuits respectively as in [Fig. 3]. The parity-checking of the inputs (a,b,c) is calculated as  $(a \text{ xor } b \text{ xor } c)$  and the majority-voting of the inputs (a,b,c) is determined as  $(ab \text{ or } bc \text{ or } ca)$  are known as sum and carry out respectively [9] [10].

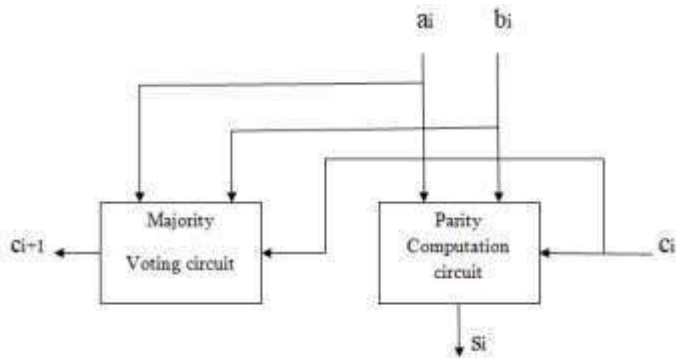


Fig.3: Single-bit full adder.

### Majority-voting (MV) circuits

The different majority-voting circuits are studied and are implemented in the place of a carry out of a full adder in a carry-save adder structure.

### Using conventional, NAND, and NOR gates

The majority-voting circuits are implemented using conventional method, NAND gates and NOR gates as in [Fig. 4a, 4b and 4c] respectively [11]. The NAND and NOR gates are very often used in CMOS VLSI circuits for better area, power and delay trade-offs.

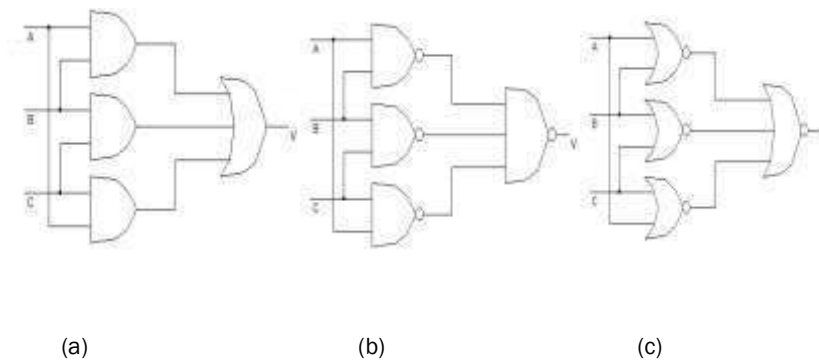


Fig. 4. Using (a) Conventional (b) NAND and (c) NOR gates.

### Using carry look-ahead adder fundamental

The carry out of a full adder is implemented as  $(a \oplus b)c + (ab)$  as in CLA concept. This is shown in [Fig.5]. The  $a \oplus b$  and  $ab$  terms are referred as 'propagate' and 'generate' respectively. If  $a \neq b$  and carry in =1, then the carry out = 1, which is based on the propagate term. If  $a = b = 1$ , then the carry out =1, which is based on the generate term [12].

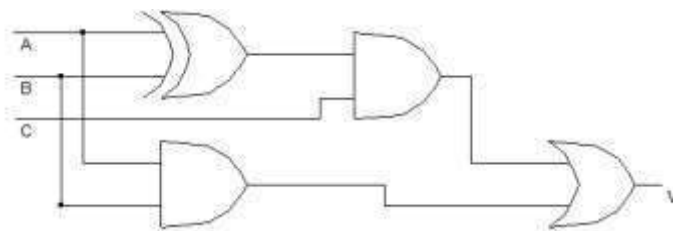


Fig. 5: MV circuit using CLA principle.

### Using Multiplexers, XOR and OR gates

The MV circuit can be designed using multiplexer and XOR gate as in Figure 6a. If  $A \neq B$ , then the majority becomes the third input; otherwise, the output is either B or A. The majority function can also be computed using Mux, AND and OR gates as in [Fig. 6b]. If the first input bit is equal to zero, then the MV output is computed as B and C, else it is determined as A or B [12].

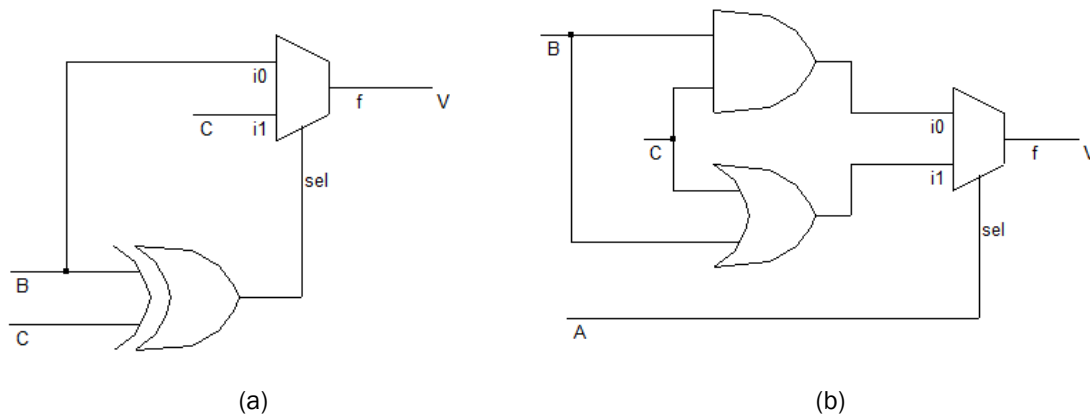


Fig.6: Using (a) Mux and XOR gate and (b) Mux, AND and OR gates.

#### Using 2-to-1 and 4-to-1 Multiplexers

The MV circuit can be designed only using 2-to-1 multiplexers as in [Fig.7a]. The [Fig. 7b] shows the majority function schematic using 4-to-1 multiplexer. If  $A = B = 0$ , then the output becomes as '0' and if  $A = B = 1$ , then the output is '1'. If  $A \neq B$ , then the majority output becomes as the third input 'C' [12].

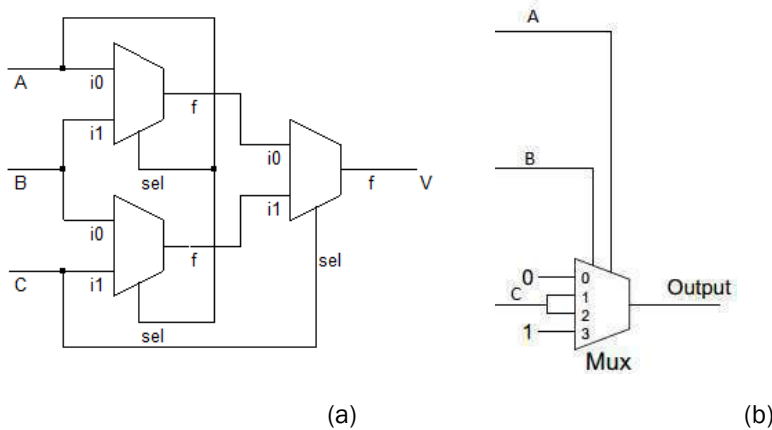


Fig. 7: Using (a) 2-to-1 Muxes and (b) 4-to-1 Muxes.

#### Using AND, NAND, OR and Inverter gates

The carry out of a full can also be design using the equation (1) and the schematic is shown in [Fig. 8a] using AND, NAND, OR and Inverter gates which is referred to as ANOI in this study.

$$v = (\overline{AB})(A + B)C + AB \quad (1)$$

The MV circuit output can also be determined using the equation (2) and the schematic is shown in [Fig. 8b] using AND, OR and Inverter gates which is referred to as AOI in this study.

$$v = (\overline{ABC}) + (A + B)C \quad (2)$$

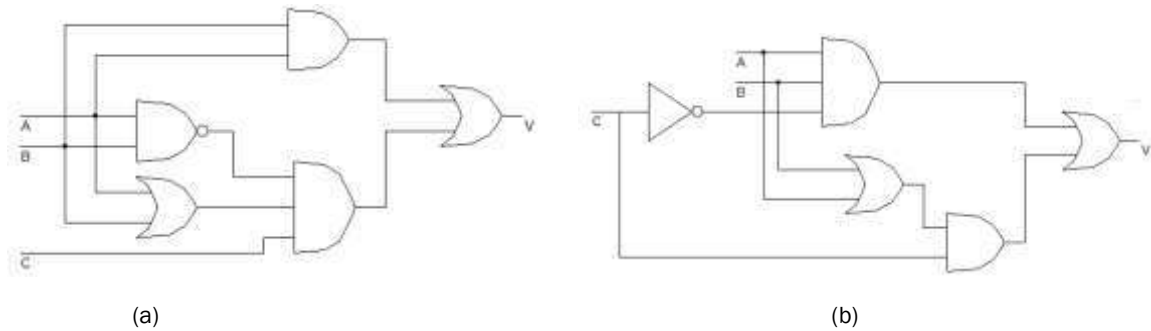


Fig. 8: Using (a) AND, NAND, OR and Inverter (b) AND, OR and Inverter

### FINAL SUM COMPUTATION METHODS OF CSA

Multi-operand addition using CSA has two important stages as “carry-save stages” and “final stage” to compute the overall sum. This section exemplifies the final stage using ripple-carry adder, carry look-ahead adder and carry select adder to determine the final output sum.

#### Sum output using RCA

In this study, the final sum output using RCA is referred in this study as “CSA-RCA”. The carry from the previous stages are considered here and propagated within the last stage to find the final sum output value. The general schematic of  $k$ -bit RCA is shown in [Fig. 9]. It is apparent that this circuit offers more delay due to the rippling effect of the carry which is shown in the diagram [2] [4].

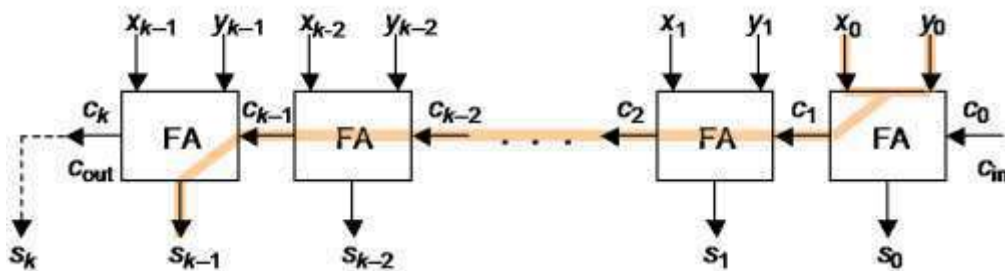


Fig. 9:  $k$ -bit ripple-carry adder.

#### Sum output using CLA

The last stage is replaced with carry look-ahead adder circuit and is referred to as “CSA-CLA”. The carry out is calculated in advance based on the “propagate” and “generate” terms instead of depending on the previous carry. Since the rippling effect is reduced, this circuit should offer better performance compared with the RCA combination. The schematic of 4-bit CLA is shown in [Fig. 10]. The VHDL portion of a CLA stage with the addition of four 8-bit numbers is shown in Figure 11. If  $a_0 = b_0 = 1$  (i.e.,  $g_0 = 1$ ), then the  $c_1$  is computed as ‘1’ based on the *generate* term. If  $p_0 = 1$  and  $c_0 = 1$ , then the  $c_1$  is computed as ‘1’ based on the *propagate* term. The CLA circuit is constructed based on the following equation (3).

$$C_{i+1} = (A_i \oplus B_i)C_i + A_i B_i = P_i C_i + G_i \quad (3)$$

For a 4-bit CLA circuit, these carry terms can be computed as,

$$\begin{aligned} C_1 &= P_0 C_0 + G_0 \\ C_2 &= P_1 C_1 + G_1 = P_1(P_0 C_0 + G_0) + G_1 \\ C_3 &= P_2 C_2 + G_2 = P_2(P_1 P_0 C_0 + P_1 G_0 + G_1) + G_2 \\ C_4 &= P_3 C_3 + G_3 = P_3(P_2 P_1 P_0 C_0 + P_2 P_1 G_0 + P_2 G_1) + G_3 \end{aligned} \quad (4)$$



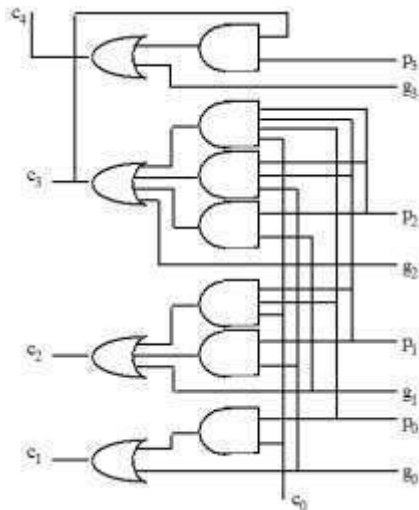


Fig.10: A 4-bit carry-look ahead adder.

.....

```

p0 <= m16 xor m17; g0 <= m16 and m17; c11 <= (p0 and cin1) or g0; s1 <= p0 xor cin1;
p1 <= m18 xor m19; g1 <= m18 and m19; c21 <= (p1 and c11) or g1; s2 <= p1 xor c11;
p2 <= m20 xor m21; g2 <= m20 and m21; c31 <= (p2 and c21) or g2; s3 <= p2 xor c21;
p3 <= m22 xor m23; g3 <= m23 and m23; c41 <= (p3 and c31) or g3; s4 <= p3 xor c31;
p4 <= m24 xor m25; g4 <= m24 and m25; c51 <= (p4 and c41) or g4; s5 <= p4 xor c41;
p5 <= m26 xor m27; g5 <= m26 and m27; c61 <= (p5 and c51) or g5; s6 <= p5 xor c51;
p6 <= m28 xor m29; g6 <= m28 and m29; c71 <= (p6 and c61) or g6; s7 <= p6 xor c61;
p7 <= m15 xor m30; g7 <= m15 and m30; cout <= (p7 and c71) or g7; s8 <= p7 xor c71;
    
```

Fig. 11: Final sum using ripple-carry adder in VHDL.

.....

### Sum output using CSeA

The carry-select adder can also be used in the last stage to produce the final sum and this topology is referred to as “CSA-CSeA”. This is used especially when adding more number of bits. The basic schematic of a CSeA is shown in [Fig. 12]. The [Fig. 13] shows the VHDL portion of the addition of four 8-bit numbers using carry-select adder stage [5] [6].

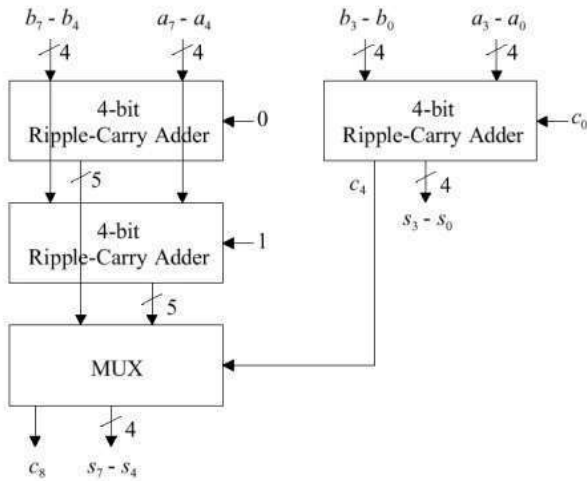


Fig.12: A 8-bit carry-select adder.

```
s4 <= ((not c4) and s50) or (c4 and s51);
s5 <= ((not c4) and s60) or (c4 and s61);
s6 <= ((not c4) and s70) or (c4 and s71);
s7 <= ((not c4) and s80) or (c4 and s81);
c8 <= ((not c4) and c80) or (c4 and c81);
```

Fig.13: Find final sum using carry-select adder in VHDL.

## RESULTS AND DISCUSSION

This paper demonstrate the addition of four 4-bit, 8-bit, 16-bit, 32-bit and 64 numbers and thus obtain a comparative analysis with the performance metrics like power, delay and area in each design. All the circuits are implemented on Altera FPGA EP4CE115F29C7 device (i.e., DE2-115) using Quartus II synthesis software tool with VHDL to obtain simulation results [13] [14]. The timing verification is done using the Time Quest timing analyzer, which is a part of Quartus II software bundle. The functional and timing verification results are shown in [Fig. 14] and [Fig. 15] respectively for the addition of four 32-bit numbers.

Name	Value at 0 ps	0 ps	30.0 ns	20.0 ns	30.0 ns	40.0 ns	50.0 ns	60.0 ns	70.0 ns	80.0 ns	90.0 ns	100.0 ns	110.0 ns	120.0 ns
A	U 3750647593		3750647593			2733685057			3225268067			2373267971		
B	U 4170893477		4170893477			3267638413			3822173945			2286769410		
C	U 3148267623		3148267623			2743973623			3343811744			3957773412		
D	U 3842578067		3842578067			1649537986			2800528677			3267768025		
cn0	B 0													
cn1	B 0													
Output	U 14912386760		14912386760			6099855383			12191782433			35180546114		

Fig. 14: Functional verification for the addition of four 32-bit numbers.

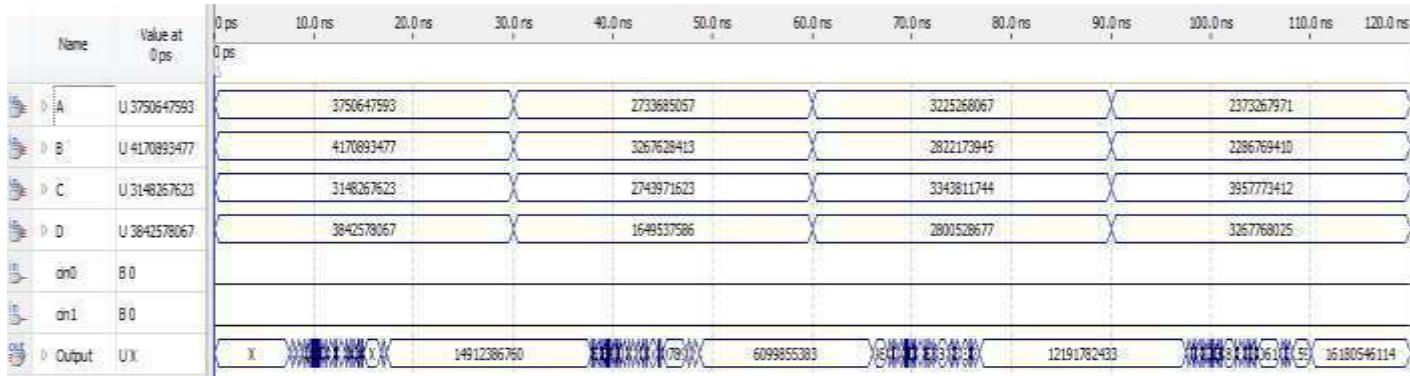


Fig. 15: Timing verification for the addition of four 32-bit numbers.

The utilization summary of LEs, critical path delay and power dissipation results for the addition of four 64-bit numbers are shown in [Fig. 16, 17 and 18] respectively. It is apparent that the CSA-CSeA method produce lower delay at the cost of area. For example with Mux-XOR majority voting, the CSA-CSeA approach produces 72.623 ns which is lower as compared with CSA-CLA (97.479 ns) and CSA-RCA (133.033 ns) at the cost of more LEs (384). Among the ten majority-voting circuits, it is also shown that the Mux-and-OR majority voting circuit offers lower delay as 100.965 ns and lower power dissipation as 187.79 mW using CSA-RCA approach.

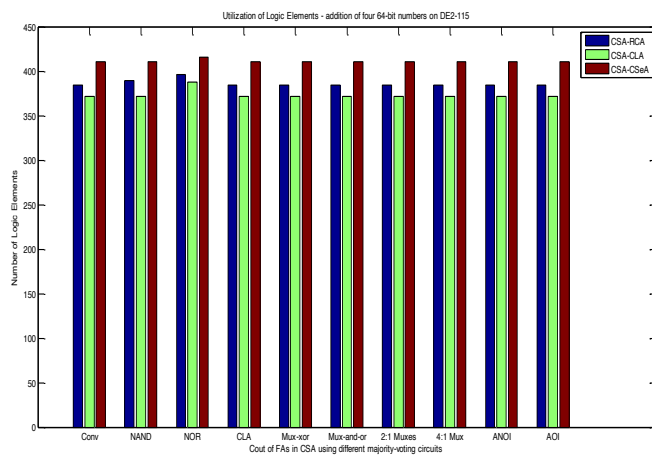


Fig. 16: Utilization of LEs for the addition of four 64-bit numbers.

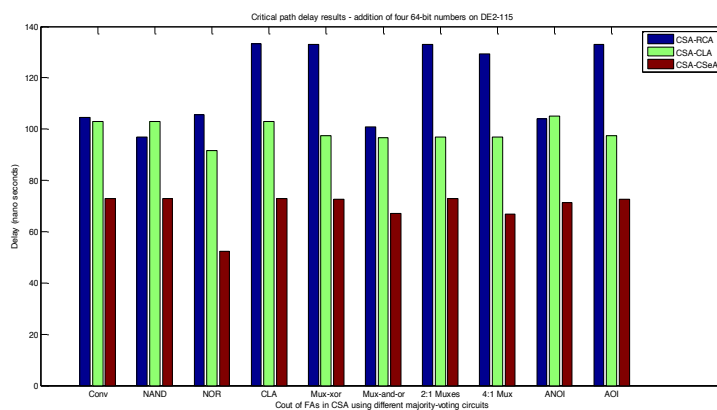


Fig. 17: Critical path delay for the addition of four 64-bit numbers.

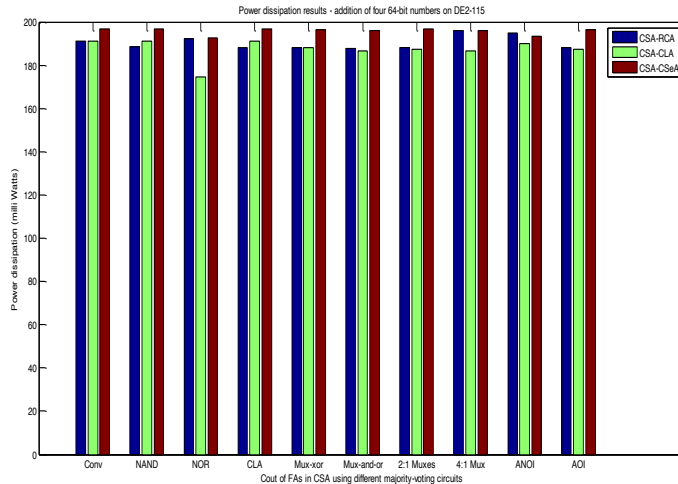


Fig. 18: Power dissipation results for the addition of four 64-bit numbers.

The research findings are summarized as follows. Among the different final stage circuits, the CSA-CSeA approach offers a lower delay, the CSA-CLA approach produces low power dissipation and the CSA-RCA approach consumes less number of logic elements. Among the majority-voting circuits, NAND based circuit offers lower delay and Mux-OR based circuit produces a better power dissipation.

## CONCLUSION

This paper exemplifies the carry-save adder utility for the multi-operand addition with plenty of recipes with the majority-voting circuits instead of a regular full adder. Each design trade-off would be different from others. The best optimum circuit can be chosen depending on the applications and requirements. This work further can be extended to by modifying the final sum calculation stage using 4:2 compressor circuits to enhance the performance and better results. Similarly, the parity-circuit portion in a regular full adder can be considered to modify like using two half adders for example.

## CONFLICT OF INTEREST

There is no conflict of interest.

## ACKNOWLEDGEMENTS

We thank SASTRA University for providing financial support for this research work under the Research and Modernization fund - R&M/0034/SEEE-014/2013-14.

## FINANCIAL DISCLOSURE

None

## REFERENCE

- [1] Dejan Markovic, Robert W. Broderson. DSP Architecture Design Essentials. US: Springer publishers, 2012.
- [2] Uwe Meyer-Baese. Digital Signal Processing using Field Programmable Gate Arrays. Springer-Verlag Berlin Heidelberg, 2007.
- [3] James E. Stine. Digital Computer Arithmetic Datapath Design using Verilog HDL. Springer publishers, 2012.
- [4] Mark Owen. Practical Signal Processing. Cambridge University press, 2007.
- [5] Real-time fault-tolerance with hot-standby topology for conditional sum adder. Atin Mukerjee and Anindya Sundar Dhar. 2015. Microelectronics Reliability, 55: 704-712.
- [6] An implementation of area and power efficient digital FIR filter for hearing aid applications. Balaji, V.S. and Har Narayan Upadhyay. 2015. Journal of Optoelectronics and Advanced Materials, 9: 657-662.
- [7] Uyemura JP. [2006] Introduction to VLSI Circuits and Systems. India: Wiley India publishers.
- [8] Kiat-Seng Yeo, Kaushik Roy. [2009] Low Voltage, Low Power VLSI Subsystems. India: Mc-Graw Hill Education India
- [9] FPGA Implementation of Fast Adder. Hamid MM. Kamboh and Shoab A. Khan. s.l: IEEE Press, 2012. International Conference on Computing and Convergence Technology, pp. 1324-1327.
- [10] An Area Efficient and Low Power Multiplier using Modified Carry Save Adder for Parallel Multipliers. S. Murugeswari and S. Kaja Mohideen. s.l: Springer: International Joint Conference AIM/CCPE 2012, Communications in Computer and Information Science, pp. 446-450.
- [11] CMOS VLSI Design of Low Power SRAM Cell Architectures with new TMR: A Layout Approach. Elamaran, V. and Har Narayan Upadhyay. 2015. Asian Journal of Scientific Research, 8: 466-477.
- [12] Majority function computation using different voter circuits - a comparative study. V Elamaran, et al. 2015. International Journal of Pharmacy and Technology, 7: 9764-9773.
- [13] B Stephen Brown, V Zvonko. [2012] Fundamentals of Digital Logic with VHDL Design. Mc-Graw Hill publishers,
- [14] R Woods, J McAllister, Dr. Ying Yi and Gaye Lightbody [2008]. FPGA-based Implementation of Signal Processing Systems. Wiley-Blackwell publishers,

ARTICLE

# EXPERIMENTAL ANALYSIS OF SEQUENTIAL CLUSTERING ALGORITHM ON BIG DATA

Ajay Kumar and Shishir Kumar\*

Dept. of Computer Science & Engineering, Jaypee University of Engineering & Technology, Guna (MP), INDIA

## ABSTRACT

In the past decade, commercial and scientific organization generates a large volume of data. Clustering of Big data finds application in many areas. For example, in pattern recognition, information extraction, image processing, computational statistics, and data mining. Over the years, we find many methods in the literature for clustering large data set and most of these methods uses, a distance based similarity measures to assign data points to a cluster. This paper considers the case of finding the cluster in big data that cannot fit into the physical processor memory or the data is accessible in batches. In the present work, we have modified the distance-based similarity measure to discover the similarity between an unlabeled data point and a cluster for assignments of cluster label to unlabeled data points. The data points first sampled according to available physical memory and then passed to the next step for further processing. We have used the k-means algorithm and its variants to assign the class or label to the first sample into a legitimate cluster. Also, we have compared the results with sequential k-means, batched-mode k-means, and online k-means algorithm for the clustering of the big data set. Our experimental results based on running time and the quality of the clusters shows the viability of proposed work.

## INTRODUCTION

In recent years, we have seen that commercial and scientific organization generates a large volume of data. Clustering of such data finds application in many areas. However, clustering of large data set requires a different approach than traditional clustering algorithm because this data set may not fit into the processor's physical memory. Another situation that may challenge the clustering algorithm is the use of different data access model when the data is available in a stream, increments, or in batches [1].

The primary need of the clustering algorithm to handle above situation is to reuse the clustering results on the addition of new data to the existing dataset in the form of batches or according to the data access model. Liberty et al. show three type of data access model for the handling of a large dataset, the offline mode, stream mode and online mode [1].

In the offline access mode, the data points are accessible ahead of time, and the data access model is unrestricted. Therefore, finding the optimal solution is hard. Recently, with an end goal to make adaptive sampling methods more scalable, Bahmani et al. presented k-means|| algorithm that decreases the number of passes required for the data, and empowers enhanced parallelization [2].

In the streaming model, the data is processed in one pass and keep a small amount of information about the data. In any case, it must yield cluster centers when the stream ends. This limited data access model requires new algorithmic thoughts for clustering. In this model, the new data points get their cluster with the help of previously computed centers [3, 4].

An online k-means algorithm must allocate points to cluster throughout the run of the algorithm. In this model, data points arrived one by one in an arbitrary order. At the point when new point arrives, the algorithm should either include it in one of the current clusters or create another cluster. This setting is entirely harder than the streaming model. From another viewpoint, the online algorithm can be convertible to a streaming model. Also, one has to keep enough statistics for every cluster so that it can be used toward the end of the stream [1].

Due to simplicity and ease of implementation, the k-means algorithm and its variants are used to cluster large dataset in the numerical domain [5]. In this method, every cluster is drawn by a center that is computed by the mean value of the entire data points present in the cluster [6]. The algorithm uses a straightforward distance measure to give a suitable cluster label to each non-clustered data points.

We see that the Euclidean distance measure from the mean value of other data points in the cluster is not adequate for a non-uniformly distributed cluster. Therefore, there is a need to address similarity measures based on the distribution of data objects in a cluster. In this paper, we have analyzed the use of a new similarity measure in light of the spread (largest and least value of every cluster) of data in every cluster and its mean value (centroids). The algorithm, named as Incremental Batched Clustering Algorithm (IBCA), gives a suitable cluster level to each non-clustered data point that is coming as batches or stream mode.

In this work, we have divided the task of assignments of cluster label to a non-clustered data point in three stages: batch creation, cluster analyses, and data labeling phase. In batch formation stage, we have sampled an appropriate size of data according to the main memory of the system. In cluster analysis stage, a suitable clustering algorithm, for example, k-means, k-means++, k-medoids and fuzzy c-mean, is applied on the dataset to get the initial cluster representative. In data labeling stage, based on the new

### KEY WORDS

Clustering, Sequential k-means, online k-means, Incremental clustering, k-means, k-means++

Published: 2 December 2016

\*Shishir Kumar

Email: dr.shishir@yahoo.com  
Tel.: +91-9407327719



similarity coefficient, each unlabeled data point gets an appropriate cluster label corresponding to the maximal resemblance. The experiments on the benchmark datasets show the effectiveness of the proposed framework. We have also analyzed the effect of the initial seed selection of the k-means algorithm on a large dataset.

The rest of paper is organized as follows. In Section 2, the related works are reviewed. In Section 3, the problem statement and several variants of k-means are presented. Section 4 describes our proposed method and Section 5 illustrates experimental setup and results. In Section 6, we conclude the paper.

## RELATED WORKS

Several methodologies have been documented in the literature for the study of the structure of large data sets [7]. Many applications need clustering of datasets that is too large to fit into the usable physical memory, or the clustering data is available in batches. Both the circumstances influence the need for incremental clustering algorithm [8].

The investigation of incremental clustering has begun with Hartigan's clustering algorithm that makes utilization of a threshold value to decide if a data objects can be put in a current cluster or it should form another cluster independently [9]. Several other algorithms use a sample data having a size equivalent to accessible physical memory [10].

The BIRCH clustering algorithm is well known for the clustering of streaming data. This algorithm has two stages: in the initial step, it examines the database and after that builds a tree comprising data of clusters. In the next step, BIRCH prunes the tree by eliminating of sparse nodes and producing new unique cluster. However, the technique has a drawback of limited memory of its leaves. In addition, the algorithm will not execute well if the cluster does not have spherical shapes because the BIRCH algorithm controls the cluster's boundary by applying the approximation of diameter [11].

The maximum margin clustering uses one data point at one time to decide which cluster the new data point has a place [12]. In another approach, a distance based incremental clustering technique that can discover clusters of arbitrary shapes and sizes in dynamic datasets have been introduced in [13]. Incremental clustering is also referred as a single pass clustering while the conventional algorithm is similar to multi-pass clustering. The thought is to cluster a manageable amount of data and preserve the results for the next block until all the data blocks are processed [8].

Shindler et al. consider the k-means issue where the data is too large to be stored in physical main memory and data must be acquired sequentially [14]. They introduce an improved algorithm for the k-means in a streaming model. Ester et al. have modified DBSCAN algorithm that is appropriate for clustering where dataset are often updated [15].

Aaron et al. demonstrated a dynamic incremental k-means clustering algorithm to discuss seeding issue, the sensitivity of the algorithm to the order of the data, and the number of clusters for the k-means algorithm [16]. Om and Sangam introduced a hybrid data-labeling algorithm for clustering mixed datasets [17]. This algorithm utilizes distance comparability measures for the numerical data to give cluster level to unlabeled data points.

Based on literature survey we observe that most of the method uses a distance based similarity measure for clustering large datasets. In the next section, we present the k-means and its variants that are used for handling large dataset.

## K-means and related

The traditional k-means algorithm is simple optimization model in unsupervised learning process [6]. Given the set,  $D = \{x_1, x_2, \dots, x_n\}$ , of n data points in  $R^n$ , the objective is to minimize the cost of discovering k clusters,  $C = \{c_1, c_2, \dots, c_k\}$ , with k center,  $\{m_1, m_2, \dots, m_k\}$  by using equation-1.

$$V(C) = \sum_{i=1}^n \min_{j=1}^k \|x_i - m_j\|^2 \quad (1)$$

Where  $m_j$ , is the mean of the cluster,  $ck$ . The norm  $\|*\|$  can be any vector norm on  $R^n$ . Minimizing the squared error is an NP-hard problem [18]. The k-mean technique is an iterative process and often terminates near a local minimum, but it is very sensitive to the initial set of centers. Algorithm-1 shows the working of the k-means algorithm.

### Algorithm 1 : k-means (R, k)

**Step 1.** Select k first centers  $\{m_1, m_2, \dots, m_k\}$  randomly from R

**Step 2.** Repeat  
**Step 3.** Partition R into k subsets,  $\{c_1, c_2, \dots, c_k\}$ , such that  $R_i, 1 \leq i \leq k$ , contains all points whose nearest center is  $m_i$   
**Step 4.** Replace the current set of centers by a new set of centers  $\{m_1, m_2, \dots, m_k\}$ , such that center  $m_i, 1 \leq i \leq k$ , is the center of gravity of  $R_i$   
**Step 5.** Until the set of centers has not changed

Clustering method expects that the whole data set is available ahead of time. In a few cases, it is possible that the data is large and cannot match the memory of the processor, or the data is available in batches, so a substitute technique must be adapted. The k-means and various other iterative optimization algorithms related to the k-means algorithm uses one of two fundamental modes of data access model for dealing large data, batch mode, and on-line mode. In an online mode or sequential mode, the parameters of the cluster are recalculated at every addition of new data points of the training set. Similarly, in batch mode, the data is accumulated with time, and a while later the clustering is performed on each batch of data. The last centers of cluster  $i$  are utilized as the initial center for the next approaching batch  $i+1$  [19]. In the sequential k-means, the data points are assigned to a cluster and immediately update the cluster centers. Because of the substantial overhead of recalculating centers, the resource requirement of sequential k-means may be a restrictive element. Even so, in specific situations, the data may appear one at a time. In these cases, it may be desirable to update the results per data occurrence as opposed to waiting for the aggregation of the whole data set.

In the next sub-section, we discuss various variants of k-means algorithm documented in the literature that is dealing with large data. Further to this, we also analyze the effect of initial seed selection methods on the quality of clustering results on the sequential k-means algorithm.

### The Sequential Block K-means Algorithm

The sequential block mode is a trade-off between the stringent computational prerequisites of the sequential k-means and the need to work on data online. For this situation, the clustering happens on accumulated block of data. Every block is going through  $l$  epoch of k-means where the last centers of block  $l$  are utilized as the initial center for block  $l+1$ . In many cases  $l=1$ . In this sense, the algorithm uses another multistage clustering, for example, the pyramid k-means algorithm [19, 16]. The block sequential algorithm employed in an iterative manner where on each iteration performs  $l$  epochs of k-means on a single block of data elements at once.

### Single Pass k-means

Single Pass k-means (SQKM) is an adaptation of the online fuzzy c-means algorithm discussed in [10]. Give  $N$  be the number of data objects in a dataset, which is too large to fit in main memory; let  $n$  signify the number of points that can be stacked into memory. SQKM divides the  $N$  points in the big dataset into  $s$  pieces of small data as  $s = \frac{N}{n}$ . Further, k-means algorithm is used to find  $k$  groups from these segments.

The first set of data now replaced by the k-weighted means,  $\{m_{w,i} : 1 \leq i \leq k\}$ , where the weights are the numbers of data objects in every group,  $\{w_i = |X_i| : 1 \leq i \leq k\}$ . These  $k$  weighted centroids are then converged with the next data segment. Followed by applying weighted k-means (WKM) to this combined set with the centroids from the past k-means run. The procedure is repeated until the entire dataset is stacked and processed. In the wake of acquiring the last  $k$  centroids, the big data are labeled according to the similarity measures. The two most vital disclaimers about its effectiveness are:

- At every step the SQKM faces same limitation and problem as the k-means algorithm and
- The output is obviously subject to the way big data are divided in  $s$  sample. Each chunk or sample of SQKM is treated as one input, and thus SQKM is sequential.

### K-MEANS++ Clustering Algorithm

The k-means algorithm is sensitive to the initial set of center. To improve the quality of k-means algorithm k-means++ algorithm [20] was introduced. It chooses the initial set of center with probability proportional to its squared distance from the nearest center already chosen. The k-means++ algorithm for choosing  $k$  initial center is given in Algorithm-2

#### Algorithm 2: k-means++ (R, k)

Step 1. choose an initial center  $m_1$  uniformly at random from R  
 Step 2.  $M \leftarrow m_1$   
 Step 3. for  $i = 2$  to  $k$   
 Step 4. choose the next center  $m_i$  at random from R, where the probability of each  $r \in R$  is given by  $D^2(r, M)/\text{cost}(R, M)$

Step 5.  $M \leftarrow M \cup m_i$ ,  
 Step 6. repeat  
 Step 7. Partition R into k subsets  $\{c_1, c_2, \dots, c_k\}$ , such that  $R_i, 1 \leq i \leq k$ , contains all points whose nearest center is  $m_i$   
 Step 8. replace the current set of centers by a new set of centers  $\{m_1, m_2, \dots, m_k\}$ , such that center  $m_i, 1 \leq i \leq k$ , is the center of gravity of  $R_i$   
 Step 9. until the set of centers has not changed

### Partitioning about medoids (PAM)

Partitioning about medoids (PAM) cluster the data objects about k medoids. The algorithm takes the instance of the steepest ascent hill climber, using a direct swap neighborhood operation. Best objects are picked in each iteration that conveys the best clustering result. The objective function uses the sum of the distance from each object to the closest medoid. As the search time of the algorithm is slow, the initial set of medoids builds in a greedy fashion. Starting with an empty set of medoids, data objects are added one at a time until k medoids have been selected. At each step, the new medoid is chosen to minimize the objective function.

### PROPOSED WORK

Most of the partitioning clustering techniques method makes use of the Euclidean distance between the cluster centers and the data points to allocate a data point into the cluster. In this paper, we propose new similarity measures for the sequential k-means clustering. The algorithm is abbreviated as Incremental Batched Clustering Algorithm (IBCA) and is capable of handling large and streaming numerical data.

The sequential k-means algorithm divides the N points in the big dataset into “s” pieces of small data. On the arrival of a new data point, the algorithm uses the previously computed centroids for the assignment of cluster label. The process is repeated until the entire dataset is stacked and processed. Often the similarity measures that are used in handling sequential data is based on the Euclidean distance between the cluster representative and the data objects. However, this strategy does not consider the spread of data inside the group for appointing the cluster level to unlabeled data points. Upon arrival of a data point,  $X_i$  the sequential k-means algorithm uses the similarity measures defined in equation-2 to provide cluster label to data point  $X_i$  [21].

$$D_{(X_i, C_j)} = \sum_{i=1}^n \min_{j=1}^k \|X_i - C_j\|^2 \tag{2}$$

Where  $D_{(X_i, C_j)}$  is the distance of data object  $X_i$  with cluster center  $C_i$ .

Now consider the case where a data point arrives in unexpected order. In the sequential approach, the first block of data is divided into two clusters having centroids  $C_1$  and  $C_2$  with the help of traditional k-means algorithm. Now on the arrival of a new data point  $X_i$ , following two possibilities is possible which are shown in the [Fig. 1] and [Fig. 2].

- If the distances between  $X_i$  and cluster centers are equal, then the algorithm is not able to decide the correct cluster label of data point  $X_i$ .
- If  $X_i$  is close to the boundary points of cluster  $C_1$  or  $C_2$ . In this case, we have to check  $D_{\max}(X_i, C_1) < D_{\max}(X_i, C_2)$ .

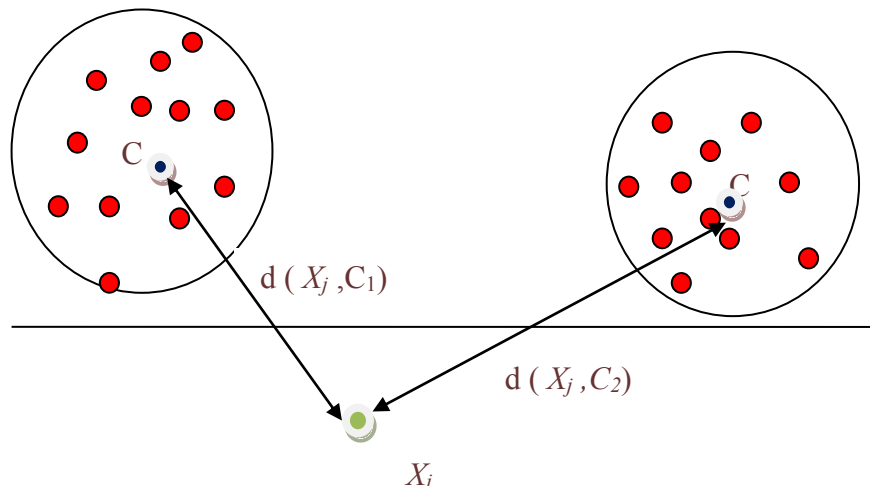


Fig. 1: First Case when  $d(X_i, C_1) = d(X_i, C_2)$ , i.e., distance from the centroids are equal.

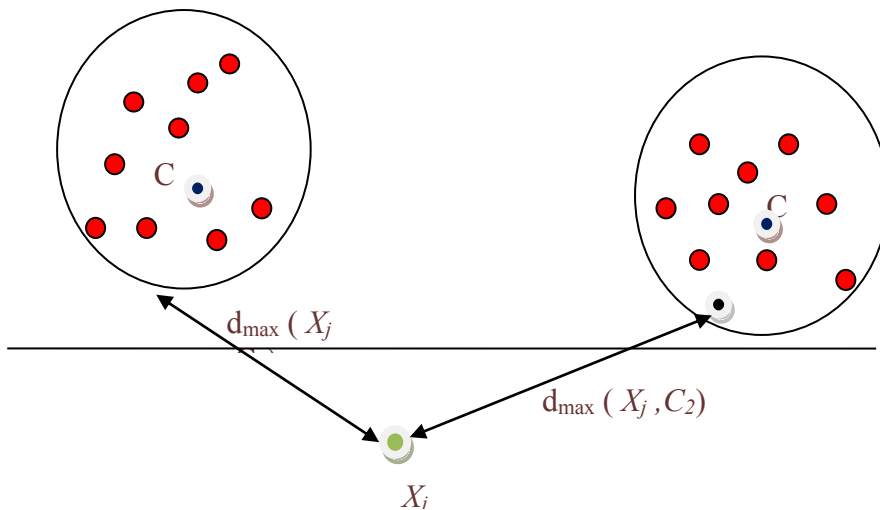


Fig. 2: The Second case when the new data point is close to the boundary points of a cluster.

Therefore, to discover a similarity coefficient for the unlabeled data on cluster  $C_i$  Euclidian distance method is used. Equation-3 gives the Euclidian distance between an unlabeled data point  $x_j$  and mean estimation of cluster  $c_i$ .

$$D_{mean}(x_j, c_i) = \sum_{j=1}^n \min_{i=1}^k \|x_j - mean(c_i)\|^2 \quad (3)$$

Where,  $D_{mean}(x_j, c_i)$  is the Euclidean distance between the unlabelled data point  $x_j$  and the centroid of the cluster  $c_i$ . The  $mean(c_i)$  represents the mean value of all the data points in the cluster  $c_i$  or centroids.

Similarly, the equation-4 and 5 gives the Euclidian distance between an unlabeled data point  $x_j$  and the nearest boundary points of a cluster  $C_i$ .

$$D_{max}(x_j, c_i) = \sum_{j=1}^n \min_{i=1}^k \|x_j - max(c_i)\|^2 \quad (4)$$

Where,  $D_{max}(x_j, c_i)$  represents the Euclidean distance between the unlabelled data point,  $x_j$  and the maximum value of cluster  $c_i$ .

$$D_{min}(x_j, c_i) = \sum_{j=1}^n \min_{i=1}^k \|x_j - min(c_i)\|^2 \quad (5)$$

Where,  $D_{min}(x_j, c_i)$  represents the Euclidean distance between the unlabelled data point  $x_j$  and the minimum value of cluster  $c_i$ .

So based on the above cases equation-6 shows a new similarity measure (SC) between the new incoming data points  $x_j$  and the cluster  $c_i$ .

$$SC(x_j, c_i) = \min(D_{mean}(x_j, c_i) + D_{max}(x_j, c_i) + D_{min}(x_j, c_i)) \quad (6)$$

We have considered the mean and spread of the data inside the cluster as a similarity measures to give cluster labeled to unlabeled data points. The proposed approached is explained with the help of exam.1.

**Example-1:** Consider the artificial dataset given in [Table 1]. The dataset comprises of two numerical attribute A1, A2, and having nineteen data samples. These data samples are divided into three cluster  $c_1$ ,  $c_2$ , and  $c_3$ . Each cluster has five data points. Based on similarity coefficient described in equation-6, the cluster label to unlabelled data points  $x_{16}$ ,  $x_{17}$ ,  $x_{18}$ , and  $x_{19}$  in clusters  $c_1$ ,  $c_2$ , and  $c_3$  are obtained as follows:

$$SC(x_{16}, c_1) = \min(D_{mean}(x_{16}, c_1) + D_{max}(x_{16}, c_1) + D_{min}(x_{16}, c_1)) \\ = 18.04217 + 24.73863 + 15.65248 = 58.43328241$$

According to the above-calculated similarity coefficient values, we can assign  $c_1$  cluster label to,  $x_{16}$  since the distance between the data point and the value of SC is minimum as compared to other clusters. For other unlabeled data points, a similar approach has been used and it is summarized in [Table 2]. Final cluster assignment to unlabelled data points is given in [Table 3].

The example shows that our proposed similarity coefficient preserves the characteristics of clustering, i.e., both high intra-cluster similarity and small inter-cluster similarity.

Table 1: Artificial dataset

Data point	A1	A2	Cluster
X <sub>1</sub>	11	52	c1
X <sub>2</sub>	13	45	c1
X <sub>3</sub>	14	44	c1
X <sub>4</sub>	15	57	c1
X <sub>5</sub>	19	40	c1
X <sub>6</sub>	31	60	c2
X <sub>7</sub>	35	62	c2
X <sub>8</sub>	34	71	c2
X <sub>9</sub>	39	73	c2
X <sub>10</sub>	30	78	c2
X <sub>11</sub>	61	51	c3
X <sub>12</sub>	64	56	c3
X <sub>13</sub>	67	58	c3
X <sub>14</sub>	72	59	c3
X <sub>15</sub>	76	55	c3
X <sub>16</sub>	25	33	?
X <sub>17</sub>	33	39	?
X <sub>18</sub>	36	73	?
X <sub>19</sub>	16	51	?

Table 2: Distance matrix of unlabelled data points w.r.t mean

		C <sub>1</sub>	C <sub>2</sub>	C <sub>3</sub>	Cluster assignment
D <sub>mean</sub>	X <sub>16</sub>	18.04217	35.80894	44.99822	C <sub>1</sub>
	X <sub>17</sub>	20.49195	30.25029	36.01722	C <sub>1</sub>
	X <sub>18</sub>	33.34247	39.42436	11.65504	C <sub>3</sub>
	X <sub>19</sub>	3.757659	24.75237	30.1171	C <sub>1</sub>
D <sub>max</sub>	X <sub>16</sub>	24.73863	47.12749	57.24509	C <sub>1</sub>
	X <sub>17</sub>	22.80351	39.45884	47.42362	C <sub>1</sub>
	X <sub>18</sub>	23.34524	5.830952	42.37924	C <sub>2</sub>
	X <sub>19</sub>	6.708204	35.4683	60.53098	C <sub>1</sub>
D <sub>min</sub>	X <sub>16</sub>	15.65248	27.65863	40.24922	C <sub>1</sub>
	X <sub>17</sub>	22.02272	25.23886	30.46309	C <sub>1</sub>
	X <sub>18</sub>	41.40048	21.40093	33.30165	C <sub>2</sub>
	X <sub>19</sub>	12.08305	9.486833	45	C <sub>2</sub>

Table 3: Sum of distance matrix and final cluster assignment for unlabelled data points

	C <sub>1</sub>	C <sub>2</sub>	C <sub>3</sub>	Cluster labeled
X <sub>16</sub>	58.43328	110.5951	142.4925	C <sub>1</sub>
X <sub>17</sub>	65.31817	94.94799	113.9039	C <sub>1</sub>
X <sub>18</sub>	98.08818	66.65624	87.33593	C <sub>2</sub>
X <sub>19</sub>	22.54891	69.7075	135.6481	C <sub>1</sub>

Given X data points, the proposed algorithm incrementally arrives at a cluster solution upon receiving a new data point, X<sub>j</sub> as follows:

- Step 1.** Compute the sample data from the sequential data X, s= (n/p), p is the available physical memory, n is the number data point.
- Step 2.** Normalize the X by min-max normalization algorithm.
- Step 3.** Apply k-means (or any other partitioned clustering algorithm) clustering algorithm on sample dataset X to create C<sub>i</sub> partition. Assigned obtained centroid as Centroid<sup>old</sup> and cluster label as Cluter\_label<sup>old</sup>



- Step 4.** Find the minimum, maximum, and means of each cluster  $C_i$
- Step 5.** Upon receiving a new data point  $X_i$ , assign a cluster label as  $i$  by using the similarity coefficient defined in equation-6.
- Step 6.** Obtained Centroid<sup>new</sup>
- Step 7.** Update the centroid<sup>old</sup> = Centroid<sup>new</sup> and append the cluster label to Cluter\_label<sup>old</sup>.
- Step 8.**  $X=X+1$ ; go to step 5.

The pseudo code of the proposed algorithm is given in [Fig. 3].

**Algorithm:** IBCA

**Input:** Dataset  $X$ , number of cluster  $k$

**Output:** Cluster labeled to unlabeled of data points

$(n \times m) \leftarrow \text{size}(X)$

Compute the sample data size,  $s = (n/p)$ ,  $p$  is the available physical memory

Initialize the variable seed as  $k \times m$  array

Initialize min\_data\_cluster, max\_data\_cluster, distance as an  $(k \times m)$  empty array

Load  $X$  as an  $s$  sized sample dataset

Apply any clustering algorithm on sample dataset to create partitions

Assign obtained centroid to seed array

for  $i=k+1$  to  $n$  do

    for  $j=1$  to  $k$  do

        Compute the minimum, maximum and mean value of the  $i$ th numerical attribute on  $j$ th cluster and assign these value to min\_data\_cluster[ $i$ ][ $j$ ], max\_data\_cluster[ $i$ ][ $j$ ], and mean\_data\_cluster[ $i$ ][ $j$ ] respectively

    end

for  $p=1$  to  $L$  do

    initialize max\_similarity=0

    for  $i=1$  to  $k$

        find the similarity between a  $P^{\text{th}}$  unlabelled data points and a  $i$ th cluster according to similarity coefficient (6)

        if max\_similarity < similarity then

            max\_similarity=similarity

            label= $p$

        end

    end

    assign label value to unlabelled data points as cluster label

end

**Fig. 3:** The pseudo-code of the proposed algorithm.

## EXPERIMENTAL SETUP AND RESULTS

We ran the proposed algorithm on several datasets. The datasets are taken from the UCI machine learning repository, and the summaries of their characteristics are given in [Table 4] [22]. The dataset  $s_1$ ,  $s_2$ ,  $s_3$ , and  $s_4$  are artificial datasets consisting of Gaussian clusters with the same variance but increasing overlap. Some of these datasets is available on the web page <https://cs.uef.fi/sipu/datasets> as mentioned in the literature [23]. All the experiments are performed on Intel Core™ i3-2348M machine with 2GB of RAM.

**Table 4:** Data Set description

Dataset	Data Set Characteristics	Number of features	Number of data objects	Number of Clusters
Iris	Multivariate	4	150	3
Wine	Multivariate	13	178	3
Thyroid	Multivariate	5	215	3
WDBC	Multivariate	32	569	2
s1-s4	Artificial	2	5000	15

We have compared the performance of the proposed method with other variants of sequential k-means algorithm. We have used running time, Dunn's, and Davies-Bouldin (DB) index as parameters for the comparison of experimental results. Several runs of each algorithm have been performed, and most significant digits of the result are shown.

The Dunn's index measure is used to find the compactness of the data points within the cluster and cluster's separation (minimum distance between clusters). The maximum value of the index represents

the right partitioning. The Davies-Bouldin index (DB) criterion is based on a ratio of within-cluster and between-cluster distances. A Smaller value of DB shows a better clustering solution [24].

First, we made running time analysis of the proposed method (IBCA) with Block-Mode-k-means, Online-k-means, and Sequential-k-means. By analyzing, the results, we have observed that the proposed approached have better time complexity with Sequential k-means and its other variants for the data set used in the experiments, see [Fig. 4]. We have also analyzed the seeding issue of the k-means algorithm and find that the running time is higher than the proposed work, but the quality can be improved significantly by choosing proper initial centers.

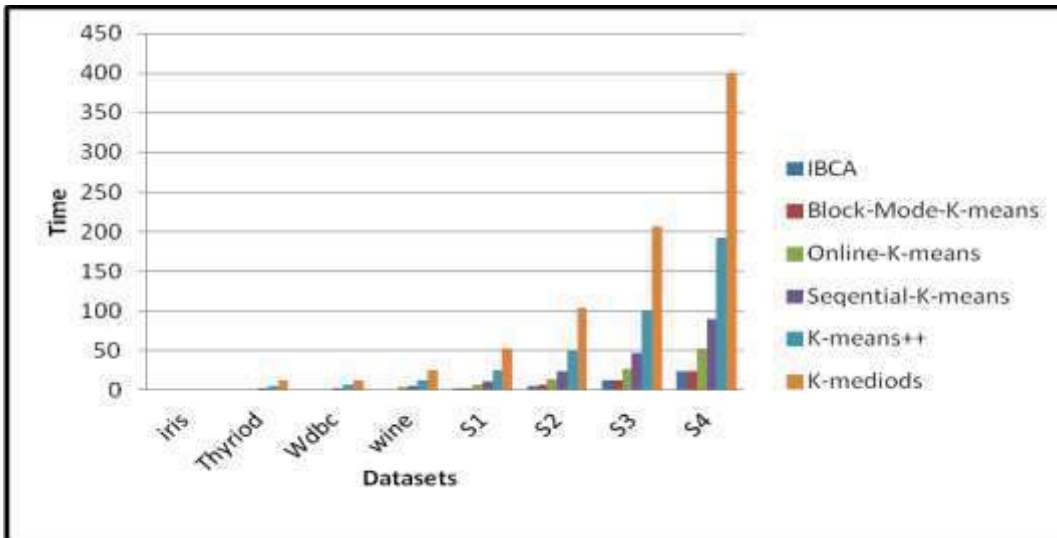


Fig. 4: Running time analysis of different variants of Sequential k-means algorithm.

As mentioned in the proposed approached the first block of data is clustered with the k-means algorithm can have poor clustering results due to a random selection of initial centers. Therefore an initialization algorithm k-means++ and k-medoids has been used in the initial phase. However, with the good initial guess of centroids consume some amount of time compared to other algorithms, but the quality of the cluster is good.

The next set of experiment examines the quality of clustering results on various dataset mentioned in the [Table 4]. Results on these data sets are tabulated in the [Table 5-12]. The experimental results show that the quality of the clustering results of the proposed algorithm is equivalent to the traditional sequential k-means algorithm except for the dataset S1 see Table-9. However, other algorithms perform better than the proposed algorithm, but the running cost of these algorithms is high; see [Fig. 5] and [Table 5-12].

Table 5: Comparative results on the iris dataset

Sample Size		15%	25%	50%	75%	100%
Dunn	IBCA	<b>0.776</b>	<b>0.9449</b>	<b>1.3442</b>	<b>1.2427</b>	<b>1.2124</b>
	Block-Mode-K-means	2.0197	1.3261	1.4959	1.3375	2.0279
	Online-K-means	2.0197	1.5961	2.1545	1.9433	1.994
	Sequential-K-means	<b>0.776</b>	<b>0.9449</b>	<b>1.3442</b>	<b>1.2427</b>	<b>1.2124</b>
	K-means++	2.219	1.4856	1.5067	1.8818	1.6197
	K-medoids	2.219	1.6488	1.4959	1.252	1.9557
DB	IBCA	0.9714	1.283	0.699	0.6673	0.6466
	Block-Mode-K-means	0.7004	0.6694	0.656	0.6593	0.7629
	Online-K-means	0.7004	0.649	0.6894	0.7209	0.7043
	Sequential-K-means	0.9714	1.283	0.699	0.6673	0.6466
	K-means++	0.5114	0.5956	0.641	0.7269	0.7812
	K-medoids	0.5114	0.6401	0.656	0.6494	0.7622

Table 6: Comparative results on the iris dataset

Sample Size		15%	25%	50%	75%	100%
Dunn	IBCA	0.6907	0.6821	0.783	0.715	0.673
	Block-Mode-K-means	1.1739	0.6364	0.8521	0.9842	1.3211
	Online-K-means	1.1699	0.6415	0.8926	1.0284	1.2896
	Sequential-K-means	0.6907	0.6821	0.783	0.715	0.673
	K-means++	1.3304	0.65	1.4457	0.9607	1.2934

	K-medoids	1.0369	0.6148	0.9629	1.0635	1.2934
DB	IBCA	2.3034	2.1126	1.8226	1.7863	1.865
	Block-Mode-K-means	1.5655	1.7807	1.8474	1.857	1.3683
	Online-K-means	1.4912	1.7821	1.9328	1.6605	1.188
	Sequential-K-means	2.3034	2.1126	1.8226	1.7863	1.865
	K-means++	0.9941	1.7547	1.1976	1.8361	1.3746
	K-medoids	1.747	1.8287	1.6531	1.4858	1.3746

**Table 7:** Comparative results on the thyroid dataset

Sample Size		15%	25%	50%	75%	100%
Dunn	IBCA	<b>1.382</b>	<b>1.2703</b>	<b>1.2955</b>	<b>0.7612</b>	<b>0.8163</b>
	Block-Mode-K-means	1.3711	1.295	1.4407	0.6743	1.4785
	Online-K-means	1.1973	1.2043	1.1764	0.697	1.4785
	Sequential-K-means	1.382	1.2703	1.2955	0.7612	0.8163
	K-means++	1.3821	1.247	1.3719	2.0212	1.4785
	K-medoids	1.2612	1.2138	1.1245	0.6743	1.4812
DB	IBCA	0.8864	1.304	1.3246	2.3526	1.692
	Block-Mode-K-means	1.0319	1.3567	1.3497	0.8977	0.7712
	Online-K-means	1.2869	1.0813	1.1516	0.8867	0.7712
	Sequential-K-means	0.8864	1.304	1.3246	2.3526	1.692
	K-means++	1.0377	1.3829	1.3264	0.7543	0.7712
	K-medoids	1.3343	1.3413	1.4192	0.8889	0.7591

**Table 8:** Comparative results on the Wdbc dataset

Sample Size		15%	25%	50%	75%	100%
Dunn	IBCA	1.1907	1.0946	1.1667	1.2507	1.2609
	Block-Mode-K-means	1.2707	1.1479	1.2403	1.26	1.281
	Online-K-means	1.2707	1.1644	1.2403	1.2594	1.2526
	Sequential-K-means	1.1907	1.0946	1.1667	1.2507	1.2609
	K-means++	1.2707	1.1479	1.2403	3.0377	1.2727
	K-medoids	1.2707	1.1644	1.2403	1.2599	1.2526
DB	IBCA	1.432	1.4879	1.4218	1.3247	1.3138
	Block-Mode-K-means	1.3388	1.4304	1.337	1.308	1.3093
	Online-K-means	1.3388	1.4167	1.337	1.3083	1.3205
	Sequential-K-means	1.432	1.4879	1.4218	1.3247	1.3138
	K-means++	1.3388	1.4304	1.337	0.6383	1.3123
	K-medoids	1.3388	1.4167	1.337	1.3081	1.3205

**Table 9:** Comparative results on the S1 dataset

Sample Size		15%	25%	50%	75%	100%
Dunn	IBCA	0.0434	0.0429	0.0958	0.0992	0.1262
	Block-Mode-K-means	0.6396	0.572	0.5384	0.5308	0.5361
	Online-K-means	0.856	1.3119	1.1437	1.4073	4.1649
	Sequential-K-means	1.1144	0.8647	0.672	0.7699	0.9218
	K-means++	1.3588	1.2671	1.0654	1.2126	0.5689
	K-medoids	0.649	0.6163	0.5797	0.4326	0.4884
DB	IBCA	1.1144	0.8647	0.672	0.7699	0.9218
	Block-Mode-K-means	0.6292	0.7492	0.5244	0.4113	0.3685
	Online-K-means	0.6688	0.6497	0.5373	0.4185	0.3103
	Sequential-K-means	0.0434	0.0429	0.0958	0.0992	0.1262
	K-means++	0.572	0.6521	0.5375	0.3991	0.3812
	K-medoids	0.7194	1.2003	1.0195	1.4404	0.5075

**Table 10:** Comparative results on the S2 dataset

Sample Size		15%	25%	50%	75%	100%
Dunn	IBCA	<b>0.059</b>	<b>0.0836</b>	<b>0.1142</b>	<b>0.1766</b>	<b>0.216</b>
	Block-Mode-K-means	0.5403	0.2731	1.0723	0.44	0.4402
	Online-K-means	1.0036	1.3485	1.1676	1.0043	0.8079
	Sequential-K-means	<b>0.059</b>	<b>0.0836</b>	<b>0.1142</b>	<b>0.1766</b>	<b>0.216</b>
	K-means++	1.113	1.0976	1.3025	0.7557	0.8944
	K-medoids	0.7646	1.1433	1.3437	1.1472	0.7811
DB	IBCA	0.7464	1.0436	0.7911	0.7799	0.7587
	Block-Mode-K-means	0.6532	0.6729	0.5079	0.5297	0.5748
	Online-K-means	0.7687	0.7557	0.6258	0.495	0.4731

	Sequential-K-means	0.7464	1.0436	0.7911	0.7799	0.7587
	K-means++	0.735	0.7254	0.6134	0.5707	0.5398
	K-medoids	0.7429	0.7054	0.6002	0.5154	0.6024

**Table 11:** Comparative results on the S3 dataset

Sample Size		15%	25%	50%	75%	100%
Dunn	IBCA	<b>0.0602</b>	<b>0.1643</b>	<b>0.2089</b>	<b>0.3142</b>	<b>0.4914</b>
	Block-Mode-K-means	0.9009	1.1579	1.2956	1.7059	1.3395
	Online-K-means	1.0932	1.3964	1.4017	1.4246	1.4246
	Sequential-K-means	<b>0.0602</b>	<b>0.1643</b>	<b>0.2089</b>	<b>0.3142</b>	<b>0.4914</b>
	K-means++	0.9422	1.3489	1.1727	1.7691	1.2206
	K-medoids	1.0335	1.4559	1.3767	1.3117	2.3305
DB	IBCA	0.9687	0.8973	0.8483	0.7616	0.7421
	Block-Mode-K-means	0.7107	0.7161	0.7131	0.633	0.6753
	Online-K-means	0.6666	0.7699	0.7149	0.6355	0.6355
	Sequential-K-means	0.9687	0.8973	0.8483	0.7616	0.7421
	K-means++	0.7874	0.7674	0.7116	0.6319	0.6335
	K-medoids	0.6929	0.7318	0.7121	0.6763	0.5164

**Table 12:** Comparative results on the S4 dataset

Sample Size		15%	25%	50%	75%	100%
Dunn	IBCA	0.1991	0.1189	0.1258	0.158	0.2634
	Block-Mode-K-means	0.6495	1.1921	0.9446	1.1518	1.3645
	Online-K-means	0.9852	1.3183	1.2853	1.2128	1.8504
	Sequential-K-means	0.1991	0.1189	0.1258	0.158	0.2634
	K-means++	1.1877	1.5787	1.5168	1.6513	1.7998
	K-medoids	0.5339	0.9537	1.4689	1.5466	1.5538
DB	IBCA	0.8064	0.7998	0.8714	0.859	0.8131
	Block-Mode-K-means	0.7108	0.7036	0.7518	0.7325	0.6596
	Online-K-means	0.6802	0.6723	0.7119	0.658	0.5596
	Sequential-K-means	0.8064	0.7998	0.8714	0.859	0.8131
	K-means++	0.6326	0.6841	0.6847	0.6578	0.6002
	K-medoids	0.6892	0.742	0.6477	0.6177	0.641

## SUMMARY

In this work, we propose an efficient method for clustering large data that does not fit into the system available physical memory. The key idea in handling the large dataset is to divide it into a fixed sample size and then perform clustering on each sampled data. We have used results of the previously computed cluster along with its boundary point to assign the cluster labeled to unlabeled data points. A series of experiments are performed on the benchmark datasets suggest that the proposed work can be utilized as an alternative to sequential k-means for clustering large data set as it has better running time complexity and similar cluster quality outcome. The Proposed IBCA algorithm competes with sequential k-means along the time and accuracy dimensions

### CONFLICT OF INTEREST

There is no conflict of interest.

### ACKNOWLEDGEMENTS

None

### FINANCIAL DISCLOSURE

None

## REFERENCES

- [1] Edo Liberty, Ram Sriharsha, and Maxim Sviridenko. [2016] an Algorithm for Online K-Means Clustering. Proceedings of the Eighteenth Workshop on Algorithm Engineering and Experiments (ALENEX). 81-89
- [2] Bahmani, Bahman, et al. [2012] Scalable k-means++. PVLDB. 622-633.
- [3] Ailon, Nir, Jaiswal, Ragesh and Monteleoni, Claire. [2009] Streaming k-means approximation. NIPS. 10-18.
- [4] Ackermann, R Marcel, et al. [2012] StreamKM++: A clustering algorithm for data streams. ACM Journal of Experimental Algorithmic.17(2):1-30
- [5] Wu X, et al. [2007] Top 10 algorithms in data mining. Knowledge and Information System. 14(1): 1-37.
- [6] MacQueen, J. [1967]5th Berkeley symposium on mathematical statistics and probability. 281-297.
- [7] Jain AK. [2010] Data clustering: 50 years beyond k-means. Pattern Recognition Letters. 31: 651-666.

- [8] Gupta C, Grossman R. [2004] A Single Generalized Incremental Algorithm for Clustering. The Fourth SIAM International Conference on Data Engineering. 234-242.
- [9] Hartigan JA. [1975]. Clustering Algorithms. New York: John Wiley & Sons.
- [10] Hore, Prodip, et al. [2009] A Scalable framework for segmenting magnetic resonance images. J. Signal Process. Syst., 183-203.
- [11] ZHANG T, RAMAKRISHNAN R, LIVNY M. [1996] an efficient data clustering method for very large databases. In Proceedings of the ACM SIGMOD. International Conference on Management of Data (SIGMOD '96). 103-114.
- [12] Saradhi V Vijaya, Abraham P Charly. [2016] Incremental maximum margin clustering. Pattern Analysis and Applications. 19(4): 1057-1067.
- [13] Patra, Bidyut kumar, et al. [2013] Distance based Incremental Clustering for Mining Clusters of Arbitrary Shapes. Pattern Recognition and Machine Intelligence. 229-236.
- [14] Shinder, Michael, Wong, Alex and Meyerson. [2011] Fast and Accurate k-means For Large Datasets. NIPS. 2375-2383.
- [15] Ester, M, et al. [1998] Incremental Clustering for Mining. Proceedings of the 24th International. Conference on Very Large Databases (VLDB'98). 323-333.
- [16] Bryant Aaron, et al. [2014] Dynamic Incremental K-means Clustering. IEEE, International Conference on Computational Science and Computational Intelligence. 308-313.
- [17] Ravi Sankar, Sangam ,Hari, Om. [2014], Hybrid data labeling algorithm for clustering large mixed data type. Journal of intelligent information system, 1-21.
- [18] NP-hardness of Euclidean sum-of-squares clustering. Aloise, D, et al. [2009], Machine Learning, pp. 245-248.
- [19] Tamir DE, Park C , Yoo B. [2007] The Validity of Pyramid K-means. Proc. SPIE conference on Optics and Photonics / Optical Engineering and Applications. 1225-1233.
- [20] Arthur D, Vassilvitskii, S. New Orleans LA. [2007] K-means++: the advantages of careful seeding. ACM-SIAM Symposium on Discrete Algorithms, Society for Industrial and applied Mathematics. 1027-1035.
- [21] Chakraborty, S and Nagwani, N.K. [2011] Analysis and study of Incremental K-Means clustering algorithm. International conference in High Performance Architecture and Grid Computing. 338-341.
- [22] Lichman M. {UCI} Machine Learning Repository. [2013] <http://archive.ics.uci.edu/ml>.
- [23] Franti P, Virmajoki, O. [2006] Iterative shrinking method for clustering problems. Pattern Recognition. 761-765.
- [24] Mirkin, B. [1996] Mathematical Classification and clustering. Springer.

ARTICLE

# AUTOMATIC SEGMENTATION OF LIVER TUMOUR IN CT IMAGES USING SPATIAL FCM AND UNIFIED LEVEL SET METHOD

D. Selvathi<sup>1</sup>, S. Priyadarsini<sup>2\*</sup>

<sup>1</sup>Dept. of Electronics and Communication Engineering, Mepco Schlenk Engineering College, Sivakasi, INDIA

<sup>2</sup>Dept. of Computer Science and Engineering, P.S.R Engineering College, Sivakasi, INDIA

## ABSTRACT

An organ that is vital in order to survive is the liver. It is however quite prone to several diseases such as hepatic tumours. These tumours are routinely investigated by the use of Computed Tomography (CT) mainly for the evaluation of primary and secondary hepatic tumours prior to surgery. In the case of large amount of data however, it is challenging to do a manual segmentation of the CT images. Here, fully automated techniques that require minimal or no supervision remove the need for manual segmentation. This paper evaluates Spatial Fuzzy C Means (FCM) clustering as compared to unified level set method to segment the liver from CT images.

## INTRODUCTION

The liver constitutes for one of the vital organs present in the human body. It carries out several functions such as detoxification, synthesis of protein and manufacturing of bio chemicals essential for digestion. The liver lies in the right upper quadrant of the abdomen just below the diaphragm. As the liver carries out several functions and due to its location in the abdomen it has been noted to be prone to masses. Here the masses may be either benign or malignant. The detection of these masses are now reliant on the advancements made in imaging modalities such as Magnetic Resonance Imaging (MRI), CT, and digital mammography to name a few. This technology serves to image the many complexities of the human anatomy [1]. In this regard, CT allows for the surgeon to determine the presence, size, location and extent of involvement, making CT the most preferred for hepatic tumours. From the abdominal CT, the liver has been previously segmented using various techniques like FCM, graph cut and adaptive threshold. Along the same lines a researcher JeongjinLeea et al [2] depicted a level-set method for segmentation. This technique involves the use of level-set speed images that determine the initial hepatic boundary. This is done by coupling the level-set speed images to a two-step Seeded Region Growing (SRG). Of the two steps, in the first step if the iteration number of the specified curvature is determined to be too small then the SRG segregates the CT images into a smaller number (also with the increase in the iteration number). From this, the liver boundary is seen to be smoother and can be more easily detected. The calculation time is also increased.

Graph cuts were developed by Jean Stawiaski et al [3] for the purpose of image segmentation. This technique use the graphs based on input data and find a global optimal cut. The graph is constructed by each voxel being assigned with a node. This algorithm was seen to have issue with locating the liver border as the border is darker than the rest if the liver and hence it marks the liver on the whole as a tumour. The accuracy hence was lowered. Adaptive threshold along with morphological was proposed by S.S.Kumar et al [4] for image segmentation of the liver. He also proposed the FCM for the segmentation of hepatic tumours. It was determined that the FCM only measures the grey area values hence decreasing the accuracy. On the other hand, Fast Discrete Curvelet Transform (FDCT) gives textural information of the extracted tumour by making use of artificial neural network classifier. The classification rate thus obtained was 93.3%. Artificial neural networks however need a more diverse training in real time situations. Classification with local binary pattern images for categorising normal and abnormal liver images with cancer was proposed by Vijayalakshmi et al [5]. Non- overlapping segments of 8X8 of liver images are obtained. Further, to extract the features of texture and other appropriate features Legendre moments and forward selection algorithm is applied. The images are then classified using the neighbourhood minimum distance decision rule and Euclidean distance classifier. Hsue et al [6] ascertained that computer aided detection using growing algorithm can be used for liver segmentation of CT images. Following this, the CT images are transformed into a digital signal through DWPD (Discrete Wavelet Packet Decomposition) after which REDUCT sets are employed to segregate the given features and reach a classification.

Xing Zhang et al [7] evaluated automatic segmentation with the employ of optimal surface detection using a statistical shape model. This technique uses the concepts of graph theory that enables for the shape of the liver to be localised using a Hough transform after which the shape model deforms in order to conform to the shape of the liver. A brute force manner is then applied for the scale and rotation of the object. This manner however is associated with a high cost and requires a 6-D parameter. YrjöHäme et al [8] proposed semi-automatic liver tumour segmentation with a hidden Markov field model measure. It uses a non-parametric distribution. Post processing is also including as part of the technique to curtail the overflow to the adjacent tissue. The accuracy is decreasing for low contrast images. Sergio Casciaro et al [9] made a

**KEY WORDS**  
Spatial FCM, Clustering,  
Tumor, Liver, Unified  
Level Set (MEA)

Published: 2 December 2016

\*Corresponding Author  
Email:  
priyaraaja26@gmail.com



comparative study on two methods namely graph cut method, active contour method for liver segmentation. For 3D liver images, both the techniques proved efficient and it was proved for tumour segmentation. This method results in high computation time. Xiaoqi Lu et al [10] proposed modified region growing method in which the source images are pre-processed using a non-linear mapping method for liver segmentation which highlights the liver region. Bing Nan Li et al [11] proposed a unified level set method (LSM) tumour segmentation. This method avoids boundary leakage. It overcomes the disadvantage of both region based LSM and edge based LSM and provides high accuracy of 97%.

Liver segmentation through constrained convex variation model was tested by Jialin Penget al [12]. This method was associated with over segmentation as it was involved in categorising those structures that had weak borders as well.

Li C et al [13] proposed a level set model with likelihood and constraint for segmentation of the liver shape. The method was however found to be only useful for the healthy liver. Xiao Song [14] proposed removing the ribs, spine and kidney structures along with a smooth filter to enhance the contrast of images by a thresholding operation. Besides this, the researcher also proposed a FMM (Fast Marching Method) with an automatic seed point process of selection. ABC (Artificial bee colony) using a clustering optimisation algorithm to segment liver from CT images was verified by Abdalla Mostafa [15]. Here the centroids from each cluster are calculated using mathematical morphological operations. This enables for the removal of sharp edges of other organs as well as flesh regions. Following this enhancement of the image was achieved by using growing approaches. Nuseiba et al [16] proposed a Distance Regularization Level Set (DRLS) model that employs a contour method which is edge-based for liver segmentation. The main advantage is that it guides the direction of the contour to evolve with the contours of the liver. Xuechen li et al [17] proposed spatial fuzzy clustering for liver segmentation coupled with the level set method. In this method, spatial constraints are included in the objective function which is minimised through spatial FCM which optimises the membership function resulting in an accuracy of 99.86%.

## MATERIALS AND METHODS

This paper depicts the modules for segmenting the tumour from the liver in CT images in figure 1. In this work, spatial FCM is used for liver segmentation from abdominal CT images. This method helps in accurate segmentation. Then the tumour from the segmented liver is extracted using Unified Level Set Method and spatial FCM and the comparison is made between the techniques.

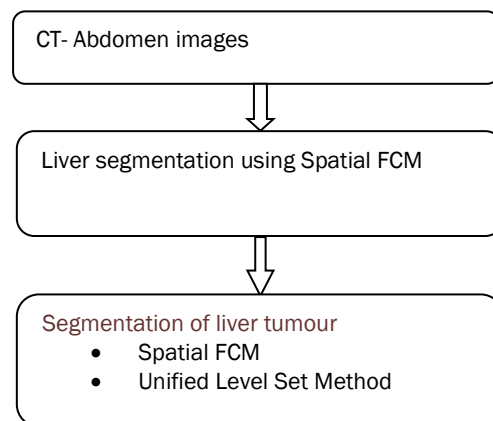


Fig. 1: Proposed methodology.

### Liver segmentation

The segmentation of liver is difficult due to the fact that the CT image includes other organs like spleen, pancreas, kidney etc. which are very close to the liver. The liver is extracted from the CT image using Spatial FCM clustering. It is an iterative optimization algorithm which aims to reduce the objective function. Initially the algorithm starts with FCM clustering which then incorporates spatial constraints in the membership function and then the iteration proceeds.

The process of fuzzy clustering implies each data point to be belonging to more than one cluster and not as if all points belong to a single cluster as a whole. Hence, clustering points may be found to be less in the cluster edges and more at the core centre (when the points in the centroid are as close, it implies minimisation of cost function and hence pixels away from the centroid are of high membership values). The membership function reveals the pixel probability of pixels in a specific cluster. However, the standard FCM utilises the value of grey level intensity which could be overcome in the spatial FCM which encompasses the pixel level spatial information.

Spatial FCM algorithm is presented as ,

Let  $X=(x_1, x_2, \dots, x_n)$  denotes an image with  $n$  pixels to be segregated into  $c$  clusters

1. Initialize the membership matrix ( $u_{ij}$ )
2. Select the number of clusters
3. Calculate cluster centre using,

$$C_i = \frac{\sum_{j=1}^n u_{ij}^m x_j}{\sum_{j=1}^n u_{ij}^m} \quad (1)$$

The parameter  $m$  controls the fuzziness of the resulting partition.

4. Update the Membership matrix as

$$U_{ij} = \frac{1}{\sum_{k=1}^c (d_{ij} / d_{kj})^{2/(m-1)}} \quad (2)$$

Where  $d_{ij} = ||c_i - x_j||$  represents the distance between the individual cluster center and pixel value i.e Euclidean distance.

5. The objective function is defined as

$$J = \sum_{i=1}^c \sum_{j=1}^n u_{ij}^m d_{ij}^2 \quad (3)$$

6. The spatial function is defined as

$$h_{ij} = \sum_{k \in NB(x_j)} U_{ik} \quad (4)$$

where  $NB(x_j)$  represents a square window centered on pixel  $x_j$  in the spatial domain.

7. The spatial function is incorporated in to the membership function as

$$U_{ij}' = \frac{u_{ij}^p h_{ij}^q}{\sum_{k=1}^c u_{ij}^p h_{ij}^q} \quad (5)$$

Where,  $p$  and  $q$  are parameters to control relative importance of spatial and membership function. Convergence is identified by making a valid comparison between all changes that occurs are the centre of the cluster in a dual step mode. The liver region is segmented and is fed as input to the tumour extraction phase.

### Tumour segmentation

From the segmented liver, tumour is extracted using spatial FCM and unified level set method. The unified level set method is discussed in this section. Edge based LSM is applicable only for CT images with clear and distinct boundaries. Region based LSM is applicable even for CT images not having clear boundaries but it is not applicable to detect object of interest with low contrast. To overcome the disadvantage, a unified level set method is proposed where boundary leakage can be avoided. This method integrates image gradient, region competition and prior information for CT liver tumour segmentation. The probabilistic distributions of liver tumours are estimated by fuzzy clustering and are utilized to improve the object indication function, defined by the directional balloon force and regulated region competition.

The algorithm for unified level set method is as follows

1. Assign the controlling parameters ( $\alpha, \beta, \gamma, \lambda$ ). ( $\alpha, \beta, \gamma, \lambda$  value ranges from 0 to 1).
2. Estimate the object of interest ( $P_{rk}$ ).
3. Compute the object indication function and signed balloon function.

$$E(\gamma, g_i, g_p) = \exp(-\max\{\gamma g_i, (1-\gamma)g_p\}) \quad (6)$$

$$\text{Where } g_i = \frac{g(\omega) - \min(g(\omega))}{\max(g(\omega))}$$

$$g(w) = \frac{1}{1 + |\nabla(G_\sigma * w)|^2}$$

$G_\sigma * w$  represents the convolution of image with Gaussian kernel.

$$G(\beta, \sigma_0, P_{rk}) = [1 - 2\beta(1 - P_{rk})] \sigma_0 \quad (7)$$

4. Initialize the dynamic interface

$$\phi_0 = -4\epsilon[0.5 - (P_{rk} > 0.5)] \quad (8)$$

5. Compute the mean curvature  $k$ , dirac function  $\delta_\tau(\phi)$ , heaviside function ( $H_\epsilon(\phi)$ ).

6. Compute the force of region competition.

$$R = P_{rk} - \sum_{j \neq k} P_{rj} \quad (9)$$

7. Evolve the dynamic interface with temporal step size.

$$\phi(v, t + \Delta t) = \phi(v, t) + \Delta t F \quad (10)$$

$$= \alpha \delta(\phi) E(k + \lambda G) + (1 - \alpha) \delta(\phi) R \quad (11)$$

8. Repeat from step 5 until the result is satisfactory.

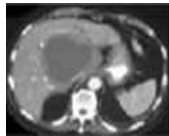
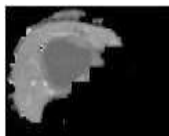
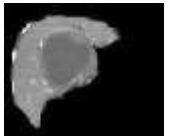

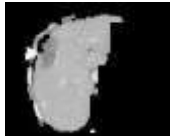

## RESULTS AND DISCUSSION

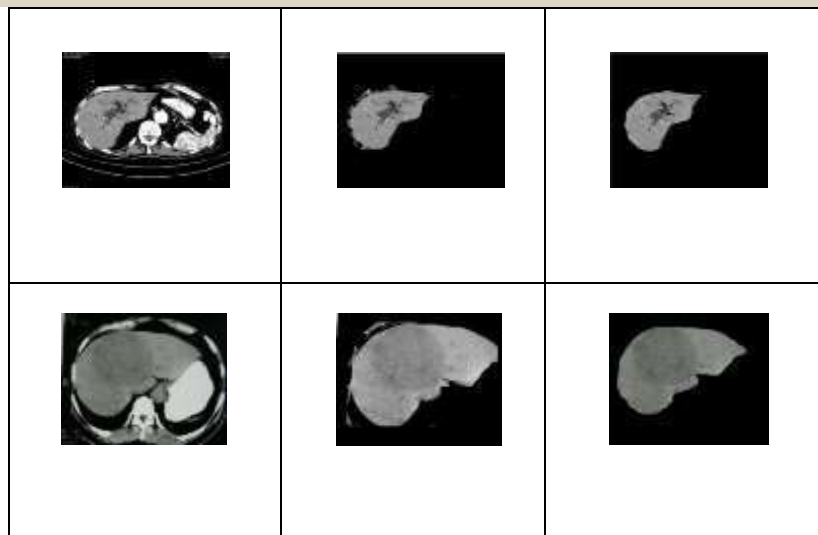
Several sources such as scan centre, internet along with corresponding ground truths for segmentation was used to collect CT images for the research. The liver segmentation and tumour of the abdominal CT images can be analyzed qualitatively and quantitatively by comparing with the ground truth from medical experts to evaluate the performance. The qualitative is done by visual analysis. Accuracy, sensitivity and specificity are calculated for quantitative analysis. These are the terms which statistically measure the performance of the test.

### Liver segmentation

Liver segmentation from the abdominal CT image is carried out using Spatial Fuzzy C Means clustering method. Twenty one images, out of 4 sample images, the corresponding segmented liver images and ground truth images are shown in [Table 1] and the quantitative results is shown in [Table 2].

**Table 1:** Liver segmentation using spatial FCM

Abdominal	Segmented Liver image	Ground Truth Image
		
		



**Table 2:** Liver Segmentation using Spatial FCM–Quantitative Analysis

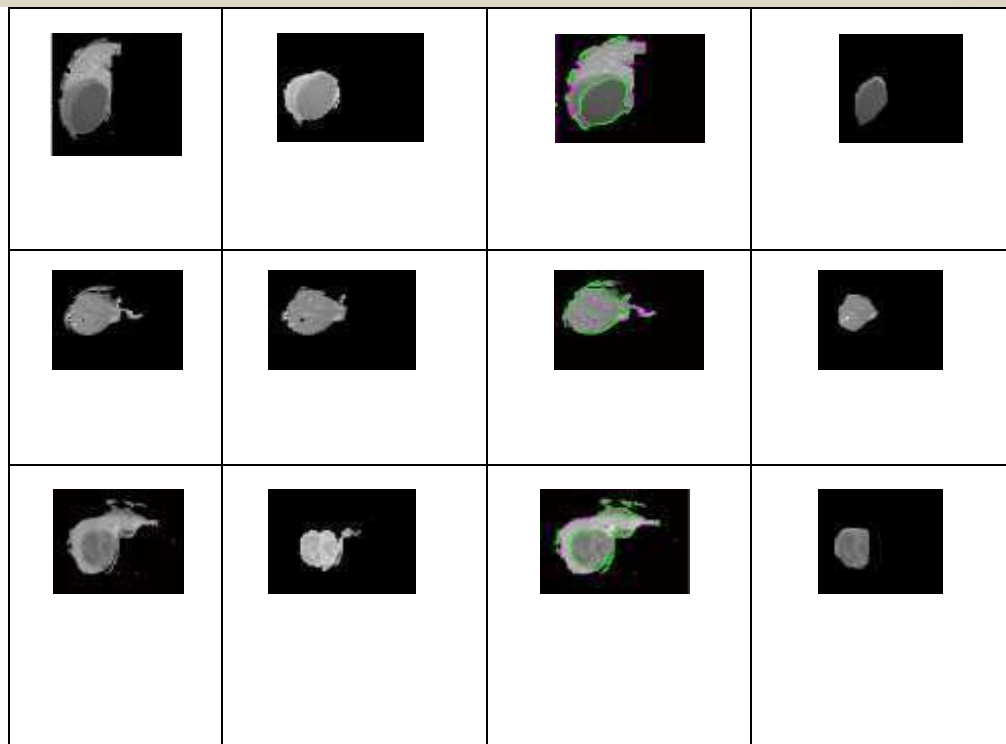
Image	Sensitivity (%)	Specificity (%)	Accuracy (%)
1	90.3	89	96
2	89	87	95.3
3	92	89.5	97.8
4	91.3	90.2	97.3

### Tumour segmentation

The tumour region is extracted from the segmented liver using Spatial Fuzzy C Means technique and Unified Level Set Method. Out of twenty sample liver images, 4 images are corresponding segmented tumour images for both the techniques. Ground truth images are shown in [Table 3] and the quantitative result is shown in [Table 4].

**Table 3:** Liver tumour segmentation using spatial FCM and unified level set method

Segmented Liver Image	Liver tumour segmentation using Spatial FCM	Liver tumour segmentation using Unified level set method	Ground truth image



**Table 4:** Liver Tumour Segmentation using Spatial FCM and unified level set Method - Quantitative Analysis

Image	Unified level set method			Spatial FCM		
	Sensitivity (%)	Specificity (%)	Accuracy (%)	Sensitivity (%)	Specificity (%)	Accuracy (%)
1	92.5	90	95	93	93.2	97.5
2	89.3	88.7	93.5	93.9	92	95.2
3	82.7	77.2	85.5	94.3	95	97.8
4	89.5	88.2	93.6	92.7	94.5	96.3

## CONCLUSION

In this research, the liver segmentation and tumour segmentation is implemented. The automatic liver and tumour segmentation proves to be efficient which can make computation feasible and less time consuming. The liver segmentation accuracy ranges from 91.4-97.8% which is achieved by means of spatial FCM, for tumour segmentation, accuracy ranges from 91-98.3% which is achieved by means of spatial FCM and for accuracy ranging 85-96.5% is achieved by using unified level set method.

**CONFLICT OF INTEREST**  
There is no conflict of interest.

**ACKNOWLEDGEMENTS**  
None

FINANCIAL DISCLOSURE

None

REFERENCES

- [1] Torfinn Taxt, Arvid Lundervold, Jarle Strand, Sverre Holm. [1998] Advances in Medical Imaging. International Conference on Pattern Recognition.
- [2] Jeongjin Leea, Namkug Kimb, Ho Leea, Joon Beom Seob, et al. [2007] Efficient Liver Segmentation Using A Level-Set Method With Optimal Detection Of The Initial Liver Boundary From Level-Set Speed Images. International Journal on Computer Methods and Programs in Biomedicine, 88( 1):26-38.
- [3] Jean Stawiaski, Etienne Decenci ere and Francois Bidault. [2008] Interactive Liver Tumor Segmentation Using Graph-cuts and Watershed. International Conference on Medical Image Computing and Computer Assisted Intervention.
- [4] SS Kumar, RS Moni.[2010] Diagnosis of Liver Tumor from CT Images using Fast Discrete Curvelet Transform.International Journal on Computer Science and Engineering (IJCS), 02(04): 1-6.
- [5] Vijayalakshmi B, Subbiah Bharathi. [2016] Classification of CT liver images using local binary pattern with LegendreMoments. CURRENT SCIENCE, 110( 4).
- [6] Ching-Hsue,Cheng,Liang-Ying Wei. [2016] Rough Classifier based on Region Growth Algorithm for identifying Liver CT image.Journal of Applied Science andEngineering,19(1):65-74.
- [7] Xing Zhang, Jie Tian, Kexin Deng, Yongfang Wu and Xiuli Li [2010] Automatic Liver Segmentation Using A Statistical Shape Model With Optimal Surface Detection. IEEE Transaction on Biomedical Engineering, 57(10).
- [8] Yrjö Häme and Mikka pollari.[2012] Semi-automatic liver tumor segmentation with hidden Markov measure field model and non-parametric distribution estimation. International Journal on Medical image Analysis, 16(1): 140-149.
- [9] Sergio Casciaro, Roberto Franchini, Laurent Massoptier, et al..[2012] Fully Automatic Segmentation Of Liver And Hepatic Tumors From 3-D CT Abdominal Images: Comparitive Analysis of Two Automatic Method. IEEE Sensors Journal, 12( 3).
- [10] Lu, Xiaoqi, Jianshuai Wu, Xiaoying Ren, Baohua Zhang, and Yinhui Li.[2014] The study and application of the improved region growing algorithm for liver segmentation. Optik - International Journal for Light and Electron Optics, 125( 9): 2142–2147.
- [11] Bing Nan Li, Chee Kong Chui, Stephen Chang, Sim Heng Ong .[2012] A New Unified Level Set Method For Semi-Automatic Liver Tumor Segmentation On Contrast-Enhanced CT Images. International Journal on Expert Systems with Applications, 39:9661-9668.
- [12] Jialin Peng, Ye Wang and Dexing Kong.[2013]Liver Segmentation Using Constrained Convex Variational Model.International Journal on Pattern Recognition Letters.
- [13] Li C, Wang X, Eberl S, Fulham M, Yin Y, Chen J, Feng DD.[2013] A likelihood and local constraint level set model for liver tumor segmentation from CT volumes.IEEE transactions on biomedical Engineering, 60(10).
- [14] Xiao Song, Ming Cheng, Boliang Wang, Shaohui Huang, Xiaoyang Huang, and Jinzhu Yang.[2013] Adaptive fast marching method for automatic liver segmentation from CT images. Medical Physics, Vol. 40, No. 9.
- [15] Abdalla Mostafa, Ahmed Fouad, Mohamed Abd Elfattah.[2015] CT Liver Segmentation using Artificial Bee Colony Optimization. Procedia Computer Science. 60: 1622-1630.
- [16] Nuseiba M. Altarawneh, Suhuai Luo, Brian Regan, Changming Sun.[2015] A modified distance regularized level Set model for liver segmentation from ct images. Signal & Image Processing: An International Journal (SIPIJ) 6(1).
- [17] Xuechen Li, Suhuai Luo, Jiaming Li.[2013] Liver Segmentation from CT Image Using Fuzzy Clustering and Level Set. International Journal of Signal and Information Processing, 4: 36-42.



## ARTICLE

# CONCURRENT ERROR DETECTION WITH SELF-CHECKING MAJORITY VOTING CIRCUITS

V. Elamaran<sup>1\*</sup>, VR. Priya<sup>2</sup>, M. Chandrasekar<sup>1</sup>, Har Narayan Upadhyay<sup>1</sup>

<sup>1</sup>Department of ECE, School of EEE, SASTRA University, Thanjavur, INDIA

<sup>2</sup>Department of CSE, SRC Campus, SASTRA University, Kumbakonam, INDIA

## ABSTRACT

The reliability of a system can be improved by designing it with relevant fault-tolerant approaches. The hardware redundancy is often used technique to mitigate errors in a system by placing duplicate copies of original modules. The faults are masked using this kind of passive redundancy approach instead of detecting errors with the help of majority voting circuit. So the reliability of this voter is more important. This study exemplifies five different self-checking voter circuits by means of computing majority and minority and with relevant additional logic in each. Self-checking voter circuits are implemented using mirror concept, mux-and-or approach, mux-xor approach, conventional approach and Manchester carry style. The critical path delay, power dissipation, layout area, number of transistors and figure-of-merit (FOM) are the performance metrics for a comparative study. Simulation results are obtained using Microwind layout editor tool with 120 nm, 90 nm and 70 nm CMOS process technologies. The approach using Manchester carry obtain better FOM (78.85), least layout area (227.0  $\mu\text{m}^2$ ), lower power dissipation (8.464  $\mu\text{W}$ ) as compared with other circuits. The Mux-and-or circuit obtains lower critical path delay (0.420 ns) as than other approaches.

## INTRODUCTION

Business-critical applications demand fault-tolerant system designs so that the transactions don't fail especially in stock exchange, banking and other time-shared systems. For example, the unavailability of ATM service should be 10 hours per year; unavailability of airline reservation should be around 1 minute per day [1]. These applications require very high reliability so that the probability of failure rate is close to zero. The identification of faults/errors and repairing the faulty modules are not possible in applications like spacecrafts and satellites [2].

The reliability improvement is achieved through fault-tolerant approaches. It does not mean that fault-tolerant systems have always high reliability; this depends upon the probability of error occurring in a system [3]. We can design a system to tolerate any single error, but the poor reliability may occur if the probability of such error is too high. But fault-tolerance helps to improve the system reliability by obtaining correct outputs under the environment with software or hardware errors. A system can be designed with high quality components to reduce the failure rate; the system cannot function if the hardware components fail [1].

If there is a possibility of quick repairing faulty components, the availability of a system is improved. Reliability would depend on an interval of time whereas the availability would depend on an instant of time [4]. By reducing the mean-time-to-repair, the reliability of a system is improved. Applications like Supercomputer servers should have high availability for example the unavailability is 10 days per year. Telecommunication service is an example where the unavailability should be around 5 minutes per year [1].

The safety of a system is more important i.e., it is safe if it operate correctly or it is in the safe state during the occurrence of failures [4] [5]. Applications like banking, railway signaling, nuclear energy demand high safety during the operation time. The safety operations are like money should not be distributed if any doubt (banking); Reactor should be stopped if there is any problem; all signal indicators should glow red (railway signaling) [1].

The ability of a system to serve its intended level of service to the customers is known as "dependability". The dependability of a system can be improved by fault removal, fault tolerance, fault prevention and fault forecasting. The faults, errors and failures are the dependability impairments. The sole objective of a system is to increase the dependability of a system [6-8].

This paper is organized as follows. The section 2 contains materials and methods of five self-checking majority voter circuits with critical path delay findings. The section 3 discuss simulation results of power dissipation and layout area used in all designs. The conclusions are made in the section 4.

## MATERIALS AND METHODS

Self-checking voter circuits are designed and simulated using Microwind and DSCH software tools. DSCH is a digital schematic editor tool whereas the Microwind is a layout editor tool [9-12]. Schematics which are designed using DSCH are converted in to Verilog hardware description language (HDL) script. The Verilog scripts are then compiled using Microwind tool to generate a corresponding layout.

### KEY WORDS

CMOS, Fault-tolerance, Majority function, Self-checking, VLSI design, Voter circuits.

Published: 2 December 2016

\*Corresponding Author

Email:  
elamaran@ece.sastra.edu

### Self-checking voter (SVC) using mirror concept

In this study, self-checking voter circuits are implemented by comparing majority computation and minority computation logic outputs; if they are different there is no error in the circuit [13]. The majority value is computed using  $(AB+BC+CA)$  expression, whereas the minority value is computed using the same expression but with complement inputs as in [Fig. 1].

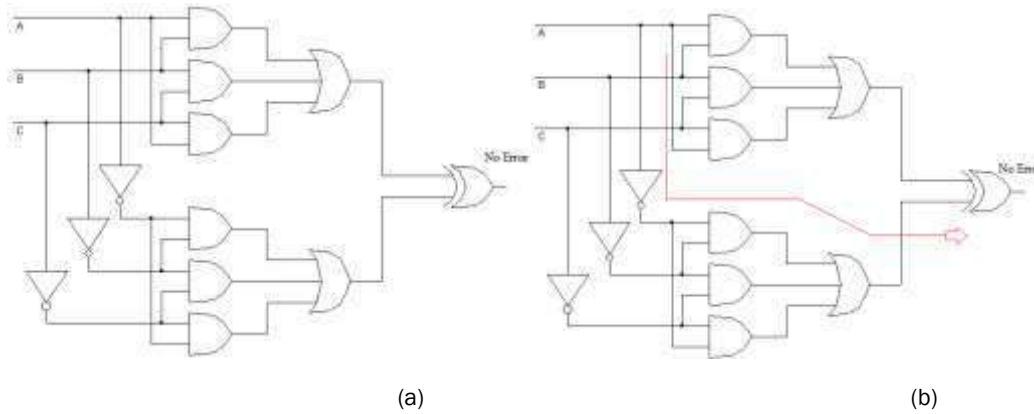


Fig. 1: SVC using mirror concept.

The critical path delay is evaluated as in [Fig. 1b]. This circuit requires one inverter (0.17 ns), one AND gate (0.16 ns), one OR gate (0.13 ns) and one XOR gate (0.16 ns) for the critical path; hence the total delay is 0.62 ns.

### Self-checking voter (SVC) using mux-and-or

If  $A=0$ , then the majority becomes “BC” else “B+C”. Similarly, if  $A=0$  then the minority becomes “ $\overline{BC}$ ”, else “ $\overline{B+C}$ ” as in [Fig. 2]. The critical path of this circuit requires one AND gate (0.16 ns), 1 mux (0.1 ns) and one XOR gate (0.16 ns); hence the total delay is 0.420 ns as portrayed in [Fig. 2b].

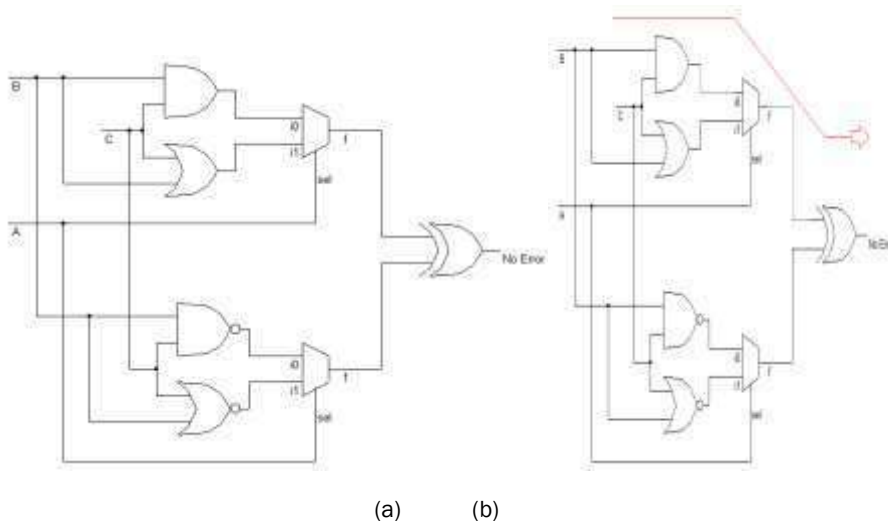


Fig. 2: SVC using mux-and-or.

### Self-checking voter (SVC) using mux-xor

If  $B=C$ , then the majority becomes “B” else “A”. The minority value is computed using similar concept as in [Fig. 3]. The critical path of this circuit requires one XOR gate (0.16 ns), one mux (0.1 ns), one inverter (0.1 ns) and one more XOR gate (0.16 ns); hence the total delay is 0.520 ns as depicted in [Fig. 3b].

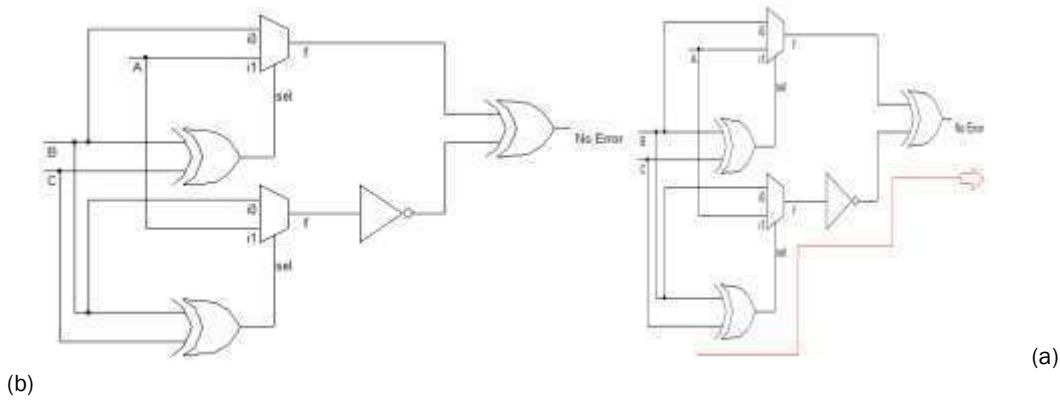


Fig. 3: SVC using mux-xor.

### Self-checking voter (SVC) using conventional method

The majority and minority values are computed using conventional method “ $AB+BC+CA$ ” by NAND/NOR gates as in [Fig. 4]. The critical path of this circuit requires one NAND2 gate (0.16 ns), one NAND3 gate (0.16 ns) and one XOR gate (0.16 ns); hence the total delay is 0.480 ns as shown in [Fig. 4b].

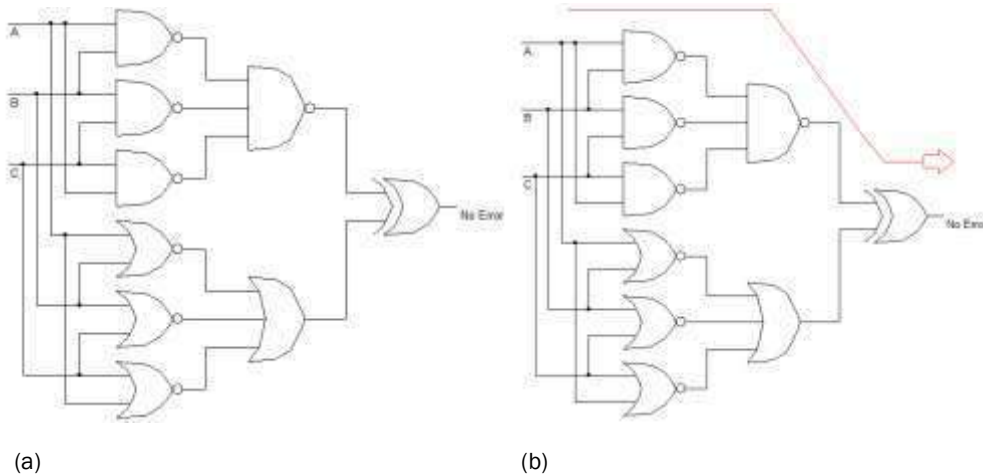


Fig. 4: SVC using conventional method.

### Self-checking voter (SVC) using Manchester carry chain

The Minority value is computed using Manchester carry chain and the minority value is computed using mux-xnor principle as in [Fig. 5] [14]. The Manchester carry chain algorithm is described as follows:

- i) If A and B are different, then the minority value becomes  $\bar{C}$ .
- ii) If  $A=B=1$ , then the minority becomes 0.
- iii) If  $A=B=0$ , then the minority becomes 1.

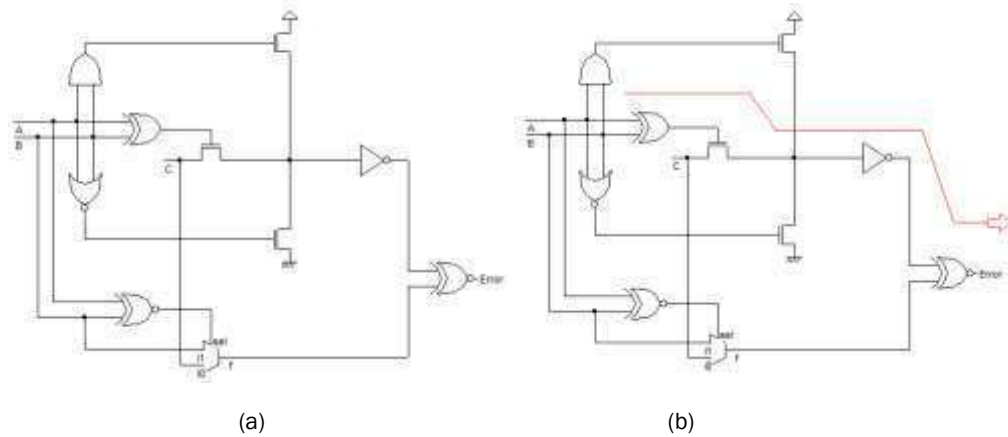


Fig. 5: SVC using Manchester carry chain.

## RESULTS AND DISCUSSION

The power dissipation and layout area results are discussed in this section. An another performance metric is a figure-of-merit (FOM) is expressed as in Equation (1),

$$FOM = \frac{1}{Power \times Delay \times Area} \quad (1)$$

Since applications demand low power, less area and high performance, an optimized VLSI design should have a high FOM [4].

### Power dissipation results

The circuit functionalities are verified in both using DSCH tool and Microwind tool with schematic and layout respectively [15]. The power dissipation simulation results of self-checking voter circuits are obtained in [Fig. 6] in 120 nm, 90 nm and 70 nm process technologies. In 120 nm foundry, SVC using Manchester carry chain consumes power of 8.464  $\mu$ W which is less as compared with remaining circuits.

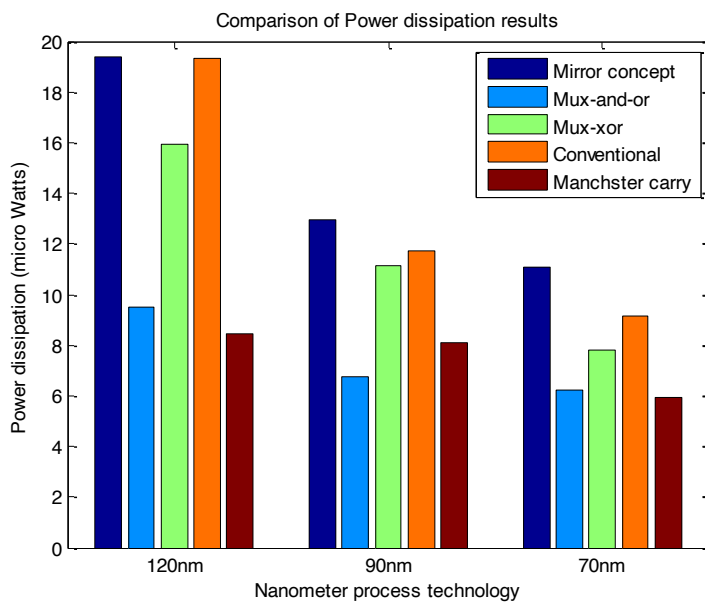


Fig. 6: Power dissipation results.

### Critical path delay results

The critical path delay results of self-checking voter circuits are obtained in [Fig. 7] in 120 nm process technology. SVC using mux-and-or had lower delay as 0.420 ns than others.

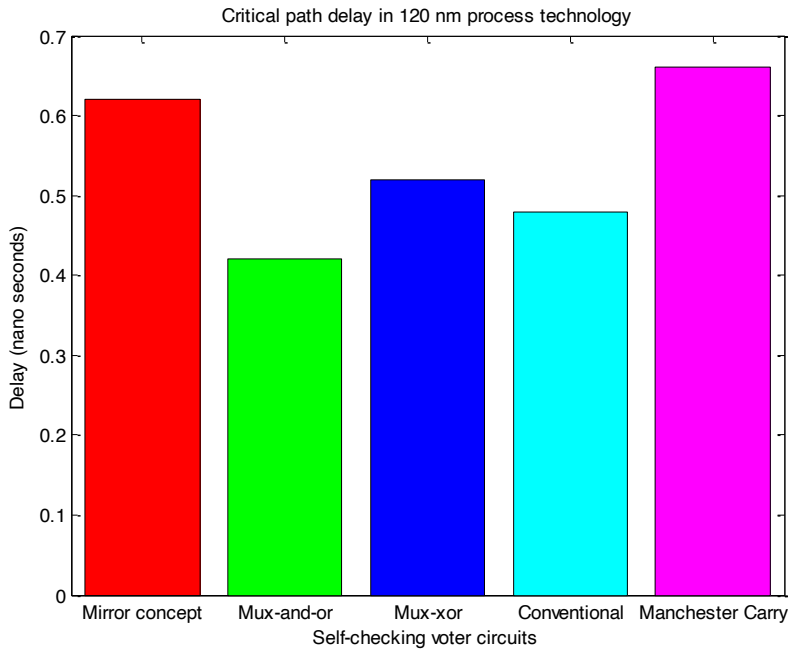


Fig. 7: Critical path delay results.

### Layout area results

Self-checking voter circuits using conventional (AB+BC+CA) method obtain less layout area in all 120 nm, 90 nm and 70 nm process technologies as in Figure 8; whereas SVC using Manchester carry chain stands next with low area. In 120 nm foundry technology, SVC using conventional had 170.4  $\mu\text{m}^2$  and SVC using Manchester carry chain had 227.0  $\mu\text{m}^2$ .

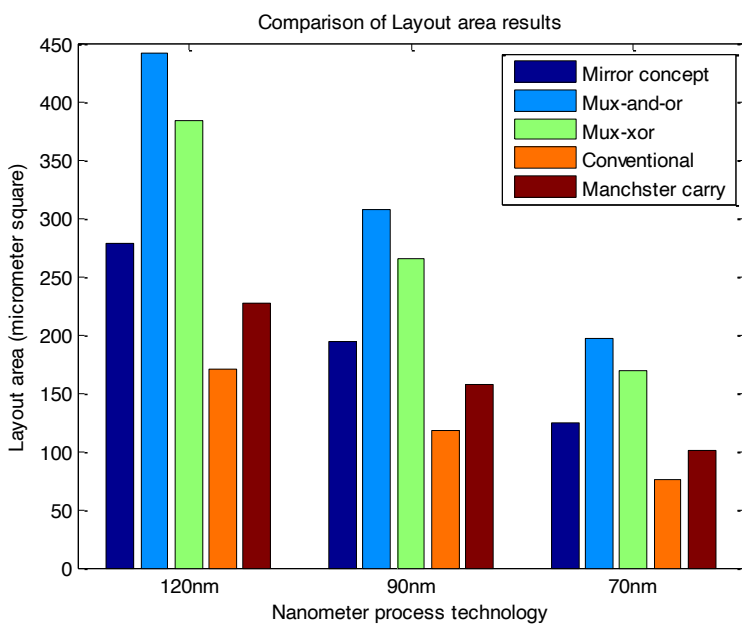


Fig. 8: Layout area results.

### Figure-of-merit results

FOM results are obtained using the Equation (1) and are plotted in [Fig. 9] in 120 nm process technology. The SVC using Manchester carry chain had a better FOM as  $78.85 \times 10^5$  than other designs.

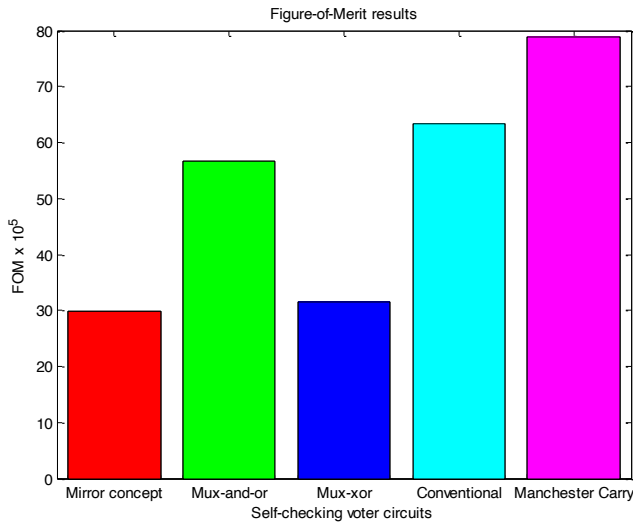


Fig. 9: Figure-of-merit results.

### Total number of transistors and failure rate

Failure rate ( $\lambda$ ) of a circuit is determined using  $\sqrt{g}$ , where  $g$  is the total number of logic gates or transistors in a design. It is obvious that the design is good if it contains few number of logic gates in order to have a lower failure rate. The reliability of a system is improved by reducing failure of rate.

The total number transistors and the corresponding failure rate results are obtained in [Fig. 10 and 11] respectively. Results show that the SVC using mux-xor design requires only 32 transistors (16 nMOS and 16 pMOS) with the lower failure rate as 5.6568 than other circuits. The SVC using mux-and-or design stands second best method with 38 transistors and 6.1644 failure rate. The SVC using mirror concept had a higher failure rate due to more number of transistors (64).

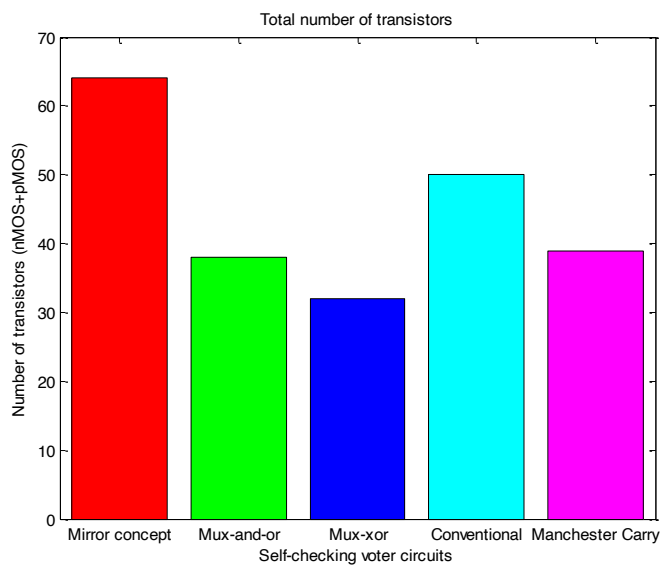


Fig.10: Results of total number of transistors in SVC.



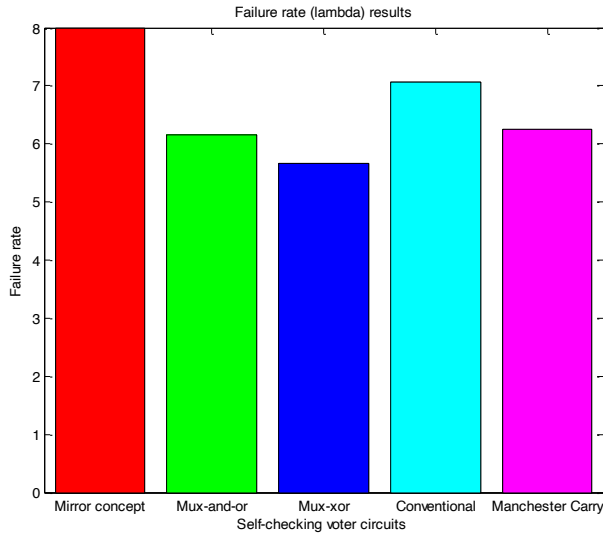


Fig. 10: Failure rate results.

## CONCLUSION

In the current semiconductor technology evolution, reliability of microelectronic circuits play a vital role in any system design. The hardware redundancy is often used to remove or mask faults/errors in a circuit by incorporating redundant modules. The fault masking can be done using the majority voter circuits in a triple modular redundancy (TMR) system for better reliability. The TMR system fails if the voter circuit does not function correctly. This study exemplifies five difference self-checking voter circuits along with a comparative analysis in area, power and delay results. In real time, some applications may demand low power; some may demand high performance; few require less area. So, the trade-off is important for many applications. Designers may able to achieve low power circuits but at the cost of area or performance and vice versa. This work can be further extended self-checking five input majority voter circuits; 7-input majority voter circuits, etc.

### CONFLICT OF INTEREST

There is no conflict of interest.

### ACKNOWLEDGEMENTS

None

### FINANCIAL DISCLOSURE

None

## REFERENCES

- [1] Dubrova E.[2013] Fault-Tolerant Design. New York: Springer Science+Business Media.
- [2] Lala PK. [2001] Self-Checking and Fault-Tolerant Digital Design. Morgan Kaufmann publishers.
- [3] Koren I, Mani Krishna C. [2013] Fault-Tolerant Systems. Morgan Kaufmann publishers.Design of a novel fault-tolerant voter circuits for TMR implementation to improve reliability in digital circuits.
- [4] Kshirsagar KV, Patrikar RM. [2009] Microelectronics Reliability, 49: 1573-1577.
- [5] Majority function computation using different voter circuits – a comparative study. V Elamaran, et al. 2015. International Journal of Pharmacy and Technology, 7: 9764-9773.
- [6] Balasubramanian P. [2016] ASIC-based design of NMR system health monitor for mission/safety-critical applications. SpringerPlus, 5: 1-16.
- [7] Elamaran V, Har Narayan Upadhyay. [2015] CMOS VLSI Design of Low Power SRAM Cell Architectures with new TMR: A Layout Approach. Asian Journal of Scientific Research, 8: 466-477.
- [8] Elamaran V, Har Narayan Upadhyay. [2015] Low Power Digital Barrel Shifter Datapath Circuits using Microwind Layout Editor with High Reliability. Asian Journal of Scientific Research, 8: 478-489.
- [9] Hari Hara Subramani S. et al. [2014] Low-energy, low power adder logic cells: A CMOS VLSI Implementation. Asian Journal of Scientific Research, 7: 248-255.
- [10] Elamaran V. et al. [2015] A handy approach for teaching and learning digital VLSI design using EDA tools. International Journal of Pharmacy and Technology, 7: 9935-9944.
- [11] Rajesh KSSK. et al. [2014] CMOS VLSI design of low power comparator logic circuits. Asian Journal of Scientific Research, 7: 238-247.
- [12] Pradhisha R. et al. [2015] FPGA Implementation of Self-testing Logic gates, Adders, Multipliers.. Indian Journal of Science and Technology, 8: 1-6.

- [13] Balasubramanian P, Maskell J.L. [2015]. A distributed minority and majority voting based redundancy scheme. *Microelectronics Reliability*, 55: 1373-1378.
- [14] Uyemura, J.P. *Introduction to VLSI Circuits and Systems*. India: Wiley India publishers, 2006.
- [15] Sayapaneni P, Elamaran V. [2014]s.l.: IEEE Press, A comparative study on low power adders using Microwind EDA tool. *International Conference on Computational Intelligence and Computing Research*, pp. 1-5.

ARTICLE

# AN AREA EFFICIENT FIRST ORDER POLYNOMIAL CONVOLUTION INTERPOLATION FOR VISUAL COMMUNICATION SYSTEMS

C. John Moses<sup>1\*</sup>, D. Selvathi<sup>2</sup>

<sup>1</sup>Dept. of ECE, St. Xavier's Catholic College of Engineering, Nagercoil, INDIA

<sup>2</sup>Dept. of ECE, Mepco Schlenk Engineering College, Sivakasi, INDIA

## ABSTRACT

Image interpolation is widely used in various visual communication systems like digital television broadcasting, digital cameras, tablets, mobile phones and display devices. A better quality of the image can be obtained by using image interpolation with higher order polynomials which require complex computations. In addition to high performance, an area efficient implementation is preferred for a variety of consumer applications. The first order polynomial convolution interpolation (FOPCI) is an algorithm in which the first order polynomial is used to reduce the complexity and to maintain the image quality. This work uses low area weighting coefficient generator for FOPCI. The proposed low complexity very large scale integration (VLSI) architecture is implemented on Virtex VI field programmable gate array (FPGA). The proposed architecture works with 171 look-up tables (LUTs) and generates interpolated pixel at 0.402 ns. Further, clamp filtering technique is added as a pre-filter to increase the image quality. The experimental results show that the proposed FOPCI produces higher peak signal to noise ratio (PSNR) as 69.17 dB by comparing with other interpolation techniques. Thus, area efficient first order polynomial convolution image interpolation architecture is created by reducing number of components and by improving interpolated image quality, which is intended for visual communication systems with high image quality. Image

## INTRODUCTION

Low bandwidth and restricted channels are one of the supreme stimulating concerns that all the nations in this world is facing. Ever since signals and data to be directed via a channel are obtainable in vast expanse and restricted volume of band is allocated to every nation, multimedia data needs to be compressed at the source and expand at the destination so as to send multiple data. This compression and expansion may cause distortion of data and occasionally even produces false reconstruction at the destination. If the network is wireless, the condition flush develops poorer. Much noise enters the network along with the signals and attempt to depreciate the signal. If a digital image is directed via a wireless network it has to be compressed at the transmitter due to limited channels. At the receiver it may possibly get distorted due to the occurrence of noise and through image expansion it might get differed from its unique form. Several features of images are barely visible to eye, they must be frequently transformed before display. Image enhancement is a technique for improving the image quality which ensures increase in image vision and makes the image adjust to be treated by computer. It improves some data inside the image selectively and limits the other ones. To rebuild or expand the image to become the original form, interpolation is done [1].

Image interpolation is an art of rescaling low-resolution image to a high-resolution version, and it has become a very active area of research in image processing. The interpolation that estimates the intermediate values of a set of discrete samples has been used extensively in the field of digital photography, computer vision, computer graphics, medical imaging, consumer electronics like digital television and personal mobile devices and it also used in visual information processing system [2]. Interpolators based on approximations of the ideal sinc kernel (pixel replication, bilinear, bi-cubic, and higher order splines) are commonly used for their flexibility and speed, but these approaches frequently contribute to blurring and ringing artifacts, jagged edges and unnatural representation of the curves of constant intensity in processed images.

In recent years, many high-quality adaptive image interpolation techniques have been proposed. These novel methods greatly improve image quality by some efficient techniques, such as bilinear interpolation with sharpening spatial filter [3], linear space-variant edge detector [4], edge-weighted scheme [5] and pre-filters [6]. These methods produce better image but the major drawbacks is computational complexity, a large chip area and high hardware cost. Additionally, in past decade, many non-adaptive interpolation techniques have also been developed to reduce the chip area such as bi-cubic [7], extended linear [8], linear [9] efficient bi-cubic [10], piecewise linear convolution [11] first order polynomial convolution interpolation [12] and region of interest method [13]. Non-adaptive image interpolation performs in a fixed pattern for every pixel and this technique is fixed the irrespective of the input image features [14]. This work deals with polynomial convolution interpolation with first order and low complexity weighting coefficient generator to reduce the chip area. Furthermore, this work concentrates on improving the image quality by using clamp filter.

Reconfigurable hardware like FPGA is widely used for rapid prototyping digital signal processing [15] and digital image processing. Very large scale integration (VLSI) architecture is designed and evaluated by

**KEY WORDS**  
image scaling, weighting coefficient, computational complexity, FPGA, convolution interpolation

Published: 2 December 2016

**\*Corresponding Author**  
Email:  
erjohnmoses@gmail.com  
Tel.: +91 999403747

using FPGAs [16]. This work presents FPGA implementation of low computation complexity image interpolation based on the first order polynomial convolution kernel [12].

The remaining portion of this paper is organized as follows. Section 2 analyses different non-adaptive and adaptive image interpolation techniques, Section 3 describes that the interpolation based on the first order polynomial convolution kernel, Section 4 deals with FPGA implementation of the proposed low-complexity image interpolation, Section 5 provides experimental analysis of both existing first order polynomial and the proposed interpolation methods and Section 6 presents the conclusion.

## RELATED WORKS

In non-adaptive image interpolation methods, certain computations are performed indiscriminately to the whole image for scaling regardless of its contents. Among the various non-adaptive interpolation algorithms, the nearest neighbour and bilinear interpolations are simple [17], but, they have undesirable blurring and block effects. Polynomial interpolation methods have been studied quite extensively in the image processing literature of the past three decades [18]. An example of such methods is cubic convolution interpolation method. The cubic convolution interpolation function is more accurate than the nearest neighbour or linear interpolation methods [19]. For convolution based interpolation, the sinc-approximating kernel with higher-degree spline can produce better results at an increase in computational cost [20].

FPGA-based bi-cubic interpolation is proposed by Maganda and Estrada [7] for digital image scaling. The hardware architecture of this interpolation is implemented on Xilinx Virtex-II FPGA with 890 configurable logic blocks (CLBs). An efficient bi-cubic convolution interpolation architecture is presented by Lin et al [10], which decreases the computational complexity of generating coefficients. The hardware architecture of this bi-cubic convolution interpolation operates at 279 MHz with 30643 gates in a  $498 \times 498 \mu\text{m}^2$  chip. The FPGA implementation needs only about 437 logic blocks but the bi-cubic algorithm [7] requires about 890 logic blocks. Pang et al [21] proposed a bi-cubic interpolation with an adaptive sharpening filter to reduce the blurring effects. The VLSI architecture of this interpolation utilizes 695 logic elements and obtains an average PSNR increase of 1.5 dB. A novel image scaling algorithm is presented by Huang et al [5] using convolution interpolation kernel with a bilateral error-amender and an edge-weighted scheme. This provides average PSNR of 43.31 dB for image enlargement. VLSI architecture of an area efficient convolution based image interpolation is presented by Moses and Selvathi [16]. This work presents FPGA implementation of convolution kernel-based interpolation for digital image scaling. This method produces the PSNR of 51.55 dB for the image of 'aerial' ( $512 \times 512$ ) for the up-scaling ratio of 2 after 1/2 downscaling. The FPGA implementation of this method requires 336 LUTs. Lee & Park [22] presented a high performance low area up-scaling using Lagrange interpolation, which produces higher visual quality on interpolated image over the bi-cubic interpolation. This method uses sharpening filter technique to improve the quality of the interpolated image by enhancing edge regions. This method achieves an average SSIM as 0.8406 by using edge detection and sharpening filter with Lagrange interpolation for 2 x scaling. However, it achieves only 0.7006 SSIM for 3x scaling.

An extended linear image interpolation for real time applications is proposed by Lin et al [8]. The hardware architecture of this interpolation is implemented on the Virtex-II FPGA, and implemented with TSMC 0.13 $\mu\text{m}$  standard cell library. The high speed architecture is simulated at 267 MHz operating frequency with 26200 gates in a  $452 \times 452 \mu\text{m}^2$  chip is capable of producing digital image interpolation for high definition television (HDTV) in real-time. A linear interpolation is proposed by Lin et al [9], which reduces the efforts of generating coefficient. The hardware architecture of this algorithm is also implemented on Virtex -II FPGA with 379 logic blocks (LBs). This architecture wants about 26200 gates and achieves higher PSNR (33.12 dB) for the test image (airplane). A piecewise linear convolution interpolation, with third-order approximation, is presented by Lin et al [11]. The number of CLBs used by Virtex - II FPGA for bi-cubic (Maganda and Estrada 2005) and this algorithm are 437 and 393 respectively. This interpolation scheme provides higher PSNR (49.53 dB) than the bi-cubic (46.38 dB) for the test image (airplane) of scaled from 3/4 downscaling after 4/3 upscaling. An efficient extended linear image interpolation is implemented by Lin et al [23] by using Virtex-II FPGA and TSMC 0.13 technologies. This uses 25980 gates at 267 MHz in TSMC 0.13 and the FPGA implementation uses only about 379 CLBs but the bi-cubic [7] needs about 437 CLBs. This method provides higher PSNR (35.29 dB) than the bi-cubic [7] for the test image (tank) for 3/2 upscaling after 2/3 downscaling. Huang & Chang [24] presented an adder-based stepwise linear interpolation (ABSI) for digital signal processing. The hardware architecture of this method uses simple operators such as compare, shift and add. This technique achieves similar interpolation quality with conventional multiplier-based linear interpolation (MBLI), but it requires less area and consumes low power. This method achieves the highest PSNR of 32.34 dB.

An adaptive interpolation technique is presented by Chen et al [6] using clamp filter and a sharpening spatial filter as pre-filters to reduce the blurring and aliasing effects of the bilinear image interpolation algorithm. This architecture is implemented on FPGA, TSMC 0.18 $\mu\text{m}$  and TSMC 0.13 $\mu\text{m}$  technologies. This scheme utilizes 9.28 K gates and 9.27 K and 9.28 K gates on FPGA and on TSMC 0.18 $\mu\text{m}$  and TSMC

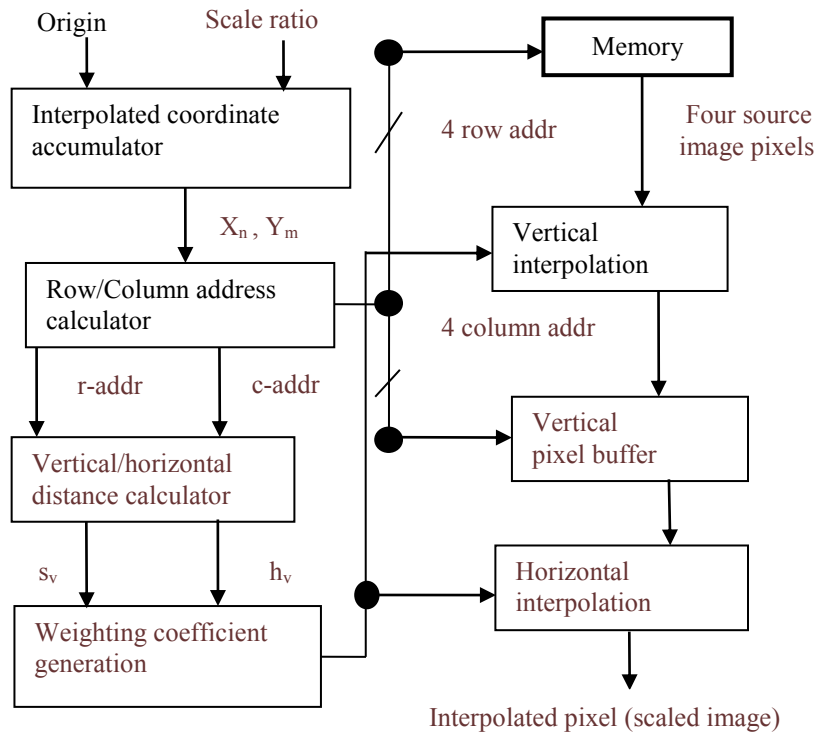
0.13 $\mu$ m respectively. This method improves average image quality by 0.42 dB over other adaptive interpolation techniques. VLSI architecture of a high quality image scalar is proposed by Chen [3] using a sharpening spatial filter, a clamp filter, and a bilinear interpolation technique. The VLSI design of this scalar can operate at 280 MHz with 6.08-K gate counts. This work can also achieve an average PSNR of 28.54 dB for image scaling. Another low complexity adaptive edge-enhanced image interpolation technique is also presented by Chen [4] using bilinear interpolation and sharpening spatial filter as a pre-filter and a linear space-variant edge catcher. This work achieves an average PSNR of 34.26 dB for image scaling. This PSNR value is higher than the previous Chen's proposal [3] due to the usage of adaptively edge catching technique. The VLSI architecture of this interpolation uses 6.67 K gate count and achieves about 280 MHz by using the TSMC 0.13  $\mu$ m VLSI technologies.

Li and Yu [13] presented a block region of interest method for FPGA implementation of image interpolation algorithm. In this method, a block region of interest is used for large image reconstruction using 2D sinc interpolation. The hardware architecture of this method is realized by pipelining on Virtex 7 FPGA with 187680 LUTs, 288272 registers. First-order polynomial convolution interpolation (FOPCI) for real-time digital image scaling is presented by Lin et al [12]. The kernel of the proposed method is built up of the first-order polynomials and it approximates the ideal sinc-funtion in the interval [-2, 2]. The architecture is implemented on the Virtex-II FPGA, and the VLSI architecture has been designed and implemented with the TSMC 0.13  $\mu$ m standard cell library. The number of adders and subtractors used to generate weighting coefficients in the architecture is less than that of bi-cubic interpolation [7].

The proposed FOPCI uses low complexity WCG to reduce the number of arithmetic elements in the interpolation. The various area dependent parameters like look-up tables (LUTs), configurable logic blocks (CLBs) of earlier low complexity interpolator for multimedia applications [5], [10] and [16], existing FOPCI [12] and proposed architectures for visual communication systems are evaluated by using Xilinx system generator. Further, it improves the image quality by using clamp filter.

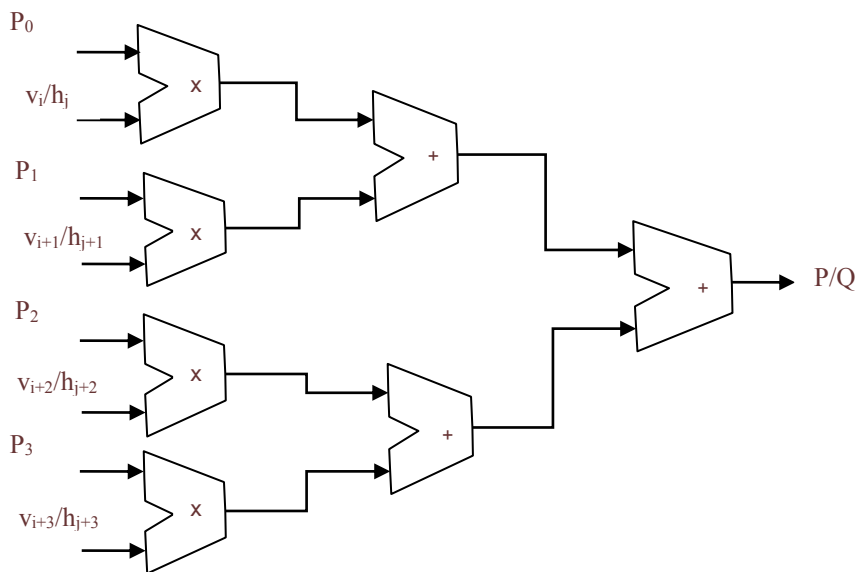
#### First order polynomial convolution interpolation

The block diagram of the hardware architecture for digital image scaling is shown in [Fig. 1], which includes Coordinate Calculation Unit, Memory Bank, weighting co-efficient generator (WCG), Vertical and Horizontal Interpolation units and Virtual Pixel Buffer [12]. The coordinate calculation unit includes interpolated coordinate accumulator, row/column address calculator and vertical and horizontal distance calculator. The coordinate of the interpolated point Q ( $x_n$ ,  $y_m$ ) is obtained in the interpolation coordinate calculator. In the circuit of row/column address calculator, the operation of vertical or horizontal address orientation is controlled by the vertical/horizontal signal. This signal determines the vertical ( $y_m$ ) and the horizontal ( $x_n$ ) coordinates. If the signal vertical/horizontal is vertical, then the row addresses and the vertical interval  $s_v$  can be obtained. Otherwise, the column addresses and the horizontal interval  $h_v$  can be found. The vertical distance calculator calculates the distance between the source pixel and the virtual interpolated pixel. Similarly, the horizontal distance calculator calculates the distance between the virtual interpolated pixel and the final interpolated pixel.



**Fig. 1:** Block diagram of the hardware architecture for digital image scaling

The most important computation in convolution-based scaling is the calculation of interpolation weighting coefficients. By using low area WCG [25] an area efficient FOPCI can be implemented. [Fig. 2] shows the vertical/horizontal interpolation unit used for image scaling. The vertical interpolation unit performs interpolation in column wise manner to produce virtual pixel. The horizontal interpolation unit performs interpolation for these virtual pixels to produce interpolated pixel. The virtual pixels created from vertical interpolation are stored in the virtual pixel buffer, as shown in [Fig. 1], they are accessed in the process of horizontal interpolation.



**Fig. 2:** Vertical/Horizontal Interpolation unit.

As shown in [Fig. 2] the vertical and horizontal interpolations have the same operation, but they have to execute in parallel to accelerate scaling speed.



### PROPOSED FOPCI

A low complexity hardware for image interpolation is proposed by reducing the computational complexity of weighting coefficient generator. To verify the performance of the proposed hardware architecture of image interpolation, the interpolation circuit is connected with image preprocessing and post processing circuit as shown in [Fig. 3].

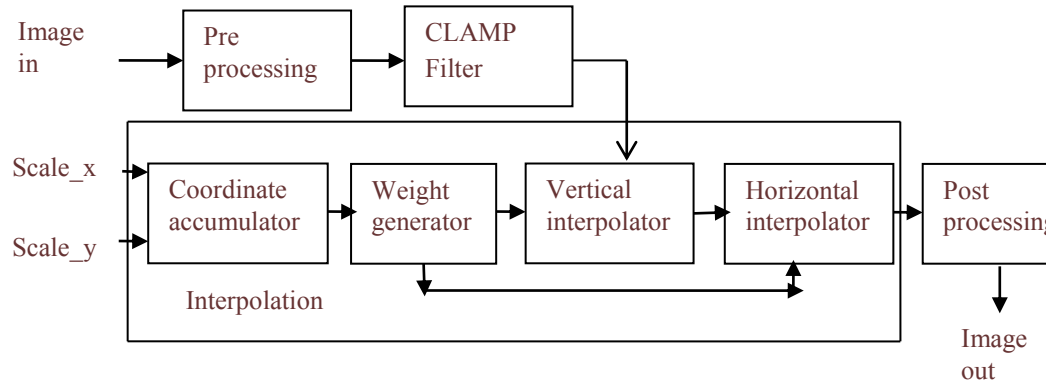


Fig.3: Block diagram of the proposed interpolation method.

Image preprocessing in Matlab simulink helps in providing input to FPGA as specific test vector array which is suitable for FPGA bitstream compilation using system generator [26].

To reduce the area of the VLSI architecture of FOPCI [12], an optimized design of weighting coefficient generator (WCG) is used. The most computational effort in the proposed WCG is the reduction of number of arithmetic elements. The simplified WCG includes only two adders, three dividers and four subtractors [25]. The proposed filtering technique for the improvement of interpolation is implemented by Clamp Filter as shown in [Fig. 3]. Clamp filter is a low-pass filter which is used for smoothing discontinuous edges and decreasing block effect caused by the interpolation method. An example of a 3x3 kernel for a clamp filter is shown in equation (1).

$$Kernel\ c = \begin{bmatrix} 1 & 1 & 1 \\ 1 & C & 1 \\ 1 & 1 & 1 \end{bmatrix} \quad (1)$$

where, C is a clamp parameter that can be set according to the characteristics of the images. The clamp filter is stable when the clamp parameter C is varied between 6 and 30 [6]. The new pixel value is computed based on the array of the clamp filter as

$$P'(i,j) = \left[ P(i,j) * \begin{bmatrix} 1 & 1 & 1 \\ 1 & C & 1 \\ 1 & 1 & 1 \end{bmatrix} \right] \div (C \div 8) \quad (2)$$

### RESULT AND DISCUSSION

The performance of scaling algorithm is evaluated based on two categories such as quality/quantitative measure and hardware performance measure. Quantitative measure specifies the quality of the interpolated image based on PSNR. The PSNR is estimated by using equation (5) [6].

$$MSE = \frac{1}{MN} \sum_{m=0}^{M-1} \sum_{n=0}^{N-1} [P(i,j) - P'(i,j)]^2 \quad (3)$$

where, MSE is the mean square error M and N are the width and height of the actual input image. P (i,j) is original input image and P'(i,j) is interpolated output image.

$$PSNR = 10 \log_{10} \frac{MAX^2}{MSE} \quad (4)$$

When the pixels are represented by eight bits per sample, the maximum value of each pixel (MAX) is 255. Therefore, the quality tends to be expressed in dB with a PSNR given as

$$PSNR = 10 \log_{10} \frac{255^2}{MSE} \quad (5)$$

The quality measure of various interpolation methods is evaluated by using MATLAB. For testing the quality of scaling algorithms, images from USC-SIPI database of size (512 × 512) are selected. [Fig. 4] shows the test images from the USC-SIPI database considered for experimentation. The images are tank, girl, pepper, pirate, livingroom, boat, house, san-diego (aerial), pepper and stream and bridge. [Fig. 5] shows the sample interpolated image. [Table 1] lists the PSNR of different interpolation methods respectively.



Fig. 4: Input images considered for experimentation.



(a) Input image

(c) Upscaled image by 2

Fig. 5: Sample interpolated image.

Table 1: PSNR of various interpolation methods for upscaling ratio of 2 after 1/2 downscaling

Image	Interpolation Methods					
	Bicubic [10]	Bilinear [4]	Convolution based [5]	Bicubic [21]	FFOPCI [12]	Proposed
Tank	56.23	56.74	65.31	68.34	68.50	69.17
Girl	55.13	50.56	64.63	67.15	67.46	67.91
Pepper	53.28	49.22	62.21	64.60	64.95	65.11
pirate	54.67	46.31	58.21	61.33	61.75	62.17
Living room	52.46	45.00	55.17	58.08	58.54	59.09
Boat	52.17	44.54	55.92	58.90	59.35	59.77
House	49.25	40.34	52.97	55.86	56.35	56.88
San-diego	49.59	39.41	50.91	54.24	54.78	55.48
Mandrill	50.78	41.89	50.72	53.57	53.79	54.22
Stream and Bridge	48.93	41.27	49.71	52.75	52.99	53.61

The results shown in [Table 1] demonstrate that the PSNR value is high (69.17 dB) for the test image ‘tank’ by using the proposed method. To evaluate the performance of the proposed image interpolation, the proposed architecture and the existing architectures are simulated, synthesized and implemented for Virtex xc6 vsx315tff1156-3 by using MATLAB Simulink and Xilinx ISE 14.5. [Table 2] shows the comparison of different device utilization factors of previous low complexity interpolation methods and the proposed FOPCI methods.

**Table 2:** Comparison of VLSI design parameters of proposed methods with other interpolation techniques

Parameters	Interpolation Methods					
	Bicubic [10]	Convolution based [5]	Convolution based [16]	FFOPCI [12]	Proposed A (without filter)	Proposed B (with filter)
Target device	Virtex xc6 vsx315tff1156-3					
Number of LUTs	198	364	336	191	171	260
Number of LUTs used as logic	175	351	330	176	147	213
Number of LUT flipflop pairs used	235	387	336	192	137	137
Number of occupied slices	63	102	84	74	57	87

Based on [Table 2], the proposed FOPCI without filter utilizes only 171 LUTs, which is much less than the previous works FFOPCI [12], Convolution based [5] and [16] and bicubic [10]. Further, the proposed FOPCI with filter utilizes only 260 LUTs, which is much less than the previous low complexity algorithms [5] and [16]. Comparing the proposed two methods, the method B costs 89 LUTs more than method A due to an additional clamp filter. However, it increases the quality by over 0.66 dB. To encapsulate, this work contributed in designing high-performance and high quality interpolation architecture of VLSI circuit for many visual communication systems.

## CONCLUSION

This paper proposes an area efficient VLSI architecture of cubic convolution kernel-based interpolation for digital image scaling. The operation of the proposed architecture without filter requires five additions, four subtractions four multiplications and three divisions. Therefore, the number of arithmetic elements in the proposed architecture is much less than the other interpolation methods. Further, the proposed architecture with clamp filter increases the interpolated image quality with reasonable amount of LUTs. Consequently, the proposed VLSI architecture has solved the problem of computation complexity for generating weighting coefficients for image interpolation and furthermore, simplified the hardware for FPGA implementation and reduced the chip area. Additionally, the image quality is improved by using clamp filter to reduce block effects of the interpolation. Thus, the proposed work is an area efficient high quality image interpolation for many compact visual communication systems.

### CONFLICT OF INTEREST

There is no conflict of interest.

### ACKNOWLEDGEMENTS

None

### FINANCIAL DISCLOSURE

None

## REFERENCES

- [1] Apurva Sinha, Mukesh Kumar, Jaiswal A.K , Rohini Saxena. [2014] Performance analysis of high resolution images using interpolation techniques in multimedia communication system”, Signal and Image processing, An international journal (SIPIJ), 5(2): 39-49, , April
- [2] Feilong Cao, Miaomiao Cai, Yuanpeng Tan. [2015] Image interpolation via low-rank matrix completion and recovery”, IEEE Trans. Circuits and systems for video technology, 25(8) :121-1270.
- [3] Chen SL[2013]“VLSI Implementation of a Low-Cost High

- Quality Image Scaling Processor", IEEE Trans. Circuits and Systems-II Express Briefs, 60(1):31-35.
- [4] Chen SL. [2013] VLSI implementation of an adaptive edge-enhanced image scalar for real-time multimedia applications", IEEE Trans. Circuits and systems for video technology, 23( 9): 1510-1522.
- [5] Chien-Chuan Huang, Pei-Yin Chen,[ 2012] Member, IEEE, and Ching-Hsuan Ma, A Novel Interpolation Chip for Real-Time Multimedia Applications, IEEE Trans. circuits and systems for video technology, 22(10):1512-1525.
- [6] Chen SL, Huang HY, Luo CH, [2011] A low-cost high-quality adaptive scalar for real-time multimedia applications," IEEE Trans. Circuits Syst.Video Technol, 21(11): 1600–1611,
- [7] Nuno-Maganda M A, Aris-Estrada MO. [2005] Real-time FPGA based architecture for bi-cubic interpolation: An application for digital image scaling. Proceedings of international conference on reconfigurable computing and FPGAs, pp. 1-8.
- [8] Chung-chi Lin, Ming-hwa Sheu, Huann-keng Chiang, Zeng-chuan Wu, Jia-yi Tu and Chia-hung Chen. [2008] A Low-cost VLSI Design of Extended Linear Interpolation for Real Time Digital Image Processing" International Conference on Embedded Software and Systems (ICESS2008), 196-202.
- [9] Chung-chi Lin, Ming-hwa Sheu, Huann-keng Chiang, Wen-kai Tsai, Zeng-chuan Wu.[ 2008]"Real-Time FPGA Architecture of Extended Linear Convolution for Digital Image Scaling, International conference on ICECE Technology, pp. 381-384.
- [10] Chung-chi Lin, Ming-hwa Sheu, Huann-keng Chiang, Chishyan Liaw, Zeng-chuan Wu. [2008] The Efficient VLSI Design of BI-CUBIC Convolution Interpolation for Digital Image Processing" in Proc. IEEE Int. Symp. Circuits Syst., pp. 480-483.
- [11] Chung-chi Lin, Chishyan Liaw, Ching-tsornng Tsai. [2010] A Piecewise Linear Convolution Interpolation with Third-order Approximation for Real-time Image Processing, IEEE Conf. pp. 3632-3637.
- [12] Chung-chi Lin, Ming-hwa Sheu, Chishyan Liaw, and Huann-keng Chiang.[ 2010] Fast First-order Polynomials Convolution Interpolation for Real-Time Digital Image Reconstruction, IEEE Trans. Circuits and Systems for Video Technology, 20(9): 1260-1264.
- [13] Lin Li , Feng Yu, [2015]Block region of interest method for real-time implementation of large and scalable image reconstruction", IEEE signal processing letters, 22(11): 1908-1912.
- [14] John Moses, CD. Selvathi, Anne Sophia VM.[2014] VLSI architectures for image interpolation-A survey", Hindawi publishing corporation, VLSI Designarticle ID 872501:10.
- [15] Lanping Deng, Kanwaldeep Sobti, [2011] Accurate area, time and power models for FPGA-based implementations Journal of signal processing systems, Springer, 63: 39-50.
- [16] John Moses C, Selvathi D. [2014]VLSI architecture of an area efficient image interpolation", International journal of engineering and technology, 6( 2): 1120-1131.
- [17] Lehmann TM, Gönner C, Spitzer K. [1999] Survey: interpolation methods in medical image processing, IEEE Trans. Medical Imaging, 18(11): 1049–1075.
- [18] Erik Meijering, Michael Unser. [2003] A note on cubic convolution interpolation,. IEEE Trans. image processing. 12( 4): 477-479.
- [19] Robert TG.[ 1981] Keys, Cubic convolution interpolation for digital image processing, IEEE Trans. on acoustics, speech, and signal processing, 29(6):. 1153-1160.
- [20] Erik HW Mijering, Wiro J Niessen,Max A.[ 2001] Viergever, Quantitative-based methods for medical image interpolation", Elsevier, Medical image analysis, 5: 111-126.
- [21] Zhi-Yong Pang, Hong Zhou Tan, Di-Hu Chen, [2013] An Improved Low-cost Adaptive Bicubic Interpolation Arithmetic and VLSI Implementation", Acta Automatica Sinica, Elsevier, Science Direct,39( 4):.407-417.
- [22] Lee J , Park IJ. [2016], High performance low area video upscaling architecture for 4K UHD video', IEEE Transactions on Circuits and Systems II: Express Briefs, 99: 1-5.DOI: 10.1109/TCSII.2016.2563818
- [23] Chung-Chi Lin, Ming-Hwa Shen, Huann-Keng Chiang, Chishyan Liaw, Zeng-Chuan Wu and Wen-Kai Tsai, [ 2010 ]An Efficient Architecture of Extended Linear Interpolation for Image processing", Journal of Information Science and Engineering, 26: 631-648.
- [24] Huang, CH & Chang, CY 2016, 'An area and power efficient adder-based stepwise linear interpolation for digital signal processing', IEEE Transactions on Consumer Electronics, 62( 1): 69-75.
- [25] .Selvathi, D & Moses, CJ (2015), 'An area efficient weighting coefficient generation architecture for polynomial convolution interpolation', Progress in systems engineering, Advances in intelligent system, Springer, proceedings of the twenty-third international conference on systems engineering, University of Nevada, Las Vegas, USA, pp. 495-500.
- [26] Allin Christe S, Vignesh M, Kandaswamy A. [2011]An Efficient FPGA Implementation of MRI Image Filtering and Tumour Characterization Using Xilinx System Generator, International Journal of VLSI Design and Communication Systems (VLSICS), 2(4): 95-109, December

# ENGINE KNOCK DETECTION BASED ON WAVELET PACKET TRANSFORM AND SPARSE FUZZY LEAST SQUARES SUPPORT VECTOR MACHINES (SFLS-SVM)

A Uma Mageswari\*, R Vinodha

Department of Electronics and Instrumentation Engineering, Annamalai University, Chidambaram, INDIA

## ABSTRACT

The intensity of knock detection techniques is detected by using the combination of microphone sensors and sequence of filtering techniques, which are identified the type of engine vibration sound. However, the other knock detection methods, such as using wavelet transform and support vector machines, are failed to accurate time detection and the exact identification. This paper proposed wavelet packet transform (WPT) and sparse fuzzy least squares support vector machines (SFLS-SVM) techniques for better accurate time detection and the exact identification. WPT acts as a tool to analyze the characteristics of the knock signals in the decomposition levels. To find the exact intensity of knock detection, sparse fuzzy least squares support vector machines (SFLS-SVM) is introduced. SFLS-SVM works efficiently in the stepwise selection, forward expansion phase and backward exclusion phase for every step. The SFLS-SVM algorithm is extremely fast as compared with the Fourier transform (FT), Wavelet Transform (WT) and Wavelet Packet Transform (WPT)

## INTRODUCTION

Now-a-days, Engine control systems are intended to minimize fatigue emissions while increasing power and fuel economy. The capability to increase power and fuel economy by optimized spark timing for a given air ratio or fuel ratio is restricted by engine knock. Detecting engine knock and controlling combustion timing to tolerate an engine to keep running at the knock threshold gives the best power and mileage. Typical ignition occurs when a gaseous combination of air and fuel is ignited by the spark plug and blazes easily from the position of ignition to the cylinder walls.

The competence efficiency is an imperative parameter for an engine. The competence efficiency of the engine is enhanced with an augment in compression ratio (CR) as predicted by thermodynamic study of best motor engine cycles. Yet, raising the CR also enhances the susceptibility to knock [1]. The condition with specific temperatures and weights of pressure in an engine cylinder after the spark ignition, the clean gas zone, situated in front of the fire front might produce one or more auto ignitions and some of them disintegrate into non-linear pressure weights waves or knock [2].

Most importantly engine knock causes the majority of the unusual burning in an engine [3], for instance polluting, exasperating passengers by the uncomfortable metallic noises and obliterating engine parts in extreme knock condition. In this way, early detection of knock is most important to lessen pollution and other issues.

There are a few disadvantages of the filtering concepts. Extracting the knock segment split into the resonance frequencies by basic pass-band filters is not adequate both to appraise the knock and to enhance the signal-to-noise ratio (SNR). Additionally the values of resonance frequency are capacity of the crank angle, and the vicinity of noise, like cam shocks, is complex to evacuate. With a specific end goal to overcome those issues, time-frequency approaches [4-7], the short-time Fourier transform (STFT), the promising method wavelet transform [8-10], are modified by number of researchers. Support vector machine (SVM) [11-12] is proposed method that intends to solve classification pattern issues, where it is utilized to discover a hyperplane  $h \cdot x$  that can isolate two class designs with the greatest edge. This is because maximizing the two-class edges is proportionate to minimizing the upper bound on the model's simplification error. Because of the high computational complexity usually concerned in illuminating the Quadratic Programming (QP) issues in the dual-space in SVM, least-squares support vector machine (LS-SVM) was proposed by changing the inequality limitations in conventional SVM with a two- standard.

This paper proposed wavelet packet transform (WPT) and sparse fuzzy least squares support vector machines (SFLS-SVM) techniques for better accurate time detection and the exact identification. WPT acts as a tool to analyze the characteristics of the knock signals in the decomposition levels. To find the exact intensity of knock detection, sparse fuzzy least squares support vector machines (SFLS-SVM) is introduced. SFLS-SVM works efficiently in the stepwise selection, forward expansion phase and backward exclusion phase for every step. The SFLS-SVM algorithm is extremely fast as compared with the SVM. Section-II describes the wavelet packet transform (WPT); Section-III explains sparse fuzzy least squares support vector machines; Section-IV describes the proposed method algorithm; Section-V discusses the result, and finally concludes the paper in section-IV.

## WAVELET PACKET TRANSFORM (WPT)

Wavelet packets are a specific linear combination of wavelets. They appearance bases that hold a lot of the orthogonality, smoothness and area properties of their parent wavelets[13]. The coefficients in the

### KEY WORDS

Knock Detection, wavelet packets transform (WPT) and sparse fuzzy least squares support vector machines (SFLS-SVM)

Published: 2 December 2016

\*Corresponding Author

Email: mdumamageswari@gmail.com



direct combinations are processed by a recursive method, with the outcome that developments in wavelet-packet bases have less computational complexity.

As of late, the WPT has been proposed as an important new device in signal analysis and processing. Wavelet transform is a high-quality solution in the both frequency domains and time domains, synchronously, and can remove more information in the time domain at unusual frequency bands. The WPT has been utilized for on-line monitoring of the process. The WPT can decompose the existing signal into different levels in distinctive time windows and frequency bands; the components, subsequently, can be considered as feature elements of the original signal.

To decompose an existing signal, which is a one-dimensional (1-D) discrete-time signal, an easy and quick method is required for calculation of WT coefficients of the signal. In the first level of wavelet decomposition, a signal can be decomposed into an approximation and detail coefficients, confirmed in [Fig. 1]. In second level of wavelet decomposition, the coefficient of the approximation is again decomposed into approximation and detail coefficients, and then it repeats the level of procedure.

In WPT, approximations coefficients and details coefficients can be part, demonstrated in [Fig. 2]. In WPT theory, the low pass coefficient (approximation coefficient) component and high pass coefficient (detail coefficient) component outputs can be iterated into further separating. Accordingly, the WPT achieves more than one wavelet packet at a specified scale at the importance of high pass filter. Anyhow the low pass filter does again at every level in wavelet transform. The final level of the wavelet packet decomposition is the time representation of the signal. At every last level, the tradeoff between resolutions of the both time and frequency can be expanded. Subsequently, the WPT acquires an exact frequency resolution than the WT.

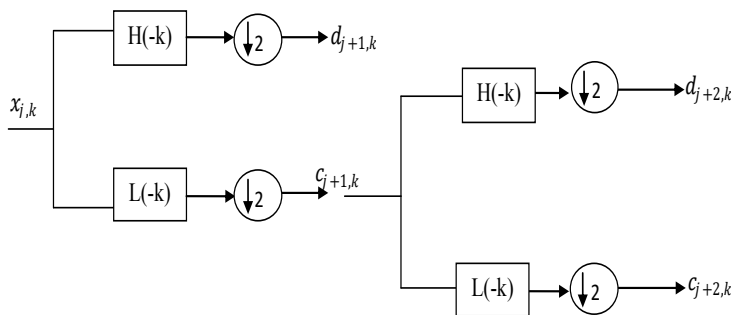


Fig. 1: Decompositions of wavelet transform.

For a predefined succession of signals  $x_{j;n} \in K$  at scale  $j$ , the approximation coefficients can be effected by filtering  $x_{j;n}$  with the low-pass wavelet filter  $L = \{l_t\}$  and then sub inspected by two

$$c_{j+1,k} = \sum_n l_{n-2k} x_{j;n} \quad (1)$$

Because of low-pass filtering, a few details would have been lost from  $x_{j;n}$ , which could be registered by filtering  $x_{j;n}$  with the high-pass wavelet filter  $H = \{h_t\}$  and then sub sampled by two

$$d_{j+1,k} = \sum_n d_{n-2k} x_{j;n} \quad (2)$$

Here  $d_{j+1,k}$  is the detail coefficient.

For that reasons, mathematical equations (1) and (2) are measured as a decomposition signal onto an orthogonal, and measured the reconstruction can be summed up the orthogonal projections.

$$x_{j;n} = \sum_n l_{n-2k} c_{j+1,k} + \sum_n h_{n-2k} d_{j+1,k} \quad (3)$$

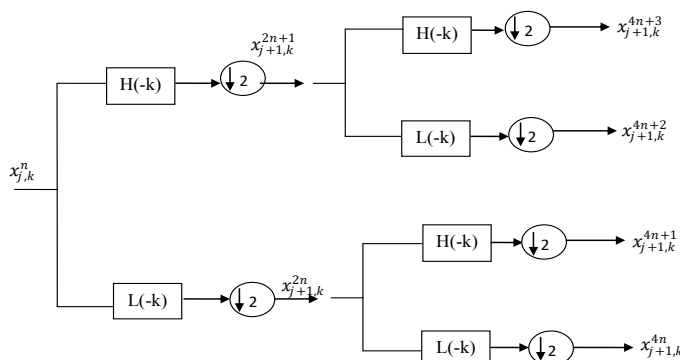


Fig. 2: Decompositions of wavelet packets transformation.

Here, filters  $h_t$  and  $l_t$  are supposed to satisfy



$$h_t = (-1)^t h_{1-t}, \sum_n h_t = \sqrt{2}, \sum_n h_t h_{t+2\varepsilon} = \delta_{0,\varepsilon},$$

$$\delta_{0,\varepsilon} = \begin{cases} 1, & \varepsilon = 0 \\ 0, & \varepsilon \neq 0 \end{cases}$$

Here  $t \in \mathbb{Z}, \varepsilon \in \mathbb{Z}$ .

In WT, every single level can be decomposed by transient the preceding approximation coefficients as high pass filters (HPF) and low pass filters (LPF). In any case, WPT decomposit, both the high frequency and low frequency coefficients have been decomposed. The WPT coefficients equations can be distinct as

$$x_{j+1,k}^{2j} = \sum_n l_{n-2k} x_{j,n}^1 \quad (4)$$

$$x_{j+1,k}^{2j+1} = \sum_n h_{n-2k} x_{j,n}^1 \quad (5)$$

The reconstruction can be done as

$$x_{j,n}^1 = \sum_n l_{n-2k} x_{j+1,k}^{2j} + \sum_n h_{n-2k} x_{j+1,k}^{2j+1} \quad (6)$$

Here,  $l$  is the space serial number in scale  $j$ . For  $j$  scale decomposition, the WPT decomposition makes  $2^j$  sets of coefficients rather than  $j + 1$  sets of coefficients for the WT. On the other hand, due to the down sampling process the number of coefficients is still same and no redundancy is there.

For effortlessness and efficiency, a node  $x_{j+1,k_{j+1}}^{2j}$  or  $x_{j+1,k_{j+1}}^{2j+1}$  can be written as the linear combination of the nodes at scale  $j$ . From the equations (4) and (5), it can be characterized as

$$x_{j+1,k_{j+1}}^{2j} = \frac{\sqrt{2}}{2} (x_{j,k_j}^1 + x_{j,k_{j+1}}^1) \quad (7)$$

$$x_{j+1,k_{j+1}}^{2j+1} = \frac{\sqrt{2}}{2} (x_{j,k_j}^1 - x_{j,k_{j+1}}^1) \quad (8)$$

Here,  $k_j = 0, 1, \dots, H = \{h_0, h_1\}, L = \{l_0, l_1\}, l_0 = \frac{\sqrt{2}}{2}, l_1 = \frac{\sqrt{2}}{2}, h_0 = \frac{\sqrt{2}}{2}, h_1 = -\frac{\sqrt{2}}{2}$ . it can be seen that  $k_j = \lfloor \frac{k_0}{2^j} \rfloor$ .

### SPARSE FUZZY LEAST SQUARES SUPPORT VECTOR MACHINES (SFLS-SVM)

Aspire of this paper is that a new fuzzy rule-based system is developed based on a SFLS-SVM learning mechanism with the representation structure appeared in [Fig. 3].

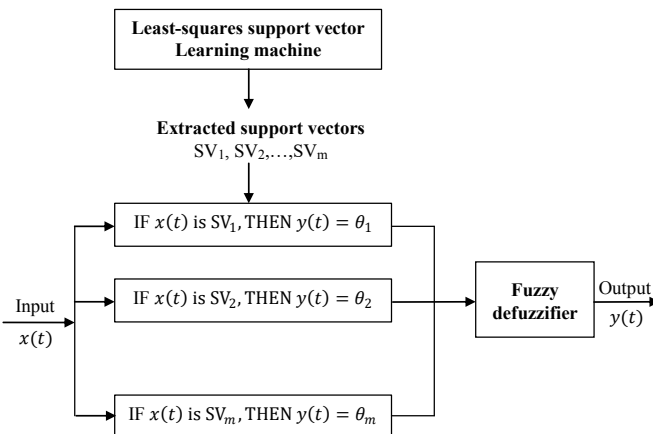


Fig. 3: The structure of the sparse fuzzy least squares support sector machines (SFLS-SVM).

Comparative as in SVM-based fuzzy systems [13], the fuzzy basis function (9) is selected as the mapping function (11) in the solution of SFLS-SVM. Comparative as in SVM-based fluffy frameworks [13] (where the portion capacity in SVMs is identified with the fluffy premise work), the fluffy premise capacity (9) is picked as the mapping capacity (11) in our proposed arrangement of SFLS-SVM,

$$N_i(x(t); W) = \frac{\mu_i(x(t); c_i; \sigma_i)}{\sum_{i=1}^m \mu_i(x(t); c_i; \sigma_i)} \quad (9)$$

Where  $W = [c_1^T, \sigma_1^T, \dots, c_m^T, \sigma_m^T]^T$  denotes the premise parameters vector.  $\mu_i(x(t); c_i; \sigma_i)$  is the Gaussian membership function; which is defined in eq. (10)

$$\mu_i(x(t); c_i; \sigma_i) = \prod_{j=1}^n \exp \left\{ -\frac{1}{2} \left( \frac{x_j(t) - c_{i,j}}{\sigma_{i,j}} \right)^2 \right\} \quad (10)$$

Where  $c_{i,j}$  is the centre of the  $i^{th}$  membership function with regard to the  $j^{th}$  input ( $j = 1, \dots, n$ ); i.e.,  $c_i = [c_{i,1}, \dots, c_{i,n}]^T \in \mathbb{R}^n$  and  $\sigma_{i,j}$  is the standard deviation of the  $i^{th}$  membership function with regard to the  $j^{th}$  input ( $j = 1, \dots, n$ ); i.e.,  $\sigma_i = [\sigma_{i,1}, \dots, \sigma_{i,n}]^T \in \mathbb{R}^n$ .

i.e.,  $\varphi_i(x(t)) = N_i(x(t); W)$ , to combine the two methods into a new sparse Least Square Support Vector Machine based fuzzy rule-based system. Note that normally the denominator of the fuzzy basis function (FBF) is uninvolved since the number of fuzzy rules is unknown in advance. There is no contravention of the soul of a fuzzy inference (FIS) system as depicted in [20], where the standard rule premises decide the certainty values for all rules, while the rule consequents allot the outcome of the inference system with the certainty values for the relating rules. Therefore, the support vectors extracted from the SFLS-SVM learning mechanism can be useful in producing the fuzzy IF-THEN rules that compare to the FBFs. In this way, the fuzzy systems can give suitable speculation capability over concealed information as in case of SFLS-SVM. Contrasting from the conventional Least Square SVM (LS-SVM) where all training samples serve as the SVs, a novel SFLS-SVM learning mechanism is proposed to generate rule determination in a fuzzy rule-based system. The average weighted defuzzification strategy can then be utilized to compute the general output of the fuzzy rule-based system, such that

$$f(x(t); W; \theta) = \sum_{i=1}^m N_i(x(t); W) \theta_i \quad (11)$$

Where  $\theta = [\theta_1, \dots, \theta_m]^T$  denotes the consequent parameter vector.

## THE PROPOSED METHOD ALGORITHM FOR KNOCK DETECTION

1. The knock signal is defined as

$$x(t) = s(t) + n(t) = \sum_{p=1}^P a_p w_p(t) \cos(2\pi(\alpha_p t^2 + \beta_p t) + \phi_p) + n(t) \quad (12)$$

2. The wavelet packet transform can be defined as  $\phi_{2n} = \sqrt{2} \sum_k h_k \phi_n(2t - k)$  and  $\phi_{2n+1} = \sqrt{2} \sum_k g_k \phi_n(2t - k)$ . Here, the wavelet packets given by  $\phi_{njk}(t) = 2^{j/2} \phi_n(2^j t - k)$ .

3. The efficient learning mechanism of the SFLS-SVM is detailed as follows.

Step 1): Initialization. To start the learning process, the candidate pool  $\Psi_0 = [\varphi_1, \dots, \varphi_m]$  is first generated by using all the training patterns as the potential rules or Support Vectors. Note that the initially selected pool  $\Phi_0$  is an empty matrix. The number of selected regressors is set to  $k = 0$  and the two vectors  $b^1 = [\varphi_1^T y, \dots, \varphi_m^T y]$  and  $d^1 = [\varphi_1^T \varphi_1, \dots, \varphi_m^T \varphi_m]$  are initialized.

Step 2): Forward expansion phase. The main task here is to select the most significant regressor from the candidate pool and to update the corresponding variables for the operations ahead.

1) According to the contribution of each candidate regressor computed

from  $\Delta \tilde{J}_{k+1}(\varphi_i) = \frac{1}{2\mu} \frac{(b_i^{k+1})^2}{d_i^{k+1} + \mu}$ ,  $i = k + 1, \dots, m$ , the one with the largest objective reduction is selected

as the next regressor to be added into the regression matrix  $\varphi_{k+1} = [p_1, \dots, p_{k+1}]$ , i.e.,  $p_{k+1} = \arg \max_{i=k+1}^m \Delta \tilde{J}_{k+1}(\varphi_i)$ . The corresponding regressor  $p_{k+1}$  is then removed from the candidate pool and  $\Psi_{k+1} = [\varphi_{k+2}, \dots, \varphi_m]$  set.

2) While all the previous  $k$  rows remain unchanged, the  $(k + 1)^{th}$  row of matrix  $A$  is calculated using  $a_{k,j}$ .

$$\text{Where } a_{k,j} = \begin{cases} \mu a_{i,j} / (a_{i,j} + \mu) - \sum_{j=i+1}^{k-1} a_{j,k} a_{j,i} / (a_{j,j} + \mu), & i = 1, \dots, k-1, \\ p_k^T p_k - \sum_{j=1}^{k-1} a_{j,k}^2 / (a_{j,j} + \mu), & i = k, \\ p_k^T \varphi_i - \sum_{j=i+1}^{k-1} a_{j,k} a_{j,i} / (a_{j,j} + \mu), & i = k+1, \dots, m. \end{cases} \quad (13)$$

3) The two vectors  $b^{k+2}$  and  $d^{k+2}$  are updated with entries from  $k + 2$  to  $m$  by using  $b^{k+1}$  and  $d^{k+1}$ , employed for selecting the  $(k + 2)^{th}$  regressor from the candidate pool.

Step 3): Backward exclusion phase. The main purpose of this phase is to re-evaluate the contribution of each of the previously selected regressors.

1) The entries from  $1$  to  $k + 1$  for the two vectors  $c^{k+1}$  and  $h^{k+1}$  are updated, while the correspondingly remaining values in the two vectors are inherited from  $b^{k+2}$  and  $d^{k+2}$ .

2) The criterion  $\Delta \tilde{J}_{k+1}(p_r) = \min_{i=1}^k \Delta \tilde{J}_{k+1}(p_i) < \max_{i=1}^k \Delta \tilde{J}_{k+1}(\varphi_i)$  is used to decide whether to remove a regressor from the selected pool or not, and to determine which one is to be removed. If the criterion is not met, then set  $k = k + 1$  and go to Step 4). Otherwise, moves to the next step.

3) The regressor  $p_r$  is shifted to the last column of  $\varphi_{k+1}$  using a total of  $k - r + 1$  interchanges between two adjacent previously selected regressors. Thus, a new regression context of  $A \in \mathbb{R}^{(k+1) \times m}$ ,  $b^{k+2} \in \mathbb{R}^m$ ,  $c^{k+1} \in \mathbb{R}^m$ ,  $d^{k+2} \in \mathbb{R}^m$ , and  $d^{k+1} \in \mathbb{R}^m$  is produced as if  $p_r$  was the last selected regressor in the regression matrix  $\varphi_{k+1}$ .

4) The criterion  $\Delta \tilde{J}_{k+1}(p_r) < \max_{i=k+2}^m \Delta \tilde{J}_{k+1}(\varphi_i)$  is used to decide whether to remove a regressor from the selected pool or not. If none has to be removed, then set  $k = k + 1$  and the algorithm moves to Step 4). Otherwise, it goes to the next step.

5) The regressor  $p_r$  is removed from the selected pool and returned to the candidate pool, i.e.,  $\Phi_k = [\phi_1, \dots, \phi_k]$  and  $\Psi_k = [\psi_1, \dots, \psi_k]$ . The regression context  $A \in \mathbb{R}^{k \times m}$ ,  $b^{k+1} \in \mathbb{R}^m$ ,  $c^k \in \mathbb{R}^m$ ,  $d^{k+1} \in \mathbb{R}^m$ , and  $h^k \in \mathbb{R}^m$  are then updated and the index  $k$  is set to  $k - 1$ .

Step 4): The learning process will terminate if some stopping criterion is met, such as a certain number of regressors have been selected or some tolerance value has been met. Similar to the stopping criterion commonly used in training neural networks and support vector machines, the tolerance for the maximum ratio of objective value reduction is used here. In detail, if the ratio  $(J_k - \min_{i=1}^k J_{k+1}(\phi_i))/J_k$  is less than a very small positive tolerance value ( $\rho$ ), the generalization performance of the fuzzy systems will not be greatly improved by adding a new regressor. It should be noted that the stopping criterion used here is an important measure for the trade-off between the training accuracy (performance) and the model complexity (sparseness and interpretability) of the obtained fuzzy systems. If the stopping criterion is not met, the algorithm returns to Step 2).

4. Finally, the output of the sparse fuzzy least square support vector machine detects the knock.

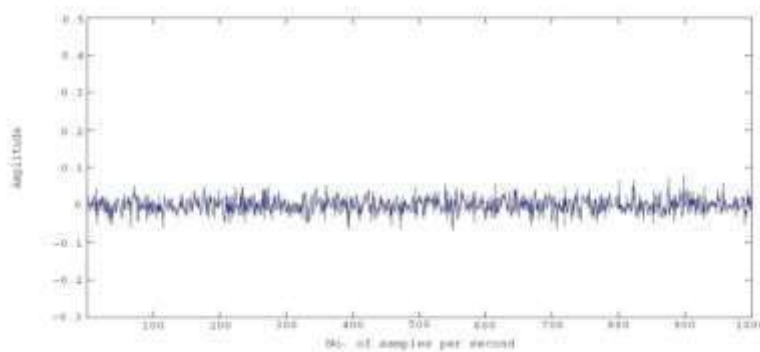
## RESULTS TS AND DISCUSSION

[Table 1] describes the characteristics of the EF7 turbocharged engine. IKCO EF engines are 4 cylinder engines. The general structure of the engine is close to the PSA Group's Peugeot TU5JP4. EF7 turbocharged engine has 1648 cc displacement with 78.560 mm bore and 85 mm stroke. This engine was presented as EF7 dual-fuel at Engine Expo Stuttgart Germany in 2008.

**Table 1:** Description of the engine characteristics

Description	Value	Unit
Engine Model	EF7 turbocharged, gasoline	-
Displacement	1648	CC
Bore	78.56	Mm
Stroke	85	Mm
Compression ratio	11.1	-
Gasoline injection pressure	3.5	bar
Maximum power	215@2500rpm – 4500rpm	Nm
Maximum torque	110@5500 rpm	kW
Number of cylinders	4	-

The input knock signal, described in eq. (12) is applied to wavelet packet transform; the low frequency coefficient of the wavelet packet transform is applied to the SFLS-SVM for detect the knock signal. [Fig.4] shows the waveform of the input knock signal. Fig.5 shows the resultant waveform of the detected knock signal.



**Fig. 4:** Input knock signal.

[Table 2] compares the knock detection error rate of the proposed method with the other techniques. As compared with the other knock detection techniques, the proposed method gets better results than Fourier Transform, Wavelet Transform and Wavelet Packet Transform.

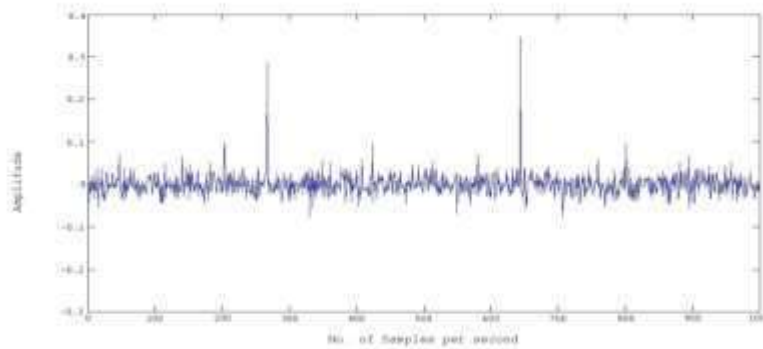


Fig. 5: Detected output of the knock signal.

Table 2: Comparison knock detection error rate of the proposed method with other techniques

Knock Detection Techniques	1000 revolution per minute Sampling Rate				
	150	200	250	300	350
Fourier Transform	74.60%	75.37 %	77.95%	77.34%	76.45%
Wavelet Transform	75.86%	76.43%	79.17%	78.05%	77.23%
Wavelet Packet Transform	77.85%	78.50%	81.25%	80.56%	79.42%
<b>PROPOSED</b>	<b>80.20%</b>	<b>81.5%</b>	<b>84.01%</b>	<b>83.7%</b>	<b>82.88%</b>

## CONCLUSION

This paper concluded an advanced approach of knock detection by using WPT and SFLS-SVM techniques. This proposed method determines a knock index which represents the engine knock tendency. Due to the statistical behavior of knock, the proposed method not much focused knock detection on an every cycle. Hence, in the proposed method is applied up to two levels of the WPT which extracts statistical information of the acquired signals, then applied to the SFLS-SVM. As compared with the results of the other knock detection techniques, the proposed method gets better result. In future enhancement, mostly concentrate to reduce the complexity of the SFLS-SVM algorithm as well as focused on output smoothing.

**CONFLICT OF INTEREST**  
There is no conflict of interest.

**ACKNOWLEDGEMENTS**  
None

**FINANCIAL DISCLOSURE**  
None

## REFERENCES

- [1] Hudson C, Gao X, Stone R. [2001] Knock measurement for fuel evaluation in spark ignition engines. Fuel, (80):395-407.
- [2] Olivier Boubal .[2000]Knock detection in automobile engines. EEEE instrumentation & measurement magazine ,3(3):24-28.
- [3] Olivier Boubal , Jacques Oksman.[2000] Knock acoustic signal estimation using parametric inversion. IEEE transactions on instrumentation and measurement, 49(4): 890-895.
- [4] Boland MD, Zoubir AM.[1997] Identification of time-varying non-linear systems with application to Knock detection in combustion engines.Speech and Image Technology for Computing and Telecommunications, Proceeding of IEEE ,2.:799-802.
- [5] Konig D.[1996] Application of time-frequency analysis for captured at Knock.IEEE International Conference on Acoustics,ICASSP-96, Speech, and Signal Processing,5:2746 - 2749 .
- [6] Matz G, Halawatsch F.[1998] Time-frequency methods for signal detection with application to the detection of knock in car engines. Proceedings of IEEE on Statistical Signal and Array Processing, 196-199.
- [7] Samimy B, Rizzoni G.[1994] Time-frequency analysis for improved detection of internal combustion engine Knock. Proceedings of the IEEE/SP International Symposium on Time-Frequency and Time-Scale Analysis, 178-181.
- [8] Molinaro F, Castanie F, Denjean A. [1992] Knocking reconition in engine vibration signal using the wavelet transform. Proceedings of the IEEE-SP International Symposium, 353 -356.
- [9] Thomas JH, Dubuisson B.[1996] A diagnostic method using wavelets networks application to engine knock detection.IEEE International Conference on Systems, Man and Cybernetics, 1: 244-249.
- [10] Cortes C ,Vapnik V, [1995] Support-vector networks.Mach. Learn, 20,(3):273–297.
- [11] Adankon M, Cheriet M, Biem A.[2011] Semisupervised learning using bayesian interpretation.Application to LS-SVM, IEEE Trans. Neural Netw,22(4):513–524.
- [12] Cody MA, Dobb's J. [1992] The fast wavelet transform. 16–28 .
- [13] Chiang JH, Hao PY.[2004] Support vector learning mechanism forfuzzy rule-based modeling. A new approach, IEEE Trans. Fuzzy Syst, 12(1):1–12.

# FAULT DIAGNOSE OF INDUCTION MOTOR USING NOVEL LEAST SQUARE FUZZY TOTAL MARGIN SUPPORT VECTOR MACHINE

S. Jaya<sup>1\*</sup>, R. Vinodha

Research Scholar, Department of Electronics and Instrumentation Engineering,  
Annamalai University, INDIA

## ABSTRACT

Induction motor plays an extremely vital part in the industrial developments due to its more reliable and regular integration in the commercial instruments and numerous applications. In regular situations, its process is reliable, however in irregular situations its process gets faults which can generate huge undesirable losses. To diagnose the faults in induction motors, a novel least square fuzzy total margin support vector machine (LS-FTM-SVM) is utilized. For stationary signals and non-stationary signals, Wavelet Packet Transform (WPT) is utilized to detect and extract the fault feature vectors. LS-FTM-SVM classifies the induction motor. This proposed method, LS-FTM-SVM is solved set of linear equations, and is computationally less intensive than other SVM methods.

## INTRODUCTION

**KEY WORDS**  
Energy coupling, wireless parameters.

The fault diagnosis of induction motor is great importance in production lines. This method can consider the maintenance cost and the some failures by allowing the fault detection of catastrophic faults [1]. A fault is defined as any types of malfunction of components, which may occur in a system and fault will reduce the performance of the system. Fault detection is the process which may be instructed as something is a problem in the system and needs to be repaired. The fault isolation is detected which fault occurs among the possible faults.

Induction motors are one of the most broadly used machines on which, depending on the industrial production process. Faults of these vital equipments can cause financial loss to the production plans which stimulate the researchers to consider and improve the efficient fault diagnosis systems for these rotary equipments [2]. In our work, the fault diagnosis of induction motors has been proposed which is classified as namely model based, signal based and data based. Induction motors are generally used in rotary machinery systems may be included machinery parts and used some industrial applications due to their arrogance, the maintenance cost is low and need low maintenance requirements [3]. The induction motors are well designed faults to be inherent due to the stresses involved in the conversion of electrical energy to mechanical energy and vice versa. The faults of induction motors may not only cause of interference of product operation, but also raise the cost, reduce the product quality and effect safety of operators.

Published: 2 December 2016

Our method of detection faults can reduce the breakdown and minimize the maintenance time. The machine availability and reliability can be increased in the same time. In regular situations, its process is reliable, however in irregular situations its process gets faults which can generate huge undesirable losses. To diagnose the faults in induction motors, a novel least square fuzzy total margin support vector machine (LS-FTM-SVM) is utilized. Wavelet Packet Transform (WPT) is used to determine and extract the fault feature vectors in the stationary and non-stationary signals. Our proposed technique divides the induction motor. This proposed method of LS-FTM-SVM is explained some linear equations, and is computationally less intensive than other SVM methods.

## BASICS OF SVM CLASSIFIER

The SVM has performed well even when it was used to solve the nonlinear problems with high dimensions with small training samples. The SVM classifier is better one compared than ANN classifier. The ANN classifier has the principle of risk minimization. In ANN, conventional empirical risk minimization is used to reduce the error on training dataset. But in SVM classifier, the risk minimization is used to decrease the upper bound of the expected risk. The SVM is based on statistical learning theory and it is a learning machine [4]. The SVM can be stated as follows: first map the input vectors into the features, space and it's have higher dimension which is relevant with to the kernel function. In the first step, the feature space is obtained and it's designed a hyperplane which separates two classes. This approach can be continued to multi-class problems.

\*Corresponding Author  
Email:  
mdjayaeece@gmail.com

The SVM has been successfully applied in many fields, including classification, recognition, regression analysis and forecast. It gives a unique solution and strongly regularized method suitable for ill-posed problems. The SVM is used to detect the optimal hyperplane by reducing the upper bound of the generalization error and it will be increasing the distance, margin, hyperplane and the data [5]. The SVM uses the preprocessing strategy in learning by mapping input space X to a high-dimensional feature space F. The fault diagnosis is basically a kind of pattern recognition method used in practical applications. There



is a given sample set  $G = \{(x_i, y_i), i = 1, \dots, n\}$  each sample  $x_i \in \mathbb{R}^d$  belongs to a class by  $y_i \in \{+1, -1\}$ . The boundary can be expressed as:

$$\omega x + b = 0$$

Where  $\omega$  is a weight vector and  $b$  denoted by bias. The decision function can be used to categorize any data point in either class 1 or 2:

$$f(x) = \text{sgn}(\omega x + b)$$

The optimal hyperplane dividing the data can be found as a solution to the following constrained optimization problem:

Minimize

$$\frac{1}{2} \|\omega\|^2$$

Subject to

$$y_i [(\omega x_i) + b] - 1 \geq 0, i = 1, \dots, n$$

Introducing Lagrange multipliers  $\alpha_i \geq 0$ , the optimization can be written as,

Maximize

$$L(\omega, b, \alpha) = \sum_{i=1}^n \alpha_i - \frac{1}{2} \sum_{i,j=1}^n \alpha_i \alpha_j y_i y_j (x_i x_j)$$

Subject to

$$\alpha_i \geq 0$$

$$\sum_{i=1}^n \alpha_i y_i = 0$$

The decision function can be found as follows:

$$f(x) = \text{sgn} \left( \sum_{i=1}^n \alpha_i y_i (x_i x) + b \right)$$

If the input linear boundary space is not enough to divide into two classes properly. In the higher dimension, the boundary will produce a hyperplane which may allow linear separation.

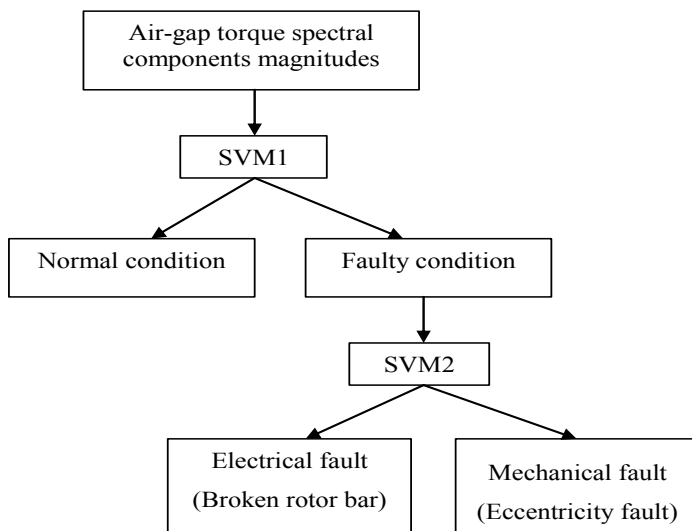


Fig. 1: Shows SVM classifiers based on Induction motor fault diagnostic model.

The SVM is accomplished by using a transformation  $\Phi(x)$  to map the data from the input space to feature space. The kernel function can be defined as,

$$K(x, y) = \phi(x)\phi(y)$$

The above equation can be mentioned the kernel functions are used in linear functions, polynomial functions, radial functions, radial basis and signed functions. The Advantages of SVM is to produce the accurate classifiers, less over-fitting and robust to noise. The disadvantage of SVM is a binary classifier and it can be used in multi-class classification, pairwise classifications [6]. The SVM classifier is computationally expensive and it will be running slow.



## PROPOSED WORK

An LS-FTM-SVM modeling method, as indicated in [Fig. 2] is improved for time varying, nonlinear processes across multiple working region. This method combines the advantage of local LS-FTM-SVM modeling and global regularization and it captures the local dynamics in each working region [7] [8]. The global regularization is used to reduce the global error. This technique may secure the continuity and smoothness between the LS-FTM-SVM models and avoid the over-fitting of our method. Thus, the method improved here may effectively complex processes across the multiple region.

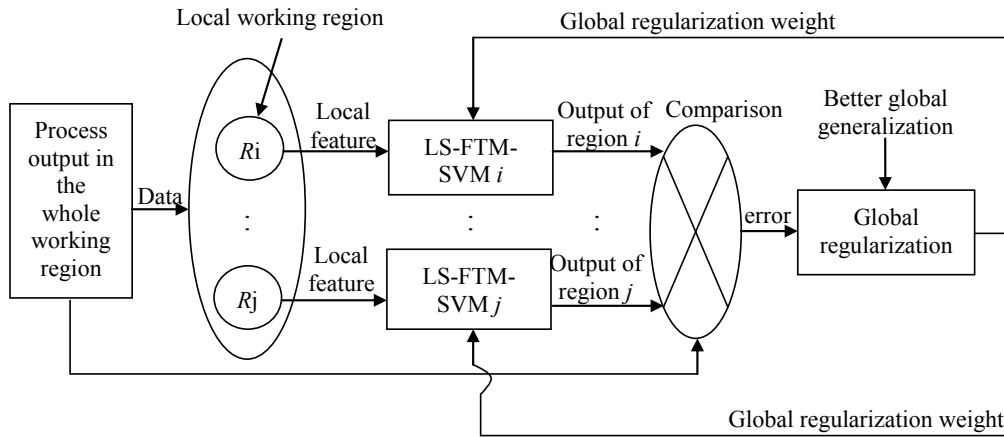


Fig. 2 : Novel LS-SVM modeling method.

### Pseudo code of the LS-FTM-SVM algorithm

A useful classifier called LS-FTM-SVM classifier is proposed in our paper. In our work, a binary classification problem is represented by  $\{(r_1, y_1), (r_2, y_2), \dots, (r_L, y_L)\}$ , where  $r_i \in \{-1, 1\}$  denotes an  $n$ -dimensional data points, for  $i=1, 2, \dots, L$ . The input is given by,

$$D = \{R, Y\} = \{r_i, y_i\}_{i=1}^L \text{ is the training set} \quad (1)$$

The training set divides into two sets are namely as the fuzzy positive training set  $S_f^+$  and the fuzzy negative training set  $S_f^-$ .

The above set following as:

$$S_f^+ = \{r_i, y_i\}_{i=1, \dots, L_p + 1, \dots, L_p + L_n} \text{ and } L_p + L_n = L. \quad (2)$$

Fuzzification of the training set is follows:

$$\mu_i^+ = f_{lim}^{con}(r_i), \mu_i^- = f_{lim}^{con}(r_i) \quad (3)$$

(3) Choose  $i$  such that

$$\mu_i^+ C_2^+ < \mu_i^+ C_1^+ \text{ and } \mu_i^- C_2^- < \mu_i^- C_1^- \quad (4)$$

In the above equation (4), the  $C_1^+$  and  $C_1^-$  are the weights for positive and negative surplus variables, respectively. The restrains for this maximization problem are the same as those in the dual form of the linear case. By means of taking the mean value of  $b^*$ , we can estimate the optimal value of  $b^*$  can follow:

$$b^* = \frac{L_p \sum_{r_i \in A_f^+} + \sum_{j=1}^L a_j y_j k(r_i, r_j) + L_n \sum_{r_i \in A_f^-} \sum_{j=1}^L a_j y_j k(r_i, r_j)}{-L_p L_n} \quad (5)$$

Calculate

$$\sum_{i=1}^L a_i y_i K(r_i, r) + b^* \quad (6)$$

Where  $A_f^+$  and  $A_f^-$  are the subsets of  $S_f^+$  and  $S_f^-$ , respectively.

### Global regularization and parameter optimization

In our proposed method, the global regularization employed in the LS-FTM SVM techniques. Given an input training set  $\{x_{ij}, y_{ij}\}_{i=1, j=1}^{kn}$ , where  $x_{ij}$  and  $y_{ij}$  Are the get input and  $l$  is the output of the local working region, respectively, the optimization problem may be written as:

$$\begin{aligned} & \min_{\omega, \omega_i, e_{ij}} \sum_{i=1}^k \left( \frac{R_i}{2} \|\omega_i\|^2 \right) \\ & + \sum_{i=1}^k \left( \frac{\lambda_i}{2} \|\omega_i - \omega\|^2 \right) + \sum_{i=1}^k \left( \frac{\gamma_i}{2} \sum_{j=1}^n e_{ij}^2 \right) \\ & y_{ij} = \omega_i^T \varphi_i(x_{ij}) + b_i + e_{ij}, j = 1, \dots, n; i = 1, \dots, k \end{aligned} \quad (7)$$

Where  $e$  is the modeling error;  $\omega$  is the global weight vector;  $\sum_{i=1}^k \frac{R_i}{2} \|\omega_i\|^2$  denotes the local regularization that assures the generalization and over-fitting the proposed LS-FTM SVM model in each local region [9].

The proposed model has the following advantages:

1. This method recognizes the local dynamics.
2. The proposed method also locates the interaction between the adjacent local regions and develops the local and global generalization.
3. The method reduces the global error.

In this work, the local and global weight vectors are optimized. The linear SVM classification method is used to transform the optimization problem into a convex optimization problem. This problem can be easily solved by using the proposed method. Let  $v_i = \omega_i - \omega$ , such that  $\omega_i = v_i + \omega$ . The global optimization problem can be written as

$$\begin{aligned} & \min_{\omega, v_i, e_{ij}} \sum_{i=1}^k \left( \frac{R_i}{2} \|\omega + v_i\|^2 \right) \\ & + \sum_{i=1}^k \left( \frac{\lambda_i}{2} \|v_i\|^2 \right) + \sum_{i=1}^k \left( \frac{\gamma_i}{2} \sum_{j=1}^n e_{ij}^2 \right) \\ & y_{ij} = (v_i + \omega)^T \varphi_i(x_{ij}) + b_i + e_{ij}, \\ & j = 1, \dots, n; i = 1, \dots, k \end{aligned} \quad (8)$$

In the above equation (7),  $R$ ,  $\lambda$  and  $\gamma$  are regularization parameters and  $\sum_{i=1}^k \left( \frac{\gamma_i}{2} \sum_{j=1}^n e_{ij}^2 \right)$  is the mentioned the global error which is to minimize the entire working region.

Define

$$\tilde{\omega} = \left[ \sqrt{R_1} (v_1 + \omega)^T, \dots, \sqrt{R_k} (v_k + \omega)^T, \sqrt{\lambda_1} v_1^T, \dots, \sqrt{\lambda_k} v_k^T \right]^T \quad (9)$$

$$\tilde{r}_{ij} = \left[ 0^T, \dots, \frac{x_{ij}^T}{R_i}, \dots, 0^T, 0^T, \dots, \frac{x_{ij}^T}{\sqrt{\lambda_i}}, \dots, 0^T \right]^T \quad (10)$$

Where the  $i$  th and  $(k+i)$  th components of  $\frac{r_{ij}^T}{\sqrt{R_i}}$  and  $\frac{r_{ij}^T}{\sqrt{\lambda_i}}$  respectively.

The equation (7) mentioned optimization problem that may be converted into convex optimization problem follows:

$$\begin{aligned} & \min_{\tilde{\omega}, e_{ij}} J(\tilde{\omega}, e_{ij}) = \frac{1}{2} \|\tilde{\omega}\|^2 + \sum_{i=1}^k \left( \frac{\gamma_i}{2} \sum_{j=1}^n e_{ij}^2 \right) \\ & y_{ij} = \tilde{\omega}^T \tilde{\varphi}_i(\tilde{x}_{ij}) + b_i + e_{ij}, j = 1, \dots, n; i = 1, \dots, k \end{aligned} \quad (11)$$

To solve the optimization equation, a Lagrangian may be written as:

$$\begin{aligned} & \Gamma(\tilde{\omega}, b_i, e_{ij}, a_{ij}) = \\ & J(\tilde{\omega}, e_{ij}) - \sum_{i=1}^k \sum_{j=1}^n a_{ij} \{ \tilde{\omega}^T \tilde{\varphi}_i(\tilde{x}_{ij}) + b_i + e_{ij} - y_{ij} \} \end{aligned} \quad (12)$$

Where  $a_{ij}$  denotes the Lagrange multiplier. The conditions are,

$$\frac{\partial \Gamma}{\partial \tilde{\omega}} = 0, \frac{\partial \Gamma}{\partial b_i} = 0, \frac{\partial \Gamma}{\partial e_{ij}} = 0, \frac{\partial \Gamma}{\partial a_{ij}} = 0. \quad (13)$$

The kernel function is applied by output equations. From the above equation, the resulting of proposed model for function estimation is

$$f(x) = \sum_{i=1}^k \sum_{j=1}^n a_{ij} y_i k(\tilde{r}_i, \tilde{r}_{ij}) + b^* \tag{14}$$

Here,  $\tilde{x} = \left[ 0^T, \dots, \frac{x^T}{\sqrt{\lambda_t}}, \dots, 0^T, 0^T, \dots, \frac{x^T}{\sqrt{\lambda_t}}, \dots, 0^T \right]^T$ ; then  $i$  th an  $(k+i)$  th components of  $\frac{x^T}{\sqrt{\lambda_t}}$  and  $\frac{x^T}{\sqrt{\lambda_t}}$  respectively. In above,  $x$  denotes the  $i$  th region, the other components are zero.

By solving this equation using the proposed LS-FTM-SVM technique, the output  $f(x)$  can be obtained. Our proposed method is solved set of linear equations, then it is computationally less intensive and to improve the modeling accuracy of a strongly nonlinear system compared other SVM methods.

## RESULTS

In this section, LS-FTM-SVM classifier is used to get fault diagnosis result. LS-FTM\_SVM classifier methods require training data sets that are produced using real time simulator. In this work, totally 1365 training data sets are used for training LS-FTM-SVM classifier network. Twelve different fault modes and fault free modes are diagnosed using binary classifiers. The deviation of the testing data from training data is the maximum available within the upper and the lower bounds of the training data set. Totally 428 data sets are used for the testing. In our proposed method is compared with some other local classifier [10] [11]. The architecture and neuron number are designed to achieve high accuracy classification using neural networks. The performances of two classifiers are compared. [Fig. 3] mentioned block diagram of the proposed model.

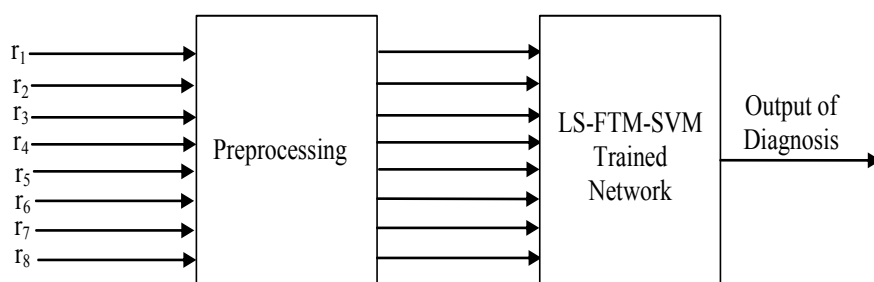


Fig. 3: Block diagram of fault diagnosis using LS-FTM-SVM classification.

Our proposed model used for diagnosing the faults, are prone to concern and practical noises. The uncertainties are due to recognizing fault free model and mathematical equations are possible for practical system. The measurement system has also uncertainty and noises. So, the performance of the proposed method needs to be verified in the presence of noises. The distributed random noise is added during testing and training is done in the absence of noise. The testing data is added with uniformly distributed random noise  $U(-a,a)$ . The magnitude value of 'a' is 5%, 10%, and 20% of the testing value of the absence of noise. The fault diagnosis performance of classifiers is shown in Table.1. It can be noticed from the LS-FTM-SVM based classifier has better accuracy and more robust against noises than the some other classifiers.

Table1: Performance of the proposed classifier

Percentage of Noise	Motor Speed (rpm)	Number of Testing data	Diagnosed Data using LS-FTM-SVM	Diagnosed Data using neural network	Diagnosis Accuracy (%)	
					Local LS-SVM	LS-FTM-SVM
20	200	426	419	412	94.8	94.4
10	400	426	416	410	94.3	96.7
5	700	426	411	403	96.6	98.5
0	900	426	408	382	87.9	99.8

## CONCLUSION

This paper discusses the classifier based fault detection and diagnosis schemes of system by classifying the residual patterns. SVM is a new machine-learning tool for classification, which is powerful for the practical problem with complex system machines. Our proposed method used to diagnose and detect the faults in the induction motor. And also our method is to improve the diagnosis accuracy is compared to some other SVM classifier. The Table.1 mentioned above the percentage of noise is increased and the

diagnosis accuracy will be decreased. The diagnosed fault accuracies have estimated at motor speed 200rpm, 400rpm, 700rpm and 900rpm respectively. The results indicate that the proposed LS-FTM-SVM model can be used in diagnosing induction motor faults.

**CONFLICT OF INTEREST**  
There is no conflict of interest.

**ACKNOWLEDGEMENTS**  
None

**FINANCIAL DISCLOSURE**  
None

## REFERENCES

- [1] Om Prakash Yadav, Dheeraj Joshi, GL Pahuja. [2013] Support Vector Machine based Bearing Fault Detection of Induction Motor. *Indian Journal of Advanced Electronics Engineering*. 1(1):34-39.
- [2] Van Tung Tran, Robert Cattley, Andrew Ball, Bo Liang, Simon Iwnicki. [2013] Fault Diagnosis of Induction Motor Based on a Novel Intelligent Framework and Transient Current Signals. *Chemical Engineering Transactions*.33.
- [3] Md Rifat Shahriar, Tanveer Ahsan and UiPil Chong. [2013] Fault diagnosis of induction motors utilizing local binary pattern-based texture analysis. *Euraship Journal on Image and Video processing*. Springer.29.
- [4] Don-Ha Hwang, Young-Woo Youn, Jong-Ho Sun, Kyeong-Ho Choi , Jong-Ho Lee and Yong-Hwa Kim.[2015] Support Vector Machine Based Bearing Fault Diagnosis for Induction Motors Using Vibration Signals. *J Electr Eng Technol*.10, 30-40.
- [5] Samira Ben Salem, Khmais Bacha, Abdelkader Chaari.[2012] Support Vector Machine-based Decision for Induction Motor Fault Diagnosis using Air-Gap Torque Frequency Response. *International Journal of Computer Applications* (0975 - 8887).38(5).
- [6] Fang Wu, Shen Yin and Hamid Reza Karimi. [2014] Fault Detection and Diagnosis in Process Data Using Support Vector Machines. *Journal of Applied Mathematics*. Hindawi. 2014, Article ID 732104, 9.
- [7] E.M.Cimpoesu, B.D.Ciubotaru, Dan Stefanoiu. [2013] Fault Detection and diagnosis Using Parameter Estimation with Recursive Least Squares. *Conference: Control Systems and Computer Science (CSCS)*.
- [8] Yassine Amirat, Mohamed Benbouzid, Tianzhen Wang, Sylvie Turri. [2014] Performance Analysis of an EEMD-based Hilbert Huang Transform as a Bearing Failure Detector in Wind Turbines.*IEEE ICGE 2014*,193-198.
- [9] Xinjiang Lu, Bi Fan ;Minghui Huang. A Novel LS-SVM Modeling Method for a Hydraulic Press Forging Process With Multiple Localized Solutions. *Industrial Informatics, IEEE Transactions on* 11(3): 663 - 670.
- [10] Mahendra Kumar, I.N.Kar. Fault Diagnosis of an Air-Conditioning system Using LS-SVM". *Springer*. 5909:555-560.
- [11] Xinli Wang , Jiangang Lu , Qinmin Yang , Wenjian Cai . [2013] Performance evaluation of packed tower liquid desiccant dehumidifier based on LSSVM. *Control and Automation (ICCA), 2013 10th IEEE International Conference on*. 987 - 990.

## ARTICLE

# SYNCHRONIZED ROBUST AUDIO WATERMARKING BASED ON FWHT

N.V. Lalitha<sup>1\*</sup>, Ch. Srinivasa Rao<sup>2</sup>, PVY. JayaSree<sup>3</sup>

<sup>1</sup>Dept. of Electronics and Communication Engineering, GMR Institute of Technology, Rajam, A.P. INDIA

<sup>2</sup>Dept. of Electronics and Communication Engineering, JNTU-K University, Vizianagaram, A.P. INDIA

<sup>3</sup>Dept. of Electronics and Communication Engineering, GIT, GITAM University, Visakhapatnam, A.P. INDIA

### ABSTRACT

Digital audio watermarking is the key solution to provide copyright protection and copy protection. Many watermarking schemes are available in the literature but these fail either in providing imperceptibility or robustness or synchronization. The watermarking scheme based on Fast Walsh Hadamard Transform (FWHT) with a synchronization code is proposed in this paper. Digital audio is segmented into two parts; synchronization code is inserted in the first part and Gaussian map encrypted watermark is embedded into the FWHT coefficients of digital audio in the second part. The experimental results on a standard database demonstrate that the proposed scheme has imperceptibility of 23.30 dB to 29.83 dB, payload is 1638.4 bps and Gaussian map is used to provide security to the watermark. As well, our watermarking scheme resists desynchronization attacks such as Signal addition, Subtraction, Cropping and Time Scale Modification (TSM) attack up to  $\pm 5\%$ . The scheme also withstands echo attack in a better manner when compared with state-of-art schemes.

### INTRODUCTION

Digital audio watermarking can be used successfully for audio copyright protection and copy protection. Based on state-of-art, audio watermarking techniques are broadly classified into two types: time domain [1] and frequency domain techniques [2]. Time domain techniques are simple but less robust to signal processing attacks. Frequency domain techniques are somewhat complex and it provides robustness to signal processing attacks [3]. Synchronization attacks are the major issue in digital audio watermarking [4], ex: cropping, signal addition, signal subtraction and Time Scale Modification (TSM). Many state of art audio watermarking algorithms are available but have not reported synchronization attack [5-8] and few algorithms have reported synchronization attack [9-13]. Major contribution of our work is to provide robustness against desynchronization attacks and mainly concentrated on TSM attack. Robustness is also provided to signal processing attacks and more light is thrown on echo-attack. In this paper, audio is segmented; synchronization code and watermark both are inserted in each segment. Fast Walsh Hadamard Transform (FWHT) [14] is used for insertion of scrambled watermark image with the help of Quantization Index Modulation (QIM) [15-16] method to provide blind extraction. Due to FWHT, computational complexity is reduced [17] and it is much faster than the FFT.

### MATERIALS

Walsh-Hadamard transform (WHT) is a non-sinusoidal, orthogonal transformation technique. The signal is decomposed with a set of basis functions called Walsh functions which are rectangular or square waves with values of +1 or -1. WHT returns sequency values. The fast version of WHT is Fast Walsh-Hadamard Transform (FWHT). FWHT is faster to calculate because it uses only real additions and subtractions requires less storage space, while the FFT requires complex values and more storage space. The FWHT is able to represent signals with sharp discontinuities more accurately using fewer coefficients than the FFT. Due to its symmetric property, the calculation process of both FWHT and the inverse FWHT is similar. The FWHT and IFWHT for a signal  $x(n)$  of length  $N$  are defined in equations (1)-(2):

$$y(n) = \frac{1}{N} \sum_{i=0}^{N-1} x(i)WAL(n,i) \quad \dots (1)$$

$$x(n) = \frac{1}{N} \sum_{i=0}^{N-1} y(i)WAL(n,i) \quad \dots (2)$$

where  $i = 0, 1, \dots, N - 1$  and  $WAL(n,i)$  is Walsh function.

### PROPOSED AUDIO WATERMARKING METHOD

In this proposed work, total audio 'A' is divided into segments for synchronization code and watermark insertion. With the help of logistic chaotic sequence, synchronization code is generated and it is inserted at the starting of each segment. For increasing the security, watermark must be pre-processed with the help of Gaussian map encryption method.

#### KEY WORDS

Audio Watermarking,  
Synchronization, Fast Walsh  
Hadamard Transform, Time  
Scale Modification

Published: 2 December 2016

#### \*Corresponding Author

Email:  
lalithanarla.ece@gmail.com  
lalitha.nv@gmrit.org  
Tel.: +91-9985001587

### Synchronization code generation

To overcome the problem of synchronization attacks in audio watermarking process, synchronization code must be inserted before the watermark. In the literature, synchronization code is generated using Bernoulli shift map [9], Piece-Wise Affine Markov (PWAM) map [12], Barker code [18-19]. In this paper, to generate  $L_{syn}$  length synchronization code, logistic chaotic method is used.

$$L_{n+1} = \gamma L_n (1 - L_n) \quad \dots (3)$$

Where  $L_n$  is the initial value in the range  $0 < L_n < 1$  and  $\gamma$  is the real parameter.

$$S_n = \begin{cases} 1 & \text{if } L_n > 0.5 \\ 0 & \text{otherwise} \end{cases} \quad \dots (4)$$

Where  $S_n$  is the synchronization code and  $n$  is varies from 1 to  $L_{syn}$ .

### Watermark image pre-processing

In this paper,  $M \times M$  size watermark image is pre-processed with the help of Gaussian map chaotic encryption method, to increase the security and it is defined as follows:

$$P_{n+1} = e^{(-\alpha P_n^2)} + \beta \quad \dots (5)$$

Where  $P_n$  is the initial value in the range of 0 to 1.  $\alpha$  and  $\beta$  are the real parameters.

$$G_n = \begin{cases} 1 & \text{if } P_n > \frac{1}{4} \\ 0 & \text{otherwise} \end{cases} \quad \dots (6)$$

$M \times M$  size watermark image is converted to one-dimensional vector  $W_n$  and this is encrypted with  $G_n$  with the help of below equation.

$$E_n = G_n \oplus W_n \quad \dots (7)$$

### Watermark embedding process

The  $L_{syn}$  length synchronization code followed by  $M \times M$  size pre-processed watermark image is embedded into the audio signal is shown in [Fig.1].

Embedding procedure steps are given below:

Step 1: Digital audio signal is segmented and each segment length depends on size of the image and length of the synchronization code.

Step 2: Each segment is again divided into two parts.

Step 3: Synchronization code is generated and inserted directly into the first part, pre-processed watermark is embedded into FWHT coefficients of the second part, using QIM method is as follows:

$$e(i) = \begin{cases} \text{round} \left[ \frac{x(i)}{Q} \right] Q, & \text{if } E_i = 0 \\ \left( \text{floor} \left[ \frac{x(i)}{Q} \right] Q \right) + \frac{Q}{2}, & \text{if } E_i = 1 \end{cases} \quad \dots (8)$$

Where  $x(i)$  is direct audio sample for part 1, Fast Walsh Hadamard transformed audio coefficient for part2,  $Q$  is the embedding strength and  $e(i)$  is the embedded coefficient of corresponding audio coefficient.

Step 4: For part 2 Inverse Fast Walsh Hadamard Transform is applied, resultant part1 and part 2 segments are combined to get watermarked audio segment.

Step 5: Repeat the steps 2 to 4 for all the segments and combined them to get watermarked audio.



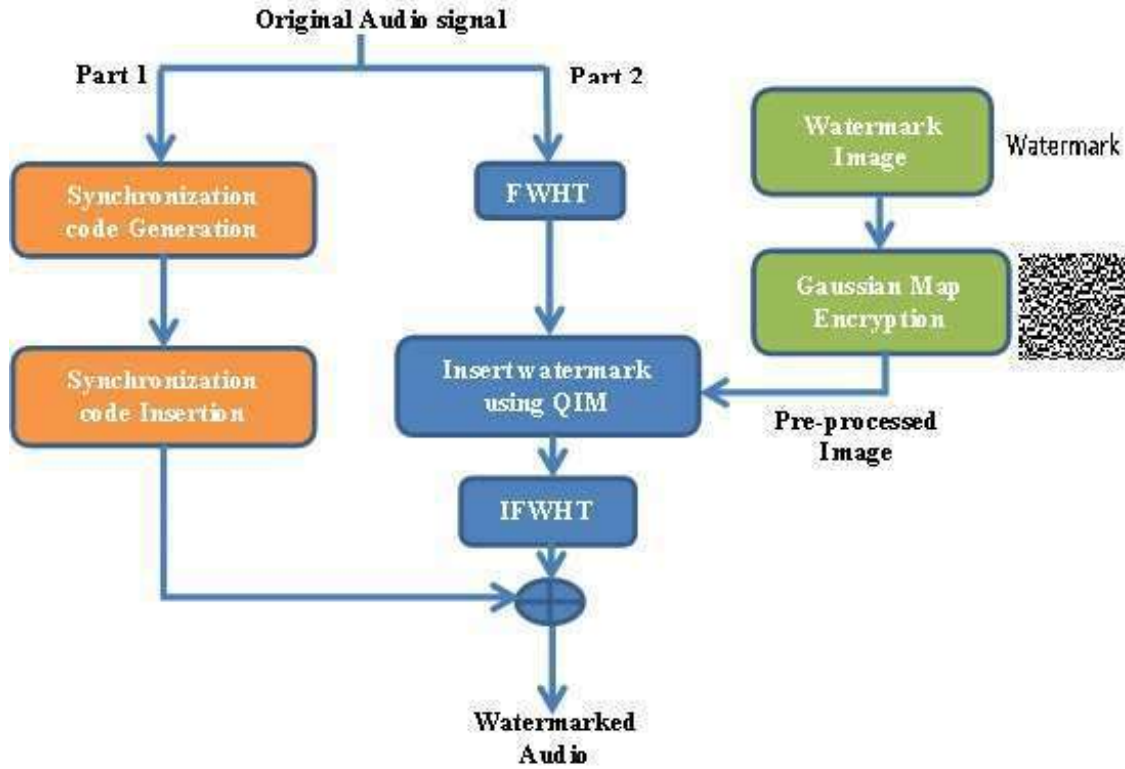


Fig. 1: Process flow of Watermark and Synchronization Code Embedding.

### Watermark extracting process

De-synchronization attack dislocates the watermark. To identify the correct position of watermark, synchronization code is inserted into the time-domain. The watermark extraction steps are given below:  
Step 1: Search for the synchronization code in the watermarked audio with the help of below equation.

$$S'_n = \begin{cases} 1 & \text{if } \frac{Q}{4} \leq x'(n) \leq \frac{3Q}{4} \\ 0 & \text{otherwise} \end{cases} \quad \dots (9)$$

Where  $S'_n$  is the extracted synchronization code and  $x'(n)$  is attacked watermarked audio.

Step 2: Calculate the similarity between extracted and original synchronization code with the help of below equation.

$$NC = \frac{\sum_{k=1}^n S_n(k)S'_n(k)}{\sqrt{\sum_{k=1}^n S_n(k)^2} \sqrt{\sum_{k=1}^n S'_n(k)^2}} \quad \dots (10)$$

If the similarity is above the threshold, the samples after the synchronization code contains valid watermark.

Step 3: Apply FWHT on those samples of size  $M \times M$ .

Step 4: Extract the binary sequence from the FWHT coefficients.

$$E'_n = \begin{cases} 1 & \text{if } \frac{Q}{4} \leq \text{mod}(y'(n), Q) < \frac{3Q}{4} \\ 0 & \text{otherwise} \end{cases} \quad \dots (11)$$

Where  $y'(n)$  is FWHT coefficient and  $E'(n)$  is the extracted binary sequence.

Step 5: Apply Gaussian map decryption process, to extract the binary image.

### RESULTS

Four different audio signals of 10 seconds i.e. pop, rock, jazz, folkcountry [20] are considered to evaluate the performance of the proposed algorithm based on FWHT. The frequency and quantization rates of mono

audio signals are 44,100 KHz and 16-bits per sample respectively. 128 X 128 binary image is considered as a watermark image. 128 bit synchronization code is inserted to resist the de-synchronization attacks. To assess the performance of the proposed algorithm, two performance metrics are used i.e. imperceptibility and robustness.

### Imperceptibility

Imperceptibility means perceptual quality measure. SNR is used to assess the imperceptibility between original audio and embedded audio.

$$SNR = \frac{\sum_{n=1}^L x^2(n)}{\sum_{n=1}^L (x(n) - x'(n))^2} \quad \dots (12)$$

Where  $x(n)$  is the original audio signal,  $x'(n)$  is the embedded audio signal and L is the length of the audio. It is evident from [Table 1] that SNR ranges from 23.3080 dB to 29.8364 dB for the four signals and meets the IFPI requirement.

**Table 1:** SNR values for different audio signals

Type of an audio signal	SNR in dB
POP Music	23.3080
ROCK Music	24.7160
JAZZ instrumental audio	24.8193
FOLK COUNTRY	29.8364

### Robustness

Robustness means ability to extract the watermark even after the attacks are applied on watermarked audio signal. Generally, these attacks are signal processing operations. Some signal processing attacks that are evaluated in this paper are: (a) Resample: Watermarked audio sampling frequency 44.1KHz is sampled to 22.05 KHz and then resampled to 44.1 KHz. (b) Lowpass filter: Watermarked signal is passing through lowpass filter with cut-off frequency 16 KHz. (c) Requantization: 16-bit watermarked audio is first quantized with 8-bit then requantized back with 16-bit. (d) Random Noise: Random noise with 40dB SNR is applied to Watermarked signal. (e) & (f) Additive White Gaussian Noise: 60dB and 50dB AWGN is applied. (g), (h) and (i) Jittering: one sample is removed in every 100000, 50000 and 10000. (j) Invert: Watermarked audio sample amplitudes are inverted.

To calculate the robustness over signal processing attacks, a performance measure BER is used with the help of below equation.

$$\text{Bit Error Rate (BER)} = \frac{\text{Number of error bits}}{\text{Total number of bits}} \quad \dots (13)$$

**Table 2:** BER for four classes of audio signals

Attack	(a)	(b)	(c)	(d)	(e)	(f)	(g)	(h)	(i)	(j)
POP	0.2363	0.2473	0.0040	0	0	0.0412	0	0	0.4542	0
ROCK	0.3397	0.3739	0.0051	0	0	0.0427	0	0	0.4915	0
JAZZ	0.2415	0.1750	0.0039	0.00006	0	0.0445	0	0	0.4238	0
FOLK COUNTRY	0.3480	0.4333	0.0050	0	0	0.0432	0	0	0.4894	0

[Table 2] shows the robustness in terms of BER for different attacks mentioned as (a) to (j). Some de-synchronization attacks are also applied to check the resistance of the algorithm over these. These de-synchronization attacks are signal addition, signal subtraction, cropping (starting, middle, ending), Time Scale Modification (-5% to +5%). In our work, more concentration is paid for de-synchronization attacks and the performance in terms of BER, Precision and CC are given in [Table 3].

**Table 3:** Robustness for Desynchronization Attacks

Type of Audio	Type of attack	Without Synchronization			With Synchronization		
		BER	Precision	CC	BER	Precision	CC
POP	Signal addition	0.2007	0.7993	0.2698	0	1	1
	Signal subtraction	0.2007	0.7993	0.2698	0	1	1
	Start cropping	0.1630	0.8370	0.3595	0	1	1

	Middle cropping	0	1	1	0	1	1
	End cropping	0	1	1	0	1	1
	TSM (-5%)	0.5049	0.4951	0.0043	0.4235	0.5765	0.0445
	TSM (-4%)	0.4980	0.5020	-0.0007	0	1	1
	TSM (-3%)	0.4969	0.5031	-0.0051	0	1	1
	TSM (-2%)	0.4969	0.5031	-0.0051	0	1	1
	TSM (-1%)	0.4969	0.5031	-0.0051	0	1	1
	TSM (+1%)	0.4969	0.5031	-0.0051	0	1	1
	TSM (+2%)	0.4997	0.5003	0.0012	0	1	1
	TSM (+3%)	0.4988	0.5012	0.0090	0	1	1
	TSM (+4%)	0.4950	0.5050	-0.0048	0	1	1
	TSM (+5%)	0.5065	0.4935	-0.0055	0.3333	0.6667	0.1385
ROCK	Signal addition	0.0356	0.9644	0.7263	0	1	1
	Signal subtraction	0.0358	0.9642	0.7257	0	1	1
	Start cropping	0.0244	0.9756	0.7816	0	1	1
	Middle cropping	0	1	1	0	1	1
	End cropping	0	1	1	0	1	1
	TSM (-5%)	0.4999	0.5001	-0.0096	0.3383	0.6617	0.1314
	TSM (-4%)	0.4999	0.5001	-0.0096	0	1	1
	TSM (-3%)	0.4999	0.5001	-0.0096	0	1	1
	TSM (-2%)	0.4999	0.5001	-0.0096	0	1	1
	TSM (-1%)	0.4999	0.5001	-0.0096	0	1	1
	TSM (+1%)	0.4981	0.5019	0.0046	0	1	1
	TSM (+2%)	0.5087	0.4913	-0.0038	0	1	1
TSM (+3%)	0.5016	0.4984	-0.0071	0	1	1	
TSM (+4%)	0.4972	0.5028	-0.0036	0	1	1	
TSM (+5%)	0.4993	0.5007	0.0062	0.3766	0.6234	0.1082	
JAZZ	Signal addition	0.0786	0.9214	0.5598	0	1	1
	Signal subtraction	0.0786	0.9214	0.5599	0	1	1
	Start cropping	0.0566	0.9434	0.6302	0	1	1
	Middle cropping	0	1	1	0	1	1
	End cropping	0	1	1	0	1	1
	TSM (-5%)	0.5043	0.4957	-0.0083	0.3998	0.6002	0.0813
	TSM (-4%)	0.4987	0.5013	-0.0075	0	1	1
	TSM (-3%)	0.4960	0.5040	-0.0089	0	1	1
	TSM (-2%)	0.4966	0.5034	-0.0028	0	1	1
	TSM (-1%)	0.4997	0.5003	-0.0052	0	1	1
	TSM (+1%)	0.4997	0.5003	-0.0052	0	1	1
	TSM (+2%)	0.4997	0.5003	-0.0052	0	1	1
TSM (+3%)	0.4997	0.5003	-0.0052	0	1	1	
TSM (+4%)	0.4987	0.5013	-0.0075	0	1	1	
TSM (+5%)	0.4926	0.5074	-0.0021	0.3867	0.6133	0.0768	
FOLKCOU NTRY	Signal addition	0.0997	0.9003	0.5156	0	1	1
	Signal subtraction	0.0997	0.9003	0.5156	0	1	1
	Start cropping	0.0908	0.9092	0.5199	0	1	1
	Middle cropping	0	1	1	0	1	1
	End cropping	0	1	1	0	1	1
	TSM (-5%)	0.5027	0.4973	0.0079	0	1	1
	TSM (-4%)	0.5016	0.4984	-0.0071	0	1	1
	TSM (-3%)	0.5016	0.4984	-0.0071	0	1	1
	TSM (-2%)	0.5016	0.4984	-0.0071	0	1	1
	TSM (-1%)	0.5016	0.4984	-0.0071	0	1	1
	TSM (+1%)	0.5016	0.4984	-0.0071	0	1	1
	TSM (+2%)	0.5001	0.4999	0.0090	0	1	1
TSM (+3%)	0.4969	0.5031	-0.0051	0	1	1	
TSM (+4%)	0.5001	0.4999	0.0122	0	1	1	
TSM (+5%)	0.4962	0.5038	0.0065	0.3507	0.6493	0.1138	

In [9], the authors analyzed TSM attack upto  $\pm 1\%$ , TSM attack upto  $+4\%$  in [10] and upto  $\pm 1\%$  in [12] is reported. As well the robustness against echo attack is compared with other state-of-art methods and is tabulated in Table 4.

**Table 4:** Echo attack analysis w.r.t BER

Echo Attack	Existing Methods	Proposed
Delay 100ms Decay 50 %	Ali Al-Haj (2014) [13] -- 0.748	0.0299
Delay 100ms Decay 40 %	Ali Al-Haj (2014) [13] -- 0.731	0.0268
Delay 10ms Decay 10 %	B.Lei et al. (2012) [9] -- 0.007	0.0118
Delay 98ms Decay 41 %	V.Bhat K at al (2010) [11] -- 0.020	0.0292
Delay 1s Decay 10 %	B.Lei et al. (2013) [21] -- 0	0

## Data Payload

Data payload means the number of bits that are embedded and extracted from the audio stream. It is measured in bits per second (bps). In this paper,  $128 \times 128 = 16384$  bits are embedded into 10 sec audio signal. So, data payload in this scheme is 1638.4 bps.

## CONCLUSION

Many of the watermarking schemes fail either in providing imperceptibility or robustness or synchronization. To overcome this, a watermarking scheme based on Fast Walsh Hadamard Transform (FWHT) with a synchronization code is proposed in this paper. Sequency and symmetric properties of FWHT are exploited to make the scheme to be more robust with less computational effort. The experimentation is performed on a standard database and imperceptibility of 23.30 dB to 29.83 dB and a payload of 1638.4 bps are achieved. Gaussian map is used to provide security to the watermark. The use of synchronization code can resist desynchronization attacks such as Signal addition, subtraction, Cropping and Time Scale Modification (TSM) attack up to  $\pm 5\%$ . The scheme is also robust to echo attack in a better manner when compared with state-of-art schemes.

### CONFLICT OF INTEREST

None

### ACKNOWLEDGEMENTS

None

### FINANCIAL DISCLOSURE

None

## REFERENCES

- [1] Bassia P, Pitas I, Nikolaidis N. [2001] Robust audio watermarking in the time domain, IEEE Transactions on Multimedia, 3(2):232-241.
- [2] Wu S, Huang J, Huang D, Shi YQ. [2005] Efficiently self-synchronized audio watermarking for assured audio data transmission, IEEE Trans. Broadcasting, 51(1):69-76.
- [3] Al-Haj A, Mohammad A, Bata L. [2011] DWT-Based Audio Watermarking, The International Arab Journal of Information Technology, 8(3):326-333.
- [4] Bhat KV, Sengupta I, Das A. [2010] An adaptive audio watermarking based on the singular value decomposition in the wavelet domain, Digital Signal Processing, 20:1547-1558.
- [5] Dhar PK, Shimamura T. [2014] Audio watermarking in transform domain based on singular value decomposition and Cartesian-polar transformation, International Journal of Speech Technology, 17:133-144.
- [6] Fallahpour M, Megias D. [2014] Secure logarithmic audio watermarking scheme based on the human auditory system, Multimedia Systems, 20:155-164.
- [7] Wang J, Healy R, Timoney J. [2011] A robust audio watermarking scheme based on reduced singular value decomposition and distortion removal, Signal Processing, 91:1693-1708.
- [8] Hu HT, Hsu LY. [2016] Incorporating Spectral Shaping Filtering into DWT-Based Vector Modulation to Improve Blind Audio Watermarking, Wireless Personal Communications, :1-20.
- [9] Lei B, Soon IY, Zhou F, Li Z, Lei H. [2012] A robust audio watermarking scheme based on lifting wavelet transform and singular value decomposition, Signal Processing, 92:1985-2001.
- [10] Lei BY, Soon IY, Li. [2011] Blind and robust audio watermarking scheme based on SVD-DCT, Signal Processing, 91:1973-1984.
- [11] M.Fallahpour, D.Megias, [2015] Audio Watermarking Based on Fibonacci Numbers, IEEE/ACM Transactions on Audio, Speech and Language Processing, 23(8):1273-1282.
- [12] Lei B, IYSoon, Tan E, [2013] Robust SVD-Based Audio Watermarking Scheme With Differential Evolution Optimization, IEEE Transactions on Audio, Speech and Language processing, 21(11):2368-2378.
- [13] Ali Al-Haj, [2014] A dual transform audio watermarking algorithm, Multimedia Tools and Applications 73: 1897-1912.
- [14] Beauchamp KG. [1984] Applications of Walsh and Related Functions: with an Introduction to Sequency Theory, Academic Press, :295-300, London
- [15] Bhat KV, Sengupta I, Das A.[2008] Audio Watermarking Based on Quantization in Wavelet Domain. In: Lecture Notes in Computer Science,5352:235-242.
- [16] Chen B, Wornell G. [2001.] Quantization Index Modulation: A class of provably good methods for digital watermarking and information embedding, IEEE Transactions on Information Theory, 47:1423-1443,
- [17] Dhavale SV, Deodhar RS, Patnaik LM. [2011] Walsh Hadamard Transform Based Robust Blind Watermarking for Digital Audio Copyright Protection, Communications in Computer and Information Science, 250:469-475.
- [18] Zhao H, Wang F, Chen Z, Liu J. [2014] A Robust Audio Watermarking Based on SVD-DWT, Elektronika Ir Elektrotechnika, Vol.20, No.1, pp. 75-80,.
- [19] Wang XY, Zhao H, [2006] A Novel Synchronization Invariant Audio Watermarking Scheme Based on DWT and DCT. IEEE Transactions on Signal Processing, 54(12):4835-4840.
- [20] <http://www-ai.cs.uni-dortmund.de/audio.html>
- [21] B Lei, IY Soon, Ee-Leng T. [2013] Robust SVD-Based Audio Watermarking Scheme with Differential Evolution Optimization. IEEE Transactions on Audio, Speech and Language Processing, 21(11).

ARTICLE

# FEED FORWARD WITH BACK PROPAGATION (FFBP) CLASSIFICATION FOR FINDMELANOCYTES IN THE SKIN EPIDERMIS AREA

E Kaveri\*, T Chakravarthy, PV Arivoli

Department of Computer Science, A.V.V.M. Sri Pushpamcollege, Poondi, Tanjore, INDIA

## ABSTRACT

One of the most modern assessments of medical research is dermatology that concerned with the skin disease treatment and diagnosis. Skin disease detection process develops one of the key issues in image processing operation and the necessary skin image classification system required for early detection of skin diseases. However in skin diseases finding process has one of the major problems which is analyzing the melanocytes in the skin epidermis area due the reason is the melanocytes are very similar to keratinocytes. Thus, in this paper proposes an efficient a melanocytes diagnosis system using image processing operation. The texture analysis of skin histopathological images such as Asymmetry, Border Irregularity, Color, Diameter, Evolving(ABCDE) is used for image feature extraction process with the help of Gray Level Co-occurrence Matrix (GLCM). Before done the feature extraction process the noises are removed by using Gaussian Filter and Dull Razor filter then segmentation is done with the help of Edge-Based Technique and finally, classification is done by using Feed Forward with Back Propagation (FFBP) pixel-wise classification using supervised learning rule such as Delta learning rule. The FFBP classifier that uses a feature space derived from texture analysis values. The experimental results shows that the effectiveness of proposed system to enhance the melanocytes recognition with higher accuracy as well as accurately identified melanocytes area.

## INTRODUCTION

Skin cancer is one of the most malignant and frequent sort of skin cancer and most aggressive types of skin cancer is melanoma [1]. The early detection of melanoma is vital to reduce this cancer mortality [2] [3]. Different kinds of techniques are used to dynamically diagnosis the melanoma and different kinds of authors are presented their proposed techniques in different ways. One of the emerging technique is confocal microscopy this technique can give pathological examination and initial diagnosis process and a cellular level view of the disease is processed by using the histopathology sides.

Basically the skin anatomy has two fundamental layers such as dermis (the inner layer) and epidermis (the outer layer). Typically the outer layer such as epidermis is made up of round cells named basal cells, scale-like cells name squamous cells, and flat. The epidermis comprises melanocytes which are in lower part of skin. The melanocytes are noting but pigment cell that are found in the produce melanin and epidermis, the pigment which provides the skin its real color. When the skin is showed to the sun, high pigments are produced by the melanocytes which cause the skin to darken or bronzed is direct to cause melanoma which is can be of Malignant or Benign. The melanoma cancer is cause by abnormal growths of melanocyte which spreads or invades to other parts of body with abnormal control. The melanoma is divided into Acral Lentiginous Melanoma, Lentigo malignant Melanoma, Nodular Melanoma and Superficial Spreading Melanoma. Thus, to minimize the death rate essential to diagnose at this early stage. Thus, in this paper proposes an efficient a melanocytes diagnosis system using image processing operation. The texture analysis of skin histopathological images such as Asymmetry, Border Irregularity, Color, Diameter, Evolving(ABCDE) is used for image feature extraction process with the help of Gray Level Co-occurrence Matrix (GLCM). Before done the feature extraction process the noises are removed by using Gaussian Filter and Dull Razor filter then segmentation is done with the help of Edge-Based Technique and finally, classification is done by using Feed Forward with Back Propagation (FFBP) pixel-wise classification using supervised learning rule such as Delta learning rule. The FFBP classifier that uses a feature space derived from texture analysis values.

## RELATED WORK

Author [4] proposes a method named as Human skin detection method. For this the skin image preprocessing and smoothing approaches are combined and skin image's RGB mean values that combine to 2-D histograms and GAUSSIAN method. This approach is makes use of automatic detection of color skin medical image. The experimental result shows that the Gaussian method obtains the promising result in over human skin detection.

Author [5] proposes a system for skin melanoma analyzing by using histopathological image. In epidermis area finding the melanocytes in epidermis is a significant process and difficult process also. Thus, author proposes a novel technique for detection of the melanocytes in epidermis area. The proposed technique based on radial line scanning, this process is used for estimated the halo region and from all the keratinocytes has to detect melanocytes is this process by using nuclei approach. Experimental evaluation based on 40 different histopathological images it comprises 341 melanocytes and the experimental results are showing a superior performance.

### KEY WORDS

Skin Diseases, Texture Analysis, Edge-Based Technique, ABCDE feature extraction, Feed Forward with Back Propagation (FFBP), Gaussian Filter, Delta learning rule and Dull Razor filter, Gray Level Co-occurrence Matrix (GLCM).

Published: 2 December 2016

\*Corresponding Author  
Email:  
ekaveri125@gmail.com



Melanoma is sort of dangerous skin disease; it can be diagnosed only in its early stage but using normal conventional dermatological approach is difficult one. Thus, author [6] proposes an image processing approach by using an efficient segmentation algorithm named a radial search method to obtain the true of lesion region in dermoscopy skin images. The thresholding method is applied in segmentation process and finds the edge using radial search process. The radial search approach is called as semiautomatic method and it's requires the manual initialization to start the process. Finally the three types of features are extracted from the segmented image such as border, color and asymmetry.

Author [7] proposes method for recognizing human skin diseases by using automated system based on texture analysis. The spatial distributions of hemoglobin and melanin in human skin are divided by independent component. The texture features are obtained from Gray Level Run Length Matrices. Finally, the classification process is done by using Minimum Distance Classifier. The experimental result are using DERMNET database which contain 350 images and recognition rate show the promising results in term of classification.

Author [8] presents a novel approach for skin cancer analysis and detection from the cancer affected image. The image enhancement and denoising process by using Wavelet Transformation and the Asymmetry, Border irregularity, Color, Diameter (ACBD) rules are used for histogram analysis. Finally, the classification process is done by using Fuzzy inference system. The pixel color is used for determine the final decision of skin cancer type, decision may be two stages like malignant stage and begin stage of skin cancer.

### Skin image classification

This section provides an overview of the proposed method for identifying the melanoma skin cancer with the help of differentiating the melanocytes and keratinocytes. The step by step process of the proposed approach is presented in [Fig.1].

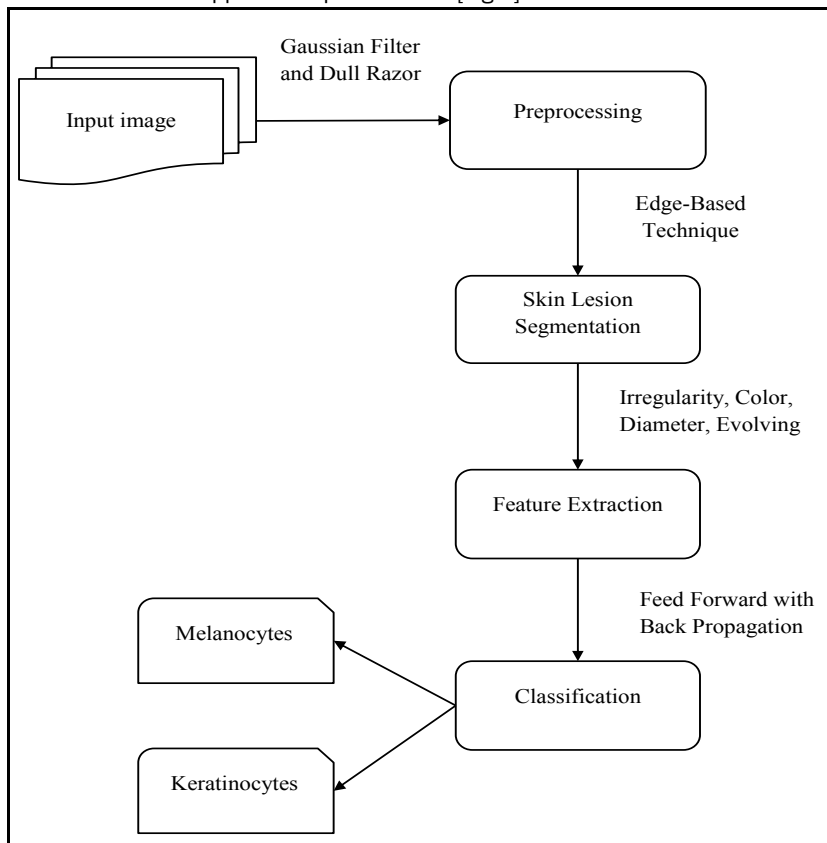


Fig. 1: Skin image classification.

#### Preprocessing

The main objective of pre-processing is to improve the given image quality and remove unwanted noise and effects from the image which is contain three different kinds of processes [9].First stage in the skin cancer detection system is the skin image. The skin image is in digital format is given as input to the system. Next stage is preprocessing which includes denoising and hairs removal.

In this work useGaussian Filter and Dull Razor filter for noise removing and hair removing operation. After preprocessing the image is directed to the segmentation process which is used to separates the normal skin from suspicious lesion [10] [11]. There are some specific features used to differentiate the



melanocytes and keratinocytes part in the skin image. Asymmetry, Border Irregularity, Color, Diameter, Evolving (ABCDE) based feature extraction process is done here.

### Hair removal

The Dull Razor filter is used for hair removal operation in given color image which replaced the hair pixels by neighboring pixels is process is as follows.

### Dull razor algorithm

#### Input

Skin images with hair.

#### Output

Skin images without hair.

The images obtained in RGB color format with 256\*512 sizes. The RGB images are changed into gray color image utilizing the following transformation

$$Gray = 0.2989 * R + 0.5870 * G + 0.1140 * B \quad (4.1)$$

In preprocessing stage the average filter is used, average filter is a low pass filter and is considerably easy for de-noising the images. The function of average filter is computed as

$$g(x, y) = 1/M \sum_{(x,y) \in S} f(x, y) \quad (2)$$

Where  $S$  denotes neighborhood of pixel  $(x,y)$  and  $M$  denotes the number of pixels in neighborhood  $S$ .

Step 1: It recognizes the dark hair locations by a formalized gray-scale morphological closing operation. Closing operation simply defined as dilation after erosion process utilizing the same structuring element for both process. The main input of this process is a given image is to be a structuring element and closed. The process of a graylevel dilation followed by graylevel erosion is defined as Graylevel closing.

$$f \cdot b = (f \oplus b) \ominus b \quad (3)$$

Step 2: The about equation is used to differentiate the hair pixels shapes as long and thin structure, and substitutes the verified pixels by a bilinear interpolation. [Fig. 2] shows the effects of filling in closing gaps and holes which describe as closing operation.

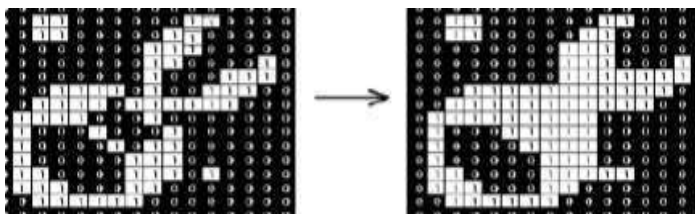


Fig. 2: Closing operation.

Step 3: After that start the smooth operation for replaced hair pixels with an adaptive median filter is defined as follows

$$f_{(i,j)}^{(n)} = \int_{(i,j)}^{(n-1)} \text{if } |X_n^{(n-1)} - m_{ij}^{(n-1)}| < T \quad (4)$$

Where,  $T$  is defined as pre-defined threshold value. The impulse detection process senses the noise even at great exploitation level setting which means here use the flag matrix value as 1 wherever noise occurs. Final Dull Razor Filter operation results is shown in [Fig. 3].

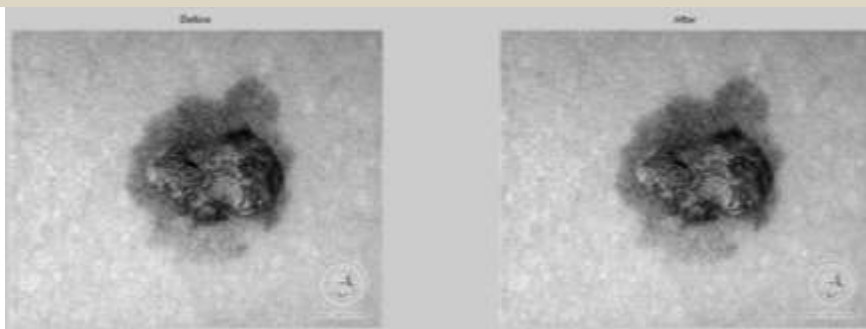


Fig. 3: Dull razor filter.

### Gaussian filter

Assume the Gaussian parameters are Kis signified as the number of distributions,  $\omega_{(i,t)}$  is a weight associated to the  $i^{\text{th}}$  standard deviation  $\Sigma_{(i,t)}$  values with Gaussian at time  $t$  and mean  $\mu_{(i,t)}$ ,  $\eta$  is signified as a density function of Gaussian probability is formulated by using follows equation

$$\eta(X, \mu, \Sigma) = \frac{1}{(2\pi)^{n/2} |\Sigma|^{1/2}} e^{-\frac{1}{2}(X-\mu)\Sigma^{-1}(X-\mu)} \quad (5)$$

Assume that the skin image RGB color features of are independent and it have the some identical differences. Thus, the closing operation matrix is defined as follows

$$\Sigma_{i,t} = \sigma_{i,t}^2 I \quad (6)$$

At the end of this process got noise removed skin image is as shown in [Fig. 4].

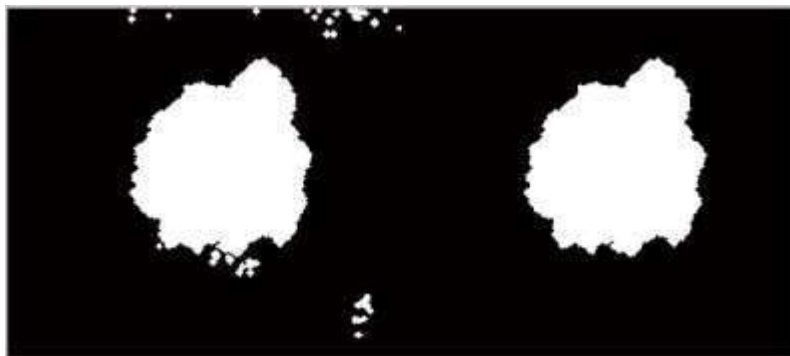


Fig. 4: Before and after gaussian filter.

### Edge-based technique

After the preprocessing work segmentation process start with the help of Edge-Based Technique which is segmented based on specific edge regions by finding the edge pixels and which is connect by using contours[12]. Basically, the boundaries are characterize by edge, the edge is gratefully helpful in process with boundaries and regions and as an edge point is transition given gray level skin image which is liked with a point [13]. Typically, the edges happened on the boundary between two different kinds of regions. Here have to consider the gradient point in the edge direction which is pixel's intensity is increases rapidly. The image gradient is defined as follows

$$\nabla f = \left[ \frac{\partial f}{\partial x}, \frac{\partial f}{\partial y} \right] \quad (7)$$

The edge strength is provided by the gradient magnitude

$$\|\nabla f\| = \sqrt{\left(\frac{\partial f}{\partial x}\right)^2 + \left(\frac{\partial f}{\partial y}\right)^2} \quad (8)$$

The gradient direction is computed by using following equation

$$\theta = \tan^{-1} \left( \frac{\partial f / \partial y}{\partial f / \partial x} \right) \quad (9)$$

Asymmetry, border irregularity, color, diameter (ACBD)

There are some identical features that differentiate melanocytes and keratinocytes for finding benign melanoma or malignant melanoma which task is used to find the feature vector. Here, use three sorts of feature such as texture, shape and color with the help of Asymmetry, Border irregularity, Color, Diameter (ACBD) using Gray Level Co-occurrence Matrix (GLCM).

Table 1: GLCM structure properties

Contrast	$\sum_{r=1, c=1}^{row, col} (i - j)^2 P_{ij}$
Correlation	$\frac{1}{\sigma_i \cdot \sigma_j} \sum_{r=1, c=1}^{row, col} (i - \mu_i)(j - \mu_j) P_{ij}$
Homogeneity	$\frac{1}{(1 + (i - j))} \sum_{r=1, c=1}^{row, col} P_{ij}$
Energy	$\sum_{r=1, c=1}^{row, col} P_{ij}^2$

The GLCM structure properties are shown in [Table 1] which is characterize the texture in terms of skin physical variation.

Asymmetry is one of the significant features for understanding the correct shape with the help of symmetry, which is very helpful in pattern analysis. In case, the shape is totally symmetrical means which ratio is defined as 1. As these asymmetries are increases means the ratio is closer to 0. Asymmetry Index is defined by using following equation

$$AI = \frac{\Delta A}{A} \times 100 \quad (10)$$

Where, **A** is defined as the area of the whole given skin Image. **ΔA** is defined as the region difference between lesion area and total image.

The skin segmentation is tending to have irregular borders with notches and sharp edges. Melanocytes area tends to have smooth borders. In case the shape is fully symmetrical which ratio is defined as 1, otherwise the ratio is closer to 0. The Irregularity index is defined as a perimeter (P) and function of area (A) is defined as follows

$$IR = \frac{4\pi A}{P^2} \quad (11)$$

Basically color features are defined as standard derivation, skewness and mean and these features are obtained by utilizing Color Moment (CM) descriptor

$$\mu_i = \frac{1}{N} \sum_{j=1}^N f_{ij} \quad (12)$$

$$\sigma_i = \left( \frac{1}{N} \sum_{j=1}^N (f_{ij} - \mu_i)^2 \right)^{\frac{1}{2}} \quad (13)$$

$$\gamma_i = \left( \frac{1}{N} \sum_{j=1}^N (f_{ij} - \mu_i)^3 \right)^{\frac{1}{3}} \quad (14)$$

Where  $f_{ii}$  is the color value of the  $i$ 'th color component of the  $j^{th}$  image pixel and  $N$  is the total number of pixels in the image.  $\gamma_i, \sigma_i, \mu_i (i = 1,2,3)$  defined as the skewness, standard deviation and mean of each channel of given image respectively.

### Feed forward with back propagation

In this work the Feed Forward with Back Propagation (FFBP) is trained with Delta learning rule using 3X3 to 5 X5 input images. The FFBP has one input and output layers, here the hidden layer's nodes were started from as a template which means is similar to any kind of image processing operation for example sobel templates or kirsch. Here the templates are examined by using the Taylor series coefficients. From this results can be found the sharp edges with trained data. In this FFBP process the hidden layers of a network receives the signals from given input layer over a connection links which is weighted, performs the transmission and computation results as message to the output layer which are connected with the help of connection link weight  $w_{11}, w_{12}, \dots, w_{pm}$ . The network indent layer is as an output layer or another input layer in its place it acts as output or input layer depends on the processing situation. The FFBP is shown in [Fig. 5]

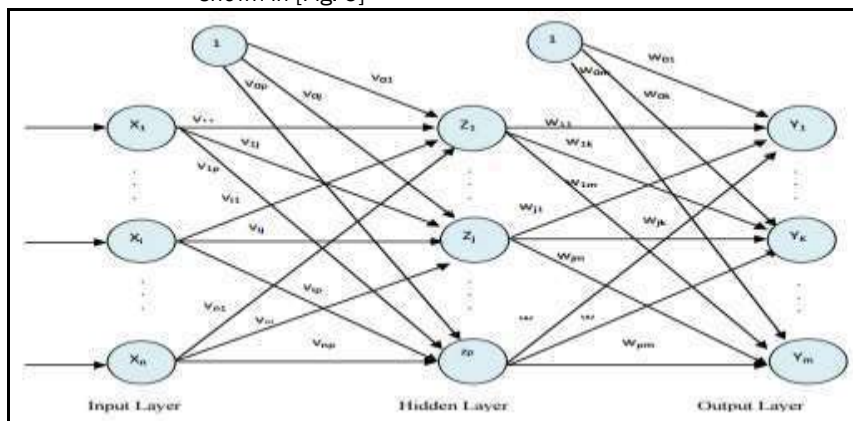


Fig. 5: Feed forward with back propagation.

Neural Network is trained by utilized Delta Rules which is also named as Backpropagation Rule [14]. The back propagation network training process includes three different kinds of process. Starting process is feed forward stage which has hidden node  $Z_i$  is obtain the input signals is defined as the  $x_1, x_2, \dots, x_n$  from these input nodes  $x_i$  over the connection weights  $v_{11}, v_{12}, \dots, v_{np}$  is used to calculate the final input as the product sum of the given input weights and signal which means  $Z_{ini} = v_{0i} + \sum x_i v_{ii}$  employs an activation function to generate the proper response and lastly sends these signals to the output node  $Y_k$ .

This process is similar to hidden node, each and every output nodes  $Y_k$  is obtain the signals  $z_1, z_2, \dots, z_p$  from the each and every hidden node  $Z_i$  over the  $w_{11}, w_{12}, \dots, w_{pm}$  compute the final input  $y_{ink} = w_{0k} + \sum z_i w_{ik}$  employs an activation function to yield the network output. An activation function which is utilized at both the output layer and hidden layer is a sigmoid function which means  $f(x) = 1/(1 + \exp(-x))$ .

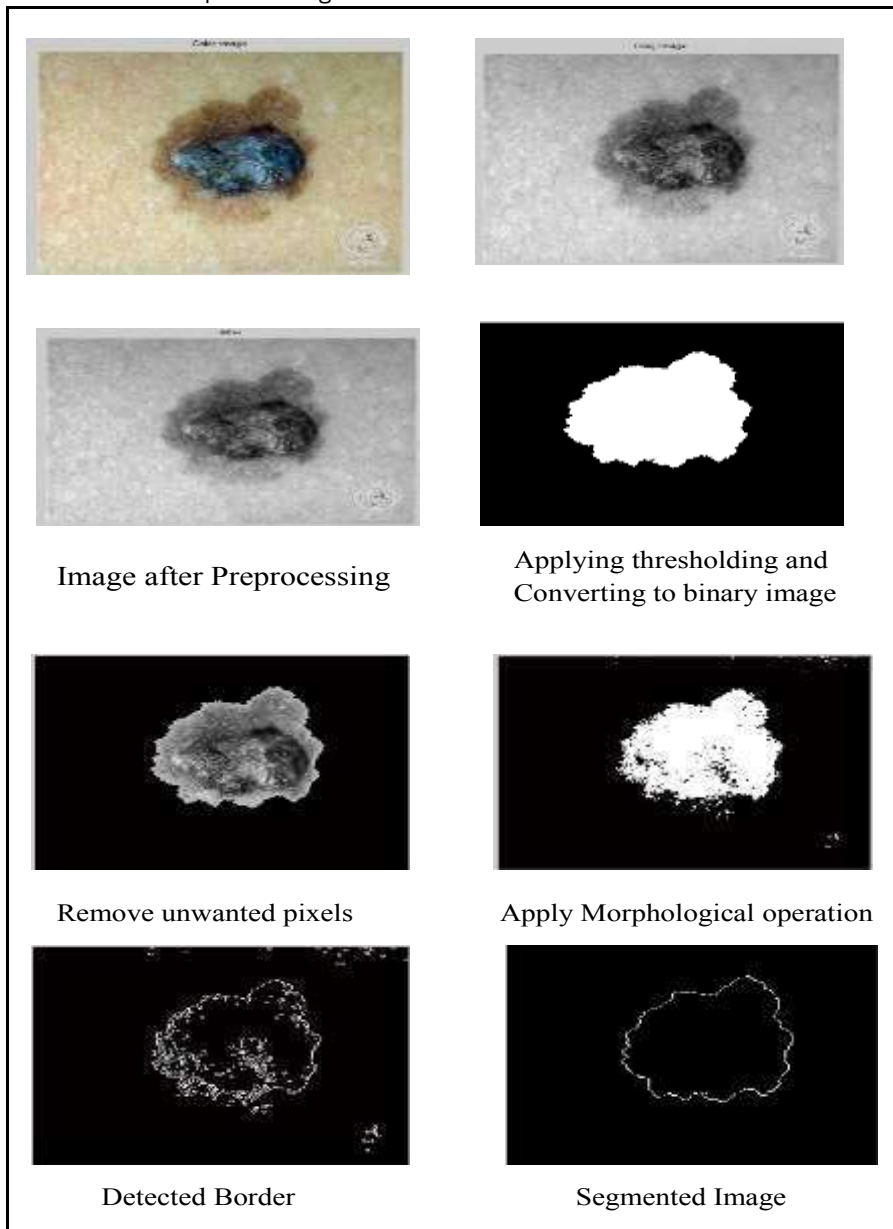
Once the response of the network is computed after that each and every output node compares its response with the given target function  $t_k$  to define the related error. Depends on these error the factor  $\delta_k$  is defined as  $\delta_k = (t_k - y_k) * f'(y_{ink})$ . The value  $\delta_k$  is utilized to distribute the error at  $Y_k$  which is return back to all the hidden nodes which are linked to  $Y_k$ . As same as factor  $\delta_i$  is calculated as  $\delta_i = \delta_{ini} * f'(z_{ini})$  for each and every hidden node  $Z_i$  to transmit errors back to input layer.

When all the  $\delta$  factors are propagated and defined to appropriate layers, after that the weights are simultaneously adjusted. The adjustment of the weight from the hidden node to output node depends on the  $\delta_k$  as  $\Delta w_{ik} = \alpha \delta_k z_i$  and  $\delta_i$  as  $\Delta v_{ii} = \alpha \delta_i x_i$ . So, the new weights between hidden node and input node are  $v_{0i}(new) = v_{0i}(old) + \Delta v_{0i}$  and  $v_{ii}(new) = v_{ii}(old) + \Delta v_{ii}$  and the weights between output nodes and hidden nodes are  $w_{0k}(new) = w_{0k}(old) + \Delta w_{0k}$ ,  $w_{ik}(new) = w_{ik}(old) + \Delta w_{ik}$ . This procedure is continued until attain the end condition. The end condition may be the number of epochs it has reached or reduce the Mean Square Error (MSE). The least MSE is calculated by using following equation

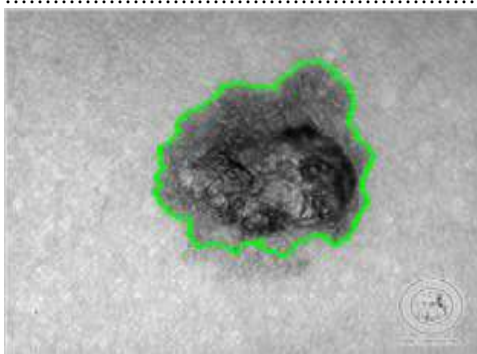
$$MSE = 0.5 \sum (t_k - y_k)^2 \tag{15}$$

### RESULTS AND DISCUSSION

Evaluation of FFBPclassification was undertaken by comparing the epidermis and dermis regions with true epidermis regions.



**Fig. 6:** Implemented results.



**Fig. 7:** Final segmented image.

The implemented results are shown in [Fig. 6] and final segmented image is presented in [Fig. 7].

### Database

In this proposed work, collected the skin disease image from the websites [15] [16] and [17], which contain approximately 20 images which are separated into different types of classes. In the database, the images are in .JPEG format. In the preprocessing stage, the images are treated as 300 X 300 dimensions. Additionally, the images are collected in different types of backgrounds.

### Performance metrics

The total number of pixels in each skin biopsy image was utilized to define the True Negative (TN), True Positive (TP), False Negative (FN) and False Positive (FP) fractions. Correspondingly, the different fractions can be considered as follows:

$$FN = (imageArea - A_s) \cap A_w \quad (16)$$

$$FP = A_s \cap (imageArea - A_w) \quad (17)$$

$$TP = A_s \cap A_w \quad (18)$$

$$TN = (imageArea - A_s) \cap (imageArea - A_w) \quad (19)$$

These fractions were utilized as the percentage specificity, sensitivity and accuracy of the automated segmentation.

$$specificity = \frac{TN}{(TN + FP)} \times 100 \quad (20)$$

$$Sensitivity = \frac{TP}{(TP + FN)} \times 100 \quad (21)$$

$$Overall Accuracy = \frac{(TP + TN)}{(TP + FP + FN + TN)} \quad (22)$$

The accuracy measurement measures the percentage of biopsy skin image pixels correctly classified as epidermis and non-epidermis.

## RESULTS

**Table 2:** Skin features

Asymmetry	Border irregularity	Color	Diameter
5.5223	0.4857	1.0722	0.5506
5.5365	0.4674	1.0718	0.5726
3.5239	0.7705	1.080	0.6175
2.562	0.7212	1.0371	0.8526

[Table 2] shows the skin features values in term of ABCD features, various skin structures are analysis in the this technique and the classification results shows the proposed method an effective tool in identifying skin diseases.



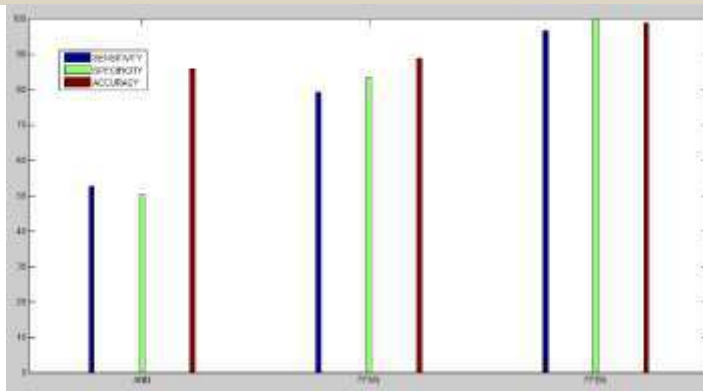


Fig. 8: Comparison of classification algorithms.

[Fig. 8] shows the different types of algorithms are compared in terms of performance metrics such as sensitivity, specificity and Accuracy. The proposed method shows the promising result to compare with other existing algorithms.

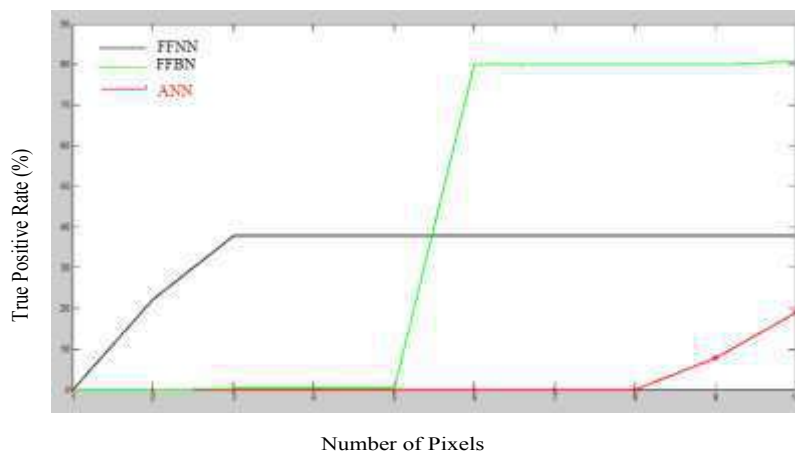


Fig. 9: True positive rate (TPR).

[Fig. 9] shows the comparison results of existing FFNN, ANN and proposed FFBN algorithm in terms of TRP. The proposed method shows promising results to compare with their existing algorithm because of very poor performance in differentiated the melanocytes from the keratinocytes by the utilizing the biopsy skin image.

## CONCLUSION

This paper successfully proposes an efficient a melanocytes diagnosis system using image processing operation. The texture analysis of skin histopathological images such as ABCDE is used for image feature extraction process with the help of GLCM. Before done the feature exaction process the noises are removed by using Gaussian Filter and Dull Razor filter then segmentation is done with the help of Edge-Based Technique and finally, classification is done by using FFBN pixel-wise classification using supervised learning rule such as Delta learning rule. The experimental results shows that the between classification results when compared with other existing classification algorithms.

### CONFLICT OF INTEREST

None

### ACKNOWLEDGEMENTS

None

### FINANCIAL DISCLOSURE

None

## REFERENCES

- [1] Maglogiannis I, Doukas C. [2009] Overview of advanced computer vision systems for skin lesions characterization, IEEE Trans. Inf. Technol. Biomed, 13(5): 721-733.
- [2] Martín JM, Rubio M, Bella R, Jordá E, Monteagudo C. [2012] Complete Regression of Melanocytic Nevi: Correlation Between Clinical, Dermoscopic, and Histopathologic Findings in 13 Patients, Elsevier journals, 103(5): 401-410.
- [3] Gang Zhang, Jian Yin, Xiangyang Su, Yongjing Huang, Yingrong Lao, Zhaohui Liang, ShanxingOu, Honglai Zhang. [2014] Augmenting Multi-Instance Multilabel Learning with Sparse Bayesian Models for Skin Biopsy

- Image Analysis,Hindawi Publishing Corporation BioMed Research International, Article ID -305629:13.
- [4] Thomas A, Josephine MS, Jeyabalaraja V. [2014] Human Skin Detection from Image using Gaussian Algorithm",International Journal of Computing Algorithm, 03: 1035-1038.
- [5] Cheng Lu, Muhammad Mahmood, Naresh Jha, Mrinal Mandal. [2013] Detection of melanocytes in skinhistopathological images using radial line scanning, Pattern Recognition, Elsevier journals, 46:509–518.
- [6] Nandini MN, MS Mallikarjunaswamy. [2014] Detection of Melanoma Skin Disease using Dermoscopy Images, International Journal of Electronics Communication and Computer Technology (IJECCCT),4 (3).
- [7] Arivazhagan S, NewlinShebiah R, Divya K, Subadev MP. [2012] Skin Disease Classification by Extracting Independent Components,Journal of Emerging Trends in Computing and Information Sciences, 3(10).
- [8] Nilkamal S Ramteke, Shweta V Jain. [2013] Analysis of Skin Cancer Using Fuzzy and Wavelet Technique – Review & Proposed New Algorithm,International Journal of Engineering Trends and Technology (IJETT), 4 (6).
- [9] Tao Xu, Yunhong Wang, Zhaoxiang Zhang, Pixel-wise skin colour detection based on flexible neural tree,Image Processing, IEEE, 751 – 761.
- [10] Robert Amelard, Jeffrey Glaister, Alexander Wong, David A Clausi. [2015] High-Level Intuitive Features (HLIFs) for Intuitive Skin Lesion Description",IEEE Transactions On Biomedical Engineering, 62(3).
- [11] Maciel Zortea, Thomas R Schopf, Kevin Thonb, Marc Geilhufe, KristianHindberga, Herbert Kircheschc, Kajsa Møllersenb, Jörn Schulz a, Stein Olav Skråvsethb, Fred Godtliebsena. [2013] Performance of a dermoscopy-based computer vision system for the diagnosis of pigmented skin lesions compared with visual evaluation by experienced dermatologists,Artificial Intelligence in Medicine, Elsevier.
- [12] Omar Abuzagheh, Buket D Barkana, MiadFaezipour. [2015] Noninvasive Real-Time Automated Skin Lesion Analysis System for Melanoma Early Detection and Prevention", IEEE Journal of Translational Engineering in Health and Medicine, 3.
- [13] P Keerthana, P Saranya. [2014] Multiscale Diffusion based image classification method in non-linear filtering,International Journal of Inventions in Computer Science and Engineering,1(11).
- [14] Rajasekaran S, AVijayalakshmi Pai G. Neural Networks, Fuzzy logic, and Genetic Algorithms synthesis and Applications, Eastern Economy Edition
- [15] <http://www.opticomdataresearch.com/melanoma.htm>
- [16] [https://challenge.kitware.com/#challenge/n/ISBI\\_2016%3A\\_Skin\\_Lesion\\_Analysis\\_Towards\\_Melanoma\\_Detection](https://challenge.kitware.com/#challenge/n/ISBI_2016%3A_Skin_Lesion_Analysis_Towards_Melanoma_Detection)
- [17] <http://homepages.inf.ed.ac.uk/rbf/DERMOFIT/Dhavale>

## ARTICLE

FUZZY BASED SELECTION OF DWT FEATURES FOR AUTOMATIC  
SPEECH RECOGNITION SYSTEM FOR MAN MACHINE  
INTERACTION WITH CS-ANN CLASSIFIERSunanda Mendiratta<sup>1\*</sup>, Neelam Turk<sup>2</sup>, Dipali Bansal<sup>3</sup><sup>1</sup>YMCA University of Science and Technology, Faridabad, INDIA<sup>2</sup>Department of Electronics, YMCA University of Science and Technology, Faridabad, INDIA<sup>3</sup>Department Faculty of Engineering and Technology, Manav Rachna International University, Faridabad, INDIA

## ABSTRACT

Man machine interaction is the most commonly used technology in Computer Aided Systems and comes under various fields. Among them man machine interaction with automatic speech recognition is the advanced technology in this era. There are several technologies are put forward by several researchers but each of them has its own backlogs. In this paper we have proposed a methodology for man machine interaction system with automatic speech recognition by Means of fuzzy based Discrete Wavelet Transform (DWT) feature extraction and Artificial neural network with Cuckoo search optimization (CS-ANN) classifier. Here the input is first preprocessed using a sequence of preprocessing steps and then features are extracted from that by Means of DWT. After this the optimum number of features are selected by Fuzzy logic and finally the speech signals are recognized by training the ANN where the optimization is done through CS algorithm. The proposed methodology is implemented on MATLAB platform and the experimental results are presented and validated under different conditions.

## INTRODUCTION

Speech signals contain a gigantic measure of data and can be depicted as having various levels of data. Voice based interfaces hold the way to understand this accomplishment. In this connection, Automatic speech recognition (ASR) systems in distinctive languages pick up significance [1]. ASR is an imperative undertaking in digital signal processing related applications. It is the procedure of automatically changing over the spoken words into written text by the PC framework [2]. In the course of recent decades speech recognition has made across the broad innovative advances in numerous fields, for example, call steering, automatic translations, data looking, data entry and so on [3]. Speech recognition has been expert by consolidating different algorithms drawn from diverse disciplines, for example, statistical pattern recognition, signal processing and semantics and so forth [4]. The percentage of the imperative uses of speech recognition are security gadgets, household apparatuses, PDAs, ATM machines and PCs [5]. Speech processing is one of the energizing zones of signal processing. The objective of speech recognition field is to create method and framework to produce for speech data to machine [6]. In view of significant development in statically displaying of speech, automatic speech recognition today find far reaching application in task that require human machine interface, for example, automatic call processing [7].

Speech recognition can be generally partitioned into two stages: feature extraction and classification [8]. Even though noteworthy advances have been made in speech recognition innovation, it is still a troublesome issue to outline a speech recognition framework for speaker-free, nonstop speech [9]. One of the crucial inquiries is whether the majority of the data important to recognize words is preserved while feature extraction stage. In the event that imperative data is lost during this stage, the execution of the accompanying classification stage is naturally handicapped and can never measure up to human ability [10]. Feature extraction can be comprehended as a stage to decrease the dimensionality of the input information, a diminishment which definitely prompts some data loss. Normally, in speech recognition, we partition speech signals into frames and extract features from every frame [11]. During feature extraction, speech signals are changed into an arrangement of feature vectors. At that point these vectors are exchanged to the classification stage. For instance, for the case of dynamic time warping (DTW), this succession of feature vectors is contrasted with reference information set. For the instance of hidden Markov models (HMM), vector quantization may be connected to the feature vectors [12-13], which can be seen as a further stride of feature extraction. In either case, data loss during the move from speech signals to a succession of feature vectors must be kept to a minimum [14].

In different many-sided application, for example, speech recognition where the frameworks are created in light of genuine information, handling an extensive number of features is successive. Be that as it may, a significant number of the features are not pertinent to the issue of interest. Moreover, various features demand a lot of calculations, which back off the general procedure. Under these circumstances, naturally releasing insignificant features is important to accomplish a model that is exact and dependable in taking care of the issue at hand [15-16]. Also, utilizing the feature selection method lessens the computational expense, which improves the reaction time of the procedure. Feature selection (FS) is a standout amongst the most profitable research territories and has pulled in a lot of consideration in the course of recent decades. For the FS undertaking, two surely understood

## KEY WORDS

Man-Machine interaction, Automatic speech recognition, Sampling, Hamming window, Harmonic decomposition, Discrete Wavelet Transform, Fuzzy model, Artificial Neural Network, Cuckoo search

Received: 7 September 2016  
Accepted: 29 September 2016  
Published: 2 Dec, 2016

## \*Corresponding Author

Email:  
sunandamendiratta712@gmail.  
com  
Tel.: +91-9677002684

strategies for feature assessment are utilized. The first uses distance metrics to quantify the cover between distinctive classes [17]. Under this system, probability thickness functions of the example appropriation can likewise be considered. Thus, the subset for which the normal overlap is insignificant is considered as an answer. In the Meantime, intra-and in addition between class distances can be measured by considering the fuzziness and Entropy of the features [18]. During that time system, classification errors in light of the feature subset candidates are assessed. Therefore, the subset with insignificant misclassification is chosen as an answer. A few techniques in [19] have been thought about and has been actualized for the variable selection. In the Meantime, utilizing flexibilities to characterize the optimization issue is useful. For this reason, fuzzy set theory is utilized to classify the adaptabilities for the objective functions. This strategy prompts accomplishing additional exchange off to tackle this issue. Fuzzy optimization systems have been every now and again utilized as a part of the optimization of clashing objectives [20].

In this paper, we have proposed an automatic speech recognition system for the man machine interaction with DWT based feature extraction and ANN classifier optimized with Cuckoo search (CS) algorithm. The remaining of the paper is structured as follows: Section 2 gives the recent works related to the speech recognition system proposed by several researches recently. Section 3 gives in detail the proposed methodology and the processes associated with the proposed work. Section 4 discusses about the experimental results and discussion of our proposed methodology and finally section 5 concludes our paper.

## RELATED WORKS

Kaya H et al. [21] have extended a recent discriminative projection based feature selection method using the power of stochasticity to overcome local minima and to reduce the computational complexity. The approach assigned weights both to groups and to features individually in many randomly selected contexts and then combined them for a final ranking. The efficacy of the method was shown in a recent paralinguistic challenge corpus to detect level of conflict in dyadic and group conversations. They advanced the state-of-the-art in this corpus using the INTERSPEECH 2013 Challenge protocol.

Cumani S, and Laface P et al. [22] have validated that a very small subset of the training pairs was essential to train the original PSVM model, and proposed two methods that permitted removing most of the training pairs that were not necessary, without damaging the precision of the model. This permitted intensely decreasing the computational resources and memory necessary for training, which became possible with enormous datasets comprising many speakers. They had evaluated these methods on the extended core situations of the NIST 2012 Speaker Recognition Estimation. Their consequences displayed that the precision of the PSVM trained with an appropriate number of speakers was 10%-30% better associated to the one attained by a PLDA model, reliant on the testing conditions. Since the PSVM precision expanded with the training set size, but for large numbers of speaker PSVM training did not scale well, their selection methods became applicable for accurate training discriminative classifiers.

To optimize a feature vector, Chatterjee S and Kleijn W. B et al. [23] had developed a new framework such that it imitates the human auditory system behavior. In an offline manner the optimization was conceded out on the basis of assumption that the local geometries of the feature vector domain and the perceptual auditory domain must be analogous. Along with a static spectral auditory model, using this principle they optimized and modified the static spectral Mel frequency cepstral coefficients (MFCCs) without regarding any feedback from the speech recognition system. Then the work was prolonged to comprise spectro-temporal auditory properties into manipulating a new dynamic spectro-temporal feature vector. Making use of a spectro-temporal auditory model, the dynamic feature vector was designed and optimized to integrate the human auditory response behavior across frequency and time. They exhibited that an essential development in automatic speech recognition (ASR) performance was achieved for any environmental condition, clean in addition to noisy.

Dikici E et al. [24] have presented some directions to enhance discriminative language modeling performance for Turkish broadcast news transcription. They used and compared three algorithms, namely, perceptron, MIRA and SVM, both for classification and ranking. They applied thresholding as a dimensionality reduction technique on the sparse feature set, and some sample selection strategies to decrease the complexity of training. In this paper, they also extended the earlier results by including the SVM classifier and classification and ranking versions of the MIRA algorithm for completeness. They also increased the feature space by incorporating higher order -grams, presented the relationship between ranking versions of perceptron and SVM, and gave a thorough statistical analysis and comparison of the results.

Pan S. T, and Li X. Y [25] have focused on field-programmable gate array (FPGA)-based robust speech measurement and recognition system, and the environmental noise problem was its main concern. To accelerate the recognition speed of the FPGA-based speech recognition system, the discrete hidden Markov model was used here to lessen the computation burden inherent in speech recognition. Furthermore, the empirical mode decomposition was used to decompose the measured speech signal contaminated by noise into several intrinsic mode functions (IMFs). The IMFs were then weighted and summed to reconstruct the original clean speech signal. Unlike previous research, in which IMFs were selected by trial and error for specific applications, the weights for

each IMF were designed by the genetic algorithm to obtain an optimal solution. The experimental results in this paper revealed that this method achieved a better speech recognition rate for speech subject to various environmental noises.

SPEECH RECOGNITION SYSTEM WITH DWT BASED FEATURE EXTRACTION AND CS-ANN CLASSIFIER

In the context of speech recognition, the recognition of the speech signal is done by extracting more relevant features that clearly characterizes the signal. Though there are several methods are employed in feature extraction, the incorporation of artificial intelligence in this field will produce better results. In this paper, we proposed a methodology for man machine interaction using Discrete wavelet transform (DWT) based features along with novel fuzzy based feature selection method and Hybrid Cuckoo search – Artificial neural network (CS-ANN) classifier for automatic speech recognition system. The proposed method consists of three stages. They are Signal Preprocessing, Fuzzy based DWT and Classification. Initially, the input recorded speech signal is preprocessed for removing noise and to detect the word. Then, the preprocessed signal is subjected to feature extraction process by using discrete wavelet transform applied to the speech signal where the preprocessed speech signal is decomposed into various frequency channels using the properties of wavelet transform. Here, in our proposed method, we are employing 8-level multi resolution wavelet transform so that at each decomposed level eight types of features like Mean, Standard Deviation, Skewness, Kurtosis, Entropy, Shannon Entropy, Log energy Entropy and Renyi's Entropy of the speech signal are extracted. Since, we are using 8-level DWT so the number of features extracted is high. So, a Fuzzy model is used to select the optimal features from speech signals which are extracted by DWT. Finally, the selected optimal set of features is used for training of Artificial neural network (ANN) classifier and then based on these features the spoken work is recognized and the corresponding text will be displayed. In order to improve the classification accuracy of the ANN the weights of the neural networks is optimized by using the Cuckoo search (CS) algorithm. The proposed method is implemented in the Matlab working platform and the results are compared with the previous methods under different conditions.

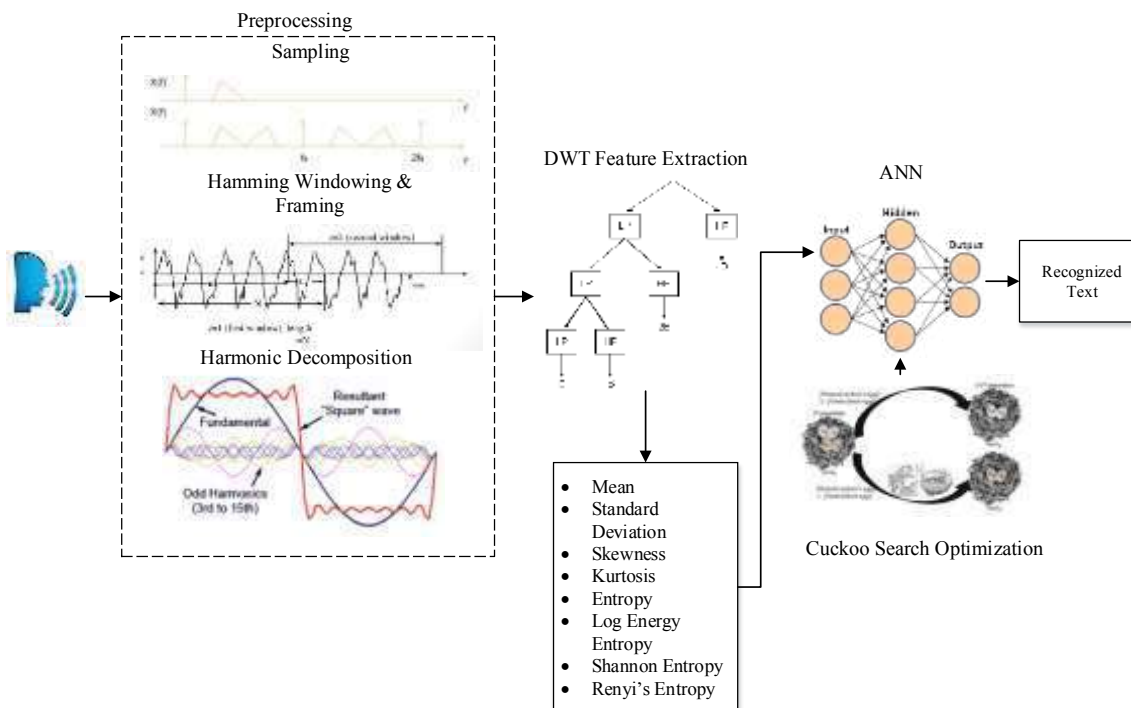


Fig.1: Block diagram of the proposed speech recognition system.

As shown in the above [Fig. 1], the input speech signal is initially undergoing some sequence of preprocessing steps as sampling the signal, producing frames by Hamming windowing process and denoising of the signal through the Harmonic decomposition process with Harmonic decomposition method. After preprocessing, the specified features from the signal is extracted through DWT and from the extracted features only the optimum number of features is chosen by Fuzzy Inference System (FIS). The optimally extracted features then employed in the training procedure of the ANN in which the optimization of the neural network is done through the CS optimization algorithm. Each of these processes are explained in detail in the following sections. Consider that the database  $D$ , contains 'N' number of speech signals as mathematically represented as  $D = \{s_1, s_2, \dots, s_N\}$ . From this the signal  $s_i, i = 1, 2, \dots, N$  is taken out and further operations are applied as discussed in the following sections.



### Preprocessing of input speech

The input speech signal produced by the human talk, normally processed using some preprocessing techniques in order to make the signal to be suitable for further operations being applied to the signal. The purpose preprocessing the speech signal is to facilitate the signal processing, eliminate the silent frequencies and to remove the noises. Each of these preprocessing is performed through the following steps.

### Sampling of the speech signal

The sampling of the speech signal  $S_i$  is performed to facilitate further operations on the speech signal by converting it into a digital format. Several types of sampling methods are available, but for processing the speech signal we have employed a Band pass Sampling method as the input signal in our methodology is of band pass type. For the band pass signals the spectrum of the signal  $S(\omega)$  will be zero for the range of frequencies except  $f_1 \leq f \leq f_2$ . In general the frequency  $f_1$  of the band pass signal is non-negative and will be greater than zero also the aliasing effect is zero when  $f_s < 2f_2$ , where  $f_s$  is the sampling frequency which is calculated using the equation (1).

$$f_s = \frac{1}{T} \quad (1)$$

where,  $T = \frac{m}{2f_2}$  is the sampling interval and hence the equation (1) is modified as in equation (2).

$$f_s = \frac{2f_2}{m}, m < \frac{f_2}{B} \text{ and } f_s = \frac{2KB}{m}, f_2 = KB \quad (2)$$

where,  $B$  = Bandwidth of the signal

$m$  =Number of Replications used in the sampling process (Can be any integer till  $f_s \geq 2B$ )

The sampled spectrum of the speech signal  $S_i$  of bandwidth  $B$  and the minimum sampling rate  $f_s$  is given by equation (3).

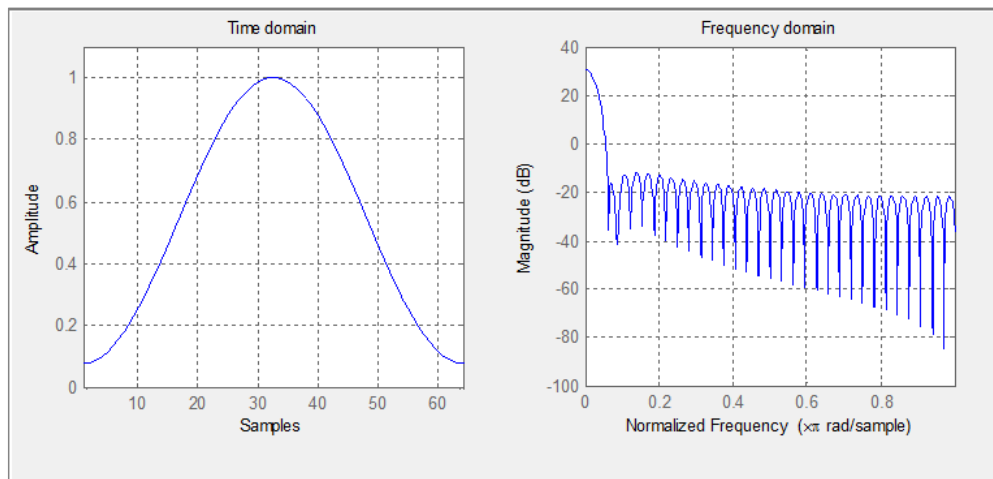
$$S_s(\omega) = \frac{1}{T} \sum_{i=1}^N \sum_{n=-\infty}^{\infty} S_i(\omega - 2nB) \quad (3)$$

where,  $n$  = time instant in discrete level, after sampled the points from the input speech signal, the samples are converted into frames by using Hamming window and this is explained in the following process.

### Framing and Windowing

The input signal produced may contain some silent sounds which are not necessary in the speech recognition system to recognize that signal. Hence the signal is converted into frames with the which smooth the progress of signal analysis. In the process of framing the signal is converted into frames with the period of 20-30 ms applied at 10 ms intervals with an overlap of 50% between adjacent frames and this is referred to as short time spectral analysis. Here, we are employing Hamming window in the process of windowing which results in number of frames of the speech signal. Hamming window is the famous windowing technique usually preferred in speech signal processing as it has its own benefits. The process of windowing with Hamming window on speech signal is explained as follows;





**Fig.2:** L point Hamming Window in Time and Frequency Domain (L=64).

In the above [Fig. 2], the L point Hamming window in time and frequency domain is displayed where L is the length of the window and it is considered here as 64. The Hamming window is generally represented as given in the equation (4) [26].

$$w(n) = 0.54 - 0.46 \cos\left(\frac{2\pi(n-1)}{N}\right) \quad (4)$$

where,  $N$  = Number of samples in each frame which is equal to L, L-1 or L+1.

In the process of windowing and framing, the sampled signal is initially divided into frames with the specified time intervals and then the hamming window is applied to each frame to produce the signal which is free from discontinuities. Consider that the input speech sample is represented as  $s_i(n)$  for the  $i^{th}$  sample, then the resulting frames after processed by the hamming window is given by the equation (5).

$$y_i(n) = \sum_{i=1}^S w(n) s_i(n) \quad (5)$$

where, S = Total number of frames produced  
 $s_i(n)$  =  $n^{th}$  sample from the spectrum  $S_s(\omega)$

The resulting S number of frames produced by the equation (5) is the speech frequencies which are free from the discontinuities. These frames further enhanced by the reduction of noise present and this is performed by the Harmonic decomposition process as explained in the following section.

### De-noising frames by Harmonic decomposition

After converting the speech samples into frames without discontinuities the noise present in these samples is removed using denoising method and the type of noise present in the speech signal is the harmonic noise. Hence, the Harmonic decomposition [27] method is employed here as the noise reduction technique in which the input speech sample is decomposed into its fundamental as well as harmonic components. After, decomposing the speech sample into the components the order of the components which are greater than three could be ignored. The speech sample obtained from the windowing function is then denoised  $y_{di}(n)$  by correlating it with the fundamental and harmonic components up to the order of three which is given mathematically in equation (6).

$$y_{di}(n) = \sum_{i=1}^S \sum_{j=1}^3 (y_i(n) * h_j) \quad (6)$$

where,  $y_{di}(n)$  = Denoised sample

$h_j$  = Harmonic Levels of the input speech sample

Thus, the correlated signal produced are free from harmonic noise by filtering out the harmonic component after reconstruction. The preprocessed speech samples are then given to the feature extraction phase, in which the features for

the speech signal to aid the classification in recognition phase. The feature extraction phase is given in the following section.

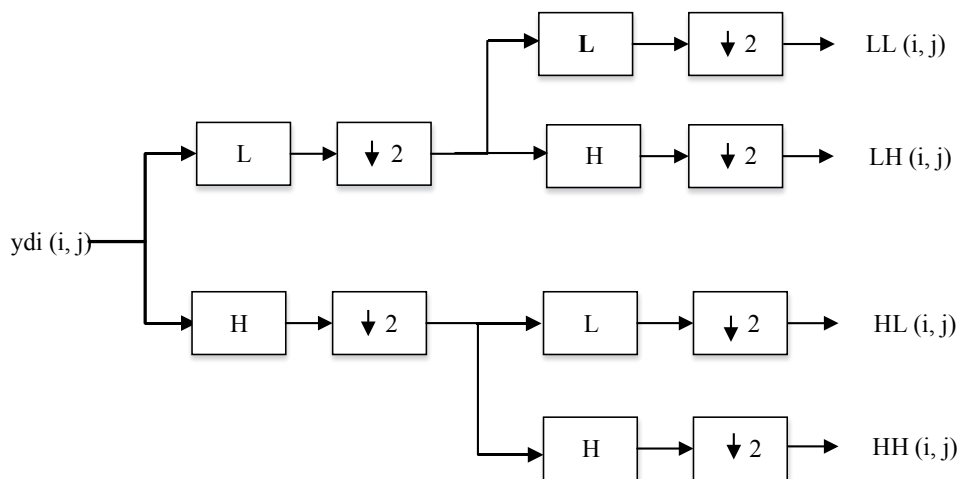
### Fuzzy Based DWT feature extraction

After, producing the de-noising signal of the speech input the features are extracted from the preprocessed signal for the purpose of recognizing the speech by training the classifier in the classification stage. There are several techniques are used to extract the features from the speech signal but the incorporation of artificial intelligence could produce most suitable features for the recognition of the speech signal. Hence in our proposed methodology, a novel fuzzy based DWT feature extraction is employed where eight different types of features are extracted such as Mean, Standard Deviation, Skewness, Kurtosis, Entropy, Shannon Entropy, Log energy Entropy and Renyi's Entropy from the signal using DWT feature extraction with eight level decompositions. After the features are extracted most of them not having necessary details to recognize the signal so that the fuzzy model is used to select the most suitable features. The process of DWT of extracting the features and the feature selection through the fuzzy model is detailed as follows.

### DWT in feature extraction

A linear transformation that operates on a data vector is discrete wavelet transform (DWT) whose length is an integer power of two, converting it into a statistically diverse vector of identical length. In image compression and signal processing the wavelet transform has obtained an extensive acceptance. A signal's multi-resolution depiction is offered by the DWT which is very beneficial in examining "real-world" signals and therefore this transformation is accepted to excerpt the speech signal features in our proposed approach. Basically, by a DWT a distinct multi-resolution depiction of a continuous-time signal is acquired. It converts a series  $a_0, a_1, \dots, a_n$  into one low pass coefficient series known as "approximation" and one high pass coefficient series known as "detail".  $n/2$  is the Length of each series. In actual life conditions, such transformation is implemented recursively on the low-pass series till the preferred number of repetitions is attained.

The function is not incessant and henceforth not differentiable. Daubechies wavelets are the families of wavelets whose inverse wavelet transforms are adjoint of the wavelet transform i.e. they are orthogonal. Using Daubechies wavelets the wavelet transform result in gradually finer discrete samplings making use of recurrence relations. Each resolution scale is double that of the earlier scale. From data compression range to signal coding the discrete wavelet transform has wide range of applications. Hence, it is a device that divides data into varied frequency modules, and then each component with a resolution accorded to its scale is considered. DWT is calculated with a cascade of filters ensued by a factor of two sub-sampling. In [Fig. 3] the fundamental DWT architecture is shown.



**Fig. 3:** General architecture of the 1-level DWT.

In the above [Fig. 3] the one level DWT is shown in which the speech signal is first split into low and high frequency bands with the Low pass and High Pass filters as given by the impulse responses denoted by  $g(m)$  and  $h(m)$  respectively and this is given in equations (7) and (8) and they are divided further to produce two low frequency bands and two high frequency bands and this is the complete one level decomposition by DWT. The  $\downarrow$  symbol denotes the down sampling of the filtered element.

$$l_{i+1}(m) = \sum_{n=-\infty}^{\infty} y_{di}(n-2m)g(m) \tag{7}$$

$$h_{i+1}(m) = \sum_{n=-\infty}^{\infty} y_{di}(n-2m)h(m) \tag{8}$$

The process given in equations (7) and (8) can be continued until the required level of decomposition is reached by extending the architecture as given in the [Fig 3]. The DWT's major feature is a function of multi scale representation. At different levels of resolution given function can be examined using the wavelets. The DWT is also orthogonal and could be invertible. In our proposed methodology we have employed 8-level DWT and hence the filtered coefficients produced for each signal is 32 from these coefficients we will extract the features mentioned above as in the following manner.

**Mean,  $\mu$**

The Mean value of the filtered coefficients is calculated at each level of the decomposition. If the low and high frequency components of level  $k$  is represented as  $l_{lk}, l_{hk}, h_{lk}$  and  $h_{hk}$  respectively, then the Mean value is calculated as given in equation (9).

$$Mean, \mu = \frac{1}{n} \sum (l_{ik} + h_{ik}), \quad i = l \& h; n = 4 \tag{9}$$

**Standard Deviation,  $\sigma$**

The Standard Deviation of the calculated filtered coefficients can be measured from the variance of the coefficients and it is the measure how the sample in the signal is far from the Mean value. The variance and the Standard Deviation from that is calculated as given in equations (10) and (11).

$$Variance, \sigma^2 = \frac{1}{n} \sum (x_i - \mu)^2 \tag{10}$$

$$Standard\ deviation, \sigma = \sqrt{\frac{1}{n} \sum (x_i - \mu)^2} \tag{11}$$

**Skewness,  $s$**

A significant distribution parameter is symmetry. Based on the definition, a skewed variable Mean is not situated at the distribution center. It might be observed that two signal segments can have the same Mean and Standard Deviation but diverse values for Skewness. Skewness is conveyed as in equation (12).

$$Skewness, s = \frac{E(x_i - \mu)^3}{\sigma^3} \tag{12}$$

$k$   $s$

$$Kurtosis, k = \frac{E(x_i - \mu)^4}{\sigma^4}$$

$H(s_n)$

$\{s_1, s_2, \dots, s_n\}$

$$P(s_n) = P_n, 0 \leq P_n \leq 1, \sum P_n = 1$$

$$I(s_n) = -\log P_n$$

$I(s_n)$

$$H(s_n) = E[I(s_n)] = -\sum P_n \log P_n$$

$H_{sh}(s_n)$

$$H_{sh}(s_n) = \frac{H(s_n)}{\log m}$$

$m$

$H_{\log}(s_n)$

$$H_{\log}(s_n) = -\sum (\log(P_n))^2$$

$$H_{Ren}(s_n) = \frac{1}{1-\alpha} \sum (\log(P_n)^\alpha)$$

### Fuzzy based feature selection

The wavelet features extracted as above are larger in number and such large quantity is not necessary to recognize the input signal. For that purpose the feature selection process is usually conducted after the feature extraction phase and the most common feature reduction techniques used are Principal Component Analysis (PCA), Isomap techniques etc. But these techniques consumes more time and results in considerable information loss. Hence including the human intelligence can produce apt features that are used better for the recognition of the speech signal and in our proposed methodology we select the required features by means of fuzzy logic. Here the method we have engaged is the fuzzy feature estimation index for a set of features which is described in terms of membership values indicating the degree of similarity between two features.

In fuzzy based feature selection, the parameter called evaluation index is calculated between a set of features based on the calculated membership functions. Initially the degree of membership  $\mu_{uv}$  is measured between the feature sets  $u$  and  $v$ . With that membership function the evaluation index is measured and the feature sets which are having a minimum value of index is selected in training the neural network. The membership function  $\mu_{uv}$  for the features is calculated as given in equation (19).

$$\mu_{uv} = \begin{cases} \left(1 - \frac{d_{uv}}{D}\right), & \text{if } d_{uv} \leq D \\ 0, & \text{otherwise} \end{cases} \quad (20)$$

In equation (20),  $d_{uv}$  is the Euclidean distance which measures the similarity between the two features and  $D$  is the minimum distance between any given two features. The distance,  $d_{uv}$  is calculated as in equation (21).

$$d_{uv} = \sqrt{(u-v)^2} \quad (21)$$

And finally the evaluation index of the membership function is measured for all the features in the feature space as in equation (22).

$$e = \frac{1}{s(s-1)} \sum_u \sum_v \mu_{uv}(1 - \mu_{uv}) \quad (22)$$

Where,  $s$  is the number of feature samples present in the respective feature space. This fuzzy evaluation index is determined for all of the eight features and then finally the respective features which are having minimum value of the index is considered in the further recognition process. After selecting the optimum features from the feature space the training and the testing of the ANN is carried out in the next stage in which the optimization of the network is done by Means of Cuckoo search algorithm and the process involved in this stage is detailed in the following section.

### Recognition of speech with CS-ANN classifier

The optimally selected features from the feature extraction is then used for training the ANN for the purpose of recognizing the speech signal, but in normal back propagation algorithm is used for the optimization of weight function between the links. But here we have employed CSO algorithm to produce fair optimization of the network and the steps of this training procedure is given as follows after giving the basic introduction about ANN.

### Artificial neural network (ANN)

A distinctive artificial neural network (ANN) has two types of basic constituents. They are neurons which are processed elements and links which are interconnections between neurons. Each link has a weighting parameter. From other neurons each neuron gets stimulus, progress the information, and an output is produced. Neurons are classified to input, output and hidden neurons. The input and output layers, are called the first and the last layers correspondingly, and the enduring layers are called hidden layers. Consider in the  $k^{th}$  layer the number of neurons as  $n_k$ . Let, the weight of the link is represented as  $w_{ij}^k$  between the  $j^{th}$  neuron of the  $(k-1)^{th}$  layer

and the  $i^{th}$  neuron of the  $k^{th}$  layer. If for each neuron  $w_{i0}^k$  is an additional weighting parameter, signifying the bias in the  $i^{th}$  neuron of the  $k^{th}$  layer. Before the neural network training the weighting parameters are initialized. In a systematic manner they are iteratively updated during training. Once the neural network is finished, the weighting parameters remain stable throughout the neural network usage as a model.

The training process of an ANN is to modify the biases and weights. The most prevalent technique to train, feed forward ANNs in numerous domains is the back-propagation (BP) learning. Though, one drawback of this method, which is a gradient-descent method, is that it necessitates a differentiable neuron transfer function. Also, as neural networks create intricate error surfaces with multiple local minima, instead of a global minimum the BP inclines to converge into local minima. In modern years, many enhanced learning algorithms have been proposed to overwhelm the handicaps of gradient-based methods. Because of conventional numerical methods' computational shortcomings in resolving complex optimization problems, researchers may depend on meta-heuristic algorithms. Over the last eras, numerous meta-heuristic algorithms have been applied successfully to several engineering optimization problems. For many complex real-world optimization problems, better solutions have been delivered by them in comparison with conventional numerical methods. Here we are employed Cuckoo Search optimization as a Meta heuristic algorithm for optimizing the ANN, the reason for this is explained in the next consecutive section.

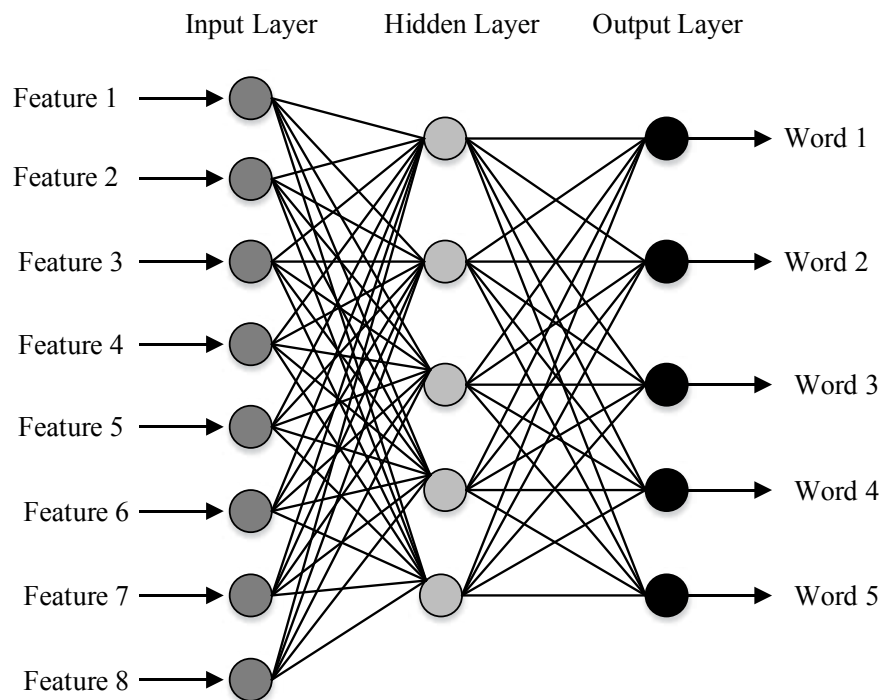


Fig. 4: Basic architecture of an ANN.

As given in the [Fig. 4] above, the input features are fed with the input layer at each input neuron. With this input the basis function is calculated at the hidden neurons present in the hidden layer with a weighting function assigned to the each link between the input layer and the hidden layer. Then the basis function is calculated at each output neuron of the output layer separately. These steps are repeated with another sample of the same words present in the signal and if any error produced Means the weighting function is optimized by Means of the CSO algorithm. The training and testing procedure of the ANN in recognizing the spoken words is explained as follows and the type of NN used here is the Feed Forward Neural Network (FFNN).

#### Training of ANN

Step 1. Define the selected features from the fuzzy evaluation index as the input neurons. We have employed eight types of features in recognizing the word and the fuzzy based feature selection technique will produce two best feature values for each type. Therefore, totally 16 feature values will be produced for training the NN as the input neurons.

Step 2. Then the basis function at each input neuron is to be calculated for each of the hidden neurons with the weighting function. This basis function calculation is given by the equation (23).

$$I_b = \sum_{j=1}^J u_j w_{jk}^i \quad (23)$$

where,  $J$  = Number of input neurons

$u_j$  = Value of feature at each input neuron

$w_{jk}^i$  = weight value of the link between input neuron  $j$  and hidden neuron  $k$

Step 3. After calculating the basis functions at the input neurons the activation function is calculated from that at each hidden neuron as given by the equation (24).

$$A_k = (1 + \exp(-I_b))^{-1} \quad (24)$$

Step 4. Once the activation function is measured by each hidden neuron Means, the basis function of each of the output neurons is determined. This basis function calculation at the output side is given in equation (25).

$$O_b = \sum_{k=1}^K A_k w_k^o \quad (25)$$

where,  $w_k^o$  = Weight value between the links of hidden neuron and output neuron.

The basis function produced at output side is the expected output to be produced at the recognizer. Sometimes, the value at the output neuron may deviate from the actual output and this is called learning error and denoted by the equation (26).

$$\text{Learning Error, } E_L = \frac{1}{2} (O_{act} - O_{obt})^2 \quad (26)$$

where,  $O_{act}$  = Actual Output

$O_{obt}$  = Obtained Output

Step 5. Optimization of Weight coefficients

The Cuckoo search optimization is employed in this part to select the corresponding weight coefficients so that the produced learning error is zero. Hence the fitness function used here is the learning error constrained to the weighting functions. The steps employed in the CSO algorithm are given in the following part.

### Cuckoo search Optimization in Output, Weight Updating

Yang and Deb in 2009, developed a Cuckoo search algorithm which is one of the modern optimization algorithms that replicates some cuckoo species' breeding performance. Modern studies have exposed that CS is possibly far more effective than PSO and GA[28]. So that the CS algorithm is employed here for the optimization of the neural network to produce the zero learning error. The nature of the cuckoo search algorithm is detailed as follows.

#### *Cuckoo proliferation approach*

In communal nests some cuckoo species lay their eggs, though moderately a number of species employ in the obligate brood parasitism by laying their eggs in the host birds' nests (frequently other species). The brood parasitism principally falls into three classes, namely intra specific brood parasitism, cooperative breeding and the nest take over. After the eggs are laid, if the host birds could discover that the eggs are not their own, they would either destroy the alien eggs or abandon their nests and new nests are built somewhere else; while some female cuckoo species can lay their eggs very specified in mimicry in pattern of the host bird's eggs. This lowers the probability of their eggs being discovered.

Many researches have presented that many insects and animals flight behavior might follow some distinctive characteristics of lévy flights. A common concern of lévy flights and random walk so as to attain new solution is offered in (27) and (28).

$$x^{i+1} = x^i + \beta \oplus Levy(\lambda), \quad \beta > 0 \quad (27)$$

$$Levy(\lambda) = t^{-\lambda}, \quad 1 \leq \lambda \leq 3 \quad (28)$$

where,  $x^{i+1}$  = New solutions (Here, learning rate)

By random lévy walk ,some of the new solutions must be produced around the finest solution. Though, a significant fraction of new solutions must be formed by far field randomization. This would assure the algorithm not to be trapped in local optimums. So as to model the standard cuckoo search algorithm, the ensuing three idealized rules are developed.

- ✓ Just one egg at a time is laid by each cuckoo, and in a arbitrarily chosen nest it is dumped.
- ✓ The finest nests with high quality of eggs (solutions) would carry over to the next generation (algorithm iteration).
- ✓ The available number of host nests is constant, and each cuckoo's egg can be discovered by the host bird with the probability of  $P_a \in [0, 1]$ .



Conferring to these three rules, the fundamental stages of CS can be précised as the pseudo code signified in [Fig. 5].

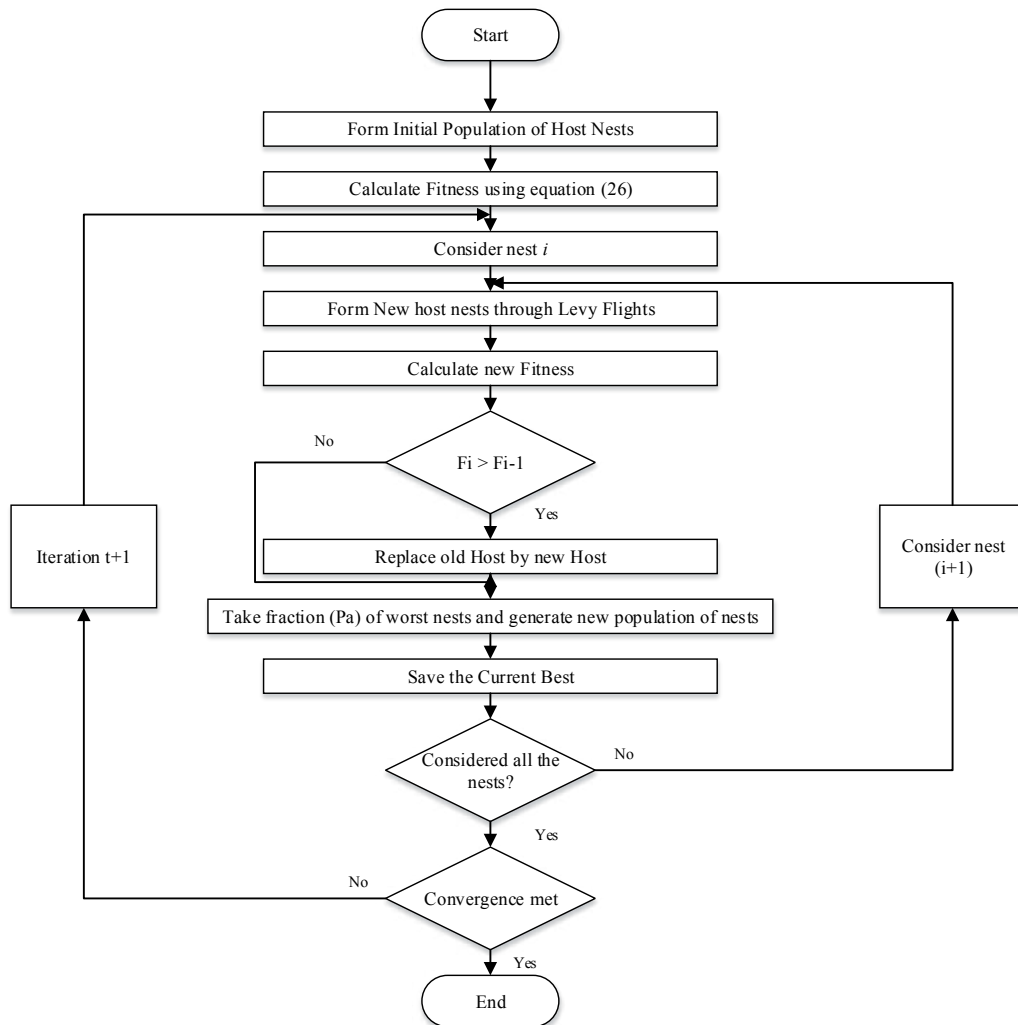


Fig. 5: Cuckoo search Algorithm.

As given in the flowchart depicted in [Fig. 5] above, initially the population (host nests) is defined with the weight coefficients as given in the section 3.3.1.1. After that the fitness function is calculated here the fitness function is the learning error of the neural network and the objective is the minimization of the error with best weighting coefficients. Once the fitness is calculated means the new host nests are formed through the levy flights by considering nest 'i' and the fitness is calculated again. Then the calculated fitness value is compared with the one which is obtained in the previous stage and if the current one is better means the old host nest will be replaced with the newest one. Else the fraction of worst nests are taken to form the new population of nests. The best solution obtained till the process will be stored and if all the nests are considered or the maximum number of iterations are reached means the algorithm will be stopped and the best solution will be returned. Otherwise it will continues until are the nests are considered or else the maximum number of iterations reached. The weight coefficients are optimized in this way and the network is trained to produce the corresponding output values. After training the network with the maximum number of training samples the testing of the network is carried out and the testing procedure involved here is explained in the next section.

### Testing of ANN

The testing procedure is also similar to that of the training of the neural network except that the learning error and hence the optimization is not done here. In the training stage the NN is trained to produce the words as recognized in the speech signal and in testing, the recognition performance of the network is validated. The experimental set up employed in our proposed work, the results, comparison with other works and the corresponding discussions are given in the experimental part.

## RESULT AND DISCUSSION

In this paper, we have proposed a methodology of the ASR system for the man machine interaction with fuzzy based DWT feature extraction and the ANN optimized with the CSO algorithm. The proposed work is implemented in the working platform of MATLAB of version R2013a with the system configurations of Intel core i3 processor, 4GB RAM and Windows 8 Operating system. In this section, the dataset used in our proposed work, the results of the proposed method, the comparison results as well the discussions about the improvement of work is presented.

### Dataset

In this paper, we use the Grid corpus [29] as a small-vocabulary ASR task to evaluate all approaches. The Grid database consists of 34,000 sentences that were uttered by 34 speakers, i.e., 1000 sentences per speaker. The task of the Grid corpus is to recognize sentences from a small vocabulary (51 words) with a fixed grammar of the form: command-color-preposition letter-digit-adverb. We have taken 100 speech data from the database among them 80% is used for training the recognizer and 20% is for testing the recognizer. The structure of the sentences in the grid database is given in the following [Table 1].

**Table 1:** Sentence Structure in Grid database

Command	Color	Preposition	Letter	Digit	Adverb
Bin	Blue	At	a-z (Except 'w')	0-9	Again
Lay	Green	By			Now
Place	Red	On			Please
Set	White	With			Soon

### Preprocessing results of the speech signal

From this signal the preprocessing steps are applied to produce the enhanced version and to be suitable for the application of further operations. Initially, sampling of the signal is done to produce the sampled data at a sampling frequency of  $f_s = 10$  kHz. After sampling, frames are produced with Hamming windowing at the specified intervals in section 3.1.2 and then noise present in the signals are removed with Harmonic Level decomposition. The preprocessing result of the sample signal from the database is given in the [Fig. 6] below.

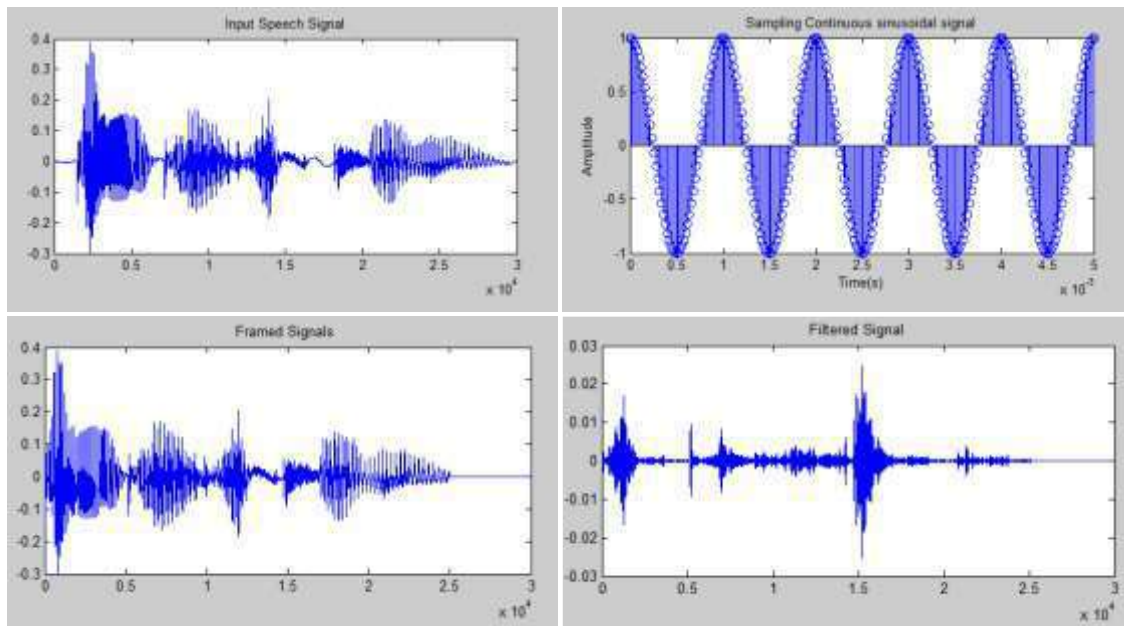


Fig. 6: Preprocessing result of the sample speech signal.

In [Fig. 6], the top left corner shows the original speech signal, the sampled signal produced is given in the top right corner, the frames of the signal is given in bottom left corner and the filtered signal is shown in the bottom right corner. After that eight different feature coefficients are extracted through 8-level DWT, which are totally 64 coefficients for each signal. From this two feature coefficients are selected optimally per each type of feature using the fuzzy model. The decomposed signal obtained with DWT feature extraction is shown in the following [Fig. 7].

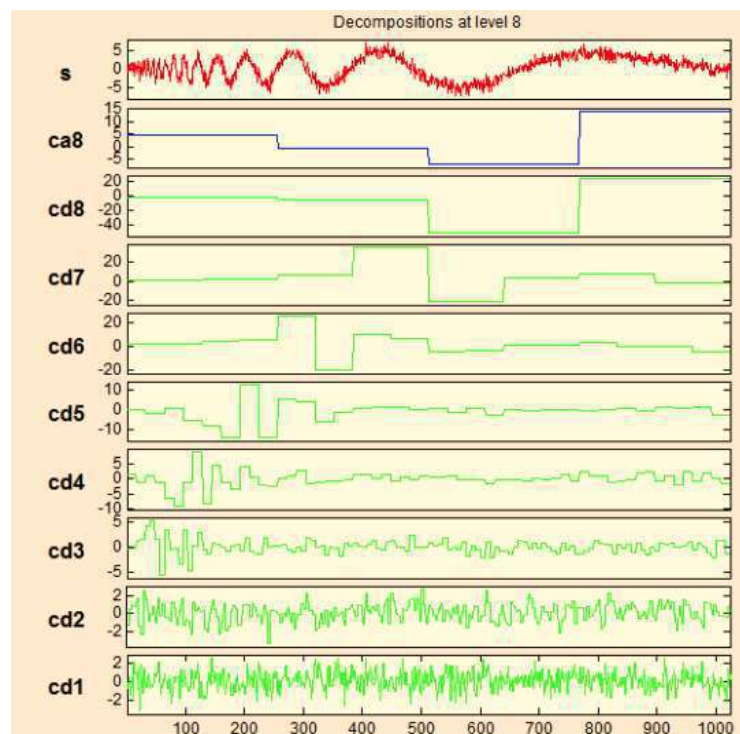


Fig.7: Eight level decomposition of the original speech signal by DWT.

The eight type of features calculated from these decomposition levels for the speech signal '  $S_i$  ' is tabulated in the following [Table 2].

**Table 2:** Feature values of the signal  $S_i$  by DWT

Type of Feature	Feature Value
Mean	65.6667
Standard Deviation	58.0108
Skewness	-2.7095
Kurtosis	6
Entropy	0.5441
Shannon Entropy	-4.5223e+5
Log energy Entropy	99.9938
Renyi's Entropy	-6.9389e^-16

Then the selected features from [Table 2] are used to train the NN in which the learning error is corrected by optimizing the weights at output neuron through CSO algorithm. The results of the speech recognition are given in the next section.

### Results of recognition

In this section the results of our proposed speech recognition system for man machine interaction are presented. The performance of our proposed methodology is evaluated here based on the performance metrics such as recognition accuracy, word error rate, sensitivity, specificity, true positive rate and false positive rate.

#### Recognition accuracy

Recognition accuracy is defined as the performance metric which is used to measure the performance of a recognition system. The recognition accuracy  $R_a$ , is simply calculated using the following equation (29).

$$R_a = \frac{\text{Number of recognized words}}{\text{Total number of words}} \quad (29)$$

The greater the recognition accuracy of the system, the greater its recognition performance.

#### Word Error Rate (WER)

Word error rate is also the performance measure used to measure the recognition system performance. This is calculated directly from the equation (29) and given in equation (30).

$$WER = 1 - R_a \quad (30)$$

The lower the WER the better the performance of the speech recognition system.

#### Sensitivity

A measure of the capability of a method to properly recognize positive samples is sensitivity. It could be computed using the subsequent equation.

$$\text{Sensitivity} = \frac{TP}{TP + FN} \quad (31)$$

The sensitivity value ranges between 0 and 1, where 1 and 0 mean best and worst recognition of positive samples, correspondingly.

#### Specificity

A measure of the ability of a method to recognize properly negative samples is specificity. It might be computed using the following equation.

$$\text{Specificity} = \frac{TN}{TN + FP} \quad (32)$$

The specificity value ranges between 0 and 1, where 0 and 1 refers to worst and best appreciation of negative samples, correspondingly.

**False positive rate (FPR)**

It is the existence rate of positive test results in matters do not known to have the behavior for which an individual is being tested. The FPR is computed as in the following equation (33).

$$FPR = \frac{FP}{FP + TN} \tag{33}$$

**False Negative rate (FNR)**

It is the occurrence rate of negative test results in subjects referred to have the performance for which an individual is being verified. The FNR is computed as in the following equation (34).

$$FNR = 1 - TPR \tag{34}$$

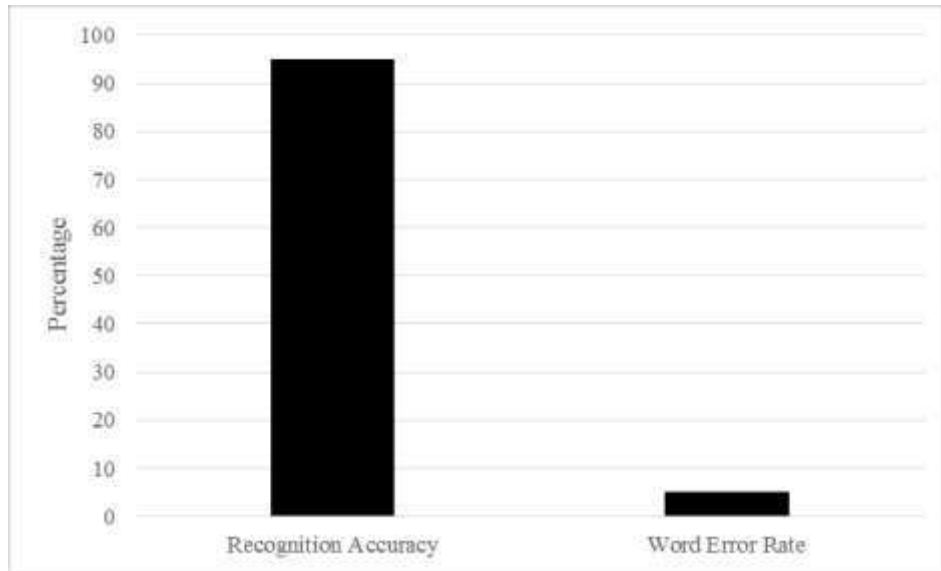
**ROC Curve**

ROC curve clearly depicts the characteristic of any of the recognition system and it is the curve drawn between the TPR and FPR of the system. The ROC of our proposed methodology is shown in [Fig. 9]. The results of our proposed methodology in terms of these performance metrics are given in [Table 3] as well as in [Fig. 8].

**Table 3:** Results of Proposed Methodology

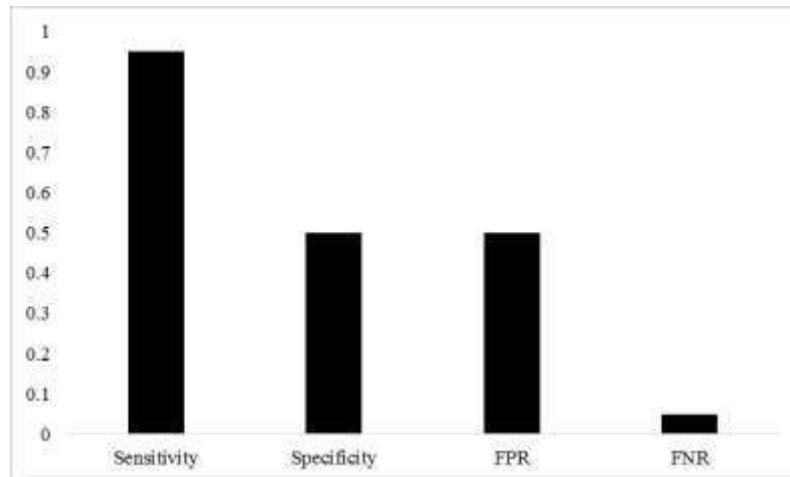
Performance Metric	Result
Recognition Accuracy (%)	95%
Word Error Rate (%)	5%
Sensitivity	0.95
Specificity	0.5
False Positive Rate (FPR)	0.5
False Negative Rate (FNR)	0.05

The results of our proposed methodology in terms of recognition accuracy and word error rate is represented graphically in the following [Fig. 8].



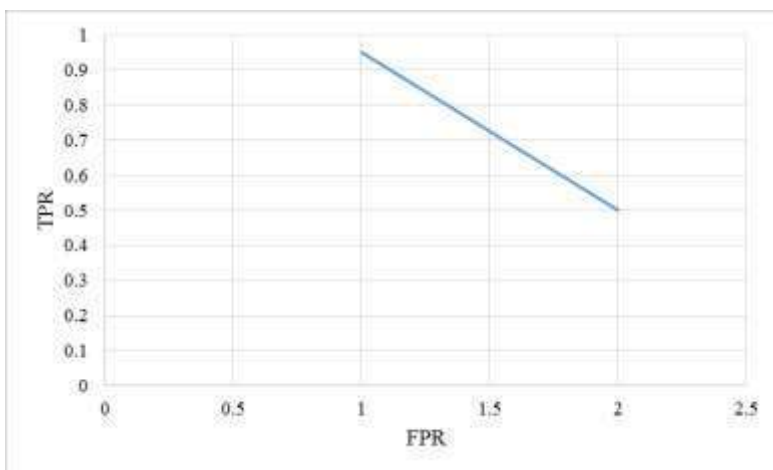
**Fig.8:** Performance of proposed methodology in terms of recognition accuracy and word error rate.

The performance of the recognizer is more understood by the performance metrics such as sensitivity, specificity, FPR and FNR for that the results obtained with our methodology is 0.95, 0.5, 0.5 and 0.05 respectively. This shows that most of the words are correctly recognized by our proposed methodology each signal. The results of our proposed method in terms of these parameters is presented in the following [Fig. 9].



**Fig. 9:** Performance of proposed methodology in terms of Sensitivity, Specificity, False Positive Rate (FPR), False Negative Rate (FNR).

The corresponding ROC graph is presented in the following [Fig. 10]. It is the graph drawn between Sensitivity and FPR.



**Fig. 10:** ROC curve of our proposed methodology.

In order to prove the efficiency of our proposed methodology, it is compared with different techniques in terms of the performance metrics and this is presented in the following section.

### Performance Comparison

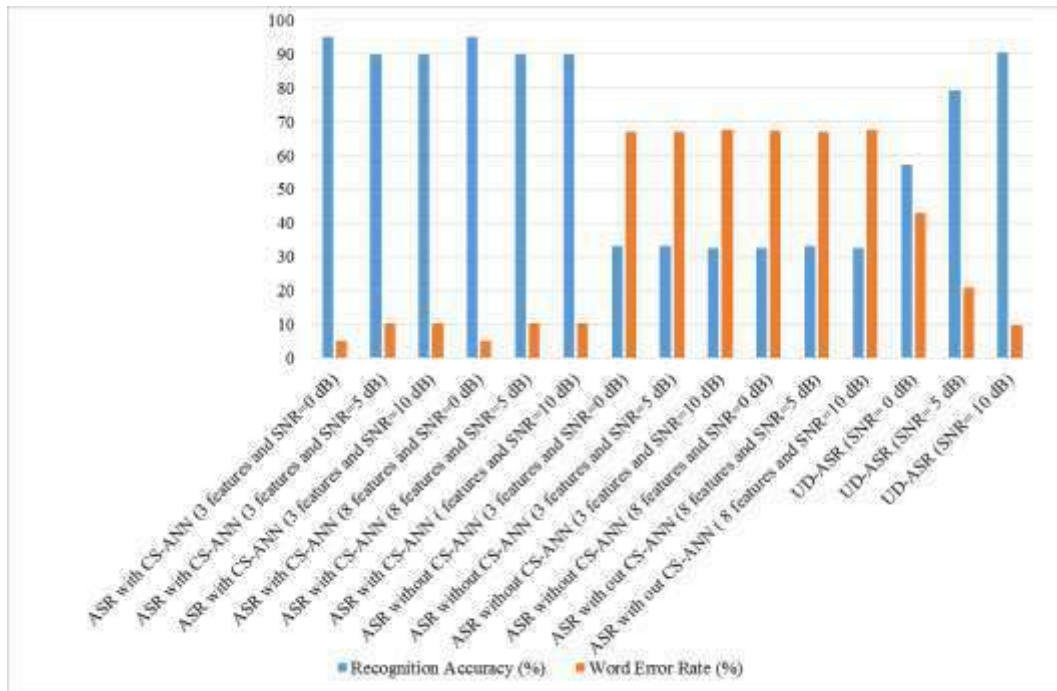
The performance of our proposed man machine interaction system is validated with speech recognition with conventional back propagation and uncertainty-decoding based ASR [30] under the presence of babble noise at different levels with minimum and maximum number of features. The performance comparison results are given in [Table 4] and in [Fig.11].



**Table 4:** Performance Comparison of Proposed Methodology with other techniques

Performance Metric	Method														
	Proposed ASR with CS-ANN						ASR without CS-ANN						Uncertainty-decoding based ASR (UD-ASR) [30]		
	With 3 features (SNR in DB)			With 8 features (SNR in DB)			With 3 features (SNR in DB)			With 8 features (SNR in DB)			UD-GHF Decoding (SNR in DB)		
	0	5	10	0	5	10	0	5	10	0	5	10	0	5	10
Recognition Accuracy (%)	95	89.83	89.83	95	89.83	89.83	33.16	33.16	32.5	32.67	33.16	32.5	57.14	79.20	90.40
Word Error Rate (%)	5	10.17	10.17	5	10.17	10.17	66.84	66.84	67.5	67.33	66.84	67.5	42.86	20.8	9.6

The performance comparison results as given in the [Table 3] can be best understood by the result as given in the following [Fig. 11].



**Fig. 11:** Performance Comparison of Proposed Methodology (ASR with CS-ANN), ASR without CS-ANN and Uncertainty decoding based ASR with other techniques.

From the results of our proposed methodology as well as its comparison with the existing techniques the recognition rate achieved by our system is better than other methods such that the recognition accuracy is 95% with zero level of Babble noise and even after increasing the noise levels to 5 and 10 dB the accuracy of recognition is better than the method without optimization. Similarly UD-ASR method has the recognition accuracy

of 57.14%, 79.20% and 90.40% with the noise levels of 0 dB, 5 dB and 10 dB respectively and the discussion about these results is given in the following section.

## DISCUSSION

The results shown in the [Tables 2-3] and in [Fig. 7-10] clearly depicts that better performance results are obtained with our proposed man machine interaction system for ASR compared with other techniques. The recognition rate achieved with our system is 95% which is better than the method proposed in [30] and without CS-ANN. This is clearly depicted in table 3 as well as in [Fig. 8], such that the system without CS algorithm in optimizing the ANN yields poor recognition results than the system with CS as well as the existing method [30]. However the accuracy of our proposed method is better than the method which we are taken into consideration even in the presence of babble noise at different levels, but the method in [30] achieved lower results compared to ours in lower SNR levels. The recognition results also shows that most of the words in the testing phase is identified clearly and hence the lower word error rate. Hence our proposed Fuzzy based DWT feature extraction produce better recognition and accuracy of the ASR system at low SNR levels and the accuracy level is maintained even the SNR level is increased which shows the efficiency of proposed method in achieving better accuracy results. The comparison result given in [Table 3] also shows that with the use of our proposed feature selection method the accuracy levels remains a stable one and with the CS-ANN classification the accuracy level is increased. In addition to that the optimization algorithm we have employed and the extracted features also have the major impact in recognizing the words as given by the comparison results.

## CONCLUSION

In this paper we have proposed a methodology for man machine interaction system in ASR systems through fuzzy based feature selection and ANN optimized with CS optimization algorithm. The speech signals are initially converted into samples, frames using Hamming window and the noise levels are suppressed by harmonic decomposition. Next eight different features are extracted from the speech signal through DWT and the most relevant features selected by Means of fuzzy logic. The selected features are employed in training the NN in which the optimization of the network is performed by CSO algorithm. The experimental results are presented and compared with conventional technologies under various conditions and the results shows the efficiency of our proposed methodology. The experimental results given in section 4.3 reveals that the proposed ASR can achieve the recognition accuracy of 95% with lower word error rate of 5% which shows the betterment of our proposed work. The recognition accuracy achieved by our method is 95% with SNR level of babble noise at 0 dB, 89.83% at both the SNR levels of 5 dB and 10 dB respectively and it is a better result compared to the uncertainty decoding based method.

### CONFLICT OF INTEREST

There is no conflict of interest between the authors regarding the manuscript.

### ACKNOWLEDGEMENTS

None

### FINANCIAL DISCLOSURE

No financial contribution for my manuscript.

## REFERENCES

- [1] Harrag A. [2015] Nature-inspired feature subset selection application to arabic speaker recognition system, *International Journal of Speech Technology* 18(2): 245-255.
- [2] El Ayadi M, Kamel MS, Karray F.[2011] Survey on speech emotion recognition: Features, classification schemes, and databases, *Pattern Recognition* 44(3): 572-587.
- [3] Furui S. [2010] History and development of speech recognition, In *Speech Technology*, Springer US, 1-18,.
- [4] Yang B, Luggner M.[2010] Emotion recognition from speech signals using new harmony features, *Signal processing*, 90(5): 1415-1423.
- [5] Patel I, Rao YS. [2010] A frequency spectral feature modeling for hidden markov model based automated speech recognition, In *Recent Trends in Networks and Communications*, Springer Berlin Heidelberg, 134-143.
- [6] Barker J, Vincent E, Ma N, Christensen H and Green P. [2013] The PASCAL CHiME speech separation and recognition challenge, *Computer Speech & Language* 27(3): 621-633.
- [7] Goh C ,Leon K. [2009] Robust computer voice recognition using improved MFCC algorithm, In *Proceedings of International Conference on New Trends in Information and Service Science*, 835-840.
- [8] Hinton G, Deng L, Yu D, Dahl GE, Mohamed AR, Jaitly N, Kingsbury B. [2012] Deep neural networks for acoustic modeling in speech recognition: The shared views of four research groups, *IEEE Signal Processing Magazine* 29(6): 82-97.
- [9] Siniscalchi S. M, Yu D, Deng L, Lee CH [2013] Exploiting deep neural networks for detection-based speech recognition, *Neuro computing*, 106:148-157.
- [10] Dahl GE, Yu D, Deng L, and Acero A. [2012] Context-dependent pre-trained deep neural networks for large-vocabulary speech recognition, *IEEE Transactions on Audio, Speech, and Language Processing* 20(1): 30-42.
- [11] Lee C, Hyun D, Choi E, Go J, Lee C.[2003] Optimizing feature extraction for speech recognition, *IEEE Transactions on Speech and Audio Processing* 11(1): 80-87.
- [12] Al-Alaoui M A, Al-Kanj L, Azar J, Yaacoub E. [2008] Speech recognition using artificial neural networks and hidden

- Markov models", IEEE Technology and Engineering Education (ITEE) 3(3): 77-86.
- [13] Xi X, Lin K, Zhou C, and Cai J. [2005] A new hybrid HMM/ANN model for speech recognition, In Artificial Intelligence Applications and Innovations, Springer US, 223-230.
- [14] Besson P, Popovici V, Vesin JM, Thiran JP, Kunt M. [2008] Extraction of audio features specific to speech production for multimodal speaker detection, IEEE Transactions on Multimedia 10(1): 63-73.
- [15] Jensen R and Shen Q. [2007] Fuzzy-rough sets assisted attribute selection, IEEE Transactions on Fuzzy Systems 15(1): 73-89.
- [16] Alcalá R, Gacto MJ, and Herrera F. [2011] A fast and scalable multi-objective genetic fuzzy system for linguistic fuzzy modeling in high-dimensional regression problems, IEEE Transactions on Fuzzy Systems, 19(4): 666-681.
- [17] Weinland D, Ronfard R and Boyer E. [2011] A survey of vision-based methods for action representation, segmentation and recognition, Computer Vision and Image Understanding 115(2): 224-241.
- [18] Zamani B, Akbari A, Nasersharif B and Jalalvand A [2011] Optimized discriminative transformations for speech features based on minimum classification error, Pattern Recognition Letters 32(7): 948-955.
- [19] Chandrashekar G, and Sahin F. [2014] A survey on feature selection methods, Computers & Electrical Engineering, 40(1): 16-28.
- [20] Mirhassani SM, Ting HN. [2014] Fuzzy-based discriminative feature representation for children's speech recognition, Digital Signal Processing 31:102-114.
- [21] Kaya H, Ozkaptan T, Salah AA, Gurgen F. [2015] Random discriminative projection based feature selection with application to conflict recognition, IEEE Signal Processing Letters 22(6): 671-675.
- [22] Cumani S, and Laface P. [2014] Large-scale training of pairwise support vector machines for speaker recognition, IEEE/ACM Transactions on Audio, Speech and Language Processing (TASLP) 22(11):1590-1600.
- [23] Chatterjee S, Kleijn WB.[2011]Auditory model-based design and optimization of feature vectors for automatic speech recognition, IEEE Transactions on Audio, Speech, and Language Processing 19(6): 1813-1825.
- [24] Dikici E, Semerci M, Saraçlar M, Alpaydın E.[2013] Classification and ranking approaches to discriminative language modeling for ASR", IEEE Transactions on Audio, Speech, and Language Processing 21(2): 291-300.
- [25] Pan ST and Li XY. An FPGA-based embedded robust speech recognition system designed by combining empirical mode decomposition and a genetic algorithm, IEEE Transactions on Instrumentation and Measurement 61(9): 2560-2572.
- [26] Meseguer NA. [2009] Speech analysis for automatic speech recognition.
- [27] T Yuvaraja, M Gopinath.[2014] Fuzzy Based Analysis of Inverter Fed Micro Grid inslating Operation International Journal of Applied Engineering Research ISSN 0973-4562 Volume 9, Number 22 (2014) pp. 16909-16916.
- [28] Yuvaraja Teekaraman\*, Gopinath Mani.[2015]Fuzzy Based Analysis of Inverter Fed Micro Grid in Islanding Operation-Experimental Analysis International Journal of Power Electronics and Drive System (IJPEDS) 5(4): 464~469
- [29] T Yuvaraja, K Ramya. Implementation of Control Variables to Exploit Output Power for Switched Reluctance Generators in Single Pulse Mode Operation IJE TRANSACTIONS A: Basics 29(4): 505-513.

ARTICLE

# IMPLEMENTING AUTOMATIC BRAIN ABNORMALITY DETECTION SYSTEM USING REACTIVE OPTIMIZED CONVOLUTION NEURAL NETWORKS

Arjunan Kavitha<sup>1\*</sup> and Vellingiri Krishnaveni<sup>2</sup>

<sup>1</sup>Department of Electronics and communication Engineering, Faculty of Information and communication Engineering Hosur, INDIA

<sup>2</sup>Department of Electronics and communication Engineering, Faculty of Information and communication Engineering, Coimbatore, INDIA

## ABSTRACT

Epilepsy is a standout amongst the most perilous neurological ailments which make the epileptic seizure excessively numerous individuals on the planet. The seizure has been difficult to detectable because it may be occurred by brain injuries, brain tumors, birth defects, infection of the brain, stroke and genetic mutation. The difficulties present in the epilepsy have been effectively recognized by using the Electroencephalogram (EEG) because it captures the brain electrical activities in various conditions with effective manner. Several researches use the EEG for detecting the brain abnormalities but still they have some issues like error rate, performance of the system, sensitivity and specificity. So, in this paper develops the automatic brain abnormality detection system using the EEG measure. Initially the recorded EEG signal is preprocessed by applying the common average singular value referencing approach. Then the noise removed EEG is decomposed with the help of the Multi Resolution Second Generation Wavelet transform. From the segmented signal various invariant and entropy features are extracted and the dimensionality of the feature is further reduced with the help of the Memetic redundancy feature selection approach. The selected features are classified by using the Reactive optimized convolution neural networks. Then the efficiency of the proposed system is evaluated with the help of the various EEG dataset like CHB-MIT Scalp EEG Database and European database in terms of the error rate, sensitivity, specificity and accuracy.

## INTRODUCTION

In the creating scene, epilepsy in one of the significant demise causes ailment because of the imperceptible issues, for example, cerebrum wounds, mind tumors, birth abandons, disease of the mind, stroke and hereditary change present in the human cerebrum [1]. As indicated by the different scrutinizes studies, 80% individuals kicked the bucket in light of the epilepsy issue which was demonstrated by the best perustration. The quantity of the general population passings are expanded from 1990 to 2013 in light of the fact that, in 1990 the 112,000 people groups are kicked the bucket because of epilepsy seizure though in, 2013 116,000 people groups are kicked the bucket which demonstrates that number of death proportion is expanded often [2]. Further the overview obviously demonstrates that the most epilepsy seizure is influenced in the time of more youthful grown-ups because of the different weights and 5-10% of the seizure is influenced by the age 80 which is still dubious. This reviews are unmistakably demonstrates the epilepsy is more risky when contrasted with the other malady because of the imperceptible manifestations. In this way, the trouble present in the seizure is examined from utilizing the Electroencephalogram, fMRI, CT thus on [3]. Among the different mind movement measure EEG dissect the cerebrum exercises with high exact way in light of the fact that the EEG catch the electrical exercises regarding the milliseconds which implies, the EEG recognize the single neuron action change with precise way when contrasted with the other mind action measure.

The EEG has been recorded by putting the quantity of anodes on the scalp up to specific day and age to breaking down the different mind exercises like backhanded marker, capacity of the cerebrum, persistent perfusion levels are checked continuously[4]. The recorded EEG sign is examine the diverse sorts of seizures, for example, Primary summed up seizures, Partial seizures with precise way by utilizing the different sign handling and machine learning strategies. The example EEG recorded setup is appeared in the [Fig. 1].

In this way, the different looks into use the changed philosophies like autonomous segment investigation, wavelet change, Fourier change, bolster vector machine, neural systems are utilized to examine the epilepsy [5]. These methodologies are proficiently perceiving the seizure however it has a few troubles like mistake rate and precision additionally the strategies are hard to handle the vast measure of dataset. Along these lines, the creator builds up the programmed cerebrum variation from the norm discovery framework utilizing the responsive based neural systems for beating the issues present in the current anomaly recognition strategies.

The remaining of the paper is organized as follows; section 2 provides the related works made on the epilepsy detection using the EEG signal. Section 3 discusses that the proposed system methodologies and the related architecture. Section 4 provides the results and discussions. Finally, section 5 concludes the proposed work.

### KEY WORDS

Epilepsy,  
Electroencephalogram,  
CHB-MIT, Scalp EEG

Received: 3 Oct 2016  
Accepted: 9 Dec 2016  
Published: 18 Dec 2016

### \*Corresponding Author

Email:  
arjunankavithaphd@gmail.com

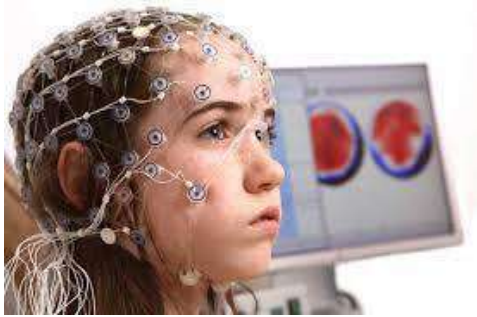


Fig. 1: EEG Capturing Setup.

## RELATED WORKS

In this section reveals that the various research opinions about the brain abnormality detection system. Juarez-Guerra et al., [6] developing the automatic seizure detection system using the discrete wavelet and neural networks. The author analyzes the recorded EEG signal and decomposes the signal into different bands. From the decomposed signal various overlapping features are efficiently retrieved with the help of the Maximal overlap discrete wavelet transform. The extracted features trained by feed forward neural networks which uses the optimized training function. The efficient training function leads to analyze the abnormal feature set easily and the efficiency of the system is evaluated in terms of using the university of bonn dataset which achieves the highest accuracy with three fold cross validation.

Zainuddin et al [7] introducing the wavelet based neural networks for detecting the epilepsy disease. Author analyzes the recorded EEG signal using the wavelet method and the sub bands are extracted. From the extracted sub bands various features like standard deviation, minimum, maximum values are derived according to the wavelet co-efficient. The extracted features are fed into the neural network to analyze the abnormal features. The classified results are evaluated with the help of the Freiburg EEG database which ensures the high sensitivity rate and minimum error rate when compared to the other methods.

Yatindra Kumar et al., [8] analyzing the dangerous epilepsy disorder using the ApEn neural networks with minimum error rate. The captured EEG signal is preprocessed and the different coefficients are evaluated with the help of the discrete wavelet transform. From the wavelet coefficients various approximation values are derived. The derived features are fed into the feed forward neural networks to analyze the various abnormalities like dementias, partial seizure, primary seizure, stroke, brain injuries. At last the performance of the system is evaluated with the help of the experimental results and discussions. Thus the proposed system ensures the minimum error rate and maximum recognition accuracy while analyzing the abnormal features.

Yatindra Kumar [9] discussing the various machine learning and sampling techniques to diagnosis the seizure from the recorded EEG signal. The recorded signal is analyzed in terms of the optimum allocation sampling and random sampling techniques. The analyzed signal is evaluated in terms of applying the both rough set and OS set. From the analyzed data signal 11 different statistical features are extracted which are fed into the various classifiers like K-nn, SVM and MLP classifier which analyze the abnormal disease with efficient manner. Then the efficiency is evaluated using the experimental results and discussions. According to the various authors discussions, the proposed seizure detection system is created for overcoming the accuracy and database issue which are explained in the following section.

## PROPOSED METHODOLOGIES

In the advancing scene, epilepsy is one of the perilous illness which prompts slaughter the general population in light of the imperceptible indications. At that point the troublesome seizure has been proficiently related to the assistance of the EEG cerebrum estimations. In this way, in this paper use the two diverse EEG databases to be specific, CHB-MIT Scalp EEG Database and European database with viable way. The proposed framework incorporates the four distinct strides, for example, preprocessing, highlight extraction, highlight determination and seizure characterization which are utilized to dissect and recognize the epilepsy in the human cerebrum. At that point the proposed framework square graph is appeared in the [Fig. 2].



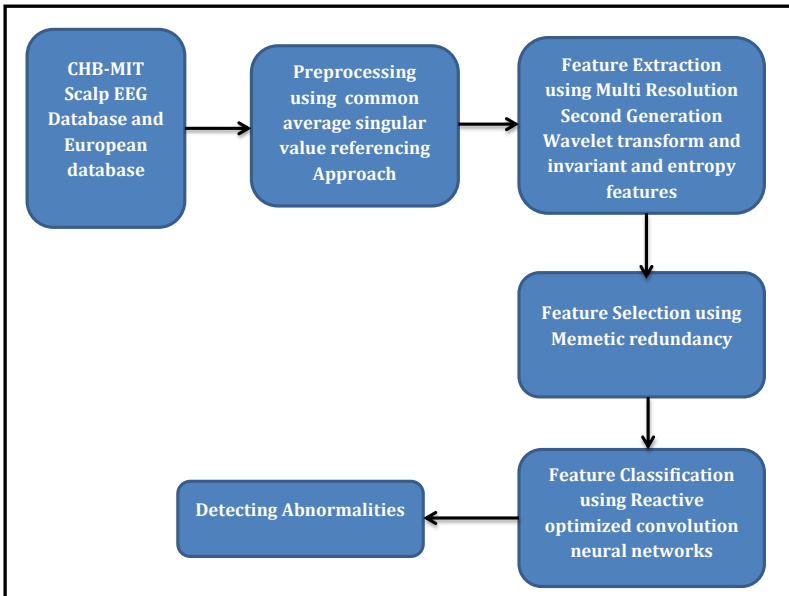


Fig. 2: Proposed system architecture.

### EEG preprocessing

The first stage of the seizure detection is preprocessing because the recorded EEG signal has several unwanted information which reduces the entire system performance [10]. So, in this paper uses the common singular value referencing approach for eliminating the entire unwanted information from the EEG signal with effective manner. Initially the common referencing method is applied to all EEG electrodes for removing the unwanted feature also enhances the signal to noise ratio. The average or mean value of the each electrodes are removed from the set of electrodes as follows,

$$CzCAR = C_z - (Fp_1 + AF_3 + F_7 + \dots F_z + MA_1 + MA_2)/34 \quad (1)$$

After removing the average mean electrode the filtering technique such as the singular value method is applied to remove all the additional noise present in the EEG signal. The method considered the total EEG signal into the  $m \times n$  matrix which consists of three matrix that is represented as follows,

$$M = U \Sigma V^* \quad (2)$$

Where  $U$  is the  $m \times m$  matrix of the left orthogonal matrix that is represented as the  $U = [u_1, u_2, \dots, u_m]$  and  $\Sigma V^*$  is the rectangular diagonal matrix and the conjugated transpose the  $V V^* = [v_1, v_2, \dots, v_n]$  of the  $n \times n$  real matrix of the right orthogonal matrix which is represented as follows,

$$AA^t = U \Sigma V^* V \Sigma U^t = U \Sigma^2 U^t \quad (3)$$

Where  $AA^t$  is the eigen vectors of columns of  $m \times m$  matrices

$$A^t A = V \Sigma U^t U \Sigma V^t = V \Sigma^2 V^t \quad (4)$$

Where  $A^t A$  eigen vector of  $n \times n$  matrix column

$\Sigma$  is the singular value which is having the non-negative values that is represented

As,

$$\Sigma = \text{diag}(\sigma_1, \sigma_2, \dots, \sigma_n) \quad (5)$$

Where,  $\sigma$  is the singular value of the  $A$

According to the matrix the first value is direction of the greatest data variants and other values are orthogonal direction of the data. Finally the rotation operation is performed for analyze and the highest ranked electrode features are eliminated successfully.



At last the bipolar and unipolar direction of electrodes also removed, which is completely eliminated the unwanted electrode feature successfully. The preprocessed EEG signal is fed into the next feature extraction stage.

### Feature extraction

The second phase of the seizure discovery procedure is highlight extraction. Before extricating the component from the EEG flag, the preprocessed EEG sign is decayed into various groups for determining the proficient elements. The sign disintegration [11] is finished with the assistance of the multi determination second era wavelet. At first the sign is investigated in an alternate heading for social affair the part of data additionally diminishing the data misfortune while disintegrating the EEG signal. The second era wavelet change, investigate the sign and sifting the EEG into various groups with the assistance of the lifting plan. The method analyzes the preprocessed signal and decomposes into detailed and the approximate band which eliminates the unwanted information. During the decomposition process, the given input EEG signal is spilt into the odd and even samples like  $\gamma_1$  and  $\lambda_1$  which is used for decomposition process. According to the sample details, the detailed coefficient value is retrieved from the signal using the even value of the signal in the multi direction.

$$\gamma_2 = \gamma_1 - P(\lambda_1) \quad (6)$$

After deriving the detailed coefficients the approximate coefficients are retrieved as follows,

$$\lambda_2 = \lambda_1 + U(\gamma_2) \quad (7)$$

From the above eqn P represented as the prediction operator and U is the updating operator which is used to analyze the detailed and approximate coefficient with efficient manner. This way of decomposing process enhance and fastest the decomposing methodology while analyzing the EEG. after decomposing the EEG signal various invariant and entropy features are extracted. The invariants analyze the decomposed EEG signal [12] with the relative position of the key features because the particular key feature does not change from one human brain measure to other. During the feature extraction process it has following steps like key point detection, key point location, orientation assignment and keypoint descriptors. The key point detection combines to work with the Gaussian filter which analyze the maximum and minimum value of the each sub band which is calculated as follows,

$$D(x, y, \sigma) = L(x, y, K_i\sigma) - L(x, y, K_j\sigma) \quad (8)$$

Where  $D(x, y, \sigma)$  the difference of the Gaussian filter band is  $L(x, y, K\sigma)$  is the convolution value of the band,  $I(x, y)$  is the Gaussian blur value,

$$L(x, y, K\sigma) = G(x, y, k\sigma) * I(x, y) \quad (9)$$

After retrieving the key point from the signal, point location is estimated which is done with the help of the Taylor series which is estimated as follows,

$$D(x) = D + \frac{\partial D}{\partial x} x + \frac{1}{2} \frac{\partial^2 D}{\partial x^2} x^2 \quad (10)$$

Finally the orientation has been assigned as follows, which is used to identify the direction of the particular key point is measured by the magnitude and orientation estimation.

$$m(x, y) = \sqrt{(L(x+1, y) - L(x-1, y))^2 + (L(x, y+1) - L(x, y-1))^2} \quad (11)$$

$$\theta(x, y) = \text{atan2}(L(x, y+1) - L(x, y-1), L(x+1, y) - L(x-1, y)) \quad (12)$$

Where,  $m(x, y)$  = magnitude of the key band  
 $\theta(x, y)$  = orientation the key point band

Finally the key point descriptors are extracted by analyzing the key point detector and the orientation assignment process. In which the decomposed signal key descriptors various features are extracted which are listed in the [Table 1].

Table 1: List of features

Features	Related Formula
Entropy	$\sum_{i=0}^{n-1} -\ln(P_{ij}) P_{ij}$

Variance	$\sum_{i=0}^{n-1} \sum_{j=0}^{n-1} (i - \mu)^2 \cdot p(i, j)$
Mean	$\sum_{i=0}^{2(n-1)} i \cdot p_{x+y}(i)$
Standard Deviation	$\sqrt{\left( \sum_{i=0}^{2(n-1)} i \cdot p_{x+y}(i) \right)^2}$

The extracted features are fed into the next feature selection process which is done with the help of the Memetic redundancy feature selection method which is discussed as follows.

### Feature selection

The third phase of seizure recognition procedure is highlight choice which is finished with the assistance of the Memetic repetition approach. The element area [13] strategy breaks down the common data estimation of the specific element and the closeness of the elements is evaluated utilizing the mimetic methodology. From the figured shared data esteem, normal quality is taken for every element and the related class with the successful way which is computed as takes after,

$$D(S, c) = \frac{1}{|S|} \sum_{f_i \in S} I(f_i; C) \quad (13)$$

Where S represented as the redundancy value of the particular feature set average value of the particular mutual information between the two different features which is defined as follows,

$$R(S) = \max_S \left[ \frac{1}{|S|} \sum_{f_i \in S} I(f_i; C) - \frac{1}{|S|^2} \sum_{f_i, f_j \in S} I(f_i; f_j) \right] \quad (14)$$

Amid the normal figuring process, the two distinct components are proficiently picked by qualities of the specific element which finished with the assistance of mimetic procedure. The comparability is evaluated in the all bearing utilizing the specific element qualities like, component significance, effect of the elements et cetera. Subsequently the ascertained contrast worth is investigated against the base esteem and picked the base diverse quality considered as the upgraded highlights which are sustained into the following seizure classifier with the powerful way.

### Seizure classification

The last stride of the seizure discovery calculation is seizure grouping which is finished with the assistance of the responsive streamlined convolution neural systems [14]. The convolution neural system is one of the managed neural systems; it comprises of four distinct layers, for example, convolution layer, pooling layer, corrected unit layer and lose layer. Every layer plays out their one capacity for acquiring the ideal yield when contrasted with other neural system in light of the fact that these layers are capacity to prepare even the clamor information. In the convolution layer [15], the greater part of info has been acknowledged from the element choice procedure which is dissecting the diverse course as far as measuring the three distinct parameters. Profundity, side and zero cushioning. In the wake of investigating these parameters pooling layer dissect the most extreme pooling estimation of every component which are nourished into the corrected unit esteem which computes the every element esteem by applying the actuation capacity. Since the enactment or learning capacity decides how quick and how exact the strategy orders the components with least mistake rate. In the wake of applying the enactment work, the blunder rate has been evaluated by contrasting the genuine quality and the related expected worth. On the off chance that the progressions happens, the weight and predisposition quality is redesigned persistently by utilizing the receptive enhancement strategy since it decreases the whole framework blunder rate with compelling way. At the time of output estimation process every layer input is multiplied its related weight value and bias value need to be added. The output calculation is done by using the following way,

$$\text{Net output} = \sum_{i=1}^N x_i * w_i + b \quad (15)$$

Then the updating of the weights and bias or done with the help of reactive method because it easy to analyze features with every direction and objective manner. So, the objective of the feature weight and bias is estimated as follows,

$$f(x) = (f_1(x), f_2(x), \dots, f_k(x))^t \quad (16)$$

According to the above objective function, the weights are updated continuously with previous value. After that the features are trained with the help of the sigmoid, Gaussian function. Then the network analyze all the inputs present in the network with effective manner and effectively classifies the seizure feature

successfully also maximum recognition rate. The efficiency of the proposed system is evaluated using the following experimental results and discussions.

### Statistical analysis

Statistical analysis was done using SPSS 20.0 v. Descriptive analysis was done to estimate the percentage of microorganisms and Chi Square test was done to assess the difference in proportions. Level of significance was taken at  $p < 0.05$ .

## RESULTS AND DISCUSSIONS

In this research work with two different databases such as CHB-MIT scalp EEG dataset and European Database is used for analyzing the efficiency of the proposed system. The CHB-MIT database consists of 256 recorded EEG signals [16] which are captured from the 22 different subjects whose age and sex has been varied. The next EEG database is European EEG [17] database which consists of 225 scalp recordings which are collected from the 275 patients which are used for our research purpose. By using these databases, the seizure features are trained up to 80% and the remaining 20% of the seizure is detected accurately in testing phase successfully. Then the performance of the proposed system is evaluated in terms of the accuracy, sensitivity and specificity.

### Performance metrics

#### Sensitivity

Sensitivity [22] is used to measure how the proposed system correctly classifies the true positive.

$$\text{Sensitivity} = \frac{\text{True Positive}}{\text{True Positive} + \text{False Negative}} \quad (17)$$

Where True positive is successfully or correctly identified the seizure value and the False Negative is successfully rejected incorrect value.

#### Specificity

Specificity [23] is used to measure how the proposed system correctly classifies the false values.

$$\text{Specificity} = \frac{\text{True Negative}}{\text{True Negative} + \text{False Positive}} \quad (18)$$

Where True negative is successfully or correctly rejected value and false positive is successfully rejected value.

#### Classification

Classification accuracy [24] is the measure which is used to estimate how the proposed system successfully classified the number of heart beats in the correct manner which is determined as follows,

$$\text{Classification Accuracy} = \frac{\text{Number of instances correctly classified}}{\text{Total number of instances}} \quad (19)$$

#### Performance analysis

The performance of the proposed reactive optimized convolution neural network is compared with the exiting methods correlation feature selection, particle swarm optimization, genetic algorithm. The feature selection process increases the overall seizure detection process which is shown in the [Fig. 3].

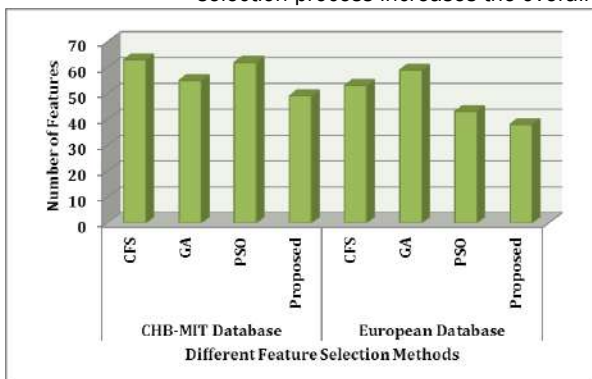


Fig. 3: Performance of various feature selection methods.

[Fig. 3] clearly depicted that the proposed Memetic redundancy feature selection method selects the optimal features from the large collection of dataset when compared to the existing methods. In addition the proposed method works well on both dataset which is means it provides the efficient results on different type of EEG data. The optimized features improve the overall efficiency of the seizure detection system. This efficient feature reduces the entire system error rate which is shown in the [Fig. 4].

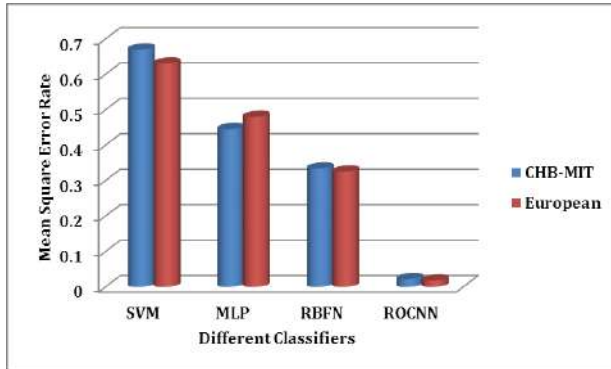


Fig. 4: Error value of the various classifiers.

The above [Fig. 4] depict that the proposed classifier reduces the entire system error rate which means it exactly identifies the seizure feature when compared to the other methods. Then the efficiency of the system is evaluated using the sensitivity, specificity of the proposed system which is shown in the [Fig. 5].

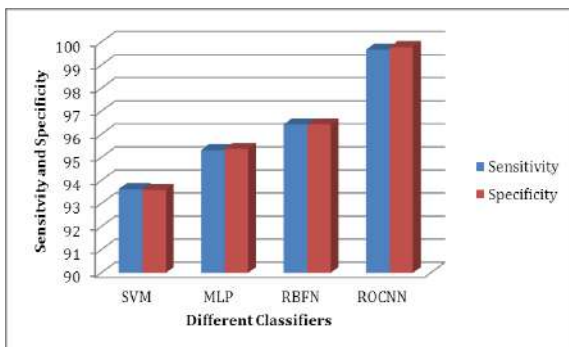


Fig. 5: Sensitivity and specificity.

[Fig. 6] shows the accuracy of different classification techniques, the proposed approach ROCNN attains 99.88 % accuracy overall, while the SVM, MLP; RBFN attains 94.6 %, 95.37% and 95.93%.

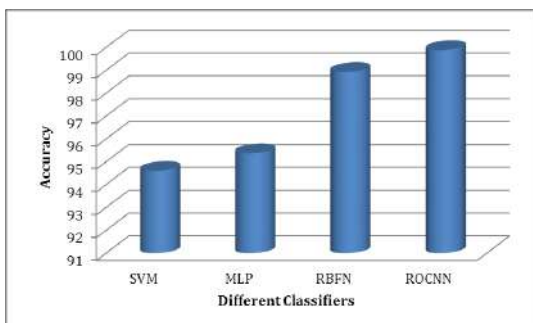


Fig. 6: Accuracy.

Thus the proposed system efficiently classifies the seizure epilepsy diseases when compared to the other traditional and existing methods like a support vector machine, Multilayer Perceptron and Radial Basis Function Networks. Further the proposed system resolves the existing researches drawbacks also reduces the entire dimensionality of the feature set. This minimum feature set reduces the entire error rate also increase the seizure recognition rate up to 99.88%.

## CONCLUSION

This paper analyzes and implementing the automatic seizure detection system using the reactive optimized convolution neural networks. Initially the EEG signal noise removed by applying the common singular value reference which evaluates the each electrode present in the recorded EEG signal. From the preprocessed EEG signal, the different EEG signal band is decomposed with the help of the multi resolution second generation wavelet transform which analyze the signal in terms of different direction. From the decomposed signal, invariant and entropy features are extracted and the dimensionalities of the features are reduced with the help of the Memetic redundancy feature selection method. The selected features are efficiently classified using the proposed classifiers and the efficiency is evaluated with the help of the CHB-MIT and European database in terms of mean square error rate, sensitivity, specificity and accuracy.

**CONFLICT OF INTEREST**  
There is no conflict of interest.

**ACKNOWLEDGEMENTS**  
None

**FINANCIAL DISCLOSURE**  
None

## REFERENCES

- [1] Ramoser H, Muller-Gerking J, Pfurtscheller G. [2000] Optimal spatial filtering of single trial EEG during imagined hand movement, *IEEE Trans. Rehabil. Engg.*
- [2] Ali S, AlMejrad. [2010] Human Emotions Detection using Brain Wave Signals: A Challenging, *European Journal of Scientific Research.* 44(4).
- [3] Fabien Lotte, Cuntai Guan. [2011] Regularizing Common Spatial Patterns to Improve BCI Designs: Unified Theory and New Algorithms, *IEEE Trans. On Biomedical Engg.* 58(2).
- [4] Araki S, Sawada H, Mukai R, Makino S. [2005] a novel blind source separation method with observation vector clustering, *Proc. of IWAENC2005.*
- [5] Kameswara Rao T, Rajya Lakshmi M, Prasad TV. [2012] an Exploration of Brain Computer Interface and Its Recent Trends, *Int. J. of Advanced Research in Artificial Intelligence.* 1(8).
- [6] Juarez-Guerra, Alarcon-Aquino V, Omez-Gil. [2013] Epilepsy Seizure Detection in EEG Signals Using Wavelet Transforms and Neural Networks, *Information and System Science engineering.*
- [7] Enamul Kabir, Siuly, Yanchun Zhang. [2016] Epileptic seizure detection from EEG signals using logistic model trees, *Brain Informatics.*
- [8] Zainuddin Z, Huong LK, Pauline O. [2012] on the use of wavelet neural networks in the task of epileptic seizure detection from electroencephalography signals, *ProcComput. Sci.* 11(2012), 149–159.
- [9] Yatindra Kumar, Dewal ML, Anand RS. [2014] Epileptic seizures detection in EEG using DWT-based ApEn and artificial neural network, *Signal, Image and Video Processing.* 8(7):1323-1334 in *Elesvier.*
- [10] Siuly Siuly, Enamul Kabir, Hua Wang, Yanchun Zhang. [2015] Exploring Sampling in the Detection of Multicategory EEG Signals, *Computational and Mathematical Methods in Medicine.* Article id. 576437.
- [11] Iosif Mporasa, Vasiliki Tsirkab, Evangelia I, Zacharackia, Michalis Koutroumanidis, Mark Richardson, Vasileios Megalooikonomou. [2015] Seizure detection using EEG and ECG signals for computer-based monitoring, analysis and management of epileptic patients, *Expert Systems with Applications.* 42(6).
- [12] Nabeel Ahammad, Thasneem Fathima, Paul Joseph. [2014] Detection of Epileptic Seizure Event and Onset Using EEG, *BioMed Research International Volume.*
- [13] Feng Gu, Julie Greensmith, Robert Oates, Uwe Aickelin. [2009] PCA 4 DCA: The Application Of Principal Component Analysis To The Dendritic Cell Algorithm, In 9th Annual Workshop on Computational Intell. (UKCI). 7-9.
- [14] Ali S, AlMejrad. [2010] Human Emotions Detection using Brain Wave Signals: A Challenging, *European Journal of Scientific Research.* 44(4).
- [15] Fabien Lotte. [2009] Study of Electroencephalographic Signal Processing and Classification Techniques towards the use of Brain-Computer Interfaces in Virtual Reality Applications, *Docteur De L'institut National Des Sciences Appliquées De Rennes Mention Informatique.*
- [16] <https://www.physionet.org/pn6/chbmit/>.
- [17] [http://www.epilepsiae.eu/project\\_outputs/european\\_database\\_on\\_epilepsy](http://www.epilepsiae.eu/project_outputs/european_database_on_epilepsy)